

THE JOURNAL OF PHYSICAL CHEMISTRY

(Registered in U. S. Patent Office)

CONTENTS

E. G. Prout and P. J. Herley: The Thermal Decomposition of Irradiated Permanganates.....	961	tion and Molecular Structure in Liquids. XLVII. The Dielectric Relaxation of Quinoline, Isoquinoline, and Several Monosubstituted Biphenyls in a Very Viscous Solvent.....	1105
G. A. Parks and P. L. de Bruyn: The Zero Point of Charge of Oxides.....	967	Hideo Imai and Paul Delahay: Faradaic Rectification and Electrode Processes. III. Experimental Methods for High Frequencies and Application to the Discharge of Mercurous Ion.....	1108
Victor K. La Mer: The Solubility Behavior of Hydroxylapatite. Sidney I. Miller: Models for Isotope Rate Effects in Displacement, Dissociation, Elimination, and Addition Reactions.....	978	P. W. M. Jacobs, F. C. Tompkins, and V. R. Pai Verneker: The Photochemical Decomposition of Barium Azide.....	1113
Keiji Naito and Toshio Suzuki: The Mechanism of the Extraction of Several Proton Acids by Tri- <i>n</i> -butyl Phosphate.....	983	Clarence J. Wolf and A. C. Stewart: Radiation Chemistry of Octamethylcyclotetrasiloxane.....	1119
Keiji Naito and Toshio Suzuki: The Mechanism of the Extraction of Several Uranyl Salts by Tri- <i>n</i> -butyl Phosphate.....	989	Ralph P. Seward: Hydrazinium Bromide as a Solvent.....	1125
Stanley J. Gill and Guy V. Ferry: Ion Exchange Kinetics of Polyelectrolytes under Steady-State Electrolysis across a Porous Frit.....	995	Douglas Henderson, Henry Eyring, and Dale Felix: The Significant Structure Theory of Liquid Hydrogen in its Various Ortho-Para and Isotopic Forms.....	1128
Guy V. Ferry and Stanley J. Gill: Transference Studies of Sodium Polyacrylate under Steady-State Electrolysis.....	999	Alfred V. Celiano, Michael Cefola, and Philip S. Gentile: Chemistry of Coordination Compounds. IV. Enol Stability of β -Diketones and the Rate of Formation of Monoenolato-copper(II) Ions.....	1132
M. M. Faktor: Standard Free Energy of Formation of Monogermane.....	1003	Tomlinson Fort, Jr.: Adsorption and Boundary Friction on Polymer Surfaces.....	1136
A. S. Tombalakian, H. J. Barton, and W. F. Graydon: Electroosmotic Water Transport across Ion-Exchange Membranes.....	1006	George S. Hammond, Nicholas J. Turro, and Peter A. Leermakers: The Mechanisms of Photoreactions in Solution. IX. Energy Transfer from the Triplet States of Aldehydes and Ketones to Unsaturated Compounds.....	1144
C. L. Sutula and L. S. Bartell: Structure and Molecular Orientation in Multimolecular Films of Long-Chain <i>n</i> -Hydrocarbon Derivatives.....	1010	George S. Hammond and Peter A. Leermakers: Mechanisms of Photoreactions in Solution. X. Relative Efficiencies of Various Quenchers in the Photoreduction of Benzophenone.....	1148
G. Myron Arcand and William R. Carroll: Extraction of Sodium Thiocyanate from Aqueous Solutions by Tributyl Phosphate.....	1014	John E. Gordon: Proton Magnetic Resonance and Infrared Spectra of Some Ion-Exchange Resin-Solvent Systems.....	1150
Harold W. Kohn: Deuterium Exchange on Silica Gel Initiated by Cobalt-60 Irradiation.....	1017	C. D. Wagner: Radiation-Polymerization of Ethylene: Evidence for Ion-Molecule Condensation.....	1158
P. Debye and B. Chu: Spectrophotometry and Light Scattering on Supported Platinum.....	1021	Norman H. Nachtrieb: Magnetic Susceptibility of Some Liquid Metals, Molten Salts, and their Solutions.....	1163
Fred A. Cafasso, Harold M. Feder, and Irving Johnson: Partition of Solutes between Liquid Metals. I. The Aluminum-Cadmium System.....	1028	W. C. Meyer and A. C. Albrecht: A Quantitative Study of a One-Electron Photooxidation in a Rigid Medium.....	1168
James J. Christensen and Reed M. Izatt: Thermodynamics of Proton Dissociation in Dilute Aqueous Solution. II. Heats of Proton Dissociation from Ribonucleotides and Related Compounds Determined by a Thermometric Titration Procedure.....	1030	Charles R. Boston and G. Pedro Emith: Spectra of Dilute Solutions of Bismuth Metal in Molten Bismuth Trihalides. I. Evidence for Two Solute Species in the System Bismuth-Bismuth Trichloride.....	1178
C. A. Bishop and L. K. J. Tong: The Kinetics of the Keto-Enol Tautomerism of Benzoylacetonilide.....	1034	Arnold Reisman and Joan Mineo: Compound Repetition in Oxide-Oxide Interactions: The System $\text{Li}_2\text{O}-\text{V}_2\text{O}_5$	1181
Sang Up Choi and John E. Willard: The Radiolysis of Chloro-, Bromo-, and Iodobenzenes with Cobalt-60 γ -Rays.....	1041	NOTES	
Bernard J. Wood and Henry Wise: The Kinetics of Hydrogen Atom Recombination on Pyrex Glass and Fused Quartz.....	1049	Harold W. Kohn: Surface Carbonium Ions Produced by Irradiating Silica Gel.....	1185
Hiroshi Fujita and Etsuji Maekawa: Viscosity Behavior of the System Polymethyl Acrylate and Diethyl Phthalate over the Complete Range of Composition.....	1053	Sherril D. Christian and M. W. C. Dharmawardhana: A New Method for the Determination of Self-Association Constants of Carboxylic Acids in Solution.....	1187
Richard M. Noyes: Some Conditions for Validity of Statistical Thermodynamic Treatments of Reaction Kinetics.....	1058	W. J. Le Noble, James LuValle, and Asa Leifer: The Strength of Butyric and <i>o</i> -Toluic Acids.....	1188
John G. Schmidt and R. F. Trimble: The Stability Constants of the Mono- and Dipyrzinesilver Complexes.....	1063	Alfred Narten: Separation Factors in the NO-NOBr System.....	1189
A. J. Zielen and J. C. Sullivan: Effects of Solution Composition on the Potentials of the Couples: Np(V-VI) , Fe(II-III) , Hg(0-I) , and Hg(I-II)	1065	J. C. Rohrer and J. H. Sinfelt: Catalytic Hydrogenolysis of Benzene and Toluene.....	1190
Frank Millich and Melvin Calvin: Coacervation of Salts of Polyvinylsulfonic Acid as Induced by Heavy Metal Ions.....	1070	George Van Dyke Tiers: Fluorine Nuclear Magnetic Resonance Spectroscopy. IX. <i>cis</i> - and <i>trans</i> -2-Chloroheptafluorobutene-2. The Assignment of Shielding Values and Spin-Spin Coupling Constants in Fluoroolefin Spectra.....	1192
Guy Waddington, J. C. Smith, K. D. Williamson, and D. W. Scott: Carbon Disulfide as a Reference Substance for Vapor-Flow Calorimetry; the Chemical Thermodynamic Properties.....	1074	J. C. Rohrer and J. H. Sinfelt: Interaction of Hydrocarbons with $\text{Pt-Al}_2\text{O}_3$ in the Presence of Hydrogen and Helium.....	1193
Thomas Gillespie and Ralph M. Wiley: On the Determination of London-van der Waals Constants from Suspension and Emulsion Viscosity and Surface Energy Data.....	1077	Paul Delahay and Akiko Aramata: Ionic Association and Correlation between Double Layer Structure and Electrode Kinetics.....	1194
J. A. Cahill and A. D. Kirshenbaum: The Density of Liquid Copper from its Melting Point (1353° K.) to 2500° K. and an Estimate of its Critical Constants.....	1080	Lohr A. Burkardt: The System 2,4,6-Trinitrotoluene-1,3,5-Trinitrobenzene.....	1196
J. F. Connolly: Ideality of <i>n</i> -Butane: Isobutane Solutions.....	1082	Leonard C. Labowitz: Water-Rich Equilibria in the System $\text{CH}_3\text{COONa}-\text{CH}_3\text{COOH}-\text{H}_2\text{O}$	1197
J. M. Thorp: The Dielectric Behavior of Vapors Adsorbed on Porous Solids.....	1086	J. D. McCullough and Irmela C. Zimmermann: Thermodynamic Studies of the Iodine Complexes of α -Trithiane, Thiacyclohexane, and Thiacyclopentane in Carbon Tetrachloride Solution.....	1198
Joseph B. Levy: The Thermal Decomposition of Paschotic Acid Vapor.....	1092	John L. Margrave, Adli S. Kanaan, and Donald C. Pease: The	
James R. Nash and William H. Hamill: The Effect of Hydrogen Iodide on the Radiolysis of Cyclohexane- d_{12}	1097		
Milton Tamres and Scott Searles, Jr.: The Iodine Complexes of Some Saturated Cyclic Sulfides.....	1099		
Ernest N. DiCarlo and Charles P. Smyth: Microwave Absorp-			

Contents continued on inside front cover

THE JOURNAL OF PHYSICAL CHEMISTRY

(Registered in U. S. Patent Office)

W. ALBERT NOYES, JR., EDITOR

ALLEN D. BLISS

ASSISTANT EDITORS

A. B. F. DUNCAN

EDITORIAL BOARD

A. O. ALLEN
C. E. H. BAWN
J. BIGELEISEN
F. S. DAINTON

D. D. ELEY
D. H. EVERETT
S. C. LIND
F. A. LONG

J. P. McCULLOUGH
K. J. MYSELS
J. E. RICCI
R. E. RUNDLE

W. H. STOCKMAYER
E. R. VAN ARTSDALEN
M. B. WALLENSTEIN
W. WEST

Published monthly by the American Chemical Society at 20th and Northampton Sts., Easton, Pa. Second-class postage paid at Easton, Pa.

The *Journal of Physical Chemistry* is devoted to the publication of selected symposia in the broad field of physical chemistry and to other contributed papers.

Manuscripts originating in the British Isles, Europe, and Africa should be sent to F. C. Tompkins, The Faraday Society, 6 Gray's Inn Square, London W. C. 1, England.

Manuscripts originating elsewhere should be sent to W. Albert Noyes, Jr., Department of Chemistry, University of Rochester, Rochester 20, N. Y.

Correspondence regarding accepted copy, proofs, and reprints should be directed to Assistant Editor, Allen D. Bliss, ACS Office, Mack Printing Company, 20th and Northampton Sts., Easton, Pa.

Advertising Office: Reinhold Publishing Corporation, 430 Park Avenue, New York 22, N. Y.

Articles must be submitted in duplicate, typed, and double spaced. They should have at the beginning a brief Abstract, in no case exceeding 300 words. Original drawings should accompany the manuscript. Lettering at the sides of graphs (black on white or blue) may be pencilled in and will be typeset. Figures and tables should be held to a minimum consistent with adequate presentation of information. Photographs will not be printed on glossy paper except by special arrangement. All footnotes and references to the literature should be numbered consecutively and placed in the manuscript at the proper places. Initials of authors referred to in citations should be given. Nomenclature should conform to that used in *Chemical Abstracts*, mathematical characters be marked for italic, Greek letters carefully made or annotated, and subscripts and superscripts clearly shown. Articles should be written as briefly as possible consistent with clarity and should avoid historical background unnecessary for specialists.

Remittances and orders for subscriptions and for single copies, notices of changes of address and new professional

connections, and claims for missing numbers should be sent to the Subscription Service Department, American Chemical Society, 1155 Sixteenth St., N. W., Washington 6, D. C. Changes of address for the *Journal of Physical Chemistry* must be received on or before the 30th of the preceding month. Please include an old address label with the notification.

Claims for missing numbers will not be allowed (1) if received more than sixty days from date of issue (because of delivery hazards, no claims can be honored from subscribers in Central Europe, Asia, or Pacific Islands other than Hawaii), (2) if loss was due to failure of notice of change of address to be received before the date specified in the preceding paragraph, or (3) if the reason for the claim is "missing from files."

Subscription rates (1962): members of American Chemical Society, \$12.00 for 1 year; to non-members, \$24.00 for 1 year. Postage to countries in the Pan-American Union \$0.80; Canada, \$0.40; all other countries, \$1.20. Single copies, current volume, \$2.50; foreign postage, \$0.15; Canadian postage \$0.10; Pan-American Union, \$0.10. Back volumes (Vol. 56-65) \$30.00 per volume; foreign postage, per volume \$1.20, Canadian, \$0.40; Pan-American Union, \$0.80. Single copies: back issues, \$3.00; for current year, \$2.50; postage, single copies: foreign, \$0.15; Canadian, \$0.10; Pan-American Union, \$0.10.

The American Chemical Society and the Editors of the *Journal of Physical Chemistry* assume no responsibility for the statements and opinions advanced by contributors to THIS JOURNAL.

The American Chemical Society also publishes *Journal of the American Chemical Society*, *Chemical Abstracts*, *Industrial and Engineering Chemistry*, International Edition of *Industrial and Engineering Chemistry*, *Chemical and Engineering News*, *Analytical Chemistry*, *Journal of Agricultural and Food Chemistry*, *Journal of Organic Chemistry*, *Journal of Chemical and Engineering Data*, *Chemical Reviews*, *Chemical Titles*, *Journal of Chemical Documentation*, *Journal of Medicinal and Pharmaceutical Chemistry*, *Inorganic Chemistry*, *Biochemistry*, and *CA — Biochemical Sections*. Rates on request.

Heat of Formation of Difluorosilylene	1200
A. S. Dworkin, H. R. Bronstein, and M. A. Bredig: The Electrical Conductivity of Solutions of Metals in their Molten Halides. V. Praseodymium-Praseodymium Trichloride	1294
Morton A. Golub: Intermolecular Energy Transfer in Polyethylene-Polybutadiene Blends during γ -Irradiation	1202
George W. Black and Benon H. J. Bielski: The Radiation-Induced Oxidation of 4- <i>t</i> -Butylpyrocatechol in Aqueous Solutions	1203
Daniel Cubicciotti: The Bismuth-Sulfur Phase Diagram	1233
Harry Goya, John L. T. Waugh, and Harry Zeitlin: The Color of Mercuric Iodide on Alumina	1206
Marianne K. Bernett and W. A. Zisman: Wetting Properties of Acrylic and Methacrylic Polymers Containing Fluorinated Side Chains	1207
E. Gil-Av and J. Herling: Determination of the Stability Con-	

stants of Complexes by Gas Chromatography	1208
John L. Margrave: The Heat of Formation of $BF_3(g)$	1209
Charles M. Apt, Frederick F. Margosian, Ivan Simon, Jay H. Freeland, and Raymond M. Fuoss: Pressure Dependence of Electrolytic Conductance in Toluene	1210
John O. Edwards, Khairat M. Ibne-Rasa, Etsuyo Itokawa Choi, and Colin L. Rice: Kinetic Deuterium Isotope Effect in the Nitrosation of Aniline. The Deuterium Isotope Effect on Three Equilibrium Constants	1212
COMMUNICATIONS TO THE EDITOR	
Robert W. Esser and Bruce G. Hobcock: The Ionization Potential of Hydrogen Disulfide (H_2S_2)	1214
H. P. Leftin, M. C. Hobson, and J. S. Leigh: The Effect of Gases on the Electron Spin Resonance Spectrum of Chemisorbed Diphenylethylene	1214

THE JOURNAL OF PHYSICAL CHEMISTRY

(Registered in U. S. Patent Office) (© Copyright, 1962, by the American Chemical Society)

VOLUME 66

JUNE 28, 1962

NUMBER 6

THE THERMAL DECOMPOSITION OF IRRADIATED PERMANGANATES

BY E. G. PROUT AND P. J. HERLEY

Chemistry Department, Rhodes University, Grahamstown, South Africa

Received May 29, 1961

The thermal decomposition of unirradiated Li and Na permanganates, and Li, Na, and Cs permanganates pre-irradiated by γ -rays, has been investigated. A comparative study of the magnitude of the irradiation effect with the permanganates of the alkali metals precludes the creation of incipient nuclei by the Compton recoil effect. The formation of essential sites is assumed to occur as a result of cationic displacement following multiple ionization by γ -rays.

Introduction

Considerable changes in the thermal decomposition of the permanganates of potassium,¹ rubidium,² and silver³ have been observed after preirradiation by high energy (~ 1.1 Mev.) γ -rays. The "induction periods" were shortened and the maximum velocities were increased. The experimental results have been explained by assuming that during irradiation the cations are displaced to interstitial positions by collision with Compton electrons and by photoelectric recoil. During the period of slow reaction the point defects migrate, and the Wigner energy released on recombination of the interstitials and vacancies causes decomposition in small regions of the crystal. The centers of decomposed material grow and ultimately fracture the crystal. Thereafter, reaction proceeds in an accelerating manner by the Prout-Tompkins mechanism.⁴

Assuming a constant displacement energy, the density of displaced ions, and consequently the irradiation effect, should depend on the atomic weight of the cation. A detailed study of pre-irradiation effects with other permanganates, *viz.*, lithium, sodium, and cesium permanganates, therefore was made and the effect of the variation in atomic weight was examined.

Experimental

Sodium permanganate was prepared by mixing a solution of 4.61 g. of A.R. NaCl in 50 ml. of water with one of 10.0 g. of AgMnO₄ in 1.2 l. of water. Both solutions were at 35°. The mixture was cooled to 5°, and the filtrate from the precipitated AgCl was concentrated to 10 ml. at 35° under re-

duced pressure. Purple-black needle shaped crystals (0.5 × 3.0 mm.) were formed on cooling to 18°. Analysis showed that the formula was NaMnO₄ · 3H₂O.

Lithium permanganate was prepared by mixing equal volumes (300 ml.) of aqueous solutions containing respectively 30.8 g. of A.R. LiClO₄ and 30.5 g. of A.R. KMnO₄. Both solutions were at room temperature. The precipitated KClO₄ was filtered and the procedure for crystallization was as for NaMnO₄. Black needle shaped crystals (0.5 × 6.0 mm.) of formula LiMnO₄ · 3H₂O were obtained.

The two permanganates were dehydrated *in vacuo* over P₂O₅ at 70° for 2 hr. Analysis showed that less than 1% H₂O remained and the specimens contained 99.0% NaMnO₄ and 99.1% LiMnO₄. Dehydration produced no apparent change in the single crystals, but X-ray analysis showed the presence of aggregates of crystallites 10⁻³ to 10⁻⁶ cm. in diameter. The dehydrated specimens were stored over P₂O₅ and extreme care was taken to prevent contact with moist air during handling.

The preparation of cesium permanganate, the high vacuum apparatus, and the procedure have been described elsewhere.⁵ The temperature control was $\pm 0.03^\circ$. Whole crystals were ground to a fine powder in an agate mortar. Approximately 20 mg. each of CsMnO₄ and NaMnO₄ and 10 mg. of LiMnO₄ were used in a run. Normalization to a common final pressure was done for comparative purposes.

Pre-irradiations were carried out at 25° in the spent fuel facility at Harwell (γ -ray energy 1.1 Mev., flux 4.0 Mrad hr.⁻¹) on specimens sealed in Pyrex ampoules.

Results

Decomposition of Unirradiated LiMnO₄ and NaMnO₄.—A knowledge of the decomposition of unirradiated LiMnO₄ and NaMnO₄ was necessary before studying the effect of γ -ray irradiation.

The *p-t* plots for ground and whole specimens are sigmoid (Fig. 1 and 2). Those for the decomposition of whole crystals of LiMnO₄ show a marked, reproducible, period of slow reaction obeying the equation

$$p = k_1 t + c \quad (1)$$

(1) E. G. Prout, *J. Inorg. & Nuclear Chem.*, **7**, 368 (1958).
(2) E. G. Prout and P. J. Herley, *ibid.*, **16**, 16 (1960).
(3) E. G. Prout and M. J. Sole, *ibid.*, **9**, 232 (1959).
(4) E. G. Prout and F. C. Tompkins, *Trans. Faraday Soc.*, **40**, 488 (1944).

(5) P. J. Herley and E. G. Prout, *J. Chem. Soc.*, 3300 (1959).

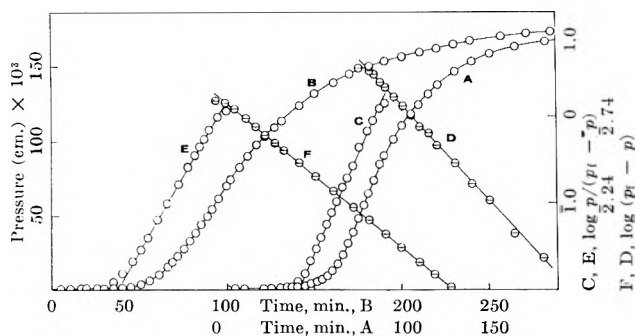


Fig. 1.—Curves A and B, pressure–time plots for decomposition of whole and ground crystals unirradiated LiMnO_4 at 105° ; lines C and E, plots of $\log [p/(p_t - p)]$ vs. t for curves A and B, respectively; lines D and F, plots of $\log (p_t - p)$ vs. t for curves A and B, respectively.

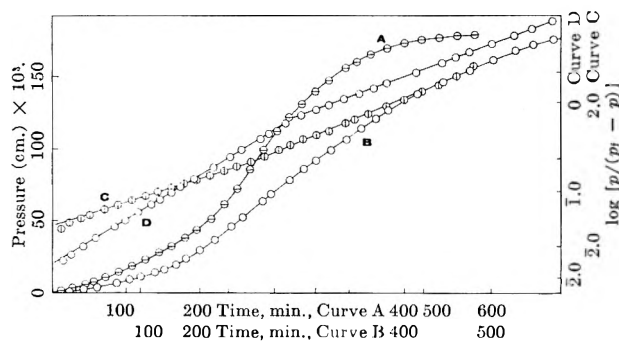


Fig. 2.—Curves A and B, pressure–time plots for decomposition of unirradiated whole and ground crystals NaMnO_4 at 135° , respectively; lines C and D, plots of $\log [p/(p_t - p)]$ vs. t for curves A and B, respectively.

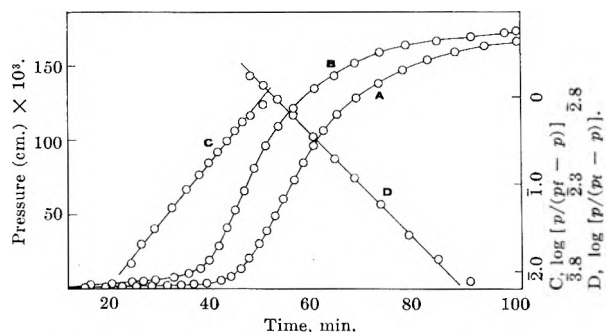


Fig. 3.—Curve A, pressure–time plot for decomposition of unirradiated whole crystals LiMnO_4 at 110° ; curve B, pressure–time plot for decomposition of irradiated whole crystals LiMnO_4 (dose, 111.0 Mrad) at 110° ; lines C and D, plots of $\log [p/(p_t - p)]$ vs. t , and $\log (p_t - p)$ vs. t , respectively, for curve B.

This period is unaffected by grinding.

The plots for NaMnO_4 do not show a well defined period of slow reaction. Almost the whole plot is described by the Prout–Tompkins equation

$$\log [p/(p_t - p)] = kt - c \quad (2)$$

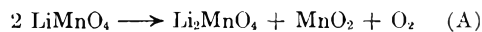
where k has two values, k_2 (acceleratory) and k_3 (decay), and p_t is the final pressure.

In the analysis of the LiMnO_4 plots eq. 2 was valid over the acceleratory period if the origin was taken at the p, t values corresponding to the end of the slow reaction. The decay period conformed to the equation

$$\log (p_t - p) = k_4 t + c \quad (3)$$

Typical analyses are shown in Fig. 1 and 2.

Reproducibility of results was satisfactory (Table I). The Arrhenius plots of $\log k_{1,2,3}$, or k_4 against $1/T^\circ\text{K}$. are well defined straight lines, and the derived activation energies are given in Table II. The “single” crystals did not appear to fracture during decomposition and the final color was black. The average percentage decompositions for whole and ground crystals calculated using the equations



were 87.7 and 85.7, respectively. Pre-irradiation with ultraviolet light had no effect.

Decomposition of Pre-irradiated LiMnO_4 .—Pronounced changes in the kinetics of ground and whole crystals of LiMnO_4 were obtained only with γ -ray doses greater than 100 Mrad. The induction period, in each case, was reduced to a very short but variable one. Figure 3 illustrates typical results for whole crystals. Those for ground crystals were similar. No disintegration or change of color of the “whole” crystals was visible during decomposition.

The curves for whole and ground crystals were analyzed as for the unirradiated decompositions and a typical analysis is shown in Fig. 3. Reproducibility was satisfactory (Table I). The activation energies derived from the plots of $\log k_2$ and $\log k_4$ against $1/T^\circ\text{K}$. are given in Table II.

The isotope Li^6 undergoes the nuclear reaction (n, α) with the production of an α -particle of energy 2.06 Mev. and a tritium atom of energy 2.74 Mev. The effect of such an energetic release on the subsequent thermal decomposition of LiMnO_4 was determined by irradiating in BEPO (Harwell) (30° , thermal neutron flux 2×10^{11} n. cm. $^{-2}$ sec. $^{-1}$) for five days. Gas was generated in the silica ampoule, and the crystals changed to a brown color. They did not color water and on heating at 110° *in vacuo* no gas was evolved. It was presumed that decomposition was complete. This particular phenomenon is still under investigation.

Decomposition of Pre-irradiated CsMnO_4 and NaMnO_4 .—The decomposition of unirradiated CsMnO_4 has been studied⁵ and shows a period of slow reaction followed by one of rapid acceleration which in turn passes into a decay stage. The first stage is described by

$$p^{1/2} = kt + c \quad (4)$$

The acceleratory and decay stages obey the Prout–Tompkins equation.

The changes in the thermal decomposition of whole and ground crystals of CsMnO_4 and NaMnO_4 after varying γ -ray doses are shown in Fig. 4–7. The p - t plots for the decomposition of irradiated NaMnO_4 , whole or ground, consist of a slow reaction obeying eq. 1, followed by a curve of complex shape. The plots for irradiated whole crystals of CsMnO_4 show a similar slow reaction, but this is absent for ground crystals; the main effect is a steady decrease in the duration of the acceleratory period with increasing dose.

Reproducibility of results was good (Table I). No mass effect was found since the rate constants

TABLE I
REPRODUCIBILITY OF VELOCITY CONSTANTS FOR THREE CONSECUTIVE RUNS
Units: k_1 , cm. min.⁻¹; $k_2, 3, 4, 5$ min.⁻¹; k_6 , (cm. min.⁻¹)^{1/2}
Constants × 10²

Substance	k_1	k_2	k_3	k_4	k_5	k_6
Unirradiated LiMnO ₄ :						
Whole crystals, 110°	10.08	10.15	10.09	6.83	6.86	6.90
Ground crystals, 115°	11.51	11.31	11.49	9.16	9.23	9.28
Irradiated LiMnO ₄ :						
Whole crystals, 110°						
11 Mrad			7.90	7.84	7.77	
Ground crystals, 110°			3.70	3.76	3.79	
Unirradiated NaMnO ₄ :						
Whole crystals, 150°			2.24	2.28	2.19	2.11
Ground crystals, 155°			4.89	4.82	4.78	3.30
Irradiated NaMnO ₄ :						
Whole crystals, 140°						
10 Mrad	0.0469	0.0479	0.0461	6.82	6.90	6.86
Ground crystals, 140°						
10 Mrad	.0617	.0624	.0633	4.51	4.60	4.67
Irradiated CsMnO ₄ :						
Whole crystals, 250°	.0281	.0271	.0286	4.81	4.85	4.82
3.3 Mrad						
Ground crystals, 250°						
3.3 Mrad			4.12	4.19	4.21	4.70
						4.83
						4.66
						7.48
						5.91
						6.03
						1.91
						3.34
						3.36
						1.96
						1.91
						1.86
						2.42
						2.50
						2.56
						2.05
						2.16
						2.21
						1.28
						1.18
						1.31
						4.59
						4.63
						4.65
						1.25
						1.21
						1.78
						1.71
						1.80

TABLE III
ACTIVATION ENERGIES FOR NaMnO₄ (KCAL. MOLE⁻¹).
ESTIMATED ACCURACY ±1.5 KCAL. MOLE⁻¹

Sub-stance	Dose, Mrad	Specimen	E, k_1	E, k_2	E, k_3	E, k_4	E, k_5	E, k_6
NaMnO ₄	0	Whole	28.6
	0	Ground	31.3
	48.0	Whole	29.8	36.5	34.0	36.5	31.4	30.5
	10.0	Whole	30.5	33.7	36.5	35.6	34.2	31.4
	48.0	Ground	30.0	33.3	35.1	31.0	31.1	31.1
	10.0	Ground	31.2	33.7	36.0	31.9	33.9	31.9

TABLE II
ACTIVATION ENERGIES FOR LiMnO₄ AND CsMnO₄ (KCAL. MOLE⁻¹). ESTIMATED ACCURACY ±1.5 KCAL. MOLE⁻¹

Substance	Dose, Mrad	Specimen	E, k_1	E, k_2	E, k_3	E, k_4
LiMnO ₄	0	Whole	22.8	32.4	..	31.6
	0	Ground	22.6	33.3	..	30.4
	111.0	Whole	..	36.4	..	37.4
	111.0	Ground	..	35.1	..	31.8
CsMnO ₄	106.0	Whole	38.3	34.7	37.9	..
	3.3	Whole	35.6	35.1	34.2	..
	0.26	Whole	29.2	33.7	36.0	..
	106.0	Ground	..	41.9	36.5	..

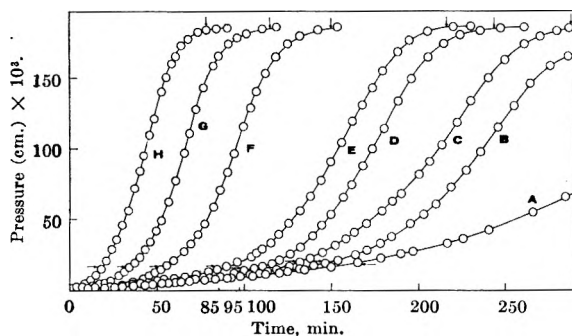


Fig. 4.—Pressure-time plots for decomposition of irradiated whole crystals CsMnO_4 at 240° ; dose in Mrad.: A, 0; B, 0.13; C, 0.26; D, 1.2; E, 3.3; F, 10.0; G, 36.0; H, 106.0; arrows show the fit of Prout-Tompkins equation.

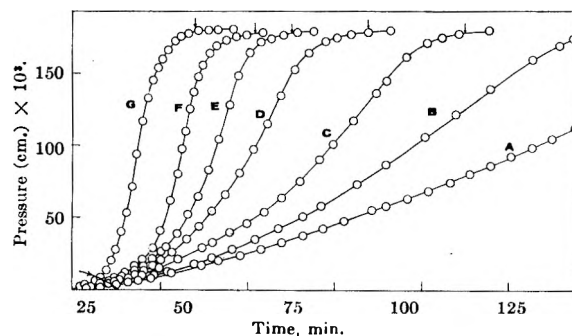


Fig. 5.—Pressure-time plots for decomposition of irradiated ground crystals CsMnO_4 at 250° ; Dose in Mrad: A, 0; B, 0.13; C, 1.2; D, 3.3; E, 10.0; F, 36.0; G, 106.0; arrows show the fit of Prout-Tompkins equation.

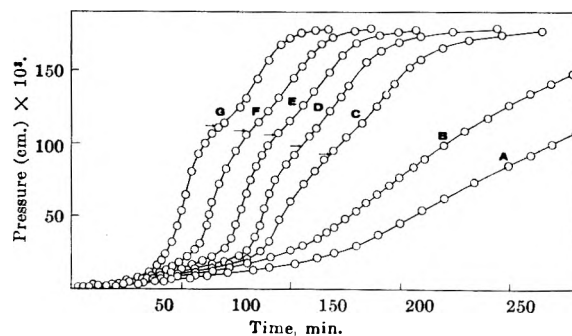


Fig. 6.—Pressure-time plots for decomposition of irradiated whole crystals NaMnO_4 at 140° ; dose in Mrad: A, 0; B, 0.5; C, 4.0; D, 6.5; E, 10.0; F, 20.0; G, 48.0; arrows mark the point O.

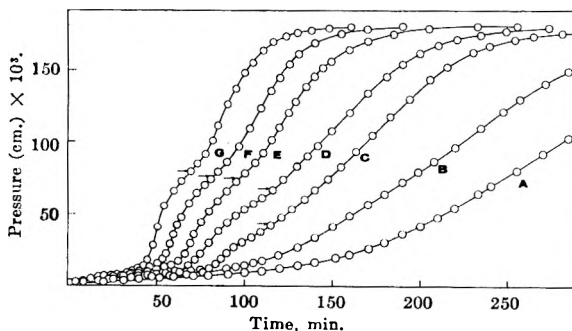


Fig. 7.—Pressure-time plots for decomposition of irradiated ground crystals NaMnO_4 at 140° ; Dose in Mrad: A, 0; B, 0.5; C, 4.0; D, 6.0; E, 10.0; F, 20.0; G, 48.0; arrows mark the point O.

were independent of mass for a given dose and decomposition temperature. The irradiation effects could not be annealed by heating CsMnO_4 at 150° and NaMnO_4 at 70° for 10 hr. Crystals of decomposing NaMnO_4 did not appear to disintegrate. Specimens of pre-irradiated whole crystals of CsMnO_4 were withdrawn at various times during decomposition (curve D, Fig 4) and examined microscopically. Explosive disintegration began when acceleration of the reaction commenced and was complete shortly after this (between $t = 85$ min. and $t = 95$ min. in Fig. 4). The final particle size varied within the range 0.02–0.01 mm. in diameter. The final size for unirradiated whole crystals was 0.07 mm. in diameter.

The variation of the duration of the slow reaction (I) with dose (τ) is given by

$$\log \tau = kI + c \quad (5)$$

for the decomposition of whole crystals of CsMnO_4 and whole and ground crystals of NaMnO_4 . Interruption of the decomposition of unirradiated whole crystals after a definite time, irradiating in the γ -ray source for a constant dose, and then continuing the decomposition was studied as for KMnO_4 , AgMnO_4 , and RbMnO_4 . The results were similar for NaMnO_4 and CsMnO_4 and the curves obtained for the former are shown in Fig. 8. The percentage decomposition, as calculated from the appropriate equations A or B, showed no regular variation with γ -ray dose. The average values for NaMnO_4 and CsMnO_4 were 86 and 91%, respectively.

The plots in Fig. 4 and 5 for CsMnO_4 are best fitted by the Prout-Tompkins equation. The extent of applicability of the equation is indicated, and is best for ground crystals; for whole crystals the equation does not apply over the initial portion of the acceleratory period. Activation energies for various γ -ray doses were determined for the slow reaction, the acceleratory period, and the decay period and are given in Table II. All the Arrhenius plots were good straight lines.

An example of the analysis of the curves for irradiated whole crystals of NaMnO_4 is illustrated in Fig. 9. After the initial reaction the curve is seen to consist of two sigmoid plots above and below the point O. The lower curve has a short period of acceleration given by

$$\log p = k_2 t + c \quad (6)$$

followed by a decay region obeying

$$(dp/dt)^{1/2} = k_3 t + c \quad (7)$$

The upper curve is analyzed by transferring the origin to O and applying the Prout-Tompkins equation. A good fit is obtained, with the usual two constants, k_2 and k_3 . The plots for ground crystals are similarly analyzed. The point O is shown by the arrows in Fig. 6 and 7. Activation energies for various doses were determined from the variation of the rate constants with temperature and are given in Table III. The Arrhenius plots again were good.

Comparison of the Effects of Pre-irradiation on the Decomposition of Permanganates.—Decomposition temperatures were determined for unirradiated Li, K, Rb, Cs, Ag, and Ba permanga-

nates such that the period of slow reaction occupied 100 ± 2 min. Specimens were decomposed at these temperatures after pre-irradiation (10 Mrad). The resulting $p-t$ plots for K, Rb, Cs, and Ag permanganates are shown in Fig. 10. The irradiation effects for Ba and Li permanganates were small and the plots are not shown. It was not possible to apply this method to NaMnO_4 since the decomposition of unirradiated crystals does not exhibit a slow reaction. Consequently, the decomposition temperature for irradiated NaMnO_4 was that at which the decomposition of the unirradiated crystals attained maximum velocity at the same time as unirradiated CsMnO_4 (with slow reaction = 100 min.)

There is no systematic variation of the irradiation effect with increasing atomic weight, and the irradiation effect is as great with NaMnO_4 as with CsMnO_4 .

Discussion

Unirradiated LiMnO_4 and NaMnO_4 .—The kinetics of the decomposition of unirradiated LiMnO_4 and NaMnO_4 can be explained by assuming that acceleration of the reaction proceeds by the Prout-Tompkins mechanism.

This mechanism originally was proposed to explain the kinetics of decomposition of KMnO_4 and the Prout-Tompkins equation was derived theoretically on the basis of a branching mechanism for the reaction. In the acceleratory period the surface array of product molecules produces lateral strains which are relieved by cracks along which nuclear reaction is favored. The reaction therefore spreads into the crystal down these crevices and covers the inner surfaces and the reaction proceeds through the solid by a system of branching planes of decomposed material. These ultimately interfere, and after the time of maximum velocity the rate is controlled by the number of unchanged permanganate molecules which are contiguous to product molecules.

The formation of a surface layer of product of critical thickness is rapid for NaMnO_4 , but slow with LiMnO_4 , as evidenced by the marked "induction period" with the latter. Decay occurs by the Prout-Tompkins mechanism for NaMnO_4 , but with LiMnO_4 the reaction consists of the decomposition of isolated blocks of material in which the probability for decomposition is proportional to the amount of substance undecomposed.

Formation of Point Defects by γ -Rays.—Interaction of γ -rays with matter occurs principally by three mechanisms: the photoelectric effect, the Compton effect, and pair production. For reactor γ -rays and γ -rays from cobalt and fission product sources, the Compton effect has the largest cross-section.⁶ Dienes and Vineyard⁷ have shown that for γ -rays of 1 Mev. or less the number of atoms displaced $\text{cm.}^{-3} \text{sec.}^{-1}$ is a maximum in the very light elements and declines rapidly with increasing atomic number becoming zero for 1 Mev. γ -rays

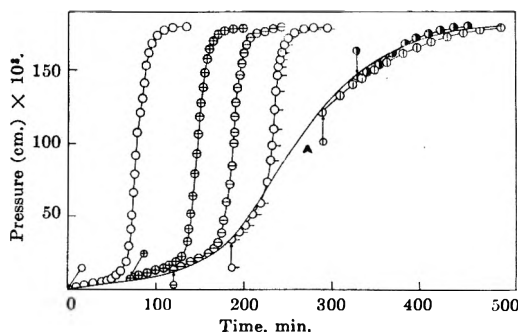


Fig. 8.—Curves showing the effect of interrupting a decomposition (temperature, 140°) at time shown by appropriate arrow, irradiating in γ -ray source (dose, 49.2 Mrad), and then continuing decomposition with original $t = 0$ min.; times of interruption in min. as indicated by arrows: A, uninterrupted; \odot , 0; \oplus , 70; \ominus , 118; \circ -, 180; \odot , 285; \bullet , 335.

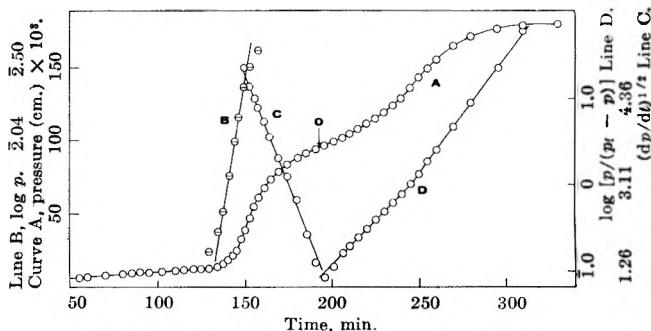


Fig. 9.—Analysis of pressure-time plot for decomposition of irradiated whole crystals NaMnO_4 (dose, 48.0 Mrad; temperature, 130°): curve A, p vs. t ; line B, $\log p$ vs. t ; line C, $(dp/dt)^{1/2}$ vs. t ; line D, $\log [p/(p_t - p)]$ vs. t , with origin at O.

and a displacement threshold of 25 ev., at atomic weight about 125.

Thus, the absence of a systematic decrease in the effect of preirradiation on the subsequent thermal decomposition of the permanganates, and the pronounced effect with CsMnO_4 , preclude the possibility that the irradiation effect primarily is due to the formation of displaced cations as a result of interaction with Compton electrons. Displacement by photoelectric recoil only, in the case of CsMnO_4 , would produce too small a concentration of defects, since the photoelectric effect is not dominant and it must be remembered that not every photoelectric absorption will displace the atom since the distribution of the emitted electrons with respect to the incoming γ -ray has to be taken into account.

However, the displacement mechanism proposed by Varley⁸ provides a satisfactory explanation of the irradiation effects with the permanganates. Irradiation of ionic solids, such as the alkali halides, with charged particles or γ -rays strips electrons from the anions, which become positive ions of multiple charge situated in an environment normally occupied by negative ions. Coulombic repulsion between the stripped ions and their neighbors eject the "anions" to interstitial sites where they recover all but one of the electrons lost. Another possibility is the ejection of a neighboring cation from the vicinity of the multiply ionized anion. This cation will occupy an interstitial posi-

(6) R. D. Evans, "The Atomic Nucleus," McGraw-Hill Book Co., New York, N. Y., 1955.

(7) G. J. Dienes and G. H. Vineyard, "Radiation Effects in Solids," Interscience Publ., New York, N. Y., 1957.

(8) J. H. O. Varley, *J. Nuclear Energy*, 1, 120 (1954).

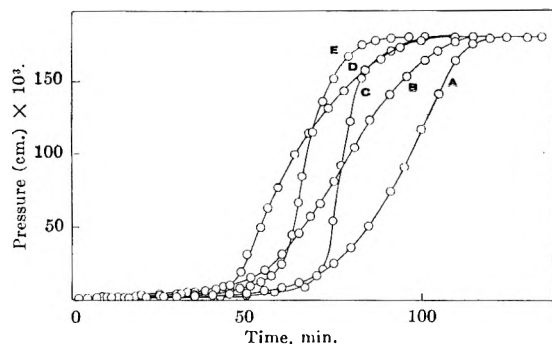


Fig. 10.—Pressure-time plots for decomposition of irradiated whole crystals of different permanganates, dose 10.0 Mrad; end of slow reaction for unirradiated whole crystals at 100 min.; A, RbMnO₄; B, CsMnO₄; C, NaMnO₄; D, AgMnO₄; E, KMnO₄.

tion as a positive ion. Durup and Platzman⁹ have suggested that multiple ionization may occur through the ejection of an inner electron followed by an intra-atomic Auger cascade, with a probability close to unity.

In the permanganates multiple ionization is more probable for the permanganate ions than for the cations because of the larger number of atoms exposed to the γ -rays. If a model of several unit cells of the KMnO₄ crystal structure is examined it is apparent that, spatially, the cations have greater freedom of movement than the anions. Consequently, we consider that coulombic repulsion between the cations and multiple ionized MnO₄ groups will eject the former to interstitial positions between MnO₄⁻ groups. This displacement mechanism will result in a high density of defects (interstitial cations and vacancies) and will account for the pronounced irradiation effects more satisfactorily than the mechanism formerly proposed. While the effects fundamentally are due to the cation, its identity is relatively unimportant, which is in accord with the experimental results. The migration of defects on heating and release of Wigner energy during the slow reaction are as before.¹ Displacement resulting from multiple ionization will explain the enormous effect after pre-irradiation of KMnO₄ crystals for 3 min. with highly ionizing protons (145 Mev.).

Pre-irradiated Li, Na, and Cs Permanganates.—The insensitivity of LiMnO₄ to pre-irradiation resembles that found for Ba(MnO₄)₂,¹⁰ where the results were explained by suggesting that the product could accommodate itself in the lattice without causing fracture. A requisite for a large irradiation effect is that fracture occurs at the end of the slow reaction with the formation of new crystal surfaces.

The decompositions of pre-irradiated whole and ground CsMnO₄ resemble those for RbMnO₄. If the above displacement mechanism is introduced, then the conclusions drawn for RbMnO₄ hold for CsMnO₄.

The irradiation effect with NaMnO₄ is complex but can be attributed to the small crystallite size. Fracture of the crystallites at the end of the slow reaction may occur, despite the absence of any

(9) J. Durup and R. L. Platzman, *Discussions Faraday Soc.*, "Radiation Effects in Inorganic Solids," (1961).

(10) E. G. Prout and P. J. Herley, *J. Phys. Chem.*, **65**, 208 (1961).

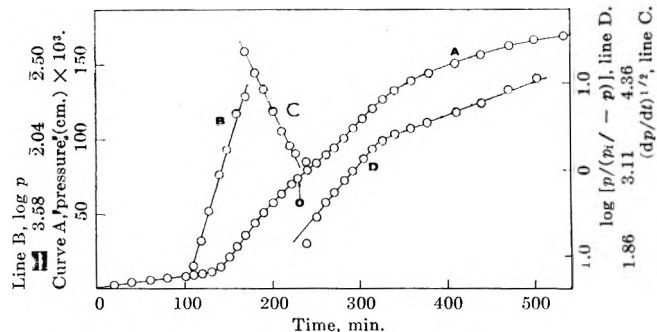


Fig. 11.—Curve A, pressure-time plot for decomposition of irradiated, finely ground, RbMnO₄ at 250°; dose, 49.2 Mrad; line B, $\log p$ vs. t ; line C, $(dp/dt)^{1/2}$ vs. t ; line D, $\log [p/(p_i - p)]$ vs. t , with origin at O.

fracture of the "single crystal." The short acceleration is due to the production of fresh surfaces, followed by rapid surface decomposition. The layer of product on the approximately spherical particles will thicken by the inward progression of the reaction. Because of the large number of small particles the rate of gas evolution will show a marked decay character and should be described by eq. 4.¹¹ The activation energy calculated from the plot of $\log k_6$ against $1/T^\circ\text{K}$. is equal to $2/3 E_6$ where E_6 is the activation energy associated with the reaction. The value given in Table III is E_6 . (All other E values in Table III are those obtained directly from the Arrhenius plots). At O the critical thickness of the product is attained and reaction then occurs by the Prout-Tompkins mechanism. The reduction in particle size on fracture will be less the smaller the concentration of defects, *i.e.*, the lower the dose. This explains the decrease in the value of the pressure at O with decreasing dose. The point O is lower with ground than with whole crystals. This may be due to sintering during grinding. The importance of small crystal size in determining the form of the p - t curve is supported by the plot obtained for the decomposition of RbMnO₄ crystals which were ground for several days prior to pre-irradiation (Fig. 11). The extremely small particle size produced a curve of the same form as for NaMnO₄.

The plots of $\log k_1$ against $1/T^\circ\text{K}$. for a fixed dose should yield a value for the activation energy of migration of the point defects.¹ The average values for CsMnO₄ and NaMnO₄ are 1.07 and 1.32 ev., respectively, which are in accord with the values obtained for the permanganates previously studied.

Figure 8 shows that acceleration of the decomposition by a reaction arising from "irradiation" nuclei is independent of the reaction commencing at nuclei present during the decomposition of unirradiated material.

The degree of fit of the Prout-Tompkins equation in the pre-irradiated decompositions of lithium and cesium permanganates is consistent with the supposition that after fracture by "irradiation" nuclei, reaction proceeds by the Prout-Tompkins mechanism. Activation energies for the decomposition of a given permanganate, irradiated or

(11) P. J. Griffiths and J. M. Grocock, *J. Chem. Soc.*, 3380 (1957).

unirradiated, are in sufficient agreement to suggest that the same chemical reaction occurs after the slow reaction.

Acknowledgment.—The authors wish to thank

the Council for Scientific and Industrial Research (South Africa) for a grant to cover the cost of irradiation and for a scholarship held by P. J. H. during the investigation.

THE ZERO POINT OF CHARGE OF OXIDES¹

BY G. A. PARKS AND P. L. DE BRUYN²

Department of Metallurgy, Massachusetts Institute of Technology, Cambridge 39, Massachusetts

Received June 26, 1961

The zero point of charge (z.p.c.) of the electrical double layer of free charges at reversible interfaces is defined, and the experimental methods for determining this parameter are discussed. Adsorption isotherms of H⁺ and OH⁻ ions on crystalline ferric oxide precipitates as obtained by acid and base potentiometric titrations are reported. From these studies at various ionic strengths (KNO₃ indifferent electrolyte), the z.p.c. of α -hematite is established at pH 8.5. A model of the double layer at the Fe₂O₃-aqueous solution interface is developed. This model is based on the dissociation of surface hydroxyl groups formed by hydration of the virgin surface. In addition, it is shown that the z.p.c. may be determined by considering the adsorption of metal hydroxo-complex ions from solution. According to this analysis it is found that for Fe₂O₃ the z.p.c. agrees with the pH of minimum solubility of the oxide and with the isoelectric pH as determined by the positively and negatively charged Fe(III) hydroxo-complexes in solution. Although limited experimental data are available, this analysis may be applied to other oxide systems.

Introduction

Depending on the mechanism by which free charges are distributed across a solid-solution interface, two basic types of electrochemical double layers may be distinguished. A reversible double layer is the result of transfer of potential-determining ions across the two-phase boundary. In contrast, the completely polarizable double layer is established by imposing by an external potentiometer circuit a potential difference (to the interface) so that all charge species have meaningful concentrations only in one of the two bulk phases. Equilibrium studies of double layers on AgI,^{3,4} Ag₂S,^{5,6} and liquid mercury⁷ in contact with aqueous electrolyte solutions have illustrated the similarity in structure and in the magnitude of the electrical properties of these two types of double layer systems.

The most important parameter which may be used to describe a double layer of free charges is its zero point of surface charge (z.p.c.). For a reversible double layer system the surface charge, (σ_s) may be expressed by the relation

$$\sigma_s = F(z_+ \Gamma_+ + z_- \Gamma_-) \quad (1)$$

where F is the Faraday constant; z_+ (z_-) the valence including sign; and Γ_+ (Γ_-) the adsorption density of the potential-determining ionic species. The z.p.c. then is expressed by the condition that σ_s be zero and will be determined by a particular value of the activity ($a_{+(0)}$ also $a_{-(0)}$) of the potential-determining ions in the solution phase. For reversible interfaces the concept of a surface charge is less unambiguous than that of a completely polarized system. This follows because a certain

arbitrariness is introduced in assigning the potential-determining ions only to the solid side of the interface.⁸ By allowing the concentration of the indifferent electrolyte in the solution to exceed greatly that of the potential-determining electrolyte, the uncertainty in the physical significance of σ_s is avoided.

The potential difference, ψ_0 , across the double layer of free charges may be related to the e.m.f. (E) of a reversible cell which uses as one of the reversible electrodes the solid to be studied. By suitable choice of a reference electrode, one may write

$$\psi_0 = E - E_0 \quad (2)$$

where E_0 is the e.m.f. of the cell at the z.p.c. From (2) it follows that⁹

$$\psi_0 = \frac{RT}{z_+ F} \ln(a_+/a_{+(0)}) = \frac{RT}{z_- F} \ln(a_{-(0)}/a_-) \quad (3)$$

Both relations 2 and 3 are only valid in the absence of any specific interaction between the solid surface and the ions derived from the supporting electrolyte or between the surface and non-ionized molecules in solution. In the presence of finite amounts of such solute species, the z.p.c. also will be a function of their activities.

To locate the z.p.c. for a reversible double layer system, the activity ($a_{i(0)}$) of the potential determining species (i) must be determined by experiment. From potentiometric titrations of a finely divided suspensor of a heteroionic solid, the surface charge and thus also the z.p.c. may be determined. In addition to this adsorption method, the z.p.c. also may be located by first determining the zero point of any property which depends on the presence of an electrical double layer. Thus the absence of the suspension effect between a settled suspension and the supernatant

(1) Parts of this paper are based on a dissertation by G. A. Parks in partial fulfillment of the requirements for the degree of Doctor of Philosophy, M.I.T.

(2) Associate Professor of Metallurgy, M.I.T.

(3) E. L. Mackor, *Rec. trav. chim.*, **70**, 763 (1951).

(4) J. Lijklema, *Kolloid-Z.*, **175**, 129 (1961).

(5) W. L. Freyberger and P. L. de Bruyn, *J. Phys. Chem.*, **61**, 586 (1957).

(6) I. Iwasaki and P. L. de Bruyn, *ibid.*, **62**, 594 (1958).

(7) D. C. Grahame, *J. Am. Chem. Soc.*, **76**, 4819 (1954).

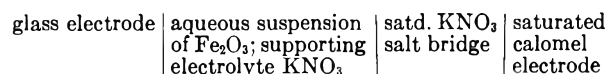
(8) J. Th. G. Overbeek, *Natl. Bur. Standards (U. S.)*, Circ. 524, 1953, p. 213.

(9) Equation 3 should not be interpreted to indicate a zero potential difference across the reversible interface; it only defines the zero point of potential across a double layer of free charges.

solution, the zero point of any electrokinetic property, and the maximum flocculation rate also may be used to evaluate the z.p.c., if specific adsorption effects are eliminated.¹⁰

This paper deals with the evaluation of the z.p.c. of crystalline oxides and in particular with Fe₂O₃. In contrast to studies with AgI and Ag₂S solids, most inorganic solids do not function satisfactorily as reversible electrodes. A direct identification of the potential-determining species is, therefore, not possible. However, by definition the potential-determining species for Fe₂O₃ are the ionic constituents of the lattice (Fe³⁺ and O²⁻) and ions, in particular, H⁺ and OH⁻, which are in equilibrium with them. Accordingly, a potentiometric titration of a ferric oxide precipitate in a reversible cell which employs a glass electrode as one of the electrodes should yield information on the z.p.c.

The Zero Point of Charge of Ferric Oxide.—The z.p.c. of ferric oxide was determined by the adsorption method which was used so successfully for AgI and Ag₂S. A potentiometric titration of an aqueous suspension of Fe₂O₃ was performed at several ionic strengths (10⁻⁴ to 1 M) and at 21° in the reversible cell



As titrants, 0.1 N solutions of KOH and HNO₃ were used. These solutions were prepared from Acculute standard volumetric solutions (Anachemica Chemicals Ltd.) by dilution with double-distilled conductivity water. The alkaline solution was stored in polyethylene bottles to avoid silicate contamination. Potassium nitrate was chosen as supporting electrolyte because the anions NO₃⁻ and ClO₄⁻ are least likely to complex Fe(III).¹¹ A Beckman saturated calomel electrode connected to the titration cell through a KNO₃ saturated salt bridge and a Beckman general purpose glass electrode served as the two electrodes. The salt bridge, introduced to prevent chloride contamination, was identical in design to the asbestos-wicked bridge used in Beckman calomel electrodes except that the lower end of the bridge was filled with solid KNO₃ crystallized *in situ*. Leakage of KNO₃ into the cell from the bridge was rapid enough so that below 10⁻² M control of ionic strength was possible only by removal of the bridge after each measurement. A Model G Beckman pH meter was used to determine the pH of the system.

The titration cell was a flat-bottomed 500-ml. Pyrex jar with a rubber stopper through which passed the electrodes, a thermometer, a microburet, and an inlet and outlet for purified nitrogen gas. Nitrogen was used to purge the cell and buret of CO₂. Mixing of the suspension was provided by a Teflon-covered magnetic stirrer. The apparatus was kept at constant temperature by pumping thermostated water through a jacket around the cell and through a rubber tube wrapped around the calomel electrode. Owing to the high resistance of the cell at low ionic strength, all parts of the equipment including the pH meter case were carefully grounded.

The ferric oxide precipitate was prepared by hydrolyzing Baker and Adamson reagent grade Fe(NO₃)₃ at the boiling point. About 100 g. of the salt added to one liter of conductivity water was boiled under reflux conditions for 18 days. To ensure that the hydrolysis product was α-Fe₂O₃ and not α-FeOOH (goethite), the HNO₃ formed by hydrolysis was prevented from escaping by vaporization.¹² The precipitate was washed by centrifuging and decantation with conductivity water. Usually the washing was done under flocculated conditions by adding KOH to give a pH of about 9. Examination of the washed ferric oxide by X-ray diffraction verified it to be rhombohedral α-hematite.

(10) H. R. Kruyt, "Colloid Science," Vol. I, Elsevier Publ. Co., New York, N. Y., 1952, p. 231.

(11) J. C. Bailar, "The Chemistry of the Coordination Compounds," Reinhold Publ. Corp., New York, N. Y., 1956.

(12) F. G. Smith and D. J. Kidd, *Am. Mineralogist*, **34**, 403 (1949).

Spectrographic analysis of the precipitate revealed no major impurity.

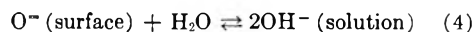
The titration procedure consisted of adding between 250 and 300 g. of a stock suspension of Fe₂O₃ (about 3 to 5 g. of Fe₂O₃) to the cell. Most commonly a series of titrations was started at ionic strength 10⁻³ and pH 9.3, and small increments of acid were made. The pH range 5 to 10 was covered. The approach to equilibrium was fast (less than 20 min.) in the high alkaline and in the acid pH range but in the vicinity of the z.p.c. and near the equivalence point (pH 7) equilibration times as high as 4 hr. were experienced. The adsorption density (Γ) of OH⁻ and H⁺ or rather the excess of one species over the other (Γ_{H⁺} - Γ_{OH⁻}) was determined by the difference between total added base or acid and the equilibrium OH⁻ and H⁺ concentration in solution. The reproducibility and reversibility of the adsorption curves was well established. In all, a large number of tests were made at different ionic strengths in the narrow pH range 9.5 to 7 and a limited number of tests over the wider range pH 5 to 10. A typical adsorption curve is shown in Fig. 2, where the adsorption density of OH⁻ and H⁺ ions in moles/g. is plotted against pH.

From the results presented in Fig. 1 one may conclude that OH⁻ and H⁺ ions are potential-determining for Fe₂O₃ and that KNO₃ acts as an indifferent electrolyte. The best value of the z.p.c. of Fe₂O₃ at 21° as determined by the intersection of the adsorption curves is pH 8.5 (pOH 5.67). Especially in the titration tests over a narrow pH range, a shift in the intersection of the curves at higher ionic strength toward more acid pH values was observed. The maximum observed spread was about 0.25 pH unit. Van Laar¹³ observed a spread in the z.p.c. of AgI of 0.13 pAg unit in the same concentration range of 10⁻⁴ to 1 N KNO₃.

The characteristic shapes of the differential capacity *vs.* surface change curves as obtained by differentiation of the adsorption curves are shown in Fig. 2. The minimum in the capacity at low ionic strength at the z.p.c. so characteristic of the double layers on AgI, Ag₂S, and mercury also is present. The general shape of the capacity curves for Fe₂O₃ is similar to those for the other two solids and liquid mercury. The absolute value of the differential capacity in μfarad/cm.² is not given because a reliable measure of the specific surface was not available. To bring the differential capacity on Fe₂O₃ in line with those observed on Hg, AgI, and Ag₂S, a specific surface of about 60 m.²/g. is indicated, whereas attempts to determine the surface area by BET measurements and negative adsorption measurements of Mg²⁺ at pH 6 gave values smaller by a factor of 4.

In Table I the z.p.c. of ferric oxide as determined by the authors is compared with results of other investigators who used electrokinetic methods. With the exception of measurements on the natural and ignited products, the agreement is quite good, especially since the precipitates and sols were made from different starting materials.

Origin of Charge at Oxide Surfaces.—Within the pH range covered in the potentiometric titration of the ferric oxide suspension, the potential-determining role of OH⁻, and therefore also H⁺ ions, is reasonably well established. The charge transfer reaction by which the double layer is established at any oxide surface and which is in agreement with the potential-determining role of OH⁻ and H⁺ may be written, as suggested by Verwey¹⁷



Most investigators¹⁸⁻²² of the properties of the oxide—

(13) J. A. W. van Laar, thesis, University of Utrecht, Department of Physical Chemistry, 1952.

(14) S. A. Troelstra and H. R. Kruyt, *Kolloid-Z.*, **101**, 182 (1942).

(15) F. Hazel and G. H. Ayres, *J. Phys. Chem.*, **36**, 2930 (1931).

(16) P. G. Johansen and A. S. Buchanan, *Australian J. Chem.*, **10**, 398 (1957).

(17) E. J. Verwey in "Colloid Chemistry," Vol. VII, J. Alexander, ed., Reinhold Publ. Corp., New York, N. Y., 1950.

(18) R. Zsigmondy and E. B. Spear, "Chemistry of Colloids," John Wiley and Sons, Inc., New York, N. Y., 1917.

(19) D. J. O'Connor and A. S. Buchanan, *Australian J. Chem.*, **6**, 278 (1953).

TABLE I
 ZERO POINT OF CHARGE OF FERRIC OXIDE

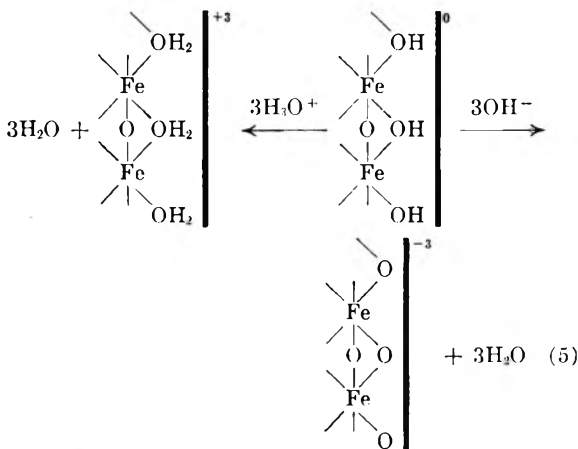
Material	Method of preparation	Observation technique	pH	Investigator
Sol (α -Fe ₂ O ₃)	React FeCl ₃ ·6H ₂ O with NH ₄ OH. Washed ppt. heated with water in autoclave (150–160°, ±5 atm.)	Micro-electrophoresis	8.3	Troelstra ¹⁴
Sol	Hydrolysis of FeCl ₃ . Dialyze ppt. for 5 days at 90°	Micro-electrophoresis	8.6	Hazel and Ayres ¹⁶
Precipitate (α -Fe ₂ O ₃)	Hydrolysis of Fe(NO ₃) ₃ at boiling point	Adsorption	8.5	Present authors
Precipitate Ignited	Reaction of FeNH ₄ (SO ₄) ₂ with ammonia. Washed ppt. ignited at 850° in air for 2 hr.	Micro-electrophoresis	8.0 6.5	Johansen and Buchanan ¹⁶
Natural	Ground in iron mortar washed with dilute HCl, dried at 120°		6.7	

aqueous solution interface suggest that the mechanism by which the surface charge is established may be viewed qualitatively as a two-step process; surface hydration followed by dissociation of the surface "hydroxide."

The hydration step may be visualized as an attempt by the exposed surface atoms to complete their coordination shell of nearest neighbors. Exposed cations accomplish this by pulling an OH⁻ ion or water molecule and the oxygen ions by pulling a proton from the aqueous phase. The net result is that the surface now is covered by a hydroxyl layer with the cations buried below the surface.

In α -Fe₂O₃, which has the corundum structure, six oxygen atoms form an octahedral group around the Fe atom and each O atom is coordinated with four Fe atoms.²³ The hydrated, uncharged surface of this oxide then may be represented schematically as in Fig. 3. The argument that hydroxyl ions take part in this process is given support by the observation that part of the water vapor adsorbed by Fe₂O₃ appears as hydroxyl groups in infrared spectra.²⁴

The process by which a surface charge is established may be viewed either as an adsorption of H⁺ and OH⁻ ions or as a dissociation of surface sites which may assume a positive or negative charge. This mechanism may be represented schematically as



(20) D. J. O'Connor, P. G. Johansen, and A. S. Buchanan, *Trans. Faraday Soc.*, **52**, 229 (1956).

(21) R. K. Iler, "The Colloid Chemistry of Silica and Silicates," Cornell Univ. Press, Ithaca, N. Y., 1955.

(22) A. M. Gaudin and D. W. Fuerstenau, *Trans. A.I.M.E.*, **202**, 66 (1955).

(23) W. L. Bragg, "Atomic Structure of Minerals," Cornell Univ. Press, Ithaca, N. Y., 1937.

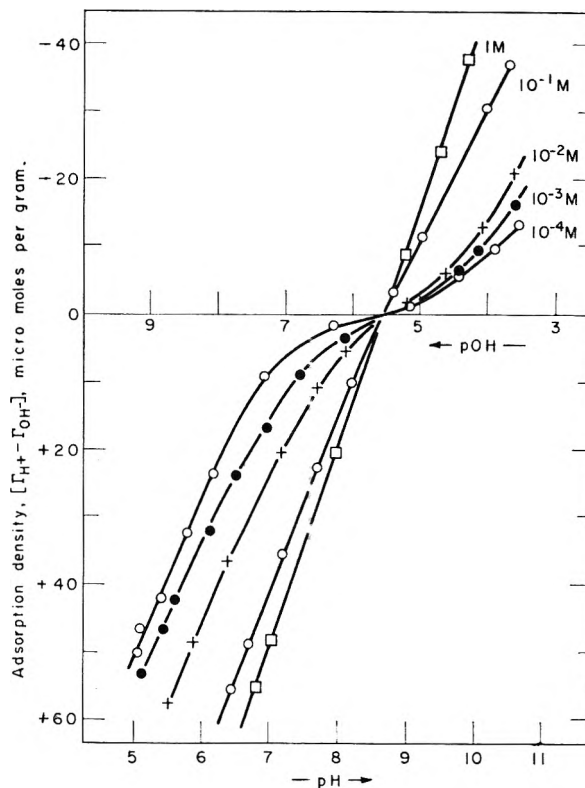


Fig. 1.—Adsorption density of potential determining ions on ferric oxide as a function of pH and ionic strength: temperature, 21°; indifferent electrolyte KNO₃.

Since adding OH⁻ to the uncharged surface would increase the Fe(III) coordination number to seven, which is not likely to occur, the negative surface probably results from removal (desorption) of H⁺ from the surface. In any event experimental adsorption measurements cannot distinguish between the adsorption of a hydroxyl ion or the desorption of a hydrogen ion. This model also suggests why the metal ion (Fe⁺⁺⁺) plays no active potential-determining role; it is buried under the surface. Only when the protective layer is stripped off at quite acid pH values will the concentration of ferric ions in solution become appreciable.

The zero point of charge may be related, therefore, to the pH of the solution when the adsorption densities of H⁺ and OH⁻ ions are equal or when by dissociation an equal number of positively and

(24) O. Glemser and G. Rieck, *Z. anorg. u. allgem. Chem.*, **297**, 175 (1958).

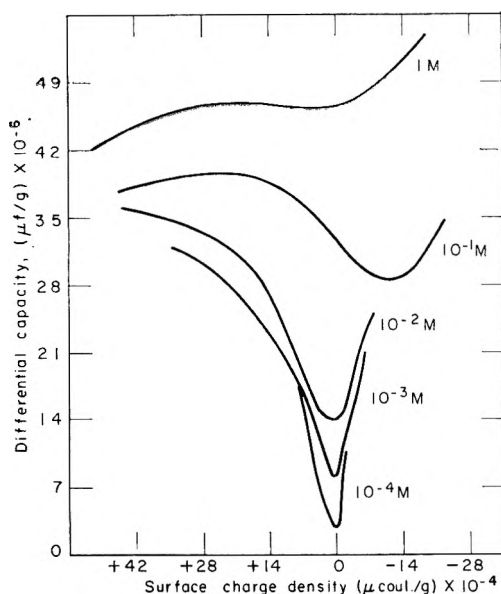


Fig. 2.—Differential capacity of ferric oxide as a function of surface charge: temperature, 21°; indifferent electrolyte KNO_3 .

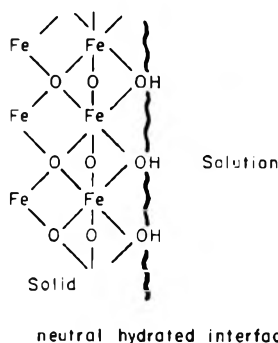
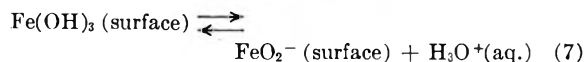
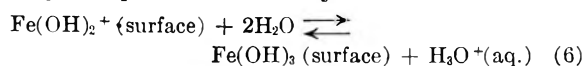
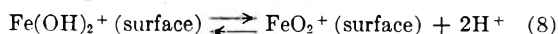


Fig. 3.—Schematic illustration of an uncharged hydrated ferric oxide surface.

negatively charged surface sites are exposed. The surface reactions involved in the establishment of a surface charge and the electrical double layer may be represented formally as



In these reactions $\text{Fe}(\text{OH})_3(\text{surface})$ represents the uncharged surface or rather a surface adsorption site which by adsorbing a proton becomes positive ($\text{Fe}(\text{OH})_2^+$) or by desorbing a proton becomes negative (FeO_2^-). From (6) and (7) it follows that the surface site ($\text{Fe}(\text{OH})_3$) has amphoteric properties, thus $\text{Fe}(\text{OH})_3$ may be regarded as the conjugate base of the acid site, $\text{Fe}(\text{OH})_2^+$, or as the conjugate acid of the base, FeO_2^- . By adding reactions 6 and 7, the important result is obtained that



for which the equilibrium constant

$$K_1 = \frac{[\text{FeO}_2^- (\text{surface})]}{[\text{Fe}(\text{OH})_2^+ (\text{surface})]} \times \left(\frac{\gamma_-}{\gamma_+} \right) \times a_{\text{H}^+}^2 \quad (9)$$

measures the strength with which the ferric oxide surface binds protons. If the ratio of the activity

coefficients (γ_- , γ_+) of the two surface sites is about unity, then it follows from (9) that the magnitude of K_1 is determined by the pH of the z.p.c. (pH 8.5) as obtained from Fig. 1. Thus, K_1 is equal to 10^{-17} , a result which shows that the proton is strongly bonded to the surface. It is interesting to note that this approach to the evaluation of the z.p.c. of ferric oxide is similar to the procedure used for determining the isoelectric pH of proteins in solution. Furthermore, the electrochemical behavior of the Fe_2O_3 -solution interface at different ionic strengths, as illustrated by Fig. 1, is very similar to that of the titration curves of proteins in aqueous solutions.²⁵

The Relationship between Z.p.c. and the Point of Minimum Solubility.—As written, the surface reaction 8 also suggests that as an alternative to the surface dissociation mechanism, the establishment of the surface charge may be explained by the adsorption from solution of the hydroxo-complex species, FeO_2^- (or $\text{Fe}(\text{OH})_4^-$) and $\text{Fe}(\text{OH})_2^+$. Indeed for negligible differences in the adsorbability of these two species the activity ratio of the surface sites may be replaced by the activity of the species in the aqueous solution which is in equilibrium with solid Fe_2O_3 . Subject to these conditions the z.p.c. will be determined by the pH of the aqueous solution for which the activities of the aqueous species, $\text{Fe}(\text{OH})_4^-$ and $\text{Fe}(\text{OH})_2^+$, are equal.

At this point it is worthwhile to interrupt the discussion of the z.p.c. of Fe_2O_3 to recall an important characteristic of complex solutions. If a group of positive and negative complexes of the same central ion is considered independently of any other ionic species in solution, this group will be electroneutral when

$$\sum z_+ c_+ = \sum z_- c_-$$

where z_+ (z_-) is the net charge of a positive (negative) complex and c_+ (c_-) the concentration of the positive (negative) complex. The ligand concentration (or activity, to be exact) at which this condition is satisfied determines the *isoelectric point* of the complex solution.^{26,27} Furthermore, when the complex system includes a solid phase in equilibrium with the solution, the isoelectric point (i.e.p.) of the solution corresponds to the point of *minimum solubility* of the solid. A clear and lucid proof of this observation has been given by Beck.²⁷ Figure 4 illustrates the relation between the i.e.p. of an aqueous solution in contact with solid Ag_2O and the point of minimum solubility of the solid.

The existence of a number of positive Fe(III) hydroxo-complexes has been well established and their stability constants are known. Although the presence of a negative complex, $\text{Fe}(\text{OH})_4^-$ (or FeO_2^-), in highly alkaline solutions has been known, it is only recently that Lengweiler, Buser, and Feitknecht²⁸ were able to determine from total

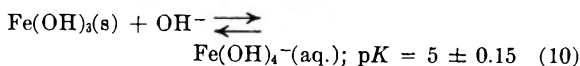
(25) R. K. Cannan, A. H. Palmer, and A. C. Kibrick, *J. Biol. Chem.*, **142**, 803 (1942).

(26) L. P. Hammett, "Solution of Electrolytes," McGraw-Hill Book Co., New York, N. Y., 1936.

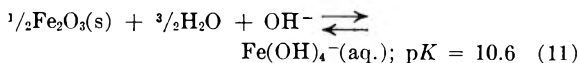
(27) M. T. Beck, *Acta Chim. Acad. Sci. Hung.*, **4**, 227 (1954).

(28) H. Lengweiler, W. Buser, and W. Feitknecht, *Helv. Chim. Acta.*, **44**, 796 (1961).

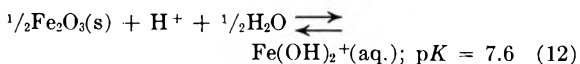
solubility measurements of $\text{Fe}^{59}(\text{OH})_3$ the equilibrium constant for the reaction



in the presence of 3 M NaClO_4 . From a knowledge of the standard free energy of formation (ΔG_f°) of solid $\text{Fe}(\text{OH})_3$ and Fe_2O_3 ,²⁹ the equilibrium constant for the reaction



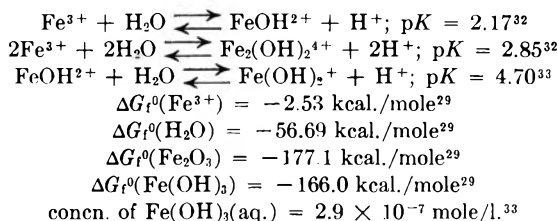
may be calculated. The corresponding reaction for the monovalent positive complex is



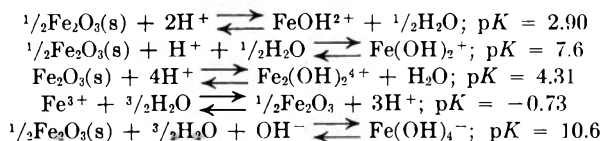
In Fig. 5 the composition of the aqueous solution in equilibrium with solid Fe_2O_3 is demonstrated by a plot of log concentration³⁰ against pH. All pertinent thermodynamic data used in constructing Fig. 5 are summarized in Table II. The isoelectric point of the complex solution is seen to lie at a pH of 8.5. Furthermore, in the vicinity of this pH, the concentration of the two monovalent complex species far exceeds that of the polyvalent species. The minimum solubility of Fe_2O_3 also falls at pH 8.5. Because of the high concentration of the undissociated species³¹ ($\text{Fe}(\text{OH})_3$), the minimum is not as sharply defined as that of Ag_2O .

TABLE II

THERMODYNAMIC DATA USED IN CONSTRUCTING FIG. 5



The above thermodynamic information was used to determine the constants for the reactions



The most striking feature of Fig. 5 is the fact that the i.e.p. of the complex $\text{Fe}(\text{III})$ solution agrees so well with the measured z.p.c. The exact agreement suggested by the experimental data must, however, be viewed as a fortuitous circumstance. Nevertheless, it may be concluded that the available experimental data suggest that the equilibrium constants for reaction 8 and its analog

(29) W. M. Latimer, "Oxidation Potentials," 2nd Edition, Prentice-Hall, Inc., New York, N. Y., 1952.

(30) For the positive complexes the values for all constants have been extrapolated to zero NaClO_4 concentration.

(31) H. Langweiler, W. Buser, and W. Feitknecht (*Helv. Chim. Acta*, **44**, 805 (1961)) present quite conclusive evidence that the concentration of undissociated $\text{Fe}(\text{OH})_3$ in solution is lower by a hundredfold factor than that indicated in Fig. 5. However, this will have relatively little effect on the sharpness of the solubility minimum.

(32) R. M. Milburn, *J. Am. Chem. Soc.*, **79**, 537 (1957).

(33) A. B. Lamb and A. G. Jacques, *ibid.*, **60**, 1215 (1938).

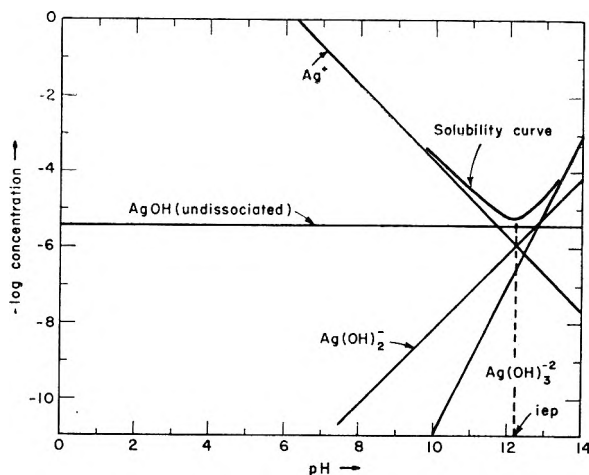


Fig. 4.—Variation of the concentration of silver-bearing species with pH in an aqueous solution in equilibrium with solid Ag_2O . (The data used in constructing this figure were taken from ref. 27 and 46.)

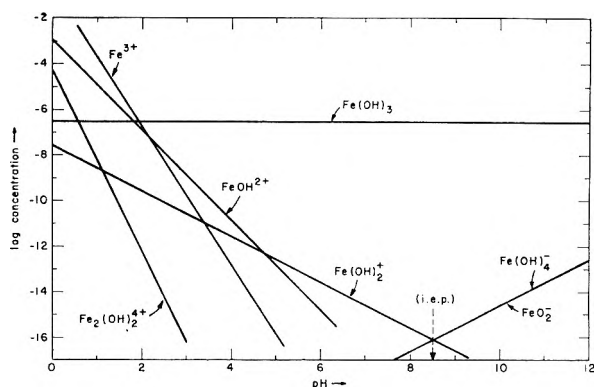


Fig. 5.—Concentration of various $\text{Fe}(\text{III})$ -bearing species in an aqueous solution in equilibrium with solid hematite ($\alpha\text{-Fe}_2\text{O}_3$).

(combination of reactions 11 and 12) in the bulk solution phase are approximately equal. As pointed out previously, this conclusion in turn suggests that the adsorbabilities of the species $\text{Fe}(\text{OH})_2^+$ and FeO_2^- are approximately equal and thus the z.p.c., i.e.p., and the point of minimum solubility fall at the same pH value.

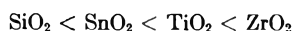
Since the solubility of a solid in a liquid phase and the establishment of an electrical double layer of free charges at the solid-liquid interface both are dependent on the same physico-chemical process—transfer of charged species across the interface, the coincidence of the z.p.c. and the point of minimum solubility perhaps is not unexpected. The maximum in the interfacial tension (or the electrocapillary maximum for a polarizable interface) lies at the z.p.c. because, due to electrostatic repulsion, less work is required to increase the surface area of a charged interface reversibly than that of an uncharged interface. This equality of z.p.c. and the point of maximum surface tension follows directly from thermodynamics. One might reason that the point of minimum solubility of a solid also should coincide with the z.p.c. since the reversible work required to move a cationic potential-determining species from a positively charged surface (or an anion from a negative surface) into

the solution phase should be less than that required for the same transfer process at a surface which has the same number of oppositely charged sites. Whether the equality of z.p.c. and i.e.p. has the same fundamental significance as that of the z.p.c. and the electrocapillary maximum must await further experimental verification.

A comparison between the measured z.p.c. and the i.e.p. of a solution of hydroxo-complexes may be extended to all oxides. In Table III the available data on a few oxides are collected. Z.p.c. measurements made on oxides for which no solubility data are available and estimates of the z.p.c. for some oxides based only on solubility measurements and complex stability constants also are included in this table.

Table III shows the paucity of available information to make this comparison between the z.p.c. of the oxide surface and the i.e.p. of the complex solution in equilibrium with the solid phase. Some of the natural anhydrous oxides and ignited precipitates (*e.g.*, Al_2O_3 , Fe_2O_3) give z.p.c. values, as determined by electrokinetic measurements, which do not agree too well with the minimum solubility observations and the z.p.c. of the crystalline precipitates. This may be due to lack of equilibrium with the solvent due to incomplete hydration of the surface, a possibility which was avoided in our experiments.

The increasing pH of the z.p.c. with decreasing charge of the cation in going from the MO_3 type oxide to the M_2O type may be explained qualitatively by the decreasing polarizing power of the cations of lower positive charge. The more acidic in nature the surface MOH group, the tighter the bonding between M and O—thus the acid pH values of z.p.c. shown by the MO_2 type oxides. Within this oxide group the variation of the pH of the z.p.c. may be explained by Pauling's³⁴ concept of electronegativity. A decreasing difference in electronegativity between the oxygen and M atom should correlate with an increasing tendency toward acid dissociation of the MOH group. According to this criterion the pH of the z.p.c. for MO_2 oxides should increase in the order



because the electronegativity differences increase from 1.7 for SiO_2 to 2.0 for ZrO_2 .

Since the electronegativity of an element is not a truly invariant property because it depends on the type of bonding and electrical environment,⁴⁷ it is not too helpful in explaining the change in z.p.c. values of the other oxide types. The Al^{3+} cation is less polarizable than Cr^{3+} or Fe^{3+} because it has the electronic configuration of a noble gas, whereas the two transition element cations do not have this structure. Al_2O_3 therefore should be a stronger acid than either Fe_2O_3 or Cr_2O_3 . The lower pH value of the z.p.c. for Al_2O_3 than for Fe_2O_3 suggested in Table III is in agreement with this conclusion.

Conclusions

1. The approximate location of the z.p.c. of metal oxides may be predicted from a knowledge

(34) L. Pauling, "Nature of the Chemical Bond," Cornell Univ. Press, Ithaca, N. Y., 1945, p. 58.

TABLE III
COMPARISON OF THE pH OF Z.P.C., I.E.P., AND MINIMUM SOLUBILITY FOR VARIOUS OXIDES

Solid	pH		Comment	Ref.
	Z.p.c.	Min. solubility I.e.p. (calcd.)		
WO_3	0.43	0.43	a,e	35
SiO_2	<2		b,e,f	37, 38, 16
SnO_2	4.5 (5.5-7.3)		a,e b,e	16 16
TiO_2	6.7 6 (4.7)		b,f a,e b,c,e	39 16 16
ZrO_2	~4		b,g	38
Al_2O_3	6.94 ± 0.37 (8.4) (9.45)		a,e b,e b,f	40 16 41
		7.7		42
Fe_2O_3	8.5 (6.5-6.7)		a,b,c,e,g,h (See Table I)	See Fig. 5
Cr_2O_3	7.03 ± 0.2		a,e	43
HgO		8.1		44
ZnO		8.8		45
CdO		9.3		45
Ag_2O	11.2 (pAg 4.8)		d,e	10
		12.17 (pAg 5.9)		46

^a Precipitated product. ^b Natural product. ^c Ignited precipitate. ^d Z.p.c. determined on silver powder, which was probably superficially oxidized. ^e Z.p.c. by electrophoresis. ^f Z.p.c. by streaming potential. ^g Z.p.c. by electroosmosis. ^h Z.p.c. by absorption of potential-determining ions.

of the minimum solubility of the solid and the i.e.p. of the solution of metal hydroxo-complexes. This relationship between z.p.c. and i.e.p. has been reasonably well established for Fe_2O_3 in aqueous solutions of KNO_3 .

2. A model of the double layer at oxide surfaces is in agreement with the known tendency of the metal cation toward hydroxo-complex formation in solution. Much can, therefore, be learned about the bonding characteristics and dissociation of the adsorption sites and the underlying solid from the structure and chemical stability of hydroxo-complexes in solution.

3. The approach to the electrochemical study of oxide surface may be extended to non-oxide systems.

Acknowledgments.—The experimental study of

(35) W. Hückel, "Structural Chemistry of Inorganic Compounds," Elsevier Press, New York, N. Y., 1950, p. 202.

(36) S. E. S. El Wakkad and H. A. Rizk, *J. Phys. Chem.*, **61**, 494 (1957).

(37) H. C. Li and P. L. de Bruyn, to be published.

(38) E. J. W. Verwey, *Rec. trav. chim.*, **60**, 625 (1941).

(39) G. Purcell, Dissertation, Department of Mineral Preparation, Pennsylvania State Univ., 1961.

(40) S. N. Tewari and S. Ghosh, *Acad. Sci. India (Allahabad), Proc.*, **A21**, 41 (1952).

(41) H. J. Modi and D. W. Fuerstenau, *J. Phys. Chem.*, **61**, 640 (1957).

(42) K. H. Gayer, L. Thompson, and O. T. Zajicek, *Can. J. Chem.*, **36**, 1268 (1958).

(43) S. N. Tewari and S. Ghosh, *Acad. Sci. India (Allahabad), Proc.*, **A21**, 29 (1952).

(44) K. Emerson and W. M. Graven, *J. Inorg. & Nuclear Chem.*, **11**, 309 (1959).

(45) J. Bjerrum, G. Schwarzenbach, and L. G. Sillén, "Stability Constants—Part II, Inorganic Ligands," The Chemical Society, London, 1958.

(46) H. L. Johnston, F. Cuta, and A. B. Garrett, *J. Am. Chem. Soc.*, **55**, 2311 (1933).

(47) W. Gordy and W. J. Orville Thomas, *J. Chem. Phys.*, **24**, 439 (1956).

ferric oxide, which led to many of the ideas expressed here, was supported by the United States Atomic Energy Commission under Contract No. AT(30-1)-956. The authors wish to acknowledge

Mr. S. Uchida for performing some of the potentiometric titrations on Fe_2O_3 . The interest shown and the valuable comments made by Dr. J. Th. G. Overbeek also are gratefully acknowledged.

THE SOLUBILITY BEHAVIOR OF HYDROXYLAPATITE

BY VICTOR K. LA MER

Columbia University, New York 27, N. Y.

Received June 30, 1961

Hydroxylapatite, a salt of a weak acid, undergoes hydrolysis in aqueous solution yielding a solid surface complex having the formula $\text{Ca}_2(\text{HPO}_4)(\text{OH})_2$. The curious and complicated solubility data become explicable when it is recognized that it is this surface complex, and not hydroxylapatite, which is dominating the solubility equilibrium. A recalculation of the data of Levinskas and Neuman obtained in 0.165 *M* NaCl to simulate biological conditions show that the solubility of hydroxylapatite responds precisely to additions of phosphate ions and calcium ions, as demanded by the solubility product principle for a medium of constant ionic environment. It is unnecessary to complicate the treatment in such solvents by calculating hypothetical individual ion activity coefficients. Aqueous NaCl (0.165 *M*) is a solvent of such biological importance that it should be taken as a standard solvent of reference in which all activity coefficients are assigned a value of unity, thus postponing the difficult and sometimes impossible problem of extrapolating the data to pure water as the solvent of reference.

Introduction

Hydroxylapatite is assigned the formula $\text{Ca}_{10}(\text{PO}_4)_6(\text{OH})_2$. In recent years it has become the focus of attention that has been directed toward all of the basic calcium phosphates for the elucidation of the processes of calcification in general and for dentistry in particular. Hydroxylapatite now is recognized as the most important of the inorganic compounds in the structure of bones and teeth.

Forty years ago, Shipley, Kramer, and Howland made the important observation that whenever the product of the total calcium by the total phosphate in the blood fell below a certain range of values, both expressed in milligrams, the subject would develop rickets; if this empirical product was above the critical range, no rickets developed.

Holt, La Mer, and Chown (H. L. and C.)¹ suggested that a more intelligible chemical interpretation could be made if the empirical product were replaced by the stoichiometric ion products calculated for the particular solid phase being precipitated in the presumed calcification process. Such computations would represent the correct and proper physicochemical measure of whether or not the system was undersaturated, supersaturated, or in equilibrium with the solid phase in question.

Research along these lines still is being prosecuted. It is complicated by the fact that, even today, we still have no method for calculating the individual ion activity coefficients that is not open to objection when ions of high and opposite charge are involved, as is the case for $\text{Ca}_3(\text{PO}_4)_2$ and hydroxylapatite. The problem is complicated further *in vivo* by the unknown extent of chelation of Ca^{++} by the proteins of the blood serum. It will be shown below that the simple equations of Debye and Hückel have been used improperly; they are inadequate for precise calculations for such ions in aqueous media and are of no value in the presence of protein.

It is one of the purposes of this paper to show how these complications of interpretation can be avoided by properly planned experimental work.

Precipitation of Basic Calcium Phosphate in Titrations.—To avoid the complications of hydrolysis in the interpretation and to ascertain the particular solid phase present for which an ion product should be calculated, H. L. and C. titrated dilute orthophosphoric acid (H_3PO_4) with saturated lime water. They measured, at successive stages of the reaction, the *pH*, using the hydrogen electrode, and analyzed the co-existing solid phase for Ca and P.

When one equivalent of $\text{Ca}(\text{OH})_2$ had been added, the solid phase was dicalcium phosphate, for which the atomic Ca/P ratio is unity; solubility equilibrium was established quickly and constant values were obtained for the ion product (Ca^{++}) ($\text{HPO}_4^{=}$) since the ionic strength remained sensibly constant over the range of *pH* and Ca^{++} ion concentration involved. These values were sensitive to the addition of foreign neutral salts. However, they proved to be in agreement with theory, as we now know they should be, for a symmetrical bivalent salt,^{2,3} for which relatively simple equations are applicable in accordance with the consequences of the extended form of the Debye-Hückel interionic attraction theory.

When the addition of more than one equivalent of $\text{Ca}(\text{OH})_2$ had been passed, the *pH* increased slowly over the range 5 to 7; the Ca/P ratio progressively increased from the value valid for CaHPO_4 through a continuous series of values which approximated that of $\text{Ca}_3(\text{PO}_4)_2$ [Ca/P = 1.5] and finally to that of hydroxylapatite [Ca/P = 1.667] or their mixtures.

Equilibrium was reached slowly in the basic region. However, after 18 days of continuous shaking at 38°, reproducible values, which had remained constant for some days, were obtained. They were taken as representing an equilibrium

(1) L. E. Holt, Jr., V. K. La Mer, and H. B. Chown, *J. Biol. Chem.*, **64**, 509 (1925); see p. 534 for recognition of the limitations of the D-H theory and p. 510 that the basic calcium phosphates hydrolyze when added to water.

(2) I. A. Cowperthwaite and V. K. La Mer, *J. Am. Chem. Soc.*, **53**, 4333 (1931).

(3) V. K. La Mer and W. G. Parks, *ibid.*, **53**, 2040 (1931); see also ref. 12 for new data on CaHPO_4 , MgHPO_4 , and BaHPO_4 .

state. Agreement with the general predictions of the limiting form of the Debye-Hückel equations were of a correct order of magnitude but exact agreement was not obtained. This was hardly to be expected in the light of researches then under way in the Columbia Laboratories dealing with the peculiar and specific behavior of the activity coefficient of high valence ions.⁴

In 1925, the behavior of ions of high and unsymmetric valence type presented an intriguing theoretical problem in physical chemistry which just was being formulated in the Copenhagen and Columbia University laboratories.²⁻⁴ This problem has not been adequately solved theoretically at the present time, despite the extensive work that has been expended upon it. In the light of later theoretical contributions of Guggenheim,^{5a} of Brønsted,^{5b} and of Onsager⁶ it is questionable whether the problem ever can be solved satisfactorily. The solubility data on many simple salts like $\text{La}(\text{IO}_3)_3$, the unsymmetric cobaltamines, etc., furnish, however, incontrovertible evidence⁷ of the magnitude and importance of the highly specific behavior of such salts. The specific behavior usually has been ignored since it cannot be calculated from simple equations. In the paper of H. L. and C. individual ion activity coefficients were not calculated because we recognized at that time that they could not be computed from the simple Debye-Hückel equations.⁸

The solubility product calculations of H. L. and C. for $\text{Ca}_3(\text{PO}_4)_2$, although executed correctly in principle, nevertheless are open to two valid criticisms.

(a) Shortly after publication of their work, it was shown by X-ray investigations that $\text{Ca}_3(\text{PO}_4)_2$ does not exist as such in bones and teeth, but exists rather as an hydroxylapatite structure for which compound the ion product should have been calculated. Strangely, none of the critics, interested in the problem of calcification, ever took the trouble

(4) (a) V. K. La Mer and C. F. Mason, *J. Am. Chem. Soc.*, **49**, 410 (1927); (b) see also J. N. Brønsted and V. K. La Mer, *ibid.*, **46**, 555 (1924), where the Debye-Hückel limiting laws and the ionic strength principle were confirmed but restricted in the generality of application (see p. 558) by the electric type effect.

(5) (a) E. A. Guggenheim, *J. Phys. Chem.*, **33**, 842 (1929); **34**, 1540 (1930); (b) J. N. Brønsted, *Z. physik. Chem.*, **143**, 301 (1929).

(6) Lars Onsager, *Chem. Revs.*, **13**, 73 (1933). The question is discussed in Harned and Owen, "Physical Chemistry of Electrolytic Solutions," 2nd Ed., A.C.S. monograph 95, p. 34.

(7) V. K. La Mer and F. H. Goldman, *J. Am. Chem. Soc.*, **51**, 2632 (1929); see Fig. 1, p. 2638. See also ref. 4a, 4b. Also V. K. La Mer and R. W. Fessenden, *ibid.*, **54**, 2351 (1932).

(8) In passing, we note that the calculation procedure employed by H. L. and C. has been misunderstood in the current literature⁹ for reasons which are neither cogent nor correct: namely, that H. L. and C. erred in not calculating and using individual ion activity coefficients. The further criticism of Hodge,¹⁰ that since the hydrogen electrode often exhibits electrode poisoning, it may have yielded invalid results for H. L. and C., also is not convincing. Holt,^{10 et al.}, have found that the quinhydrone electrode checks the results of the hydrogen electrode.

(9) G. J. Levinskas, Dissertation for the degree of Ph.D., University of Rochester, N. Y., 1953, pp. 14-15. The calculation (pp. 115-121) of the individual ion activities (also quoted in ref. 14, Table 1-1, page 7), violate the restriction quoted in the text. $\gamma_{\text{Ca}^{++}}$ (0.165 μ CaCl_2) is not necessarily the same as $\gamma_{\text{Ca}^{++}}$ (0.165 μ NaCl), etc., even though the ionic strengths are the same and similarly for their calculations for phosphate ions.

(10) L. E. Holt, Jr., J. A. Pierce, and C. N. Kajdi, *J. Colloid Sci.*, **9**, 409 (1954); see pp. 413.

to calculate the ion product for hydroxylapatite from these data until Rootare, Carpenter, and Deitz¹¹ did so in 1961. This important paper, which emphasizes many further complications, is responsible for reviving the writer's interest in the problem of calcification after a lapse of thirty-six years.

(b) The concentrations of HPO_4^- , and particularly PO_4^{3-} , ions are very sensitive to the values of the three dissociation constants of H_3PO_4 chosen for the calculations. The values of these constants available to H. L. and C. in 1925 have been superseded by more precise values determined by methods which also are recognized as more accurate in principle,^{12,13} since they do not involve cells with liquid junctions.

It becomes important, therefore, to recognize for what follows, that the recalculations of the data of H. L. C. by Rootare, Deitz, and Carpenter (R. D. C.), using modern values of the dissociation constants, and most particularly by applying them in accord with their new approach to the perplexing problem of the solubility behavior of hydroxylapatite, yield solubility products which are constant over most of the basic region investigated by H. L. C. Furthermore, they are also in remarkably good agreement with the measurements of R. D. C. obtained by a different procedure.

Solubility Behavior of Hydroxylapatite.—Within the past decade, an opposite approach has been emphasized; namely, to investigate the solubility of crystalline hydroxylapatite by dissolving this compound in water containing various ions. The results have been startling and paradoxical. For example, Levinskas and Neuman¹⁴ find that (a) The solubility measured, either in terms of total Ca or total P, depends strongly upon the solid content of the slurry; *i.e.*, upon the amount of solid phase per unit of the leaching solution.

(b) The composition of the saturated solution does not agree with the formula of the saturating salt $\text{Ca}_{10}(\text{PO}_4)_6(\text{OH})_2$. Instead, the Ca/P ratio of the solution varies with the solid content of the slurry. They call behaviors (a) and (b) "incongruent solubility."

(c) The solubility of hydroxylapatite does not respond to additions of calcium and phosphate ions as it should after corrections for the individual ion activity coefficients have been made. (Table III of ref. 14.)

They conclude "There was no simple relation between calcium and phosphate concentrations after equilibration."

In a later chapter we shall show from a recalculation of the data of L. and N. that the conclusion they draw that "no ion product can be calculated" that is constant over a range of HPO_4^- and Ca^{++} additions is unwarranted. Instead, it will be shown that their data conform very closely to the solubility product principle when treated properly.

(11) H. M. Rootare, V. R. Deitz, and F. G. Carpenter, *ibid.*, **17**, 179 (1962).

(12) L. F. Nims, *J. Am. Chem. Soc.*, **55**, 1946 (1933).

(13) R. G. Bates and S. F. Acree, *J. Research Natl. Bur. Standards*, **30**, 129 (1943).

(14) G. J. Levinskas and W. F. Neuman, *J. Phys. Chem.*, **59**, 164 (1955).

These conclusions of L. and N. are surprising; they have furnished the motivation for a monograph¹⁵ by Neuman and Neuman (N. and N.) which seems to have attained considerable currency in biological circles. In that monograph N. and N. advance radically new theories of solubility and of nucleation as explanations for the aberrant solubility of hydroxylapatite and the role it plays in calcification. These theories are in direct conflict with the teachings of physical and colloid chemistry.¹⁶

A critical review, testing the validity of these theories (ref. 15, chap. 2), is accordingly in order before further research on calcification processes based upon them can be accepted. However, it seemed more logical that one should first re-examine the data and calculations to ascertain if any of these new theories really are needed for an explanation of the paradoxical results observed. In other words, are classical concepts sufficient? Have the classical concepts been adequately tested and treated?

Several suggestions have been offered for these marked aberrations from simple solubility behavior for hydroxylapatite; namely, (1) the solid phase was impure, (2) substitution and exchange occurred within the lattice, and (3) equilibrium was not established. None of these explanations is adequate in themselves to explain all of the facts that now are available. Although no specimen of hydroxylapatite has ever been prepared which is entirely free from impurities, the sample used by L. and N. was crystalline and one of the purest available at that time.

The researches of earlier investigators have shown that hydroxylapatite reaches solubility equilibrium slowly. However, L. and N. found with their finely divided product, whose surface area was 60 m.², that with a rotation of 21.6 r.p.m. "a reproducible end-point was reached promptly and remained unchanged, within experimental error from 1 to 77 days." Most important of all, L. and N. demonstrated that the same values could be approached from undersaturation and from supersaturation; a generally accepted criterion that an equilibrium state to within the perceptible experimental limits has been reached. (Table I, ref. 14.)

In an extensive study, employing twelve preparations of hydroxylapatite under a variety of conditions, Rootare, Deitz, and Carpenter¹¹ (R. D. and C.) have confirmed the paradoxical findings (1) and

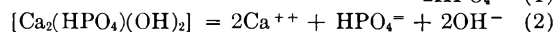
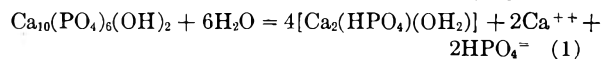
(15) Neuman and Neuman, "The Chemical Dynamics of Bone Mineral," University of Chicago Press, [Library of Congress No. 58-5491], 1958.

(16) For example, Neuman and Neuman (ref. 15, pp. 25 on) resurrect an old paper by Knapp [Trans. Faraday Soc., 17, 457 (1922)] in which a plausible equation is developed, purporting to show that electric charges on small particles will modify profoundly their solubility in addition to the Kelvin effect of particle size. It would indeed be strange, and most important for the proper development of colloidal theory, if chemists, well versed in the effects of electric charge on simple ionic systems, had been unaware for forty years of such a fundamental factor as N. and N. believe to be the case. Space does not permit a discussion of the various reasons why the Knapp equation has never been accepted. We refer the interested reader to Alexander and Johnson's "Colloid Science," (Oxford Press, 1949, Vol. 1, pp. 36-38, 87-90) where the effect of electrical charge has received attention and is rejected as inconsequential in the solubility of colloids.

(2) of L. and N. In addition they find that: (4) An increase in ionic strength by "spectator ions," such as Na⁺ and Cl⁻, leads to a decrease in solubility! (5) The ionic strengths of the solution prepared from water extracts alone has a greater than expected effect and the solubility increases with increase in ionic strength. (6) The molar ratio of calcium to total phosphate in the extracts is not constant at the hydroxylapatite value (1.667). It approaches this value only as a large fraction of the material is dissolved.

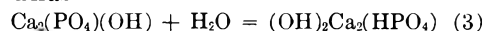
Obviously, the Debye-Hückel equations of electrostatic interaction have in some cases the wrong sign as in (4) and are quite inadequate to explain the effects of foreign ions in (5).

Hypothesis of Surface Complex [Hydrolysis].—R. D. and C.¹¹ offer a simple explanation which appears to resolve almost all of these paradoxes. They postulate that the terminal phosphate ions of hydroxylapatite undergo hydrolysis when the solid is immersed in water. The release of ions by this reaction and the simultaneous formation of a surface complex accounts for the apparent "solubility." The following reactions are employed



The complex $[\text{Ca}_2(\text{HPO}_4)(\text{OH})_2]$ formed by reaction 1 rapidly covers the exposed surface of hydroxylapatite with a strong (hydrogen?) bonding to the underlying structure which contributes to its stability. With a specific surface of 60 m.² per g. a sufficient amount of the surface complex forms to dominate the equilibrium.

Arnold (see ref. 11) also had suggested, as early as 1950, that hydroxylapatite in neutral or alkaline solution would possess a surface group having the formula $\text{Ca}_2(\text{PO}_4)(\text{OH})$. The hydrated form of this group is the surface complex postulated in eq. 1 and 2. Thus



Both reactions 1 and 2 yield calcium and phosphate ions in solution, but in different proportions.

If hydroxylapatite is prepared from the melt and placed in water, reaction 1 occurs and the Ca/P ratio is unity. On the other hand, if hydroxylapatite is prepared by precipitation and/or redispersed in water, the solid presumably would already be covered with complex and also be subject to the adsorption of other extraneous ions. The important controlling factor is the variation in solid to water ratio (ref. 11).

When both reactions 1 and 2 contribute equally to the solution process, the molar ratio of calcium to phosphate in solution should approach 1.67, as is found to be the case by R. D. and C.

If the solubility equilibrium is dominated by eq. 1 the equilibrium constant reduces to the square of the activity product of CaHPO_4 , i.e., of dicalcium phosphate. Thus, using p for the negative logarithm eq. 1 yields

$$pK(\text{eq. 1}) = 2p_{\text{Ca}^{++}} + 2p_{\text{HPO}_4^{=}} + 4p[\text{Ca}_2(\text{HPO}_4)(\text{OH})_2] \quad (4)$$

and reduces to eq. 5

$$= 2p_{\text{Ca}^{++}} + 2p_{\text{HPO}_4^{=}} = -2 \log a_{\pm}(\text{CaHPO}_4) \quad (5)$$

since the activities of the solid surface complex, of solid hydroxylapatite, and of H_2O are constant.

This simple hypothesis, corresponding to equations 1 and 5, is tested in Table I. The log of the geometric mean molality product of Ca^{++} and HPO_4^- proves to be a constant (see last two columns of Table I) within the limits of experimental error of the reliable data over the range of variables. *The constancy of this ion product does not require that the solution be in equilibrium with a solid phase of $CaHPO_4$; it means only that eq. 1 is operating and that eq. 4 and 5 are confirmed. The value 0.36×10^{-3} for this ion product is below the saturation value for $CaHPO_4$.*

Principle of Constant Ionic Environment.—If correct computations of individual ion activities are not possible with presently existing equations, how can one treat the data? It is the purpose of this chapter to explain in more detail, since the method used by H. L. and C. has not been understood, how one can treat the data of L. and N. and dispense with this unnecessary complication.

In their Table III, L. and N. equilibrate a fixed amount of solid hydroxylapatite (1 g.) with 1 l. of 0.165 *m* NaCl solution modified by additions of $CaCl_2$ or NaH_2PO_4 arranged to give initial concentrations of these salts extending by decadic intervals over a wide range of the variables. The initial state is specified in col. 2 of our Table I. After equilibrating for $9\frac{1}{3}$ days—which proved to be an adequate length of time—the solutions were ultracentrifuged and the supernatant liquid analyzed. The final Ca and total P content in 10^4 mole/l. units are given in columns 3 and 4, along with the pH as measured by a glass electrode.

The design of these experiments, their execution, and the analytical work appear to meet all the requirements necessary for the calculation of equilibrium solubility product constants, except for the absolute values of the pH.

NaCl (0.165 *m*) was used as the solvent to simulate biological conditions. The addition of NaCl, instead of complicating matters, actually simplifies the interpretation since the ionic strength at equilibrium remained virtually constant at 0.166 to 0.167, the additions of $CaCl_2$ or of NaH_2PO_4 being insufficient to change the ionic strength appreciably.

From an extensive series of measurements involving solubilities and e.m.f.'s published before the appearance of the Debye-Hückel theory, Brønsted^{17,18,19} developed and verified the principle of constant ionic environment; namely, that the *activity coefficients of all ions present in small amount remain constant when dissolved in a solution containing an inert neutral salt in much larger constant amount.* This means that when the concentrations of the ions present in small amount are varied, their activity coefficients remain constant; their absolute values being determined solely by some

(17) J. N. Brønsted, *D. Kgl. Danske Videnskab. Selskab-Skrifter*, [7] **XII**, 241 (1915); **III**, 9 (1920) (in English).

(18) J. N. Brønsted, *Z. physik. Chem.*, **103**, 307 (1922) (with Kai Pedersen). Further papers are cited and interpreted in ref. 19 (p. 519-523).

(19) V. K. La Mer, "Recent Advances in the Ionization Theory as Applied to Strong Electrolytes," *Trans. Am. Electrochem. Soc.*, **51**, 507 (1927). Data confirming the principle are given in this reference.

function of the constant total concentration. This principle demands a constant stoichiometric solubility product (mean ionic molality product) for the saturating salt [the surface complex] as a thermodynamic consequence for the entire range of the data in Table III.

It is most important to recognize that Brønsted's principle remains valid even when ions of high and unsymmetric valence type are involved; whereas, the principle of ionic strength developed later by Lewis and Randall as well as the Debye-Hückel equations often break down completely when ions of high and unequal valence type are present even in highly dilute solutions. For example,⁷ the activity coefficient of $La(IO_3)_3$ (solubility = 0.00089 *m*) differs by a factor of 200% in a 0.10 μ solution of K_2SO_4 compared to a 0.10 μ solution of KCl; *i.e.*, $\gamma_{La(IO_3)_3(K_2SO_4)}$ does not equal $\gamma_{La(IO_3)_3(KCl)}$ at the same ionic strengths. The bearing on solutions containing Ca^{++} , HPO_4^- , $PO_4^{=}$, and similar ions is obvious.

This means that the common practice of computing component ion activities by multiplying stoichiometric concentrations by individual ion activity coefficients calculated from tables, as L. and N. have done, *can be a treacherous procedure.* The practice is acceptable only when care is taken to ascertain that the tabulated activity coefficients, particularly of the higher valence types of salts, actually have been referred to the specific total ionic environment chosen and have not been computed from Debye-Hückel equations or simply on the basis of the G. N. Lewis ionic strength principle, both of which are not of general validity under the circumstances.

The second dissociation constant of H_3PO_4 dominates the equilibria of interest in the pH ranges studied; namely

$$K_{2A} = \frac{m_{H^+} m_{HPO_4^-}}{m_{H_2PO_4^-}} \times \frac{\gamma_{H^+} \gamma_{HPO_4^-}}{\gamma_{H_2PO_4^-}} \quad (6)$$

which yields for *Z* the ratio of the molalities of HPO_4^- and $H_2PO_4^-$ ions

$$\log Z = \log \frac{m_{HPO_4^-}}{m_{H_2PO_4^-}} = \left[K_{2A} \times \frac{\gamma_{-}}{\gamma_{=}} \right] \times \frac{1}{a_{H^+}} \quad (7)$$

or

$$p[Z] = Y - pH \quad (8)$$

where $Y = p [K_{2A} \times \gamma_{-}/\gamma_{=}]$. Equation 8 is a working formula for determining the concentrations of the phosphate ions.

Nims,¹² as well as Bates and Acree,¹³ have made detailed and thermodynamically correct determinations of K_{2A} which should yield the values of *Y* to within the undetermined, but constant, activity ratio $\gamma_{-}/\gamma_{=}$. Since the ionic environment is constant, $\gamma_{-}/\gamma_{=}$ may be assigned arbitrarily a value of unity for the solvent 0.165 *m* NaCl as a reference state. They find $K_{2A} = 7.198$ (B. and A.) and 7.206 (L. F. N.), which averages to 7.204 when corrected to 24°.

A precise value of *Y* is of little value here because $\gamma_{-}/\gamma_{=}$ is unknown and the pH values measured by Levinskas¹⁴ leave much to be desired in respect to absolute values. There is an undetermined junction (or asymmetry) potential between the glass electrode and the reference electrode, which

TABLE I

CALCULATION OF STOICHIOMETRIC ION PRODUCT $[Ca^{++}][HPO_4^-]$ FOR HYDROXYLAPATITE DISSOLVED IN AQUEOUS 0.165 *m* NaCl (μ RANGED FROM 0.166-0.167 EXCEPT FOR LAST TWO POINTS) AT 24°

$$Y = p \left[K_{2A} \times \frac{\gamma_{H_2PO_4^-}}{\gamma_{HPO_4^-}} \right] = 7.20. \quad p[Z] = 7.20 - pH. \quad \text{Data from Table III of Levinskas and Neuman (ref. 14)}$$

Exp. No.	Initial 10 ⁴ mole/l. of added Ca	Final 10 ⁴ mole/l.		pH	Z	10 ⁴ mole/l. [HPO ₄ ⁻]	10 ⁸ [Ca ⁺⁺]/[HPO ₄ ⁻]	p(m _±) CaHPO ₄
		Ca	P					
1	25	25.4	0.144	6.27	0.118	0.0149	0.38	4.21
2	25	22.2	.159	6.32	.133	.0188	.42	4.20
3	2.5	3.17	.465	6.68	.302	.117	.37	4.22
4	2.5	3.17	.400	6.76	.363	.107	.34	4.24
5	0.25	1.38	.629	6.80	.398	.179	.25	4.30
6	0.25	1.24	(.604)	6.58	.240	(.117)	(.15)	(4.41)
7	...	1.14	.697	6.69	.309	.164	.19	4.37
8	P	1.21	.675	6.95	.563	.243	.29	4.27
9	0.322	1.02	.891	6.87	.468	.284	.29	4.27
10	.322	1.13	.849	6.84	.436	.258	.29	4.27
11	3.22	0.594	3.21	7.24	1.10	1.68	(1.00)	(4.00)
12	3.22	0.160	3.20	7.29	1.23	1.77	(1.35)	(3.94)
13	32.2	.178	32.9	7.86	4.57	2.70	0.48	4.16
14	32.2	.163	32.0	7.90	5.01	2.77	0.44	4.18
Av. (11) = 0.36 × 10 ⁻⁸								4.21

TABLE II

COMPARISON OF ION PRODUCTS (AS GEOMETRIC MEAN MOLALITIES) $A = p(m_{\pm})(CaHPO_4)$; $B = p(m_{\pm})(Ca_2HPO_4 \cdot (OH)_2)$ USING DIFFERENT VALUES OF $Y = p \left[K_{2A} \times \frac{\gamma_{H_2PO_4^-}}{\gamma_{HPO_4^-}} \right]$ FOR HYDROXYLAPATITE AS INDICATED

Data from Table III of Levinskas and Neuman at 24° in 0.165 *m* NaCl.

Exp. Av.	Y = 7.20			Y = 6.92			Y = 7.40		
	A	B	B - A	A	B	B - A	A	B	B - A
1-2	4.21	5.37	1.17	4.16	5.31	1.15	4.30	5.34	1.04
3-4	4.23	5.38	1.14	4.14	5.28	1.14	(4.63)	(5.36)	(0.73)
5-6	4.35	5.47	1.12	4.23	5.34	1.11	4.44	5.40	0.96
7-8	4.32	5.45	1.14	4.19	5.35	1.16	4.39	5.34	0.95
9-10	4.27	5.44	1.17	4.19	5.35	1.16	4.35	5.39	1.04
11-12	(3.97)	(5.25)	(1.28)	(3.76)	(5.12)	(1.36)	(4.03)	(5.16)	(1.13)
13-14	4.17	5.20	1.02	3.65	4.71	1.00	3.71	4.86	1.1
Av. ⁶	4.26		1.13			1.12			

must be evaluated before exact comparison with measurements using the Nims type of galvanic cells can be made. King and Prue²⁰ in a recent paper have re-emphasized these shortcomings of the glass electrode. It also should be emphasized that the Pallman Effect (see p. 184, 185 of Vol. I, Kruyt, "Colloid Science," Elsevier, 1952) introduces very serious errors in the measurement and interpretation of pH whenever a slurry is involved. The pH that is effective is the value corresponding to that for the localized part of the solution between the charged particles of the slurry which often differs by as much as several pH units (!) from that of the supernatant liquid *in equilibrium with the slurry*. For these reasons we have chosen to assign arbitrary values to the pH in terms of Y in the neighborhood of 7.20 and ascertain the effect of the choice of Y upon the constancy of the calculated stoichiometric products (m_{\pm}) (Table I).

Of the values tested, Y = 6.76, 6.92, 7.06, 7.20, and 7.40, only Y = 7.20 yielded constant ion products for experiments 1-12 which also included no. 13 and 14. In the other trials the products either were inconstant or passed through a maximum, with no. 13 and 14 always much smaller than the preceding values. This is illustrated in part in Table II.

To complete the calculation in Table I, $p[Z] = Y - pH$; $Z/(1 + Z) =$ fraction of the total phosphate as HPO_4^- . All activity coefficients are assigned an arbitrary value of unity in the standard solvent of reference, 0.165 *m* NaCl. The mean molality constants at equilibrium are defined in Table II as

$$A = p[m_{\pm}(CaHPO_4)] \text{ and } B = p[m_{\pm}(Ca_2HPO_4 \cdot (OH)_2)] \quad (9)$$

The constancy of A for CaHPO₄, equal to 4.26 ± 0.05, in Table I over the entire range of concentration of added CaCl₂ or Na₂HPO₄ is in accord with the demands of eq. 1 for hydroxylapatite when dissolved in 0.165 *m* NaCl to maintain a constant environment.

It will be noted, however, that the mean molality product B given in Table II is an equally good constant. The differences (B - A) are constant over the range of concentrations studied and for the Y values of 7.20 and 6.92 are nearly identical.

In contrast to A, the value of B is to be interpreted as a *solubility product constant* applicable to the hydroxylapatite-water system, since B refers to the solid surface complex $[Ca(HPO_4)(H_2O)_2]$ which is in solubility equilibrium with the solution.

W. E. Brown and his associates,²¹ in papers which have just come to hand, also re-assess the solubility questions of hydroxylapatite. In none of these papers is any reason given for doubting the applicability of the solubility product principle, despite complications that exist for hydroxylapatite.

Conclusions

The solubility data for hydroxylapatite in aqueous media exhibit many paradoxical behaviors which have defied simple interpretations on well established classical principles. It is shown that these inexplicable results arise primarily from the failure to recognize that hydroxylapatite, although a very insoluble salt, nevertheless hydrolyzes in water forming a more stable and insoluble surface complex $[\text{Ca}_2\text{HPO}_4(\text{OH})_2]$ and liberating at the same time Ca^{++} and HPO_4^- ions in equal proportions. It is this hydrolysis reaction which dominates the solubility and not hydroxylapatite.

When the solubility data for hydroxylapatite in 0.165 *M* NaCl, as recorded by Levinskas and Neuman, (L. and N.), are recalculated, it is found that the ion molality product for this surface complex is constant over a wide range of CaCl_2 and of Na_2HPO_4 additions, thus confirming the applicability of the solubility product principle for this system.

In addition to neglecting the important influence

(21) E. C. Moreno, W. E. Brown, and G. Osborne, *Soil Sci. Soc. U.S.A. Proc.*, **24**, 94, 99 (1960); *Soil Sci.*, **90**, 51 (1960).

of hydrolysis, the failure of L. and N. to confirm the solubility product principle can be attributed in part to a combination of two further factors; namely (a) improper calculations of individual ion activity coefficients and (b) improperly standardized values of the pH when measured by the use of a glass electrode.

When solubility is measured in a medium of constant ionic environment (0.165 *m* NaCl) it is unnecessary and confusing to complicate the interpretation by attempting to compute such controversial quantities as individual ion activity coefficients, particularly when ions of high valence and opposite signs are present. The theories of "aberrant solubility" advanced by Neuman and Neuman to explain the solubility results of L. and N. not only violate accepted principles of physical and colloid chemistry but likewise become unnecessary.

The ion product $(\text{Ca}^{++})(\text{HPO}_4^-)$ is also constant for this system over a wide range of CaCl_2 and Na_2HPO_4 additions. The constancy of this ion product is a concomitant of the hydrolysis reaction; it does not require that the solution which is saturated in respect to the surface complex also be saturated in respect to solid CaHPO_4 ; in fact it is undersaturated.

Acknowledgment.—The author is indebted to Drs. Victor Deitz and Walter E. Brown for helpful correspondence in the preparation of this paper.

MODELS FOR ISOTOPE RATE EFFECTS IN DISPLACEMENT, DISSOCIATION, ELIMINATION, AND ADDITION REACTIONS¹

BY SIDNEY I. MILLER

Department of Chemistry, Illinois Institute of Technology, Chicago 16, Illinois

Received July 10, 1961

Detailed calculations of isotope rate factors, k/k' , for representative reactions, *e.g.*, dissociation, displacement, elimination, and addition are presented. Various approximations for three-center, reactant-like, product-like, and complete models of the activated complex were tested. At 27°, some results are as follows: for methyl iodide in SN_1 reaction, $k_{12}/k_{13} = 1.05$, $k_{\text{H}}/k_{\text{D}} = 1.53$; for methyl iodide with iodide ion in SN_2 reaction, $k_{12}/k_{13} = 1.17$, $k_{\text{H}}/k_{\text{D}} = 0.70$; for *sym*-tetrachloroethane with iodide in dechlorination (E2), $k_{\text{H}}/k_{\text{D}} \approx 1.6$; for chlorine addition to 1,2-dichloroethene, $k_{\text{H}}/k_{\text{D}} \approx 0.8$. The linear three-center model for an SN_2 activated complex was unsatisfactory for cases in which one of the masses was polyatomic.

Apart from a few reports, models for isotope rate effects, particularly for organic species, have been highly simplified.² For primary isotope effects the simple approach often has been adequate. However, to account for small primary or secondary isotope effects, more complete models of activated complexes are needed. Here it is assumed that the theory of absolute reaction rates is applicable and that the geometry and vibration frequencies³ of each reaction species can be de-

scribed. On this basis we report fairly detailed calculations for the important processes, displacement (SN_2), dissociation (SN_1), halogen elimination (E2), and addition.

Isotope Rate Effects in Model Systems.—The isotope rate factor of the reaction, $\text{A} + \text{B} \rightarrow \text{Products}$, in which species A may have labeled atoms (indicated by primes), may be written

$$\frac{k}{k'} = \frac{\nu_{\text{L}\ddagger} K\ddagger}{\nu_{\text{L}\ddagger'} K\ddagger'} = \frac{Q_{\text{A}'} Q_{\ddagger}}{Q_{\text{A}} Q_{\ddagger'}} \left(\frac{m\ddagger'}{m\ddagger} \right)^{1/2} \quad (1)$$

In the language of absolute reaction rate theory, $\nu_{\text{L}\ddagger}$ is the vibration of the transition state which leads to decomposition and is proportional to $(m\ddagger)^{-1/2}$; $m\ddagger$ is the effective mass along this coordinate; the equilibrium constant $K\ddagger$ and the partition functions are complete. For the calculations, (1) is conveniently used in the equivalent forms^{2,4}

(1) (a) Presented in part at the 130th National Meeting of the American Chemical Society, Atlantic City, N. J., September, 1956.

(b) Related paper: W. G. Lee and S. I. Miller, *J. Phys. Chem.*, **66**, 655 (1962).

(2) L. Melander, "Isotope Effects on Reaction Rates," The Ronald Press Co., New York, N. Y., 1960. Since this volume reviews the field, we shall limit our citations.

(3) (a) E. B. Wilson, J. C. Decius, and P. C. Cross, "Molecular Vibrations," McGraw-Hill Book Co., Inc., New York, N. Y., Chap. 8;

(b) G. Herzberg, "Infrared and Raman Spectra of Polyatomic Molecules," D. Van Nostrand Co., Inc., New York, N. Y., 1945.

$$\ln \frac{k}{k'} = \frac{1}{2} \ln \frac{m^{\pm'}}{m^{\pm}} + \frac{3}{2} \ln \frac{M' M^{\pm}}{M M^{\pm'}} + \frac{1}{2} \ln \frac{I_x' I_y' I_z'}{I_x I_y I_z} \frac{I_x^{\pm} I_y^{\pm} I_z^{\pm}}{I_x^{\pm'} I_y^{\pm'} I_z^{\pm'}} \quad (2a)$$

$$+ \sum_{3n \pm - 6} \left(\frac{\Delta u_i}{2} + \ln \frac{1 - e^{-u_i}}{1 - e^{-u_i'}} \right) - \sum_{3n \pm - 6} \left(\frac{\Delta u_i^{\pm}}{2} + \ln \frac{1 - e^{-u_i^{\pm}}}{1 - e^{-u_i^{\pm'}}} \right)$$

$$\ln \frac{k}{k'} = \frac{1}{2} \ln \frac{m^{\pm'}}{m^{\pm}} + \sum_{3n \pm - 6} \left(\frac{\Delta u_i}{2} - \ln \frac{u_i'(1 - e^{-u_i})}{u_i(1 - e^{-u_i'})} \right) - \sum_{3n \pm - 6} \left(\frac{\Delta u_i^{\pm}}{2} + \ln \frac{u_i^{\pm'}(1 - e^{-u_i^{\pm}})}{u_i^{\pm}(1 - e^{-u_i^{\pm'}})} \right) \quad (2b)$$

M = molecular weight; $I_x I_y I_z$ = product of the principal moments of inertia; $u = h\nu/kT$; ν = fundamental frequency; $\Delta u = u - u'$. One term in eq. 2, the one assumed to be most involved in the reaction coordinate, that is

$$\frac{\Delta u_i^{\pm}}{2} + \ln \frac{u_i^{\pm'}(1 - e^{-u_i^{\pm}})}{u_i^{\pm}(1 - e^{-u_i^{\pm'}})} \quad (3)$$

usually is dropped on the basis that u_i^{\pm} and $u_i^{\pm'}$ are similar and small. For some transition states a multivibrational reaction coordinate seems appropriate and several such terms should be dropped.

To a good approximation, Bigeleisen's succinct $G(u)$ function, in which all terms of eq. 2 but $(m^{\pm}/m^{\pm'})^{1/2}$ are collected, normally gives the same result as (2).⁵ There were several reasons for using (2). First, the moments of inertia and molecular weights had to be found; in any case, they probably can be assigned more accurately than the vibration frequencies. More important, the $G(u)$ function is less reliable for the higher (hydrogenic) frequencies.^{2,5} Finally, it seemed necessary to display for typical processes the "components" of the isotope effect. The temperature independent part of the isotope rate factor, which usually has been identified with $(m^{\pm'}/m^{\pm})^{1/2}$, clearly includes contributions from the molecular weight and moment of inertia ratios as in eq. 2a or from the vibration frequency product $\Pi u_i/u_i'$ as in (2b). In the most approximate calculations of k/k' , all but the zero point energy terms are ignored. It turns out that the contributions of each term of eq. 2 are significant in certain systems.

The evaluation of k/k' from eq. 2 required detailed descriptions of both reactants and transition states. Table I lists the processes that were considered. Note that the reactants are simple molecules and information on them is available. The molecular weight term of (2) offered no problem. In general, the moment of inertia ratios were not very sensitive to small changes in geometry and need not be discussed further. To obtain the vibration frequencies a number of accessible models for transition states were considered. What follows is a review of these models.

(4) V. Gold and D. P. N. Satchell, *Quart. Revs.* (London), **9**, 51 (1955).

(5) J. Bigeleisen and M. Wolfsberg, "Theoretical and Experimental Aspects of Isotope Effects in Chemical Kinetics" in "Advances in Chemical Physics," Vol. I; I. Prigogine, editor, Interscience Publishers, Inc., New York, N. Y., 1958, p. 15; J. Bigeleisen and M. G. Mayer, *J. Chem. Phys.*, **15**, 261 (1947); J. Bigeleisen, *ibid.*, **17**, 675 (1949).

Despite considerable discussion, the method of evaluating $m^{\pm'}/m^{\pm}$ is not clear.^{5,6} In the rupture of a given bond of a polyatomic species, should one use the masses of the bonded atoms or the bonded fragments? For secondary isotope effects the dilemma is immediate. On a "mass of the atoms" approach, isotopic substitution in the fragments cannot lead to an isotope effect in the rate process. On the "mass of the fragments" approach, such isotopic substitution, e.g., D for H, may contribute significantly to m^{\pm} in a relatively light species, e.g., CH₃, or insignificantly in a heavy species, e.g., C₂H₅Br₄. In the calculations, both approaches were used, although the mass of the fragments method was favored. However, it is desirable to obtain m^{\pm} from the potential surface⁷ and this approach also was used where feasible.

The following linear three-center transition state, A⁻¹B⁻²C, has been described.⁸ Using a general quadratic potential function one obtains the relations³

$$\begin{aligned} \lambda_1 + \lambda_2 &= f_1\mu_A + f_2\mu_C + (f_1 + f_2 - 2f_{12})\mu_B \\ \lambda_1\lambda_2 &= (f_1f_2 - f_{12}^2)(\mu_A\mu_B + \mu_A\mu_C + \mu_B\mu_C) \\ \lambda_3 &= (\mu_B/d_1^2 + \mu_B(1/d_1 + 1/d_2)^2 + \mu_C/d_2^2)d_{12}^2f_\phi \end{aligned} \quad (4)$$

in which $\lambda = 4\pi\nu^2$; $\lambda_1, \lambda_2,$ and λ_3 are the symmetric, unsymmetric, and doubly degenerate modes, respectively; ν = vibration frequency; f = force constant, ϕ = bond angle; d = bond distance, $d_{12}^2 = d_1d_2$; μ = reduced mass, $\mu_A = 1/M_A$, etc. In order to make λ_2 small (zero) and have it correspond to the bond breaking mode, $f_1f_2 \approx f_{12}^2$ is assumed.⁸ Provided force constants and a geometry of the transition state are assumed, λ_1 and λ_3 can be calculated. Now

$$\lambda_2/\lambda_2' = (\nu_2/\nu_2')^2 = m^{\pm'}/m^{\pm} \quad (5)$$

so that

$$\frac{m^{\pm'}}{m^{\pm}} = \frac{\lambda_1'(\mu_A\mu_B + \mu_A\mu_C + \mu_B\mu_C)}{\lambda_1(\mu_A'\mu_B' + \mu_A'\mu_C' + \mu_B'\mu_C')} \quad (6)$$

For the linear species A-B-A the corresponding expressions are

$$\lambda_1 = (f_1 + f_{12})\mu_A \quad \lambda_2 = (f_1 - f_{12})(\mu_A + 2\mu_B) \quad \lambda_3 = 2f_\phi(\mu_A + 2\mu_B) \quad (7)$$

$$m^{\pm'}/m^{\pm} = (\mu_A + 2\mu_B)/(\mu_A' + 2\mu_B') \quad (8)$$

To the extent that the three-center model of the activated complex is valid, this is a consistent and rigorous approach to $m^{\pm'}/m^{\pm}$.

In a second "complete" model of the activated state, vibration frequencies were assigned to the activated state by analogy with similar molecules. For example, the activated complex I...CH₃...I was assumed to be a bipyramid with the carbon-iodide bonds perpendicular to the plane of the hydrogen atoms. The symmetry (D_{3h}) modes of vibration and symmetry coordinates of such a species have been discussed by Ziomek.⁹ Molecules such as methyl iodide, methylene iodide, vinyl iodide, diiodoethene, methane, ethylene, etc., as

(6) (a) P. E. Yankwich and R. M. Ikeda, *J. Am. Chem. Soc.*, **82**, 1891 (1960); **81**, 1532 (1959); (b) K. R. Lynn and P. E. Yankwich, *ibid.*, **83**, 53 (1961).

(7) M. Wolfsberg, *J. Chem. Phys.*, **33**, 21 (1960).

(8) (a) D. R. Herschbach, H. S. Johnston, K. S. Pitzer, and R. E. Powell, *J. Chem. Phys.*, **25**, 736 (1956); (b) F. Westheimer, *Chem. Revs.*, **61**, 265 (1961).

(9) J. S. Ziomek, *J. Chem. Phys.*, **22**, 1001 (1954).

well as the three-center models provided a basis for the choice of vibration frequencies. Several small and fairly obvious adjustments in a few of the frequencies could raise or lower k/k' . In all cases, internal consistency in the assignments to isotopically labeled species was imposed by the Teller-Redlich product rule.³

In the third or "product" model, an activated state was identified with an immediate product. For example, the dissociation of methyl iodide was assumed to give either a planar or pyramidal methyl carbonium ion and frequencies were assigned accordingly; instead of the usual one, three frequencies have been dropped from the activated complex. In the elimination reactions of the tetrachloro- and tetrabromoethanes, the *trans*-dihaloethenes were taken to be activated complexes. In going to these complexes, the reactant "loses" six vibrations. The foregoing models are "product-like" and almost complete.

Finally, a "reactant-like" activated complex was tested. By comparing the kinds of vibration frequencies, *e.g.*, stretching, bonding, etc., in related symmetry classes, one can find those in the reactant missing in the product, or *vice versa*. These "disappearing" frequencies can be used to obtain an isotope rate factor if all of the other frequencies are assumed to cancel between reactant and activated complex. Such a model was used in the dissociation of methyl iodide and in the dehalogenation of the tetrahaloethanes. Thus, $\nu_2(a_g)$, $\nu_7(b_g)$, $\nu_8(b_g)$, $\nu_{12}(a_u)$, $\nu_{13}(a_u)$, and $\nu_{14}(b_u)$ of the reactant, *trans*-tetrabromoethane, are absent in the product, *trans*-dibromoethene.¹⁰

Analogous models of transition states have been used fairly successfully in a variety of systems, for example, the association of ammonia and boron trifluoride,¹¹ the acid cleavage of $\text{CH}_3\text{OCH}_2\text{CH}_2\text{HgI}$,¹² and the reduction of sulfate to sulfide.¹³

Calculations

In this section are presented the essential data on which the calculations are based. The results of these calculations are given in Table I. Each process is numbered so as to correspond with the entries in the table where the reactants and transition states are indicated. The processes were dissociation (SN1) 1-4, displacement (SN2) 5-10, and elimination (E2) 11-14. For each assumed model the terms in eq. 2 as well as the over-all k/k' are listed individually. Only deuterium and carbon 13 isotope substitutions were considered.

The following were used: r , bond length in Å (angstrom); \angle , bond angle in degrees; I , principal moment of inertia in amu. Å.²; ν , in cm.⁻¹; all force constants in md./Å. To conserve space, the units have been omitted from the text and ν^\pm have been given simply as ν . The one or more frequencies

along the reaction coordinate involved in terms such as eq. 3 will be indicated as "dropped."

1. SN1.—A single frequency, ν_3 of methyl iodide,¹⁴ drops from the "diatomic" or two-center model to give the activated complex. Incidentally, $(\mu'/\mu)^{1/2} \approx \nu_3/\nu_3'$.

2. SN1.—The vibrational assignments of methyl iodide were taken from the literature^{14a}—the more recent assignments would not affect our results appreciably.^{14b} Moments of inertia for methyl iodide were calculated for a tetrahedral molecule with r_{CH} 1.09 and r_{CI} 2.10. These also will be used in models 3 and 4. In this model, all frequencies but ν_3 and $\nu_6(e)$ are assumed to cancel between methyl iodide and the transition state. Further, the vibration product terms as determined in eq. 2 differ grossly from the more plausible values in model 4.

3. SN1.—In this model the molecular weight and moment of inertia ratios were taken from model 4. The activated complexes were otherwise identical with possible products, *e.g.*, methylcarbonium ions. Thus, three vibrations ν_3 and $\nu_6(e)$ of methyl iodide are dropped in the complex. For pyramidal methyl, $\angle \text{HCH}$ 109°28', r_{CH} 1.09; for $\text{C}^{12}\text{H}_3^+$, $I_x = I_y = 1.9155$, $I_z = 3.1931$, ν_1 3020, ν_2 949, $\nu_3(e)$ 3062, $\nu_4(e)$ 1526; for C^{13}H_3 , $I_x = I_y = 1.9205$, $I_z = 3.1931$, ν_1 3010, ν_2 945, $\nu_3(e)$ 3052, $\nu_4(e)$ 1520; for CD_3 , $I_x = I_y = 3.7219$, $I_z = 6.382$, ν_1 2258, ν_2 720, $\nu_3(e)$ 2285, $\nu_4(e)$ 1054. For planar methyl, $\angle \text{HCH}$ 120, r_{CH} 1.07; for $\text{C}^{12}\text{H}_3^+$, $I_x = I_y = 1.731$, $I_z = 3.462$, ν_1 3019, ν_2 949, $\nu_3(e)$ 3106, $\nu_4(e)$ 1444; for $\text{C}^{13}\text{H}_3^+$, $I_x = I_y = 1.731$, $I_z = 3.462$, ν_1 3019, ν_2 945, $\nu_3(e)$ 3096, $\nu_4(e)$ 1438; for CD_3 , $I_x = I_y = 3.4599$, $I_z = 6.9198$, ν_1 2130, ν_2 720, $\nu_3(e)$ 2345, $\nu_4(e)$ 1078.

4. SN1.—The complete activated complex, $\text{H}_3\text{C} \cdots \text{I}$, had $\angle \text{HCH}$ 115, r_{CH} 1.08, r_{CI} 2.4 with ν_3 dropped; for $\text{H}_3\text{C}^{12} \cdots \text{I}$, $I_x = I_y = 80.108$, $I_z = 2.5018$, ν_1 2995, ν_2 1150, $\nu_4(e)$ 3062, $\nu_5(e)$ 1482, $\nu_6(e)$ 441; for $\text{H}_3\text{C}^{13} \cdots \text{I}$, $I_x = I_y = 85.00$, $I_z = 3.5018$, ν_1 2985, ν_2 1140, $\nu_4(e)$ 3052, $\nu_5(e)$ 1476, $\nu_6(e)$ 440; for $\text{D}_3\text{C} \cdots \text{I}$, $I_x = I_y = 97.02$, $I_z = 6.999$, ν_1 2196, ν_2 837, $\nu_4(e)$ 2285, $\nu_5(e)$ 1065, $\nu_6(e)$ 332.

5. SN2.—This involves a diatomic reactant CI and a linear transition state, $\text{I} \cdots \text{C} \cdots \text{I}$, with r_{CI} 2.4, f_1 1.9, f_2 0.1, ν_1 225.5, and ν_2 dropped. For $\text{I} \cdots \text{C}^{12} \cdots \text{I}$, $\nu_3(e)$ 101.4; for $\text{I} \cdots \text{C}^{13} \cdots \text{I}$, $\nu_3(e)$ 97.6.

6. SN2.—This differed from model 5 only insofar as the different central mass led to different ν_3 frequencies. For $\text{I} \cdots \text{C}^{12}\text{H}_3 \cdots \text{I}$, $\nu_3(e)$ 91.1; for $\text{I} \cdots \text{C}^{13}\text{H}_3 \cdots \text{I}$, $\nu_3(e)$ 88.3; for $\text{I} \cdots \text{C}^{12}\text{D}_3 \cdots \text{I}$, ν_3 83.6.

7. SN2.—For the bipyramid, $\text{I} \cdots (\text{CH}_3) \cdots \text{I} < \text{HCH}$ 120, $\angle \text{ICH}$ 90, CH 1.07, r_{CI} 2.3; for $\text{I} \cdots \text{C}^{12}\text{H}_3 \cdots \text{I}$, $I_x = I_y = 1344.4$, $I_z = 3.462$, ν_1 3030, ν_2 529, ν_4 1351, $\nu_5(e)$ 3272, $\nu_6(e)$ 1444, $\nu_7(e)$ 1105, $\nu_8(e)$ 716; for $\text{I} \cdots \text{C}^{13}\text{H}_3 \cdots \text{I}$, $I_x = I_y = 1344.4$, $I_z = 3.462$, ν_1 3030, ν_2 529, ν_4 1346, $\nu_5(e)$ 3261, $\nu_6(e)$ 1439, $\nu_7(e)$ 1101, $\nu_8(e)$ 716; for $\text{I} \cdots \text{CD}_3 \cdots \text{I}$, $I_x = I_y = 1346.2$, $I_z = 6.9198$, ν_1 2254, ν_2 500, ν_4 1015, $\nu_5(e)$ 2304, $\nu_6(e)$ 1175, $\nu_7(e)$ 955, $\nu_8(e)$ 507.

(14) (a) R. B. Bernstein, F. F. Cleveland, and F. L. Volz, *J. Chem. Phys.*, **22**, 193 (1954); P. F. Fenlon, F. F. Cleveland, and A. G. Meister, *ibid.*, **19**, 1561 (1951); (b) W. T. King, I. M. Mills, and B. Crawford, *ibid.*, **27**, 455 (1957).

(10) (a) E. A. Piotrowski, S. Sundaram, F. F. Cleveland, and S. I. Miller unpublished data on the *sym*-tetrabromoethanes; (b) J. M. Dowling, P. G. Puranik, A. G. Meister, and S. I. Miller, *J. Chem. Phys.*, **26**, 233 (1957).

(11) G. B. Kistiakowsky and C. E. Klots, *ibid.*, **34**, 712 (1961).

(12) M. M. Kreevoy and L. T. Ditsch, *J. Am. Chem. Soc.*, **82**, 6127 (1960).

(13) A. G. Harrison and H. G. Thode, *Trans. Faraday Soc.*, **53**, 1648 (1957).

Only ν_3 was dropped. In activated complexes of 7b, the two degenerate vibrations ν_7 and ν_8 were changed in the three species to 716 and 530, 714 and 530, 622 and 375, respectively.

8a. SN2.—This was a linear mass of the fragments model of the transition state with $r_{\text{CI}} 2.4$, $r_{\text{CO}} 1.7$, $f_{\text{CI}} 1.9$, $f_{\text{CO}} 3.0$, $f_{\phi} 0.3$ and with ν_2 dropped. For $\text{H}_2\text{O} \cdots \text{C}^{12}\text{H}_3 \cdots \text{I}$, $\nu_1 568$, $\nu_3(\text{e}) 427$; for $\text{H}_2\text{O} \cdots \text{C}^{13}\text{H}_3 \cdots \text{I}$, $\nu_1 567$, $\nu_3(\text{e}) 417$; for $\text{H}_2\text{O} \cdots \text{C}^{12}\text{D}_3 \cdots \text{I}$, $\nu_1 566$, $\nu_2(\text{e}) 399$.

8b. SN2.—This was similar to 8a except for two force constants $f_{\text{CO}} 4$ and $f_{\phi} 0.5$. The frequencies changed as follows: in $\text{H}_2\text{O} \cdots \text{C}^{12}\text{H}_3 \cdots \text{I}$, $\nu_1 668$, $\nu_3(\text{e}) 551$; in $\text{H}_2\text{O} \cdots \text{C}^{13}\text{H}_3 \cdots \text{I}$, $\nu_1 666$, $\nu_3(\text{e}) 538$, in $\text{H}_2\text{O} \cdots \text{C}^{12}\text{D}_3 \cdots \text{I}$, $\nu_1 662$, $\nu_3 515$.

9. SN2.—The transition state here is analogous to that of model 5. For $\text{I} \cdots \text{CH}_3 \cdots \text{Br}$, $r_{\text{CI}} 2.4$, $r_{\text{CBR}} 2.0$, $f_{\text{CI}} 1.9$, $f_{\text{CBR}} 2.2$, $f_{\phi} 0.1$. The frequencies of the reactant were $\nu_3 = 611$ from CH_3Br and $\nu_3 = 578$ from CD_3Br .¹⁵ The frequencies of $\text{I} \cdots \text{CH}_3 \cdots \text{Br}$ were $\nu_1 271$ and $\nu_3(\text{e}) 222$ and of $\text{I} \cdots \text{CD}_3 \cdots \text{Br}$ were $\nu_1 270$ and $\nu_3(\text{e}) 204$.

10. SN2.—This process is analogous to that in 9. Because of the large central mass, the three-center treatment does not lead to significant shifts in the frequencies of isotopic species of $\text{I} \cdots (\text{Br}_2\text{CHCHBr}) \cdots \text{Br}$. The frequencies of the reactant were 586 from $\text{C}_2\text{H}_2\text{Br}_4$ and 569 from $\text{C}_2\text{D}_2\text{Br}_4$.^{10a}

11. 12. E2.—Because of the complexity of the reaction coordinate, we were unable to assign a value to the effective mass ratio other than unity. Superficially, at least, the E2 process $\text{I} \cdots \text{Cl} \cdots \text{C} \cdots \text{C} \cdots \text{Cl}$ involves no isotopic substitution. The vibration frequencies of *sym*-tetrachloroethane (the *trans*-rotomer) and of *trans*-dichloroethene generally were available¹⁶; however, we estimated $\nu_8 116$, $\nu_{10} 91$ for tetrachloroethane, and $\nu_2 1265$, $\nu_7 966$, $\nu_8 738$, $\nu_9 114$, $\nu_{10} 88$, $\nu_{14} 2233$, $\nu_{15} 965$, $\nu_{16} 688$, $\nu_{17} 349$, and $\nu_{18} 288$ for the corresponding deuterium compound. For 11, the 18 frequencies of reactant and 12 frequencies of the activated complex (actually the product) were used in eq. 2b. For 12, six disappearing frequencies of tetrachloroethane, ν_2 , ν_7 , ν_9 , ν_{12} , and ν_{14} were used in eq. 2b; ν_{13} , the unobserved twisting frequency, was assumed to cancel in the reactants and the other frequencies were assumed to cancel between reactant and activated complex.

13. 14. E2.—The treatment is the same as 11 and 12. The *trans* reactant *sym*-tetrabromoethane and product *trans*-dibromoethene frequencies are known.¹⁰

Discussion

Where possible, the results as summarized in Table I will be compared with literature reports. In several cases such data were unavailable, in others it was not clear whether the data applied to comparable processes. What will be emphasized here is a set of predictions of k/k' for several important reaction types. Some "reasonable"

models fail. Whether the remaining models are adequately valid or useful must be judged by the results.

Processes 1–4 are for heterolytic (SN1) processes of methyl iodide in a polar medium. However, it is believed that similar k/k' values would apply to homolytic cleavage. The effect of a polar medium, e.g., water, in solvation or as an attacking nucleophile probably would reduce k/k' as is implied in process 8. Bender and Hoeg report $k_{12}/k_{14} = 1.09$ at 25° for the silver ion promoted dissociation of methyl iodide¹⁷; presumably, $k_{12}/k_{13} \approx 1.045$. Reports on the solvolysis of several alkylsulfonates^{18–20} indicate $k_{\text{H}}/k_{\text{D}} = 1.10 - 1.20$ or 10–20% per α -deuterium substitution. Klemm and Bernstein report $k_{12}/k_{13} = 1.010$ for the pyrolysis of methyl iodide at 486°.²¹

Although the two-center model for the SN1 activated complex makes fair predictions of k/k' , these are surely fortuitous. Models 2 and 3 exaggerate $k_{\text{H}}/k_{\text{D}}$. However, the agreement between the complete model 4 of the SN1 activated complex and the reported data is good. Model 4 was an outgrowth of models 2 and 3 and their relationship is instructive. It is sufficient to point out here that along with ν_3 of methyl iodide, the degenerate ν_6 bendings contributed significantly to k/k' . The importance of bending contributions in such systems has been pointed out by Streitwieser, et al.¹⁸

Processes 5–7b are displacements (SN2). For the reactions of hydroxide ion, triethylamine, and pyridine with methyl iodide at 25°, $k_{12}/k_{14} = 1.09$, 1.10, and 1.14, respectively¹⁷; presumably, $k_{12}/k_{13} \approx 1.06$. For the reactions of hydroxide and cyanide with methyl iodide at 31°, $k_{12}/k_{13} = 1.035$ and 1.074.⁶ The attack of water on the methyl halides gives $k_{\text{H}}/k_{\text{D}} = 0.90$ at ca. 80° or ca. 0.96 per α -hydrogen.²² The reaction of methanol or methoxide ion with methyl *p*-bromobenzenesulfonate gives $k_{\text{H}}/k_{\text{D}}$ in this range.²⁰ In short, the literature data require $k_{12}/k_{13} > 1$ and $k_{\text{H}}/k_{\text{D}} < 1$ for the displacement reaction. (For the sake of comparison, it is assumed that the nucleophiles iodide, cyanide, water, etc., will give similar $k_{\text{H}}/k_{\text{D}}$.) By an appropriate blend of the ideal SN1 and SN2 models, it should be possible to approximate intermediate characteristics of the activated complex. For example, the substitution reactions of 2-bromopropane²³ with ethoxide ion at 25° and *n*-propyl iodide^{22a} with water at 90° have $k_{\text{H}}/k_{\text{D}} \approx 1.00$.

The three-center mass of the atoms model (5) can be discarded because it inevitably gives $k_{\text{H}}/k_{\text{D}} = 1$. Clearly, models 6 and 7a bracket k/k' : in 6,

(17) M. L. Bender and D. F. Hoeg, *J. Am. Chem. Soc.*, **79**, 5649 (1957); M. L. Bender and G. J. Buist, *ibid.*, **80**, 4304 (1958).

(18) A. Streitwieser, R. H. Jagow, R. C. Fabey, and S. Suzuki, *ibid.*, **80**, 2326 (1958).

(19) (a) K. Mislav, S. Borčić, and V. Prelog, *Helv. Chim. Acta*, **40**, 2477 (1957); (b) W. H. Saunders, S. Asperger, and D. H. Edison, *J. Am. Chem. Soc.*, **80**, 2421 (1958).

(20) R. R. Johnson and E. S. Lewis, *Proc. Chem. Soc.*, 52 (1958).

(21) R. F. Klemm and R. B. Bernstein, *J. Am. Chem. Soc.*, **82**, 5987 (1960).

(22) (a) K. T. Lefek, J. A. Llewellyn, and R. E. Robertson, *ibid.*, **82**, 6315 (1960); (b) *Can. J. Chem.*, **38**, 1505 (1960); (c) J. A. Llewellyn, R. E. Robertson, and J. M. W. Scott, *ibid.*, **38**, 222 (1960).

(23) V. J. Shiner, *J. Am. Chem. Soc.*, **74**, 5285 (1952).

(15) H. B. Weissman, R. B. Bernstein, S. E. Rosser, A. G. Meister, and F. F. Cleveland, *J. Chem. Phys.*, **23**, 544 (1955).

(16) (a) J. P. Zietlow, F. F. Cleveland, and A. G. Meister, *ibid.*, **24**, 142 (1956); (b) K. S. Pitzer and J. L. Hollenberg, *J. Am. Chem. Soc.*, **76**, 1493 (1954); H. J. Bernstein and D. A. Ramsay, *J. Chem. Phys.*, **17**, 556 (1949).

TABLE I
 CALCULATED ISOTOPE RATE FACTORS FOR MODELS OF ACTIVATED COMPLEXES

No. ^a	Process ^b	Model ^c	$(m' \pm / m \mp)^{1/2}$	$\prod \mu_i' / \mu_i \mp$	$\ln(1 - e^{-u_i})^e$	ZPE ^f	k_{12}/k_{13}^g	k_H/k_D^h
1	$H_3CI \rightarrow (H_3C) \dots I$	Two	1.029	0.9679	1.007	1.042	1.045	
			1.080	0.9319	1.016	1.090		1.116
2	$H_3CI \rightarrow CH_3^+ + I^-$	Reactant	1.029	0.9602	1.009	1.059	1.056	
			1.080	0.5292	1.074	3.093		1.90
3a	$H_3CI \rightarrow \text{pyramidal-}CH_3^+ + I^-$	Product	1.029	0.9897	1.008	1.052	1.080	
			1.080	1.035	1.058	2.670		3.16
3b	$H_3CI \rightarrow \text{planar-}CH_3^+ + I^-$	Product	1.029	0.9897	1.008	1.078	1.106	
			1.080	1.035	1.060	3.532		4.19
4	$H_3CI \rightarrow H_3C \dots I$	Complete	1.029	0.9897	1.007	1.032	1.058	
			1.080	1.035	1.553	0.8752		1.521
5	$I^- + CI \rightarrow I \dots C \dots I^-$	Three	1.039	1.045	0.9490	1.023	1.054	
			1.000	1.000	1.000	1.000		1.00
6	$I^- + H_3CI \rightarrow I \dots (CH_3) \dots I^-$	Three	1.031	1.028	0.9583	1.028	1.044	
			1.089	1.107	0.8858	1.052		1.123
7a	$I^- + H_3CI \rightarrow I \dots (CH_3) \dots I^-$	Complete	1.031	1.055	1.008	1.083	1.188	
			1.089	1.252	0.9380	0.3515		0.456
7b		Complete	1.031	1.055	1.003	1.032	1.125	
			1.089	1.252	0.8425	0.603		0.703
8a	$H_2O + H_3CI \rightarrow (H_2O) \dots (CH_3) \dots I$	Three	1.028	1.018	0.9922	0.9895	1.027	
			1.082	1.073	0.9724	0.947		1.069
8b			1.026	1.019	0.9965	0.9723	1.014	
			1.077	1.077	0.9859	0.9032		1.033
9	$I^- + H_3CBr \rightarrow I \dots (CH_3) \dots Br^-$	Three	1.087	1.120	0.9181	0.9933		1.11
10	$I^- + Br_2CHCHBr_2 \rightarrow$ $I \dots (Br_2CHCHBr) \dots Br^-$	Three	1.00	0.971	1.005	1.037	1.012	
11	$I^- + \text{trans-}Cl_2CHCHCl_2 \rightarrow$ $I \dots Cl \dots (CHClCHCl) \dots Cl^-$	Product	1.00	0.829	1.040	1.356	1.17	
			1.00	0.829	1.046	1.256		1.08 ^t
12		Reactant	1.00	0.609	1.047	3.419	2.18	
			1.00	0.609	1.056	2.502		1.61 ⁱ
13	$I^- + \text{trans-}Br_2CHCHBr_2 \rightarrow$ $I \dots Br \dots (CHBrCHBr) \dots Br$	Product	1.00	0.539	1.328	1.302	0.93 ^j	
14		Reactant	1.00	0.623	1.049	2.682	1.75 ^j	

^a See Calculations section for a detailed description. ^b The activated complex but not the products is indicated. Parentheses enclose fragment masses. The temperature is 27° unless otherwise noted. ^c Two-center, product-like, reactant-like, and complete models of activated complexes are indicated. ^d This is the term $\prod_{3n-6} \mu_i' / \mu_i / \prod_{3n \mp -6} \mu_i \mp / \mu_i \mp$. ^e This includes all terms of this form. ^f Zero point energy term $e^{\Delta \mu_i / 2} / e^{\Delta \mu_i / 2}$. ^g k/k' for carbon 12 vs. carbon 13. ^h k/k' for hydrogen vs. deuterium substitution. ⁱ 127°. ^j 81°.

k_{12}/k_{13} is low and k_H/k_D is high; in 7a, k_{12}/k_{13} is high and k_H/k_D is low. Model 6 is a fairly inflexible three-center model. 7a is the better model because it is complete and allows adjustment. This has been done in the complete model 7b in which agreement with the experimental data is much improved.²²

In a formal sense models 6, 8, 9, and 10 are simply three-center systems in which variations in the mass and the force constants have been tested. Compared to 6 and 9, 8 shows the effect of an increased force constant and a decreased mass in an end fragment. In 10, there is the effect of a large central mass in which the deuterium is swamped. Of these processes, 8, the attack by water (or hydroxide) on methyl iodide, is most readily compared with experiment.^{6,17,22} In order to change the calculated values of k/k' , adjustment of the bending constant f_ϕ is most effective. In 8b, the upper reasonable limits of the range in the force constants appears to have been reached

but the experimental k/k' were not generated. Worse still, k_{12}/k_{13} and k_H/k_D were shifted from 8a to 8b in parallel fashion: the experimental results require that k_{12}/k_{13} be increased and k_H/k_D decreased.^{6,17,22} We conclude, therefore, that the three-center model is insufficiently flexible or subtle when one of the fragments is polyatomic.

Processes 11–14 are *trans*-eliminations (E2). The secondary isotope effect $k_H/k_D = 1.06$ in the dehydrobromination of 2-bromopropane with ethoxide ion at 25°²³ and $k_H/k_D = 1.06$ at 25° in the deoxymercuration of β -methoxyethylmercuric iodide¹² are related processes. The iodide-promoted debromination of tetrabromoethane apparently is an elimination reaction: $k_H/k_D = 1.28$ at 81–111° and has a negative temperature coefficient.^{1b}

In 11–14 there is an element effect on k/k' between the chloro and bromo compounds. Since six vibrational modes weigh heavily in the assumed models, it is probable that the change in k/k' results from a cumulative effect of moderate shifts in sev-

eral frequencies. Such a variation in the secondary isotope rate factor in E2 reactions has yet to be tested experimentally. Between product-like 11 and 13 and reactant-like 12 and 14 must lie estimates of, say, *ca.* 1.4 at 100° and *ca.* 1.3 at 81° for the chloro and bromo compounds, respectively. A negative temperature coefficient in k_H/k_D is predicted. It is fortuitous that these results check the available data for tetrabromoethane.^{1b} Though detailed, these models for E2 reactions are still crude and only moderately successful. Further refinement clearly is necessary.

The reverse processes to 11–14 are halogen additions for which k/k' would be inverse to those given. That is, for debromination, k_H/k_D is predicted to be *ca.* 1.3 and for bromine addition *ca.* 0.77 at 81°. This agrees generally with the report on the bromine addition to stilbene at -78° for which $k_H/k_D = 0.87$.²⁴

In summary, the results in Table I may be re-

(24) D. B. Denney and N. Tunkel, *Chem. & Ind. (London)*, 1383 (1959).

garded as an exercise in the adjustment of theoretical models of activated complexes to experimental data. Of course, this adjustment generally is possible because the disposable parameters are many. Even so, the linear three-center model failed when the fragments were polyatomic and should be discarded in these cases. However, extensive experimental data, the Teller-Redli rule, the use of k_{12}/k_{13} as well as k_H/k_D isotope effects, and the temperature coefficient of k/k' tend to narrow the choice of a model and give it some validity. It also is clear that all four terms of (2) may be important in assessing k/k' ; some of these have more often than not been ignored. Finally, the use of the results in Table I in making mechanistic distinctions^{9a} or even in planning a mechanism study, *e.g.*, hydrogen *vs.* carbon isotopic substitution, should be evident.

Acknowledgment.—We wish to thank Prof. R. B. Bernstein for several helpful discussions and Dr. W. G. Lee for doing the calculations on models 13 and 14.

THE MECHANISM OF THE EXTRACTION OF SEVERAL PROTON ACIDS BY TRI-*n*-BUTYL PHOSPHATE

BY KEIJI NAITO AND TOSHIO SUZUKI¹

Japan Atomic Energy Research Institute, Tokai, Ibaraki-ken, Japan

Received July 18, 1961

The distribution equilibria of several proton acids (HNO₃, HCl, HClO₄, HOAc, H₂SO₄, H₂C₂O₄, H₃PO₄) between aqueous and TBP phases were measured. The mechanism of extraction of these acids was confirmed as a reaction between acid ions and TBP molecules, and the formation of the complexes, HNO₃·TBP, HNO₃(TBP)₂, HCl·TBP, HCl(TBP)₃, HClO₄(TBP)₃, HOAc·TBP, and H₂C₂O₄(TBP)₂, was confirmed. The order among the extractabilities of these acids suggests that the extractability may be correlated with the hydration energy of the anion.

Introduction

The extraction of mineral acids by TBP (tri-*n*-butyl phosphate) already has been the subject of investigations by a few workers. Alcock, *et al.*,¹ Peppard, *et al.*,² Tuck,³ and Naito⁴ have made detailed studies of the extraction of nitric acid, and the formation of the complex HNO₃·TBP was confirmed. Pagel, *et al.*,⁵ Peppard, *et al.*,² and Baldwin, *et al.*,⁶ studied the extraction of hydrochloric acid by TBP. Recently Hesford, *et al.*,⁷ have reported new results on the extraction of HCl, HNO₃, H₂SO₄, HClO₄, and HF by TBP, and concluded the formation of HCl·TBP, HNO₃·TBP, H₂SO₄·TBP, and HClO₄·TBP. Kertes⁸ also has made a detailed study on the system of HCl-H₂O-TBP, and concluded the formation of the two species: [(TBP)₂HCl(H₂O)₆] at lower acid concentration and [TBP(HCl(H₂O)₃] at higher acid concentration.

The present authors⁹ worked on the TBP extractions of HNO₃, HCl, HClO₄, HOAc, H₂SO₄, and H₃PO₄ independently from the work of Hesford, *et al.* This paper presents the results of the work in comparison with those of previous workers.

Experimental

Reagents.—The TBP was purified by refluxing with 0.5% aqueous sodium hydroxide according to the method shown by Alcock, *et al.*¹ The other reagents used were all of A. R. grade.

Equipment and Method.—The measurements of distribution equilibrium always were made at constant temperature of 25° using a thermostated water-bath controlled to within ±0.1°. The centrifuge tubes containing the sample solution were shaken in the water-bath for about 4 hr. Then, the two phases were separated by a centrifuge. The samples for analysis were taken from each phase.

The concentration of acids was determined by titration using an auto-titrator equipped with a glass electrode. For the samples of low acid content of HCl, HClO₄, or H₃PO₄, the neutron activation method also was employed, and the samples were irradiated in the JRR-1 Reactor. In the case of HCl and HClO₄ samples, the γ -peak height of ³⁸Cl at 1.60 Mev. was compared with that of a standard sample by using the 256-channel pulse height analyzer. In the case of H₃PO₄ samples, the β -activity of ³²P ($\beta_{max} = 1.707$ Mev.) was measured by the gas flow type 2π counter. The calibration curves obtained for both cases showed very good linearity.

- (1) K. Alcock, *et al.*, *Trans. Faraday Soc.*, **52**, 39 (1956).
- (2) D. F. Peppard, *et al.*, *J. Inorg. & Nuclear Chem.*, **3**, 215 (1956).
- (3) D. G. Tuck, *J. Chem. Soc.*, 2783 (1958).
- (4) K. Naito, *Bull. Chem. Soc. Japan*, **33**, 363 (1960); **33**, 894 (1960).
- (5) H. A. Pagel, *et al.*, *Anal. Chem.*, **21**, 1150 (1949).
- (6) W. H. Baldwin, *et al.*, *J. Phys. Chem.*, **63**, 118 (1959).
- (7) E. Hesford and H. A. C. McKay, *J. Inorg. & Nuclear Chem.*, **13**, 156 (1960).
- (8) A. S. Kertes, *ibid.*, **14**, 104 (1960).

(9) K. Naito and T. Suzuki, "The Mechanism of the Extraction of Several Acids by TBP," presented at the Japan Chemical Society meeting, Tokyo, April 5, 1960.

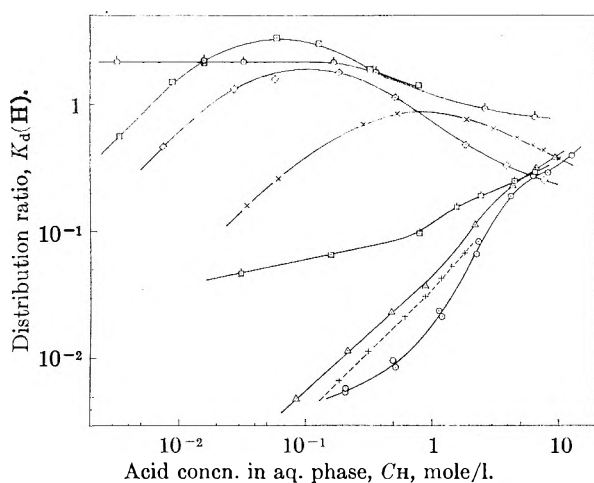


Fig. 1.—Influence of acid concentration upon the distribution ratio at various acid concentrations, TBP 100%, 25°: \square , $\text{H}_2\text{C}_2\text{O}_4$; \circ , HOAc ; \diamond , HClO_4 ; \times , HNO_3 ; \square , H_3PO_4 ; Δ , HCl ; $+$, HCl ; \circ , H_2SO_4 .

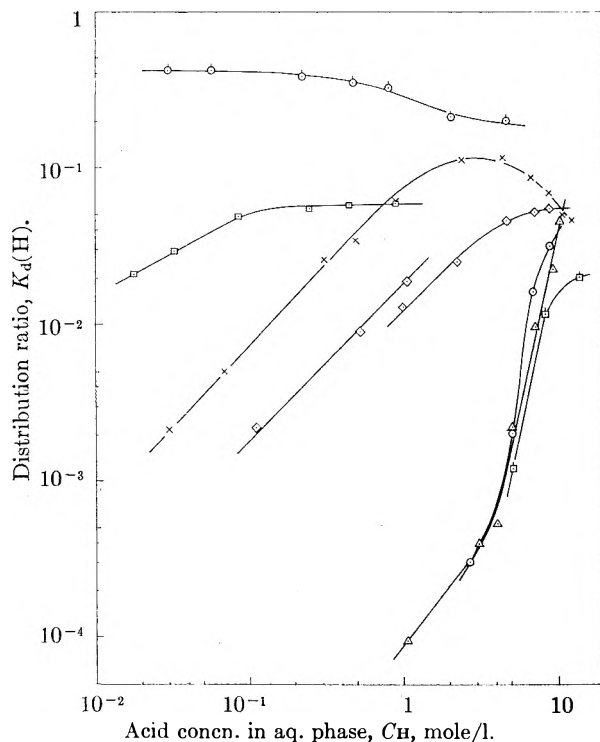


Fig. 2.—Influence of acid concentration upon the distribution ratio at various acid concentrations, TBP 20% (diluted with CCl_4), 25°: \circ , HOAc ; \square , $\text{H}_2\text{C}_2\text{O}_4$; \times , HNO_3 ; \diamond , HClO_4 (straight line, diluent, benzene); \circ , HClO_4 (curved line); \circ , H_2SO_4 ; Δ , HCl ; \square , H_3PO_4 .

The water content of the TBP phase was determined by Karl Fischer titration.

Notation.—The notation used here is

H_mX = protic acid (H^+ = proton, X^{m-} = anion)

C_H and C_X = the equilibrium total concn. in aqueous phase of H and X

f_{\pm} = mean activity coefficient in aqueous phase of the acid H_mX

α_H = degree of dissociation of the acid

K_d = distribution ratio (= total concn. in organic phase / total concn. in aqueous phase)

Results and Discussion

Distribution Equilibrium.—The measurement of the distribution ratio, K_d , of these acids was made

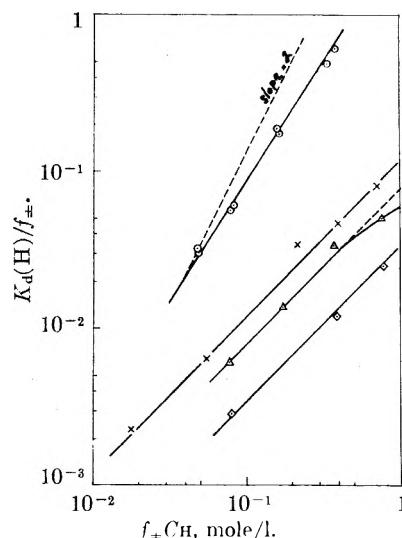


Fig. 3.—Determination of μ in case the salting agent is absent, 25°: \circ , H_2SO_4 (TBP 100%); \times , HNO_3 (TBP 20% diluted with CCl_4); Δ , HCl (TBP 100%); \diamond , HClO_4 (TBP 20% diluted with benzene).

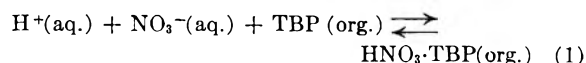
at various acid concentrations. The results obtained are shown in Fig. 1 and 2.

Figure 1 shows the results for the case of TBP used without dilution. In this figure, the dotted line indicates the distribution equilibrium curve of HCl obtained by Pagel, *et al.*,⁵ and it shows that their K_d values are somewhat lower than those of this investigation. The reason for the discrepancy is not clear, though our data were determined by the neutron activation method and theirs by titration. The K_d values of HCl in the high concentration region, however, are in good agreement with the results of previous workers. The K_d values for HNO_3 , HCl , HClO_4 , H_2SO_4 are in good agreement with those of Hesford, *et al.*, except a few points in low concentrations of HClO_4 and H_2SO_4 .

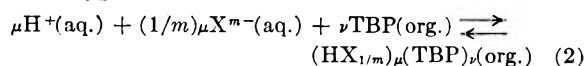
Figure 2 shows the results for 20% (vol.) TBP solution diluted with carbon tetrachloride. In the case where the activation analysis was employed, however, benzene was used instead of carbon tetrachloride as the diluent, because a trace amount of dissolved carbon tetrachloride may cause some inaccuracy in the precise determination of ^{38}Cl .

The behavior of these acids in distribution equilibrium as shown in Fig. 1 and 2 is to be explained from the mechanism of extraction of these acids.

Analysis of the Mechanism of Extraction.—The mechanism of the extraction of nitric acid by TBP has been confirmed as⁴



So, it is expected that the mechanism of the extraction of the other acids also is explained by the same type of reaction as



This mechanism can be confirmed by determining the values of μ and ν as integers without contradiction. The method of analysis has been presented

by this author,⁴ and the outline of this method is shown in the Appendix.

(1) **Determination of μ .**—It is convenient to divide the problem into two cases—strong acids and weak acids.

(a) **The Case of Strong Acids.**—The value of μ of eq. 2 is determined as follows. In the case where there is no salting agent present, the slope obtained by plotting $\log K_d(H)/f_{\pm}$ against $\log (f_{\pm}C_H)$ indicates the value of $(1 + n/m)\mu - 1$ as shown in Appendix eq. ii. Figure 3 shows the result of this analysis. The slopes obtained for HNO₃, HCl, and HClO₄ indicate that $\mu = 1$ for each case. The slope for H₂SO₄ is about 3/2, and then μ is obtained as 5/3. Though it is close to 2, in this case, the value of μ is not an integer. This may be coming from the fact that the measurement is made at the high concentration region (0.5–2.5 M) of H₂SO₄, where the activity of water changes markedly with the change of the acid concentration. Since the complex formed is hydrated, as shown later, the activity of water affects the extraction equilibrium. Accordingly the measurement made at the high concentration region of the acid will not give the exact value of μ . This effect is observed also in the region of higher concentration of HCl.

In the case where the salting agent exists the slope of the curve obtained by plotting $\log K_d(H)$ against $\log C_H$ indicates the value of $\mu - 1$, according to eq. iii of the Appendix. The result obtained is shown in Fig. 4. It is reconfirmed from these curves that $\mu = 1$ for HNO₃, HCl, and HClO₄, and that $\mu = 2$ for H₂SO₄.

(b) **The Case of Weak Acids.**—In the case of weak acids (H₃PO₄, HOAc, and H₂C₂O₄), the analysis also is valid by using the degree of dissociation, α_H , instead of the activity coefficient, f_{\pm} . The value of α_H , however, should be treated as a function of the acid concentration, because it changes sensitively with the change of the acid concentration even at the low concentration region.

In case there is no salting agent present, the following equation is derived, corresponding to eq. ii of the Appendix

$$K_d(H) = \text{const} (\alpha_H)^{(1+1/m)\mu} (C_H)^{(1+1/m)\mu-1} \quad (3)$$

The value of α_H is obtained easily from the dissociation constant, K , as

$$\begin{aligned} \text{when } C_H/K_1 \gg 1: \alpha_H &\approx (K_1/C_H)^{1/2} \\ \text{when } C_H/K &\ll 1: \alpha_H \approx 1 \end{aligned}$$

by neglecting the dissociations of the second and third stages, which are very small compared with that of the first stage. The dissociation constants for acetic, oxalic, and phosphoric acids are given in Table I.

TABLE I

DISSOCIATION CONSTANTS OF WEAK ACIDS			
Acid	K_1	K_2	K_3
HOAc	1.75×10^{-5}
H ₂ C ₂ O ₄	5.90×10^{-2}	6.40×10^{-5}
H ₃ PO ₄	7.52×10^{-3}	6.23×10^{-8}	5×10^{-13}

It should be noticed that although the oxalic

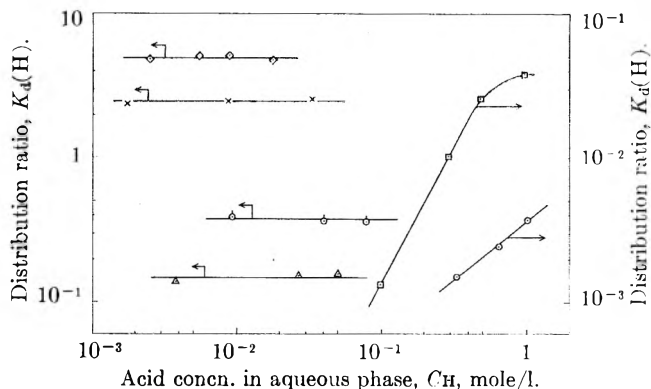


Fig. 4.—Determination of μ in case the salting agent is added, 25°: \diamond , HClO₄-NaClO₄ (5 M); \times , HNO₃-NaNO₃ (1 M); \circ , HOAc-KOAc (1 M); Δ , HCl-NaCl (4 M); \square , H₂C₂O₄-K₂C₂O₄ (0.2 M); \circ , H₂SO₄-Na₂SO₄ (1.5 M).

acid is a weak acid at high concentration, the α_H (of the first stage) approaches unity on dilution.

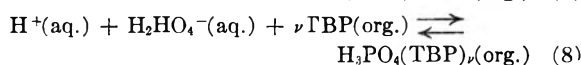
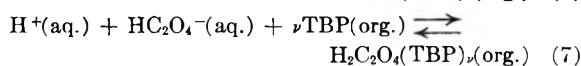
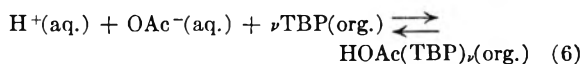
Equation 3 becomes

$$\text{when } \alpha_H = (K_1/C_H)^{1/2}, K_d(H) = \text{const}(C_H)\mu^{-1} \quad (4)$$

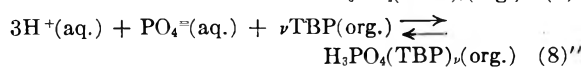
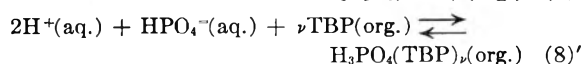
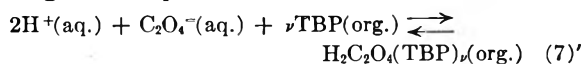
$$\text{when } \alpha_H \approx 1, K_d(H) = \text{const}(C_H)^{\mu-1} \quad (5)$$

It is observed from Fig. 1 and 2 that the K_d values of HOAc and H₃PO₄ at low acid concentration are nearly constant, so that μ is obtained as $\mu = 1$ by eq. 4. The concentration dependence of K_d of oxalic acid shows that as the concentration decreases the slope approaches unity and as the concentration increases the slope approaches zero. Accordingly μ is determined as 1, in this case, by eq. 4 and 5.

Then, the mechanisms of extraction of these acids are confirmed as



These mechanisms also are expressed in the following way, since the dissociations of each stage are in equilibrium.



In the case where the salting agent exists, this equation is derived corresponding to eq. iii of the Appendix

$$K_d(H) = \text{const}(\alpha_H)\mu(C_H)^{\mu-1}(C_X)^{\mu/m} \quad (9)$$

The value of α_H , in this case, is obtained roughly as K_1/C_X for the case of addition of OAc⁻, HC₂O₄⁻, and H₂PO₄⁻ ion, or as $2K_2/C_X$ for addition of C₂O₄²⁻ and HPO₄²⁻ ion. Thus eq. 9 becomes

$$K_d(H) = \text{const}(C_H)^{\mu-1} \quad (10)$$

because C_X is kept constant. Then, the slope of the curve obtained by plotting $\log K_d(H)$ against $\log C_H$ indicates the value of $\mu - 1$. Figure 4

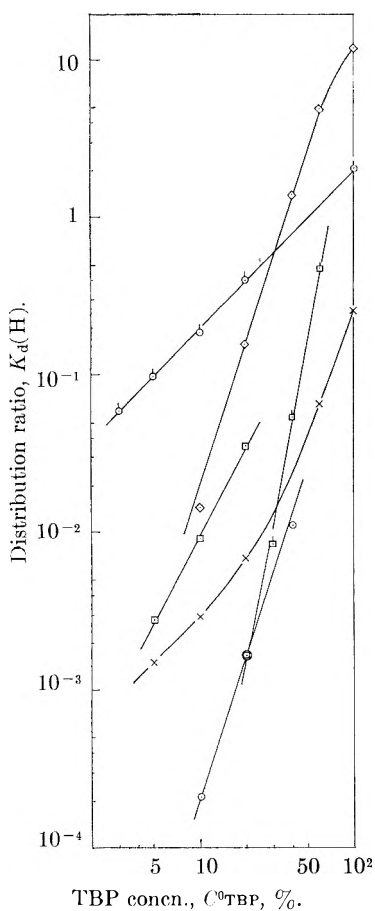


Fig. 5.—Determination of ν in the system of TBP-CCl₄, 25°: \circ , HOAc (0.05 ~ 0.5 M); \diamond , HClO₄-NaClO₄ (5 M); \square , H₂C₂O₄ (0.01 M); \times , HNO₃ (0.1 M); \triangle , H₃PO₄ (3.3 M); \circ , H₂SO₄ (5 M).

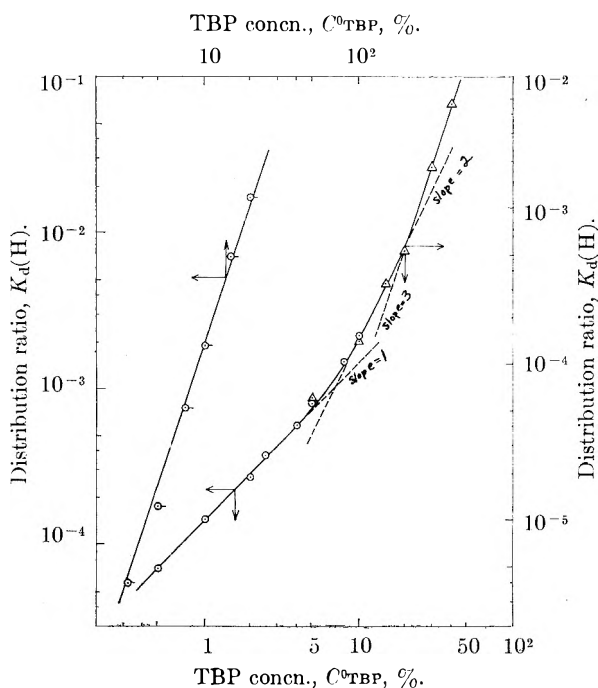


Fig. 6.—Determination of ν of HCl and HClO₄ in the system of TBP-CCl₄, 25°: \circ , HClO₄ (2 M); \triangle , HCl (4 M).

indicates that $\mu = 1$ for HOAc and $\mu = 2$ for H₂C₂O₄. The mechanisms of the extraction of these acids are confirmed again as eq. 6 and 7'.

(2) **Determination of ν .**—The value of ν is determined by plotting $\log K_d(H)$ against $\log C^0_{TBP}$, as shown in the Appendix, where C^0_{TBP} denotes the initial concentration of TBP in the organic phase. The result of the analysis is shown in Fig. 5, where carbon tetrachloride is used as a diluent. From this figure the values of ν are obtained as $\nu = 1$ or 2, 3, 3, 5(?), 1, and 2 for HNO₃, HClO₄, H₂SO₄, H₃PO₄, HOAc, and H₂C₂O₄, respectively.

The result obtained for the system of HCl-TBP is shown separately in Fig. 6, where the data obtained under two different acid concentrations are combined to form one curve. These acid concentrations are chosen in order to make the concentration of HCl extracted as low as possible. It is observed from Fig. 6 that the monosolvate, HCl·TBP, is formed at low TBP concentration (<5% TBP), and the trisolvate, HCl(TBP)₃, is formed at high TBP concentration (>20% TBP). In the region of intermediate TBP concentration (5% < TBP concn. < 20%), it is not clear whether the disolvate is formed or not.

In Fig. 6, the solvent dependence of K_d for the system of HClO₄-TBP in the region of low TBP concentration also is shown. It should be noticed that the solvation number ($\nu = 3$) is not changed even at very low TBP concentration.

As pointed out in the Appendix, this treatment is valid only under the condition that the TBP concentration is low. However, the use of carbon tetrachloride as a diluent makes the treatment possible even at high TBP concentration, say up to ~60% TBP, as will be shown later.¹⁰ This is also observed from Fig. 5 and 6 where the linearity holds in all cases except HNO₃ and HCl. Accordingly, it may be preferable to conclude that in the case of HNO₃, $\nu = 1$ for low TBP concentration and $\nu = 2$ for high TBP concentration; and in the case of HCl, $\nu = 1$ for low TBP concentration and $\nu = 3$ for high TBP concentration.

Although Hesford, *et al.*, reported the formation of the complexes HCl·TBP, HNO₃·TBP, H₂SO₃·TBP, and HClO₄·TBP by considering the solubilities of each species in organic phase, this simple picture does not hold in every case, as pointed out by Glueckauf.¹¹

The formation of the disolvate of HCl suggested by Kertes can not be confirmed clearly in this work.

(3) **Salting Effect.**—The addition of a salt to an extraction system usually brings an increase of K_d value, so that the salt is called a salting-out agent. The explanation of this effect is that the addition of a salt (M_mX_n) results in the increase of the concentration of anion (X^{m-}); then the equilibrium of eq. 2 is shifted to the right.

In the case of weak acids, however, it was found that the salting-out effect is not always observed on the addition of salt. Figure 7 shows the salting effect for the extraction of weak acids (HOAc

(10) K. Naito and T. Suzuki, *J. Phys. Chem.*, **66**, 989 (1962).

(11) E. Glueckauf, *Ind. Chim. Belg.*, **23**, 1215 (1958).

and $\text{H}_2\text{C}_2\text{O}_4$). In this figure, the addition of KOAc brings up no salting effect, and the addition of $\text{K}_2\text{C}_2\text{O}_4$ shows even a salting-in effect. This can be explained by using eq. 9 as follows. For HOAc-KOAc systems, $\alpha_{\text{H}} = K_1/C_{\text{X}}$, $m = 1$, and $\mu = 1$; thus eq. 9 becomes

$$K_{\text{d}}(\text{H}) = \text{const.} \quad (11)$$

so that a constant value of $K_{\text{d}}(\text{H})$ is to be obtained irrespective of the concentrations of acid and salt added. This is observed evidently in Fig. 7, 1, and 2. For the $\text{H}_2\text{C}_2\text{O}_4$ - $\text{K}_2\text{C}_2\text{O}_4$ system, $\alpha_{\text{H}} = 2K_2/C_{\text{X}}$, $m = 2$, and $\mu = 2$; then eq. 9 becomes

$$K_{\text{d}}(\text{H}) = \text{const. } C_{\text{H}}/C_{\text{X}} \quad (12)$$

so that the value of $K_{\text{d}}(\text{H})$ is to be inversely proportional to the concentration of salt added when C_{H} is kept constant. One can observe in Fig. 7 that this relation is held roughly.

The same effect is observed in the case of phosphoric acid, namely, little salting effect by addition of NaH_2PO_4 and salting-in effect by addition of Na_2HPO_4 .

Consequently, the salting effect for a weak acid extraction system is interpreted as follows. In this case, the addition of salts does not bring only an increase of anion concentration but also a decrease of proton concentration. Then, if both effects are canceled out the distribution ratio is obtained as a constant, and if the latter effect predominates over the former effect the salting-in effect is observed.

(4) **Partition of Water.**—The water content in the TBP phase changes as the acid is extracted. The change for 100% TBP is shown in Fig. 8.

Hesford, *et al.*,⁷ also presented water partition data for HCl, HClO_4 , HNO_3 , and H_2SO_4 systems which are in fairly good agreement with our results.

The change of water content in TBP phase is given as

$$dN_{\text{w}}/dN_{\text{A}} = \lambda - \nu \quad (13)$$

assuming that TBP saturated with water (TBP· H_2O) is replaced by the complex formed $(\text{H}_m\text{X} \cdot (\text{TBP})_{\nu}(\text{H}_2\text{O})_{\lambda})$, where N_{w} and N_{A} represent the number of water and acid molecules in the organic phase.

The hydration number λ of the complex can be calculated from this relation where the value $dN_{\text{w}}/dN_{\text{A}}$ is obtained from the initial slope in Fig. 8. So the values of λ for the complexes of $\text{H}_2\text{C}_2\text{O}_4$, HOAc, HNO_3 , HClO_4 , H_2SO_4 , H_3PO_4 , and HCl are determined roughly as 0.5, 1, 1, 4.5, 4.5, 4.5, and 7, respectively.

(5) **Infrared Spectra.**—The infrared spectra of the TBP phase give direct information concerning the formation of a complex. In the case of HNO_3 , it was observed that the band due to the P=O group at 1260 cm.^{-1} is shifted to 1208 cm.^{-1} , and this suggests a strong bonding between P=O and nitric acid.¹²

A similar shift of the P=O band also is observed in the cases of HCl, HClO_4 , H_2SO_4 , H_3PO_4 , HOAc, and $\text{H}_2\text{C}_2\text{O}_4$. The shift amounts to about $40 \sim 60 \text{ cm.}^{-1}$ for each case.

Order of Extractability.—The order among the

(12) K. Nukada, *et al.*, *Bull. Chem. Soc. Japan.*, **33**, 894 (1960).

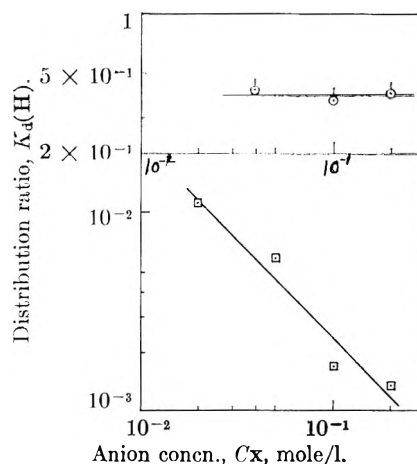


Fig. 7.—Salting effect for the systems of HOAc-KOAc (TBP 20% diluted with CCl_4) and $\text{H}_2\text{C}_2\text{O}_4$ - $\text{K}_2\text{C}_2\text{O}_4$ (TBP 100%), 25°: \circ , HOAc (10^{-2} M)-KOAc; \square , $\text{H}_2\text{C}_2\text{O}_4$ ($5 \times 10^{-3} \text{ M}$)- $\text{K}_2\text{C}_2\text{O}_4$.

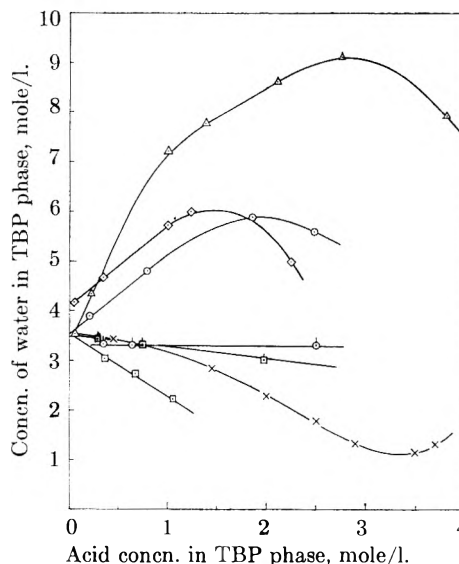


Fig. 8.—Partition of water, TBP 100%, 25°: Δ , HCl; \circ , HClO_4 ; \circ , H_2SO_4 ; \diamond , HOAc; \square , H_3PO_4 ; \times , HNO_3 ; \square , $\text{H}_2\text{C}_2\text{O}_4$.

extractabilities of the proton acids for 100% TBP is $\text{H}_2\text{C}_2\text{O}_4 \sim \text{HOAc} > \text{HClO}_4 > \text{HNO}_3 > \text{H}_3\text{PO}_4 > \text{HCl} > \text{H}_2\text{SO}_4$, as seen in Fig. 1.

It is an interesting fact that the order is closely related to the order among the hydration energies of anions.

Though the values of the hydration energies of anions have been obtained quantitatively for a few anions,¹³ these are not enough to give the order of the hydration energies of anions investigated in this work. One can estimate, however, the order among the hydration energies of anions by several methods.¹⁴ Among them, the electrostriction effect¹⁵ of the anion was employed as a measure of hydration energy. The electrostriction effect is a volume contraction of solution by dissolving an electrolyte expressed as

$$\Delta V = V_1 + V_2 - V_3 \quad (14)$$

(13) I. Benjamin and V. Gold, *Trans. Faraday Soc.*, **50**, 797 (1954).

(14) T. Sasaki, *Kagaku no Ryoiki*, **2**, 378 (1948).

(15) P. Drude and H. Nernst, *Z. physik. Chem.*, **15**, 79 (1894).

where V_1 , V_2 , and V_3 indicate the volumes of solvent, solute, and solution. The volume contraction ΔV is calculated as shown in Table II for the case of $V_1 = 1000$ ml., $V_2 =$ volume of solid electrolyte of 1 g.-equiv. (ml.), at 20°.

TABLE II

ELECTROSTRICTION EFFECT OF ANION, ΔV , (ml.)						
Anion	SO ₄ ⁻	H ₂ PO ₄ ⁻	Cl ⁻	NO ₃ ⁻	OAc ⁻	ClO ₄ ⁻
K salt	14.5	12.4	10.1	9.3	5.2	..
Na salt	18.3	..	10.0	9.3	13.1	4.8

If ΔV is the sum of $\Delta V+$ and $\Delta V-$ (where $\Delta V+$ and $\Delta V-$ are the corresponding volume contractions of cation and anion of an electrolyte), the order of the hydration energies in anions can be estimated from the order of ΔV in Table II. The order is SO₄⁻ > H₂PO₄⁻ > Cl⁻ > NO₃⁻ > OAc⁻ for the K salt, and SO₄⁻ > OAc⁻ > Cl⁻ > NO₃⁻ > ClO₄⁻ for the Na salt. The orders of both systems agree with each other except OAc⁻ ion. Concerning the reason for the disagreement of the position of OAc⁻ ion in the two systems, it is not clear whether this comes from the uncertainty of the data used or the effect of the cations. A calculation for HC₂O₄⁻ ion cannot be made because of its low solubility.

One may note that the order of ΔV is roughly inverse to the order among extractabilities of proton acids.

Baldwin, *et al.*,⁶ studied the extraction of HI, HBr, and HCl with TBP, and found the order of extractability as: HI > HBr > HCl. This is also in the inverse order of hydration energy of halide ions. It is an interesting fact that HF is extracted as well as HClO₄, as observed by Hesford, *et al.*⁷ Though F⁻ itself is a strongly hydrated ion, the anion of hydrofluoric acid in aqueous solution is mainly HF₂⁻ ion because of the strong hydrogen bonding between H⁺ and F⁻ ions. Accordingly the extractability of HF should not be correlated with the hydration energy of F⁻ ion but with that of HF₂⁻ ion, which has not been obtained yet.

The relation between extractability and hydration of an anion may be explained qualitatively as follows. The mechanism of TBP extraction is a reaction between inorganic ions and organic TBP molecules as already shown. Since the TBP molecule contains a P=O group in its structure, TBP can be regarded as a Lewis base,¹⁶ so that the extraction reaction with TBP is regarded essentially as a reaction between a Lewis acid and a Lewis base, where the base is the TBP molecule and the acid is the inorganic cation. Though it is expected that the behavior of the anion in this reaction is rather complicated, it can be reasonably assumed that the extractability will become less as the anion in the aqueous phase becomes stable. If one takes the hydration energy of the anion as a measure of its stability in the aqueous phase, we can come to

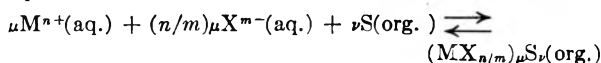
the above-mentioned relation between extractability and the hydration energy of the anion.

The order among the extractabilities of the proton acids for 20% TBP is HOAc > H₂C₂O₄ > HNO₃ > HClO₄ > HCl > H₂SO₄ ~ H₃PO₄. The reason that this order is different from the order for 100% TBP is due to the difference of solvent dependences of the acids, that is, the acids with high solvation number (*i.e.*, H₃PO₄, HClO₄, HCl, H₂SO₄, etc.) become much less extractable compared with the acids with lower solvation number (*i.e.*, HOAc, HNO₃, etc.).

Acknowledgment.—The authors would like to express their gratitude to Drs. K. Kimura, T. Nakai, T. Mukaibo, and K. Oshima for their invaluable assistance and advice in this work. They also are grateful to Prof. S. Makishima for his helpful discussion.

Appendix

The Method of Analysis for Extraction Mechanism.—The distribution equilibrium of a metal ion between the aqueous and organic phase can be expressed, in general, by the equation



where

$M_n X_n$ = inorganic solute (M^{n+} = cation, X^{m-} = anion)
 S = organic solvent (extractant)
 μ and ν = positive integers

Then, in case the concentration of the solute in the organic phase is low, and it is assumed that all the M ions in the organic phase are related to the formation of the complex, the following equation for the distribution ratio, $K_d(m)$, can be derived

$$K_d(M) = \text{const.} [(f_{\pm})^{(1+n/m)\mu} (f_s^0)^{\nu} / (f_{\text{complex}})] / [(C_M)^{\mu-1} (C_X)^{(n/m)\mu} (C_S^0)^{\nu}] \quad (\text{i})$$

where

C_M, C_X = equilibrium concn. of M and X in aq. phase
 C_s^0 = initial concn. of the solvent in organic phase
 f = activity coefficient

The experimental determination of the values of μ and ν in this equation can be made as shown below.

(1) **Determination of μ .**—In the case where the salting agent is absent, if the distribution ratio is measured under constant concentration of the solvent, one obtains

$$K_d(M) = \text{const.} (f_{\pm})^{(1+n/m)\mu} (C_M)^{(1+n/m)\mu-1} \quad (\text{ii})$$

Thus by plotting $\log [K_d(m)/f_{\pm}]$ against $\log (f_{\pm} C_M)$ the slope of the line indicates the value of $(1 + n/m)\mu - 1$, from which μ can be determined.

In the case where the salting agent exists, if the distribution ratio is measured under constant concentrations of the solvent and salting agent, equation i becomes

$$K_d(M) = \text{const.} (C_M)^{\mu-1} \quad (\text{iii})$$

It is, however, necessary to add a large amount of salting agent compared with the amount of the solute. Thus by plotting $\log K_d(M)$ against $\log C_M$ one can determine μ from the slope of the curve.

(2) **Determination of ν .**—When the distribution ratio is measured keeping the concentration of the salting agent constant (if the salting agent exists), equation i becomes

$$K_d(M) = \text{const.} [(f_s^0)^{\nu} / f_{\text{complex}}] (C_s^0)^{\nu} \quad (\text{iv})$$

Then, the value of ν is obtained by plotting $\log K_d(M)$ against $\log C_s^0$ if the measurement is made at low solvent concentration.

(16) G. N. Lewis, *J. Franklin Inst.*, **226**, 293 (1938).

THE MECHANISM OF THE EXTRACTION OF SEVERAL URANYL SALTS BY TRI-*n*-BUTYL PHOSPHATE

BY KEIJI NAITO¹ AND TOSHIO SUZUKI¹

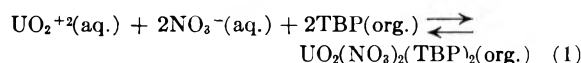
Japan Atomic Energy Research Institute, Tokai, Ibaraki-ken, Japan

Received July 18, 1961

The extraction of several uranyl salts (nitrate, chloride, perchlorate, sulfate, acetate, and phosphate) by TBP was studied. The formation of the complexes $\text{UO}_2(\text{NO}_3)_2(\text{TBP})_2$, $\text{UO}_2\text{Cl}_2(\text{TBP})_2$, $\text{UO}_2(\text{OAc})_2(\text{TBP})_2$, and $\text{UO}_2(\text{ClO}_4)_2(\text{TBP})_4$ was confirmed by partition study and infrared study. The influence of acid concentration on uranium extraction was discussed, especially for the system $\text{UO}_2(\text{ClO}_4)_2\text{-HClO}_4\text{-TBP}$. The order of the extractabilities of the uranyl salts was compared with that of the acids.

Introduction

The extraction of uranyl nitrate by TBP (tri-*n*-butyl phosphate) has been studied by many workers¹ because of its importance in the chemical processing of nuclear fuels. The mechanism of the extraction of uranyl nitrate by TBP was studied by Moore,² McKay, *et al.*,³⁻⁵ and Naito,⁶ and was confirmed as



The extraction behavior of uranyl chloride between the aqueous and TBP phase was reported by Reilly⁷ and Ishimori⁸; however, the mechanism of the extraction remains uncertain.

The extraction of uranyl perchlorate by TBP was studied recently by Hesford, *et al.*,⁹ who concluded the formation of a complex, $\text{UO}_2(\text{ClO}_4)_2(\text{TBP})_2$.

The object of the present work is to survey the extraction behavior of several uranyl salts (nitrate, chloride, perchlorate, sulfate, acetate, and phosphate) between the aqueous and TBP phase, and to reveal the mechanism of the extraction. The role of the anion during the process of uranium extraction also is to be discussed.

Experimental

Reagents.—The TBP was purified by the usual method.³ The uranyl salts used in this study were prepared by Yokozawa Chemicals, Tokyo. The other reagents used were all A. R. grade.

Equipment and Method.—The experimental techniques were essentially the same as described in the preceding paper.¹⁰ All measurements were made at a constant temperature of 25°.

The concentration of uranium was determined by the alkaline peroxide method¹¹ with a Hitachi EPU-2 spectrophotometer (at $\lambda = 400 \text{ m}\mu$). For the samples of low uranium concentration, the neutron activation method was adopted and the samples were irradiated in the JRR-1 reactor. In this case, the uranium concentration was determined by comparing the γ -peak heights of ²³⁹Np at 0.106 and 0.229 Mev. of

the samples with those of the standard sample by using the 256-channel pulse height analyser.

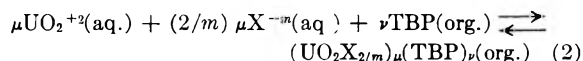
A Koken DS Type 301 spectrometer equipped with a rock salt prism was used in the infrared measurements.

Results and Discussion

Distribution Equilibrium.—The measurement of the distribution ratio, K_d , for the dilute solution of uranyl salts (nitrate, chloride, perchlorate, sulfate, phosphate, acetate) was made at various acid concentrations. In the case of the uranyl phosphate-phosphoric acid system, uranyl nitrate was used as a solute. TBP was used without dilution.

The results obtained are shown in Fig. 1. The equilibrium concentrations of uranium in the aqueous phase were maintained as low as possible; in almost all the cases, less than 10^{-3} M ; and in the cases of chloride, phosphate, and sulfate, $5 \times 10^{-3} \sim 10^{-2} \text{ M}$. The data for the high acid concentration region of the $\text{UO}_2\text{Cl}_2\text{-HCl}$ system were obtained by Ishimori, *et al.*⁸

Mechanism of Extraction. (1) **Partition Study.**—Since the mechanism of extraction of uranyl nitrate by TBP was confirmed as eq. 1, the mechanism of extraction of uranyl salts may be expressed by the general equation



where X^{-m} indicates an anion and μ and ν are integers. The mechanism can be confirmed by determining the values of μ and ν , respectively, according to the method of analysis shown in the Appendix of the preceding paper.¹⁰

The determination of the value of μ in the presence of salting agents is shown in Fig. 2, from which the values of μ are determined as $\mu = 1$ for $\text{UO}_2(\text{NO}_3)_2\text{-TBP}$, $\text{UO}_2\text{Cl}_2\text{-TBP}$, $\text{UO}_2(\text{ClO}_4)_2\text{-TBP}$, and $\text{UO}_2(\text{OAc})_2\text{-TBP}$ systems. This also is confirmed by the fact that the values of K_d for these systems are nearly proportional to the square of the acid concentration.

For the systems of uranyl acetate, phosphate, and sulfate, it is suggested that uranyl ion is complexed with the anion in the aqueous phase since the K_d values in the low acid concentration region are nearly constant.

The determination of the value of ν is shown in Fig. 3, where carbon tetrachloride is used as a diluent. The values of ν are determined as $\nu = 4, 2,$ and 2 for $\text{UO}_2(\text{ClO}_4)_2\text{-TBP}$, $\text{UO}_2\text{Cl}_2\text{-TBP}$, and $\text{UO}_2(\text{OAc})_2\text{-TBP}$ systems, respectively.

Accordingly it was confirmed by this analysis that the mechanisms of extraction by TBP for

(1) For example, R. I. Smith, TID-3502.

(2) R. L. Moore, AECD-3196 (1951).

(3) K. A. Alcock, *et al.*, *Trans. Faraday Soc.*, **52**, 39 (1956).

(4) T. V. Healy and H. A. C. McKay, *ibid.*, **52**, 633 (1956).

(5) E. Hesford and H. A. C. McKay, *ibid.*, **54**, 573 (1958).

(6) K. Naito, *Bull. Chem. Soc. Japan*, **33**, 363, 894 (1960).

(7) E. Reilly, ANL-5254 (1954).

(8) T. Ishimori and E. Nakamura, *Bull. Chem. Soc. Japan*, **32**, 713 (1959).

(9) E. Hesford and H. A. C. McKay *J. Inorg. & Nuclear Chem.*, **13**, 165 (1960).

(10) K. Naito and T. Suzuki, *J. Phys. Chem.*, **66**, 683 (1962).

(11) C. J. Rodden and J. C. Warf, "Analytical Chemistry of the Manhattan Project," (National Nuclear Energy Series VIII-1 (1950)).

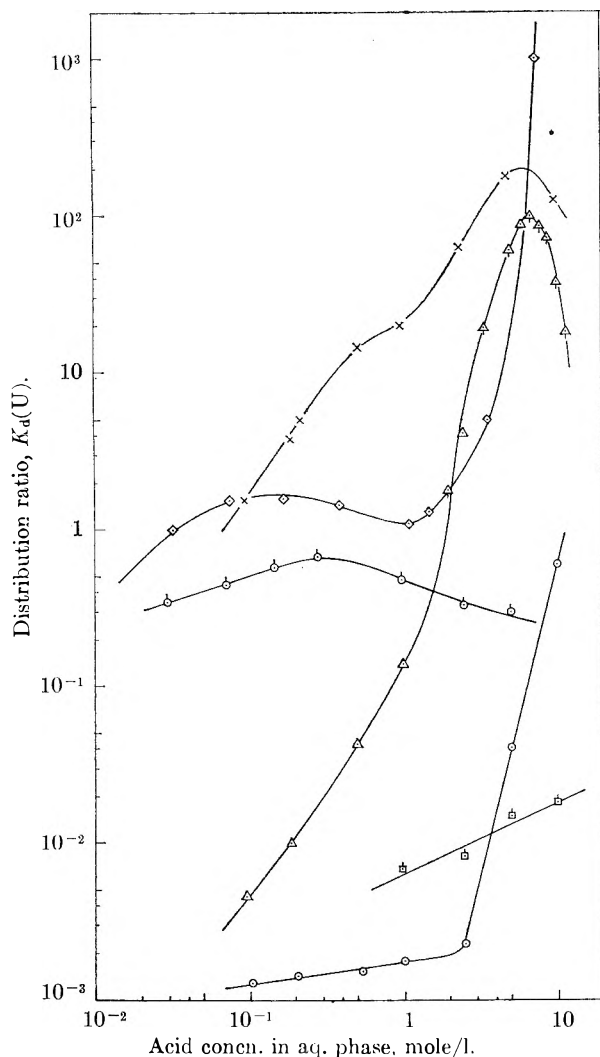


Fig. 1.—Influence of acid concentration upon the distribution ratio of uranium at various acid concentrations, TBP 100%, 25°. The data for the acid concentration of $\text{UO}_2\text{Cl}_2\text{-HCl}$ system symbolized with Δ were obtained by Ishimori, *et al.*⁸ \times , $\text{UO}_2(\text{NO}_3)_2\text{-HNO}_3$; \diamond , $\text{UO}_2(\text{ClO}_4)_2\text{-HClO}_4$; Δ , $\text{UO}_2\text{Cl}_2\text{-HCl}$; \circ , $\text{UO}_2(\text{OAc})_2\text{-HOAc}$; \square , $\text{UO}_2(\text{NO}_3)_2\text{-H}_3\text{PO}_4$.

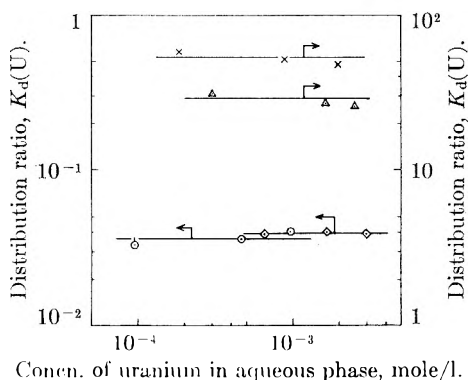


Fig. 2.—Determination of μ in case the salting agent is added, 25°: \times , $\text{UO}_2(\text{NO}_3)_2\text{-NaNO}_3$ (1 *M*) (TBP 100%); Δ , $\text{UO}_2\text{Cl}_2\text{-NaCl}$ (5 *M*) (TBP 100%); \diamond , $\text{UO}_2(\text{ClO}_4)_2\text{-NaClO}_4$ (3 *M*) (TBP 20%); \circ , $\text{UO}_2(\text{OAc})_2\text{-KOAc}$ (1 *M*) (TBP 100%).

$\text{UO}_2(\text{NO}_3)_2$, UO_2Cl_2 , $\text{UO}_2(\text{ClO}_4)_2$, and $\text{UO}_2(\text{OAc})_2$ are expressed by eq. 2, and the compositions of the complexes formed are $\text{UO}_2(\text{NO}_3)_2(\text{TBP})_2$,

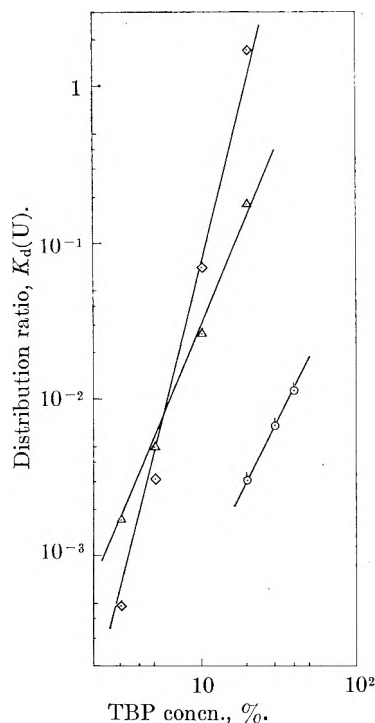


Fig. 3.—Determination of ν in the system of TBP- CCl_4 , 25°: \diamond , $\text{UO}_2(\text{ClO}_4)_2\text{-NaClO}_4$ (5 *M*); Δ , $\text{UO}_2\text{Cl}_2\text{-NaCl}$ (4 *M*); \circ , $\text{UO}_2(\text{OAc})_2\text{-KOAc}$ (1 *M*).

$\text{UO}_2\text{Cl}_2(\text{TBP})_2$, $\text{UO}_2(\text{ClO}_4)_2(\text{TBP})_4$, and $\text{UO}_2(\text{OAc})_2(\text{TBP})_2$. Though the mechanism of extraction for the systems of uranyl sulfate and phosphate also are expected to be expressed as eq. 2, the mechanism is not clearly confirmed to the present since their low K_d values make the analysis difficult.

Hesford, *et al.*,⁹ have reported the formation of a disolvate, $\text{UO}_2(\text{ClO}_4)_2(\text{TBP})_2$, at very high HClO_4 concentrations (10–12 *M*). This disagreement on the system $\text{UO}_2(\text{ClO}_4)_2\text{-TBP}$ will be discussed later.

(2) **Infrared Study.**—Although the composition of the complex formed can be determined by partition measurement as described above, we tried to determine it directly by means of infrared spectroscopy.

It is known that the absorption band due to the $\text{P}=\text{O}$ group at 1280 cm.^{-1} is shifted to the longer wave length by the formation of a complex with the inorganic salt.^{6,12} One can observe the fact that the intensity of the band due to free TBP decreases as the concentration of uranium in the TBP phase increases. Since the decrease of the concentration of free TBP corresponds to the composition of the complex formed, the composition of the complex can be determined by plotting the decrease of the concentration of free TBP against the increase of the concentration of uranium in the TBP phase.

The infrared spectra obtained for the $\text{UO}_2(\text{ClO}_4)_2\text{-TBP}$ system are shown in Fig. 4. All of the spectra were obtained by capillary samples and their thicknesses were adjusted so as to give a constant intensity in the absorption band due to CH_3 and CH_2 deformation vibration at 1470 cm.^{-1} .

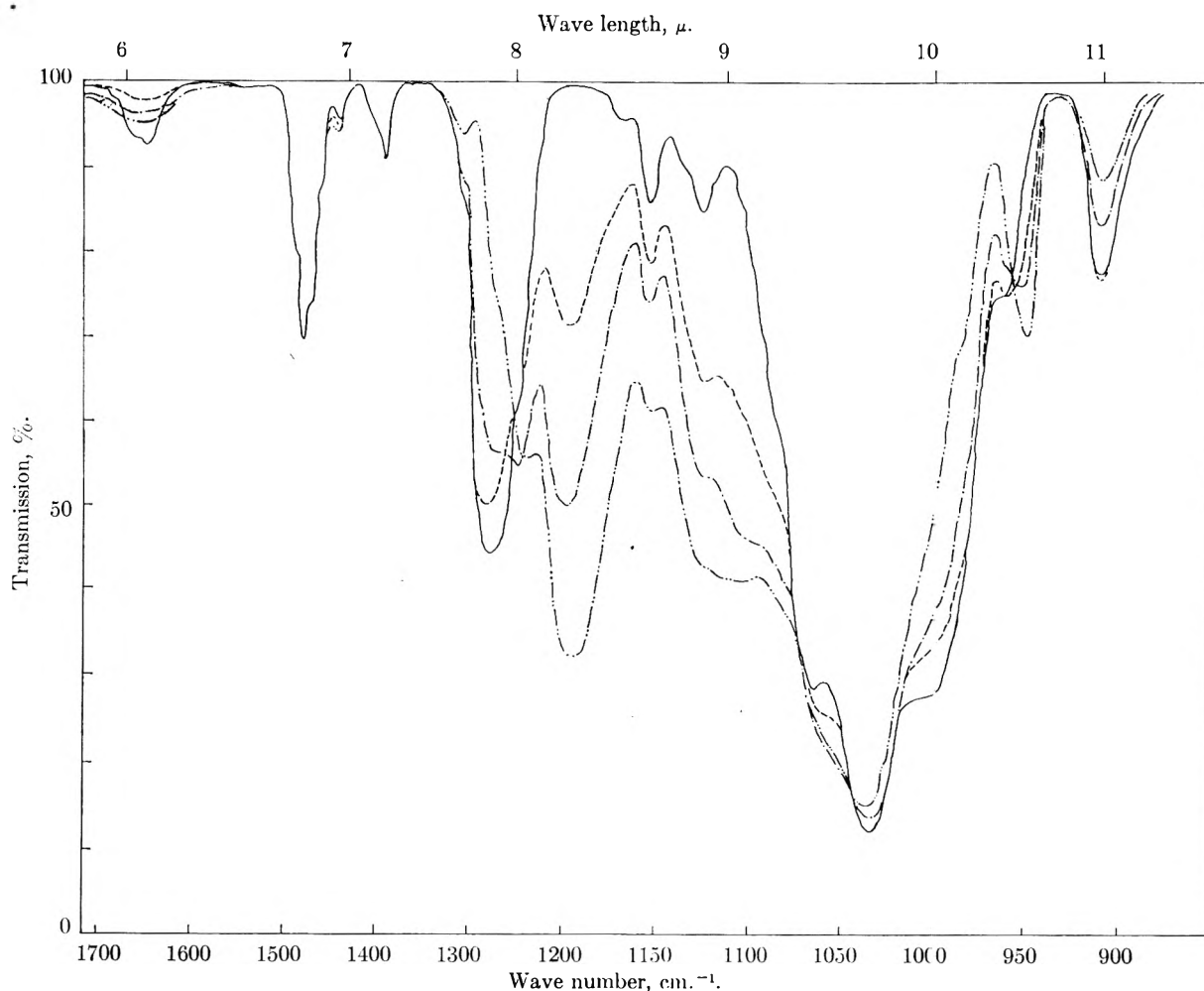


Fig. 4.—Infrared spectra for the system of $\text{UO}_2(\text{ClO}_4)_2$ -TBP, TBP 100%. Concn. of uranium in TBP phase (mole/l.): —, 0; — · —, 0.630; — — —, 0.327; - - - -, 0.169.

The samples were prepared by dissolving uranyl perchlorate crystals in the TBP phase, and the concentrations were 0.630, 0.327, and 0.169 *M*, respectively. The decrease of the concentration of free TBP with the increase of the concentration of uranium in the organic phase is shown in Fig. 5a. The initial slope is 3.8, so the solvation number, ν , in this case can be determined as $\nu = 3.8$. On the other hand, Fig. 5b gives the change of the intensity of absorption due to the formation of complex at 1195 cm^{-1} . It is observed that the intensity of this absorption band increases in proportion to the concentration of uranium in the organic phase. Similar spectra were obtained for the sample which was prepared by extracting uranium from the aqueous phase with NaClO_4 as salting agent. In this case, the value of ν was obtained as 3.9 and 4.0 in repeated measurements. Accordingly it is confirmed that the solvation number, ν , for the system $\text{UO}_2(\text{ClO}_4)_2$ -TBP is 4.

The same treatment was carried out for the system UO_2Cl_2 -TBP. The results obtained are shown in Fig. 6a and b. The samples used were prepared by dissolving the crystals in the TBP phase, and the concentrations of uranium were 0.19, 0.35, and 0.75 *M*. From Fig. 6a, the solvation number, ν , of UO_2Cl_2 is determined as $\nu = 2$.

For the system $\text{UO}_2(\text{NO}_3)_2$ -TBP, a correct determination of ν is difficult because the absorption band due to the NO_3 group overlaps with the band due to free TBP. The system $\text{UO}_2(\text{OAc})_2$ -TBP also has a similar difficulty since the absorption bands due to the acetate group overlap with the bands due to TBP.

Influence of Acid Concentration on the Extraction of Uranium.—The influence of acid concentration on the extraction of uranium seems to be complicated, as seen in Fig. 1. However, this is explainable by considering two effects—the competitive extraction of uranium and acid, and the formation of complexes with anions.

(1) **Competitive Extraction.**—The competitive extraction of uranyl nitrate and nitric acid has been discussed in detail,⁶ and it was concluded that the K_4 values of uranyl nitrate plotted against the nitric acid concentration have a maximum resulting from the competitive extraction of both.

Other acids, however, also are extractable by TBP as shown in the preceding paper,¹⁰ so the competitive extraction of uranium and acid may take place, especially in the case of easily extractable acids, for example the HClO_4 or HOAc system.

In general, in the case of the extraction of

Fig. 5a.—Optical density of the absorption due to free P=O vs. concn. of uranium in TBP phase, $\text{UO}_2(\text{ClO}_4)_2$ -TBP system, TBP 100%.

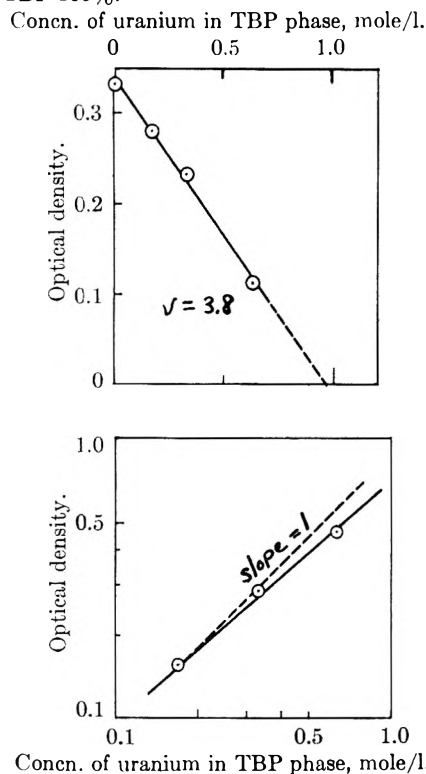
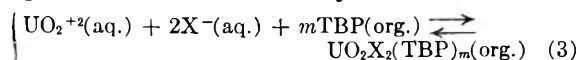


Fig. 5b.—Optical density of the absorption due to bonded P=O vs. concn. of uranium in TBP phase, $\text{UO}_2(\text{ClO}_4)_2$ -TBP system, TBP 100%.

uranium from acidic solution, these distribution equilibria hold simultaneously



In the case where the concentration of uranium is low, if one replaces the activity by the concentration in order to make the discussion simple, these simultaneous equations hold approximately

$$\left\{ \begin{array}{l} K(\text{U}) \approx K_d(\text{U})/C_{\text{H}}^2 C_{\text{TBP}}^m \quad (5) \\ K(\text{H}) \approx K_d(\text{H})/C_{\text{H}} C_{\text{TBP}}^n \quad (6) \end{array} \right.$$

where $K(\text{U})$ and $K(\text{H})$ are the equilibrium constants of uranium for eq. 3 and of nitric acid for eq. 4, C_{H} represents the concentration of acid in the aqueous phase, and C_{TBP} the concentration of free TBP in the organic phase. From eq. 5 and 6, one may obtain the equation

$$K_d(\text{U}) = [K(\text{U})/K(\text{H})]^{m/n} C_{\text{H}}^{2-m/n} K_d(\text{H})^{m/n} \quad (7)$$

Equation 7 gives the general relation between $K_d(\text{U})$ and C_{H} in the region where the uranium concentration is low. Though $K_d(\text{H})$ is also a function of C_{H} , the relation between $K_d(\text{H})$ and C_{H} is given experimentally by Fig. 1 in the preceding paper.¹⁰

It can be derived from eq. 7 that $K_d(\text{U})$ has a maximum value at $(C_{\text{H}})_{\text{max}}$ which is given by the equation

$$d \log K_d(\text{H})/d \log C_{\text{H}} = 1 - 2n/m \quad (8)$$

So, the concentration of $(C_{\text{H}})_{\text{max}}$ can be calculated

Fig. 6a.—Optical density of the absorption due to free P=O vs. concn. of uranium in TBP phase, UO_2Cl_2 -TBP system, TBP 100%.

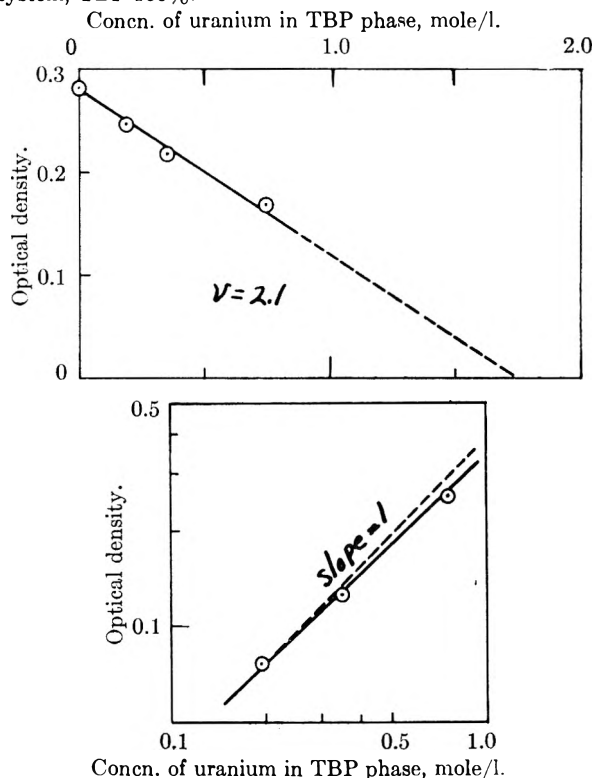


Fig. 6b.—Optical density of the absorption due to bonded P=O vs. concn. of uranium in TBP phase, UO_2Cl_2 -TBP system, TBP 100%.

from eq. 8 and Fig. 1 in the preceding paper.¹⁰ The calculated values of $(C_{\text{H}})_{\text{max}}$ for each extraction system are shown in Table I.

TABLE I
CALCULATION OF $(C_{\text{H}})_{\text{max}}$

System	m	n	$(C_{\text{H}})_{\text{max}}$ Calcd.	$(C_{\text{H}})_{\text{max}}$ Obsd.
$\text{UO}_2(\text{NO}_3)_2$ - HNO_3 (TBP concn. high)	2	2	...	5 N
$\text{UO}_2(\text{NO}_3)_2$ - HNO_3 (TBP concn. low)	2	1	4 N	5 N
$\text{UO}_2(\text{ClO}_4)_2$ - HClO_4	4	3	0.3 N	0.2 N
UO_2Cl_2 - HCl (TBP concn. high)	2	3	...	6 N
$\text{UO}_2(\text{OAc})_2$ - HOAc	2	1	0.4 N ^a	0.3 N

^a In the case of the $\text{UO}_2(\text{OAc})_2$ - HOAc system, the following equation holds instead of eq. 7, since HOAc is a weak acid and UO_2^{+2} ion complexes with OAc^- ion

$$K_d(\text{U}) = [K(\text{U})/\alpha_{\text{U}}K(\text{H})^{m/n}] C_{\text{H}}^{2-m/n} \alpha_{\text{H}}^{2(1-m/n)} K_d(\text{H})^{m/n}$$

where α_{U} and α_{H} are the fractions of the bare UO_2^{+2} ion and the free H^+ ion. Then, one obtains the following equation instead of eq. 8 by using a relation $\alpha_{\text{H}} = (K_1/C_{\text{H}})$ (where K_1 is the dissociation constant of HOAc): $d \log K_d(\text{H})/d \log C_{\text{H}} = n/m$. (in this derivation, α_{U} is assumed as a constant).

The calculated values for the systems $\text{UO}_2(\text{ClO}_4)_2$ - HClO_4 -TBP and $\text{UO}_2(\text{OAc})_2$ - HOAc -TBP are in fairly good agreement with the observed values.

For the system $\text{UO}_2(\text{NO}_3)_2$ - HNO_3 -TBP, though a maximum of $K_d(\text{U})$ is obtained from the calculation for the region of low TBP concentration, a maximum with gentle slope in Fig. 1 for the high

TBP concentration region cannot be obtained from the calculation.

For the system $\text{UO}_2\text{Cl}_2\text{-HCl-TBP}$, the maximum again cannot be obtained by calculation. This seems to indicate that the maximum is not due to the competition. However, if one adds a salt instead of an acid as a salting agent, the $K_d(\text{U})$, in this case, increases monotonously without a maximum, as shown in Fig. 7. By this fact, it may be reasonable to conclude that the maximum in the curve of $K_d(\text{U})$ for the $\text{UO}_2\text{Cl}_2\text{-HCl-TBP}$ system is caused by the competitive extraction of uranium and acid.

The reason for the disagreements between the calculation and the observation are thought to be due to the use of concentration in place of activity in the calculation. Especially, in the system $\text{UO}_2\text{-Cl}_2\text{-HCl-TBP}$, the change of the activities of the species in the organic phase must be remarkable since a large amount of water is extracted into the organic phase together with the hydrochloric acid.¹⁰

(2) **Successive Complex Formation in the Aqueous Phase.**—In the calculation described, it is assumed that the uranyl ion remains as 'free' ion in the aqueous phase. It is well known, however, that uranyl ion forms many complexes with different anions in an aqueous phase as shown in Table II.¹³

TABLE II

EQUILIBRIUM CONSTANTS FOR REACTIONS $\text{UO}_2^{++} + n\text{X}^- = \text{UO}_2\text{X}_n^{2-n}$ ($\mu = 0, 20^\circ$)

Anion	$\frac{n=1}{(\text{mole/l.})^{-1}}$	$\frac{n=2}{(\text{mole/l.})^{-2}}$	$\frac{n=3}{(\text{mole/l.})^{-3}}$
NO_3^-	0.5
Cl^-	0.8
SO_4^{2-}	50	350	2.5×10^3
OAc^-	240	2.3×10^4	2.2×10^6

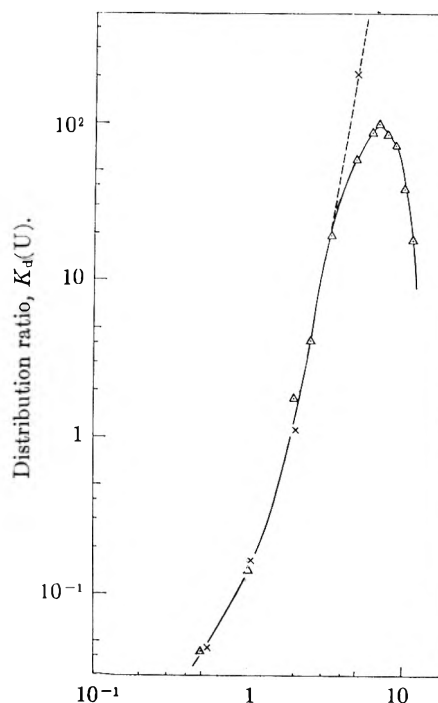
In the case where uranyl ion forms the complexes $\text{UO}_2\text{X}_n^{2-n}$ with the anion successively, the concentration of free uranyl ion, $C_{\text{UO}_2^{++}}$, is given by the equation

$$C_{\text{UO}_2^{++}} = C_U / (1 + k_1 C_x + k_2 C_x^2 + \dots) \quad (9)$$

where k_1, k_2, \dots are the stability constants of the successive complexes and C_U represents the stoichiometric concentration of uranium. Accordingly the formation of complexes with anions brings up the decrease of the concentration of free uranyl ion in the aqueous phase. It can be derived from eq. 9 that the increase of $K_d(\text{U})$ with acid concentration is suppressed by the formation of these complexes, and if a neutral complex, UO_2X_2 , predominates, the $K_d(\text{U})$ becomes nearly constant, and if the anionic complexes such as UO_2X_3^- , $\text{UO}_2\text{X}_4^{2-}$, etc., predominate, the $K_d(\text{U})$ decreases with the acid concentration (if the anionic complexes could not be extracted).

Accordingly, the formation of anionic complexes also may possibly produce a maximum in the K_d curve of uranium.

In the systems $\text{UO}_2(\text{ClO}_4)_2\text{-HClO}_4$, $\text{UO}_2(\text{NO}_3)_2\text{-HNO}_3$, and $\text{UO}_2\text{Cl}_2\text{-HCl}$, since the formation of anionic complexes with anion cannot be expected even at fairly high concentration, the acid con-

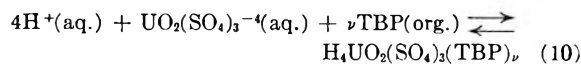


Concn. of chloride ion in aq. phase, C_{Cl} , mole/l.

Fig. 7.—The salting effect of both hydrochloric acid and lithium chloride for diluted uranyl chloride, TBP 100%, 25° : \times , $\text{UO}_2\text{Cl}_2\text{-LiCl}$; Δ , $\text{UO}_2\text{Cl}_2\text{-HCl}$.

centration dependence may be resulting mainly from the competitive extraction of uranium and acid.

In the systems $\text{UO}_2(\text{OAc})_2\text{-HOAc}$ and $\text{UO}_2\text{SO}_4\text{-H}_2\text{SO}_4$, the uranyl ion forms complexes strongly with these anions. However, in the $\text{UO}_2(\text{OAc})_2\text{-HOAc}$ system, since acetic acid is a weak acid the increase of the concentration of free acetate ion with the acid concentration is suppressed and it is easily derived that the free uranyl ion, UO_2^{++} , predominates over other species up to 1 M HOAc. Accordingly it is concluded that the effect of complex formation with anion in the system $\text{UO}_2\text{-}(\text{OAc})_2\text{-HOAc}$ is not remarkable. On the contrary, in the $\text{UO}_2\text{SO}_4\text{-H}_2\text{SO}_4$ system, it is calculated that the anionic complex, $\text{UO}_2(\text{SO}_4)_3^{4-}$, is formed completely over 1 M H_2SO_4 . Nevertheless, the value of $K_d(\text{U})$ increases rapidly with acid concentration, as seen in Fig. 1. This fact suggests that the anionic complex formed is extractable, and the mechanism of extraction at high acid concentrations is



(3) **Extraction of Uranyl Perchlorate.**—The extraction of uranyl perchlorate TBP was studied in detail by Hesford, *et al.*,⁹ and they reported the formation of a disolvate, $\text{UO}_2(\text{ClO}_4)_2(\text{TBP})_2$. This does not agree with our result, that is the formation of a tetrasolvate, $\text{UO}_2(\text{ClO}_4)_2(\text{TBP})_4$. The reason for this discrepancy is thought to be as follows. They determine the solvation number from the solvent dependence of K_d of uranium, which is the same method as we used. However, their measurement was made at a very high acid concentration, 10–12 M. At such a high acid

(13) J. J. Katz and G. T. Seaborg, "The Chemistry of Actinide Elements," John Wiley and Sons, Inc., New York, N. Y., 1957.

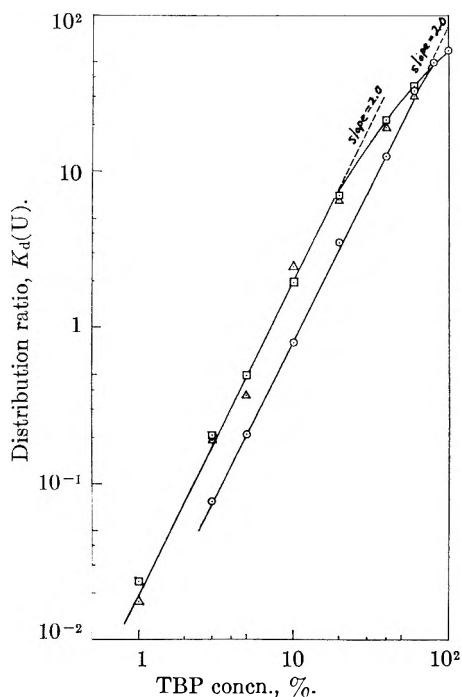


Fig. 8.—Determination of ν for $UO_2(NO_3)_2$ -TBP system in use of different solvent ($UO_2(NO_3)_2$, $2 \times 10^{-4} \sim 10^{-2} M$; HNO_3 , 0.05 M, $NaNO_3$, 1 M), 25°: O, CCl_4 ; Δ , kerosene; \square , benzene.

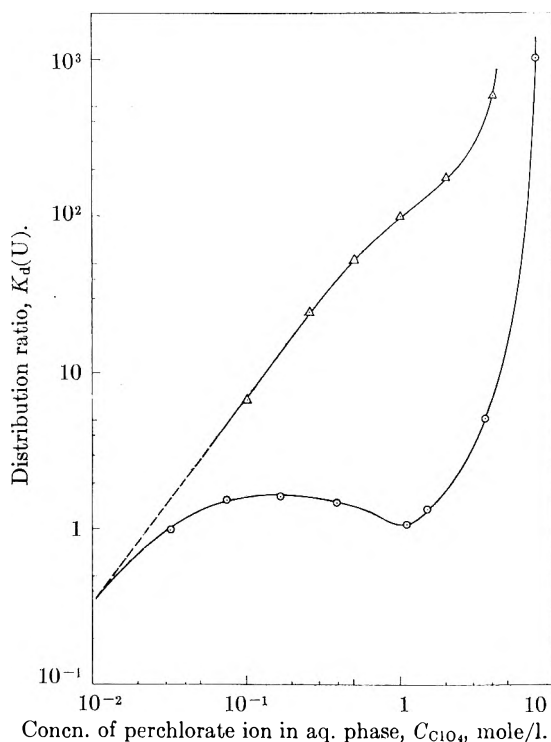


Fig. 9.—The salting effect of both perchloric acid and sodium perchlorate for diluted uranyl perchlorate, TBP 100%, 25°: Δ , $UO_2(ClO_4)_2$ -NaClO₄; O, $UO_2(ClO_4)_2$ -HClO₄.

concentration, the solvent dependence of K_d does not give the correct value of the solvation number because most of the TBP molecules are bonded with HClO₄. In the determination of the solvation number, ν , it is necessary to maintain the concentration of the solutes in the organic

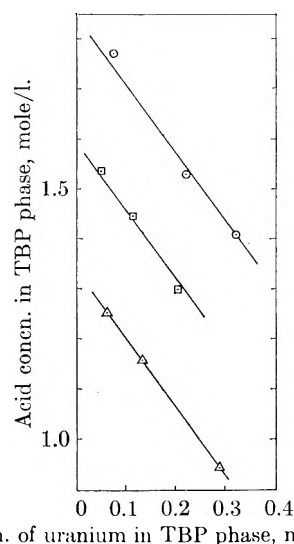


Fig. 10.—Replacement of HClO₄ by $UO_2(ClO_4)_2$ in TBP phase, TBP 100%, 25°: O, $C_H \approx 6.2 M$; \square , $C_H \approx 4.8 M$; Δ , $C_H \approx 4.1 M$.

phase as low as possible, as noted in the Appendix of the preceding paper.¹⁰ Since the solvation number in this work is obtained from the system $UO_2(ClO_4)_2$ -NaClO₄, and most of the TBP molecules in the organic phase remain free, the solvation number obtained can be considered to be correct.

The reason for the fact that only $UO_2(ClO_4)_2$ forms tetrasolvate is not clear, but it perhaps arises from the fact that $UO_2(ClO_4)_2$ is ionized appreciably in the TBP phase.⁹

In addition, the choice of the diluent also is important in the determination of the solvation number even at the higher concentration region of TBP in comparison with other diluents. For example, the solvent dependence of K_d for uranyl nitrate is shown in Fig. 8, where different diluents are used. It is obviously observed that the linearity of the solvent dependence of K_d is held up to the region of fairly high concentration of TBP, say 60% TBP.

On the maximum at 0.2 M HClO₄ in Fig. 1, Hesford, *et al.*,⁹ did not give any definite explanation, but suggested that it may arise from varying ionization of the $UO_2(ClO_4)_2$ in the TBP phase. However, it is preferable to conclude that the maximum arises from the competition of uranyl perchlorate and acid as discussed already. This also is confirmed by the observation in the salting effect of NaClO₄, which is not extracted well by TBP. Figure 9 shows the salting effect of NaClO₄ upon the distribution ratio of uranium in comparison with HClO₄. It is obvious from Fig. 9 that the K_d of the $UO_2(ClO_4)_2$ -NaClO₄ system increases monotonously without a maximum.

In the region where the acid concentration is high, however, the K_d increases rapidly again. This increase of K_d is thought to be caused by the presence of the excess acid in the TBP phase. As shown in the preceding paper,¹⁰ it is expected that a considerable amount of excess acid exists in the TBP phase equilibrated with an aqueous

HClO₄ solution of high concentration. The presence of excess acid may change the activity of the species in the TBP phase remarkably, and cause a rapid increase in the K_d .

However, even in the region of such high acid concentration it is estimated from Fig. 10 that the compositions of the complexes formed remain unchanged as UO₂(ClO₄)₂(TBP)₄ and HClO₄(TBP)₃. Figure 10 shows the replacement of HClO₄ by UO₂(ClO₄)₂ in the TBP phase, in case the concentration of acid in the aqueous phase is maintained nearly constant. In the region of high acid concentration, a linear decrease of the concentration of acid with a slope of $3/4$ is observed. This implies that the complex of acid, HClO₄(TBP)₃, in the TBP phase is replaced with the complex of uranium, UO₂(ClO₄)₂(TBP)₄, while the concentration of excess acid remains nearly constant.

Order of Extractability.—In the region where the acid concentration is low, it is possible to compare the extractabilities of the different uranyl salts, since the effect of competitive extraction or complex formation with anion can be ignored.

The order among the extractabilities of the uranyl salts in the region of low acid concentration is obtained from Fig. 1 as UO₂(ClO₄)₂ ~ UO₂(OAc)₂ > UO₂(NO₃)₂ > UO₂Cl₂ > UO₂SO₄. This order is in good agreement with the order for proton

acids, and it also is in the inverse order to the hydration energy of the anions.¹⁰

The difference of extractabilities due to the anions is useful in the extraction of uranium from sulfuric acid solution by TBP. By adding anions such as SCN⁻, ClO₄⁻, and NO₃⁻, which are weakly hydrated in the aqueous phase, uranium can be easily extracted from the aqueous phase, leaving the SO₄⁼ ion. The addition of SCN⁻ ion for the extraction of uranium from sulfuric acid solution was tried by Ross.¹⁴ Though uranium is extracted well by this method, there is the disadvantage that Fe(III) also is extracted easily and accompanies the uranium. On the other hand, the addition of NO₃⁻ ion gives a high separation factor for uranium. The addition of ClO₄⁻ ion also is effective, if TBP is used without dilution. However, if a diluent is used, the K_d of uranium decreases rapidly with dilution because of the high solvent dependence of K_d ($\nu = 4$) in this case.

Acknowledgment.—The authors would like to express their gratitude to Drs. K. Kimura, T. Nakai, T. Mukaibo, and K. Oshima for their invaluable assistance and advice in this work. They also are grateful to Prof. S. Makishima for his helpful discussion.

(14) A. M. Ross, TID-7508 (1955).

ION EXCHANGE KINETICS OF POLYELECTROLYTES UNDER STEADY-STATE ELECTROLYSIS ACROSS A POROUS FRIT¹

BY STANLEY J. GILL AND GUY V. FERRY

Department of Chemistry, University of Colorado, Boulder, Colorado

Received August 28, 1961

A theory is developed for a steady-state electrolysis method to determine the characteristics of ion binding with polyelectrolytes. The solutions of continuity equations of free and bound tagged ion electric current flow are given for the cases of one or two exchange constants. The boundary conditions simulate the porous frit method for diffusion studies. The ratio of tagged ion flows toward cathode and anode suggests a design and analysis of experiments which allow a determination of the fraction of ion binding and exchange rate constants.

Introduction

The interaction between small ions and many naturally occurring polymers, such as proteins and nucleic acids, plays a significant role in determining the configuration and chemistry of these materials. The methods used to study ionic interactions between macro and small ions have included direct determinations, such as dialysis, conductivity, and electrophoresis, as well as the indirect effects given by viscosity and light scattering.²

The electrical transference method, developed by Wall and co-workers,³ is capable of yielding not only a measure of the extent of ion binding^{3,4} but also the rates of exchange between bound and

free ions. This has been shown for the system of partially neutralized sodium polyacrylate.⁵

These studies have indicated that the rate of exchange between free and bound sodium ions is relatively slow. Wall⁶ has discussed these results in connection with the formation of a high potential ion atmosphere about the polyion. Harris and Rice⁷ have proposed a theory of ion binding based upon a more specific interaction between small ions and charged sites on the polyion.

In this paper we wish to discuss a steady-state electrolysis situation which might be used to design and interpret further experiments of polyelectrolyte ion exchange. The proposed steady-state experimental parameters with rate constants and fraction of

(1) This work was supported in part by a research grant (C-5393) from the United States Public Health Service.

(2) I. M. Klotz, "The Proteins," Vol. I, Part B, Edited by H. Neurath and K. Bailey, Academic Press Inc., New York, N. Y., 1953, Chapter 8.

(3) J. R. Huizenga, P. F. Grieger, and F. T. Wall, *J. Am. Chem. Soc.*, **72**, 2636 (1950).

(4) R. H. Doremus and P. Johnson, *J. Phys. Chem.*, **62**, 203 (1958).

(5) (a) F. T. Wall and P. F. Grieger, *J. Chem. Phys.*, **20**, 1200 (1952); (b) F. T. Wall, P. F. Grieger, J. R. Huizenga, and R. H. Doremus, *ibid.*, **20**, 1206 (1952).

(6) F. T. Wall, *J. Phys. Chem.*, **61**, 1344 (1957).

(7) F. E. Harris and S. A. Rice, *ibid.*, **58**, 725 (1954).

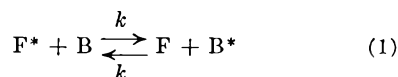
binding over that of the moving boundary experiment developed by Wall, etc.⁵ The steady-state case is analogous to the use of a swept porous frit for diffusion measurements.⁸ In this way deleterious experimental effects such as convections from electrolysis heating perhaps can be minimized.⁹

An experimental investigation of this method is presented in the following paper.

Theory

We consider a solution of polyions and small counterions. A number of the small ions are intimately associated with the polyion and are considered as bound. The remainder of the small ions are free. An exchange process of bound and free ions is imagined to take place continuously, the rate determined by a rate expression. If the charge of the free ions of interest is opposite to that of the polyion then electrolysis will cause each to flow in opposite directions. Under the conditions where the exchanging ion is tagged and a distinct boundary of highly tagged ions is formed, the distribution of tagged ions upon subsequent electrolytic flow is characterized by the exchange process and by the number bound and free. Wall and Grieger^{5a} solved this problem for the case of a moving boundary of tagged ions. We wish to apply this theory to the steady-state case in order to determine the distribution of tagged ions across a porous frit bounded by regions of different uniform tagged ion concentration. We start with the basic continuity equations of the exchange and flow process of Wall and Grieger^{5a} and solve these for the steady-state situation where the concentration of tagged ions is regarded as effectively zero on one side and very high on the other side of a frit. We first review the basic equations and apply these to a single exchange process. A similar development, which is outlined in the Appendix, is shown for the case of two exchange rates. Both of these situations are first-order simplifications for the diverse number of exchange rates probably present.

A. Differential Equations for Electrolytic Flow with Exchange (Wall and Grieger^{5a}).—We shall briefly review the case of a simple exchange process



where k is an average exchange constant, F denotes the free ion, B denotes a bound ion, and $*$ indicates a tagged species of ion. The increase in bound tagged ions at a specific location is given by

$$\frac{\partial [B^*]}{\partial t} = k[F^*][B] - k[F][B^*] \quad (2)$$

which acts as a source function in the continuity equations of the bound and free tagged ions. We shall consider only electrolytic flows of the polymeric and simple ions in one dimension. The total ion concentrations in the regions of interest are virtually uniform in view of the negligible concentrations of tagged ions.

(8) A. R. Gordon, *Ann. N. Y. Acad. Sci.*, **46**, 285 (1945).

(9) K. J. Mysels and H. W. Hoyer, *J. Phys. Chem.*, **59**, 1119 (1955).

For the one dimensional flow in the x direction the continuity equations become

$$\begin{aligned} -\frac{\partial \rho_i}{\partial t} &= v_i \frac{\partial \rho_i}{\partial x} + kn_p b_p (\rho_i - \rho_p) \\ -\frac{\partial \rho_p}{\partial t} &= v_p \frac{\partial \rho_p}{\partial x} - kn_i (\rho_i - \rho_p) \end{aligned} \quad (3)$$

where

- n_i = no. of free counterions per cc. soln.
- ρ_i = fraction of free counterions tagged
- n_p = no. of polymer ions per cc. soln.
- b_p = av. no. of counterions bound to polymer ion
- ρ_p = fraction of bound counterions tagged

The velocities are given by

$$\begin{aligned} v_i &= z_i \omega_i E \\ v_p &= z_p \omega_p E \end{aligned} \quad (4)$$

The symbols z_i and z_p denote the signed charges of the ion and polymer, and ω_i and ω_p denote the respective mobilities. The mobilities are related to the ionic equivalent conductance, λ_j , by $\lambda_j / (\mathcal{F}|z_j|)$, where \mathcal{F} is Faraday's constant.

B. Steady-State Solution.—We proceed from this point by stipulating that a steady-state has been established across the region of a frit. Then

$$\frac{\partial \rho_i}{\partial t} = \frac{\partial \rho_p}{\partial t} = 0 \quad (5)$$

and the continuity equations 3 can be written simply as

$$\begin{aligned} \frac{\partial \rho_i}{\partial x} + \gamma (\rho_i - \rho_p) &= 0 \\ \frac{\partial \rho_p}{\partial x} - \beta (\rho_i - \rho_p) &= 0 \end{aligned} \quad (6)$$

We define γ and β by

$$\gamma = \frac{kn_p b_p}{v_i} \text{ and } \beta = \frac{kn_i}{v_p} \quad (7)$$

The simultaneous equations 6 are solved¹⁰ from solutions of the form

$$\rho_i = A e^{mz}, \rho_p = B e^{mz} \quad (8)$$

which upon substitution gives the auxiliary requirement on m by the secular equation

$$\begin{vmatrix} \gamma + m & -\gamma \\ -\beta & \beta + m \end{vmatrix} = 0 \quad (9)$$

The two solutions of m are seen to be

$$m = 0, m = -(\beta + \gamma) \quad (10)$$

and the complete solutions for ρ_i and ρ_p after relating A and B are

$$\begin{aligned} \rho_i &= A_0 + A_1 e^{-(\beta+\gamma)x} \\ \rho_p &= A_0 - \frac{\beta}{\gamma} A_1 e^{-(\beta+\gamma)x} \end{aligned} \quad (11)$$

where A_0 and A_1 are constants to be determined by the boundary conditions.

C. Boundary Conditions for Bound and Free Tagged Ions.—When the motion of the polymer ions is opposite that of the tagged counterions, then a steady-state may be established which gives a variable distribution of bound and free tagged ions completely across the frit. The distribution will depend upon the direction the polymeric ions and the small ions travel. To visualize both pos-

(10) M. Morris and O. E. Brown, "Differential Equations," Revised Edition, Prentice-Hall, Inc., New York, N. Y., 1942, p. 119.

sibilities of direction consider a three-compartment cell formed by two frits as shown in Fig. 1. Let the center compartment contain a uniformly labeled concentration of tagged ions, which forms the small fraction ρ^0 of the total of that ionic species. Let the compartment and frit labeled by p denote the regions where the polymeric ions move from the center compartment upon electrolysis, and similarly the compartment and frit labeled by i as where the oppositely charged counterions move to. Again we assume that the concentration of tagged ions is negligible in the p and i compartments. The possible steady-state distribution is schematically represented in Fig. 1 by the lines describing ρ_i and ρ_p across the frits and into the center compartment, where both are assumed to be represented by ρ^0 . To simplify the discussion let both i and p frits have the same physical properties with an effective thickness L ; a distance from the left side of each frit as the origin is given by x_i and x_p . The boundary conditions can then be described by

$$\begin{aligned} \text{i frit: } x_i = 0, \rho_p = 0 \\ x_i = L, \rho_i = \rho^0 \\ \text{p frit: } x_p = 0, \rho_p = \rho^0 \\ x_p = L, \rho_i = 0 \end{aligned} \quad (12)$$

Equations 11 become

i frit

$$\begin{aligned} \frac{\rho_i(x_i)}{\rho^0} &= \frac{(\beta/\gamma) + e^{-(\beta+\gamma)x_i}}{e^{-(\beta+\gamma)L} + (\beta/\gamma)} \\ \frac{\rho_p(x_i)}{\rho^0} &= \frac{(\beta/\gamma) - (\beta/\gamma)e^{-(\beta+\gamma)x_i}}{e^{-(\beta+\gamma)L} + (\beta/\gamma)} \end{aligned}$$

p frit

$$\begin{aligned} \frac{\rho_i(x_p)}{\rho^0} &= \frac{e^{-(\beta+\gamma)L} - e^{-(\beta+\gamma)x_p}}{e^{-(\beta+\gamma)L} + (\beta/\gamma)} \\ \frac{\rho_p(x_p)}{\rho^0} &= \frac{e^{-(\beta+\gamma)L} + (\beta/\gamma)e^{-(\beta+\gamma)x_p}}{e^{-(\beta+\gamma)L} + (\beta/\gamma)} \end{aligned} \quad (13)$$

The flows of tagged ions into the i and p compartments are determined by the respective boundary values $\rho_i(x_i = 0)$, $\rho_p(x_p = L)$ of equations 13, by the concentrations of bound and free ions, and by the carrying velocities defined by v_i and v_p . The flows of tagged ions per unit area out of the respective frits into the i and p compartments are then

$$\begin{aligned} J_i &= n_i v_i \rho_i(x_i = 0) \\ J_p &= n_p b_p v_p \rho_p(x_p = L) \end{aligned} \quad (14)$$

The flows are accessible to experimental measurement by studying the change in low level tagged ion concentration in the appropriate end compartments.

Discussion

A. The Ratio of Tagged Ion Flows.—The ratio of the ion flows given by equations 14 yields a result which suggests the design of one type of experiment. Taking the ratio of the flows of equation 14 and recognizing the definitions of β and γ from equations 7 we have

$$\frac{J_p}{J_i} = \frac{\gamma_p \rho_p(x_p = L)}{\beta_i \rho_i(x_i = 0)} \quad (15)$$

The velocities as defined by equations 4 are directly influenced by the field E within the frit. For a given solution we assume that the mobilities and the charges are independent of the field strengths

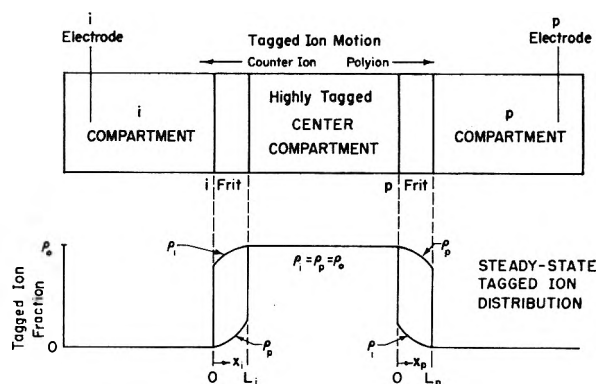


Fig. 1.—Schematic representation of tagged ion distribution with electrolysis across porous frits.

in the range where experiments will be run. This allows us to define two factors which will be independent of the field as

$$\begin{aligned} \beta' &= E\beta \\ \gamma' &= E\gamma \end{aligned} \quad (16)$$

The ratio of flows (equation 15) can then be written explicitly by using the definitions of equations 16 and the specific values of equations 13 as

$$\frac{J_p}{J_i} = (\gamma'/\beta') e^{-(\beta+\gamma)(L/E)} \quad (17)$$

A plot of the logarithm of the flow ratio *vs.* L/E would be linear if the one exchange constant theory held; the slope and the intercept enable β' and γ' to be determined. From these factors a determination of the rate constant and the fraction of ions bound is possible. The experimental conditions for equation 17 are obtained by using one frit and reversing the current.

The various factors of equation 17 can be better understood by writing this equation more explicitly using the definitions of β' and γ'

$$\frac{J_p}{J_i} = \frac{n_p b_p v_p}{n_i v_i} e^{-k \left(\frac{n_i}{v_p} + \frac{n_p b_p}{v_i} \right) L} \quad (18)$$

We observe that the flow ratio depends (among other things) on factors of length divided by the velocity of the free tagged ion and the polyion. Positive values of these terms represent the exposure times of the respective ions in the frit. They are defined by

$$t_i = \frac{L}{|v_i|} = \frac{\mathcal{F}L}{\lambda_i |E|} \quad \text{and} \quad t_p = \frac{L}{|v_p|} = \frac{\mathcal{F}L}{\lambda_p |E|} \quad (19)$$

The exposure times can be varied by using different electrolysis currents. Both t_i and t_p are proportional to the current.

Since the flows of free and bound tagged ions go in opposite directions (in the derivation v_i was chosen to have a negative value and v_p a positive value), the ratio J_p/J_i is negative. The magnitude of the ratio is given by use of the exposure times as

$$\left| \frac{J_p}{J_i} \right| = \frac{n_p b_p t_i}{n_i t_p} e^{-k(n_i t_p - n_p b_p t_i)} \quad (20)$$

or

$$\left| \frac{J_p}{J_i} \right| = \frac{n_p b_p t_i}{n_i t_p} e^{-k n_i t_i} \left(1 - \frac{n_p b_p t_i}{n_i t_p} \right) t_p \quad (21)$$

We see that a plot of $\ln |J_p/J_i|$ *vs.* t_p will have a

positive slope if the intercept $\ln[(n_p b_p t_i)/(n_i t_p)]$ is positive and a negative slope if the intercept is negative. The slope is proportional to the exchange constant. For very rapid exchange the ratio of flows may become unmeasurably large or small, depending on the intercept value. If the intercept is zero then a solution other than that given by equation 11 is required.

The fraction of ions bound can be determined from the intercept value along with the ratio t_p/t_i as

$$f_b = \frac{n_p b_p}{n_p b_p + n_i} = \frac{n_p b_p}{n_i} + 1 \quad (22)$$

$$= \left(\frac{n_p b_p t_i}{n_i t_p} \right) / \left(\frac{n_p b_p t_i}{n_i t_p} + \frac{t_i}{t_p} \right)$$

The reciprocal ratio of mobilities or ionic conductance if available could be used in place of the ratio of exposure times.

B. Frit Calibration.—Two methods for calibrating the frit are apparent from the preceding discussion. The first would be to measure directly t_p and t_i for the solution under investigation. This can be done by determining the time for radioactivity to appear across the frit when the frit originally contains non-radioactive solution. This method provides the best way to eliminate experimental variations in the frit as well as further theoretical assumptions.

A second method would involve the use of a simple electrolyte with known mobilities and specific resistance, r . The frit constant $L/|E|$ can be measured by determining the time t' for the ion of equivalent ionic conductance λ' to cross the frit. This time is given by equation 19 as

$$\frac{L}{|E'|} = \frac{t'\lambda'}{\mathfrak{F}} \quad (23)$$

Since the value of $|E'|$ is proportional to the current I and the specific resistance of the calibrating solution, we have in general

$$\frac{|E'|}{|E|} = \frac{r'I'}{rI} \quad (24)$$

which when combined with equation 23 gives

$$\frac{L}{|E|} = \frac{r'I't'\lambda'}{rI\mathfrak{F}} \quad (25)$$

Thus $L/|E|$ can be evaluated from measurements on the standard solution, conductivity, and current.

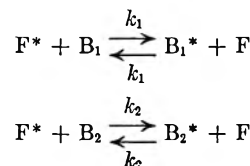
Conclusion

The theory of steady-state exchange processes during electrolytic flow reduces to simple equations when the ratio of tagged ion flows are evaluated under similar frit and current conditions. By studying this ratio for different currents, a test can be made on whether a single or a multiple rate of exchange is needed to describe the kinetics of the system. In the event the exchange is described by one or two exchange constants then an experimental evaluation of the rates is possible by this technique. The ratio of tagged ion flows extrapolated to zero frit exposure times affords a method for evaluating fractions of ion binding. The results of experiment will be described in a subsequent paper.

Appendix

Exchange Governed by Two Rate Constants

1. Equations of Continuity.—Consider the free ions exchange with the bound ions according to two exchange expressions



where tagged species is denoted by the * and the type of the bound species is either B_1 or B_2 . Let ρ_{p1} and ρ_{p2} signify the fraction of tagged bound ions held by regions 1 and 2 of the polymer, and b_{p1} and b_{p2} denote the number of ion sites per polymer molecule in the regions 1 and 2. The notation of the free ions is the same as before.

The exchange rates are then given at a point in space by

$$\frac{\partial[B_1^*]}{\partial t} = k_1 n_i n_p b_{p1} (\rho_i - \rho_{p1})$$

$$\frac{\partial[B_2^*]}{\partial t} = k_2 n_i n_p b_{p2} (\rho_i - \rho_{p2})$$

Combining these with the continuity equations and using the same assumptions as before on unidirectional flow and uniform macroscopic concentration yields the expressions

$$\frac{\partial \rho_i}{\partial t} = v_i \frac{\partial \rho_i}{\partial x} + (n_p b_{p1} k_1 + n_p b_{p2} k_2) \rho_i - n_p b_{p1} k_1 \rho_{p1} - n_p b_{p2} k_2 \rho_{p2}$$

$$\frac{\partial \rho_{p1}}{\partial t} = v_p \frac{\partial \rho_{p1}}{\partial x} - n_i k_1 \rho_i + n_i k_1 \rho_{p1}$$

$$\frac{\partial \rho_{p2}}{\partial t} = v_p \frac{\partial \rho_{p2}}{\partial x} - n_i k_2 \rho_i + n_i k_2 \rho_{p2}$$

2. Solutions under Steady-State.—We shall be concerned with finding a solution to the above equations under steady-state conditions where they reduce to

$$0 = \frac{\partial \rho_i}{\partial x} + (\gamma_1 + \gamma_2) \rho_i - \gamma_1 \rho_{p1} - \gamma_2 \rho_{p2}$$

$$0 = -\beta_1 \rho_i + \frac{\partial \rho_{p1}}{\partial x} + \beta_1 \rho_{p1}$$

$$0 = -\beta_2 \rho_i + \frac{\partial \rho_{p2}}{\partial x} + \beta_2 \rho_{p2}$$

where $\beta_1 = n_i k_1 / v_p$, $\beta_2 = n_i k_2 / v_p$

$$\gamma_1 = n_p b_{p1} k_1 / v_i, \quad \gamma_2 = n_p b_{p2} k_2 / v_i$$

Solutions to these equations are given by the forms

$$\rho_i = A e^{mz}, \quad \rho_p = B e^{mz}, \quad \text{and} \quad \rho_{p2} = C e^{mz}$$

which upon substitution yields the characteristic equation for m

$$\begin{vmatrix} m + (\gamma_1 + \gamma_2) & -\gamma_1 & -\gamma_2 \\ -\beta_1 & m + \beta_1 & 0 \\ -\beta_2 & 0 & m + \beta_2 \end{vmatrix} = 0$$

which reduces to

$$m \begin{vmatrix} 1 & -\gamma_1 & -\gamma_2 \\ 1 & m + \beta_1 & 0 \\ 1 & 0 & m + \beta_2 \end{vmatrix} = 0$$

The roots of this equation are given by

$$m_0 = 0$$

$$m_1 = \frac{-(\beta_1 + \beta_2 + \gamma_1 + \gamma_2) + \sqrt{[(\beta_1 + \beta_2 + \gamma_1 + \gamma_2)^2 - 4(\beta_1 \beta_2 + \gamma_1 \beta_2 + \beta_1 \gamma_2)]}}{2}$$

$$m_2 = \frac{-(\beta_1 + \beta_2 + \gamma_1 + \gamma_2) - \sqrt{[(\beta_1 + \beta_2 + \gamma_1 + \gamma_2)^2 - 4(\beta_1 \beta_2 + \beta_1 \gamma_2 + \beta_2 \gamma_2)]}}{2}$$

With these three roots the constants A , B , and C are interrelated and the complete solution of the equations can be written as

$$\begin{aligned}\rho_i &= A_0 + A_1 e^{m_1 x} + A_2 e^{m_2 x} \\ \rho_{p1} &= A_0 + \frac{\beta_1}{\beta_1 + m_1} A_1 e^{m_1 x} + \frac{\beta_1}{\beta_1 + m_2} A_2 e^{m_2 x} \\ \rho_{p2} &= A_0 + \frac{\beta_2}{\beta_2 + m_1} A_1 e^{m_1 x} + \frac{\beta_2}{\beta_2 + m_2} A_2 e^{m_2 x}\end{aligned}$$

3. Boundary Conditions.—We again consider boundary conditions that are very similar to the case of one exchange rate, except that now we have to stipulate ρ_{p1} and ρ_{p2} . For the sake of simplicity we shall consider the p frit has the same thickness as the i frit, and concentration fractions are shown for both frits in Fig. 2. The concentration fractions which will determine the flow of tagged ions into the i and p compartments are the boundary values $\rho_i(0)$ and $\rho_{p1}(L)$, $\rho_{p2}(L)$. With the above boundary conditions these are given as

$$\begin{aligned}\rho_i(0) &= \frac{\rho_0 m_1 m_2 (\beta_1 - \beta_2)(m_1 - m_2)}{D(\beta_1 + m_1)(\beta_1 + m_2)(\beta_2 + m_1)(\beta_2 + m_2)} \\ \rho_{p1}(L) &= \frac{\rho_0 m_1 m_2 (\beta_1 - \beta_2)[(\beta_2 + m_1)X - (\beta_2 + m_2)Y]}{D(\beta_1 + m_1)(\beta_1 + m_2)(\beta_2 + m_1)(\beta_2 + m_2)} \\ \rho_{p2}(L) &= \frac{\rho_0 m_1 m_2 (\beta_1 - \beta_2)[(\beta_1 + m_1)X - (\beta_1 + m_2)Y]}{D(\beta_1 + m_1)(\beta_1 + m_2)(\beta_2 + m_1)(\beta_2 + m_2)}\end{aligned}$$

where $X = e^{m_1 L}$, $Y = e^{m_2 L}$, and

$$D = \begin{vmatrix} 1 & X & Y \\ 1 & \frac{\beta_1}{\beta_1 + m_1} & \frac{\beta_1}{\beta_1 + m_2} \\ 1 & \frac{\beta_2}{\beta_2 + m_1} & \frac{\beta_2}{\beta_2 + m_2} \end{vmatrix}$$

As in the case of the single rate of exchange case discussion, these equations assume a particularly simple form when the ratio of flows into the p compartment and the i compartment is determined

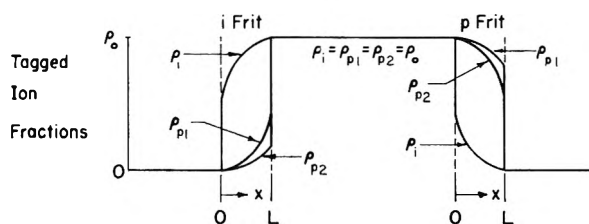


Fig. 2.—Boundary conditions and distributions of tagged ion fractions (ρ) for case of two rates of exchange.

$$\begin{aligned}\frac{J_p}{J_i} &= \frac{\gamma_1 \rho_{p1}}{\beta_1 \rho_i} + \frac{\gamma_2 \rho_{p2}}{\beta_2 \rho_i} \\ &= \frac{1}{m_1 - m_2} \left\{ \frac{\gamma_1}{\beta_1} [(\beta_2 + m_1)X - (\beta_2 + m_2)Y] + \right. \\ &\quad \left. \frac{\gamma_2}{\beta_2} [(\beta_1 + m_1)X - (\beta_1 + m_2)Y] \right\}\end{aligned}$$

which can be written as

$$\frac{J_p}{J_i} = \frac{1}{m_1 - m_2} [D_1 e^{m_1 L} - D_2 e^{m_2 L}]$$

where $D_1 = \begin{vmatrix} \frac{\gamma_1}{\beta_1} & \frac{\gamma_2}{\beta_2} \\ -(\beta_1 + m_1) & (\beta_2 + m_1) \end{vmatrix}$ and

$$D_2 = \begin{vmatrix} \frac{\gamma_1}{\beta_1} & \frac{\gamma_2}{\beta_2} \\ -(\beta_1 + m_2) & (\beta_2 + m_2) \end{vmatrix}$$

This expression reduces to that given for the single exchange case when we let k_2 and b_{p2} equal zero.

The plot suggested before of the logarithm of the flow ratio vs. L/E would generally give a curved line for the two exchange constant case. Similar conclusions can be drawn when more exchange rate processes are considered, but in general, it will be extremely difficult to evaluate anything more than the two exchange constants.

TRANSFERENCE STUDIES OF SODIUM POLYACRYLATE UNDER STEADY-STATE ELECTROLYSIS¹

BY GUY V. FERRY² AND STANLEY J. GILL

Department of Chemistry, University of Colorado, Boulder, Colorado

Received August 28, 1961

A study of ion binding with partially neutralized sodium polyacrylate using a steady-state electrolysis technique is reported. The fraction of ions bound tightly is negligible below 40% neutralization and increases to approximately 0.50 at 95% neutralization. From the nature of the technique employed, these fractions apply to bound ions which exchange slowly. A half-life of exchange of five minutes was determined for the 95% neutralized sodium polyacrylate. The strong binding is in accord with the ion pair interaction theory suggested by Harris and Rice.

Introduction

In the preceding paper³ a method for determining the rates of exchange between bound and free counterions has been discussed.

In this paper we wish to present an application of this method to the system of polyacrylic acid partially neutralized with sodium hydroxide. One finding of these experiments was the smaller values for the fraction of bound ions than had been obtained by Huizenga, Grieger, and Wall⁴ using a different

electrolysis technique. This is not inconsistent with the over-all nature of polyion binding and is discussed in the light of current theories of ion association with polyelectrolytes.⁵⁻⁸

Experimental

A. Apparatus.—A number of differently designed pieces of electrolysis equipment were constructed. The final apparatus is shown in Fig. 1. It consists of two frit bounded compartments with connections to silver-silver chloride electrodes. The porosity of the center frit was fine and the other frits coarse (Corning). Standard frits were used of approximately 2-mm. thickness and 25-mm. diameter. The

(1) This work was supported in part by P.H.S. Grant No. C-5393 from The National Cancer Institute, Public Health Service.

(2) Part of a thesis to be submitted by Guy V. Ferry in partial fulfillment of a Master of Science degree, University of Colorado.

(3) S. J. Gill and G. V. Ferry, *J. Phys. Chem.*, **66**, 995 (1962).

(4) J. R. Huizenga, P. F. Grieger, and F. T. Wall, *J. Am. Chem. Soc.*, **72**, 2636 (1950).

(5) F. T. Wall, *J. Phys. Chem.*, **61**, 1344 (1957).

(6) F. E. Harris and S. A. Rice, *ibid.*, **58**, 725 (1954).

(7) S. A. Rice and F. E. Harris, *ibid.*, **58**, 733 (1954).

(8) S. A. Rice, *Revs. Mod. Phys.*, **31**, 69 (1959).

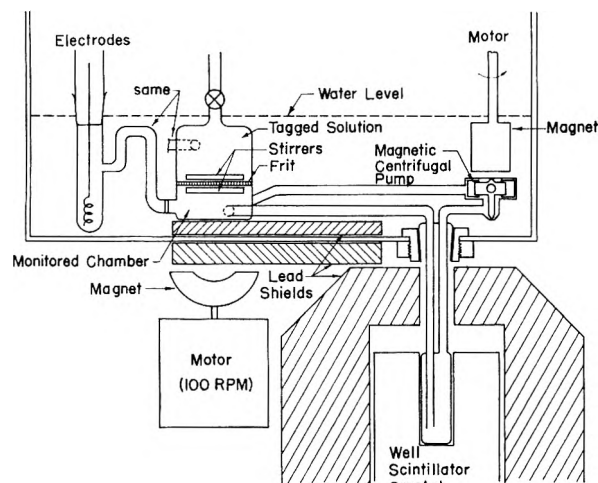


Fig. 1.—Steady state electrolysis apparatus with scintillation detector.

center frit was swept on both sides by magnetic stirrer bars, one of which was made to float.

In order to determine continuously the activity in the low level compartment, a small centrifugal pump was devised to circulate its contents through a tube that could be situated within a shielded scintillation detector. Approximately 5 cc. from a total of 40 cc. was monitored for radioactivity. The centrifugal pump was driven by the action of a rotating magnet. The apparatus was placed in a special thermostated bath, which had a tapered fitting in its base, so that the monitored tube extended beneath the bath into the scintillation detector. Additional lead shielding was placed between the highly tagged radioactive solution and the scintillation detector. In this way a background rate of about twice normal was obtained with radioactivity only in the top compartment. The efficiency of the circulating pump was tested before its incorporation in the apparatus and found to circulate the contents of the monitored compartment in less than 10 sec. under operating conditions.

Incorporation of Teflon stopcocks and Teflon sleeves for the electrode compartment connections enabled the elimination of all possible stopcock grease contamination upon the sintered frits.

The scintillation detector and associated counting apparatus consisted of a Baird Atomic γ -ray spectrometer connected to a Baird Atomic Model 432 ratemeter. The ratemeter output was recorded on a Brown recording potentiometer.

Electrolysis current was provided by a constant current regulator as described by Proctor.⁹

B. Experimental Conditions and Procedure.—The apparatus was filled with non-radioactive solution, taking special care to remove all bubbles from the apparatus and its frits. In a typical run, approximately 25 microcuries of radioactive sodium ion,¹⁰ which was contained in 0.025 cc., was added to 50 cc. of polyacrylate solution and from 6–12 hr. later this solution was exchanged with the similar but non-radioactive solution in the top compartment of the electrolysis apparatus. A few minutes were allowed for the slight thermal equilibration between the added solution and bath before starting electrolysis. Special filling procedures also were investigated in order to determine if the time of radioactive equilibration was important. The most significant of these was the direct addition of 0.025 cc. of radioactive sodium ion directly to the polyacrylate solution in the top compartment, followed by a minute of stirring, and electrolysis. No difference in crossing times or flow rates was discernible between this mode of addition and that of the equilibrated solution.

The electrode compartments were prepared by adding enough saturated KCl under the polyacrylate solution in the electrode compartment, so that the silver-silver chloride electrodes were completely immersed in KCl solution. Air was excluded when the electrodes were put in place.

(9) C. M. Proctor, *Anal. Chem.*, **28**, 2032 (1956).

(10) Carrier-free Na^{22} as sodium chloride in 0.5 *N* HCl, obtained from Nuclear Science and Engineering Corp., Pittsburgh, Pa.

The apparatus was placed in a thermostated water-bath at $25 \pm 0.05^\circ$, and the magnetic stirring equipment then was adjusted and tested for satisfactory alignment. When thermal equilibrium was achieved, radioactivity or radioactive solution was placed in the radioactive compartment. It was found that a time of crossing the frit for the free tagged sodium ion in the polyacrylate mixture could be determined directly by noting the sudden increase in the low level compartment of the monitored activity level. Similarly, after the frit was cleaned by electrolysis with non-radioactive solution in the high level compartment, the tagged solution replaced, and electrolyzed with the current reversed, a time for the polymer to cross the frit could be determined. This provides the necessary calibration data for the system under investigation. Electrolysis then was continued until a steady rate of radioactive flow was noted on the recorder chart. This was repeated for each current value and each direction of current.

During the course of a run, no more than 10% of the high level activity was removed by electrolysis. The activity in the low level compartment did not exceed 4% of that in the high level compartment.

Solutions of various degrees of neutralization of polyacrylic acid,¹¹ standardized at about 0.04 *N* with respect to monomer groups, were used in these investigations. The concentration of PAA was determined by drying an aliquot of the acid form at 120° until constant weight readings were obtained. The pH of the solutions was determined by a Beckman Model GS pH meter, and conductivity was measured using a Serfass conductivity bridge with a cell calibrated with standard KCl solutions.

C. Preliminary Observations.—Several important results were noted with earlier models of electrolysis apparatus. These results led to the apparatus described above.

It had been noticed that significant electro-osmosis with fine or medium frits could take place if the compartments on each side of the frit were open to the atmosphere during electrolysis. This effect was reduced or eliminated by the use of non-gassing electrodes. Thermal expansion was reduced by thermostating the apparatus in a water-bath.

The possible importance of electro-osmotic circulation within the frit also was investigated. The apparatus was filled with 0.01 *N* NaCl and sucrose was placed into one of the fritted compartments. The sucrose diffusing into the adjacent compartment was sampled as a function of time for a fixed current setting. The results showed that the flow of sucrose in the presence of an electric current was measurably higher but of the same order as with diffusion without any current. We concluded that electro-osmosis was not serious in such an apparatus and that an expected internal electro-osmotic circulation within the frit did not contribute to an effective transport across the frit by convection. A conclusion of this type has been discussed by Mysels and Hoyer.¹²

The heating effect within the frit for a typical solution with a specific conductance of 10^{-3} ohm⁻¹ cm.⁻¹ can be estimated by measurements of crossover times or by the resistance between electrodes placed close against the frit. Both methods gave a resistance of about 200 ohms. For a current of 0.01 amp. the voltage drop is 2 volts and the heat generated is 0.02 watt.

Stirring of frits has been studied in connection with diffusion measurements.¹³ We performed similar tests and found that radioactive sodium chloride could be pumped through a medium porosity frit, when the stirrer swept the surface of the frit. Consequently, we turned to the use of fine frits which did not give this effect. A low rate of stirring, about 100 r.p.m., also was used since the high rates with the medium frits produced noticeable pumping.

These and other initial observations were made by monitoring the radioactivity by taking small samples during the course of electrolysis. The accuracy and difficulty in determining when a steady-state condition of flow had been reached led to the development of the apparatus for continuous monitoring.

(11) We are grateful to Rohm and Haas in providing us with samples of polyacrylic acid, Acrysol, Grade A-3 (Mol. Wt.—130,000).

(12) K. J. Mysels and H. W. Hoyer, *J. Phys. Chem.*, **59**, 1119 (1955).

(13) R. H. Stokes, *J. Am. Chem. Soc.*, **72**, 763 (1950).

Calculations and Results

In the preceding paper it was shown how the use of ratios of the steady-state flows of tagged ions toward the cathode and anode could be used for investigating polyelectrolyte ion exchange. The simple one exchange constant theory seems adequate for the results we have found with sodium polyacrylate solutions.

The equation needed for the experiments performed is

$$\left| \frac{J_p}{J_i} \right| = \frac{n_p b_p t_i}{n_i t_p} e^{-k(n_i t_p - n_p b_p t_i)} \quad (1)$$

where J_p and J_i represent the flows of radioactive ions carried by the polyelectrolyte or the free ions through a frit under an electric field. The number of polyions per cc. is n_p with an average b_p counterions bound to each polyion. There are n_i free counterions (sodium) per cc. The rate of exchange is governed by a single exchange process with constant k . The time for the free sodium ions to cross the frit is t_i and the time for the tagged polyion is t_p .

As was noted in the previous paper, the intercept value, $\ln|J_p/J_i|_0$, of the plot of $\ln|J_p/J_i|$ vs. t_p has the same sign as the slope. However, if the slope is very small then its sign may be difficult to detect. Figure 2 illustrates two cases of the steady-state flows vs. current. If exchange is not taking place, or is too slow to be measured, the steady-state flows should increase proportionally with the current and a straight line should pass through the experimental points and the origin. If measurable exchange takes place, upward curvature should be present, *i.e.*, at higher currents less time is available for exchange which reduces the flow in the given direction. Only in the case of 95.0% neutralized PAA was such curvature clearly indicated. For this reason only for the 95.0% neutralized PAA is a half-life calculated. In the case of the flow for the polymer at low percentages (40 and 50) of neutralization, it was found that a straight line passing through the experimental points would not pass through the origin. This difference, detectable only where the flow of radioactivity is very small, is attributed to diffusion and possibly electro-osmotic circulation. The amount of the zero current flow is subtracted from the flow at each current measured to calculate the fraction bound. Calculations show that diffusion without current is of the same order of magnitude as the zero current flow. Calculations for diffusion against electric current are not this high. However, as was indicated previously, internal electro-osmotic circulation is of about the same order as diffusion.

A. Calculation of the Fraction Bound by t_i and t_p .—As might be expected, the times t_p and t_i were found to be inversely proportional to the current. A set of early experiments with lower accuracy shows this effect in Table I for the case of 70% neutralized 0.04 N PAA. Table II summarizes our results for solutions at different neutralizations.

The fraction bound is determined by

$$f_b = \frac{n_p b_p}{n_i + n_p b_p} \quad (2)$$

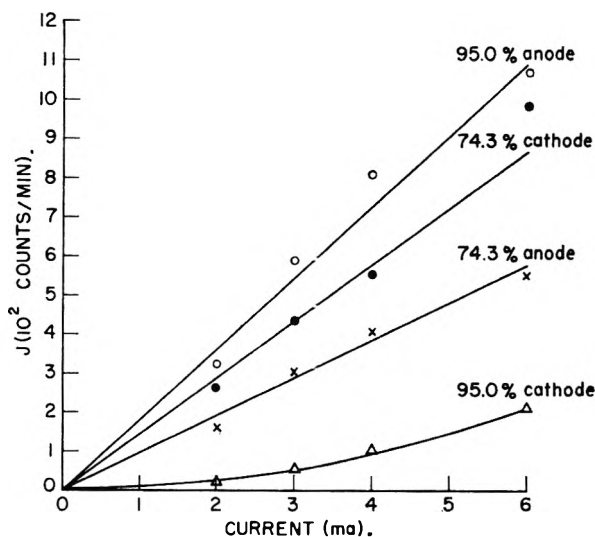


Fig. 2.—Plots of radioactive flow values vs. electrolysis current.

TABLE I
CROSSOVER TIMES AT DIFFERENT CURRENTS FOR 70%
NEUTRALIZED 0.04 N POLYACRYLIC ACID

Current, ma.	t_p , mi.	t_i , min.
6.0	5 ± 1	6 ± 1
4.0	8.5	11
2.0	17	17

TABLE II
SUMMARY OF ELECTROLYSIS RESULTS FOR VARIOUS NEU-
TRALIZATIONS OF 0.042 N POLYACRYLIC ACID

Soln. % neutral- ized	Flow ratios ($ J_p/J_i $) for given current				Times of crossing at 4 ma., min.	
	2 ma.	3 ma.	4 ma.	6 ma.	t_p	t_i
40 ^a	0.0032	0.0037	0.0020	0.0030	9.0	2.8
50 ^a	.054	.052	.050	.040	5.7	3.0
60	.18	.15	.11	.09	9.5	4.9
74	.64	.59	.51	.44	6.0	9.0
80	2.5	2.4	1.9	1.6	7.8	13.2
95	16.6	9.0	6.2	4.2	6.9	19.5

^a Flow ratios corrected for non-electrolytic flow.

for the simple case of partially neutralized polyacrylic acid. The intercept current ratio of flows gives

$$\left| \frac{J_p}{J_i} \right|_0 = \frac{n_p b_p t_i}{n_i t_p} \quad (3)$$

Combining equation 2 with 3 gives for the fraction bound

$$f_b = \frac{\left| \frac{J_p}{J_i} \right|_0}{\left| \frac{J_p}{J_i} \right|_0 + \frac{t_i}{t_p}} \quad (4)$$

The results from this calculation are found in Table III.

Several runs were made by adding the radioactivity to the PAA solution at different times before the solution was placed in the apparatus and electrolysis was started. In no case was there any discernible effect due to this change in equilibration time upon the measured crossing times or flow values.

B. Alternate Calculation of the Fraction Bound by Use of Conductivity Data.—From the previous

TABLE III
CALCULATIONS OF ION BINDING

Soln. % neutralized	$ J_p/J_i _0$	t_i/t_p	Frac. bound calcd. by A (Text)	Frac. bound calcd. by B (Text)	pH	$\kappa \times 10^3$, mho/ cm. ²
40	0.0030	0.31	0.0095	0.0044		1.10
50	.051	.53	.089	.134	5.92	1.13
60	.131	.52	.20	.24	6.44	1.26
74	.60	1.50	.29	.47	6.70	1.28
80	1.30	1.69	.44	.56	7.07	1.38
95	2.8	2.8	.51	.67	7.74	1.43

paper it has been noted that the intercept ratio is also determined by the ionic conductivities λ_i and λ_p

$$\left| \frac{J_p}{J_i} \right|_0 = \frac{n_p b_p \lambda_p}{n_i \lambda_i} \quad (5)$$

The specific conductivity, κ , of the solution is represented by

$$\kappa = N_{av}^{-1}(z_i n_i \lambda_i - z_p n_p \lambda_p) \quad (6)$$

where z_i and z_p are the free ion and polyion charges, and N_{av} is Avogadro's number.

Electroneutrality at near neutral pH's is determined by

$$z_i n_i + z_p n_p = 0 \quad (7)$$

The sodium ion balance is represented by the total sodium ion concentration n_i^0

$$n_i^0 = n_i + n_p b_p \quad (8)$$

Combining these equations to eliminate n_p , b_p , λ_p , and z_p , we arrive at n_i in terms of experimental parameters and λ_i

$$n_i = \frac{\kappa N_{av} + n_i^0 z_i \lambda_i \pm [(\kappa N_{av} + n_i^0 z_i \lambda_i)^2 - 4 z_i \lambda_i (1 - |J_p/J_i|_0) n_i^0 \kappa N_{av}]^{1/2}}{2 z_i \lambda_i [1 - |J_p/J_i|_0]} \quad (9)$$

This may be combined with the sodium ion balance equation to calculate f_b . Only the negative sign in equation 9 gives a physically permissible answer. In order to use this equation it is necessary to assume a value of λ_i for the sodium ion. Following Wall in this case we have chosen a value of 46 for λ_i at 25°. The results from this calculation are found in Table III.

The values calculated by this method depend upon several assumptions. The first is that the same free ions and polyion species determine the conductivity and determine the results given by the tagged flow experiment. If part of the bound ions undergo rapid exchange, the flow measurements would not include this fraction, whereas the conductivity measurements would. Another assumption is the choice of an ionic conductance for the sodium ion. This has been discussed recently by Martin¹⁴ and also by Wall.⁴ It was found that no single value for λ_i could be used to make the results from this calculation similar to those using t_i and t_p .

C. Calculation of the Rate Constant.—Under favorable circumstances, k may be determined from a plot of $\ln |J_p/J_i|$ vs. t_p as given by equation 1. The slope, s , of this plot is related directly to k as

$$s = -k n_i \left(1 - \frac{n_p b_p t_i}{n_i t_p} \right) \quad (10)$$

It is perhaps more informative to look at the half-life, $t_{1/2}$, of exchange.

The rate of exchange in terms of the fraction of bound tagged ions, ρ_p , is given by

$$\frac{\partial \rho_p}{\partial t} = k n_i (\rho_i - \rho_p) \quad (11)$$

where ρ_i is the fraction of free ions that are tagged.⁴ The total sodium ion content is

$$n^0 = n_i + n_p b_p \quad (12)$$

of which a total fraction ρ^0 are tagged and given by

$$n^0 \rho^0 = n_i \rho_i + n_p b_p \rho_p \quad (13)$$

With these expressions the rate process can be written as

$$\frac{\partial \rho_p}{\partial t} = k n^0 (\rho^0 - \rho_p) \quad (14)$$

and the time for loading an initially untagged polyion to a fraction $1/2$ ρ^0 would be

$$t_{1/2} = 0.693/k n^0 \quad (15)$$

The close similarity of this half-life expression with that of a pure first-order reversible reaction is due to effective constant concentrations of bound and free untagged sodium ions in the second-order exchange process.

Combining equation 15 with 10 and using (4) gives

$$t_{1/2} = - \frac{0.693[1 - |J_p/J_i|_0](1 - f_b)}{s} \quad (16)$$

For 0.0424 N PAA-95.0% neutralized with NaOH, $t_{1/2} = 4.5$ min.

Discussion

Figure 3 shows plots of fraction bound vs. per cent. neutralization plots for Wall and co-workers' results⁴ and Harris and Rice's calculations⁸ as well as our own. From the nature of the method we have employed, our fractions represent the counterions that are tightly bound, in other words those that exchange very slowly. In Wall's method the fraction includes total binding independent of the rate of exchange of various species. The difference between our fraction bound and that determined by Wall would represent counterions that are loosely bound. As the neutralization increases, the fraction of tightly bound ions increases while the fraction of loosely bound ions decreases. This idea of tightly and loosely bound ions has been suggested by Wall and co-workers to explain some of their results. Our evidence substantiates this idea.

Although the concept of various degrees of binding seems intuitively correct, the tightness of binding of the tightly bound ions is surprising. If the migration of ions to and from a bound condition within the polyion was governed by simple diffusion, such as occurs when sodium ion diffuses within a concentrated solution of sodium chloride, then the half-life of exchange would be of the order of 10^{-5} sec. to react within a region of a 500-Å. radius. Only at high degrees of neutralization could we detect a rate constant. At low degrees of neutralization, the inherent difficulty in obtain-

(14) W. H. Martin and Q. Van Winkle, *J. Phys. Chem.*, **63**, 1539 (1959).

ing sufficient accuracy did not permit the determination of a rate constant, although it must be small since the effect of current on J_p/J_i is so slight. However, the rate constant determined for 95% neutralized PAA was very similar to the estimate by Wall and co-workers.

In order to explore the observation that no difference could be detected between runs made when the activity was added directly to the radioactive compartment just before the run and when the activity was allowed to equilibrate for 12 or more hours, some preliminary runs have been made using similar solutions but with added salt. It was found that the fraction bound drops very rapidly, *i.e.*, considerably more than predicted, with the addition of very small amounts of salt. Since the radioactivity was added from a strongly ionic solution, possibly a localized space of high ionic strength would form at the point of addition and allow the radioactive sodium to exchange rapidly when first added.

At low degrees of neutralization the slope of the plot of $\ln |J_p/J_i|_0$ vs. t_p was opposite to that required by theory. A possible explanation, other than the experimental error at these low neutralizations, would be given if the fraction bound depends upon the speed with which the polymer ion were moving. An effect of this type has been noted by Wall and co-workers.¹⁵ At low degrees of neutralization the charge on the polymer would be less and thus the tightness of the binding might be less, permitting the bound ions to be torn away at higher field strengths.

(15) F. T. Wall, H. Terayama, and S. Techokumpuch, *J. Polymer Sci.*, **20**, 477 (1956).

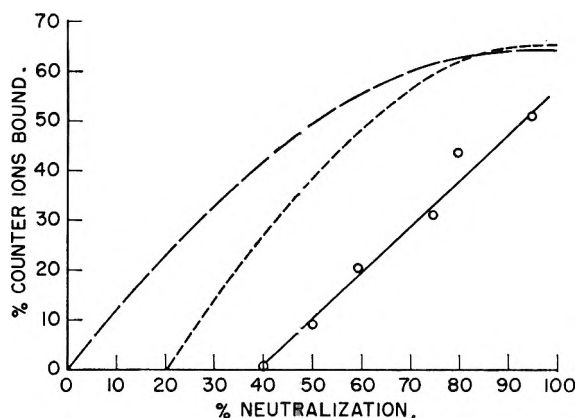


Fig. 3.—Per cent. sodium ion bound vs. per cent. neutralization; results of Wall and co-workers (— · —), calculations of Harris and Rice (---), and results from this work (O) with solid line.

The tightness of binding suggests some type of site binding similar to that suggested by Harris and Rice.^{6,7} The plot of tight fraction bound vs. per cent. neutralization follows the general theoretical predictions of Rice and Harris, who suggested specific ion pair binding between a sodium ion and a specific negatively charged group on the polymer. Their calculations showed that no binding should take place at low degrees of neutralization. This would agree with our results.

Acknowledgments.—We wish to thank both Mr. Frank Burlingame and Dr. Mancourt Downing for discussions on various aspects of this work.

STANDARD FREE ENERGY OF FORMATION OF MONOGERMANE

BY M. M. FAKTOR

Post Office Engineering Research Station, Dollis Hill, London, N.W. 2, England

Received September 4, 1961

An upper limit for the standard chemical potential of gaseous monogermane ($\mu^0_{\text{GeH}_4}$) is derived from measurements of the potentials of electrodes at which dissolved germanium species are being reduced to monogermane. Satisfactory agreement with the value of $\mu^0_{\text{GeH}_4}$ calculated from recent indirect thermochemical measurements is observed. The mechanism of reduction is discussed, tentatively, in terms of a number of volatile germanium compounds detected in the cathode gas, which had not been reported previously.

Introduction

Monogermane is a well characterized compound of germanium which recently has come to the fore in semiconductor technology. When the present work was begun no thermodynamic data for monogermane were available other than Latimer's estimated standard electrode potential¹ for the hypothetical half-reaction $\text{GeH}_4 \rightarrow \text{Ge} + 4\text{H}^+ + 4\text{e}^-$. Arguing that the compound is endothermic, and yet requires a fairly high temperature to decompose it, Latimer¹ suggest an oxidation potential of -0.3 v. or more negative.

A very recent paper by Gunn and Green² gives

(1) W. M. Latimer, "Oxidation Potentials," 2nd ed., Prentice Hall, New York, N. Y., 1952.

(2) S. R. Gunn and L. G. Green, *J. Phys. Chem.*, **65**, 779 (1961).

the standard heats of formation for a number of gaseous hydrides, including monogermane and monostannane, derived from measured heats of decomposition of the hydrides in admixture with stibine. Their values, together with available entropy data for germanium,³ hydrogen gas, and monogermane,⁴ lead to a value of $+28 \pm 0.5$ kcal. mole⁻¹ for the standard free energy of formation of monogermane. Since monogermane has been prepared repeatedly⁵⁻⁷ by electrochemical

(3) O. Kubaschewski and E. L. Evans, "Metallurgical Thermochemistry," Pergamon Press, London and New York, 1958.

(4) W. L. Jolly, "Some Problems in the Chemistry of Germanium" (thesis), Radiation Laboratory, University of California, 1952. United States Atomic Energy Commission UCRL-1638, Technical Information Service, Oak Ridge, Tennessee.

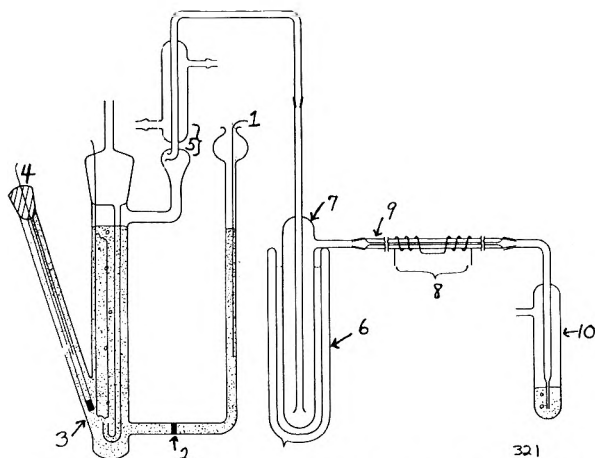


Fig. 1.—Electrolytic cell; 1, platinum anode; 2, glass sinter; 3, platinum cathode; 4, calomel electrode; 5, spray trap and water cooled condenser; 6, dewar vessel; 7, cold trap; 8, heating coils; 9, silica capillary; 10, bubbler.

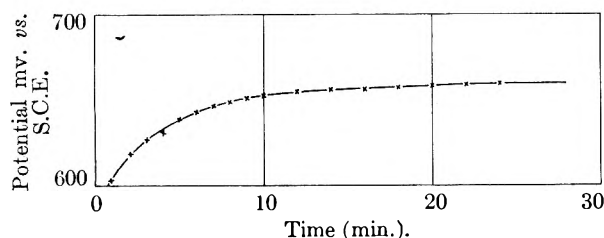


Fig. 2.—Variation of overpotential with time.

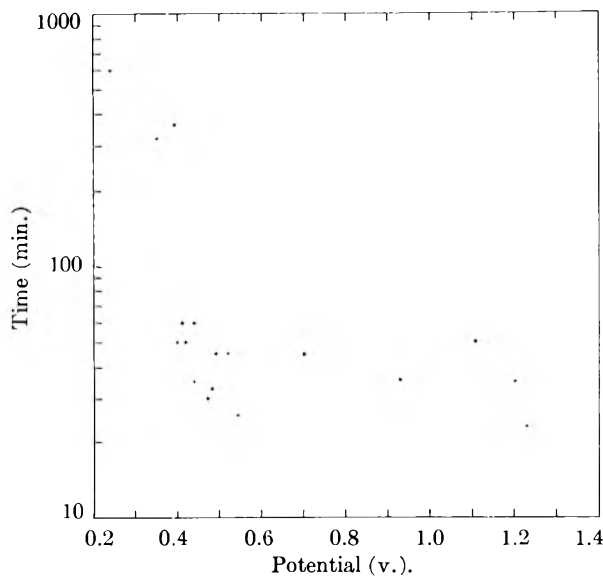


Fig. 3.—Time taken to form a standard Ge mirror vs. potential (hydrogen scale).

reduction, it should be possible to estimate an upper limit for its standard free energy of formation given sufficient information on the chemical reactions involved, the operating electrode potentials, and the monogermane content of the cathodic gases. Unfortunately, this information is not specifically available, and attempts to ascribe

(5) F. Paneth and E. Rabinowitsch, *Ber. deut. chem. Ges.*, **58**, 1138 (1925).

(6) S. A. Coase, *Analyst*, **59**, 462 (1934).

(7) J. Bardeleben, *Z. physik. Chem. (Frankfurt)*, **175**, 39 (1958).

operating potentials on the basis of reported current densities and known hydrogen overpotentials for the particular electrodes yielded an unacceptably high value for the standard free energy of formation of monogermane.⁸ A re-investigation of the electrolytic production of monogermane, with particular emphasis on the parameters needed for the computation of $\mu^0_{\text{GeH}_4}$, was clearly required. It was carried out under conditions of low pH, when the complexity of solutions containing quadrivalent germanium species is at its minimum.

Experimental

The cell used is illustrated in Fig. 1. It was immersed in a thermostat at $25 \pm 0.01^\circ$. Both the cathode and the anode compartment were filled with analytical reagent grade 2 *N* sulfuric acid, saturated with hexagonal germanium dioxide (semiconductor grade, arsenic content not more than 0.1 p.p.m.). The anode was of platinized platinum, 4 cm.² in apparent area. The cathode was either of monocrystalline germanium (both n- and p-type were used, 4 cm.² in apparent area, well etched in hydrogen peroxide), or a bright platinum sheet 45 cm.² in apparent area. The cathode potential was measured with respect to that of a saturated calomel electrode over a range of polarizing currents. A conventional d.c. potentiometer circuit, and a high impedance, constant current source, were used. The behavior of the platinum cathode potential with time is exemplified in Fig. 2.

The presence of germanium species in the cathode gas could be detected either by locally heating to 500° a silica tube carrying the evolved gas (resulting in an appearance of a mirror just beyond the point at which the heat was applied) or by collecting the yield in a suitable cold trap cooled in liquid air. The cold trap then was evacuated to a pressure of 10^{-2} mm., attached to a mass spectrometer, allowed to warm up to 0° , and the mass spectrum of the cold trap contents was investigated. Blank experiments using both methods of detection were carried out on the solutions, in the absence of germanium, to establish that the system was free from interfering materials.

At the beginning of each experiment the cell was swept out with hydrogen gas, deoxygenated by means of a commercial ("Deoxo") palladized alumina catalyst for 48 hr. Subsequently, the cell was swept for 24 hr. whenever a change in current density was carried out. During the experiments a slow stream of hydrogen was passed through the cell to prevent local and temporary build-up of gaseous cathodic products.

Results

Using p- and n-type germanium electrodes at a potential of -1.05 v. (current through the cell 40 ma.) and in the absence of added germanium dioxide, no mirror could be detected in 9.5 hr. The germanium cathodes then were replaced by a large-area bright platinum cathode and the electrolyte was saturated with hexagonal germanium dioxide. A plot of electrode potential against the logarithm of the time taken for the mirror to form is displayed in Fig. 3. As can be seen from Fig. 3 no single value can be ascribed to the slope. The large value of the slope at high overpotential is indicative of diffusion playing a part in the process. However, the lowest value at which monogermane is formed is seen to be -240 mv. (on the hydrogen scale). The reproducibility of the time taken for the formation of the mirror is tolerable at low overpotentials, but it becomes significantly worse at the higher overpotentials.

The mass spectrometric investigation of the cathodic gas clearly revealed in addition to the

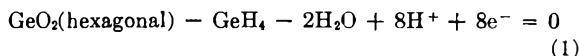
(8) J. I. Carasso and M. M. Faktor, "The Electrochemistry of Semiconductors," P. J. Holmes, Ed., Academic Press, London and New York, to be published.

monogermane spectrum covering the M/e range from 70 to 79, three other families of peaks, removed from monogermane by approximately 16, 32, and 48 mass units and decreasing in amplitude with increasing mass. Because of the low resolution of the mass spectrometer at high mass numbers, an uncertainty of ± 2 mass units attaches to the spacings between families of peaks. A comparison of these results with recent work⁹ on the mass spectrum of monogermane confirmed both the identity of the major constituent, monogermane, and the fact that the higher mass constituents are peculiar to electrolytically evolved, unpurified cathodic gas obtained under the experimental conditions described above. The higher-mass constituents were found to be relatively short-lived, their concentration decreased approximately fivefold on standing overnight at 0°, and they were not examined further.

Discussion

The failure of germanium cathodes to evolve detectable amounts of monogermane, at the potentials employed in this investigation, from a solution containing no dissolved germanium species, confirms earlier reports^{7,10} that the reaction $\text{Ge} + 4\text{H}^+ + 4\text{e}^- \rightarrow \text{GeH}_4$ is opposed by a high activation energy barrier.

Assuming that the electrolyte was in good solubility equilibrium with solid hexagonal germanium dioxide, the relevant half-reaction can be written as



for which the equilibrium electrode potential is given by

$$E = E^0 - 0.0591 \text{ pH} - 0.0074 \log P_{\text{GeH}_4} \quad (2)$$

$$\text{and } E^0 = \frac{\sum \gamma \mu}{23060n} \quad (3)$$

where the symbols have their usual meaning. For a reaction proceeding at a finite rate

$$E_{\text{obs}} > E \quad (4)$$

and the observed electrode potential (which includes an overpotential term associated with the particular reaction) corrected for the departure from standard, thus provides an upper limit for the standard electrode potential.

The correction to standard conditions was calculated on the basis of solution pH of -0.3 , and a mass of $10^{-6 \pm 1}$ g. for a barely visible germanium mirror in a capillary of 2-mm. bore. This latter value, which needs to be known only to the nearest order of magnitude, is consistent with the normal Marsch test calibration, and leads to a partial pressure of monogermane of $10^{-8 \pm 1}$ atm., at the lowest potential at which monogermane was detected, for a flow of carrier hydrogen of $0.5 \text{ cm}^3 \text{ sec}^{-1}$. Hence

$$E^0 < -0.240 \pm 0.010 - 0.059(-0.3) - 0.0074(-8 \pm 1) \text{ v.}$$

$$E^0 < -0.16 \pm 0.02 \text{ v.}$$

(9) G. P. Van der Kelen and D. F. van de Vondel, *Bull. soc. chim. Belges*, **69**, 504 (1960).

(10) M. Green and P. H. Robinson, *J. Electrochem. Soc.*, **106**, 253 (1959).

To evaluate an upper limit for $\mu^0_{\text{GeH}_4}$ by combining the above inequality with eq. 3, we require a knowledge of $\mu^0_{\text{GeO}_2(\text{hex})}$. The most recent value for this quantity, incorporating new data¹¹ on the standard entropy of hexagonal germanium dioxide which differ from previously accepted values^{1,12-14} is given⁸ as $\mu^0_{\text{GeO}_2(\text{hex})} = -114.8 \pm 0.6 \text{ kcal. mole}^{-1}$. Taking $\mu^0_{\text{H}_2\text{O}}$ as $-56.7 \text{ kcal. mole}^{-1}$ the standard chemical potential of monogermane is found to be $+28 \pm 4 \text{ kcal. mole}^{-1}$ or less positive. The agreement with the value of $28 \pm 0.5 \text{ kcal. mole}^{-1}$ reported by Gunn and Green² is satisfactory. The soundness of Latimers estimate of $+28 \text{ kcal. mole}^{-1}$ for the standard free energy of formation of monogermane is striking. These results show that the formation of monogermane, at the lowest potentials observed, takes place with an overpotential which is small compared with the experimental error.

It is interesting to compare the results of Gunn and Green² for the standard free energy of formation of monostannane with results based on the observation of the minimum potential at which monostannane is evolved at tin cathodes in acid and alkaline solutions.¹⁵ The discrepancy is some $70 \text{ kcal. mole}^{-1}$, which is attributable to a high overpotential associated with the half-reaction $\text{Sn} + 4\text{H}^+ + 4\text{e}^- \rightarrow \text{SnH}_4$. Some preliminary observations, in these Laboratories, on the Sn-SnH₄ system indicate the following: (i) in acid solutions containing no deliberately dissolved tin, monostannane is evolved at the potential values reported¹⁵; (ii) in acid solutions to which tin dioxide had been added, monostannane is evolved at lower potentials, together with volatile products of higher mass number than monostannane.

The system is complicated by the electrodeposition of tin, but the above information strongly suggest a behavior analogous to that of the germanium system.

The mechanism of reduction of dissolved germanium species to monogermane was studied by Green and Robinson¹⁰ in alkaline solution. They report explicitly, but without experimental details, that no species other than monogermane and hydrogen was detected in their cathodic gas. They did, however, detect in their solution a short-lived, highly reducing intermediate, containing germanium, which they were unable to characterize. They suggest three possible formulas for their labile intermediate: GeO_3^{3-} , HGeO_2^{2-} , or GeO_2^{2-} . In the absence of supporting evidence this suggestion is difficult to accept, involving as it does some species quite novel to the chemistry of germanium or, indeed, of the other group IV elements. An alternative reduction scheme, supported by mass spectrometric evidence, is proposed here. Orthogermanic acid, the predominant

(11) E. G. King, *J. Am. Chem. Soc.*, **80**, 1799 (1958).

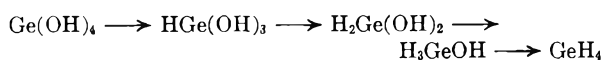
(12) W. Bues and H. Von Wartenberg, *Z. anorg. u. allgem. Chem.*, **266**, 28 (1956).

(13) W. L. Jolly and W. M. Latimer, *J. Am. Chem. Soc.*, **74**, 5757 (1952).

(14) K. K. Kelley, *Bull. U.S. Bur. Mines*, No. 477 (1950).

(15) N. deZoubov and E. Deltombe, *Proc. Intern. Comm. Electrochem. Thermodynam. and Kinet.*, 240 (1957).

dissolved species³ at low pH values, is progressively reduced as



Green and Robinson's failure to detect these intermediates in the cathodic gas suggests that the germanols may have acidic properties as have their carbon analogs and the alkyl germanium hydroxyls.

The mechanism of reduction postulated does

not involve the participation of elementary germanium among the intermediate products.

Acknowledgments.—The author is indebted to J. I. Carasso for much helpful discussion, to Miss C. M. Lovett who carried out the mass spectrometric analysis, and to J. M. McPherson for experimental assistance. Acknowledgment also is due to the Engineer-in-Chief of the British Post Office and to the Controller of Her Britannic Majesty's Stationery Office for permission to publish.

ELECTROÖSMOTIC WATER TRANSPORT ACROSS ION-EXCHANGE MEMBRANES

BY A. S. TOMBALAKIAN,¹ H. J. BARTON, AND W. F. GRAYDON

Department of Chemical Engineering and Applied Chemistry, University of Toronto, Toronto, Canada

Received September 11, 1961

A study of electroösmotic transport of water across polystyrenesulfonic acid ion-exchange membranes, having various exchange capacities and degrees of crosslinking, has been made. The results indicate that water transport by electroösmosis is a function of the internal ion concentration of the membrane pore solution and the membrane ionic form. A marked dependency of electroösmotic water transport on current density also is noted only at high current densities.

Introduction

The results of previous measurements of electroösmotic transport of water across polystyrenesulfonic acid ion-exchange membranes have been reported.² Direct measurements of water transport accompanying various cations by electroösmosis across similar membranes over a wide range of external solution concentration and current density are given in this report. This study was undertaken to obtain further experimental data on the magnitude of electroösmotic water transport across these ion-exchange membranes. The dependence of electroösmotic water transport on membrane properties such as exchange capacity, moisture content, internal ion concentration of the membrane pore solution, and membrane ionic form was determined.

Experimental

A. Membranes.—The membranes used in this work were prepared by the bulk copolymerization of the propyl ester of *p*-styrenesulfonic acid with styrene and divinylbenzene and subsequent hydrolysis to produce polystyrenesulfonic acid as described previously.³ However, instead of using a petri dish and floating it over a mercury bath in the oven, a stainless steel dish with a glass plate cover was used. This enabled the preparation of a membrane 5.25 in. long and 3 in. wide, which permitted the cutting out of various sizes of membranes as they were needed during the course of this investigation. In the oven the stainless steel dish was seated over a table which was supported by three adjustable screws. The membrane formed did not show variation in thickness more than 0.003 in.

The membranes are designated by two digits. The first digit represents the nominal exchange capacity of the membrane, while the second digit represents the mole per cent. of divinylbenzene used in the preparation of the membrane.

(1) Chemistry Department, Laurentian University of Sudbury, Sudbury, Canada.

(2) R. J. Stewart and W. F. Graydon, *J. Phys. Chem.*, **61**, 164 (1957).

(3) (a) I. H. Spinner, J. Ciric, and W. F. Graydon, *Can. J. Chem.*, **32**, 143 (1954); (b) W. F. Graydon and R. J. Stewart, *J. Phys. Chem.*, **69**, 86 (1955).

B. Membrane Moisture Content and Internal Solution Concentration.—In the past it has been customary to measure the moisture content of an ion-exchange resin by the vapor sorption method and present it as one of the main characteristics of the ion-exchange resin.^{1,3b,4}

The moisture contents of the membranes were determined at 25° in the lithium, hydrogen, sodium, and potassium forms of the resin with external solutions in the concentration range pure water to 4.0 *M*. In Table I are given the moisture contents of the membranes in the leached lithium, hydrogen, sodium, and potassium forms in contact with pure water. It can be seen from the data in Table I that the quantity of water sorbed by the membranes, in the given cationic forms of the resin, decreases in the order lithium, hydrogen, sodium, and potassium.

TABLE I

Membrane no.	MEMBRANE MOISTURE CONTENT				
	Capacity, meq./g. dry resin Na form	Moisture content, g. H ₂ O/equivalent			
		Li form	H form	Na form	K form
1-2	1.12	560	558	558	542
1-6B	0.85	282	275	280	264
1-8	1.11	227	226	224	208
1-10	1.13	202	199	198	180
1-6A	1.14		302	291	
1-4	1.40		366	362	
2-6	1.77		332	330	
1.5-6	1.32			180	
2-8	1.58			179	
3-6	2.80			274	

The internal ion concentration of the membrane pore solution may be evaluated from its capacity and moisture content. For this purpose Stewart^{3b} used the membrane exchange capacity and moisture content by the vapor sorption method. For the membranes used in this work the internal concentrations were determined both as the ratio of membrane exchange capacity to moisture content by the vapor sorption method, and as the ratio of total cation content (exchange capacity plus sorbed electrolyte) to moisture content by direct contact with solution. The difference in the internal ion concentration of the membrane pore solution evaluated by the two methods was on the average 10% and

(4) M. H. Waxman, B. R. Sundheim, and H. P. Gregor, *ibid.*, **57**, 969 (1953).

the maximum deviation between the two occurred at about 1 *M* external solution concentration, in which solutions the vapor sorption method gave values of about 15% less than the direct contact method. In general, the observed variations in internal solution concentration with membrane capacity and cross-linking by the two methods were very similar.

C. Membrane Swelling and Density.—The thickness of a surface dried 3-6 membrane was measured with a micrometer gage to 0.0001 in. following the method of Stewart.^{3b} The membrane first was allowed to come to equilibrium at 25° in water and this procedure was repeated for solution concentrations of 0.1, 0.5, 1.0, 2.0 and 4.0 *M* equally concentrated in sodium nitrate and hydrochloric acid. The membrane bulk volume in contact with the above solutions at 25° also was measured using a pycnometer. The density of the membrane was evaluated by dividing the wet weight by the bulk volume determined.

With an increase in the external solution concentration from pure water to 4.0 *M*, the density of the 3-6 membrane was found to increase from 1.326 g./ml. to 1.581 g./ml., while the membrane thickness decreased nearly 10% and the membrane bulk volume decreased by approximately 25%. This indicates that within the precision of the measurement there is no marked deviation from isotropic swelling.

D. Electroösmotic Water Transport.—Measurements of electroösmotic water transport were made using a lucite cell following the method of Stewart.² The capillaries fitted into the cell first were calibrated by the mercury weight method. The electrodes were silver rods coated with silver chloride. A current density of 1 mamp./cm.² was used.

During the measurement of water transport, the cell was placed in a water-bath controlled to 25 ± 0.1°. The heights of the solutions in both the capillary tubes were measured using a cathetometer. A measured current was passed through the cell for a time determined by a stopwatch and the changes in the heights of solutions were observed. This was repeated four times by reversing the direction of current every time. All the data reported here are average values of four individual measurements. The solutions of lithium chloride, sodium chloride, potassium chloride, and hydrochloric acid used were in the concentration range 0.05 to 4.0 *M*.

The effect of current density on electroösmotic water transport also was determined. The current densities varied from 1.076 to 107.6 mamp./cm.². In Table II are listed the observed values of water transport at different current densities. With high current densities in the range 26.9 to 107.6 mamp./cm.² the number of moles of water transferred per equivalent of transferred sodium ions decreased as the current density was increased. This decrease in water transport may be due to the polarization of the membrane at high current densities. The resultant decrease of moisture content for one membrane face would reduce the water transport value. With a current density below 1.076 mamp./cm.² all ionic forms of a membrane showed no dependence of water transport on current density.

TABLE II
EFFECT OF CURRENT DENSITY ON WATER TRANSPORT

Membrane no.	NaCl soln., moles/l.	Water transport, $\Delta V/18$			
		0.01076-1.076 mamp./cm. ²	26.90 mamp./cm. ²	53.82 mamp./cm. ²	107.6 mamp./cm. ²
3-6	0.1	7.9	7.7	7.2	6.3
	1.0	5.6	5.3	5.0	4.1
	4.0	3.3	3.2	2.8	2.2

In order to determine the extent to which the drier face of a membrane regulated the water transport, the water transport across a 3-6 membrane separating different solutions of sodium chloride over a wide range of solution concentration was determined using a current density of 1.076 mamp./cm.². The observed values of water transport are plotted in Fig. 1 against the external solution concentration together with the values of water transport representing the values for the dilute and concentrated solutions. It can be seen from Fig. 1 that the values of water transport across a membrane separating different solutions of sodium chloride fall between the values of water transport for the same membrane in contact with a dilute solution and the membrane in

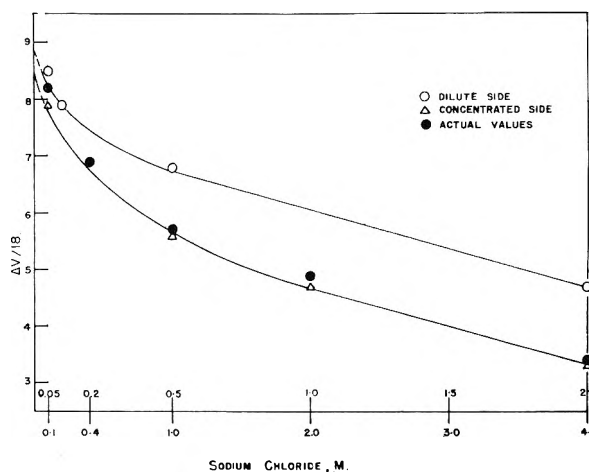


Fig. 1.—Electroösmotic water transport for a 3-6 membrane at 25°. Water transport values across the membrane separating different solutions of sodium chloride are represented by the dark circles. The upper and lower curves define the values of water transport for the membrane in contact with the dilute solutions and the membrane in contact with the concentrated solutions, respectively. The solutions of sodium chloride used were in the concentration range 0.05 to 4.0 *M*.

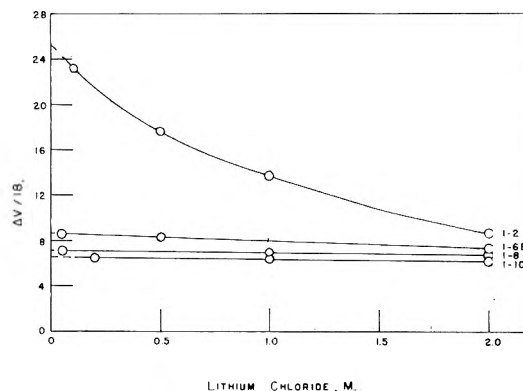


Fig. 2.—Electroösmotic water transport for various membranes using solutions of lithium chloride in the concentration range 0.05 to 2.0 *M*. The quantity $\Delta V/18$ is approximately the moles of water transported per faraday by lithium ions.

contact with a concentrated solution. The values obtained are close to the values of water transport for the membrane in contact with the concentrated solutions. This indicates that the drier face of a membrane regulates the water transport through the membrane.

Discussion

The data obtained for the volume change in one-half of the electroösmotic cell per faraday for some membranes using various solutions of lithium chloride, sodium chloride, potassium chloride, and hydrochloric acid and a current density of 1.076 mamp./cm.² are presented in Fig. 2, 3, 4, and 5, respectively. The quantity $\Delta V/18$ has been shown² to be a good approximation to the moles of water transported per faraday by sodium ions at any of the solution concentrations used. It can be seen from Fig. 2, 3, 4, and 5 that the water transport decreases with increasing external solution concentration and also in the order lithium, sodium, potassium, and hydrogen. This latter effect is consistent with the variation in the effective radii of these ions in their hydrated forms. In the

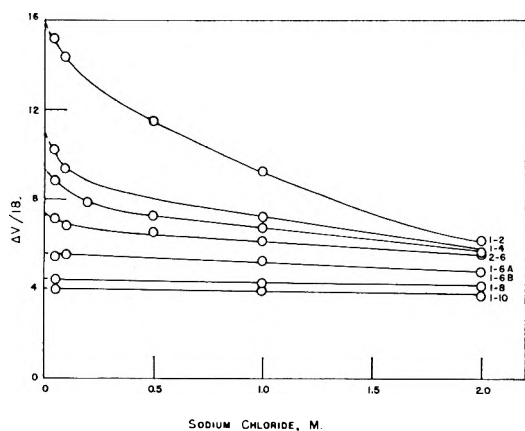


Fig. 3.—Electroosmotic water transport for various membranes using solutions of sodium chloride in the concentration range 0.05 to 2.0 *M*. The quantity $\Delta V/18$ is approximately the moles of water transported per faraday by sodium ions.

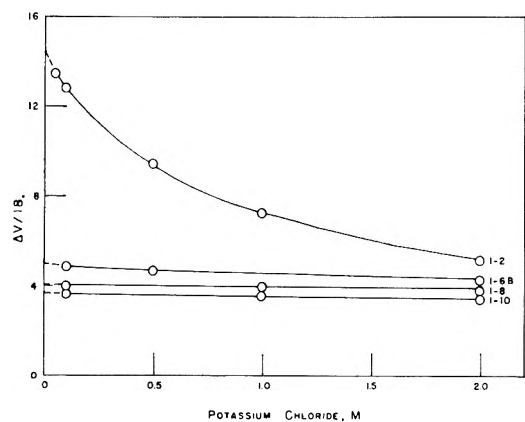


Fig. 4.—Electroosmotic water transport for various membranes using solutions of potassium chloride in the concentration range 0.05 to 2.0 *M*. The quantity $\Delta V/18$ is approximately the moles of water transported per faraday by potassium ions.

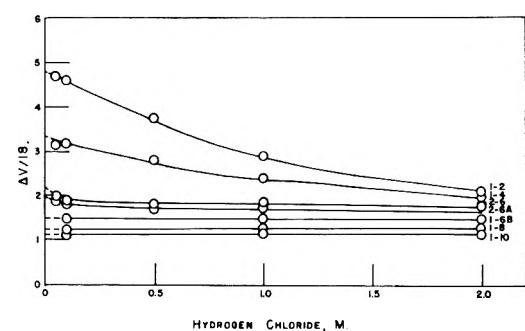


Fig. 5.—Electroosmotic water transport for various membranes using solutions of hydrochloric acid in the concentration range 0.05 to 2.0 *M*. The quantity $\Delta V/18$ is approximately the moles of water transported per faraday by hydrogen ions.

case of the high crosslinking membranes, it appears that the limiting values for water transport have been reached. The 1-10 membrane was an exceedingly "tight" membrane requiring many weeks to hydrolyze and represents very nearly the limiting condition of membrane internal solution concentration. For this membrane the values of water transport are reduced to about six moles of

water per mole of lithium, about four moles of water per mole of sodium and potassium, and about one mole of water per mole of hydrogen.

The observed variations in water transport with the external solution concentration are very similar to the variations in membrane moisture content. In general, water transport for any one ion appears to follow the moisture content^{2,5} of the membrane in that ionic form. Although the moisture content of a membrane, as shown in Table I, differs only slightly with ionic form, a large difference in water transport between lithium, sodium, potassium, and hydrogen ions is observed. The moving ion exerts the major control over the magnitude of water transport.

In Table III are given the values of the ratio of the observed water transport of one ion to the water transport of another ion for a series of membranes having nearly the same exchange capacity. It can be seen that the ratios of water transport for any two ions are quite constant regardless of membrane network tightness within the wide range of external solution concentrations investigated. This indicates that there is very little sieve effect resulting from membrane network interference.

TABLE III

Membrane no.	RATIO OF WATER TRANSPORTS					
	H/Na		Li/K		Na/K	
	0	2	0	2	0	2
1-2	0.306	0.339	1.79	1.65	1.08	1.17
1-4	.306	.332				
1-6A	.250	.298				
1-6B	.272	.317	1.82	1.72	1.17	1.10
1-8	.280	.301	1.78	1.70	1.09	1.08
1-10	.288	.307	1.81	1.76	1.10	1.10

The major determining parameters in water transport for a given ion appear to be the membrane moisture content and exchange capacity, that is, the internal concentration of the membrane pore solution. If the values of water transport for several membranes, having the same nominal exchange capacity, are plotted against the membrane equivalental moisture values (moles of water per equivalent of ion-exchange resin) over the entire range of sodium chloride solution concentration, a linear relationship between water transport and membrane equivalental moisture is observed. The slope of the line gives the ratio of water transport to membrane equivalental moisture (w_T/w_D). An empirical representation of this dependence on membrane exchange capacity is given by

$$\frac{w_T}{w_D} = 0.38(\text{Exchange Capacity})^{0.42}$$

where w_T/w_D is the ratio of water transport to membrane equivalental moisture.

In Table IV are given the observed and calculated values of the ratio of water transport to equivalental moisture for the membranes in the sodium form using the empirical relationship given above. It can be seen that good agreement is found between the calculated and observed values of the ratio of water transport to membrane equivalental mois-

(5) A. G. Winger, R. Ferguson, and R. Kunin, *J. Phys. Chem.*, **60**, 556 (1956).

ture. The over-all mean deviation of the observed values from the calculated results is 0.037. Similar ratios reported by Stewart² also have been compared to the values calculated by the equation, with a mean deviation of 0.024.

TABLE IV
RATIO OF WATER TRANSPORT TO MEMBRANE EQUIVALENTAL MOISTURE, SODIUM FORM

Membrane no.	—Sodium chloride solution— molarity				Calcd. value of w_T/w_D	Mean dev. from the calcd. value
	0	1	2	4		
1-10	0.36		0.38		0.40	-0.030
1-8	.37		.38		.40	-.025
1-6B	.36		.35		.35	+.005
1-6A	.45		.41		.40	+.030
1.5-6	.48	0.46	.44	0.43	.43	+.025
1-2	.51		.34		.39	+.035
1-4	.55		.43		.44	+.050
2-8	.45	.44	.44	.41	.46	-.050
2-6	.51		.48		.48	+.015
3-6	.57	.53	.50	.44	.60	-.090

In Table V are given similar ratios of water transport to equivalental moisture for the other membrane ionic forms. The ratios listed in Table V show a marked variation with membrane ionic form. The capacity effect for each ionic form is similar to that for the sodium form as represented by the above equation.

TABLE V
RATIO OF WATER TRANSPORT TO MEMBRANE EQUIVALENTAL MOISTURE, VARIOUS IONIC FORMS

Membrane no.	Ext. soln., moles/l.	Lithium	Potassium	Hydrogen
1-10	0	0.57	0.37	0.10
	2	.58	.40	.11
1-8	0	.57	.36	.10
	2	.56	.37	.11
1-6B	0	.55	.33	.10
	2	.56	.34	.11
1-2	0	.84	.50	.15
	2	.46	.31	.11

One might consider that interactions within a membrane during water transport, between the moving ion and water, and between the water

and membrane pore wall may be represented by a simple viscous force balance. A moving ion under the influence of an applied electric potential will exert a force on the water which will be balanced by the friction force between the water and the stationary membrane pore wall. If the forces of interaction are assumed proportional to the relative velocities, then this would lead to the relationship

$$\frac{w_T}{w_D} = \frac{f_{1W}}{f_{1W} + f_{wW}}$$

where f_{1W} is the proportionality constant representing the ratio of the forces exerted by the moving ion and the water to the velocity of the ion relative to the water, and f_{wW} is the proportionality constant representing the ratio of the forces exerted by the water and the membrane pore wall to the velocity of the water relative to the membrane pore wall.

In the simplest case this ratio (w_T/w_D) might be expected to be constant and independent of membrane parameters. However, in a series of membranes having various exchange capacities and degrees of crosslinking, the observed decrease in the value of the ratio (w_T/w_D) with decreasing membrane exchange capacity indicates an increased water-membrane pore wall viscous interaction. The dependence given by the above equation is of this sort and shows a decrease in the quantity w_T/w_D with decreasing membrane exchange capacity. Since the exchange capacity is a measure of the amount of organic membrane material per sulfonate group, the effect noted above is consistent with the view that the water-membrane pore wall viscous interactions increase with increasing amount of the organic membrane material per sulfonate group. Although some variation in the quantity w_T/w_D may be observed as a result of variation in external solution concentration and crosslinking, these effects are nearly within the present limit of experimental error, and require further study.

Acknowledgment.—The authors are indebted to the National Research Council, Ottawa, Canada, the Ontario Research Foundation, and to the Advisory Committee on Scientific Research, University of Toronto, for financial support.

STRUCTURE AND MOLECULAR ORIENTATION IN MULTIMOLECULAR FILMS OF LONG-CHAIN *n*-HYDROCARBON DERIVATIVES^{1,2}

BY C. L. SUTULA AND L. S. BARTELL

*Institute for Atomic Research and Department of Chemistry, Iowa State University, Ames, Iowa**Received September 16, 1961*

An electron diffraction study has been made of the structure and molecular orientation in multimolecular films of a variety of long-chain molecules. Films were prepared several ways, but principally by evaporating dilute solutions on metal slides. Most of the films studied were 30 to 40 molecules thick, although films considerably thinner and thicker were examined. The films were found to consist of microcrystals with 00 l planes parallel to the surface of the substrate, in agreement with previous studies. Careful measurements of the lattice parameters and crystal form were made. These showed, contrary to several previous studies involving some of the same compounds, that the molecular packing in the colloidal films was characteristic of that and indistinguishable from that occurring in the bulk crystals. Evidence is presented which indicates that the exceptional packing found in the earlier studies of thin films was the result of impurities rather than the extreme thinness. Two new methods are reported for preparing thin films with molecules aligned in a designated direction.

It is widely appreciated that the orientation and packing of anisotropic molecules at interfaces are important factors in interfacial properties such as friction, adhesion, and wettability. Numerous qualitative studies of orientation based on surface potentials, adsorption isotherms, coefficients of friction, and contact angles have been reported but none of these methods permits a very precise characterization. Electron diffraction studies, on the other hand, though restricted in applicability, are capable of yielding considerable detail about the structure of surface films. Extremely informative diffraction studies have been made by several authors, on both monomolecular and multimolecular films. Of particular interest have been several reports of multimolecular films in which molecular packing differed from that characteristic of the bulk material. The possibility that this difference arose from the colloidal character of the interfacial films deserved investigation. In addition, in studies of multilayers, sufficient attention has not always been paid to the composition of the films or their thickness, and the variety of compounds studied has been small.

The present investigation was undertaken to study molecular orientation and packing in films of several homologous series of *n*-hydrocarbon derivatives on metal slides, by electron diffraction. Particular attention was given to the purity of the compounds. Films ranging in thickness from one molecular layer to over 1000 Å. were investigated. A very helpful device, not previously used in structural studies of such films, was a polarization spectrometer capable of measuring the average thickness of the thinner films to within a small fraction of a molecular length.

The preparation of reasonably homogeneous films of 1000 Å and over was not difficult, as discussed in the following. The deposition of known numbers of molecular layers in the very thin and intermediate ranges by the Langmuir-Blodgett technique was possible with the more polar derivatives and a few examples of such films were studied. Structural results for Langmuir-Blodgett films

confirmed results of earlier published studies and will not be discussed in detail in the following. In the case of non-polar molecules, for which the Langmuir-Blodgett technique is not applicable, the attainment of homogeneous films of controlled thickness in the thinner range proved more difficult. One method which was successful in producing quite uniform films even of pure hydrocarbons from 1000 down to 30 Å. or less involved the buffing down of 1000-Å. films with soft tissue paper. It was found, however, that the mechanical shear associated with the buffing had a profound influence on molecular orientation, as will be discussed in a forthcoming paper. The present paper will be concerned, unless otherwise stated, with films which have been subjected to no externally applied mechanical shear in their preparation.

Experimental Procedure

Preparation of Surfaces.—Platinum slides and chromium plated steel slides were used as substrates for the films. They were polished by hand with increasingly smaller sizes of abrasives in the manner customary in metallurgical polishing procedures. Positive removal of abrasive particles from the metal surface was accomplished by vigorous rubbing of the entire surface of the slide with a small piece of polishing cloth in a jet of water. This was followed by rubbing with a cotton applicator in a stream of distilled water. The last traces of grease-like material remaining on the surface after the above operation were removed in the following way. Platinum slides were dried with soft tissue after rinsing and were flamed for about 1 min. at a dull red color in the oxidizing portion of a flame of a meker burner. Chromium plated slides were first wiped with tissue dampened with benzene after rinsing and were flamed in the oxidizing portion of a flame of a meker burner for a total of 5 to 7 sec. in 1-sec. steps.

Electron diffraction photographs taken of metal surfaces cleaned by the above procedure showed only the typical pattern of polished surfaces. They did not indicate the presence of abrasive or of oriented, grease-like substances. Small drops of water placed on the metal surfaces spread and gave contact angles that were approximately zero. The surfaces also gave black breath figures and films of *n*-octadecyl amine were readily formed by the drop retraction technique from 0.1% solutions of *n*-octadecylamine in cetane.

Preparation of Films.—Several methods were used in preparing films. One involved spreading a fused compound over a warm slide and allowing the material to solidify. Generally, this method gave films too thick for convenient use in electron diffraction experiments. Another method was to spread a small quantity of a solution of a particular compound over the metal slide. A film of the compound formed as the solvent evaporated. Although such films were somewhat heterogeneous in thickness, large, fairly uniform areas often were observed and were selected for detailed study.

(1) (a) Contribution No. 1061. Work was performed in the Ames Laboratory of the U. S. Atomic Energy Commission; (b) presented at the 135th National Meeting of the American Chemical Society, Boston, Massachusetts, April 6, 1959.

(2) Based on a dissertation by C. L. Sutula to the Graduate School, Iowa State University, in partial fulfillment of the requirements for the degree of Doctor of Philosophy, 1959.

In the case of the acids, a few films of Langmuir-Blodgett multilayers also were investigated. The overwhelming majority of the films studied were prepared by the second method, and averaged about 1000 Å. in thickness.

Diffraction Apparatus.—Diffraction patterns were obtained by the reflection method with a General Electric electron diffraction unit using an accelerating voltage of 35 kv. ($\lambda \cong 0.064$ Å.). Zinc oxide patterns were taken to determine the wave length of the electrons.

Measurements of Film Thickness.—A polarization spectrometer, similar to Rothen's ellipsometer,³ was used to determine the optical thickness of the thinner films. Although its greatest utility was in the second paper of this series,⁴ it is expedient to describe it here. For films less than 150 Å. thick the sensitivity of measurement was of the order of ± 1 Å. The optical arrangement and the technique of taking readings was identical to that described by Bartell, Ruch, and Betts.⁵ Langmuir-Blodgett films of neutral stearic acid and of barium stearate deposited on highly polished surfaces of platinum and of chromium plated steel were used to calibrate the instrument.

The change in optical reading between a fresh surface and a surface covered by a film was used as a measure of the thickness of the film. The substrate surface was carefully prepared for every experiment according to the method previously described, and its base optical reading was determined shortly after preparation. Immediately afterward, a film was formed on the metal surface and its thickness was estimated. Then the film was examined by electron diffraction.

In the case of films thicker than a few hundred angstroms, thicknesses were estimated visually from the color of the film.

Chemicals.—The hydrocarbons docosane through triacontane were estimated to be over 99% pure by mass spectrographic analysis performed by the Shell Development Company. The remainder of the hydrocarbons and acids melted to within a degree of the values reported in the literature. Benzene, toluene, *n*-tetradecane, acetone, and *n*-octane were used as solvents for the hydrocarbon derivatives when the films were formed by evaporation from a solution. All of the above solvents were carefully redistilled. Benzene, toluene, and acetone, evaporated drops of which after the above treatment left no film on a freshly prepared metal surface, were used without further purification. The compounds *n*-octane and *n*-tetradecane were percolated through a column of silica gel and aluminum oxide to remove polar impurities.

Results

All compounds gave well defined electron diffraction patterns except for lauric acid, which was irregularly oriented. Patterns similar to those obtained in this investigation have been reported in a number of previous studies.⁶ Several analyses of such patterns have been published.⁷⁻⁹

The diffraction data indicated that the multimolecular films were preferentially oriented and polycrystalline. The films appeared to be composed of many contiguous submicroscopic crystallites oriented with their basal (00 l) planes parallel to the plane of the substrate surface. This orientation of the crystallites (disregarding the underlying adsorbed monolayer in the case of acids^{6,7}) was found to be unrelated to the thickness of the films, occurring in films ranging in average thickness from several molecular layers to films well over

1000 Å. Nevertheless, it is fair to point out that only in the case of Langmuir-Blodgett films was there any guarantee that the crystallites diffracting the electrons were as thin as the average film thickness. Moreover, the electron beam penetrates only the top few molecular layers of any flat regions in a film, leaving unexamined the lower layers. When the films were prepared by the first two methods described above, the basal axes of the crystallites were randomly arranged in the plane of the substrate surface. Two methods were found, however, which gave films with basal planes parallel to the substrate but with molecular tilts all in virtually the same direction. These are described in the Appendix.

Electron micrographs of 1000-Å. films of stearic acid and octadecyl stearate prepared on evaporated carbon substrates confirmed the polycrystalline character of the films. Crystallites of octadecyl stearate ranged from thin, flat, well developed crystals the order of a micron in width on down through much smaller platelets and prisms closely wedged together to flat, featureless clumps. Crystallites a few tenths of a micron in diameter often had orientations strongly correlated with those as far away as several microns even though the over-all orientation in the film was random. Crystallites of stearic acid failed to show well developed faces in the micrographs, possibly because of the deleterious effects of the water used in the preparation of the microscope specimens prior to shadowing the films.

The angle which the long axis of the molecules made with the perpendicular to the plane of the substrate surface, customarily designated by ψ , was used as a measure of molecular orientation. Orientations observed in the present study are listed in Table I in terms of $\psi + 90^\circ$, a quantity which should be directly related to the crystallographic angle β for bulk crystals if 00 l planes in the films are parallel to the surface.

By means of a systematic analysis of the position and intensity of the elongated reflections occurring in the patterns, it often was possible to determine the lattice parameters a and b of the crystallites in the films. In the films investigated, reflections revealing the c -spacing were never observed on unrubbed films.¹⁰ The film results are compared in Table I with published results of investigations of bulk crystals of *n*-hydrocarbon derivatives by X-ray and electron diffraction. In the case of some substances for which no values are reported in the literature, values found by interpolation or by extrapolation using literature values for homologous substances are given. In other cases structural data for similar substances are listed. The diffraction data from several films were too incomplete for a reliable determination of the parameters of the crystallites. In these cases, the cited data from the literature gave calculated

(3) A. Rothen, *Rev. Sci. Instr.*, **16**, 26 (1945).
 (4) L. S. Bartell and C. L. Sutula, to be published.
 (5) L. S. Bartell and R. J. Ruch, *J. Phys. Chem.*, **60**, 1231 (1956); L. S. Bartell and J. F. Betts, *ibid.*, **64**, 1075 (1960).
 (6) See for example, L. H. Germer and K. H. Storks, *Proc. Natl. Acad. Sci.*, **23**, 390 (1937); Th. Schoon, *Z. physik. Chem.*, **B39**, 385 (1938).
 (7) L. H. Germer and K. H. Storks, *J. Chem. Phys.*, **6**, 280 (1938).
 (8) Z. G. Pinsker, "Electron Diffraction," Butterworths Scientific Publications, London, 1953.
 (9) C. A. Murison, *Phil. Mag.*, [7] **17**, 201 (1934).

(10) In the case of a gently buffed film of octadecanol which retained the 00 l orientation, the c spacings were observed once. Presumably crystallites were elevated above the average surface, exposing their sides as well as their top surfaces to the electron beam. The absence of 00 l reflections in the remainder of the patterns is additional evidence that crystallites were flat and smooth, with essentially no tall spires.

TABLE I

THE PARAMETERS DETERMINED FOR CRYSTALLITES FOUND IN MULTIMOLECULAR FILMS OF LONG-CHAIN, *n*-HYDROCARBON DERIVATIVES

Compound	(a)	(b)	(c)	β	$\psi + 90^\circ$	Crystal form
<i>n</i> -Octadecane (impure) ^a	90°	Orthorhombic
Homologous compound ^b	7.43	4.96	...	90°	...	Orthorhombic
<i>n</i> -Eicosane (impure) ^a	7.4	5	90°	Orthorhombic
Homologous compound ^b	7.43	4.96	...	90°	...	Orthorhombic
<i>n</i> -Docosane	Triclinic
Data from films ^a fit extrapolated results of Mazee ^c						
<i>n</i> -Tricosane ^a	5.0	7.5	90°	Orthorhombic
Smith ^d	4.97	7.48	62	90°	...	Orthorhombic
<i>n</i> -Hexacosane ^a	5.5	7.4	118°	Monoclinic
Homologous compound ^e	5.57	7.42	...	119°	...	Monoclinic
<i>n</i> -Heptacosane ^a	5.0	7.5	90°	Orthorhombic
Smith ^d	4.97	7.48	72.59	90°	...	Orthorhombic
<i>n</i> -Octacosane ^a	5.5	7.4	118°	Monoclinic
Homologous compound ^e	5.57	7.42	...	119°	...	Monoclinic
<i>n</i> -Nonacosane ^a	5.0	7.5	90°	Orthorhombic
Smith ^d	4.97	7.48	77.70	90°	...	Orthorhombic
<i>n</i> -Triacontane ^a	5.5	7.4	118°	Monoclinic
Homologous compound ^e	5.57	7.42	...	119°	...	Monoclinic
<i>n</i> -Hentriacontane ^a	5.0	7.5	90°	Orthorhombic
Smith ^d	4.97	7.48	...	90°	...	Orthorhombic
<i>n</i> -Dotriacontane (impure) ^a	7.35	5.0	90°	Orthorhombic
Homologous compound ^b	7.43	4.96	...	90°	...	Orthorhombic
Stearic acid ^a	9.40	5.0	128°	Monoclinic, form C ^k
Abrahamsson and von Sydow ^f	9.35	4.96	50.76	128°14'	...	Monoclinic, form C
Arachidic acid ^a	128-129°	Monoclinic, form C
Interpolated ^g	9.3	5.0	...	128°	...	Monoclinic, form C
<i>n</i> -Heptadecanoic acid ^a	20°	Possibly triclinic
Palmitic acid ^a	9.48	5.0	127-129°	Monoclinic, form C
Verma ^h	9.68	5.05	46.86	128°57'	...	Monoclinic, form C
Thibaud and Dupre LaTour ^h	9.41	5.00	45.9	129°	...	Monoclinic, form C
Isostearic acid ^a	130-135°	Possibly triclinic
Isopalmitic acid ^a	125°	Possibly triclinic
Lauric acid ^a	..	patterns	diffuse, no reliable data obtained
<i>n</i> -Octadecyl stearate ^a	5.56	7.53	118°	Monoclinic
<i>n</i> -Hexadecyl stearate ^a	5.65	7.40	118°	Monoclinic
<i>n</i> -Dodecyl laurate ^a	5.68	7.5	120°	Monoclinic
<i>n</i> -Cetyl palmitate by Kohlhaas ⁱ	5.61	7.42	92.8	118.7°	...	Monoclinic
<i>n</i> -Cetyl palmitate by Schoon ^j	5.60	7.49	93	119.2°	...	Monoclinic
<i>n</i> -Octadecyl alcohol ^a	4.97	7.45	49.4	90°	90°	Orthorhombic
<i>n</i> -Stearamide (impure) ^a	110°	...

^a This investigation. ^b A. Muller, *Proc. Roy. Soc. (London)*, **A120**, 437 (1928). ^c W. M. Mazee, ref. 14. ^d A. E. Smith, ref. 13. ^e H. M. M. Shearer and V. Vand, ref. 19. ^f S. Abrahamsson and E. von Sydow, *Acta Cryst.*, **7**, 591 (1954). ^g A. R. Verma, *Proc. Roy. Soc. (London)*, **A228**, 34 (1955). ^h J. Thibaud and F. Dupre LaTour, *J. chim. phys.*, **29**, 153 (1932). ⁱ R. Kohlhaas, *Z. Krist.*, **98**, 418 (1938). ^j Th. Schoon, *Z. physik. Chem.*, **B39**, 385 (1938). ^k Some films of stearic acid were found to contain crystallites of form B as well as C.

positions for reflections in the diffraction patterns which agreed well with the observed positions.

The agreement exhibited in Table I shows that the packing of the molecules in the crystallites in the films is the same, to within experimental error, as that observed in studies of larger crystals. No influence of the colloidal nature of the thinner films was observed on the packing of the molecules in the crystallites.

Discussion

Several investigators have obtained data for films similar to those reported here, including films deposited in different ways. For example, Germer and Storck^{6,7} have found crystallites of monoclinic forms A and C of stearic acid in multi-molecular Langmuir-Blodgett films of stearic

acid which gave patterns indistinguishable from those observed in the present study. Trillat and Hirsch¹¹ have found monoclinic forms A, B, and C of stearic acid in crystalline lenses of stearic acid which were formed on a water surface from benzene solutions. On the other hand, Brummage¹² has reported that crystallites in multi-molecular films of *n*-tetracosane, *n*-triacontane, and *n*-tetratriacontane were of orthorhombic form, whereas in the present investigation, films of the higher even-numbered *n*-hydrocarbons were found to exhibit monoclinic structures, provided the compounds were sufficiently pure. It seems likely that the difference can be attributed to effects of homologous impurities which are extremely

(11) J. J. Trillat and Th. V. Hirsch, *Compt. rend.*, **216** (1932).

(12) K. G. Brummage, *Proc. Roy. Soc. (London)*, **A188**, 411 (1947).

difficult to remove, and which can alter the molecular packing, as discussed below.

A. E. Smith¹³ in an X-ray study of single crystals of a series of *n*-hydrocarbons determined that the even-numbered *n*-hydrocarbons beginning with *n*-hexacosane are monoclinic at room temperature. The shorter, even-numbered *n*-hydrocarbons below and including *n*-hexacosane also may crystallize in a triclinic form. Mazee¹⁴ has found *n*-tetracosane to be triclinic at room temperature while Muller and Lonsdale¹⁵ have found a triclinic form for *n*-octadecane. Indeed, it appears for pure compounds that the orthorhombic form has been found only for the odd-numbered *n*-hydrocarbons and also for certain *n*-aliphatic alcohols.^{16,17} In this connection, Smith¹⁸ has shown that the presence of even a single homologous impurity in a concentration as low as 1% gives orthorhombic crystals for the even-numbered *n*-hydrocarbons. Also, Shearer and Vand,¹⁹ while determining the crystal structure of *n*-hexatriacontane, observed the crystals to change from an orthorhombic form to a monoclinic form upon repeated crystallization.

Analogous observations were made in the present investigation when Langmuir-Blodgett multilayers of stearic acid were deposited from a film balance with paraffined sides. Although pure stearic acid was used, it was found that if the benzene solution in which the acid was spread on the water was allowed to spread to the paraffined sides, the Langmuir-Blodgett multilayers subsequently formed sometimes were orthorhombic instead of monoclinic of form A or C. This undoubtedly was due to the contamination of the acid film on water by paraffin wax. Recently Takogi has made similar observations which he has explained, also, by contamination.²⁰ Analogous effects of impurities also were found in films formed by evaporating solutions.

The effects of impurities also may account for the results of Natta and Rigamonti²¹ who found, in disagreement with the present study of pure compounds, orthorhombic crystallites in films of many *n*-aliphatic acids, esters, ethers, etc., and suggested that the orthorhombic form was characteristic of multimolecular films of all these compounds.

Although several crystalline forms have been observed in multimolecular films of *n*-hydrocarbon derivatives, the observation of crystallites with their basal axes parallel to the plane of the substrate surface (considered to be an 00 l orientation) has been remarkably consistent. Molecular orientations observed in multimolecular, unrubbed films agree to within 1 or 2° with the angles that the molecular chains form with the 00 l planes in

the larger crystals of the compounds, as determined by previous structural investigations.²² The 00 l surface exposed by the films is then essentially a methyl surface, the surface which, for a crystal, would have the lowest free energy of the crystallographically possible faces. It undoubtedly is significant that the substances investigated above normally crystallize in thin flat plates exposing 00 l faces.²³ Whether the orientation of the crystallites deposited upon the slides was determined principally by considerations of interfacial free energy, or, somehow, by the kinetics of growth of crystallites which preferentially orient parallel to the surface is not known. It will be shown in the next paper of this series, however, that surfaces of presumably higher free energy can be induced in many of the films by mechanical shear which re-orient the molecules.

Acknowledgments.—We are deeply indebted to Dr. A. E. Smith and the Shell Development Company for samples of a series of extremely pure *n*-hydrocarbons from docosane through triacontane and to Dr. M. Senkus and the R. J. Reynolds Tobacco Company for a sample of pure *n*-hentriacontane. We wish to thank the Ohio Oil Company for its generous aid in the electron micrograph studies. It is a pleasure to acknowledge support from the American Petroleum Institute in the early phases of this investigation.

Appendix

Controlled Orientation from a Melt.—Films formed by cooling molten compounds spread over a surface were usually too thick for convenient diffraction studies. It was found, however, that the following method gave films of stearic acid with smooth regions only about 10,000 Å. thick and with molecular tilts all aligned in the same direction. Molten stearic acid was spread over the surface of a polished platinum slide at a temperature of 130–140°. If one end of the slide was held against a cold block of metal (–50°), a thin film of solid stearic acid began to form at the cold end and spread down the slide, pushing in front of it a thick wave of the molten material. The resultant film was of monoclinic form C, and the molecular chains were tilted from the normal to the surface by 38°, pointing in the direction of propagation of the wave.

Controlled Orientation from Evaporation of Solutions.—It was discovered that similar results for stearic acid could be obtained, with thinner films, by evaporating a dilute solution of the acid in acetone. If a drop of solution was spread over a clean metal slice and one end of the slide was placed against a warm surface (slightly under the boiling

- (13) A. E. Smith, *J. Chem. Phys.*, **21**, 2229 (1953).
 (14) W. M. Mazee, *Rec. trav. chim.*, **67**, 197 (1948).
 (15) A. Muller and K. Lonsdale, *Acta Cryst.*, **1**, 129 (1948).
 (16) D. A. Wilson and E. J. Ott, *J. Chem. Phys.*, **2**, 231 (1934).
 (17) D. G. Kolp and E. S. Lutton, *J. Am. Chem. Soc.*, **73**, 5593 (1951).
 (18) A. E. Smith, International Congress of the Union of Crystallography, Montreal, 1957; *Abstracts of the Communications*, **4**, 74 (1957).
 (19) H. M. M. Shearer and V. Vand, *Acta Cryst.*, **9**, 379 (1956).
 (20) S. Takogi, private communication, 1958.
 (21) G. Natta and R. Rigamonti, *At. C. Accad. Lincei*, [6] **22**, 342 (1935).

(22) It cannot be supposed that the metal slides are at all flat on an atomic scale. It then seems, at first, remarkable that molecular directions in a surface film should be related at all closely to the macro-average plane of the surface. Nevertheless, not only are experimental mean tilts to the average surface identical to the crystallographic tilts, but the scatter from the mean cannot be very many degrees, according to the diffraction patterns. In all of the films investigated the molecular packing was essentially crystalline. It must be concluded that lateral regularity is energetically more important than precise registry of the low-energy methyl ends with the surface of the substrate (or in the case of some polar derivatives, with the upper surface of the adsorbed monolayer). Electron micrographs show to within a resolving power of some tens of angstroms (roughly the molecular dimensions of the long-chain compounds) that the polished surfaces are smooth, except for scattered scratches, and undulate gently. The horizontal tops of the undulations then would be the regions most accessible to the electron beam in diffraction experiments. Viewed from this standpoint the close relation between molecular and macro directions seems not unreasonable.

(23) See, for example, S. Amenckx, *Acta Cryst.*, **8**, 530 (1955); **9**, 16 (1956); **9**, 217 (1956).

point of acetone) a thin film of solid stearic acid began to form at the warm end and spread down the slide, pushing in front of it a wave of the solution. The resultant film was

again of monoclinic form C with the molecular chains tilted 38° from the normal, pointing in the direction of propagation of the wave.

EXTRACTION OF SODIUM THIOCYANATE FROM AQUEOUS SOLUTIONS BY TRIBUTYL PHOSPHATE

By G. MYRON ARCAND¹ AND WILLIAM R. CARROLL

Department of Chemistry, Montana State College, Bozeman, Montana

Received September 22, 1961

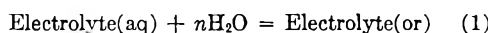
The extraction of sodium thiocyanate from aqueous solutions by tri-*n*-butyl phosphate has been studied and the data were analyzed in several different ways. Values of ΔF° and K have been calculated at 20, 30, and 40° for the complete equilibrium and for the distribution alone. Evidence indicates that a different hydrate is extracted at 20° than at the higher temperatures.

Introduction

Solvent extraction methods have been used to determine the nature of species existing in certain aqueous solutions. Yost and White² postulated the existence of H_2OsO_5 in aqueous solution, Swift, *et al.*,^{3,4} studied the extraction of iron(III) by ethers to arrive at HFeCl_4 as the predominant species in 6–8 *F* hydrochloric acid, and Arcand⁵ used an extraction method to propose arsenic(III) equilibria in hydrochloric acid solutions.

Melnick, *et al.*,⁶ investigated the extraction of ferric thiocyanate with tri-*n*-butyl phosphate (TBP) and as a result proposed $(\text{Fe}(\text{SCN})_3)_x$ as the extracted species.

Baldwin, Higgins, and Soldano⁷ investigated the extraction of various alkali metal salts by TBP and proposed an equation for the extraction



A distribution constant can be calculated if this equation is valid. The electrolyte in the aqueous phase is considered to be completely dissociated and that in the organic phase completely associated. The authors interpret n to be the primary hydration number of the cation extracted.

The present work shows that the Baldwin-Higgins-Soldano (hereafter referred to as B-H-S) analysis is valid to a point for the study of the extraction of sodium and potassium thiocyanates. However, other procedures have been developed which, in conjunction with the B-H-S approach, lead to knowledge of the composition of species in the organic phase and permit evaluation of some of the thermodynamic constants associated with the transfer of the thiocyanates from the aqueous to the organic phase.

(1) American Systems, Inc., 1625 E. 126th Street, Hawthorne, California.

(2) D. M. Yost and R. J. White, *J. Am. Chem. Soc.*, **50**, 81 (1928).

(3) R. J. Myers, D. E. Metzler, and E. H. Swift, *ibid.*, **72**, 3767 (1950).

(4) See also S. Kato and R. Isii, *Sci. Papers Inst. Phys. Chem. Research*, **36**, 82 (1939); *Chem. Abstr.*, **33**, 7232' (1939).

(5) G. M. Arcand, *J. Am. Chem. Soc.*, **79**, 1865 (1957).

(6) L. Melnick, H. Freiser, and H. F. Beeghly, *Anal. Chem.*, **25**, 856 (1953).

(7) W. H. Baldwin, C. E. Higgins, and B. A. Soldano, *J. Phys. Chem.*, **63**, 118 (1959).

Experimental

Tri-*n*-butyl Phosphate.—For most purposes, Eastman TBP was washed with 1 *F* HCl, then with 1 *F* NaOH, and finally with distilled water until the organic phase was clear and the washings neutral. Where high purity was desired, washed TBP was distilled at 3 mm. pressure, the fraction boiling between 121 and 124° being collected. The refractive index was n_{25}^D 1.4222.

Solutions.—Stock solutions were prepared from reagent grade materials. Thiocyanate solutions were standardized against AgNO_3 or KIO_3 . Fisher Chemical Company stabilized Karl Fischer reagent was used to determine water.

Distribution Measurements.—In most cases, equal volumes of aqueous solution and wet TBP were added to 60-ml. separatory funnels and placed in a constant temperature water-bath controlled to within $\pm 0.1^\circ$. Samples were shaken intermittently over a period of 5 hr. and then were allowed to stand in the bath overnight. Weighed portions of both phases were removed for analysis. The organic phases were washed 6 times with 5-ml. portions of water, the washings being collected in a volumetric flask.

For water determinations, equal volumes of aqueous solution and dry TBP were added to 60-ml. separatory funnels and placed in a constant temperature bath. Samples were shaken continuously for 2 hr. and then were allowed to stand in the bath for about 48 hr. Weighed portions of both phases were removed for analysis.

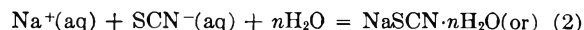
Analyses.—Aliquots of the aqueous phase acidified with HCl were titrated with standard KIO_3 in the presence of CCl_4 to determine thiocyanate.⁸ The end-point was taken as the disappearance of iodine color in the CCl_4 .

Thiocyanate concentrations in the organic phase were determined by washing the NaSCN from aliquots of the TBP and titrating the combined washings as described above.

Water in the TBP was determined by dissolving aliquots in dry methanol and titrating with Karl Fischer reagent to an amperometric end-point.⁹

Results and Discussion

The distribution data for various aqueous concentrations of sodium thiocyanate at different temperatures are shown in Table I. An attempt was made to analyze these data in several different ways, all of them based on the stoichiometric equation



Method of B-H-S.—The procedure involves plotting the quantity δ vs. $[\text{NaSCN}]_{\text{or}}$ where

$$\delta = 2 \log (\text{SCN}^-)_{\text{aq}} + n \log (\text{H}_2\text{O}) - \log [\text{NaSCN}]_{\text{or}} = \log K' + b'[\text{NaSCN}]_{\text{or}} \quad (3)$$

(8) R. Gaugin, *Anal. Chim. Acta*, **3**, 272 (1949).

(9) R. W. Freedman, *Anal. Chem.*, **31**, 1287 (1959).

where [] indicates molal concentration and () indicates mean activity. (Hereafter, NaSCN_{or} and $\text{NaSCN} \cdot n\text{H}_2\text{O}_{\text{or}}$ may be used interchangeably.) K' is the reciprocal of the equilibrium constant for eq. 2. Mean activity coefficients for the salts were taken from Harned and Owen.¹⁰

TABLE I
DISTRIBUTION OF NaSCN BETWEEN WATER AND TBP

$T, ^\circ\text{C.}$	$[\text{SCN}^-]_{\text{aq}}$ (m)	$(\text{SCN}^-)_{\text{aq}}$ (m)	$[\text{NaSCN}]_{\text{or}}$ (m)	$[\text{NaSCN}]_{\text{or}}$ $(\text{SCN}^-)_{\text{aq}}^2$
20	4.411 ± 0.006	4.212	1.321 ± 0.004	0.0746
	3.040 ± 0.007	2.504	0.931 ± 0.001	.149
	2.318 ± 0.001	1.787	.677 ± 0.001	.212
	1.963 ± 0.005	1.468	.540 ± 0.0007	.251
	1.205 ± 0.002	0.864	.2344 ± 0.0005	.312
	1.067 ± 0.008	.761	.1855 ± 0.0003	.320
	0.899 ± 0.006	.640	.1337 ± 0.0007	.327
	.728 ± 0.002	.517	.0886 ± 0.0001	.332
	.5541 ± 0.0005	.3951	.05275 ± 0.00004	.338
	.3761 ± 0.0006	.2719	.02551 ± 0.0001	.345
	.2362 ± 0.0005	.1753	.01098 ± 0.00010	.357
	.1580 ± 0.0005	.1206	.00549 ± 0.00003	.378
.1150 ± 0.0001	.0898	.00320 ± 0.00001	.397	
30	1.128 ± 0.003	.804	.1315 ± 0.0008	.204
	0.972 ± 0.004	.692	.0984 ± 0.0007	.205
	.743 ± 0.003	.528	.0581 ± 0.0005	.208
	.566 ± 0.000	.402	.0338 ± 0.0003	.210
	.3845 ± 0.0030	.2780	.0167 ± 0.0001	.216
	.2029 ± 0.0010	.1522	.00530 ± 0.00004	.229
	.1000 ± 0.0004	.0788	.00160 ± 0.00001	.259
40	1.670 ± 0.004	1.230	.1780 ± 0.0016	.1174
	1.389 ± 0.001	1.004	.1244 ± 0.0010	.1234
	1.144 ± 0.008	0.816	.0824 ± 0.0001	.1245
	0.756 ± 0.000	.537	.0370 ± 0.00011	.1280
	0.4615 ± 0.0042	.327	.01449 ± 0.00026	.1360

The value of n was determined by measuring the concentration of water in TBP which had been equilibrated with pure water and comparing with that in TBP which had been equilibrated with the salt solutions. The difference was considered to be the amount carried into the TBP as water of hydration. The mole ratio of water to salt in the TBP was taken as n . The presence of salt in the aqueous phase may change the amount of water extracted by the TBP alone; however, no information is available to show such a change. Furthermore, the value of n at any given temperature appears to be independent of the activity of salt in the aqueous phase. The values of n found at 20 and 30° were 3.2 and 1.7, respectively.

The plots made by this method are shown in Fig. 1. The linear portions of the curves are extrapolated to zero concentration to evaluate $\log K'$, from which the distribution constants are calculated. It will be noted that these plots are linear only between concentrations of about 0.02 and 0.2 m . The B-H-S procedure assumes that the extracted species is undissociated in the TBP and that the molar concentration is proportional to the activity in this phase. The drop-off at low concentrations seen in Fig. 1 is attributable to significant dissociation of the salt in the TBP. Correction for this dissociation results in straight lines from almost 0 to 0.2 m (see Fig. 1).

The constant, b' , is related to the activity corrections which may be necessary in the TBP phase. It is reasonable to assume that the logarithm of

(10) H. S. Harned and B. B. Owen, "The Physical Chemistry of Electrolytic Solutions," 2nd Ed., Reinhold Publ. Corp., New York, N. Y., 1950, p. 563.

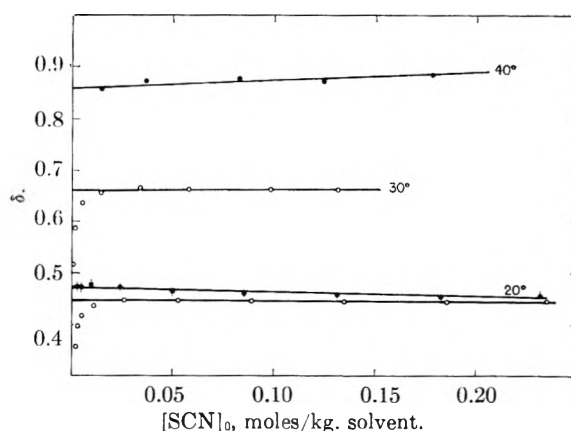


Fig. 1. Plot of eq. 3: ● is the plot corrected for the dissociation of NaSCN in the TBP.

the activity of the undissociated salt in the organic phase is directly proportional to the molal concentration in dilute solutions. However, at higher concentration, this simple linear relationship probably no longer is valid; therefore the curve becomes non-linear under those circumstances. The value of b' varies from -0.01 to 0.17 as the temperature varies from 20 to 40°, suggesting that this activity correction is not important at the lower temperatures.

D vs. $(\text{SCN}^-)_{\text{aq}}$.—The equilibrium expression for eq. 2 may be written

$$[\text{NaSCN}]_{\text{or}} \gamma_0 / (\text{SCN}^-)_{\text{aq}}^2 (\text{H}_2\text{O})^n = K \quad (4)$$

γ_0 is the activity coefficient of undissociated NaSCN in the TBP. If a quantity, D , is defined such that $D = [\text{NaSCN}]_{\text{or}} / (\text{SCN}^-)_{\text{aq}}^2$, then eq. 4 becomes

$$D \gamma_0 = K (\text{H}_2\text{O})^n \quad (5)$$

If we let $\ln \gamma_0 = h$, then

$$\gamma_0 = e^h = 1 + h + \frac{h^2}{2!} + \frac{h^3}{3!} + \dots \quad (6)$$

In this case it is found that $\ln (\text{H}_2\text{O})$ is proportional to $(\text{SCN}^-)_{\text{aq}}$, therefore

$$\ln (\text{H}_2\text{O}) = g (\text{SCN}^-)_{\text{aq}} \quad (7)$$

and

$$(\text{H}_2\text{O})^n = e^{ng(\text{SCN}^-)_{\text{aq}}} = 1 + ng(\text{SCN}^-)_{\text{aq}} + \frac{ng^2(\text{SCN}^-)_{\text{aq}}^2}{2!} + \dots \quad (8)$$

The activity of water is calculated by the graphical integration of the Gibbs-Duhem equation using the activities of aqueous NaSCN.¹¹ Combining eq. 5, 6, and 8 yields

$$D(1 + h + h/2! \dots) = K + \frac{Kn_g(\text{SCN}^-)_{\text{aq}}}{ng(\text{SCN}^-)_{\text{aq}}/2! + \dots} [1 + \dots] \quad (9)$$

At low salt concentration in TBP, $h = 0$, while higher powers of $ng(\text{SCN}^-)_{\text{aq}}$ will be negligible when $(\text{SCN}^-)_{\text{aq}}$ is less than 1. Thus eq. 9 is approximately

$$D = K + Kng(\text{SCN}^-)_{\text{aq}} [1 + ng(\text{SCN}^-)_{\text{aq}}/2] \quad (10)$$

A fairly accurate first approximation of K can be made by plotting D vs. $(\text{SCN}^-)_{\text{aq}}$. At low concentration, the second term in $(\text{SCN}^-)_{\text{aq}}$ becomes small so that extrapolation to zero concentration provides a good estimate of K . The

(11) H. S. Harned and B. B. Owen, ref. 10, eq. 1-9-10, p. 13.

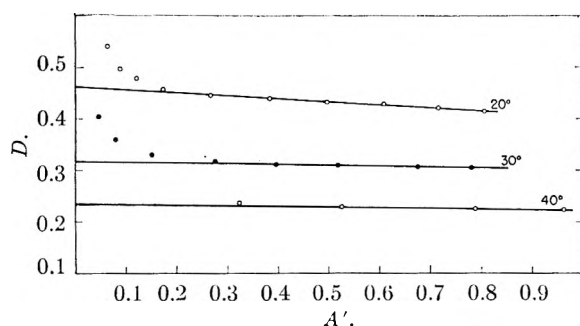


Fig. 2.—Plot of eq. 10: $A' = (\text{SCN}^-)_{\text{aq}}\{1 + ng(\text{SCN}^-)_{\text{aq}}/2\}$.

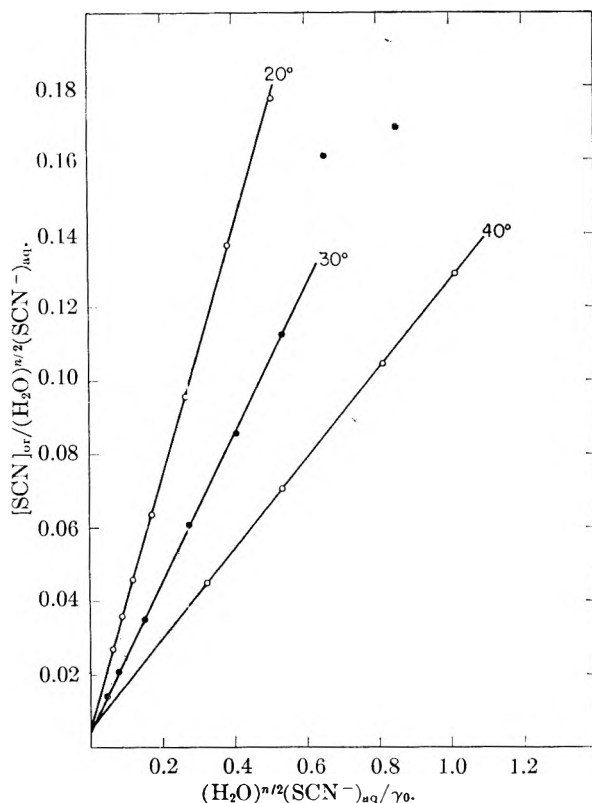


Fig. 3.—Plot of eq. 13.

slope of this straight line is Kng ; therefore an approximate value for ng can be calculated permitting a plot of D vs. $(\text{SCN}^-)_{\text{aq}}[1 + ng(\text{SCN}^-)_{\text{aq}}/2]$. Successive approximations should yield an accurate value for K . The constants so determined are very nearly the same as those determined by the B-H-S method. The final plots are shown in Fig. 2. Table II lists values of K which are the averages of these two analyses.

TABLE II

DISTRIBUTION AND DISSOCIATION CONSTANTS			
T , °C.	K	ΔF° , cal./mole	
20	0.360	595	
30	.217	920	
40	.136	1241	
			$k \times 10^4$
20°	.337	633	1.0
30°	.200	970	1.1
40°	.122	1308	2.0

^a Calculated using eq. 13.

Since a value for g can be calculated from a plot of eq. 7, the slope of the curves in Fig. 2 should yield the hydration number for the salt. Values of n calculated by this method at 20, 30, and 40° were 3.1, 1.5, and 1.7, respectively, which is quite close to those determined experimentally. These comparisons suggest that this method is at least as good as that of B-H-S; however, it must be remembered that g must be constant over the range of concentrations used.

There is considerable deviation from linearity in these plots at low concentrations, as was the case in the B-H-S plots. This is to be expected since no account was taken of dissociation of the salt in the TBP.

Some of the preliminary results on the extraction of potassium thiocyanate were analyzed using eq. 10 and the distribution constant was calculated to be 0.204 at 25°. The value of n was found to be 2.8. Comparison of these results with those for the sodium system is difficult because of the temperature differences, but the trend appears to be as expected.

Estimate of Dissociation in TBP.—The dissociation constant for sodium thiocyanate in the TBP phase may be estimated by including this factor in the equations. If eq. 5 is assumed to represent only undissociated salt in the TBP, then

$$[\text{NaSCN}]_{\text{or}} \gamma_0 = K(\text{SCN}^-)_{\text{aq}}^2 (\text{H}_2\text{O})^n \quad (11)$$

The dissociation may be represented by

$$[\text{Na}^+]_{\text{or}} [\text{SCN}^-]_{\text{or}} = k[\text{NaSCN}]_{\text{or}} \gamma_0 \quad (12)$$

Let $m = [\text{NaSCN}]_{\text{or}} + [\text{Na}^+]_{\text{or}}$, combine with eq. 11 and 12, and rearrange

$$m/(\text{SCN}^-)_{\text{aq}}(\text{H}_2\text{O})^{n/2} = K(\text{SCN}^-)_{\text{aq}}(\text{H}_2\text{O})^{n/2}/\gamma_0 + (kK)^{1/2} \quad (13)$$

A plot of $m/(\text{SCN}^-)_{\text{aq}}(\text{H}_2\text{O})^{n/2}$ vs. $(\text{SCN}^-)_{\text{aq}}(\text{H}_2\text{O})^{n/2}/\gamma_0$ should be a straight line of slope K and intercept $(kK)^{1/2}$. These plots are shown in Fig. 3 and the values of K and k are given in Table II. The values for γ_0 are calculated from the relation used in the B-H-S method

$$\log \gamma_0 = b'(\text{SCN}^-)_{\text{aq}}$$

where b' is the slope of the line given by eq. 3.

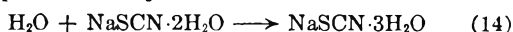
The value of k determined by this method is somewhat uncertain. However, it does compare favorably with the value determined by analysis of conductivity data. Furthermore, if the concentration of undissociated NaSCN in the organic phase is calculated using this constant, the B-H-S plot becomes linear to the lowest concentrations investigated (Fig. 1), which suggests that the values are at least of the correct order of magnitude.

Thermodynamic Quantities.—Activities have been used where available in all of the methods of data treatment and effective extrapolation to zero concentrations of solute in each phase should eliminate any error from neglect of activity coefficients in the organic phase. Consequently, the equilibrium constants so evaluated should be thermodynamic constants and should permit the calculation of the standard free energies for the distributions. These values are shown in Table II. The first group of values apply to the over-all

equilibria while the second apply only to the distribution equilibria.

We thought at first that we should be able to calculate ΔH^0 and ΔS^0 if a plot of $\ln K$ vs. $1/T$ provided a straight line. Actual deviation from a straight line turned out to be relatively small and a ΔH^0 of -9.2 kcal./mole was calculated for the distribution. However, this calculation must assume that the species extracted are the same at all temperatures. This seems unlikely when one considers the apparent change in hydration number as the temperature changes from 20 to 30°. We feel that the evidence indicates a different hydrate at 20° than at 30 and 40°. This is not in disagreement with the results of solubility measurements of alkali halides reported by Meyerhoffer.¹² Therefore, calculations of ΔH^0 could be made using only 30 and 40° points, but this evaluation would be of questionable accuracy. However, it seems probable that a value near -10 kcal./mole would be correct.

If one assumes that ΔH^0 can be calculated from the 30 and 40° points, one can determine a ΔF^0 for a postulated hydration of the salt



which would yield a value of 70 cal./mole. The di- and trihydrates are assumed, being the closest whole numbers to the experimental values of n . No information on ΔH^0 or ΔS^0 for this hydration is available.

The value of n calculated for the potassium thio-

(12) J. W. Mellor, "A Comprehensive Treatise on Inorganic and Theoretical Chemistry," Vol. 2, Longmans, Green & Co., New York, N. Y., 1922, p. 602.

cyanate system is not considered to be very accurate. The g term in eq. 7 does not seem to be quite constant over the necessary concentration range although it is nearly so. However, it seems probable that n will be nearer to 3 than to 2. This certainly would suggest that any change in hydration to a lower value of n must occur at a temperature higher than 25°. If we can assume that the hydration effect is similar for the sodium salt system, then we might reasonably look for dehydration to occur between 25 and 30°.

Work is in progress to investigate the observed change in primary hydration number. When this is completed, a more accurate evaluation of the thermodynamic quantities should be possible. At present it would seem that ΔH^0 and ΔS^0 for the transfer of the hydrated, undissociated ion-pair are about -10 kcal./mole and -35 cal./mole/deg., respectively.

It is apparent that the different methods of analyzing the distribution data all are valid to a certain extent, but may not be entirely independent of each other. Use of eq. 3 requires a value of n which may be determined experimentally or by means of eq. 10. Experimental evaluation is tedious while use of eq. 10 depends on the constancy of g . Probably the most valid approach uses eq. 13. In this case, both n and γ_0 must be known. Unless n is determined experimentally, both of the other equations must be used, (3) to determine b' (to determine γ_0) and (10) to determine n . This is probably the most powerful approach.

Acknowledgment.—This work was supported in part by a grant from Research Corporation.

DEUTERIUM EXCHANGE ON SILICA GEL INITIATED BY COBALT-60 IRRADIATION

BY HAROLD W. KOHN

Chemistry Division, Oak Ridge National Laboratory, Oak Ridge, Tennessee. Operated for the U. S. Atomic Energy Commission by Union Carbide Corporation

Received September 27, 1961

The irradiation-induced exchange of deuterated silica gel with methane and with hydrogen has been studied with Co^{60} gammas, and the yields of H_2 , HD, D_2 , and CH_3D were measured. The G -values for HD and D_2 from the hydrogen reaction based on energy absorbed by the gel were 1.5 to 1.8 and 0.6 to 1.0, respectively. Deuterated product yield increased with cumulative dose. The surprisingly high D_2 yield could be suppressed either by degassing the gel at higher temperatures before irradiation, or by lowering the temperature of the radiation reaction. These treatments left the HD yield virtually unaffected. Radiation-induced exchange with methane gave low (<0.4) yields for all hydrogen species and somewhat greater (0.6–1.6) yields for CH_3D , which increased and then decreased with increasing degassing temperature up to 585°, showing a maximum near 400°. The hypothesis that radiation-produced ions on the gel initiate reaction is discussed.

Introduction

Many studies of radiation effects on silica have been reported,¹ yet little is known about the actual radiation chemistry of the various types of silica. Such knowledge might clarify our understanding of two problems of current interest: first, the role of the solid adsorbent in transferring radiation energy to an adsorbate in systems involving high-area inorganic solid adsorbents and saturated organic adsorbates²; and second, the enhancement

of the catalytic activity of a solid by ionizing radiation.³

This paper reports the results of experiments on the irradiation-induced exchange of deuterated silica gel with hydrogen and with methane. Since it had been suggested that water might play a determining role in both energy transfer and radiation enhancement, specific attention was devoted to the effect of water as a surface contaminant.

(1) See for example, *J. Phys. Chem. Solids*, **13**, 271 (1960).

(2) A. O. Allen, *Radiation Research*, Supplement 2, 471 (1960).

(3) E. H. Taylor, H. W. Kohn, and G. E. Moore, "Large Radiation Sources in Industry," International Atomic Energy Agency, 1960, p. 119.

These exchange reactions were studied with respect to D₂O content, impurity content, temperature, and irradiation history of the silica gel.

The usual methods of studying the chemical effects of radiation on solids⁴ are not applicable to this system⁵; silica is neither readily decomposed, nor does it release any gas upon irradiation.⁶

Actually silica gel adsorbs both oxygen and hydrogen during irradiation,⁷ thus any H₂ or O₂ which might be formed would be immediately reabsorbed. Such a decomposition-readsorption cycle could change the chemical binding of an adsorbate or redistribute it on the surface or in the interior of the solid, but the cycle would not be directly detectable. Hence an indirect method such as the tracer method is indicated.

Experimental

Two types of silica gel were used in this investigation. Commercial silica gels (Davison, Fisher) contained 0.01 to 0.04% Al impurity and had surface areas of 300 to 500 m.²/g. An especially pure sample of gel was prepared by slowly hydrolyzing SiCl₄ in a polyethylene beaker with triply distilled water. This SiCl₄ was prepared from the reaction of zone-refined silicon and chlorine. It had no impurity content detectable by spectrographic analysis and had a surface area of ~600 m.²/g. Samples were generally 10 g. in containers of 30 to 50 cc. volume. After preliminary evacuation at 500°, all samples were deuterated by adding three or more successive portions of 99+% D₂O, heating after each addition, and then re-evacuating, thus deuterating all the normal OH groups on the surface.⁸ The samples finally were evacuated overnight at the temperature indicated.

Matheson 99+% methane was purified by fractionation from a Linde 4a Molecular Sieve at -185°. Mass spectrographic analysis of this material showed only traces of N₂ and of H₂. Electrolytic hydrogen passed through a "De-oxo" purifier (Baker and Company, Inc., Newark, N. J.) was similarly fractionated from silica gel at -196°. The deuterium was purified by passage through a palladium valve.

Standard high-vacuum technique (mercury diffusion pumps, liquid N₂ traps, etc.) was used. The irradiation ampoules were fitted with high-vacuum stopcocks and standard taper joints for ease in manipulation. Possible contamination by the radiolysis products of stopcock grease is unavoidable but does not appear to be a serious problem.⁹ Pressure was measured by a mercury manometer in the millimeter range and in the micron region by a Pirani-type gage using thermistors.

The irradiation ampoule was connected to a calibrated (45-cc.) volume which then was evacuated to ~10⁻⁵ mm. Reactant gas then was admitted to this volume to a pressure of 30 to 50 mm. The ampoule was cooled to -196°, and the stopcock was opened, which transferred nearly all the gas from the calibrated volume to the irradiation ampoule. The ampoule was closed, removed from the apparatus, and warmed to room temperature. It then was placed in a 700-curie Co⁶⁰ source (calibrated by ferrous sulfate dosimetry at 4.4 × 10¹⁷ e.v. g.⁻¹ min.⁻¹) for times ranging from 30 to 200 min. In all these experiments small irradiation doses were used to ensure low conversions, thus reducing the possi-

bility of the initial radiolysis products reacting with the gel or with the reactant gas.

After irradiation, the ampoule was reconnected to the apparatus and a representative sample of the gas was obtained by expansion into an evacuated bulb. In experiments involving methane, the ampoule was immersed in boiling water to promote desorption from the gel. The gas samples were analyzed by mass spectrometry. When hydrogen and methane were determined simultaneously, their respective concentrations were calculated using the ratio of signal to pressure for masses 2, 15, and 16 obtained from standard samples of methane and of hydrogen.

The yield for each species was calculated from the formula

$$G = \frac{V \times P \times 3.3 \times 10^{16} \times (\% - \%_0)}{T \times W \times 4.4 \times 10^{17}}$$

where G = 100 e.v. yield

V = volume of calibrated volume in cc.

P = pressure, in mm. of gas

$(\% - \%_0)$ = percentage of component in gas, suitably corrected for background

T = time of irradiation in min.

W = weight of adsorbent in g.

The numbers obtained probably are minimum values and our experience has indicated that their reproducibility by this method cannot be expected to be better than ±15%. Their significance is found more in their interrelationships than in their absolute values.

Experimental Results

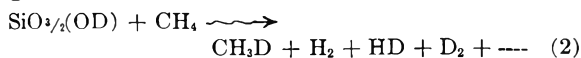
Ordinarily the exchange between irradiated silica gel and gaseous reactants such as hydrogen or methane is small and slow.¹⁰ Any appreciable exchange during irradiation therefore would imply that irradiation creates short-lived reactive intermediates, either in or on the gel. Studies of these radiation-induced exchanges were intended to reveal the presence of such intermediates, if any, and to aid in their characterization. If we represent the reactive surface portion of deuterated silica gel as SiO₂(OD), we can write chemical reactions for each set of exchange experiments. A brief summarization of experiments with appropriate equations follows.

The exchange of hydrogen with deuterated silica gel



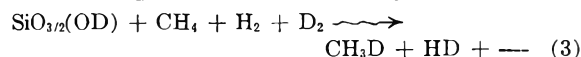
was studied with respect to irradiation history, temperature, and oxygen poisoning of the gel.

The exchange between methane and deuterated gel

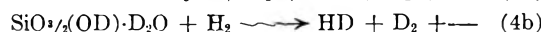
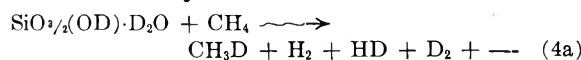


was examined with respect to gel purity, irradiation history, degassing temperature of the gel, and aging.

The exchange reaction between a 1:1 deuterium-hydrogen mixture and methane in the presence and absence of gel was examined briefly.



Finally, the exchange of methane and hydrogen with deuterated gel covered by a monolayer of molecular heavy water was measured.



(4) H. G. Heal, *Atomics and Atomic Technology*, **6**, 205, 241 (1955).

(5) Standard methods are the irradiation of the solid *in vacuo* followed by analysis of the gaseous decomposition products, and/or dissolution of the irradiated solid followed by the analysis of species in solution and in the gas phase. Direct observation by paramagnetic resonance techniques, optical spectroscopy, etc., also are useful; however, these are primarily physical rather than chemical measurements.

(6) *Radiation Research*, Supplement 2, 478 (1960).

(7) H. W. Kohn and E. H. Taylor, Abstracts of Papers, 138th National A.C.S. Meeting, 11-I, No. 28, September, 1960. See also T. F. McDonald, Thesis, Columbia University, January, 1961.

(8) R. G. Haldeman and P. H. Emmett, *J. Am. Chem. Soc.*, **78**, 2917 (1956).

(9) Mass spectrometer analyses indicated sufficient reproducibility and no detectable contaminants from the grease.

(10) H. W. Kohn and E. H. Taylor, Second International Congress on Catalysis, Paper No. 71, Paris, 1960.

Preliminary experiments were intended merely to determine whether any significant exchange between hydrogen and deuterated gel would occur during irradiation (eq. 1) at ambient (25–35°) temperature. Two deuterated silica gel samples, previously degassed at 530°, were irradiated in the presence of 20–150 mm. H₂. One sample was given 20- to 30-min. cumulative doses up to a total of 491 min.; the other was irradiated similarly to a total of 221 min. The data are represented in Fig. 1. Each sample showed a large yield of deuterium¹¹ for each 20- to 30-min. irradiation; this yield increased with uninterrupted dosage. The increase in $G_{(D)}$ appeared monotonic and reasonably reproducible, although, after the sample was kept for a week at room temperature with no irradiation, $G_{(D)}$ dropped to near its initial value. These samples when further irradiated *in vacuo* for long periods (Fig. 1) gave values for $G_{(D)}$ as high as 5.8. Varying the hydrogen pressure had no observable effect on $G_{(D)}$.

In order to measure molecular D₂ formation, one has to use a poisoned gel since even short irradiations at these dose rates convert unpoisoned silica gel to an active H₂-D₂ exchange catalyst.¹² Hence, at low conversions, most of the D₂ which might be formed would be converted to HD on the irradiated gel. The H₂-D₂ exchange could best be suppressed by poisoning the gel before each irradiation with a small amount of oxygen, since such poisoned gels apparently differed from the unpoisoned gels (compare Table I and Fig. 1) only in their inability to promote hydrogen-deuterium exchange. The yield of molecular D₂ at room temperature appears remarkably large. Results of such experiments are shown in Table I.

TABLE I

100 E.v. Co⁶⁰ γ -RAY YIELDS OF HD AND OF D₂ FROM DEUTERATED SILICA GEL

Samples were oxygen poisoned before each determination

Temp. of irradiation, °C.	$G_{(HD)}$	$G_{(D_2)}$	HD/D ₂ ^a
Sample I, pumped at 350°			
60	0.69	0.27	2.6
25	1.46	0.60	2.3
-18	1.09	1.13	8.3
-78	1.31	0.05	~75
-196	2.03	.01	~160
Sample II, pumped at 410°			
60	0.48	0.32	1.5
25	1.83	1.00	1.8
-18	0.68	0.33	2.1
-78	1.43	.21	6.8
Sample II, repumped at 585°			
25	1.61	0.03	51
-18	1.01	.02	47
-78	0.87	~.00	...

^a If equilibrium be reached, HD/D₂ should be in the neighborhood of 60 for this range of composition.

The yield of HD was not as greatly affected by the temperature of evacuation of the sample as

(11) The yield is large compared with experiments where the deuterated gel is first irradiated and hydrogen then is added. Such a G is $\sim 3 \times 10^{-2}$. Cf., Ref. 10.

(12) H. W. Kohn and E. H. Taylor, *J. Phys. Chem.*, **63**, 966 (1959).

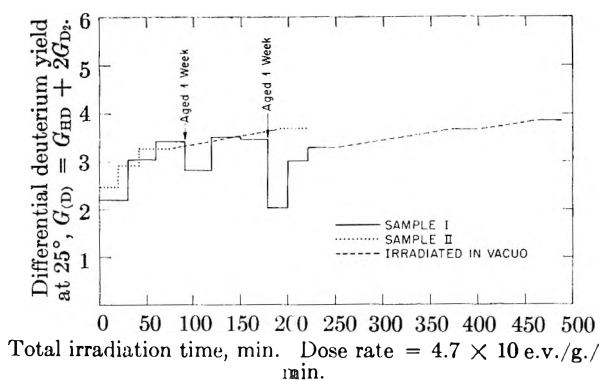


Fig. 1.—Effect of cumulative radiation on the exchange of deuterated silica gel with hydrogen. Sample I, after an additional 16 hr. irradiation, $G_D = 4.7$. Sample II, after an additional 65 hr. irradiation, $G_0 = 5.8$.

was the yield of D₂. In order to avoid the cumulative dose or aging effects previously cited, the chronological order of the experiments was not that shown in Table I, hence the yields (particularly of HD) did not change monotonically with reaction temperature. The ratio of the yields of HD relative to D₂, however, generally was increased by decreasing the reaction temperature.¹³ Apparently deuterium-containing intermediates activated by radiation can react with neighboring deuteriums, but this reaction has a higher activation energy than the reaction of this intermediate with the gas. Excessively high (585°) degassing temperature, which would seriously deplete the surface of OD groups, caused a marked lowering of the D₂ yield without similarly affecting the yield of HD.

The magnitude of reaction 1 demonstrated the existence of a radiation-produced reactive intermediate in the hydrogen-silica gel system. Further characteristics of this intermediate might best be determined by the examination of another reactive system. Experiments on the radiation-initiated exchange between deuterated silica gel and methane (reaction 2) are summarized in Table II.

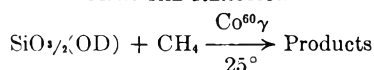
The results of these exchange experiments showed similarities to the results previously cited with hydrogen, being markedly sensitive to preconditioning of the gel. For example, increasing the degassing temperature up to some point between 375 and 420° caused an increase in CH₃D yield, whereas further temperature increases lowered this yield. Prior irradiation increased the CH₃D yield obtained from the commercial silica gel, but actually produced a slight decrease in the yield of CH₃D from the ultra-pure gel sample. Aging the pre-irradiated impure sample for one week produced a decrease of the CH₃D yield to near its initial value.

Since H₂ is formed by the radiolysis of CH₄, the CH₃D conceivably could be formed by the gas phase radiation reaction of CH₄ and the deuterium formed by reaction 1. A separate experimental check of this possibility was made by irradiating small amounts (1/2 mmole each) of hy-

(13) Exceptions are line 1 or 2 and lines 10 and 11. The analytical error in determining such small amounts of deuterium makes the last two numbers highly uncertain.

TABLE II

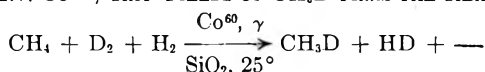
100 E.V. YIELDS OF HYDROGEN AND DEUTERATED PRODUCTS FROM THE REACTION

50 mg. of D₂O is added to deuterated gel prior to first evacuation listed in column 1

Treat-ment	Dose × 10 ²⁰ , e.v.	G _{H₂}	G _{HD}	G _{D₂}	G _{CH₃D}	
A. Effect of degassing temperature.						
Sample I, 10 g. ultra-pure silica gel						
Degass.	25°	2.6	0.27	0.44	1.6	0.21-0.25
	170°	2.6	.25	.09	0.28	0.58
	280	2.6	.25	.06	.32	.70
	340	2.6	.21	.05	.19	.72
	395	2.6	.20	.03	.11	.65
	440	2.6	.20	.03	.13	.64
	535	2.6	.19	.05	.11	.62
Sample II, 10 g. Fisher silica gel						
Degass.	25°	4.0	0.05	0.23	0.27	0.59
	160°	4.0	.10	.21	.30	.68
	250	3.5	.09	.18	.18	.77
	375	3.3	.16	.17	.04	.96
	450	2.6	.14	.04	..	.72
	530	3.7	.1569
B. Effect of continued irradiation.						
Sample I, redeuterated, degassed at 425°						
		1.7	0.36	0.05	0.09	0.59
Pre-irr.	312'	1.7	.31	.05	.15	.53
Pre-irr.	960'	2.6	.20	.07	.22	.49
Sample II, redeuterated, degassed at 420°						
		3.7	0.28	0.02	..	0.92
		3.5	.22	.11	..	0.94
Pre-irr.	100 min.	2.9	.25	.10	..	1.10
Pre-irr.	440 min.	2.9	.26	1.51
	780 min.	2.3	.25	1.57
Aged 1 week		5.3	.35	.23	0.05	0.94
Reaction at -78°		6.0	.18	.17	0.10	0.40

drogen, deuterium, and methane with and without silica gel present. The results are summarized in Table III. Thus CH₃D is formed on the gel since none is found when no gel is present.

TABLE III

100 E.V. Co⁶⁰ γ-RAY YIELDS OF CH₃D FROM THE REACTION

(Silica is not deuterated)

Irradiation time, min.	G _{CH₃D}	Adsorbent
92	0	None
130	0.05	4.4 g. Fisher degassed at 530°, Sample I
130	.17	4.4 g. Fisher degassed at 530°, Sample II
315	.11	4.4 g. Fisher degassed at 530°, Sample I
315	.05	4.4 g. Fisher degassed at 530°, Sample II
75	.69	4.4 g. Fisher degassed at 530°, Sample I
75	.21	4.4 g. Fisher degassed at 530°, Sample II
60	.67	10 g. Fisher degassed at 700°

Studies of the radiolysis of water and of the water-methane system¹⁴ have indicated that deu-

terated products (CH₃D, HD, D₂) might be formed by the radiation reaction of heavy water alone with methane or with hydrogen. However, comparison with water adsorbed on silica gel (which retains the conditions of high surface and rigidity), rather than with liquid water, would be more pertinent. To test this, two samples were prepared, each consisting of 1 g. of heavy water plus 10 g. of silica gel. This composition corresponds to a surface coverage of about a monolayer of D₂O molecules on top of the OD groups. The observed irradiation-produced exchange with methane and with hydrogen (reaction 4) is summarized in Table IV.

TABLE IV

100 E.V. Co⁶⁰ γ-RAY YIELDS FROM THE RADIATION EXCHANGE OF HEAVY WATER WITH METHANE AND WITH HYDROGENSamples: 10 g. deuterated Fisher silica gel plus 1.1 g. D₂O

Reaction	G _H	G _{HD}	G _{D₂}	G _{CH₃D}	
H ₂ + D ₂ O	..	0.39	0.27	..	Sample I
CH ₄ + D ₂ O	0.50	.40	.62	0.19	
H ₂ + D ₂ O	..	.29	.20	..	Sample II
CH ₄ + D ₂ O	.83	.76	.74	.15	
H ₂ + D ₂ O	..	.83	.43	..	Sample I, pre-irradiated 24 hr.
CH ₄ + D ₂ O	.39	.93	.56	.09	
H ₂ + D ₂ O	..	.52	.48	..	Sample II, pre-irradiated 22 hr.
CH ₄ + D ₂ O	.21	.54	.74	.13	

Intercomparison of different samples of silica gel is not always satisfactory due to the difficulty of obtaining reproducible samples. Accordingly, a series of irradiations using hydrogen and methane alternately was done on the two gel samples described in Table II. The yields of deuterated products from the hydrogen experiment always were significantly higher than the yields from the methane experiment for both samples throughout the course of nine experiments.

Discussion

A hypothesis involving ion-molecule reactions appears to be most consistent with these findings. Four facts support such a postulate. (1) Maximum deuterated-product yields for both the methane-gel system and the hydrogen-gel system occur when the gel is degassed at 400°, a procedure which leaves the gel surface about half covered with OD groups.¹⁵ (2) Deuterated-product yield for the hydrogen-gel system is consistently higher than that for the methane-gel system. (3) Deuterated-product yield for the hydrogen-gel system is appreciably greater than the amount of chemisorbed hydrogen.¹⁰ (4) Cumulative dose increases the deuterated-product yield.

Now, if reaction were initiated, for example, by radicals containing deuterium or by deuterium atoms driven from the gel surface, one would expect a maximum yield of deuterated products when the surface was fully covered, rather than half covered, with OD groups. If reaction were initiated in the substrate by electrons (the gel merely serving as a source of secondary electrons with which to bombard the substrate) one would predict higher

(14) H. Sakurai, J. Boyle, and C. Hochanadel, private communication, see also ORNL 2983, p. 28, June 20, 1960.

(15) W. K. Lowen and E. C. Broge, *J. Phys. Chem.*, **65**, 16 (1961). Such a gel although only 0.8 wt. % deuterium may be considered ~25 mole % deuterium.

yields of $\text{CH}_3\text{D} + \text{HD} + 2\text{D}_2$ from the methane-gel reaction than of $\text{HD} + 2\text{D}_2$ from the hydrogen-gel reaction. This is because criteria for comparing ionization of the two gases, *i.e.*, cross section, appearance potential, and W value, show that methane is more easily ionized than hydrogen.^{16,17}

If the appearance of deuterium in the gas phase were due to the reaction of chemisorbed hydrogen with OD groups, one of the two following conditions would occur. (1) The adsorbed hydrogen could exchange many times with OD groups during the course of the experiment. This would imply a path for catalytic exchange on the gel, but would allow the deuterated product yield to be greater than the yield of adsorption sites. (2) The adsorbed hydrogen could exchange with the OD group only once, *i.e.*, upon radiation activation. This implies no catalytic activity of the gel, but a deuterated product yield equal to the amount of chemisorbed hydrogen. Since the gel adsorbs hydrogen only during or after irradiation,¹⁸ and since the initial yield of adsorption sites is only about 1 site per 100 e.v. absorbed, and decreases with increasing irradiation,^{10,18} neither situation is in accord with the experimental facts presented here. It also is difficult to imagine how either mechanism could account for the large yields of D_2 obtained from oxygen poisoned gels. Other higher-order and multiple-step mechanisms do not appear likely in view of the lower yields obtained from some of the individual steps (reactions 3 and 4).

Most radiation chemical studies involve liquids, where the ions initially formed are not thought to persist long enough to participate in chemical reactions.¹⁹ They are quickly lost through re-

(16) S. C. Lind, "Radiation Chemistry of Gases," Reinhold Publ. Corp., New York, N. Y., 1961.

(17) F. H. Field and J. L. Franklin, "Electron Impact Phenomena," Academic Press, Inc., New York, N. Y., 1957.

(18) H. W. Kohn, *Nature*, **184**, 630 (1959).

(19) An interesting exception to this can be found in the work of Charlesby, Worrall, and Pinner (*Proc. Roy. Soc. (London)*, **A269**, 386 (1960)) on the radiation induced ionic polymerization of liquid isobutylene.

combination leading to radicals which initiate the chemical reactions.²⁰ The limited mobility of ions and electrons in silica gel (compared for example with the mobility in liquids) might preclude such rapid recombination; hence these ions might live long enough in the silica gel to initiate reaction. It is not required that such an ion contain deuterium, because any ion, under favorable energetic conditions, could transfer its charge to an adsorbed or impinging gas molecule which then could react with a neighboring deuterium atom if one be present. Carbonium ion reactions of this type on cracking catalysts are well known.²¹ The increase in the yield of deuterated products with cumulative irradiation then might be ascribed to an increase in the lifetime of ions formed in the gel by irradiation due to changes in its electronic structure produced by irradiation. However, in view of other changes in adsorptive¹⁸ and catalytic¹² properties engendered by irradiation, this last hypothesis is highly speculative.

Conclusions

Reactive deuterium-containing intermediates are formed in deuterated silica gel by irradiation. These intermediates react readily with methane and with hydrogen even though the latter gas is not adsorbed on the gel to any appreciable extent. At room temperature they also will react readily with neighboring OD groups to form molecular deuterium. Although the intermediates are not unambiguously identifiable, present evidence indicates that positive ions are principally responsible for initiating the exchange of the gel deuterium with methane, and that these ions also can account satisfactorily for the exchange with hydrogen. Radicals may perform a subordinate role in each case.

(20) "Comparative Effects of Radiation," edited by M. Burton, J. S. Kirby-Smith, and J. L. Magee, John Wiley and Sons, Inc., New York, N. Y., 1961.

(21) R. G. Haldeman and P. H. Emmett, *J. Am. Chem. Soc.*, **78**, 2922 (1956).

SPECTROPHOTOMETRY AND LIGHT SCATTERING ON SUPPORTED PLATINUM^{1,2}

BY P. DEBYE AND B. CHU

Cornell University, Ithaca, N. Y.

Received October 6, 1961

Transmission and scattering of dispersed platinum supported on catalysts are measured for visible light by utilizing an immersion technique. At one definite wave length the indices of refraction of the sample and the immersion liquid are made equal. From the extinction coefficient and the increase in the refractive index of the catalyst due to the presence of dispersed platinum, conclusions are drawn about the state of the platinum. It is found necessary to assume that part of the platinum is in an "atomic" state. The theory is substantiated by the good agreement obtained between the average radius of bulk platinum spheres by extinction measurements and by the method of light scattering.

Hydrogen adsorption and X-ray line broadening are being used for the characterization of supported

platinum. The measurement of adsorption can provide us with an average size of the platinum particles. X-Ray line broadening is restricted to the characterization of supported platinum in the crystalline state and is no good when the platinum particles are too small. Therefore, it seems worthwhile to look for a new approach which might give

(1) This work was performed as part of a research program sponsored by Esso Research and Engineering Company, Linden, New Jersey.

(2) Presented at the 140th National Meeting of the Am. Chem. Soc., Chicago, Illinois, September, 1961.

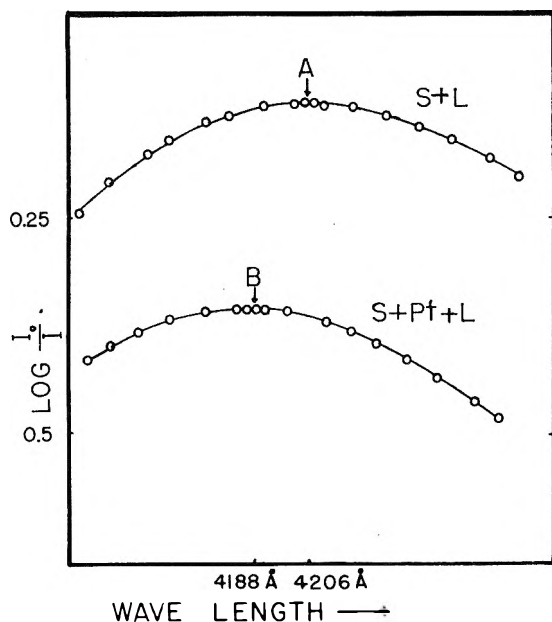


Fig. 1.—Plot of minus the logarithm of per cent. transmission *vs.* wave length of the incident light; S + L = alumina and immersion liquid; S + Pt + L = alumina plus dispersed platinum and immersion liquid.

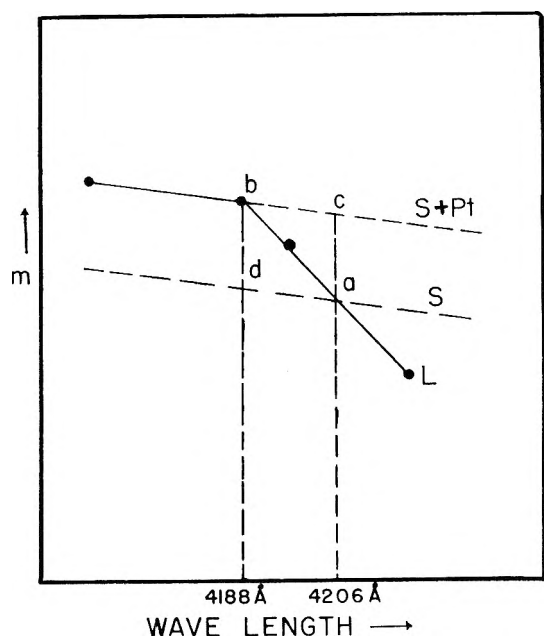


Fig. 2.—Index of refraction change due to the presence of dispersed platinum: S = alumina powder; S + Pt = alumina plus dispersed platinum; L = immersion liquid; *m* = index of refraction.

us more intimate information about the physical nature of the dispersed platinum. The purpose of this paper is to explore the possibility of characterizing supported platinum from measurements of the total turbidity and the angular dependence of the intensity of scattered light of dispersed platinum by utilizing an immersion technique.

Plan of Attack.—Our immediate problem arises from the fact that the bulky alumina will interfere with optical measurements of the supported platinum. We first must try to make alumina optically

invisible so that we see only the dispersed platinum. In theory, an isotropic powder immersed in a liquid which for one definite wave length has the same index of refraction should become optically invisible with monochromatic light of that wave length. In practice, however, the slight structural defects of the alumina lattice and adsorption of foreign molecules limit the degree of transparency. Then, it is necessary to compare results with a platinum free blank and base all calculation on excess effects.

The over-all picture of our experiment resembles the characterization of macromolecules in solution where the combination of excess extinction and the change in the index of refraction going from the solvent to the solution leads to the evaluation of molecular weight. In our case, if the index of refraction of the immersion liquid and that of the alumina are the same at a certain wave length, then, when a beam of light at that wave length passes through the solution mixture containing dispersed platinum, each platinum particle absorbs part of the incident light and also becomes the center of a scattered wave. The excess extinction depends on the number and size of the platinum particles. In addition, there is a change in the index of refraction going from pure alumina to the composite medium, alumina plus dispersed platinum.

A plot of per cent. transmission *vs.* wave length reveals a maximum transmission which indicates the match of refractive indices of powder and liquid, such as point A (or B) in Fig. 1. A shift in the maximum transmission indicates a change in the index of refraction of alumina to that of the composite medium at another wave length. The actual change in the index of refraction due to the presence of dispersed platinum is

$$\Delta m = \left[\left(\frac{dm}{d\lambda} \right)_i - \left(\frac{dm}{d\lambda} \right)_s \right] \Delta \lambda \quad (1)$$

where $\Delta \lambda$ is the wave length shift, $(dm/d\lambda)_i$ is the dispersion of component *i* at the wave length of maximum transmission, subscript (l) indicates immersion liquid, and (s) solid. Δm corresponds to *bd* or *ac* in Fig. 2.

Results

The results are listed in Tables Ia and Ib for γ -alumina plus 0.096 wt. % platinum (Catalyst 1126-108) and in Table II for η -alumina plus 2 wt. % platinum (Catalyst 1126-89).³

TABLE Ia

TRANSMISSION MEASUREMENTS ON γ -ALUMINA AND CATALYST (0.096 WT. %) ^c

Sample	λ (Å.)	$A_s = \log(I_0/I)$	<i>d</i> (cm.)	γ_{ext} (cm. ⁻¹)	<i>m</i> ₁
^a	4188	0.364	0.218	3.85	1.7093
^b	4206	0.12	0.218	1.27	1.7086
^a	3746	(1-chloronaphthalene as immersion liquid)			

^a γ -Alumina plus dispersed platinum. ^b γ -Alumina. ^c P-salt impregnation. Catalyst 1126-108.

(3) Samples were obtained by courtesy of the Esso Research and Engineering Company, Linden, New Jersey. See Appendix III for details of preparation of catalysts used.

TABLE I

LIGHT SCATTERING MEASUREMENTS ON γ -ALUMINA AND CATALYST (WITH 0.096 WT. % Pt)^a

Angle	G ₁	G ₂	G ₃	I ₁	I ₂	(I) = I ₂ - I ₁
30	76.5	82.0				
35	64.0	67.5				
40	50.1	51.6				
45	39.4	40.2				
50	32.0	32.0				
55	26.2	26.0				
60	22.3	21.0				
65	19.1	17.0				
110	9.0	11.0	7.0	503	1093	590
115	9.9	12.0	8.0	501	1026	525
120	10.1	12.5	9.1	477	992	515
130	10.2	13.5	11.0	436	956	520
140	11.0	14.9	13.0	436	921	485
150	12.1	16.0	18.0	438	900	462

G₃₀^o 5.8 6.0 36.0 36.0 36.0 Mean = 495.5

^a G₁, G₂, and G₃ are galvanometer readings of alumina, alumina plus platinum (Catalyst 1126-108), and immersion liquid, respectively; (I) is the corrected scattered intensity in relative units, $d = 0.205$ cm.; $\zeta = G$; $I = \gamma\zeta [1 + 1/\cos(\pi - \theta)]$.

TABLE II

TRANSMISSION MEASUREMENTS ON η -ALUMINA AND CATALYST (2 WT. %)^c

Sample	λ_0 (Å.)	A _s	d (cm.)	γ_{ext} (cm. ⁻¹)	m_1	Temp., °C.
^a	4299	1.50	0.218	15.9	1.7018	28.5
^b	4322	0.84	.218	8.87	1.7008	28.5
^a	4384	.73	.102	16.5	1.7010	23.0
^b	4408	.416	.102	9.37	1.7000	23.0

^a η -alumina plus platinum (Catalyst 1126-89). ^b η -alumina. ^c P-salt impregnation, calcined 10 hours at 1100°F. Catalyst (1126-89) mixed with enough pure η -alumina so that the resultant platinum content was reduced to 0.342 wt. %.

($dm/d\lambda$)_s only states the order of magnitude. The refractive index of 1-chloronaphthalene at the wave length of maximum transmission was extrapolated from values in the literature. Since ($dm/d\lambda$)_s is less than ($dm/d\lambda$)_l, the error involved for $\Delta m(\text{exp})$ is not appreciable.

	($dm/d\lambda$) _s
γ -alumina	6.4×10^{-5} for each $m\mu$ decrease in wave length
η -alumina	4.3×10^{-5} for each $m\mu$ decrease in wave length

Multiple scattering was eliminated with a reasonably thin light path. However, in calculating refractive index changes from the corresponding wave length shifts, we implicitly assume that the characteristics of alumina remain unchanged after we have dispersed platinum at its surface. Blank and catalyst must contain the same amount of foreign molecules, such as water and hydroxyl groups,⁴ and have similar structural defects. Since these assumptions do not necessarily hold under ordinary circumstances, the wave length shifts can be used only as supporting evidence in our final analysis.

Characterization of Dispersed Platinum. 1. General Discussion.—Theoretically, absorption and scattering always are governed by the Maxwell equations provided we consider the platinum with optical properties of the bulk material. If we assume the particle shape to be spherical, we can use a series expansion formula⁵ which expresses

(4) J. B. Peri and R. B. Hannan, *J. Phys. Chem.*, **64**, 1526 (1960).(5) E. Schoenberg and B. Jung, *Mit. Sternwarte Univ. Breslau*, **4**, 61 (1937); *Astron. Nachrichten*, **253**, 261 (1934).

the relationship between the extinction coefficient and a dimensionless quantity X , defined as $X = 2\pi a/\lambda_{\text{vac}}$, a being the radius of the sphere. The formula requires that the external medium is a vacuum. We have extended the theory so that we are able to calculate absorption and scattering coefficients for small absorbing spheres immersed in another homogeneous dielectric. The final formula for the excess extinction coefficient (see Appendix II for derivation) is

$$\gamma_{\text{ext}} = \frac{2\pi\Phi}{\lambda} \left(\frac{1 + 2m_1^2}{m_1^2} \right) \left\{ -\text{Im} \left(\frac{m^2 - 1}{m^2 + 2} \right) - \text{Im} \left[\frac{X^2 (m^2 - 1)^2 m^4 + 27m^2 + 38}{15(m^2 + 2)^2 m^2 + 3} \right] \right\} + \frac{4\pi\Phi X^3}{\lambda} \left| \frac{m^2 - 1}{m^2 + 2} \right|^2 + \dots \quad (2)$$

where Φ is volume fraction of platinum, m_1 and m_2 are the refractive index of immersion liquid and that of platinum, respectively, $m = m_2/m_1$, $X = 2\pi a/\lambda$, and $\lambda = \lambda_{\text{vac}}/m_1$. Im indicates that the imaginary part of the expression in brackets should be taken. m_2 is complex and accounts for the first two main absorption terms while the third term is derived from scattering. The series expansion formula is appropriate for small spheres.

No exact formula is available in the case of large spheres where the sizes are comparable to the wave length of the incident beam. γ_{ext} is roughly $n\pi a^2$, n being the number of spheres per unit volume. Since $\Phi = n(4\pi/3)a^3$, we have $\gamma_{\text{ext}} = (3\pi\Phi/2\lambda)(1/X)$.

All the information is summarized in Fig. 3, which shows a plot of γ_{ext} vs. X . The tail of the curve represents large spheres where γ_{ext} is proportional to X^{-1} . The beginning of the curve represents small spheres where γ_{ext} starts with a constant value and is expressed by the corrected formula of Schoenberg and Jung. The dotted line indicates an intermediate range of the variable X for which neither expression holds. The intercept at the ordinate is γ_{ext} (limiting), which is equal to

$$-\frac{2\pi\Phi}{\lambda} \left(\frac{1 + 2m_1^2}{m_1^2} \right) \text{Im} \left(\frac{m^2 - 1}{m^2 + 2} \right)$$

The refractive index change due to the presence of dispersed platinum in the form of limiting small spheres with optical properties of the bulk material (see Appendix II for derivation) is

$$\frac{nv}{2} \frac{1 + 2m_1^2}{m_1} \text{Re} \left(\frac{m^2 - 1}{m^2 + 2} \right) \quad (2a)$$

when $nv \ll 1$. v is the volume per particle, and Re indicates that the real part of the expression in brackets should be taken.

2. Extinction Measurements (Values from Table Ia and Appendix I).—The measured refractive index change due to dispersed platinum corresponds to about 6.4×10^{-4} . The measured excess extinction coefficient is 2.58 cm.⁻¹. A 0.096 wt. % of dispersed platinum in the form of "bulk" absorbing spheres would exhibit a limiting extinction coefficient, γ_{ext} (limiting), of no smaller than 15.62 cm.⁻¹ (eq. 2 with $X = 0$), and would contribute a shift in the index of refraction of 3.38

(6) Landolt-Börnstein, 5th Ed., 1st suppl. Vol., 1937, p. 470.

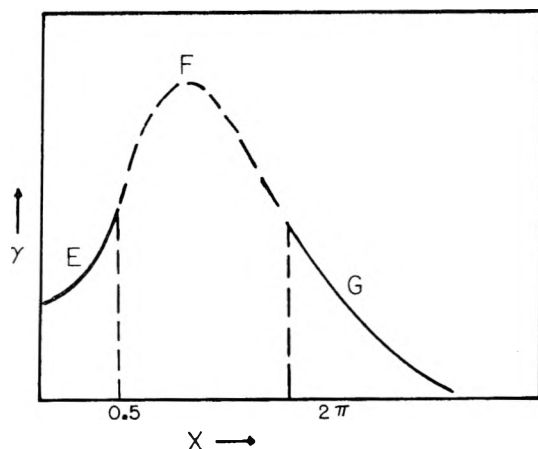


Fig. 3.—Plot of theoretical extinction coefficient vs. X : $X = 2\pi a/\lambda$; E, region where the corrected series expansion formula holds; F, intermediate range where neither theory holds; G, extinction coefficient approximately proportional to $1/X$.

$\times 10^{-4}$ (eq. 2a). The discrepancy signifies that the series expansion formula does not hold for such platinum spheres as are present in our supported catalyst. It is possible to explain the low extinction coefficient assuming platinum spheres with sizes comparable to the wave length of light. Since platinum particles grow rapidly at temperatures above 600° , we can test this assumption by measuring the change in the extinction coefficient of a heat-treated sample (at $625 \pm 25^\circ$ overnight).

The measured γ_{ext} increases to 6.16 cm.^{-1} . Figure 3 tells us that the increase in the excess extinction signifies an increase in the sizes of dispersed platinum and the smallness of bulk platinum spheres (certainly less than $0.5\lambda/2\pi$). In addition, a plot of extinction coefficient vs. time of heat treatment could tell us the growth rate of platinum spheres. We may conclude that the dispersed platinum does not have the same optical properties as the bulk material.

Spenadal and Boudart⁷ and Adler and Keavy⁸ concluded from their experiments that the tiny platinum "clusters" (or discontinuous monolayers) could be "atomic" in nature. We now assume that the total change in the index of refraction due to both "atomic" and bulk platinum is

$$\Delta m = \frac{(m_1^2 + 2)^2}{m_1} \frac{2\pi}{9} \frac{N}{A_{\text{Pt}}} c_1 \alpha_1 + \frac{c_2}{2d_{\text{Pt}}} \frac{1 + 2m_1^2}{m_1} \text{Re} \left(\frac{m^2 - 1}{m^2 + 2} \right) \quad (3)$$

in which α_1 is polarizability of atomic platinum per atom, c_1 and c_2 are the weights of atomic and bulk platinum per cc. of alumina, d_{Pt} is density of bulk platinum in g./cc., A_{Pt} is atomic wt. of platinum, and N is Avogadro's number. The first term accounts for the refractive index change due to "atomic" platinum and is derived from the Lorentz-Lorenz formula.

Suppose we equate the measured excess extinction coefficient with the limiting extinction coefficient γ_{ext} (limiting); we can calculate c_2' , defined as the weight of bulk platinum per cc. of alumina

required to account for the actual extinction when bulk platinum is in the form of limiting small spheres. In our case, $\gamma_{\text{ext}}(\text{exp}) = 2.58 \text{ cm.}^{-1}$, $c_{\text{total}} = 3.59 \times 10^{-3} \text{ g./cc.}$, and $\gamma_{\text{ext}}(\text{limiting}) = 4.35 \times 10^3 c_2' \text{ cm.}^{-1}$, therefore, $c_2' = 5.93 \times 10^{-4} \text{ g./cc.}$ We have about 83% dispersed platinum in its "atomic" state.

The polarizability of "atomic" platinum is $6.314 \times 10^{-24} \text{ cm.}^3$. The polarizability of an element in its atomic state can be estimated with the aid of the Lorentz-Lorenz expression. Refractive indices of KCl ,⁹ K_2PtCl_6 ,¹⁰ and the atomic polarization of chlorine¹¹ were taken from the literature. With eq. 3, we then get the calculated refractive index change to be 6.3×10^{-4} , which is only slightly lower than the measured 6.4×10^{-4} . The discrepancy is reasonable since we have assumed that the bulk platinum is in the form of limiting small spheres. Thus, it is justifiable to assume that part of the dispersed platinum is in an "atomic" state. The experimental findings in the wave length shift have not contradicted our theory and assumptions.

We may venture to estimate the three unknowns (c_1 , c_2 , and X) by solving three simultaneous equations, namely

$$\begin{aligned} c_{\text{total}} &= c_1 + c_2 \\ \gamma_{\text{ext}}(\text{exp}) &= \gamma_{\text{ext}}(\text{eq. 2}) \\ \Delta m(\text{exp}) &= \Delta m(\text{due to bulk Pt}) + \Delta m(\text{due to "atomic" Pt}) = \Delta m(\text{eq. 3}) \end{aligned}$$

As a first approximation, we can neglect the extinction of atomic platinum compared with that of bulk Pt because the bulk platinum has a complex dielectric constant and absorbs strongly in the visible region. The final results of our sample are

$$\begin{aligned} c_1 &= 3.08 \times 10^{-2} \text{ g./cc.} \\ c_2 &= 5.12 \times 10^{-4} \text{ g./cc.} \\ X &\cong 0.265 \text{ (by graphical soln.)} \\ a &\cong 103 \text{ \AA.} \end{aligned}$$

The average radius is about 100 \AA. Errors involved in this calculation are large since both theory and experiments are qualitative.

3. Scattering Measurements (Values from Table Ib).—The presence of an appreciable amount of dissymmetry signals the scattering of large spheres, which have sizes comparable to the wave length of the incident beam. It then is possible to estimate the distribution of sizes from a more detailed study of scattered intensity measured at different angles.

An important result from our angular measurements was that the excess scattered intensity did not fall off to zero for large values of θ , as shown in Table Ib. This means that in addition to the large inhomogeneities responsible for the great angular dependence of scattering, there are small inhomogeneities which for this wave length of 4358 \AA. would give an almost constant background scattering. Extinction measurements indicate that only one sixth of the dispersed platinum is in bulk

(9) "International Critical Tables," Vol. 7, McGraw-Hill Book Co., New York, N. Y., 1928.

(10) Raiteri, *Atti accad. naz. Lincei, Rend.*, **31**, 112 (1922); through Landolt-Börnstein.

(11) Extrapolated from W. Hückel, "Theoretische Grundlagen der organischen Chemie," Vol. 2, 1935, p. 86.

(7) L. Spenadel and M. J. Boudart, *J. Phys. Chem.*, **64**, 204 (1960).

(8) S. F. Adler and J. J. Keavy, *ibid.*, **64**, 208 (1960).

form, therefore we shall consider the more interesting small inhomogeneities.

Equation 5 in Appendix I tells us that the measured scattering coefficient for the imaginary sample which scatters the same amount of light at all angles is $3.27 \times 10^{-2} \text{ cm.}^{-1}$. Substituting it into eq. 12 in Appendix II and with $c_2 = 5.12 \times 10^{-4} \text{ g./cc.}$, then we get $X \cong 0.205$, or $a \cong 83.5 \text{ \AA.}$, which is the average radius of bulk platinum for this imaginary sample. The actual average radius of bulk platinum should be greater than 83.5 \AA. , since large inhomogeneities were entirely neglected in the calculation. We have shown that the average radius of the bulk platinum spheres by extinction measurements and by the method of light scattering has the same order of magnitude.

Catalyst with Higher Platinum Content.—We have chosen another catalyst with a 2 wt. % platinum and η -alumina as our support. The catalyst has been mixed with additional η -alumina blank so that the resultant platinum content can be reduced to 0.342 wt. %. The measured refractive index change is 9.06×10^{-4} . If we assume that all the dispersed platinum is in limiting small absorbing spheres with optical properties of the bulk material, the calculated refractive index change is 1.17×10^{-3} . Theoretically, the refractive index change is no longer precisely defined since we hardly can consider a mixture of alumina and catalyst truly composite. However, an increase in the index of refraction still indicates the presence of dispersed platinum. If γ_{ext} (limiting) = γ_{ext} (exp) = 7.1 cm.^{-1} , then we get $c_2' = 1.8 \times 10^{-3} \text{ g./cc.}$, which again is less than the measured platinum content of $1.22 \times 10^{-2} \text{ g./cc.}$ of alumina. Obviously the major fraction of dispersed platinum is still in its "atomic" state.

Conclusion

In summary, we may conclude from our measurements of the two specified samples that dispersed platinum is partially atomic in nature, creating a large specific surface area which may account for the activity of the catalyst. The remaining "bulk" platinum indicates a distribution of sizes. The average size of "bulk" platinum sometimes can be estimated, depending on the accuracy of our measurements and our assumptions on the nature of atomic (or ionic) platinum. Dispersed platinum tends to grow at temperatures above 550° . It may be noted that, as a rule, catalysts made from different procedures may have a variety of characteristics. Our catalyst samples are unique. However, we merely use these samples as illustrations of a new method for characterizing supported platinum. When the measured extinction coefficient of supported platinum is much lower than the value calculated with platinum having optical properties of the bulk material, and when the extinction coefficient increases with heat-treatment (above 550°), it is quite evident that part of the supported platinum which does not absorb light strongly must have a real dielectric constant. We have assumed a kind of "atomic" platinum which has a large polarizability and obeys the Lorentz-Lorenz formula. Because of the assumptions and the qualitative nature of both experiments and

theory, especially when a major fraction of the supported platinum is "atomic," the estimated size of the remaining bulk platinum spheres must necessarily be extremely qualitative. At most, it could give us the order of magnitude. Here we must realize that X-ray line broadening starts to play an increasingly important role. For a better understanding of the supported platinum, we feel that all existing methods of analysis, such as hydrogen chemisorption, X-ray line broadening, activity and surface area measurements, spectrophotometry and light scattering, etc., should be used on the same catalyst since it is difficult to make catalysts with exact characteristics, even from the same method of preparation.

The immersion technique can be utilized for characterizing any metal spheres dispersed at the surface of an isotropic powder. Our main difficulty comes from measurements of the wave length shift. In addition, only apparent extinction coefficients were measured. We have neglected the effect of the solid angle of scattered light reaching the photocell. The correction, which depends on particle size and concentration, is not important for qualitative discussions. Refined techniques (in vacuum drying, etc.) should give us a better estimate of the average radius of bulk platinum spheres.

Appendix I

Details of Measurement. 1. Determination of Φ .— Φ , defined as volume fraction of platinum in the light path, is

$$\frac{f d_s}{d_p}$$

with volume fraction of solid, f , = $(d_b - d_1)/d_s - d_1$; where d_b is the bulk density, d_1 is the density of immersion liquid, d_s is the density of the solid, and P is the platinum content in wt. %. The platinum content was determined spectrophotometrically by the iodide method.¹²

Sample	d_1 (g./cc.)	d_s (g./cc.)	d_b (g./cc.)	f
γ -Alumina	1.354 ^a	3.74	1.83	0.2024
η -Alumina	1.46	3.57	1.91	0.211

^a A mixture of 1-bromonaphthalene and 1-chloronaphthalene.

2. Transmission Measurements.—The powder was dried at 500° overnight to bake off adsorbed gases and vapors, and cooled in a desiccator with magnesium perchlorate and anhydrous calcium sulfate as desiccants. The sensitivity of wave length shift measurements depends on the moisture control. It is essential to exclude the powder from exposure to air, and the Beckman cell should be thermostated.

Apparent extinction coefficients were measured in a Cary Model 14 recording spectrophotometer. The normal 1-cm. Beckman cells were narrowed down to 0.102 cm. by inserting Beckman adaptors and 0.5-cm. Beckman cells to 0.218 cm. by inserting glass plates. The absorbancies ($A_s = -\log(I/I_0)$) were determined relative to a cell that contained a similar insert and the same liquid. A vial containing a small amount of the catalyst was filled with the immersion liquid *in vacuo*. Both powder and immersion liquid were transferred to the cell with a syringe and needle.

The refractive indices of alumina at different wave lengths were estimated from measurements of the wave lengths of maximum transmission of alumina immersed in two different liquids of known dispersions, namely, 1-bromonaphthalene and 1-chloronaphthalene. Refractive index measurements were made with an Abbe refractometer which was equipped with compensating Amici prisms adjusted so as to

(12) "Handbuch der analytischen Chemie," Teil IV, "Quantitative Analyse," Bd. VIIIb, achte Nebengruppe 3, p. 31; E. B. Sandell, "Colorimetric Determination of Traces of Metals," Interscience Publishers, Inc., New York, 1959, p. 728.

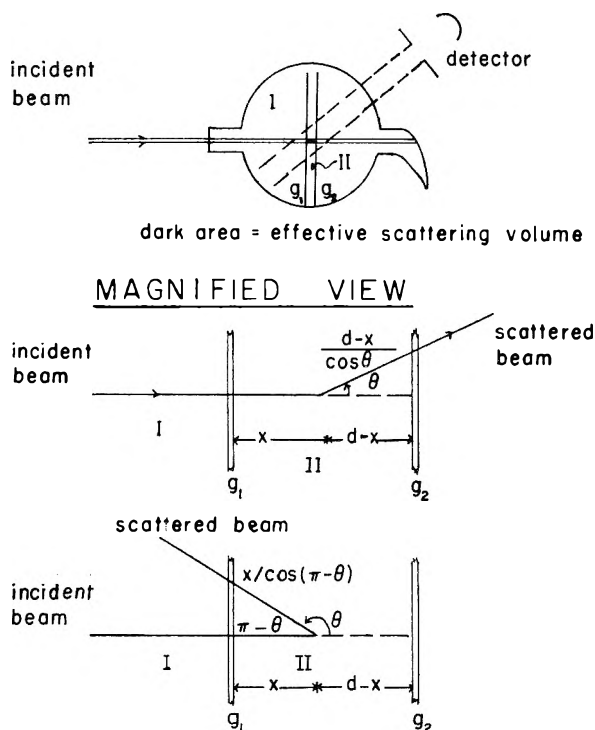


Fig. 4.—Schematic arrangement for measuring scattered light of supported platinum by using an immersion technique. Region I, immersion liquid only; region II, immersion liquid plus powder. g_1 and g_2 are thin glass plates having the same index of refraction as the immersion liquid at the wave length of maximum transmission.

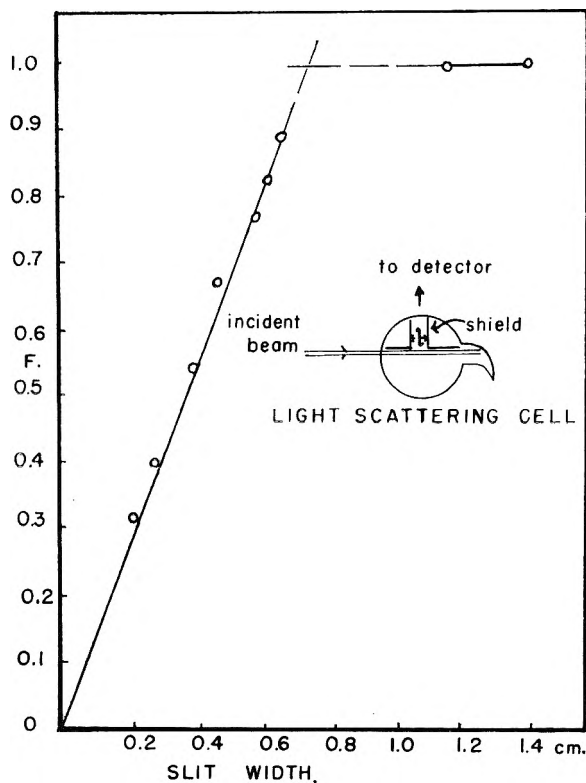


Fig. 5.—Plot of fraction of scattered intensity vs. slit width.

yield correct values of refractive index for $\lambda_{vac} = 5890 \text{ \AA}$. Refractive indices of the immersion liquid at other wave lengths were calculated with the aid of known dispersion

curves of 1-bromonaphthalene¹³ and 1-chloronaphthalene.¹⁴

3. **Light Scattering Measurements.**—The powder filled between two parallel glass plates, each 0.5 mm. thick and having the same index of refraction as the immersion liquid at 4358 Å. (near the wave length of maximum transmission), could be immersed in a light scattering cell containing the liquid. Then the angular distribution of scattered light was measured. Looking at the geometry of Fig. 4, we find

$$\zeta = \sigma \int_0^d \zeta_0 \exp\left(-\gamma x - \frac{\gamma x}{\cos(\pi - \theta)}\right) dx \cdot \frac{S}{R^2} \quad \theta > \frac{\pi}{2} \quad (4)$$

$$= \sigma \int_0^d \zeta_0 \exp\left(-\gamma x - \frac{\gamma(d-x)}{\cos \theta}\right) dx \cdot \frac{S}{R^2} \quad \theta < \frac{\pi}{2}$$

where ζ is apparent intensity of the scattered light, σ = scattering coefficient of the solid, ζ_0 = intensity of incident beam, S = cross section of the incident beam, $S dx$ = volume element of the sample, and R = distance from the volume increment to the photomultiplier. To find ζ/ζ_0 , we need a standard. Since

$$\zeta_s/\zeta_0 = \sigma_s Sl/R^2$$

where subscript (s) denotes the standard, and Sl is volume element of the standard, we get

$$\sigma = \frac{\zeta_s l}{\zeta_s} \left(1 + \frac{1}{\cos(\pi - \theta)}\right) \gamma \left[1 - \exp\left\{-\gamma \left(1 + \frac{1}{\cos(\pi - \theta)}\right) d\right\}\right]^{-1} \quad \text{for } \theta > \frac{\pi}{2}$$

When $\gamma d \gg 1$

$$\sigma = \frac{\zeta_s l}{\zeta_s} \left(1 + \frac{1}{\cos(\pi - \theta)}\right) \gamma$$

With polarized light

$$\begin{aligned} \gamma_{sca} &= \frac{8\pi}{3} (\sigma_2 - \sigma_1) \\ &= \frac{\tau_{sl}}{\zeta_s} \left(1 + \frac{1}{\cos(\pi - \theta)}\right) [\zeta_2 \gamma_2 - \zeta_1 \gamma_1] \end{aligned} \quad (5)$$

where subscript (2) indicates catalyst with platinum; (1) without platinum; γ_{sca} is the scattering coefficient for the imaginary sample which scatters the same amount of light at all angles. A 0.5% Dow Styron in toluene solution (Cornell Standard) has an excess turbidity at 90° over that of the solvent of $3.51 \times 10^{-3} \text{ cm.}^{-1}$.

$\tau_s = 3.30 \times 10^{-3} \text{ cm.}^{-1}$ (National Bureau of Standards).

Instead of calculating l from the geometry of the instrument, the width of the scattered beam that was intercepted by the receiver was determined experimentally. For this purpose, two adjustable slits were inserted into the light scattering cell at right angles with the incident beam, as shown in Fig. 5. The scattering solution was 0.5% Styron in toluene (Cornell Standard). To start with, we knew G_{90}^0 , the galvanometer reading of the standard without the two slits. The determination was made by observing the scattered intensity at 90° as the slits were narrowed. As long as the slit widths were greater than the intercepted beam width, there was no change of scattered intensity with a small decrease in slit widths. In other words, $G_{90}^0 = G_{90}(l)$, where $G_{90}(l)$ is the galvanometer reading of the standard with slit widths equal to l . On further narrowing down the slits, a point was reached where the intensity falls with decreasing slit widths; $G_{90}(l)$ is now less than G_{90}^0 . A plot of F ($G_{90}(l)/G_{90}^0$) vs. l showed a point of discontinuity. This point was taken as the intercepted beam width.

l (experimentally determined) = 0.72 cm. for our light scattering instrument.

Appendix II

Absorption by Small Spheres.^{15,16}—Let a constant

(13) W. A. Wooster, "Experimental Crystal Physics," Oxford University Press, London, 1957, p. 9; Landolt-Börnstein, Phys. Chem., Tabellen II, 1923, p. 972.

(14) K. Auwers and A. Frühling, *Ann. Chem. Liebigs*, **422**, 192 (1921).

(15) C. J. F. Böttcher, "Theory of Electric Polarization," Elsevier Publishing Co., Amsterdam, Houston, London, New York, 1952, p. 49.

(16) H. C. Van de Hulst, "Light Scattering by Small Particles," John Wiley and Sons, Inc., New York, N. Y., 1957, chapter 14.

field F be applied to an isotropic dielectric sphere of radius a and dielectric constant ϵ_2 , embedded in a homogeneous material of dielectric constant ϵ_1 .

$$\phi_1 = -Fr \cos \theta + \frac{A}{r^2} \cos \theta; \quad \phi_2 = -Br \cos \theta$$

$$\frac{\partial \phi_1}{\partial r} = -\left(F + \frac{2A}{r^3}\right) \cos \theta; \quad \frac{\partial \phi_2}{\partial r} = -B \cos \theta$$

where ϕ_1 and ϕ_2 are the potential outside and inside the sphere, respectively. The boundary conditions require that

$$\phi_1|_{r=a} = \phi_2|_{r=a}$$

$$\epsilon_1 \frac{\partial \phi_1}{\partial n} \Big|_{r=a} = \epsilon_2 \frac{\partial \phi_2}{\partial n} \Big|_{r=a}$$

We then get

$$\frac{A}{a^3} = \frac{\epsilon_2 - \epsilon_1}{\epsilon_2 + 2\epsilon_1} F; \quad B = \frac{3\epsilon_1}{\epsilon_2 + 2\epsilon_1} F$$

and

$$\phi_1 = -Fr \cos \theta + \frac{\epsilon_2 - \epsilon_1}{2\epsilon_1 + \epsilon_2} \frac{a^3}{r^3} Fr \cos \theta \quad (6)$$

$$\phi_2 = -\frac{3\epsilon_1}{\epsilon_2 + 2\epsilon_1} Fr \cos \theta \quad (7)$$

Now, if we have N particles per volume V , the number of particles per unit volume, n , is N/V , the volume v per particles is $(4/3)\pi a^3$. Since

$$\epsilon_1 = 1 + 4\pi\mathcal{C}_1; \quad \epsilon_2 = 1 + 4\pi\mathcal{C}_2$$

the total induced electric moment, M , is

$$\frac{3\epsilon_1}{2\epsilon_1 + \epsilon_2} FN \frac{4}{3} \pi a^3 \mathcal{C}_2 + \mathcal{C}_1 \left(V - N \frac{4}{3} \pi a^3 \right) F$$

and the dielectric constant of the composite medium, ϵ , is

$$1 + 4\pi\mathcal{C} = \epsilon_1 + nv \left(\epsilon_2 - \epsilon_1 \right) \frac{1 + 2\epsilon_1}{\epsilon_2 + 2\epsilon_1}$$

With the Maxwell relation, $\epsilon_1 = m_1^2$, we have the refractive index of the composite medium, m

$$m = m_1 \left[1 + \frac{nv}{2} \left(\frac{1 + 2m_1^2}{m_1^2} \right) \operatorname{Re} \left(\frac{m_2^2 - m_1^2}{m_2^2 + 2m_1^2} \right) + \dots \right] \quad (8)$$

when $nv \ll 1$. The electric and magnetic fields of a wave traveling in the x direction are proportional to $e^{ik(ct-mx)}$ where $k = 2\pi/\lambda_{\text{vac}}$, and c is the velocity of light. The Poynting vector determining the intensity of the waves is proportional to

$$e^{2k\operatorname{Im}(m)x} = e^{-\gamma_{\text{abs}}x} \quad (9)$$

Therefore the absorption coefficient (cm.^{-1}), γ_{abs} , is

$$-\frac{4\pi}{\lambda_{\text{vac}}} \operatorname{Im}(m) = -\frac{8\pi^2 na^3}{\lambda} \left(\frac{1 + 2m_1^2}{3m_1^2} \right) \operatorname{Im} \left(\frac{m_2^2 - m_1^2}{m_2^2 + 2m_1^2} \right) \quad (10)$$

where

$$\lambda = \frac{\lambda_{\text{vac}}}{m_1}$$

When the suspending medium is vacuum

$$\epsilon_1 = 1$$

$$M_{\text{vac}} = \frac{3}{2 + \epsilon_2} FN \frac{4}{3} \pi a^3 \mathcal{C}_2$$

$$m_{\text{vac}} = 1 + \frac{3nv}{2} \operatorname{Re} \left(\frac{m_2^2 - 1}{m_2^2 + 2} \right) + \dots \text{ when } nv \ll 1$$

then

$$\gamma_{\text{abs}}(\text{vac}) = -\frac{8\pi^2 na^3}{\lambda_{\text{vac}}} \operatorname{Im} \left(\frac{m_2^2 - 1}{m_2^2 + 2} \right) \quad (11)$$

The derivation of the limiting absorption coefficient of small dielectric spheres *in vacuo* could not be extended to that of dielectric spheres in another homogeneous dielectric simply by replacing m with m_2/m_1 and λ with λ_{vac}/m_1 . \mathcal{C}_1 is different from zero when the suspending medium is not vacuum. Equations 10 and 11 differ by a factor of $(1 + 2m_1^2)/3m_1^2$ when we replace λ_{vac} and $(m_2^2 - 1)/(m_2^2 + 2)$ in (11) by λ and $(m_2^2 - m_1^2)/(m_2^2 + 2m_1^2)$, respectively. The correction factor arises from the fact that we have an additional term, $\mathcal{C}_1(V - N \frac{4}{3} \pi a^3)F$, in the total induced electric moment. Further, our suspending medium has a high index of refraction. The correction factor amounts to approximately 0.78, therefore it cannot be neglected.

The scattering coefficient is

$$\gamma_{\text{scat}} = \frac{4\pi\Phi}{\lambda} X^3 \left| \frac{m_2^2 - m_1^2}{m_2^2 + 2m_1^2} \right|^2 \quad (12)$$

The final formula for the (excess) extinction coefficient is

$$\gamma_{\text{ext}} = \frac{3\pi\Phi}{2X\lambda} \left(\frac{1 + 2m_1^2}{3m_1^2} \right) \left[-\operatorname{Im} \left(4X \frac{m^2 - 1}{m^2 + 2} + \frac{4X^3}{15} \frac{(m^2 - 1)^2}{(m^2 + 2)^2} \left(\frac{m^2 + 27m^2 + 38}{2m^2 + 3} \right) \right) \right] + \frac{4\pi\Phi}{\lambda} X^3 \left| \frac{m^2 - 1}{m^2 + 2} \right|^2 + \dots$$

in which we have applied the same correction factor to the second absorption term without further justification. The error involved will not be large for qualitative discussions.

Appendix III

Preparation of Catalysts. Catalyst 1126-108: γ -Alumina Plus 0.096 Wt. % Pt.—0.1646 g. of P salt was dissolved in sufficient hot distilled water (100 ml.) to just wet 100 g. of alumina. The P salt solution was mechanically mixed into the alumina. The resulting mass was dried overnight at 250°F., and then calcined in a nitrogen atmosphere at 1100°F. for 3 hr.

Catalyst 1126-89: η -Alumina Plus 2 Wt. % Pt.—1.683 g. of P salt ($\text{Pt}(\text{NH}_3)_2(\text{NO}_2)_2$) was added to 200 ml. of hot water. Cooling of the solution precipitated out a jelly-like substance. The solution was reheated and then added to 60 g. of alumina and mixed mechanically. It was dried overnight at 250°F.; the mixture then was calcined at 1100°F. overnight in a nitrogen atmosphere.

PARTITION OF SOLUTES BETWEEN LIQUID METALS. I. THE ALUMINUM-CADMIUM SYSTEM

BY FRED A. CAFASSO, HAROLD M. FEDER, AND IRVING JOHNSON

Chemical Engineering Division, Argonne National Laboratory, Argonne, Illinois

Received October 27, 1961

The mutual solubilities of molten aluminum and cadmium have been measured and the partition of Pd, La, Ce, Pr, and U between these solvents has been examined. The partition coefficients (Al/Cd) of the lanthanons decrease in the order Ce > Pr > La. The partition coefficient of uranium and its activity coefficient in cadmium have been used to estimate the activity coefficient of uranium in aluminum solution. An approximate equation has been derived which connects the partition coefficient of a solute and its activity coefficient in each of two solvents which are partially miscible.

Studies of the partition of various solutes between immiscible liquids can serve to determine thermodynamic functions¹⁻³ as well as to provide information useful for separation processes. The aluminum-cadmium system, which has a useful miscibility gap⁴ between the melting point of aluminum (660.2°) and the boiling point of cadmium (765°), has not been examined previously in this connection. In the present investigation, the partitions of La, Ce, Pr, Pd, and U between liquid aluminum and liquid cadmium were measured. These solutes were chosen because of their occurrence in irradiated nuclear fuels and to determine whether elements as closely similar as adjacent lanthanons would show appreciable differences in behavior.

Experimental

Materials.—The purities of the metals were: aluminum, 99.99%; uranium, 99.95+%; lanthanum, 99.5%; cerium, 99+%; praseodymium, 99.5%; palladium, 99.5%.

Apparatus.—The furnace chamber, a closed-bottom stainless steel tube with an internal diameter of 4.5 in., was heated by a resistance furnace equipped with a Brown automatic temperature controller. The chamber was made vacuum tight with an O-ring sealed, water-cooled cover. The cover was provided with two sampling ports (described elsewhere⁵) and Wilson seals for a tantalum stirrer and a Morganite thermocouple protection tube. The melts were contained in 500-cc. Morganite crucibles which were positioned in the uniform temperature zone of the furnace. The melt temperatures were measured with an immersed Pt/Pt-10% Rh thermocouple and are believed to be known to $\pm 1.0^\circ$.

Procedure.—A crucible, containing about a kilogram of charge, was placed in the furnace chamber which then was evacuated and flushed several times with purified argon. A final pressure of 1100 mm. was maintained. After the charge was heated to the desired temperature, the melt was stirred for 1 hr. and allowed to settle for 1 hr. prior to sampling. The relative densities of the upper (aluminum-rich) and lower (cadmium-rich) layers are such that phase separation was rapid. Sampling pipets were inserted and filled by increase of the pressure in the chamber to 1500 mm.; they then were withdrawn from the melt and allowed to cool. In each experiment at least four samples were taken after intermediate stirring and settling periods. The Vycor pipet used to sample the upper layer has been described.⁵ Clean sampling of the lower layer posed a problem. This problem was solved by the use of a Vycor pipet drawn to a sealed point which could be broken on the bottom of the crucible. With a sealed pipet, contamination of the sample was prevented even when the upper layer was richer in solute by a factor of 10⁵.

Analyses.—Each pipet was broken and the total sample was removed for dissolution in nitric acid preparatory to analysis. Cadmium was determined by direct titration with tetraethylenepentamine (teten) and *p*-azoresorcinol as the indicator. Aluminum was determined spectrophotometrically as the oxine complex in chloroform. The oxine complex was extracted from a tetren-complexed solution to prevent cadmium interference. Palladium was determined by a spectrophotometric method.⁶ Lanthanum and praseodymium were determined by EDTA titration with xylenol orange as the indicator. In the cadmium-rich samples interference from cadmium was eliminated by mercury-cathode electrolysis and complexation with diethyldithiocarbamate. In the aluminum-rich samples aluminum interference was eliminated by precipitation with sodium hydroxide and complexation with sulfosalicylic acid. Cadmium was separated by precipitation of the rare earth with ammonia. Cerium was determined spectrophotometrically as its tartrate complex in an ammoniacal buffer. Separation from cadmium was achieved by coprecipitation of cerium with lanthanum fluoride. Separation from aluminum was achieved by coprecipitation of cerium with lanthanum hydroxide. Uranium in concentrations below 10⁻¹% in the samples was determined fluorophotometrically. Larger concentrations were determined spectrophotometrically by the dibenzoylmethane method.

Results

The mutual solubilities of liquid aluminum and cadmium as a function of temperature (Fig. 1) may be represented by the equations

$$\log X_{\text{Cd}} = 3.479 - 2.944 \times 10^3 T^{-1} \quad (1)$$

$$\log X_{\text{Al}} = 3.702 - 2.815 \times 10^3 T^{-1} \quad (2)$$

where X is the atom per cent. of the stated solute. Extrapolation of eq. 1 to the monotectic temperature (649°) gives a value of 1.7 atom % cadmium. Hardy⁷ has estimated 1.6 atom % from the maximum solid solubility at the monotectic temperature and Hansen and Blumenthal⁸ measured a value of 1.8 atom %.

Equilibrium in the partition experiments was judged to have been achieved when the concentrations of solute in successive samples taken from both layers showed no significant variations. The averaged concentrations are given in Table I. K , the partition coefficient of each solute, has been expressed by the ratio (wt. % in upper layer)/(wt. % in lower layer).

The effect of concentration and temperature on the partition of uranium was examined (Table I). No significant variations were observed; however, the magnitude of the experimental uncertainty and the small temperature range examined precluded

(1) J. Chipman and T. P. Floridis, *Acta Met.*, **3**, 456 (1955).

(2) P. J. Koros and J. Chipman, *J. Metals*, **8**, 1102 (1956).

(3) D. T. Peterson and R. Kontrimas, *J. Phys. Chem.*, **64**, 362 (1960).

(4) M. Hansen and K. Anderko, "Constitution of Binary Alloys," McGraw-Hill Book Co., Inc., New York, N. Y., 1958, second edition, p. 77.

(5) A. E. Martin, J. B. Knighton, and H. M. Feder, *J. Chem. Eng. Data*, **6**, 596 (1961).

(6) L. E. Ross, G. Kesser, and E. T. Kucera, *Anal. Chem.*, **32**, 1367 (1960).

(7) H. K. Hardy, *J. Inst. Metals*, **80**, 431 (1951-1952).

(8) M. Hansen and B. Blumenthal, *Metallwirtschaft*, **10**, 925 (1931).

TABLE I
PARTITION COEFFICIENTS IN THE ALUMINUM-CADMIUM SYSTEM

Solute	Temp., °C.	Concn. in upper layer, wt. %	Concn. in lower layer, wt. %	Partition coefficient, K	Estimated reliability, %
Palladium	680	6.35	1.07×10^{-1}	5.94×10^3	1.5
Lanthanum	686	8.31	1.80×10^{-1}	4.62×10^1	3
Cerium	680	4.63	2.48×10^{-2}	1.87×10^2	3
Praseodymium	686	7.82	4.78×10^{-2}	1.64×10^2	3
Uranium	686	4.80	3.3×10^{-5}	1.5×10^5	12
Uranium	689	3.63	2.3×10^{-5}	1.6×10^5	12
Uranium	686	2.33	1.7×10^{-5}	1.4×10^5	12
Uranium	710	4.98	3.2×10^{-5}	1.6×10^5	12

the measurement of the temperature coefficient of partition.

Discussion

Significant differences between the partition coefficients of the adjacent lanthanons, lanthanum, cerium, and praseodymium, were observed. The pattern of the variation ($Ce > Pr > La$) does not seem to be similar to that observed for partition of the metal nitrates between aqueous and organic phases⁹; however, the present data should be extended to other lanthanons to make this conclusion firm.

The observed partition of uranium permits an estimate to be made of its activity coefficient in liquid aluminum. At 686° the activity coefficient of uranium (referred to solid uranium) in dilute liquid cadmium solution can be estimated to be $1.28 \times 10^{2.10}$. At this temperature the partition coefficient $K_U(Al/Cd)$ on an atom fraction basis is 4.5×10^4 . If one neglects the mutual solubility of molten aluminum and cadmium and assumes that in each phase the activity coefficient of uranium is the same as in the pure solvent, a crude estimate of the activity coefficient of uranium in aluminum ($\gamma_{U(Al)}$) yields a value of $2.8 \times 10^{-3} = (1.28 \times 10^2 / 4.5 \times 10^4)$. However, the activity coefficients of uranium in the equilibrated phases are different from those in the pure solvents. The effects of the mutual solubility of the phases on the activity coefficients have been considered in the Appendix, and an approximate equation which takes these effects into account is derived therein. The more refined estimate gives $\gamma_{U(Al)} = 9.7 \times 10^{-4}$, with a probable reliability of 40%.

Acknowledgment.—R. J. Uhle assisted in performing the experiments. Special thanks are due to R. J. Meyer and G. Kesser for their solutions of a number of analytical problems. This research was carried out under the auspices of the Atomic Energy Commission.

Appendix

The equation connecting the partition coefficient of a solute and its activity coefficient in each of two solvents has been discussed by McKay¹¹ for the case of partial miscibility of the solvents. The application of McKay's exact method requires extensive additional measurements which cannot be made for the system under consideration. Instead, we have derived the desired equation by the following method. (Symbols are defined at the end of this Appendix.)

(9) C. A. Blake, Jr., C. F. Baes, Jr., and K. B. Brown, *Ind. Eng. Chem.*, **50**, 1763 (1958).

(10) I. Johnson and H. M. Feder, *Trans. A.I.M.E.* (in press).

(11) H. A. C. McKay, *Trans. Faraday Soc.*, **49**, 237 (1953).

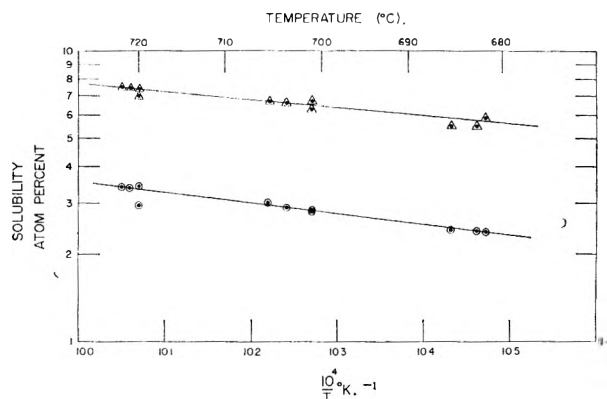


Fig. 1.—Mutual solubilities of aluminum and cadmium: \circ , cadmium in aluminum; \triangle , aluminum in cadmium.

It is assumed that the activity coefficient of a solute at low concentration in a binary solvent varies with solvent composition approximately as given by eq. 3

$$\bar{G}_2^{xs} \cong X_1 \bar{G}_{2(1)}^{xs} + X_3 \bar{G}_{2(3)}^{xs} - G_{1-3}^{xs} \quad (3)$$

Substitution of the symbols for each phase in eq. 3, subtraction, and simplification *via* the condition $X_1' + X_3' \cong X_1'' + X_3'' \cong 1$, yields

$$\bar{G}_2^{xs'} - \bar{G}_2^{xs''} = (X_1' - X_1'')(\bar{G}_{2(1)}^{xs} - \bar{G}_{2(3)}^{xs}) - (G_{1-3}^{xs'} - G_{1-3}^{xs''}) \quad (4)$$

Furthermore, since

$$RT \ln K_2 \equiv RT(\ln X_2'' - \ln X_2') = \bar{G}_2^{xs'} - \bar{G}_2^{xs''} \quad (5)$$

one obtains

$$RT \ln K_2 \cong (X_1' - X_1'')(\bar{G}_{2(1)}^{xs} - \bar{G}_{2(3)}^{xs}) - (G_{1-3}^{xs'} - G_{1-3}^{xs''}) \quad (6)$$

The evaluation of the second term on the r.h.s. can be made if it is further assumed that Raoult's law is applicable to the major constituent of each binary solvent, *i.e.*

$$\bar{G}_1' - G_1^0 = RT \ln X_1'; \quad \bar{G}_3' - G_3^0 = RT \ln X_3' \quad (7)$$

Combination of eq. 7 with the defining eq. 8 and 9

$$G_{1-3}^{xs} \equiv \Delta G_{1-3}^M - RT(X_1 \ln X_1 + X_3 \ln X_3) \quad (8)$$

$$\Delta G_{1-3}^M = X_1(\bar{G}_1 - G_1^0) + X_3(\bar{G}_3 - G_3^0) \quad (9)$$

and the mutual equilibrium condition eq. 10

$$\bar{G}_1' = \bar{G}_1''; \quad \bar{G}_3' = \bar{G}_3'' \quad (10)$$

yields

$$G_{1-3}^{xs'} - G_{1-3}^{xs''} = RT \left(X_1'' \ln \frac{X_1''}{X_1'} - X_3' \ln \frac{X_3'}{X_3''} \right) \quad (11)$$

and the final result

$$RT \ln K_2 \cong (X_1' - X_1'')(\bar{G}_{2(1)}^{xs} - \bar{G}_{2(3)}^{xs}) - RT \left(X_1'' \ln \frac{X_1''}{X_1'} - X_3' \ln \frac{X_3'}{X_3''} \right) \quad (12)$$

Equation 12 has been used for the refined estimate given in the Discussion section.

Two essential approximations have been made in the derivation of eq. 12. The approximation expressed by eq. 3 was suggested independently by Darken¹² and by Alcock and Richardson.¹³ It appears to reproduce the observed activity coefficient variation of metallic solutes in binary solvents to within 20%.¹³⁻¹⁶ The Raoult's law approximation for the binary equilibrium phases introduces a smaller error if the mutual solubilities are not excessive, say <10 atm %.

A search of the literature on partition between liquid metals has been made to find data suitable for testing eq. 4 or 12. None has been found.

(12) L. S. Darken, *J. Am. Chem. Soc.*, **72**, 2909 (1950).

(13) C. B. Alcock and F. D. Richardson, *Acta Met.*, **6**, 385 (1958).

(14) S. Z. Beer, *Trans. Met. Soc. A.I.M.E.*, **221**, 2 (1961).

(15) T. Yokokawa, A. Doi, and K. Niwa, *J. Phys. Chem.*, **65**, 202 (1961).

(16) C. B. Alcock and F. D. Richardson, *Acta Met.*, **8**, 882 (1960).

List of Symbols

X_i	= atom fraction of constituent i ; 2 = solute	\bar{G}_i	= partial molal free energy of constituent in
G_i^0	= molal free energy of constituent i in the reference state $X_i = 1$	G_i^{3s}	= excess partial molal free energy of constituent i in the binary solvent
ΔG_{1-3}^M	= molal free energy of mixing of the binary solvent	$\bar{G}_{(i)j}^{3s}$	= excess partial molal free energy of constituent i in solvent j
G_{1-3}^{3s}	= excess molal free energy of mixing of the binary solvent	Superscript ' ' = phase having constituent 1 in large excess	
		Superscript " " = phase having constituent 3 in large excess	
		K_2	= atom fraction partition ratio (distribution coefficient) of solute between " " and ' '

THERMODYNAMICS OF PROTON DISSOCIATION IN DILUTE AQUEOUS SOLUTION. II. HEATS OF PROTON DISSOCIATION FROM RIBONUCLEOTIDES AND RELATED COMPOUNDS DETERMINED BY A THERMOMETRIC TITRATION PROCEDURE¹

BY JAMES J. CHRISTENSEN AND REED M. IZATT

Department of Chemical Engineering and Department of Chemistry, Brigham Young University, Provo, Utah

Received November 1, 1961

A thermometric titration procedure is described for measurement of heats of proton dissociation, and equations are developed for determination of heats of reaction from the data which account for the various heat effects throughout the titration. A thermistor used as the temperature sensing element allows measurement of a 0.02° change with 1% accuracy. The experimental equipment is housed in an air-box whose temperature is controlled at $25 \pm 0.05^\circ$. Heats of proton dissociation are given for the pK 4 (pyrimidine N-H), pK 7 and 9 (phosphate), and pK 9 (imidazole N-H) groups when present in protonated adenine, adenosine, adenosine mono-, di-, and tri-phosphate, ribose phosphate, pyrophosphoric acid, and tripolyphosphoric acid. ΔH_n values are given as a function of μ , and ΔH_n^0 values are obtained in each case by extrapolating a plot of ΔH_n vs. μ to $\mu = 0$. ΔS_n^0 values are calculated from ΔH_n^0 and corresponding ΔF_n^0 values. The magnitude of ΔH^0 appears to be a function of the proton donor atom and the type of bonding between it and the parent molecule (e.g., O; primary, secondary, tertiary N; etc.), but not of either the pK or the nature of the parent molecule.

Introduction

Despite the importance of proton ionization in the functioning of ribonucleotides, few dissociation constant or heat of ionization data are available for them or related compounds. For this reason, a study has been initiated in this Laboratory to determine under the same experimental conditions the thermodynamic quantities associated with the stepwise removal of protons from these substances. This paper presents heats of proton dissociation determined calorimetrically at 25° and as a function of ionic strength, μ , from protonated adenine, adenosine (A), adenosine monophosphate (AMP), adenosine diphosphate (ADP), adenosine triphosphate (ATP), ribose phosphate (RP), pyrophosphoric acid, and tripolyphosphoric acid.

Rawitscher and Sturtevant² report heats determined calorimetrically in 0.1 F NaCl for proton dissociation from the pyrimidine group of adenine and A. This appears to be the only other calorimetric study involving the substances studied here. Alberty, Smith, and Bock³ report pK_a values at 25 and 38° in 0.15 F NaCl for the pyrimidine and phosphate ionizations of adenine, A, AMP, ADP, and ATP; however, heats calculated from these pK values would be unreliable because of the small temperature range covered, and the uncertainty of the pK values.

Use of a low heat capacity, rapid response thermistor as the temperature sensing device in the calorimetric measurements makes possible the determination of heats of reaction at relatively low reactant concentrations. In order to take advantage of these thermistor characteristics and to obtain a permanent record of the temperature change a modification of the thermometric titration procedure used by Jordan and Alleman⁴ has been developed. Previous work in the field of thermometric titrations has been summarized recently.⁵

Several factors are inherent in the thermometric titration method which make subsequent calculations more difficult than those using standard calorimetric data. These factors are (a) the titrant is continuously added during the time of reaction at a temperature different from that of the solution except perhaps at one point during the titration, (b) the solution concentration is continuously changing during the titration with resultant change in the heats of solution and dilution, and (c) the walls of the calorimeter are not necessarily at the same temperature as the solution during the titration. Previous investigators have noted these effects and have proposed various methods or equations which allow for them in their calculations. Jordan and Alleman⁴ proposed an extrapolation method for heat loss and heat of dilution corrections. Keily and Hume⁶ used only the initial slope of the titration curve in order to correct for heat losses and to minimize errors due to the titrant being at a different temperature than the solution. Neither of these workers has taken into account the

(1) Supported in part by NIH Grant A-3272, AEC Contract AT(04-3)-299, and a Research Corporation Grant. Presented in part at the Pacific Northwest Regional A.C.S. Meeting, June, 1960, and at the Calorimetry Conference, Ottawa, August, 1961. Part I, *J. Phys. Chem.*, **66**, 359 (1962).

(2) M. Rawitscher and J. Sturtevant, *J. Am. Chem. Soc.*, **82**, 3739 (1960).

(3) R. A. Alberty, R. M. Smith, and R. M. Bock, *J. Biol. Chem.*, **193**, 425 (1951).

(4) J. Jordan and T. G. Alleman, *Anal. Chem.*, **29**, 9 (1957).

(5) S. T. Zenchelsky, *ibid.*, **32**, 389R (1960).

(6) H. J. Keily and D. N. Hume, *ibid.*, **28**, 1294 (1956).

fact that the temperature difference between the titrant and the solution is continually changing during the course of the titration.

Equations developed in this paper take into account the effects outlined above and give a more precise method for the calculation of heats of reaction from thermometric titration data.

Experimental

Materials.—Reagent grade perchloric (Fisher), isobutyric (Eastman), butyric (Eastman), hydrochloric, and phosphoric acids; adenine (Schwarz Labs.), A (Sigma Chem. Co.), AMP (Sigma Chem. Co.), ADP (Sigma Chem. Co.), ATP (Sigma Chem. Co.), RP (Sigma Chem. Co.), $\text{Na}_2\text{H}_2\text{P}_2\text{O}_7$ (Mallinckrodt), $\text{Na}_3\text{H}_2\text{P}_3\text{O}_{10}$ (Food Machinery and Chem. Corp.), $(\text{CH}_3)_4\text{NOH}$ (Eastman), and NaOH were standardized by conventional methods for use in the determinations. Complexing between Na^+ and the pyro- and triphosphosphate groups was eliminated by substituting $(\text{CH}_3)_4\text{N}^+$ for Na^+ with a cation-exchange resin in the cases of those substances containing the $-\text{O}-\text{P}-\text{O}-\text{P}-\text{O}-$ linkage.

Thermometric Titration Apparatus.—Measurements were made in an air-bath which consisted of a cubic wooden box (two feet on a side) within another with 4 in. of insulation between the boxes. The bath temperature was maintained at $25 \pm 0.05^\circ$ by circulation of water from a 30-gal. tank through copper tubing placed on aluminum foil on the inside box surfaces. Air, constantly circulated in the box, was maintained at a constant temperature by passing it through a mesh of copper tubing containing the circulated water. A thermoregulator located in the air-bath controlled the temperature of the circulating water by actuating auxiliary heating and refrigeration units located in the water tank. The room in which the air-bath was located was maintained at a temperature of $25 \pm 1^\circ$. The calorimeter stirring motor, buret drive motors, and blower motor for circulation of conditioned air within the box were located on the outside of the bath. Titrant was delivered with a constant flow titrimer consisting of an ultra-buret (Scientific Industries, T-200), driven through precision-machined gears by two Series 500 30-r.p.m. Gleason Avery, Inc., synchronous gear motors. The buret delivered 0.00852 ml. titrant/sec. with a precision of $\pm 0.1\%$. The calorimeter was a 250-ml. dewar flask in which was placed through a tightly fitting rubber stopper the micro-buret tip, a glass stirrer (driven by a 600 r.p.m. Wes Co. stirring motor), and a thermistor (Victory Engineering Corp., 31A-6 type) in a 2-mm. o.d. glass tube. The thermistor resistance was approximately 1000 ohms at 25° and it had a temperature coefficient of $-3.9\%/^\circ$. The glass stirrer was positioned to sweep titrant immediately from the buret tip into the solution.

The thermistor was incorporated as one arm of a Wheatstone bridge whose circuits were shielded and guarded to eliminate parasitic currents. In operation, the thermistor resistance change resulted in an unbalanced bridge potential which was fed to a Minneapolis-Honeywell extended range strip chart recorder (Model 153X14-V-II-III-30-N6) having a span of 2.2 mv. with a total of five ranges giving an effective span of 11.0 mv.

Thermistor Calibration.—The thermistor resistance change as a function of temperature was determined at various applied bridge voltages by observing the thermistor response to small, accurately measured temperature changes. The temperature changes were measured by placing a 5° Beckmann thermometer and the thermistor in close proximity in a water-bath which was allowed to slowly cool through the temperature range for which the thermistor was to be calibrated. A linear relationship between temperature change (read from the Beckmann thermometer) and recorder deflection was found at each bridge voltage. The calibration covered a 1° interval. At the bridge voltage used in this study (1.4500 v.), a deflection of one scale unit on the recorder corresponded to 0.000739 or 0.15° per chart width. Thus, a temperature change of 0.02° could be measured with an accuracy of 1% and a change of 0.7° could be recorded over the five available spans of the recorder in a single titration.

Procedure.—The calorimeter and auxiliary equipment, constant rate microburet titrimer, and all solutions 48 hr. prior to use were kept in the constant temperature air-bath

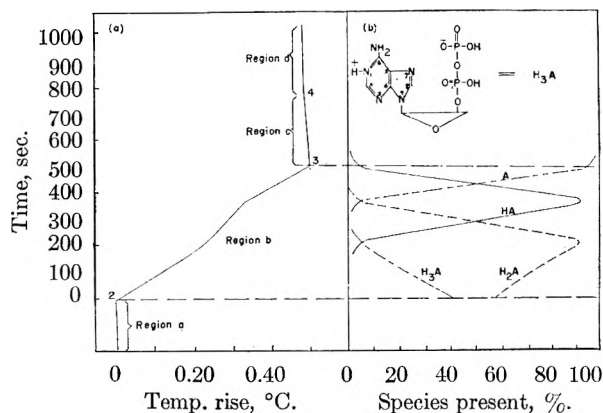


Fig. 1.—Correlation of temperature rise (a) with per cent species present; (b) in calorimeter as a function of moles base added (time) for the ADP- $(\text{CH}_3)_4\text{NOH}$ system.

in order to improve temperature control of the calorimeter and its contents and to ensure that all solutions and equipment used in the titration were at the same temperature. The titrant in all determinations was approximately 100 times more concentrated than the solution being titrated. The initial volume of the solution being titrated was always 100 ml.; however the solute concentration varied from approximately 0.05 to 0.005 F . The temperature of the solution was continuously recorded in each determination throughout the four regions of the titration curve which is described below.

Calculations.—The calculation of ΔH by the method outlined here is based on the typical thermometric titration curve obtained from the reaction of a strong acid with a strong base. The derived equations are sufficiently general, however, for the method to be extended to any system, exothermic or endothermic, so long as the concentrations of the species causing the heat changes are known. The method also can be extended to systems containing two or more reacting species, but if these systems react in the same pH region, *i. e.*, their pK values are close together, it is necessary to know the quantity of each species present in order that heats may be correctly assigned. Equations can be derived for these more complex systems, providing pK values are known, in the same manner as is done below for the single species system. These equations are not presented here because of their length and complexity.

The curve in Fig. 1a has four distinct regions: (a) titrant off—temperature change is due to stirring, power dissipated by the thermistor, and heat transfer if air-bath and solution temperatures are different; (b) titrant on—temperature change is due to heat of neutralization reactions, heat of solution of titrant, addition of titrant at a lower temperature than solution, and items in (a); (c) titrant on—neutralization reaction is completed, temperature change is due to heat of solution of titrant, addition of titrant at a lower temperature than solution and items in (a); (d) titrant off—temperature change due to items in (a). Region (b) may consist of heat effects resulting from neutralization of protons from more than one acidic group of the same substance. An example of a system involving such simultaneous equilibria is ADP. A typical titration of ADP with NaOH is shown in Fig. 1b where the % species is plotted vs. time. Distance along the ordinate or time axis is equivalent to moles NaOH added. In Fig. 1a is plotted the corresponding temperature rise as a function of time that the titrant base has been added. It is seen that the temperature rise at any point along the curve in Fig. 1a is a result of the simultaneous dissociation of protons from two ADP species (Fig. 1b) although the contribution is mainly from one species in each case. It now is possible to distribute the heat measured in region (b) among the species reacting in that region by solving appropriate simultaneous equations.

For the simple case where region (b) contains only one reacting species, the following equations are written (treating regions a and d as closed systems, *i. e.*, regions in which no mass crosses the boundaries of the calorimeter and its contents, and treating regions b and c as open systems, *i. e.*, regions in which titrant enters the calorimeter).

$$dQ - dW = dE \text{ regions a and d} \quad (1)$$

$$dQ - dW = dE + (h + U^2/2g_0 + Xg/g_0)dm \text{ regions b and c} \quad (2)$$

(For symbols used in this and succeeding equations, see section at end of article.) Expanding and integrating these equations in the usual manner with the assumptions that the neutralization reaction is essentially instantaneous, the heat capacity of the solution is independent of small temperature and concentration changes, and $C_p = C_v$ one obtains

$$Q_a = (m_a C_{p_a} + m_v C_{p_v}) \Delta T_a + W_a \quad (3)$$

$$Q_b = (m_a C_{p_a} + m_v C_{p_v} + m_{tb} C_{p_t}) \Delta T_b + m_{tb} C_{p_t} (T_2 - T_t) + \Delta H_r + \Delta H_{nb} + W_b \quad (4)$$

$$Q_c = (m_a C_{p_a} + m_v C_{p_v} + m_{tb} C_{p_t} + m_{tc} C_{p_t}) \Delta T_c + m_{tc} C_{p_t} (T_3 - T_t) + \Delta H_{nc} + W_c \quad (5)$$

$$Q_d = (m_a C_{p_a} + m_v C_{p_v} + m_{tb} C_{p_t} + m_{tc} C_{p_t}) \Delta T_d + W_d \quad (6)$$

The heat of reaction, ΔH_r , can be found from eq. 4 if Q_b , ΔH_{nb} , and T_t are known. Q_b and Q_c (eq. 4 and 5) can be evaluated in terms of known quantities Q_d and Q_a if the assumption is made that over the small temperature rise encountered in the titration the rate of heat loss from the calorimeter is directly proportional to the temperature difference between the solution and the surrounding air-bath. T_t then can be evaluated from eq. 5, and Q_b and T_t substituted in eq. 4 to give the following expression for ΔH_r in terms of known and measured quantities

$$\Delta H_r = \left\{ YA + [(Y + Z)D - YA] \frac{\Delta T_b}{\Delta T_{2-4}} \right\} \Delta \theta_b - (Y + m_{tb} C_{p_t}) \Delta T_b \quad (7)$$

$$- \frac{m_{tb}}{m_{tc}} \left\{ (Y + Z)D + [(Y + Z)D - YA] \frac{\Delta T_c}{2\Delta T_{2-4}} \right\} \Delta \theta_c - (Y + Z) \Delta T_c - \Delta H_{nc} \left\} + m_{tb} C_{p_t} \Delta T_b - \Delta H_{nb}$$

where Y is the heat capacity of the calorimeter and its contents.

Either heats of dilution ΔH_{nb} and ΔH_{nc} can be evaluated at the average ionic strength in each respective region or if heat of dilution vs. μ data are available a true average heat of dilution can be determined.

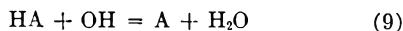
All calculations were made on an IBM 650 computer.

Equipment Calibration.— Y (eq. 7), the effective heat capacity of the calorimeter and its contents, was determined by studying a system whose ΔH_r is accurately known. The system chosen was the neutralization of a strong acid with a strong base in aqueous solution



(omitting ion charges and waters of hydration for simplicity in this and succeeding eq.) in which case ΔH^0 has been determined by a microcalorimetric procedure at $\mu = 0$ to be -13.50 ± 0.05 kcal./mole.⁷ Using this value for ΔH_r , a value of 111.53 cal./deg. was obtained for Y .

The experimental procedure was further checked by calculating the heats of neutralization at $\mu = 0$ of *n*-butyric acid, isobutyric acid, and dihydrogen phosphate ion and comparing these with results of previous studies. These heats determined as a function of reactant concentration and μ are given in Tables I and II for the reaction



Each ΔH value in Tables I and II was obtained by averaging the ΔH values from 2 to 4 determinations at the indicated μ value. The precision of the ΔH values in Tables I and II is estimated to be $\pm 0.5\%$.

The substitution of tetramethylammonium hydroxide for NaOH in the H_3PO_4 titration (Table II) made no difference in the observed heats.

ΔH_n^0 values obtained by extrapolation of ΔH_n vs. μ plots to $\mu = 0$ are given in Table III together with results of previous workers. The ΔH_n^0 values in Table III are for the reaction



(7) H. M. Papez, W. J. Canady, and K. J. Laidler, *Can. J. Chem.*, **34**, 1677 (1956).

and are obtained by subtracting -13.50 from the ΔH_n^0 measured for the reaction occurring in the calorimeter, eq. 9. The present results are seen to be in good agreement with previous work.

TABLE I

THERMOCHEMICAL DATA FOR THE TITRATION OF NaOH WITH SEVERAL ACIDS AT 25°

Titrant	NaOH formality $\times 10^2$	$\mu \times 10^3$	$-\Delta H$ (kcal./mole)
1.034 F HClO ₄	0.4634	2.30	13.62
	1.159	5.78	13.46
	2.317	11.6	13.43
	3.479	17.4	13.42
	4.634	23.1	13.35
0.678 F (CH ₃) ₂ CHCOOH	0.4634	2.30	13.99
	0.9268	4.62	14.32
	1.159	5.78	14.25
	2.317	11.6	14.18
	3.479	17.4	13.98
1.080 F CH ₃ (CH ₂) ₂ COOH	0.9268	4.62	14.40
	1.159	5.78	14.22
	2.317	11.6	14.28
	3.479	17.4	14.14
	4.634	23.1	13.98

TABLE II

THERMOCHEMICAL DATA FOR THE TITRATION OF H₂PO₄⁻ WITH BASE AT 25° ACCORDING TO THE REACTION H₂PO₄⁻ + OH⁻ = HPO₄⁻ + H₂O

Titrant	H ₂ PO ₄ formality $\times 10^2$	$\mu \times 10^3$	$-\Delta H$ (kcal./mole)
1.134 F (CH ₃) ₄ NOH	0.400	9.40	12.18
	0.500	11.9	12.00
	1.000	21.0	11.92
	1.500	30.2	11.70
	2.000	43.2	11.49
1.074 F NaOH	0.515	12.1	12.28
	1.030	21.3	11.88
	1.545	31.0	11.40
	2.060	44.1	11.36

TABLE III

COMPARISON OF ΔH_n^0 VALUES FROM PRESENT AND PREVIOUS WORK FOR PROTON DISSOCIATION FROM SEVERAL ACIDS AT 25°

Acid	ΔH_n^0	ΔH_n^0
(CH ₃) ₂ CHCOOH	-0.90 ^a	...
	-0.73 ^b	...
CH ₃ (CH ₂) ₂ COOH	-0.86 ^a	...
	-1.01 ^b	...
H ₃ PO ₄	-0.20 ^c	0.90 ^a
		0.80 ^c
		1.00 ^d

^a Present work. ^b W. J. Canady, *et al.*, *Trans. Faraday Soc.*, **54**, 502 (1958). ^c K. S. Pitzer, *J. Am. Chem. Soc.*, **59**, 2365 (1937). ^d A. K. Grzybowski, *J. Phys. Chem.*, **62**, 555 (1958).

Results

ΔH values for the ionization of water, as a function of μ , were obtained from the data in Table I, and were used to correct the measured heats, equation 9, to those represented by equation 10 at each ionic strength for the substances studied. These heats are given in Table IV (see Fig. 1b for location of N₁ and N₉ atoms). Each ΔH value in Table IV was obtained by averaging the ΔH_n values from 2

determinations at the indicated μ value. The precision of these ΔH values is estimated to be $\pm 1\%$.

TABLE IV

HEATS OF PROTON DISSOCIATION (KCAL./MOLE) AS A FUNCTION OF IONIC STRENGTH FOR REACTION 10

Compound	$\mu_1 \times 10^3$	$\frac{\Delta H_1}{(N_1-H)}$	$\mu_2 \times 10^3$	$\frac{\Delta H_2}{(P_1O-H)}$	$\mu_3 \times 10^3$	$\frac{\Delta H_3}{(N_9-H)}$
Adenine	4.92	4.88			7.72	9.39
	6.20	4.78			9.50	9.48
	12.5	4.74			19.5	9.76
	18.5	4.42			28.8	10.21
A	5.09	3.12				
	6.36	3.16				
	12.7	3.10				
	18.9	2.97				
	25.1	3.00				
AMP	3.00	4.22	11.8	-1.54		
	3.80	4.10	14.5	-1.48		
	7.62	3.78	29.0	-1.01		
	11.4	3.92	44.4	-0.59		
	15.2	3.91	59.2	-0.36		
ADP	5.60	4.06	9.58	-1.13		
	7.09	4.27	14.2	-1.13		
	14.1	4.48	28.2	-1.12		
	21.1	4.28	42.2	-0.46		
	28.0	4.83	55.6	-0.48		
ATP	19.8	3.72	36.5	-2.00		
	24.8	4.15	45.7	-0.47		
	49.7	4.13	91.5	-1.16		
	73.8	4.76	132	-1.19		
	98.0	4.50	177	-1.23		
RP			7.96	-2.74		
			9.93	-2.12		
			19.7	-2.58		
			29.5	-1.82		
			39.0	-1.86		
$H_2P_2O_7^-$	$\mu_1 \times 10^3$	ΔH_1 (pK = 7)	$\mu_2 \times 10^3$	ΔH_2 (pK = 9)		
	22.6	-0.94	41.6	-2.20		
	28.3	.20	52.0	-1.54		
	56.6	-.32	104	-1.63		
	83.7	.40	152	-1.72		
112	-.14	405	-1.70			
$H_2P_3O_{10}^{3-}$	18.8	-1.06	29.3	-3.94		
	23.5	-.88	36.0	-3.23		
	47.0	-.34	73.2	-4.28		
	70.5	-.10	110	-4.26		

pK values for assignment of the heats to the correct species in region b, Fig. 1a, were taken from the literature.^{3,8-12} These values were available at $\mu = 0$ for all substances studied here except AMP and ATP, where values determined at $\mu = 0.15$ were used without correction. The values at $\mu = 0$ were corrected by appropriate activity coefficients to concentration quotients at the ionic strength of the solution under study and used as described in the Experimental section.

(8) R. M. Izatt and J. J. Christensen, *J. Phys. Chem.*, **66**, 359 (1962), (adenine, A, ADP, RP).

(9) E. R. Tucci, E. Doody, and N. C. Li, *ibid.*, **65**, 1570 (1961), (AMP, phosphate ionization).

(10) R. M. Smith and R. A. Alberzy, *J. Am. Chem. Soc.*, **78**, 2376 (1956), (ATP, phosphate ionization).

(11) S. M. Lambert and J. I. Watters, *ibid.*, **79**, 4262 (1957), ($H_2P_2O_7^-$).

(12) J. I. Watters, E. D. Loughran, and S. M. Lambert, *ibid.*, **78**, 4855 (1956), ($H_2P_3O_{10}^{3-}$).

No pK values have been reported for the most acidic phosphate groups in ATP, ADP, AMP, and RP. It was assumed in our calculations that the pK values of these groups would be somewhat lower than the corresponding pK values in $H_5P_3O_{10}$, $H_4P_2O_7$, and H_3PO_4 which are known.¹¹⁻¹³ No heats are given for proton dissociation from these acidic phosphate groups since calculations show that negligible quantities of them are present at any time during the titration.

There is evidence in our work for proton dissociation in a pH region considerably higher than that in which the last phosphate proton is removed from A, AMP, ADP, ATP, and RP. This is consistent with the reported observation that a proton is removed at high pH from the ribose group of these substances.¹⁴ Titration of ribose with 1 *F* NaOH also showed liberation of heat although an endpoint was not reached. Since pK_a values are not available for ribose, no ΔH values were calculated.

ΔH_n^0 values for equation 10 were obtained from the data in Table IV by extrapolation of a ΔH_n vs. μ plot to $\mu = 0$. The precision of these values is estimated to be ± 0.1 kcal./mole. These values are given in Table V together with ΔS^0 values calculated from the ΔH^0 and ΔF^0 values. Since the ΔF values for AMP and ATP are calculated from pK data at μ approximately 0.15, there is some uncertainty in the ΔS values calculated using these ΔF data. On the basis of the pK change observed in ADP between $\mu = 0$ and $\mu = 0.2$ it is estimated that in AMP and ATP the corrected ΔS^0 would be approximately 2 e.u. higher for the pK 7 ionization, and 0.2 e.u. higher for the pK 4 ionization.

Discussion

Heats of Proton Dissociation.—The heats of ionization reported by Rawitscher and Sturtevant at 25° for the pyrimidine portion of adenine and A (3.990 and 3.810 kcal./mole, respectively) were determined at $\mu = 0.1$, and, therefore, are not comparable to those determined in the present study.

In the case of adenine the ΔH^0 was found to be much greater for the imidazole than for the pyrimidine N-H ionization. This increase in the ΔH^0 value reflects the essential difference in the N₁ and N₉ atoms. The N₉-H region has a higher electron density than does the N₁-H region which results in the ΔH for proton dissociation being greater for the N₉-H bond than for the N₁-H bond.

An interesting relationship is seen in Table V between the magnitude of the ΔH^0 values and the site of proton dissociation. ΔH^0 values in kcal./mole for dissociation of the pyrimidine N-H group are in the range 4.0 ± 0.9 ; while that of the imidazole N-H bond in adenine is 9.1; and those for the O-H dissociation in the phosphate groups are -0.9 ± 1.9 . (It is seen in Table III that ΔH^0 values for other OH dissociations also fall in this range.) It would be interesting to study this effect further by determining ΔH^0 for a large number of acidic groups having a variety of proton donor atoms. There are many substances of biochemical

(13) R. A. Robinson and R. H. Stokes, "Electrolyte Solutions," 2nd Edition, Butterworth, Washington, 1959, p. 520.

(14) "The Nucleic Acids," Vol. 1, E. Chargaff and J. N. Davidson, Editors, Academic Press, New York, N. Y., 1955, p. 156.

TABLE V

ΔF^0 (KCAL./MOLE), ΔH^0 (KCAL./MOLE), AND ΔS^0 (E.U.) VALUES FOR PROTON DISSOCIATION (EQUATION 10) FROM SEVERAL RIBONUCLEOTIDES AND RELATED COMPOUNDS

Compound	N ₁ -H (pK = 4)			N ₃ -H (pK = 9)			P-O-H (pK = 7)			P-O-H (pK = 9)		
	ΔF^0	ΔH^0	ΔS^0	ΔF^0	ΔH^0	ΔS^0	ΔF^0	ΔH^0	ΔS^0	ΔF^0	ΔH^0	ΔS^0
Adenine	5.7	4.9	-2.7	13.4	9.1	-14						
A	4.8	3.1	-5.7									
AMP	5.1 ^a	4.2	-3.0 ^a				8.8 ^a	-1.8	-36 ^a			
ADP	5.7	4.1	-5.4				9.5	-1.3	-36			
ATP	5.4 ^a	3.7	-5.7 ^a				9.5 ^a	-1.2	-36 ^a			
RP							9.1	-2.7	-40			
H ₂ PO ₄ ⁻							9.8	0.90	-30			
H ₂ P ₂ O ₇ ⁻							9.2	-0.3	-32	12.8	-1.7	-49
H ₂ P ₃ O ₁₀ ³⁻							8.5	-1.3	-33	12.1	-3.8	-53

^a Calculated using pK values determined at $\mu = 0.15$.³

interest in which the location of the proton donor groups is not known with certainty. If general, the above relationship could be valuable as a guide in establishing the location of proton donor groups in these substances.

Entropies of Proton Dissociation.—The relative magnitudes of the ΔS^0 values in Table V may be understood by considering the effect of eq. 10 on the cratic and unitary¹⁵ portions of ΔS^0 . The cratic portion of ΔS^0 , *e.g.*, that dealing with particle-solvent mixing, is constant for the substances studied since in the reaction under consideration the same number of particles is produced in each case. A value of 3 to 6 e.u. has been estimated (Table III, ref. b) for this cratic portion or for the purely structural factors of ΔS^0 . However, the unitary portion of ΔS^0 , *e.g.*, the portion which includes solvent particle interaction, would be expected to become more negative as the negative charge increased, resulting in increased solvent ordering capacity of the aqueous species. The data in Table V show the expected trends. The ΔS^0 values for the pyrimidine N₁-H dissociation are in the range -3 to -6 e.u., as would be expected if unitary contributions were very small. The ΔS^0 value for proton ionization from adenine, -14 e.u., is that found by previous workers (Table III, ref. b)

(15) R. W. Gurney, "Ionic Processes in Solution," McGraw-Hill Book Co., New York, N. Y., 1953.

for proton ionization from neutral molecules. The very negative ΔS^0 values in the cases of ionization of protons from the phosphate groups are consistent with the increased negative charge and solvent ordering capacity of the aqueous species.

Symbols

<i>A</i>	slope of curve in region a, Fig. 1
<i>C_p</i>	heat capacity at constant pressure per unit mass
<i>D</i>	slope of curve in region d, Fig. 1
<i>E</i>	total energy
<i>g</i>	acceleration due to gravity
<i>g_c</i>	conversion factor
<i>H</i>	total enthalpy
<i>h</i>	enthalpy per unit mass
<i>m</i>	mass
<i>Q</i>	heat
<i>T</i>	absolute temperature
<i>U</i>	velocity
<i>W</i>	work
<i>X</i>	elevation above a datum plane
<i>Y</i>	$m_a C_{p_a} + m_v C_{p_v}$
<i>Z</i>	$m_{th} + m_{tc} C_{p_t}$

Subscripts

a	region a, Fig. 1	v	calorimeter
b	region b, Fig. 1	2	point 2, Fig. 1
c	region c, Fig. 1	3	point 3, Fig. 1
d	region d, Fig. 1	4	point 4, Fig. 1
n	heat of dilution		
r	heat of reaction		
s	solution		
t	titrant		

Superscripts

⁰	infinite dilution
θ	time
μ	ionic strength

THE KINETICS OF THE KETO-ENOL TAUTOMERISM OF BENZOYLACETANILIDE

BY C. A. BISHOP AND L. K. J. TONG

Communication No. 2238 from the Kodak Research Laboratories, Eastman Kodak Company, Rochester, N. Y.

Received November 9, 1961

The rates of equilibration between the keto form of benzoylacetanilide and its anion have been measured under the influence of several acids and bases by a steady-state flow method. The specific rate constants using various phosphates and carbonates at constant $\mu = 0.375$ were shown to fit the Brönsted catalysis law. The absorption spectra of each of the species, keto, enol, and anion, were obtained and used to determine the dissociation constants of the keto and enol forms.

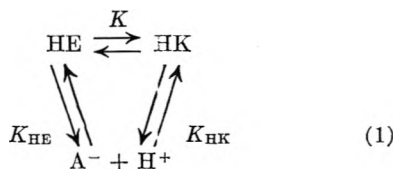
With few exceptions^{1,2} it is difficult to study the kinetics of acid-base reactions of organic compounds, since either the rate of dissociation of the acid at a convenient pH is too fast for measurement

or, where the rate is slow enough, the acid ionizes only to a minute extent. Examples of the first case are 1,3-dicarbonyl compounds, phenols, and naphthols, while most aldehydes and ketones fall into the second category.

The equilibria in keto-enol tautomerism can be expressed as acid-base reactions

(1) A. Hantzsch, *Ber.*, **32**, 575 (1899); D. Turnbull and S. H. Maron, *J. Am. Chem. Soc.*, **65**, 212 (1953).

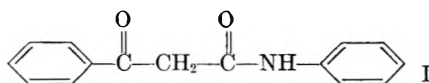
(2) S. H. Maron and V. K. LaMer, *ibid.*, **61**, 2018 (1939).



where HE, HK, and A^- represent the enol form, the keto form, and the common anion, respectively, K_{HK} and K_{HE} are the ionization constants for the keto form and the enol form, respectively, and K is the keto-to-enol equilibrium ratio.

For 1,3-dicarbonyl compounds, the rates of tautomeric equilibration are quite rapid. No observation or direct measurement of the enol-anion equilibrium has been reported, although K_{HE} (as well as K_{HK}) has been calculated in a few cases from the composite term $(K_{\text{HE}} + K_{\text{HK}})$ and the values of K which were obtained from bromination.³⁻⁵ Rates of equilibration are likewise scarce, the only ones available being ionization rates obtained by a flow method involving a secondary bromination reaction.^{6,7}

This paper reports an investigation of the kinetics of prototropic isomerization of benzoylacetanilide (structure I)



under the influence of a series of acids and bases. The measurements of the rate of ionization of the keto form and the reverse rate of association of the anion, as well as the independent determination of K_{HE} , are given. Reactions were carried out in a flow machine^{8,9} capable of obtaining ultraviolet absorption spectra of the reaction mixture under steady-state conditions at times varying from 8 msec. to 1 sec. after mixing.

Data and Results

The absorption maxima in the ultraviolet region for benzoylacetanilide in various solvents are reported in Table I. By analogy with benzoylacet-

TABLE I
ULTRAVIOLET ABSORPTION MAXIMA FOR BENZOYLACETANILIDE IN VARIOUS SOLVENTS

Solvent	Band I, $m\mu$	Band II, $m\mu$	Band III, $m\mu$
Butyl acetate	244	307	..
Cyclohexane	245	308	..
H_2O (below pH 8)	245		
H_2O (pH 12)	245		323

tone, bands I and II were assigned to the keto and enol forms, respectively,^{10,11} and band III was assigned to the anion.

- (3) K. H. Meyer, *Ann.*, **380**, 212 (1911).
- (4) G. W. Wheland, "Advanced Organic Chemistry," John Wiley and Sons, Inc., New York, N. Y., 1949, Chapter 14.
- (5) G. Schwarzenbach and E. Felder, *Helv. Chim. Acta*, **27**, 1701 (1944).
- (6) G. Schwarzenbach and C. Wittwer, *ibid.*, **30**, 669 (1947).
- (7) R. P. Bell, "The Proton in Chemistry," Cornell University Press, Ithaca, N. Y., 1959.
- (8) E. F. Caldin and F. W. Trowse, *Discussions Faraday Soc.*, no. 17, 133 (1954).
- (9) W. R. Ruby and L. K. J. Tong, unpublished work.
- (10) A. E. Gillam and E. S. Stern, "An Introduction to Electronic Absorption Spectroscopy in Organic Chemistry," Edward Arnold Publishers, Ltd., London, 1958, p. 258.

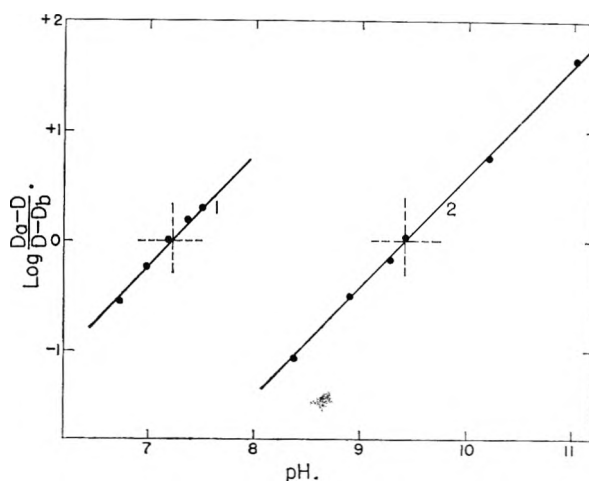


Fig. 1.—Equilibrium constants for dissociation of benzoylacetanilide: 1, enol form (HE); 2, keto form (HK).

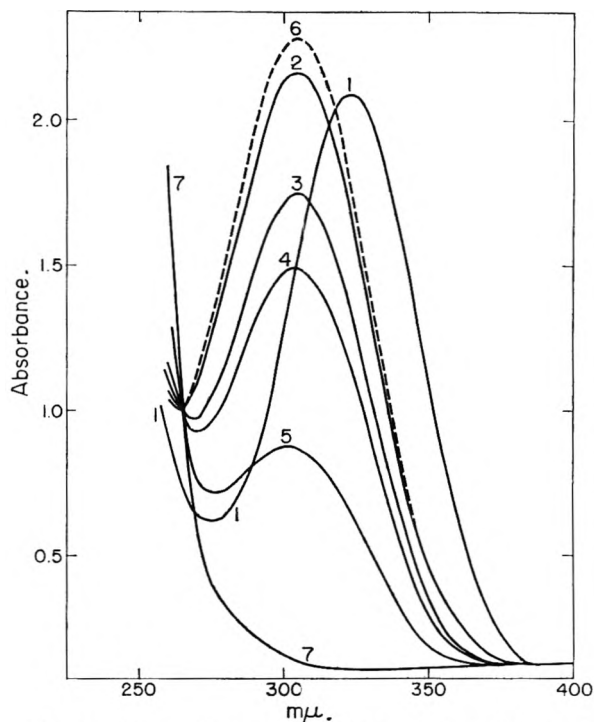


Fig. 2.—Absorption curves of benzoylacetanilide, $10^{-4} M$; 1, aqueous solution of the anion, pH 10.2; 2, anion solution 12 msec. after the addition of acidic buffer; 3, 4, 5, 7, anion solution plus acidic buffer at subsequent time intervals; 7, infinity time, identical with absorption of keto form; 6, absorption of enol at zero time.

Below pH 8 in aqueous solution, the absorption has a prominent band at 245 $m\mu$ and only negligible values between 300 and 325 $m\mu$, since the percentage of enol is very low under these conditions. The addition of a base produces a rapid increase in absorption at 323 $m\mu$, with a concurrent decrease in the 245- $m\mu$ band, showing conversion from the keto form to the anion. The equilibrium constant for the keto form, $pK_{\text{HK}} = 9.41$, was obtained from a plot of $\log (D_a - D)/(D - D_b)$ vs. pH (Fig. 1, curve 2), where D_a , D_b , and D are, respectively, the absorptions at 323 $m\mu$ of the keto form, the anion,

- (11) R. A. Morton, A. Hassan, and T. C. Calloway, *J. Chem. Soc.* 883 (1934).

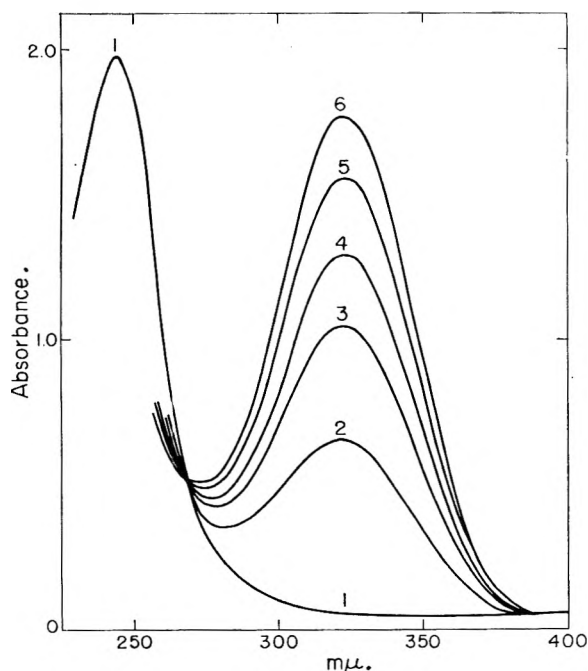


Fig. 3.—Absorption curves of benzoylacetanilide, $10^{-4} M$, at various times after mixing with pH 11 buffer: 1, aqueous solution, pH 7 (reference); 2, 12.2 msec.; 3, 23.8 msec.; 4, 35.5 msec.; 5, 59.9 msec.; 6, 1 minute.

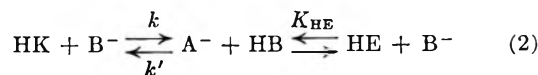
and the mixture of the two at the pH indicated. Similar results were obtained using phosphate buffer ($\mu = 0.375$) or a mixed electrolyte of the same ionic strength containing phosphate ($\mu = 0.075$) and potassium chloride ($\mu = 0.300$).

When an aqueous solution (pH 10.2) of the anion was acidified in the flow machine, a shift in $\lambda_{D_{max}}$ from 323 to 304 $m\mu$ occurred in less than 12 msec. (Fig. 2). The $\lambda_{D_{max}}$ subsequently remained constant although the absorption decreased. The 304- $m\mu$ absorption is thought to be due to the enol form because of the similarity with the position of enol absorption of benzoylacetanilide in other solvents (Table I). The enol is probably β -hydroxycinnamanilide,¹⁰ although this structure has not been definitely established.

At pH values near the pK_{HE} , the absorption curves between 300 and 323 $m\mu$ contain a single broad peak, with $\lambda_{D_{max}}$ characteristic of the pH. The $\lambda_{D_{max}}$ remained constant while the absorption decreased with time (similar to Fig. 2). This is understandable if we assume rapid equilibration between A^- and HE in a buffered medium and the absorption due to HK to be negligible. The ratio of enol to anion at these intermediate pH values can be calculated (see Experimental section). The value of $pK_{HE} = 7.22$ was determined graphically in Fig. 1. The ratio of K_{HK} and K_{HE} shows that the enol content of benzoylacetanilide in aqueous solution is 0.65%.

In neutralization reactions, the reaction rates were followed by measuring spectrophotometrically the disappearance of enol or anion with time after the acidification of the anion (Fig. 2). The rates of ionization of HK were calculated from absorption measurements after a neutral solution of benzoylacetanilide was made alkaline (Fig. 3).

The results are analyzed according to the following scheme of reactions



The ionization of the enol is too rapid to be measured in our experiments, so we assumed that equilibrium was maintained at all times

$$K_{HE} = \frac{(H^+)(A^-)}{(HE)} \quad (3)$$

The net rate of change of the keto form is

$$\frac{d(HK)}{dt} = -k(HK) + k'(A^-) \quad (4)$$

Here k and k' are pseudo-first-order rate constants dependent on the concentrations of HB and B^- , which are present in huge excess over the amide. From eq. 3 and 4 and the relationship $(HE) + (HK) + (A^-) = \text{constant}$, for a given experiment, we obtain

$$-d \ln [(HK) - (HK)_e] = k + k'\phi \quad (5)$$

where $(HK)_e$ represents the equilibrium concentrations of HK and

$$\phi = \frac{K_{HE}}{(H^+) + K_{HE}}$$

Furthermore, even though the absorption (D) is due to several species, it can be shown that

$$-2.303 \frac{d \log (D - D_\infty)}{dt} = k + k'\phi \quad (6)$$

where D_∞ is the absorption at equilibrium.

For optimum conditions, D at $\lambda_{D_{max}}$ was used. The pseudo-first-order rate constants calculated from eq. 6 are recorded in Tables IIa and IIIa for ionization reactions of the keto form with base and in Tables IIb and IIIb for neutralization reactions of the anion with acid. The data reveal the linear dependence of the ratio on buffer-ion concentration. The over-all rates can be expressed in terms of the specific rate constants for each component present. For the phosphates acting as bases

$$k = k_{PO_4^{3-}}(PO_4^{3-}) + k_{HPO_4^{2-}}(HPO_4^{2-}) + k_{H_2PO_4^{-}}(H_2PO_4^{-}) + k_{OH^{-}}(OH^{-}) + k_{H_2O}(H_2O)$$

and acting as acids

$$k' = k'_{H_3PO_4}(H_3PO_4) + k'_{H_2PO_4^{-}}(H_2PO_4^{-}) + k'_{HPO_4^{2-}}(HPO_4^{2-}) + k'_{H_3O^{+}}(H_3O^{+}) + k'_{H_2O}(H_2O)$$

To obtain the specific rate constants, several rates were measured at each pH, using different buffer-salt concentrations. Within each set of runs, the ratios of the phosphate salts were kept constant to maintain constant pH, and potassium chloride was added to maintain constant ionic strength so as to minimize general salt effects. The rate constants were plotted against the buffer ion concentration at each pH. The slopes of these plots measure the effects due to buffer ion, and the intercepts measure the effects due to solvents which include H_3O^+ and OH^- , as well as H_2O . In the case of phosphate buffers

TABLE IIa

INFLUENCE OF PHOSPHATE BUFFERS ON THE RATE OF IONIZATION OF THE KETO FORM OF BENZOYLACETANILIDE

Set no.	pH	Composition	Total buffer ion, M	Rate, sec. ⁻¹	Slope	Intercept
I	12.50	KOH	0	191.5	328	191.5
	12.04	[PO ₄ ⁻³] = 0.0625	0.0625	88.0		
		.0375	.0375	79.5		
		.0125	.0125	71.5		
II	11.55	[HPO ₄ ⁻²]/[PO ₄ ⁻³] = 1.01	.0835	35.5	170	21.3
			.0500	30.0		
			.0167	24.1		
III	11.08	[HPO ₄ ⁻²]/[PO ₄ ⁻³] = 3.0	.1000	15.2	85.6	6.80
			.0800	13.0		
			.0600	11.7		
			.0400	10.0		
			.0200	9.2		
IV	10.28	[HPO ₄ ⁻²]/[PO ₄ ⁻³] = 18.0	.1188	4.98	27.6	1.67
			.0951	4.24		
			.0713	3.64		
			.0476	2.95		
			.0238	2.47		
V	9.83	[HPO ₄ ⁻²]/[PO ₄ ⁻³] = 48.0	.1225	3.50	22.0	0.79
			.1095	3.10		
			.0735	2.40		
			.0245	1.38		
VI	9.22	[HPO ₄ ⁻²]/[PO ₄ ⁻³] = 142 [HPO ₄ ⁻²]/[H ₂ PO ₄ ⁻¹] = 502	.1244	4.50	32.3	0.53
			.0747	2.90		
			.0249	1.31		
			.0124	0.98		
VII	8.93	[HPO ₄ ⁻²]/[H ₂ PO ₄ ⁻¹] = 265 [HPO ₄ ⁻²]/[H ₂ PO ₄ ⁻¹] = 265	.1250	6.13	41.1	0.67
			.0750	4.20		
			.0250	1.66		

$$\text{slope} = k'_{\text{H}_2\text{PO}_4} \frac{(\text{H}_2\text{PO}_4)}{(\text{T})} + (k_{\text{H}_2\text{PO}_4} + k'_{\text{H}_2\text{PO}_4} \phi) \frac{(\text{H}_2\text{PO}_4^-)}{(\text{T})} + (k_{\text{HPO}_4^-2} + k'_{\text{HPO}_4^-2} \phi) \frac{(\text{HPO}_4^-2)}{(\text{T})} + k_{\text{PO}_4^-3} \frac{(\text{PO}_4^-3)}{(\text{T})} \quad (8)$$

where (T) = (H₃PO₄) + (H₂PO₄⁻¹) + (HPO₄⁻²) + (PO₄⁻³)
intercept = k'_{H₃O⁺} φ (H₃O⁺) + (k_{H₂O} + k'_{H₂O} φ)(H₂O) + k_{OH⁻}(OH⁻) (9)

For carbonate buffers, the intercept is the same as for the phosphate, however

$$\text{slope} = (k_{\text{HCO}_3^-} + k'_{\text{HCO}_3^-} \phi) \frac{(\text{HCO}_3^-)}{(\text{T})} + k_{\text{CO}_3^-2} \frac{(\text{CO}_3^-2)}{(\text{T})} \quad (10)$$

where (T) = (HCO₃⁻) + (CO₃⁻²), neglecting carbonic acid.

The slope and intercept for each set of experiments are given in Tables IIa and IIb and IIIa and IIIb. To obtain the specific rate constants (k' and k) for each of the buffer ions, the buffer ratios and experimental slopes were substituted into the appropriate equation, (8) or (10), for each set of data. Several equations resulted, each containing one or more constants. When these equations for anion neutralization below pH 7 were solved simultaneously, only the constants k'_{H₃PO₄} and k'_{H₂PO₄⁻} were obtained. The terms containing these constants were large enough to mask completely all the other terms in this region. In the equations for the ionization reactions (>pH 9), φ is unity. All

terms are therefore independent of pH, and the constants k_{PO₄⁻³} and (k_{HPO₄⁻²} + k'_{HPO₄⁻²}) were calculated directly. This last constant is composite and cannot be broken down without imposing further conditions. Applying the principle of microscopic reversibility, eq. 11 must hold

$$k_{\text{B}^-}(\text{B}^-)_{\text{eq}}(\text{HK})_{\text{eq}} = k'_{\text{HB}}(\text{HB})_{\text{eq}}(\text{A}^-)_{\text{eq}} \quad (11)$$

and it follows that

$$k_{\text{B}^-}K_{\text{HB}} = k'_{\text{HB}}K_{\text{HK}} \quad (12)$$

where K_{HB} is the ionization constant for the acid, HB, involved in the reaction. Table IV reports four of these ionization constants calculated from pH measurements of buffered systems used in the experiments. For internal consistency, all pK's were measured by the same glass electrode at μ = 0.375.

Substituting into eq. 12, we obtain

$$k_{\text{PO}_4^-3} K_{\text{HPO}_4^-2} = k'_{\text{HPO}_4^-2} K_{\text{HK}} \quad (12a)$$

$$k_{\text{HPO}_4^-2} K_{\text{H}_2\text{PO}_4^-} = k'_{\text{H}_2\text{PO}_4^-} K_{\text{HK}} \quad (12b)$$

The constants k_{HPO₄⁻²} and k'_{HPO₄⁻²} were calculated and the sum of these checked with the composite term, as calculated. All these constants are reported in Table IV, along with constants for carbonate ions, obtained in the same way.

In the pH range 7 to 9.5, the situation is more complicated. The equations contain as many as four different constants, only some of which are pH-dependent. Substitution of buffer ion ratios for this region and the rate constants calculated from the other pH regions into eq. 8 and 10 led to a calculated

TABLE IIb
INFLUENCE OF PHOSPHATE BUFFERS ON THE RATE OF NEUTRALIZATION OF BENZOYLACETANILIDE ANION

Set no.	pH	Composition	Total buffer ion, <i>M</i>	Rate, sec. ⁻¹	Slope	Intercept
VIII	8.22	$[\text{H}_2\text{PO}_4^{-1}]/[\text{HPO}_4^{-2}] = 3.37 \times 10^{-2}$	0.1275	23.8	185	1
			.0765	15.0		
			.0255	5.5		
IX	7.00	$[\text{H}_2\text{PO}_4^{-1}]/[\text{HPO}_4^{-2}] = 0.497$.1580	133.5	747	0.8
			.0948	71.5		
			.0316	26.0		
X	6.78	$[\text{H}_2\text{PO}_4^{-1}]/[\text{HPO}_4^{-2}] = 0.902$.1825	129	691	2
			.1095	75.5		
			.0365	28.6		
XI	6.00	$[\text{H}_2\text{PO}_4^{-1}]/[\text{HPO}_4^{-2}] = 4.48$.2750	76.0	269	3
			.1650	48.6		
			.1100	34.2		
			.0550	18.6		
			.0283	9.90		
XII	5.38	$[\text{H}_2\text{PO}_4^{-1}]/[\text{HPO}_4^{-2}] = 18.7$ $[\text{H}_2\text{PO}_4^{-1}]/[\text{H}_3\text{PO}_4] = 2470$.3396	35.7	95.7	2.6
			.2718	27.7		
			.2037	23.6		
			.1358	15.5		
			.0679	8.45		
			.0340	6.50		
XIII	4.38	$[\text{H}_3\text{PO}_4]/[\text{H}_2\text{PO}_4^{-1}] = 4.46 \times 10^{-3}$ $[\text{H}_2\text{PO}_4^{-1}]/[\text{HPO}_4^{-2}] = 225$.375	9.50	22.9	0.96
			.225	6.00		
			.075	2.63		
XIV	3.60	$[\text{H}_3\text{PO}_4]/[\text{H}_2\text{PO}_4^{-1}] = 2.635 \times 10^{-2}$.385	6.87	16.1	0.61
			.231	4.37		
			.077	1.85		
XV	3.21	$[\text{H}_3\text{PO}_4]/[\text{H}_2\text{PO}_4^{-1}] = 6.45 \times 10^{-2}$.400	6.36	14.2	0.66
			.240	4.126		
			.080	1.81		

TABLE IIIa
INFLUENCE OF CARBONATE BUFFERS ON THE RATE OF IONIZATION OF BENZOYLACETANILIDE

Set no.	pH	Composition	Total buffer ion, <i>M</i>	Rate, sec. ⁻¹	Slope	Intercept
XVI	11.30	$[\text{CO}_3^{-2}] = 0.125$	0.125	32.0	157.5	12.7
			.075	24.9		
			.025	16.3		
XVII	10.60	$[\text{HCO}_3^{-1}]/[\text{CO}_3^{-2}] = 0.158$.1375	16.6	95.8	3.50
			.0825	11.3		
			.0275	6.20		
XVIII	9.94	$[\text{HCO}_3^{-1}]/[\text{CO}_3^{-2}] = 0.75$.175	14.7	77.8	1.1
			.105	9.40		
			.035	3.73		
XIX	9.54	$[\text{HCO}_3^{-1}]/[\text{CO}_3^{-2}] = 2.0$.225	14.1	59.5	0.55
			.180	11.2		
			.135	8.70		
			.090	6.00		
			.045	3.11		
XX	9.10	$[\text{HCO}_3^{-1}]/[\text{CO}_3^{-2}] = 5.58$.2878	13.2	43.2	0.87
			.1725	8.45		
			.0575	3.30		

slope. The agreement between the observed and calculated slopes (Table V) over the whole range of pH's serves as a check of the accuracy of the rate constants.

The specific rate constants due to hydronium ion, hydroxide ion, and water (Table IV) were determined graphically from the intercepts. In these calculations, (H_3O^+) and (OH^-) were taken from pH measurements without corrections and K_w was

assumed to be equal to $10^{-14.00}$. From the data from Tables II and III at $\text{pH} > 10.5$, a plot of log intercept vs. pH gave a straight line with the slope equal to unity. The same line fitted the data from phosphate buffer, carbonate buffer, or KOH. The specific rate constant, k_{OH^-} , was determined from this plot. Figure 4 shows a plot of the intercept against pH for all the carbonate runs (\blacktriangle) and phosphate runs (\bullet), between pH 3 and pH 11.5.

TABLE IIIb

Set no.	pH	Composition	Total buffer ion, <i>M</i>	Rate, sec. ⁻¹	Slope	Intercept
XXI	9.02	[HCO ₃ ⁻¹]/[CO ₃ ⁻²] = 7.0	0.300	15.2	48.8	0.52
			.180	9.29		
			.060	3.50		
XXII	8.81	[HCO ₃ ⁻¹]/[CO ₃ ⁻²] = 12.0	.325	16.2	48.7	0.80
			.195	9.73		
			.065	3.55		
XXIII	8.64	[HCO ₃ ⁻¹]/[CO ₃ ⁻²] = 27.0	.350	15.8	43.7	0.53
			.210	9.75		
			.070	3.55		

TABLE IV

SPECIFIC RATE CONSTANTS FOR THE EQUILIBRATION OF BENZOYLACETANILIDE

Base	<i>k</i> , l./mole sec.	Acid	<i>k'</i> , l./mole sec.	p <i>K</i>
PO ₄ ⁻³	310	HPO ₄ ⁻²	2.2	11.56
HPO ₄ ⁻²	12	H ₂ PO ₄ ⁻¹	5750	6.71
H ₂ PO ₄ ⁻¹	Very small	H ₃ PO ₄	2.3 × 10 ⁶	2.01
CO ₃ ⁻²	105	HCO ₃ ⁻¹	35.5	9.88
HCO ₃ ⁻¹	6.6	H ₂ CO ₃	Unknown	
OH ⁻	5900	H ₂ O	0.5 ^a	
H ₂ O	Very small	H ₃ O ⁺	1.3 × 10 ⁷	

^a This value is for *k*_{H₂O}(H₂O) sec.⁻¹.

TABLE V

COMPARISON OF OBSERVED AND CALCULATED SLOPES AND CONTRIBUTIONS FROM EACH ACID AND BASE TERM

System no.	Calcd.				Sum = (calcd. slope)	Slope (obsd.)
	<i>k</i> _{PO₄⁻³} / (T)	<i>k</i> _{HPO₄⁻²} / (T)	<i>k</i> _{H₂PO₄⁻¹} × φ / (T)	<i>k</i> _{H₃PO₄} × φ / (T)		
I	310				310	328
II	154	6	1		161	170
III	77.5	9	1.5		89	85.6
IV	16.3	11.4	2.1		29.8	27.6
V	6.3	12.0	2.2		20.5	22.0
VI	2.2	12.0	2.2	11.5	27.9	32.3
VII	1.2	12.0	2.2	20.9	36.3	41.1
System no.	Calcd.				Sum = (calcd. slope)	Slope (obsd.)
	<i>k</i> _{HPO₄⁻²} (HP-O ₄ ⁻²) / (T)	<i>k'</i> _{HPO₄⁻²} (HP-O ₄ ⁻²) φ / (T)	<i>k</i> _{H₂PO₄⁻¹} (H ₂ P-O ₄ ⁻¹) / (T)	<i>k'</i> _{H₂PO₄⁻¹} (H ₂ P-O ₄ ⁻¹) φ / (T)		
VIII	11.6	1.9	170		183.5	185
IX	8.2	0.6	720		728.8	747
X	6.3	0.3	727		733.6	691
XI	2.2	0.02	267		269.2	269
XII	0.6	0	78.8	12.8	91.6	95.5
System no.	Calcd.			Sum = (calcd. slope)	Slope (obsd.)	
	<i>k'</i> _{H₂PO₄⁻¹} (H ₂ P-O ₄ ⁻¹) φ / (T)	<i>k'</i> _{H₃PO₄} (H ₃ P-O ₄) φ / (T)				
XIII	8.3	14.8		23.1	22.9	
XIV	1.4	14.2		15.6	16.13	
XV	0.5	13.6		14.1	14.2	
System no.	Calcd.			Sum = (calcd. slope)	Slope (obsd.)	
	(CO ₃ ⁻²) <i>k</i> _{CO₃⁻²} / (T)	(HCO ₃ ⁻¹) <i>k</i> _{HCO₃⁻¹} / (T)	(HCO ₃ ⁻¹) <i>k</i> _{HCO₃⁻¹} φ / (T)			
XVI	105			157	105	
XVII	90.8	4.8	0.9	96.5	95.8	
XVIII	60	15.2	2.8	78	77.8	
XIX	35	23.7	4.4	63.1	59.5	
XX	15.9	29.1	5.5	50.5	43.2	
XXI	13.1	30.5	5.8	49.4	48.8	
XXII	8.1	32	6.1	46.2	48.7	
XXIII	3.7	33.1	6.4	43.2	43.7	

At pH 9, the only significant term is due to water, *k'*_{H₂O}(H₂O). Below pH 6, the only significant term contains the rate constant *k'*_{H₃O⁺}. Both constants were determined from the most favorable regions. The hydroxide ion, hydronium ion, and water constants were used to construct the total rate curve represented by the solid curve in Fig. 4. The points fall very close to the line except at pH 5.38, 6.00, and 6.78. Here the intercepts are quite small compared with the total rates, and the error in their determination therefore was fairly large. The shaded areas are an estimate of the error.

The Brønsted catalysis law was applied to the data in Table IV. Log *k* and log *k'* were plotted vs. p*K* for the series of acids and bases used (Fig. 5).

For the acids $\log k' = \log G' - \alpha pK$ (13)

and for the bases $\log k = \log G + \beta pK$ (14)

Here, $\alpha = 0.66$ and $\beta = 0.30$, in agreement with Maron and LaMer,² who found that $\alpha + \beta = 1$ under these conditions. The ionization constants were not statistically corrected since there is doubt that such corrections are valid for phosphates and carbonates.⁷ Even if such corrections are made, the slopes change very little. The ionization constant for the carbonic acid-bicarbonate ion equilibrium was not determined, but the value of 10⁻⁴ was assumed⁷ in the plot.

Discussion

In choosing a simple mechanism (eq. 2) to fit the kinetic data, we assumed that the transformation between the keto and enol forms goes through a common anion.¹² Since the enol-anion equilibrium is very rapid, the rates of equilibration between the anion and the keto form are the rate-controlling steps.

Other mechanistic schemes also fit the kinetic data, e.g., the keto form and anion could be assumed to approach equilibrium through an enol intermediate, whereby the equilibrium reaction between the keto and the enol forms then would be the slow step involving simultaneously both an acid and a base. The kinetics then require that a solvent molecule always function as either the acid or the base, since otherwise third-order terms involving buffer ions as both acid and base would have been observed. The assumption of this more complicated mechanistic scheme would, however, add little to the picture since it is equivalent to stating that only ions and molecules solvated in certain configurations can react. The mechanism

(12) K. J. Pedersen, *J. Phys. Chem.*, **38**, 581 (1934).

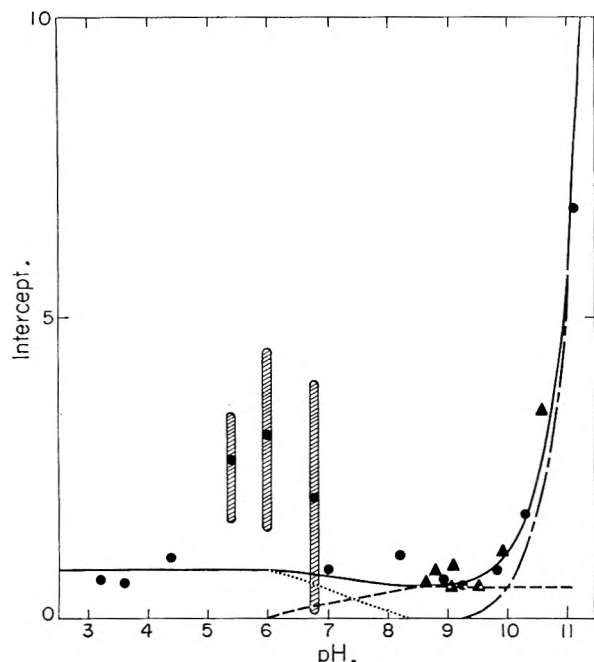


Fig. 4.—Plot of intercept vs. pH:, $k'_{H^+} [H^+] \phi$; ---, $k_{H_2O} [H_2O] \phi$; - - - -, $k_{OH^-} [OH^-]$; ———, total of the three broken curves.

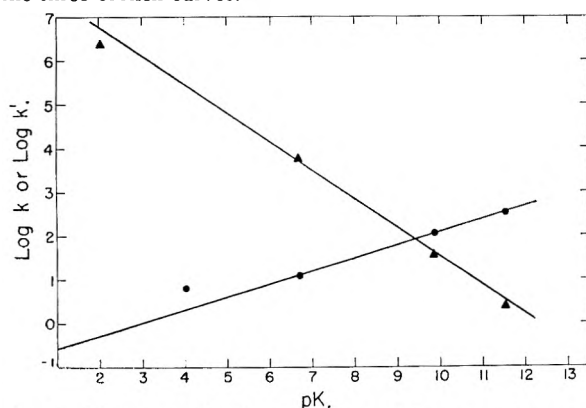


Fig. 5.—Brønsted plot for the acid and base constants of benzoylacetanilide: ●, base constants; ▲, acid constants. of direct ionization currently is held as valid for the neutralization of nitroalkanes, and the nitro-acid-automerism, although slower, appears to be entirely analogous to the keto-enol tautomerism of benzoylacetanilide.^{1,2,4,7}

The assumption of direct ionization is supported by the separation of rate constants according to the kinetic equations derived for this scheme and eq. 11, and the agreement of the observed and calculated slopes, as shown in Table V. In addition for simple acid-base reactions, Maron and LaMer² have shown from eq. 11 that the sum of the exponents of the Brønsted relationships, $\alpha + \beta$, must be equal to unity. For our data, $\alpha + \beta$ is observed to be 0.96. Therefore, the data are entirely consistent with a simple ionization reaction.

Experimental Details

Materials.—Benzoylacetanilide, m.p. 107.5–108° (lit.¹³ 106–106.5°); *Anal.* Calcd. for $C_{15}H_{13}O_2N$: C, 75.4; H, 5.48; N, 5.85. Found: C, 75.7; H, 5.8; N, 6.0.

Phosphoric acid, KH_2PO_4 , K_2HPO_4 , K_3PO_4 , $NaHCO_3$, Na_2CO_3 , and KCl were all reagent-grade chemicals.

(13) C. J. Kibler and A. Weissberger, *Org. Syntheses*, **25**, 7 (1945).

Measurement of Rates.—All experiments were carried out at $25 \pm 0.1^\circ$. The buffers were prepared by mixing appropriate volumes of H_3PO_4 , KH_2PO_4 , K_2HPO_4 , and K_3PO_4 solutions or $NaHCO_3$ and Na_2CO_3 solutions to give a final ionic strength of 0.375 in the reaction solution. In cases where the buffer ion was decreased, the ionic strength of the reaction mixture was maintained at 0.375 by dilution with potassium chloride solution.

Solutions of benzoylacetanilide ($2 \times 10^{-4} M$) were prepared by dissolving the substrate in 1 ml. of absolute ethanol and adding this solution to 1 l. of distilled water, with rapid stirring. The anion was prepared in solution as needed by adjusting the pH of the amide solution to pH 10.2 with concentrated sodium hydroxide solution. The concentration of substrate in the reaction mixtures below pH 6 had to be reduced to $2.5 \times 10^{-5} M$, owing to limited solubility.

The reaction rates were determined in a flow machine which was equipped with a scanning ultraviolet double-beam recording spectrophotometer as the analyzing component. Equal volumes of carbonyl and buffer solutions were brought together in the mixing chamber and passed through a spacer which determined the reaction time before analysis. The housing at the end of the spacer contained a quartz cell for the absorption measurements. Constant flow from the mixing chamber through the spacer ensured a steady-state concentration of reactants in the absorption cell. Combinations of spacer length and flow rate to correspond to reaction times ranging from 12 to 850 msec. were used. Several convenient reaction time intervals were used in each run. The absorption curve between 250 and 400 $m\mu$ was recorded for each time.

For reactions above pH 9, measurements of increase in density were made at 323 $m\mu$ ($\lambda_{D_{max}}$ for the anion). Below pH 9, the decrease in absorption was measured also at the position of maximum absorption, but $\lambda_{D_{max}}$ varied in this region, depending on pH. Below pH 6, $\lambda_{D_{max}} = 304 m\mu$ ($\lambda_{D_{max}}$ for the enol). In the range pH 6.0–9.0, different mixtures of anion and enol were present in a single broad peak with $\lambda_{D_{max}}$ between 304 and 323 $m\mu$.

The pH of the reaction mixture for each run was determined with a Beckman Model G pH meter and a glass electrode. The sample was taken from the flow machine. For a series of runs in which the concentration of buffer ion was changed but the ratio of buffer salts and the total ionic strength of the solution were left constant, the pH did not vary more than ± 0.02 pH unit throughout the set of experiments.

Determination of pK_{HE} .—When a solution of benzoylacetanilide ($2 \times 10^{-4} M$, pH 10.5) containing both anion and keto forms was mixed with an equal amount of phosphate buffer (pH 5.4) in the flow machine, the anion was converted to enol almost instantaneously. From the rate of disappearance of enol and extrapolation to zero time, the absorption curve for the pure enol was constructed (Fig. 2, curve 6). A curve for the anion corresponding to the same concentration as the enol was obtained by mixing equal volumes of the anion solution and pH 10.5 buffer (Fig. 2, curve 1). The concentration of the keto form present during the measurement of these curves can be neglected for the purpose of calculation since its absorption between 300 and 323 $m\mu$ is negligible. The ratio of the extinction coefficients of the anion and enol ($\epsilon_{A^-}/\epsilon_{HE}$) at two different wave lengths (from the curves) and the ratios of optical densities at the two wave lengths from curves at intermediate pH values were used to calculate (HE/A^-) as shown

$$D(\lambda_1) = \epsilon_{HE}(\lambda_1) [HE] + \epsilon_{A^-}(\lambda_1) [A^-] \quad (15)$$

$$D(\lambda_2) = \epsilon_{HE}(\lambda_2) [HE] + \epsilon_{A^-}(\lambda_2) [A^-] \quad (16)$$

where HE = concentration of enol, A^- = the concentration of anion in the mixture, ϵ_{HE} and ϵ_{A^-} are the extinction coefficients for the pure enol and the pure anion, respectively, at the wave lengths specified; and D = the observed density of the curve for the mixture at the wave length specified. Solution of eq. 15 and 16 for $\lambda_1 = 323 m\mu$ and $\lambda_2 = 304 m\mu$ yields

$$\frac{D_a - D}{D - D_b} = \frac{(HE)}{(A^-)} = \frac{\left(\frac{\epsilon_{A^-}(304)}{\epsilon_{HE}(323)}\right) \left(\frac{D_{323}}{D_{304}}\right) - \left(\frac{\epsilon_{A^-}(323)}{\epsilon_{HE}(323)}\right)}{1 - \left(\frac{\epsilon_{HE}(304)}{\epsilon_{HE}(323)}\right) \left(\frac{D_{323}}{D_{304}}\right)} \quad (17)$$

A plot of $\log [(D_a - D)/(D - D_b)]$ vs. pH is shown in Fig. 1 from which $pK_{HE} = 7.22$.

THE RADIOLYSIS OF CHLORO-, BROMO-, AND IODOBENZENES WITH COBALT-60 γ -RAYS

BY SANG UP CHOI AND JOHN E. WILLARD

Department of Chemistry of the University of Wisconsin, Madison, Wisconsin

Received November 20, 1961

G-values have been determined for the products of radiolysis of liquid C_6H_5Cl , C_6H_5Br , and C_6H_5I at room temperature and 100° , and in the presence of radical scavengers. The inorganic products are HCl from C_6H_5Cl , HBr and Br_2 from C_6H_5Br , and primarily I_2 from C_6H_5I . G_{H_2} is $<10^{-2}$. Organic products include C_6H_6 , $C_6H_5C_6H_5$, $C_6H_4X_2$, and $C_6H_5-C_6H_4X$. Apparent activation energies for the formation of all of the products are ≤ 3 kcal./mole. The yields of organic products are relatively insensitive to halogen scavengers. *G*-values for conversion of the aromatic halide to new products of molecular weight up to and including the halobiphenyls are about 2.3, 4.0, and 5.3 for the iodide, bromide, and chloride, respectively, while the corresponding values for exchange with radioiodine are approximately four equivalents per 100 e.v. in each case. In the radiolysis of C_6H_5Br and C_6H_5I , metastable products with high absorbance indices at 3750 and 4200 Å., respectively, which disappear at room temperature with a first-order rate constant of about 0.1/hr., and much more rapidly at 90° , are formed. Intense illumination of $C_6H_5Br-Br_2$ solutions with light absorbed by bromine did not form the metastable species. The results reported here for the aromatic halides are compared with known data for alkyl halides.

Introduction

This work was undertaken to compare the radiation chemistry of the halobenzenes with the radiation chemistry of the alkyl halides, and to compare the different halobenzenes with each other with respect to their radiolysis. Radiohalogen scavengers, temperature dependence, and gas chromatographic analysis for the products have been used in an endeavor to identify both the final products and the reaction intermediates. The results are discussed in the light of the extensive work which has been done on the radiolysis¹ and photolysis² of the alkyl iodides, the radiolysis of alkyl bromides,^{3,4} and the radiolysis of alkyl chlorides.⁵

The study of the radiation chemistry of the organic halides allows comparisons related to the different strengths of the carbon-halogen bonds, the different fraction of total electrons per molecule contributed by the different halogen atoms, the different activation energies for abstraction of hydrogen by the different halogen atoms, and the different activation energies for reactions of free radicals with the different hydrogen halides and halogen molecules.

Experimental

Reagents and Sample Preparation.—Chlorobenzene (Eastman white label) and iodobenzene (Eastman white label) were purified further by passing through a column of alumina and distilling on a 1-m. Todd column packed with glass helices. Bromobenzene (Baker analytical reagent grade) was purified by several methods including: (1) vigorous mechanical stirring with concentrated sulfuric acid followed by washing with bicarbonate solution and fractional distillation on a Todd column; (2) intense illumination in the presence of elemental bromine followed by bromine removal by aqueous sulfite solution; (3) washing with water, and drying over magnesium sulfate, after which oxygen

containing a few per cent. ozone was bubbled through the bromobenzene which then was washed with aqueous ferrous solution, with dilute $KMnO_4$, and with sodium hydroxide. After washing with water and drying with magnesium sulfate it was fractionally distilled with a Todd column. *G*-values for bromine production proved to be independent of the method of purification. This was true at all doses tested including the early stages of irradiation where an induction period is observed. Consequently most of the bromobenzene used in this work was purified only by fractional distillation. The bromine (Baker, reagent grade), the iodine (Mallinckrodt, analytical reagent), and the hydrogen bromide (Matheson) used as additives were used without further purification. Dry HI was prepared by the dehydration with P_2O_5 of a 55% aqueous solution of HI (Merck), as described previously.^{1b}

Samples for irradiation were degassed by four successive cycles of freezing, evacuation and melting on a vacuum line and were sealed off in the irradiation vessel. Chlorobenzene, bromobenzene, bromine, and HBr were each distilled through P_2O_5 on the vacuum line before use. Iodobenzene was pipetted directly into the irradiation vessel following distillation on the Todd column.

Irradiation and Dosimetry.—Irradiations were made with a Co^{60} source in an irradiation facility similar to that described earlier.⁶ The average intensity of the source during the period of this work was about 300 curies and it delivered about 10^6 roentgens per hour (10^{20} e.v. g^{-1} hr^{-1}) to the samples. The samples were contained either in an annular glass vessel which held 5 ml. of liquid in a 3-mm. thick annular layer around the 1-cm. diameter source, or in 6-mm. o.d. glass tubes reproducibly mounted adjacent to the source irradiation position. The rate of energy absorption by the samples was determined by ferrous sulfate dosimetry assuming a value of 15.6 ferrous ions oxidized per 100 e.v. absorbed and a molar absorptivity index of 2.24×10^3 at 3050 Å. for ferric ion in the dosimeter solution. Factors were applied for the differences in electron density between the dosimeter solution and the halobenzenes and for the added absorption occurring by the photoelectric effect in bromo and iodobenzene, as discussed previously,^{1b} and appropriate correction was made for source decay. The ratios of rates of energy absorption by chloro-, bromo-, and iodobenzene were 1, 1.29, and 1.59 on the volume basis and 1, 0.95, and 0.96 on the weight basis.

Analysis.—Analysis for bromine produced in bromobenzene and iodine produced in iodobenzene was made at frequent intervals during the course of irradiations by removing the annular irradiation vessel from the source, pouring the solution into a sidearm to which was attached a Beckman cell, and examining the solution on a Beckman spectrophotometer. The side arm normally contained a Beckman cell with a 1-cm. light path and another with a 1-mm. light path so that the halogen concentration could be followed over a wide range. The molar absorptivity indices used for bromine in bromobenzene were 231 at 3750 Å., 289 at 4000

(1) See for example: (a) E. O. Hornig and J. E. Willard, *J. Am. Chem. Soc.*, **79**, 2429 (1957); (b) R. J. Hanrahan and J. E. Willard, *ibid.*, **79**, 2434 (1957); (c) R. F. Pottier, W. H. Hamill, and R. R. Williams, *ibid.*, **80**, 4224 (1958).

(2) (a) D. L. Bunbury, R. R. Williams, Jr., and W. H. Hamill, *ibid.*, **78**, 6228 (1956); (b) R. H. Luebbe, Jr., and J. E. Willard, *ibid.*, **81**, 761 (1959).

(3) (a) R. H. Schuler and W. H. Hamill, *ibid.*, **74**, 6171 (1952); (b) J. C. W. Chien and J. E. Willard, *ibid.*, **77**, 3441 (1955).

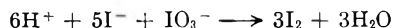
(4) R. J. Neddenriep and J. E. Willard, *J. Phys. Chem.*, **65**, 1206 (1961).

(5) (a) H. L. Benson, Jr., and J. E. Willard, *J. Am. Chem. Soc.*, **83**, 4672 (1961); (b) R. H. Wiley, W. Miller, C. H. Jarboe, Jr., J. R. Harrell, and D. J. Parish, *Radiation Research*, **13**, 479 (1960); (c) E. B. Dismukes and W. S. Wilcox, *ibid.*, **11**, 754 (1959).

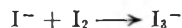
(6) R. F. Firestone and J. E. Willard, *Rev. Sci. Instr.*, **24**, 904 (1953).

Å., 302 at 4120 Å., 215 at 4500 Å., and 95 at 5000 Å. These were determined at 4 concentrations ranging from 1×10^{-3} to $5.8 \times 10^{-3} M$ by measuring the absorbancy of the solutions and then determining the bromine concentration by extraction with aqueous KI solution, followed by titration of the liberated iodine with standard thiosulfate. Molar absorbancy indices for iodine in iodobenzene determined in the same way were 340 at 4200 Å., 682 at 4500 Å., 1240 at 4920 Å., and 490 at 5500 Å. The consumption of iodine during the irradiation of chlorobenzene was followed by the change in its absorbancy. Molar absorbancy indices for iodine in chlorobenzene were determined at five concentrations from 2.6×10^{-3} to $1.3 \times 10^{-2} M$ and found to be 282 at 4500 Å., 979 at 5050 Å., and 512 at 5500 Å. Molar absorbancy indices for iodine in bromobenzene determined in the same way were 54 at 4120 Å., 366 at 4500 Å., 1060 at 5000 Å., and 529 at 5500 Å.

When it was desired to determine the amount of HCl, HBr, or HI formed during an irradiation, the annular type irradiation vessel was provided with a thin walled glass bulb on a side arm. Following irradiation, the liquid was poured from the annular vessel to the bulb, where it was sealed off while frozen with liquid air. The bulb then was broken under a known volume of distilled water and elemental bromine and organic compounds were removed from the aqueous phase by repeated extraction with carbon tetrachloride. An aliquot of the aqueous solution then was mixed with an equal volume of 2 *N* KI solution and some solid potassium iodate was added. I_3^- ion was formed in amounts stoichiometrically related to the amount of hydrogen ion in solution according to the relations



and



The I_3^- concentration was determined spectrophotometrically at 3500 Å. The molar absorbancy index of I_3^- in 1 *N* KI solution was determined both by using standard thiosulfate to determine the concentration of an I_3^- solution in 1 *N* KI solution and by preparing an I_3^- solution of known concentration by the addition of standard HCl solution to an equal amount of 2 *N* KI solution containing solid KIO_3 . The molar absorbancy indices obtained by the two methods were in excellent agreement; the values being 1.67×10^4 at 3250 Å., 2.78×10^4 at 3500 Å., and 1.92×10^4 at 3750 Å.

Analysis for chlorine in chlorobenzene was made in the same way as the analysis for the halogen acids above, after extracting the chlorine from the organic layer with a 1 *N* aqueous solution of KI.

Analysis for organic products was made by gas chromatography using a 12-ft. 4-mm. o.d. Pyrex column wound in a double spiral. It was packed with 40–60 mesh Johns-Manville C-22 firebrick coated with General Electric SF-96(40) silicone oil. The flow gas was helium. The temperature of the column was raised from room temperature to 200° at a rate of about 4°/min. during the analysis, all the connecting tubes from the column to the Gow-Mac thermal conductivity cells or the scintillation counter used for radioactivity analysis being heated to over 200° by a winding of resistance wire. When it was desired to analyze for very high boiling compounds such as biphenyl and the bromobiphenyls, a column of only 6–12 in. in length was substituted for the 12-ft. column. This column separated these compounds well at temperatures considerably lower than their boiling points. The areas of the peaks obtained from irradiated samples were used to calculate yields, the sensitivity of the apparatus being determined with known samples. The relative sensitivities for the compounds of interest were: (1) analysis of irradiated C_6H_5Br : C_6H_5Br , 1; C_6H_6 , 1.36; *p*- $C_6H_4Br_2$, 0.86; $C_6H_5C_6H_5$, 0.78; *o*- $BrC_6H_4C_6H_5$, 0.67; *p*- $BrC_6H_4C_6H_5$, 0.73. (2) analysis of irradiated C_6H_5I : C_6H_5I , 1; C_6H_6 , 1.40; $C_6H_5C_6H_5$, 0.84; *p*- $C_6H_4I_2$, 0.85; *p*- $IC_6H_4C_6H_5$, 0.76. (3) analysis of irradiated C_6H_5Cl : C_6H_5Cl , 1; C_6H_6 , 1.22; *p*- $C_6H_4Cl_2$, 0.86; $C_6H_5C_6H_5$, 0.68; *p*- $ClC_6H_4C_6H_5$, 0.70. In general, the samples used for gas chromatographic analysis consisted of 0.1 ml. irradiated in 4-mm. i.d. tubes with thin blown ends that could be broken readily by a bulb crusher

in the entrance gas stream of the gas chromatography equipment.

Organic compounds containing radiobromine introduced during irradiation in the presence of radioactive Br_2 were detected as they came off the column by the use of a well-type scintillation counter equipped to give a record on a chart recorder.⁷ The peaks on the chromatograms were identified by comparing the emergence times with those for known compounds.

The presence of hydrogen as a product was indicated by a negative peak when the effluent from the gas chromatography column was monitored by thermal conductivity with helium as the carrier gas. The amount of hydrogen was determined by *P-V-T* measurements on the non-condensable gases from irradiated samples. Mass spectrometric analysis of these gases showed that they contained only hydrogen. Samples irradiated for these analyses consisted of 0.5 ml. of liquid in 4-mm. i.d. tubes.

Solubility of HBr in Bromobenzene.—HBr was used as a radical scavenger during a number of irradiations of liquid bromobenzene. In order to know the concentration of HBr in the liquid as compared to that in the gas phase when a known number of moles of HBr was present in the reaction vessel, it was necessary to determine the Henry's law constant for HBr in bromobenzene. This was done by metering successive known amounts of HBr from a reservoir system into a system containing a known amount of magnetically stirred liquid bromobenzene and using a manometer to measure the pressure in the known volume of gas in the system. The values obtained for the constant in the expression $pressure = K \times \text{mole fraction}$ are: 7.78 mm. at 0°, 11.8 mm. at 19°, and 14.6 mm. at 27.5°.

Radioactive bromine for exchange studies was prepared by exposure of elemental bromine to the neutrons in the reactor of the Argonne National Laboratory. Br^{82} (36-hr.) was used in the present work, time being allowed for the Br^{80} isomers to decay. Radioiodine was prepared from carrier-free sodium iodide solution of the type prepared for diagnostic use by hospitals. A desired amount of inactive NaI was added to an aliquot of the solution in a tube which could be attached to the vacuum line by a ground joint. The solution was evacuated to dryness and the residue covered with powdered potassium dichromate. When this mixture was heated under vacuum, iodine was produced and could be distilled into the desired reaction vessel. The annular irradiation vessels used for studying the exchange reaction were equipped with a thin bulb in which the irradiated liquid was sealed off (while frozen in liquid air) after exposure to the Co^{60} source. The bulb then was broken under an aqueous solution of sulfite and bromide which then was vigorously shaken with a known volume of carbon tetrachloride. The aqueous and organic layers each were counted in a test-tube in a well type scintillation counter. Wall thicknesses were such that the β -rays did not count, so no correction was required for differences in density of the counting media.

Results and Discussion

Bromobenzene

Bromine and HBr Production.—The irradiation of pure bromobenzene with Co^{60} γ -rays yielded elemental bromine with an initial *G*-value of about 0.2 which gradually increased to 0.6 after the absorption of about 2×10^{20} e.v. g^{-1} . It then remained constant until the absorption of about 7×10^{20} e.v. g^{-1} , following which it gradually decreased. This induction period which seems to be reproducible with bromobenzene purified by widely varying methods is illustrated by the curve labeled "no additive" in Fig. 1.

Hydrogen bromide is also a product of the irradiation of bromobenzene as shown in Fig. 2, in which the lower curve is for an irradiation which started with pure bromobenzene, and the upper curve for an irradiation initially containing $4 \times 10^{-2} M Br_2$

(7) J. B. Evans, J. E. Quintan, and J. E. Willard, *Ind. Eng. Chem.*, **50**, 192 (1958).

A larger scale plot indicates that there may be an induction period for the production of HBr such as was observed in the production of bromine. $G(\text{HBr})$ values determined from the slopes after the absorption of 1×10^{20} e.v. g.⁻¹ are 0.43 for the pure bromobenzene and 0.65 for the bromine solution. At an absorption of about 10×10^{20} e.v. g.⁻¹ these have decreased to 0.24 and 0.27, respectively. Irradiation of the pure bromobenzene solution was continued to 38×10^{20} e.v. g.⁻¹; the G -value for the interval from 13 to 38×10^{20} e.v. g.⁻¹ was 0.13. Irradiation of the $\text{Br}_2\text{-C}_6\text{H}_5\text{Br}$ solution also was continued to 53×10^{20} e.v. g.⁻¹; the G -value for the interval from 12 to 53×10^{20} e.v. g.⁻¹ was 0.17.

In a system such as this where both Br_2 and HBr are produced there is a possibility that the two may compete for free radicals and that this competition may be affected by adding one or the other prior to irradiation. Such an effect is suggested by the upper curve of Fig. 2. It also is suggested by the influence of added bromine and of added HBr on the rate of production of bromine as shown in Fig. 1. All concentrations of added HBr tested from 0.01 to 0.06 M increase the initial rate of bromine production by the same amount, *i.e.*, to a G -value of about 2.8. As irradiation continues the increased rate falls off, becoming progressively more similar to the normal rate. The approach to the normal rate is slower, the higher the concentration of the additive. This behavior is of the type that would be expected if radicals such as phenyl radicals produced in the system can react with HBr to produce benzene and bromine atoms or with Br_2 to produce bromobenzene and bromine atoms. The decrease in $G(\text{Br}_2)$ to the same initial value for all added concentrations of Br_2 shown in Fig. 1 also is to be expected if such a competition prevails. The initial $G(\text{Br}_2)$ with added bromine is about -0.4 . The negative value suggests that there are radicals other than C_6H_5 in this system, such as $\text{C}_6\text{H}_4\text{Br}$, the net effect when these react with Br_2 to form $\text{C}_6\text{H}_4\text{Br}_2$ being to reduce the total bromine in the system. As the dose is increased and HBr builds up in the system it competes more and more effectively with Br_2 and so the rate of bromine production approaches the rate in the absence of additives. When bromobenzene with both HBr and Br_2 (0.06 M HBr, 0.04 M Br_2) added prior to irradiation was irradiated, the curve for bromine production fell between the curves for 0.01 and 0.03 M added HBr shown in Fig. 1, except at the start where the rate was slower than any of the curves without added bromine.

As further evidence as to the role of radicals in the radiolysis we have determined the rate of entry of radiobromine into organic combination when the radioactivity is initially present as Br_2 . The data for five experiments ranging from initial bromine concentrations of 0.4 to 0.02 M are shown as the plot of $\log(1 - F)$ against radiation dose in Fig. 3. G -values calculated from the initial slopes of these curves by the relation

$$G = -2.3(2[\text{Br}_2][\text{C}_6\text{H}_5\text{Br}]/(2[\text{Br}_2] + [\text{C}_6\text{H}_5\text{Br}]))(\log(1 - F)/\text{e.v. g.}^{-1})(N/1000d)(100)$$

are 6.8, 7.0, 6.1, 6.0, and 5.4 for the experiments at 0.4, 0.2, 0.04, 0.04, and 0.02 M , respectively. F is the

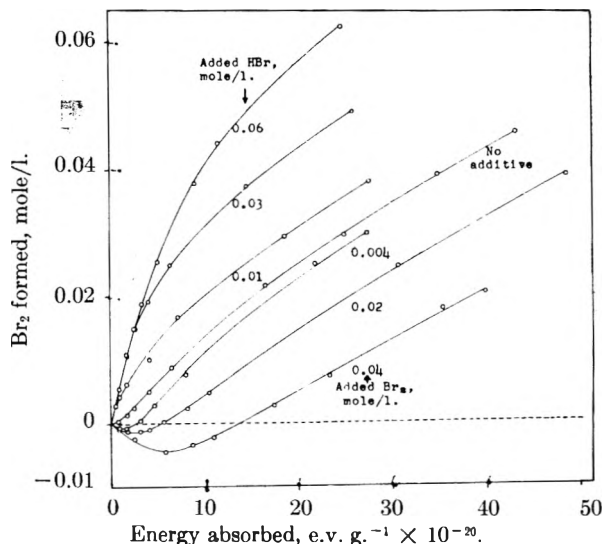


Fig. 1.—Bromine production as a function of radiation dose during the radiolysis of $\text{C}_6\text{H}_5\text{Br}$ with and without added HBr and Br_2 .

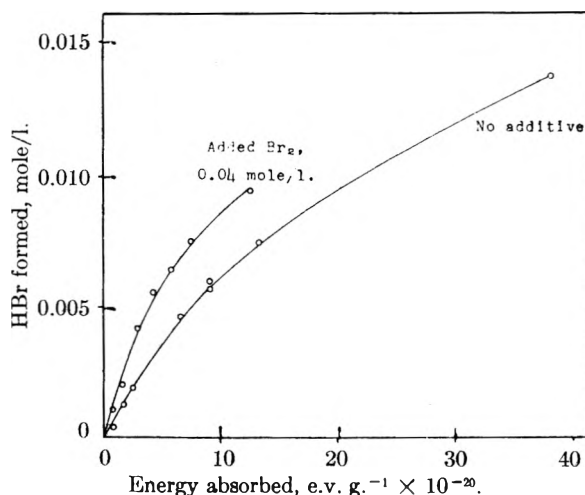


Fig. 2.—HBr production as a function of radiation dose during the radiolysis of $\text{C}_6\text{H}_5\text{Br}$ with and without added Br_2 .

fraction of equilibrium exchange obtained after the absorption of a certain e.v. g.⁻¹, based on the initial composition of the solution, N is Avogadro's number, and d is the density of the solution. The relationship used is the standard expression for the rate of isotopic exchange with the usual units of moles exchanged per liter per unit time converted to units of molecules exchanged per 100 e.v. absorbed. Each point on the curve was calculated on the assumption that all of the inorganic halogen present in the solution was present as Br_2 . Since HBr is produced this is not a correct assumption. Since bromine present as HBr presumably does not take part in the reactions which cause bromine to enter organic combination, although the Br_2 and HBr are in exchange equilibrium with each other, the slopes of the lines in Fig. 3 would be expected to decrease with increasing irradiation and this would be expected to be most apparent for the lower concentrations of bromine, which would have the highest HBr/ Br_2 ratio.

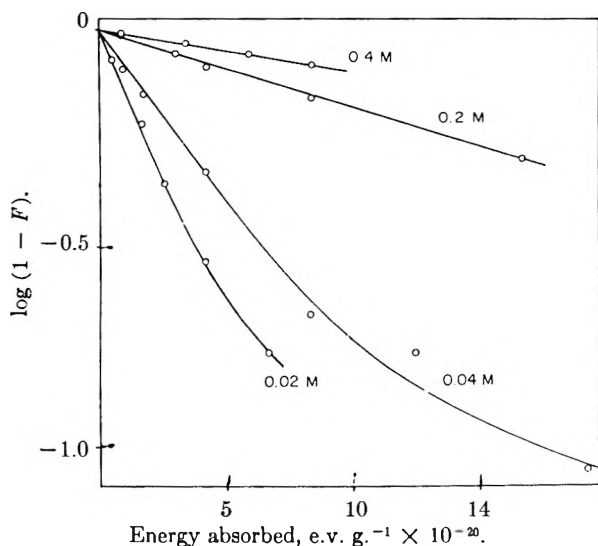


Fig. 3.—Radiation induced exchange of radiobromine with C_6H_5Br at different initial Br_2 concentrations.

If one assumes that all thermal radicals react with Br_2 when Br_2 is present initially to give the limiting rate $G(1/2 Br_2) = -0.8$, whereas all react with HBr when HBr is present initially to give $G(1/2 Br_2) = 5.6$, then the rate of radical production may be calculated to be one-half of the difference between these two values, or 3.2. The factor of one-half is required because for every radical which abstracts hydrogen from HBr there is a net contribution of 2 Br atoms to the system (one from dissociation of C_6H_5Br and one from the abstraction reaction.). The values cited above for G (exchange) are nearly twice as great as the G for radical production deduced thus from the maximum minus minimum rates. This seems to mean, as suggested earlier,^{1b} that there is a mechanism of exchange which does not involve free radicals. Hanrahan⁸ found that, with concentrations of iodine of about $2 \times 10^{-3} M$, the ratio of G exchange to G of free radical production, as determined by the maximum and minimum rates in the presence of added HI and I_2 , is greater than 1 for each of seven alkyl iodides tested. The ratios obtained were: methyl iodide, 1.64; ethyl iodide, 1.21; *n*-propyl iodide, 1.64; isopropyl iodide, 1.75; *n*-butyl iodide, 1.34; isobutyl iodide, 1.61; *sec*-butyl iodide, 2.12. We have carried out two irradiations in which radioiodine as I_2 was added to the bromobenzene prior to exposure. The G -values for incorporation of iodine were 4.8 and 4.6 equiv./100 e.v. absorbed, I_2 concentrations being 0.063 and 0.031 M , respectively. As in the case of the radiobromine, these are higher than the G of radical formation estimated from maximum and minimum rates, but it is of interest that the apparent non-radical reaction of bromobenzene with iodine has a lower efficiency than the reaction with bromine. This possibly may be because iodine atoms formed in the exchange step ($C_6H_5 + I_2 \rightarrow C_6H_5I + I$) have lower probability of abstracting an H or Br atom from another molecule than do bromine atoms.

(8) R. J. Hanrahan, Ph.D. thesis, Univ. of Wisconsin 1957, p. 148, "Mechanism of the Radiolysis of Alkyl Iodides," available from University Microfilms, Ann Arbor, Michigan.

Organic Products and Hydrogen.—To determine the predominant free radicals present in bromobenzene during radiolysis, a 0.1-ml. sample of the compound containing 0.04 M bromine labeled with Br^{82} was radiolyzed with a dose of 4×10^{20} e.v. g^{-1} and then passed through a gas chromatography column with the effluent monitored by a scintillation crystal. A large peak corresponding to bromobenzene was observed and a second peak, which was a double peak, corresponded to the three isomers of dibromobenzene. The total area of the double peak was only a few per cent. of the bromobenzene peak, indicating that most of the radicals produced in the system are phenyl radicals.

Table I shows the results of the chromatographic analyses of nine different samples of bromobenzene, four of which were irradiated at room temperature with no additive, three at room temperature with 0.1 mole/l. of Br_2 added before irradiation, and two irradiated at 100° with no additive. The results obtained from the several samples at each condition have been averaged before calculating the G -values of Table I. In each case the radiation dosage was 13.6×10^{20} e.v. g^{-1} . The average bromine concentration during the run with no additives was about $5 \times 10^{-3} M$. Concentrations even much lower than this would be sufficient to prevent essentially all intertrack reaction of free radicals and probably most interspur reactions, so the products observed may be assumed to be formed either by hot reactions or by a combination of radicals formed within the same spur. A possible exception is $C_6H_4Br_2$, which might be formed by reaction of a diffusing C_6H_4Br radical with a bromine molecule. The apparent activation energies are lower even than those normally associated with diffusion. It is interesting that this is true even for C_6H_6 , which may be formed in part by reaction of phenyl radicals with HBr competing with Br_2 . The decreased G -values (except for $C_6H_4Br_2$) for the experiments with added bromine must be due to interference of the bromine with intraspur reactions, the bromine here being present at the high concentration of 1 mole %. It would be of interest to know whether the decreased value for the bromobiphenyls in the experiments with added bromine is exactly balanced by an increase in $C_6H_4Br_2$. The experimental data of Table I probably are not sufficiently accurate to preclude the existence of such a balance. Irradiation of a 0.5-ml. sample of bromobenzene to a dose of 13×10^{20} e.v. g^{-1} produced sufficient gas non-condensable in liquid air for a pressure-volume measurement. This gas was identified mass spectrometrically as hydrogen and the G -value was calculated to be 6×10^{-3} . The same G -value was obtained from the area of the negative peaks produced on gas chromatograms by the hydrogen. In order to measure the production of hydrogen for shorter irradiations, a 5-ml. sample was exposed to 1.1×10^{20} e.v. g^{-1} . No hydrogen was found, suggesting that the G -value increases with dose, *i.e.*, with the presence of some product of the irradiation in the solution. Another 5-ml. sample was given an identical 1.1×10^{20} e.v. g^{-1} irradiation except that it contained 0.06 M dissolved HBr . $G-H_2$ was 0.033, suggesting that hydrogen may be

formed by H atoms reacting with HBr in competition with their reaction with Br₂. The possibility cannot be precluded, however, that the increase is the result of direct energy absorption by the HBr.

TABLE I

ORGANIC PRODUCTS OF THE RADIOLYSIS OF BROMOBENZENE

	G-values C ₆ H ₅ Br + 0.1 mole/l. of Br ₂ room temp.		Apparent E _{act.} kcal./ mole	
	C ₆ H ₅ Br 25°	C ₆ H ₅ Br 100°	C ₆ H ₅ Br 100°	
C ₆ H ₆	1.5	0.72	1.7	0.5
C ₆ H ₄ Br ₂	0.36	.53	0.42	.5
C ₆ H ₅ C ₆ H ₅	.25	.21	.29	.4
<i>o</i> -BrC ₆ H ₄ C ₆ H ₅	.52	.29	.64	.6
<i>p</i> -BrC ₆ H ₄ C ₆ H ₅	.32	.27	.41	.7

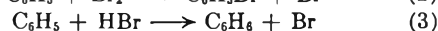
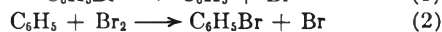
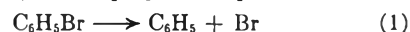
Temperature Coefficients.—As noted above the G-values for the production of organic products are only slightly different at 100° than at 25°. Single experiments on the radiolysis of bromobenzene without additives have indicated that the maximum $G(\text{Br}_2)$ at 100° is 1.4, that the initial $G(\text{HBr})$ at 100° is 1.3, and that the initial $G(\text{exchange})$ at 100° is 11. The corresponding values at room temperature are 0.6, 0.4, and 6 and the corresponding apparent activation energies 2.4, 3.4, and 1.7. Although these must be considered as only approximate values in view of the limited data they do show that all of the activation energies are low and that there are not any important thermal reaction steps of intermediates which have an activation energy greatly different from other steps competing for the same species. These activation energies are in the range normally associated with diffusion and are similar to those observed for the production of bromine in the radiolysis of CCl₃Br⁹ and for the production of iodine in the radiolysis of ethyl iodide.^{1a}

Other Tests.—To determine whether the radiolysis of bromobenzene is affected by small amounts of oxygen, an irradiation was done in the presence of 53 mm. pressure of added O₂. If the solubility of oxygen in bromobenzene is similar to that in ethyl iodide the concentration of dissolved oxygen was slightly under 10⁻³ M. The observed rate of bromine production was almost indistinguishable from that in the absence of oxygen. The data suggest that possibly there was less induction period than shown by the data of Fig. 1.

A single experiment was made in which *p*-dibromobenzene was added at a concentration of 10⁻³ M before irradiation of bromobenzene. The rate of bromine production was indistinguishable from that in experiments where there was no additive.

Mechanism.—The radiolysis of bromobenzene is similar to the radiolysis^{1b} and photolysis^{2b} of ethyl iodide in that both hydrogen halide and free halogen are produced and that these seem to compete with each other for free radicals, the predominant radical being the organic group initially combined with the halogen atom. The yield of bromine is increased by the presence of added hydrogen bromide and the yield of hydrogen bromide is

increased by added bromine, as would be expected if reactions 1, 2, and 3 play an important role.



Because of the unexplained induction period, because of the gradually decreasing G-values for both hydrogen halide and halogen as a function of dose, and because there are some deficiencies in material balances, it would be premature to attempt a rigorous quantitative correlation of the intermediate steps in this radiolysis. A very rough estimate of the ratio $k_{\text{Br}_2}/k_{\text{HBr}}$ involving the rate constants for the reactions of phenyl radicals with bromine molecules and of phenyl radicals with HBr molecules may, however, be made from the relationship^{1b}

$$\frac{k_{\text{HBr}} [\text{HBr}]}{k_{\text{Br}_2} [\text{Br}_2]} = \frac{(G(\text{Br}_2)_{\text{normal}} - G(\text{Br}_2)_{\text{min.}})}{(G(\text{Br}_2)_{\text{max.}} - G(\text{Br}_2)_{\text{normal}})} = \frac{0.6 - (-0.4)}{(2.8 - 0.6)} = \sim 0.5 = \frac{k_{\text{HBr}} G(\text{HBr})}{k_{\text{Br}_2} G(\text{Br}_2)}; \quad \frac{k_{\text{HBr}}}{k_{\text{Br}_2}} = 0.7$$

$(G(\text{Br}_2)_{\text{normal}} - G(\text{Br}_2)_{\text{min.}})$ is the $G(\text{Br}_2)$ in bromobenzene without additives which results from the reaction $\text{C}_6\text{H}_5 + \text{HBr} \rightarrow \text{C}_6\text{H}_6 + \text{Br}$, it being remembered that an additional Br atom has been liberated in forming C₃H₆. $(G(\text{Br}_2)_{\text{max.}} - G(\text{Br}_2)_{\text{normal}})$ is the G of the reaction $\text{C}_6\text{H}_5 + \text{Br}_2 \rightarrow \text{C}_6\text{H}_5\text{Br} + \text{Br}$, it being remembered that $G(\text{Br}_2)_{\text{max.}}$ was determined by using an excess of HBr which yields one Br₂ molecule per C₆H₅ radical consumed. The value obtained is 0.7, which, as would be expected, is the same order of magnitude as the value of unity for the corresponding ratio $k_{\text{HI}}/k_{\text{I}_2}$ for the reactions of ethyl radicals with HI and I₂ in the radiolysis^{1b} and photolysis^{2b} of ethyl iodide.

The G-value for exchange of radiobromine is 6. As indicated earlier this is greater than the G for the production of thermal radicals as determined from the maximum and minimum rates with additives, suggesting a contribution to exchange by a non-radical mechanism similar to that which has been observed with the alkyl iodides.^{1b,8} In ethyl iodide it has been found that this non-radical mechanism is peculiar to the radiolysis and is not available in the photolysis.^{2b} Phenyl radicals are formed by reaction 1 and probably also in part by the abstraction of bromine atoms from bromobenzene by hot bromine atoms formed in reaction 1. The G for thermal radical production is about 3.4 and therefore that for non-radical exchange is about 2.7. The total G for conversion of bromobenzene to other organic compounds in the presence of 0.1 M Br₂ (Table I) is about 2.8, so that the total G for all reactions including exchange is about 9.

C₆H₆, C₆H₄Br₂, C₆H₅C₆H₅, and C₆H₅C₆H₄Br all are formed primarily by hot processes. This is shown by the fact that they all are formed with significant G in solutions of bromobenzene where the average bromine concentration as a result of irradiation is 10⁻² M, and further is confirmed by the fact that the G still is significant in solutions with 0.1 M bromine added before irradiation. These processes either may be bimolecular reactions between an excited molecule and a normal molecule or may involve bond rupture followed by reaction of a hot radical with an adjacent molecule.

(9) R. F. Firestone and J. E. Willard, *J. Am. Chem. Soc.*, **83**, 3551 (1961).

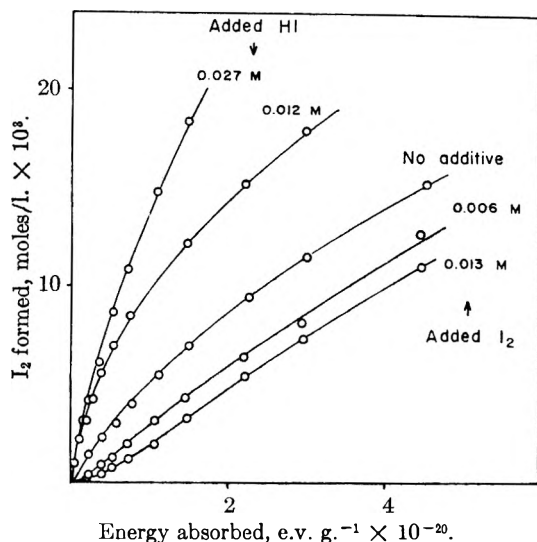


Fig. 4.—Iodine production as a function of radiation dose during the radiolysis of C_6H_5I with and without added HI and I_2 .

Additional evidence that bromobiphenyl and biphenyl are not formed as a result of encounters of thermal radicals is given by the fact that the G of biphenyl is less than 1/3 that of bromobiphenyl, even though phenyl radicals are known to be produced in much greater concentration in the solution than are C_6H_4Br radicals. The decrease in bromobiphenyl in the presence of 0.1 M Br_2 , which is a high enough concentration to cause some interference with intraspur processes, is accompanied by an increase in $C_6H_4Br_2$, as would be expected. The production of $C_6H_4Br_2$ at low bromine concentrations in all probability results from the production of C_6H_4Br radicals either by direct splitting of a hydrogen atom from an activated molecule or by abstraction of a hydrogen atom by a hot bromine atom.

It is, of course, impossible to preclude the possibility that ion-molecule reactions or electron attachment reactions contribute to the observed yields. They do not seem to be required to explain the results. In the analogous radiolysis of ethyl iodide the HI and I_2 have been found to compete for ethyl radicals on the same quantitative basis as in the photolysis of ethyl iodide, where no ions can be formed.^{1b,2b}

Iodobenzene

Table II summarizes the G -values obtained in the radiolysis of iodobenzene and Fig. 4 shows the production of iodine as a function of radiation dose both in the presence and absence of added HI and I_2 . In a very qualitative sense the results are similar to those for bromobenzene. Among the differences is the fact that even in the presence of added iodine, HI production is only a few per cent. as great as that of the other products whereas HBr production from bromobenzene is similar to that of the other products. This difference may be due to the fact that bromine atoms can abstract hydrogen atoms from solvent molecules much more readily than can iodine atoms. Another difference is in the higher G for biphenyl and the lower G for the halobiphenyl (compare Tables I and II). The

fractional decrease in the yields of these two types of compounds when free halogen initially is present in the system is qualitatively the same. It may be noted also that there is no induction period for the production of iodine in iodobenzene, the initial slope of the curve for pure iodobenzene in Fig. 4 being greater than that for longer times of irradiation.

TABLE II
SUMMARY OF G -VALUES OBTAINED IN THE RADIOLYSIS OF $C_6H_5I^a$

	G -values at 25°			G -values at 100°	Apparent $E_{act.}$ kcal./mole
	No additive	Added I_2	Added HI		
H_2	0.004	
HI	.008	0.006 ^b			
I_2	.79 (2.0)	(.4) ^c	(6.0) ^d	(3.0)	(1)
C_6H_6	.43	.32 ^e		0.78	2
$C_6H_5C_6H_5$.49	.22 ^e		.59	1
$C_6H_4I_2$.43	.39 ^e		.84	2
$C_6H_5C_6H_4I$.25	.13 ^e		.57	2
Radioiodine		(4.1), (4.6) ^f		(6.3) ^g	(1)

"exchange"

^a The G -values given are the average values at a dose of approximately 13×10^{20} e.v. g^{-1} , except for the values in parentheses, which are for a dose of about 1.5×10^{19} e.v. g^{-1} . ^b 0.013 M added I_2 . ^c 0.006 and 0.013 M added I_2 . ^d 0.012 and 0.027 M added HI, both gave the same result. ^e 0.1 M added I_2 . ^f 0.013 and 0.055 M added I_2 , respectively. Expressed as equivalents/100 e.v. ^g 0.02 M added I_2 .

It is important to note in considering the data of Table II that the G -values are a function of iodine concentration and therefore presumably would be somewhat different for different dosages.

Mechanism.—As with bromobenzene and with the alkyl iodides, $G(X_2)$ for iodobenzene is increased by added hydrogen halide and decreased by added halogen. The initial G -values with added HI appear to be independent of the concentration of HI and those with added I_2 independent of the concentration of I_2 . This suggests, as in the analogous systems studied, that HI and I_2 compete for free radicals. Since $G(HI)$ is 1% or less of $G(I_2)$ and is not increased by the addition of I_2 , it cannot be an important competitor for radicals in the system without HI added. However, there must be some reaction which competes with I_2 for radicals since $G(I_2)$ is lowered considerably by the presence of initially added I_2 at a concentration as low as 0.01 M . The most probable competition appears to be radical-radical combination. In subsequent work in this system it would be desirable to determine, if possible, the G -values for biphenyl and iodobiphenyl for very short irradiations in which the iodine concentration had not had opportunity to build up as high as in the irradiations reported in Table II. It is, however, surprising if radical-radical reactions can compete with radical-iodine reactions when measurable concentrations of iodine have been built up in the solutions. The existence of such reactions would imply that the ratio of the rate constant for reaction of phenyl radicals with iodine molecules to that for radical-radical combination is much lower than that for the analogous ratio in alkyl iodide systems since no curvature in

the iodine production curve such as that observed for iodobenzene was found for ethyl iodide and several other alkyl iodides.^{1a,1b} As with the bromobenzene, the very small effect of temperature on G -values for the products of the radiolysis of iodobenzene indicates that they are formed by hot processes utilizing the energy from the radiation or by low activation energy processes such as radical-radical combination. The fact that a substantial fraction of the yield of each of the organic products remains even for radiations carried out in the presence of 0.1 M iodine indicates that these are formed in large part by reactions which do not involve thermal radicals.

The difference between the minimum $G(I_2)$ obtained with added iodine and the maximum $G(I_2)$ obtained with added HI should be equal to the rate of production of thermal free radicals which escape their parent spurs according to the mechanisms discussed for bromobenzene and earlier for the alkyl halides.^{1b} This value of 5.6 is somewhat in excess of the G -values of 4.1 and 4.6 obtained for the exchange at iodine concentrations of 0.013 and 0.055 M , respectively.

Chlorobenzene

The G -values obtained in the radiolysis of chlorobenzene are summarized in Table III. Inspection of Table III shows immediately that the yield of simple chlorine containing product molecules is insufficient to give a material balance for chlorine. For such a material balance this equation should hold

$$2G(Cl_2) + G(HCl) + G(C_6H_4Cl_2) = G(C_6H_6) + 2G(C_6H_5C_6H_5) + G(C_6H_5C_6H_4Cl)$$

Using the values of Table III the left side of the equation totals 0.6 while the right side totals 4.0. The material balance relationship which should hold for hydrogen is $2G(H_2) + G(HCl) + G(C_6H_6) = G(C_6H_4Cl_2) + G(C_6H_5C_6H_4Cl)$. Again there is a discrepancy, the left side totaling 3.2 and the right side 1.3. It was noticed that when irradiated chlorobenzene was allowed to evaporate a non-volatile residue remained. This residue was quantitatively collected (77 mg.) from the irradiation of a 5-ml. sample of chlorobenzene with a dose of 14×10^{20} e.v. g^{-1} . Analysis by a commercial laboratory indicated that the C:H:Cl ratio was 6:4.62:1.30. From these data it could be calculated that the non-volatile residue was formed with a G -value of 4.9 phenyl groups used per 100 e.v. absorbed, the G -value for incorporation of chlorine in excess of the normal chlorine-carbon ratio in chlorobenzene was 1.5, and the G for deficiency of hydrogen was 1.9. If the 1.9 is added to the 1.3 for the right side of the hydrogen material balance equation it equals 3.2, which is the value for the left side. The added G of 1.5 for chlorine plus the original 0.6 gives a value of 2.1, which still is much short of the 4.0 needed for material balance.

When chlorobenzene containing 0.13 mole/l. of I_2 was irradiated to a dose of 1.5×10^{20} e.v. g^{-1} , the iodine concentration decreased nearly linearly as indicated by spectrophotometric measurements at 5050 Å. The initial G -value for iodine disappearance was 6.1 equiv./100 e.v. This decreases slightly over the dosage range indicated. Under nearly the

TABLE III
SUMMARY OF G -VALUES OBTAINED IN THE RADIOLYSIS OF CHLOROBENZENE^a

	G -value at 25°		G -value at 100°	$F_{act.}$ kcal./mole
	No additive	Added I_2^b		
H ₂	0.01			
Cl ₂	.006			
HCl	.25		0.72	3
C ₆ H ₆	2.9	0.46	3.6	1
C ₆ H ₄ Cl ₂	0.36	... ^c	0.49	1
C ₆ H ₅ C ₆ H ₅	.12	0.05	0.15	1
C ₆ H ₅ C ₆ H ₄ Cl	.90	0.16	1.8	2
C ₆ H ₅ I		3.3		
C ₆ H ₄ ICl		0.18		
Non-volatile product		4.9 ^e		
Radioiodine "exchange"		(4.5, 3.7) ^d		
Iodine consumption		(6.1) ^d		

^a G -values are the average values at a dose of about 14×10^{20} e.v. g^{-1} except for the exchange and iodine consumption experiments where doses in the range of 1×10^{19} to 1×10^{20} e.v. g^{-1} were used. $G(HCl)$ decreases slowly with increasing dose from 4 to 40×10^{20} e.v. g^{-1} . ^b 0.1 M except for the exchange experiments (0.04 and 0.02 M , respectively) and the iodine consumption experiment (0.013 M). ^c No peak was observed, presumably due to the superposition of a fairly large peak of C₆H₅I. ^d Expressed as equivalents/100 e.v. ^e C₆H_{4.62}Cl_{1.30} units/100 e.v.

same conditions the G -values of 4.5 and 3.7 equivalents were obtained for entrance of radioiodine into organic combination. These data indicate that some iodine is being converted to an inorganic species which does not absorb as strongly at 5050 Å. as does I_2 . It may be estimated from information in the literature that the absorbancy index¹⁰ of iodine-chloride at 5050 Å. is about 20% of that of an equal number of iodine atoms as I_2 . It appears possible that a part or all of the difference between the iodine consumption yield and the radioiodine organic yield is due to ICl formation.

Mechanism.—Because of the ease with which chlorine atoms abstract hydrogen it was expected that the chlorine yield from chlorobenzene would be very low. It might have been expected, however, that the HCl yield would be equivalent to the yield of phenyl groups incorporated in benzene and other molecules from which chlorine had been eliminated. The largest G for a reaction involving chlorine is for its appearance in the non-volatile material with a G of 1.5 equivalents/100 e.v. in excess of the chlorine ratio in C₆H₅Cl. Assuming that the commercial analysis of C₆H_{4.62}Cl_{1.3} for this material is correct, ring rupture must be involved in its formation.

The effect of added iodine on the yields of benzene and chlorobiphenyl is to cause a much greater fractional drop than is caused by added iodine in bromo- or iodobenzene. This may be because the chlorobenzene system does not produce free halogen which can cause "self-scavenging" in the absence of added scavengers.

Metastable Species

Figure 5 shows absorption spectra of bromobenzene taken before exposure to γ -radiation, immedi-

(10) (a) A. I. Popov and E. H. Schmor, *J. Am. Chem. Soc.*, **74**, 4672 (1952); (b) R. E. Buckles and J. F. Mills, *ibid.*, **76**, 4845 (1954).

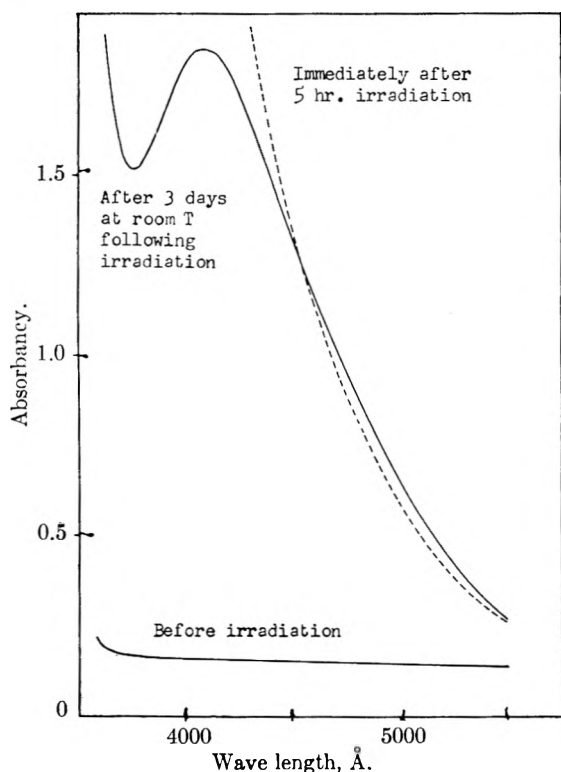


Fig. 5.—Evidence of metastable species formed during radiolysis of C_6H_5Br .

ately after exposure to 4×10^{20} e.v. g.⁻¹, and after a subsequent period of 59 hr. standing at room temperature. The curve taken after the standing period is typical of the absorption spectrum of bromine dissolved in benzene. It shows an absorption maximum at 4120 Å. which falls to a minimum at 3750 Å. before rising at shorter wave lengths due to the absorption of bromobenzene itself. Freshly irradiated bromobenzene, however, shows a continuous increase in absorption at wave lengths below 5500 Å., with a new highly absorbing species obscuring the maximum and minimum of bromine. When an irradiated solution is allowed to stand in the dark at room temperature for a day or so, the absorbancy in the region of 3700 to 4200 decreases greatly and the maximum and minimum of bromine begin to show. After several days standing the absorption becomes identical with that obtained by dissolving bromine in bromobenzene. Heating of a freshly irradiated solution at 90° for a few minutes causes the spectrum of a freshly irradiated solution to change immediately to that of bromine in bromobenzene. A similar effect is observed in radiolyzed iodobenzene but not in chlorobenzene.

When the metastable species indicated by the above observations is decomposed there is always an increase in absorbancy at wave lengths where the only absorbing species appears to be Br_2 . If it is assumed that the number of moles of bromine produced by decomposition of the metastable species (calculated from the increase in absorbancy at 5000 Å.) is equal to the number of moles of the metastable species present before decomposition, the absorbancy index of the metastable species at 3750 Å. is about 3×10^3 . On the basis of these

considerations estimates of G -values for the production of the species may be made from experimentally determined plots of the increasing absorbancy of the species as a function of radiation dose. These plots are smooth curves which indicate that in the range from 0 to 4×10^{20} e.v. absorbed per g. the G (metastable species) increases with increasing dose in bromobenzene and in bromobenzene containing 0.06 M HBr but that it decreases with dose for bromobenzene which initially contains 0.04 M Br_2 . Table IV gives estimated G -values made from the plots. The results suggest that production of the metastable species may be increased by the presence of bromine.

TABLE IV
ESTIMATED G -VALUES FOR PRODUCTION OF THE METASTABLE SPECIES

Initial conditions	Differential G	
	At 0.3×10^{20} e.v. g. ⁻¹ absorbed	At 3×10^{20} e.v. g. ⁻¹ absorbed
No additive	0.04	0.1
0.06 M HBr	0.1	0.3
0.04 M Br_2	0.6	0.3

Rate measurements on the decay of the metastable species at room temperature always give straight line plots for the log of the concentration of the species against time, indicating that the decay is first order in the concentration of the species. The first-order rate constants for three determinations of the rate of decomposition all fell in the range 0.1 ± 0.04 /hr. for the three solutions of Table IV, each of which received 4×10^{20} e.v. g.⁻¹.

Other properties of the metastable species include the following. The spectrum was not changed by opening the reaction cell to air. The absorption due to the species disappeared when the irradiated bromobenzene was washed with water and dried by passing through a magnesium sulfate column, but was only slightly reduced when the bromobenzene was washed with water and centrifuged without use of magnesium sulfate. There appeared to be no decrease in the species in iodobenzene as a result of washing with water. When 0.2 ml. of bromobenzene was irradiated with γ -rays long enough to produce an estimated 10^{17} molecules of the metastable species, the solution gave no electron paramagnetic resonance spectrum when examined under conditions when normally 10^{16} unpaired electrons might have been expected to give a pronounced signal.

In order to determine whether the metastable species could be formed by producing bromine atoms in a solution of bromine in bromobenzene, such a solution (0.4 M) was examined spectrophotometrically at hourly intervals during an intense 3-hr. illumination with visible light. During this time the absorbancy due to bromine decreased approximately equally at all wave lengths; that at 4120 Å., the maximum of bromine absorption, dropping from about 1.2 to 0.4. There was no evidence of production of a species which absorbed at 3750 Å., as does the metastable species. The illumination was carried out in a Beckman type spectrophotometer cell thermostated at 25° and exposed to a 1000-watt lamp through a copper sulfate filter and lens system.

Solutions of iodine in iodobenzene showed an absorbancy maximum at 4920 Å. and a minimum at 4200 Å. As with bromobenzene, these features were obscured in irradiated solutions by the absorbancy due to the metastable species and when the latter decomposed the iodine concentration as indicated by the absorbancy at longer wave lengths increased. After correction for I₂ produced, the increase in absorbancy at 4200 Å., due to the meta-

stable species in iodobenzene is linear with dose, in contrast to the autocatalytic effect observed with bromobenzene.

Acknowledgment.—This work was supported in part by the United States Atomic Energy Commission (Contract AT(11-1)-32) and in part by the University Research Committee with funds made available by the Wisconsin Alumni Research Foundation.

THE KINETICS OF HYDROGEN ATOM RECOMBINATION ON PYREX GLASS AND FUSED QUARTZ¹

BY BERNARD J. WOOD AND HENRY WISE

Division of Chemical Physics, Stanford Research Institute, Menlo Park, California

Received November 21, 1961

The heterogeneous recombination rate of hydrogen atoms on Pyrex glass and fused quartz has been evaluated as a function of temperature in the range from 77 to 1123°K. At room temperature and above, the catalytic activities of fused quartz and Pyrex for this reaction are comparable. A transition from first- to second-order kinetics, with respect to hydrogen atom concentration, occurs at temperatures >500 and also at temperatures <120°K. The experimental data are interpreted on the basis of two-state adsorption at low temperatures with different binding energies for the respective adsorbed states.

The wide use of Pyrex glass and fused quartz apparatus in experimental studies involving atomic hydrogen makes desirable a detailed understanding of the catalytic properties of these materials. The heterogeneous recombination of hydrogen atoms on glass has been investigated in the past,^{2,3} but the kinetic data reported did not permit a detailed analysis of the mechanism of interaction between the gaseous atomic species and the solid surface. We have investigated the rate of formation of molecular hydrogen resulting from heterogeneous atom recombination on surfaces of these materials over a broad range of temperatures.

Theoretical Analysis.—In our measurements, hydrogen atoms from an electrodeless discharge diffuse into a closed cylindrical Pyrex or fused-quartz tube, where they recombine on the wall and on the closure of the tube. By means of a catalytically active filament which approximates the closure and which can be moved axially along the tube, the relative residual atom concentration at the closed ends of tubes of various lengths is determined.³

Evaluation of the catalytic efficiency of the tube wall is based on a mathematical analysis of a model in which the removal of atoms by heterogeneous reaction is balanced by their diffusion from an atom source of constant intensity. The steady-state balance of the number of active particles n entering and leaving an arbitrary volume in a cylindrically symmetrical system is given by

$$D[\partial^2 n/\partial r^2 + (1/r)(\partial n/\partial r) + \partial^2 n/\partial x^2] = 0 \quad (1)$$

with D the diffusion coefficient, r the radial, and x the axial coordinate. At the source, *i.e.*, $x = 0$, the atom density has a uniform value

$$n(r,0) = n_0 \quad (2)$$

and no radial density gradient is exhibited at the axis of the cylinder, so that

$$\partial n/\partial r(0,x) = 0 \quad (3)$$

The catalytic activity of the cylinder wall at $r = R$ and that of the end plate located at a distance $x = L$ from the atom source are specified by additional boundary conditions. For the end plate on whose surface atom recombination takes place by a first-order mechanism

$$(\partial n/\partial x)(r,L) = -[n(r,L) k_1 R/2D] = -n(r,L)/\delta' R \quad (4)$$

On the cylinder wall

$$(\partial n/\partial r)(R,x) = -[n(R,x) k_1 R/2D] = -n(R,x)/\delta R \quad (5)$$

for a first-order heterogeneous process, and

$$(\partial n/\partial r)(R,x) = -[n^2(R,x) k_2 R/D] \quad (6)$$

for a second-order heterogeneous reaction. The symbols k_1 and k_2 represent the first- and second-order rate constants with respect to hydrogen atoms, and the dimensionless parameter δ is defined

$$\delta \equiv 2D/k_1 R^2 \text{ and } \delta' \equiv 2D/k_1' R^2$$

For the first-order reaction, boundary conditions (2) through (5) yield an analytic solution^{4,5} to eq. 1 giving the average concentration of atoms at the catalytically active closure located at $x = L$

$$(\bar{n}/n_0)_L = 4 \sum_{i=1}^{\infty} \delta' / \{ \alpha_i (1 + \delta^2 \alpha_i^2) [\sinh \alpha_i (L/R) + \delta' \alpha_i \cosh \alpha_i (L/R)] \} \quad (7)$$

In this solution the α_i 's are determined as roots of the equation $J_0(\alpha_i) = \delta \alpha_i J_1(\alpha_i)$ where J_0 and J_1 represent Bessel functions of the first kind.

For the case of second-order atom recombination⁶ on the cylinder wall, boundary condition (6), the

(1) This work was supported by Project Squid, Office of Naval Research, Department of the Navy.

(2) (a) W. V. Smith, *J. Chem. Phys.*, **11**, 110 (1943); (b) K. Tsu and M. Boudart, "International Catalysis Congress," Paris, 1960, paper No. 23.

(3) B. J. Wood and H. Wise, *J. Phys. Chem.*, **65**, 1976 (1961).

(4) H. Wise and C. M. Ablow, *J. Chem. Phys.*, **29**, 634 (1958).

(5) H. Motz and H. Wise, *ibid.*, **32**, 1893 (1960).

(6) A more detailed derivation is to be found in a forthcoming publication.

solution for the average atom density at $x = L$ becomes

$$(\bar{n}/n_0)_L = \delta' / (\delta' + U) - \sum_{i=1}^{\infty} [2B_i I_1(\beta_i) \sin \beta_i U] / \beta_i \quad (8)$$

where the β_i 's are roots of the function $\beta \delta' \cos \beta U = -\sin \beta U$, I_1 represents a Bessel function of the first kind for imaginary arguments, U , the dimensionless distance $\bar{U} = L/R$, and

$$B_i = \frac{2 \left\langle 1 + (\cos \beta_i U) - \left[2 + \left\{ (\beta_i U)^2 \left(1 + \frac{2\delta'}{\bar{U}} \right) - 2 \right\} \cos(\beta_i U) \right] \right\rangle [(\beta_i U)^{-2} \left(1 + \frac{\delta'}{\bar{U}} \right)^{-2}]}{\beta_i (\beta_i U) I_1(\beta_i) [1 + (\delta'/U) \cos^2(\beta_i U)]} \quad (9)$$

The first term on the right-hand side of eq. 8 is identical with that derived from the atom concentration profile in a cylinder of finite length with a non-catalytic wall⁴; the second term modifies the concentration profile as a result of a second-order wall reaction. Under these conditions the relative atom density at a given cross section in the cylinder no longer is independent of the absolute atom concentration at the source, n_0 . By means of this theoretical analysis the kinetics of the surface recombination reaction may be evaluated from measurements of the variation of atom density with distance, and the order of the reaction from its dependence on the absolute atom concentration at the source.

Experimental Details

A detailed description of the apparatus and technique employed in this study is contained in a previous publication.³

The results presented here are derived from experiments in four different discharge tubes and side arms with filament probes of various metals (such as Ni, Pt, W) simulating the end plate of a cylinder of variable length, and total gas pressures in the range of 30–80 μ , a pressure region where three-body gas phase reaction makes a negligible contribution to atom removal. The Pyrex discharge tubes³ were washed with chromic acid cleaning solution and rinsed thoroughly with distilled water before use. One of these, during the course of the experiments, was washed with concentrated nitric acid, then rinsed with distilled water. The quartz tube was given this latter treatment prior to its incorporation in the vacuum line. In these experiments the mode of pretreatment did not affect the catalytic activity of the surface, nor did the surface of any tube exhibit change of activity with time. Temperature control of the glass tube over the observed range of temperature was achieved with the techniques listed in Table I.

TABLE I

TEMPERATURE CONTROL OF PYREX AND QUARTZ TUBES

Temp., °K.	Mode of control
300–1123	Tube furnace with appropriately shunted segmented heating units to provide a uniform axial temperature profile
280–300	Tap water circulating through jacket on tube
210–240	Methanol circulated through copper coil immersed in Dry Ice–methanol bath, then through jacket on tube
120	Dry nitrogen blown through copper coil immersed in liquid nitrogen, then through insulated jacket on tube
77	Jacket on tube filled with liquid nitrogen

Results

For heterogeneous reactions, such as the recombination of atoms on a solid surface, it is convenient

to express the efficiency of the rate process in terms of a recombination coefficient, γ , defined as the fraction of atoms striking the surface which recombine. It follows from kinetic theory that when the rate of recombination on the wall of a tube is first order with respect to atom concentration, and mass transport to and from the surface is purely diffusional

$$\gamma_1 = 2k_1 R / \bar{c} \quad (10)$$

where \bar{c} is the mean atomic velocity.

Under similar conditions, but with atom removal at the surface governed by second-order kinetics, an atom concentration term, n , appears in the mathematical expression for the recombination efficiency, *viz.*

$$\gamma_2 = 2k_2 R n / \bar{c} \quad (11)$$

The kinetic order of the recombination reaction therefore was investigated by evaluating the dependence of the recombination coefficient on gaseous hydrogen atom concentration. In the temperature range (120–500°K.) in which the relative atom concentration profile in the tube remained independent of the atom concentration at the source, n_0 , γ_1 was evaluated directly by applying the first-order mathematical analysis³ (Table II). In temperature regions where the recombination coefficient demonstrated a dependence on source atom concentration (120°K. $> T >$ 500°K.), eq. 11 was employed to evaluate γ_2 in terms of $k_2 n_0$.

The results of such an analysis on data obtained at 77 and at 773°K. are shown, respectively, in Fig. 1 and 2. To derive values of k_2 from these data, the concentration of atoms at the source, n_0 , was estimated from the heat input to the filament located at the source.³ Assuming that each recombination on the surface involves a perfectly temperature-accommodated molecule, the concentration of atoms at the filament is

$$n_0 = 8(\Delta w) / [\gamma_1' A \bar{c} (\Delta H)]$$

where Δw is the heat input to the filament due to atom recombination, A is the geometric surface area of the filament, ΔH is the energy liberated per molecule of hydrogen formed, and γ_1' is the recombination coefficient of the surface. The actual atom density n_0 may be greater than the value derived from the measured energy transferred by the filaments, depending on the degree of energy accommodation by the solid; hence, the values of k_2 shown in Table II represent an upper limit in magnitude.

Discussion

For the surface formation of a hydrogen molecule from two hydrogen atoms two models have been postulated. One, the Rideal mechanism, involves the collision between a surface-adsorbed atom (S–H) and a gas atom, *i.e.*, $S-H + H \rightarrow S + H_2$. The second, the Hinshelwood mechanism, occurs when two surface-bound atoms recombine: $2(S-H) \rightarrow 2S + H_2$. Since either reaction path requires participation of adsorbed atoms, the rate of atom

TABLE I

AVERAGED EXPERIMENTAL VALUES OF RATE CONSTANT AND RECOMBINATION COEFFICIENT FOR THE RECOMBINATION OF HYDROGEN ATOMS ON THE WALL OF PYREX GLASS AND FUSED QUARTZ TUBES IN THE TEMPERATURE RANGE FROM 77 TO 1123°K.^c

Temp., °K.	Sur- face	First order		Second order	
		k_1 , sec. ⁻¹	γ_1	k_2 [(atoms/ cm. ³)sec.] ⁻¹	γ_2^a
77	Pyrex			3.1×10^{-12}	6.0×10^{-4}
119	Pyrex	3.2	5×10^{-3}		
209	Pyrex	1.6×10^2	2.0×10^{-3}		
238	Pyrex	1.5×10^2	1.7×10^{-3}		
294	Pyrex	5.7×10^2	5.8×10^{-3b}		
300	Quartz	2.8×10^2	2.8×10^{-3}		
345	Pyrex	5.2×10^2	5.0×10^{-3}		
370	Pyrex	8.7×10^2	8.0×10^{-3}		
416	Pyrex	6.6×10^2	5.5×10^{-3}		
476	Pyrex	1.7×10^3	1.4×10^{-2}		
527	Pyrex	1.3×10^3	9.6×10^{-3}		
773	Quartz			6.1×10^{-11}	3.7×10^{-4}
823	Quartz			5.5×10^{-11}	3.3×10^{-2}
1123	Quartz			0	0

^a Calculated from eq. 11 for $n_0 = 10^{14}$ atoms/cm.³, $R = 1.27$ cm. ^b Average value derived from 27 experiments in the pressure range 30 to 80 μ , with various atom densities and using a variety of probes. ^c An over-all accuracy of 50% is estimated for the values of γ reported.

recombination is sensitively dependent on the energies of the bonds between the adsorbate and the surface.

Recent work^{7,8} indicates the existence of two distinct binding states in the adsorption of atomic hydrogen on glass: a strongly chemisorbed state, and a weakly-bound state which becomes significantly populated at low temperatures. deBoer and van Steenis⁷ estimated, by empirical rules,⁹ the bond energies of these states to be, respectively, 44 and 5 kcal./g.-atom.¹⁰

On the basis of atom removal at a surface by the Hinshelwood and Rideal processes occurring in both adsorption states, a model may be constructed which permits over-all recombination coefficients to be calculated as a function of temperature. Briefly, the model^{7,11} specifies a steady-state condition in which the number of atoms incident on the surface is equal to the number which evaporate either as atoms or as molecules. The rates of the elementary evaporation and recombination processes are calculated on the basis of absolute rate theory. The effective recombination coefficient at a specified temperature then becomes

$$\gamma = \frac{[(v_R)_a + (v_R)_b + (v_H)_a + (v_H)_b]}{Z}$$

where Z is the collision frequency of surface-incident atoms, and the v terms represent the rate of removal of atoms by recombination per unit area of surface, the subscripts to which identify the reaction mechanism as Rideal, R, or Hinshelwood, H, and the respective adsorption state in which the reaction occurs as strongly-bound, a, or weakly-bound, b.

From such considerations the recombination

(7) J. H. deBoer and J. van Steenis, *Proc. Koninkl. Ned. Akad. Wetenschap.*, **55B**, 572 (1952).

(8) T. W. Hickmott, *J. Appl. Phys.*, **31**, 128 (1960).

(9) J. O. Hirschfelder, *J. Chem. Phys.*, **9**, 645 (1941).

(10) The latter heat includes a correction for a "roughness factor" of 2.

(11) J. H. deBoer, *Bull. soc. chim. Belges*, **67**, 284 (1958).

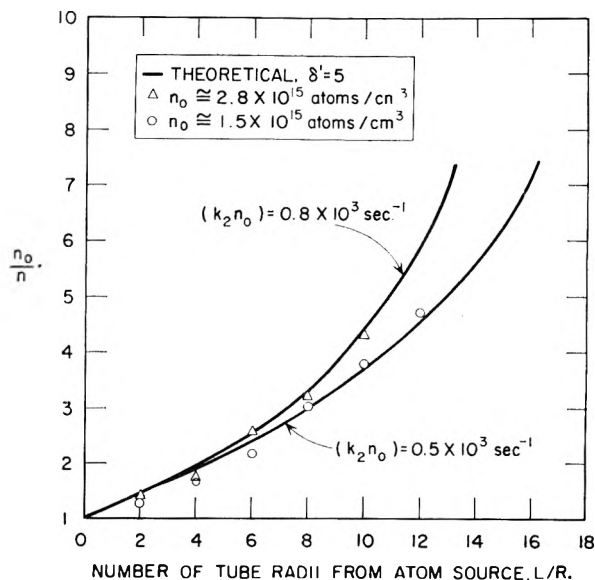


Fig. 1.—Analysis of hydrogen atom relative concentration profiles in Pyrex tube at $T = 77^\circ\text{K.}$, platinum probe.

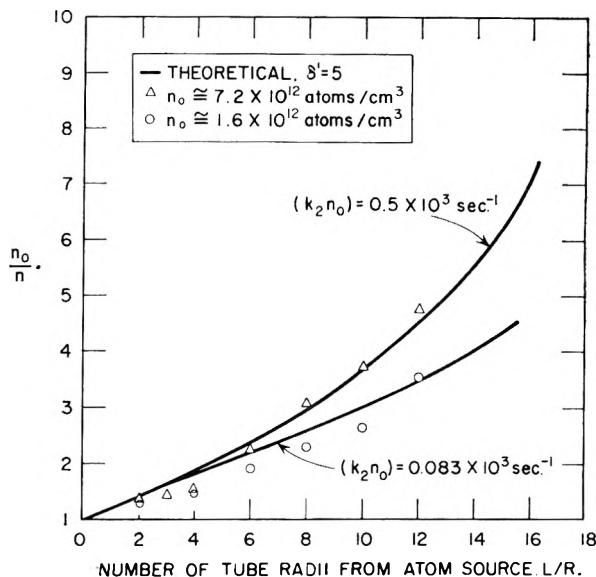


Fig. 2.—Analysis of hydrogen atom relative concentration profiles in quartz at $T = 773^\circ\text{K.}$, tungsten probe.

coefficient for hydrogen on glass would be expected to vary with temperature differently in four distinct, yet continuous, regimes. At high temperature where the strongly-bound state is incompletely occupied, the recombination process is due principally to collisions of atoms in this state as a result of surface diffusion $[(v_H)_a$ predominates]. At lower temperatures, the adsorption bond energy of the strongly-bound state is sufficient to keep the state fully occupied. Under such conditions, the recombination process will occur primarily by the reaction of gas-phase atoms colliding with adatoms to form hydrogen molecules $[(v_R)_a$ predominates]. Here the rate of surface collision and the rate of molecule production both are dependent on the gas atom population; hence the recombination coefficient will be independent of the degree of dissociation of the gas. The low temperature regime is distinguished by the presence of adatoms in the

TABLE III
CALCULATED RATES OF ELEMENTARY PROCESSES IN HYDROGEN ATOM RECOMBINATION ON GLASS

Gas-phase atom concn., atoms/cm. ³	Temp., °K.	Contribution of elementary rate processes, atoms/cm. ² sec.			
		$2SH \xrightarrow{(v_R)_a} 2S + H_2$ $E = 22.5 \text{ kcal./mole}$	$SH + H \xrightarrow{(v_R)_a} S + H_2$ $E = 2.25 \text{ kcal./mole}$	$2SH-H \xrightarrow{(v_R)_b} 2SH + H_2$ $E = 0.75 \text{ kcal./mole}$	$SH-H + H \xrightarrow{(v_R)_b} SH + H_2$ $E = 0.075 \text{ kcal./mole}$
10^{13}	500	3.0×10^{17}	5.4×10^{16}	~ 0	~ 0
	250	5.2×10^8	1.1×10^{16}	~ 0	~ 0
	120	2.6×10^{-17}	7.4×10^{12}	3.0×10^{11}	1.2×10^{10}
	77	6.4×10^{-43}	3.4×10^{10}	7.0×10^{13}	5.6×10^{12}
10^{14}	500	6.4×10^{17}	7.8×10^{16}	~ 0	~ 0
	250	5.2×10^8	1.1×10^{16}	~ 0	~ 0
	120	2.6×10^{-17}	7.4×10^{12}	3.0×10^{13}	1.2×10^{12}
	77	6.4×10^{-43}	3.4×10^{11}	7.0×10^{15}	5.4×10^{13}

Temp. range (°K.) of kinetic predominance →

>500	500-120	120-50	<50
------	---------	--------	-----

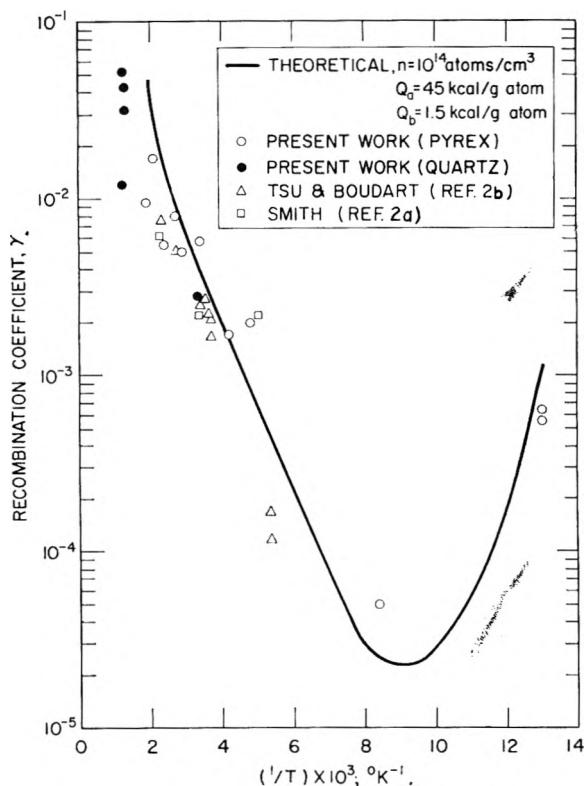


Fig. 3.—Temperature dependence of rate of hydrogen atom recombination on Pyrex glass and fused quartz surfaces. γ_2 calculated for $n = 10^{14}$ atoms/cm.³ from measured second-order rate constants.

weakly-bound state. This state becomes more heavily populated as the temperature is decreased and the predominant mode of molecule production again becomes adatom-adatom collisions, but now among atoms in the weakly-bound state $[(v_R)_b]$. As in the high temperature region, the recombination coefficient again becomes dependent on the gas-phase atom concentration, *i.e.*, a second-order reaction. When the weakly-bound state becomes nearly fully occupied, gas atom-adatom recombinations $[(v_R)_b]$ would be expected to predominate. It is apparent that at both temperature extremes the recombination coefficient approaches zero: at high temperature, because the residence time of the adatoms becomes too brief for successful encounters, and near the absolute zero because the

molecule formed does not possess sufficient energy to evaporate from the surface. Experimental evidence of such behavior at high temperature was observed (Table II, $T = 1123^\circ\text{K.}$).

The relative importance of each elementary recombination process predicted by this model is indicated quantitatively as a function of temperature and atom concentration in Table III. The activation energies, E , computed by means of Hirschfelder's rule,⁹ are based on a bond strength of $Q_a = 45 \text{ kcal./g.-atom}$ for the strongly-bound state and $Q_b = 1.5 \text{ kcal./g.-atom}$ for the weakly-bound state. The latter value is lower than that estimated by other investigators^{8,11}; however, it more closely fits our experimental results.

The temperature-dependence of the over-all recombination rate in terms of γ_1 and γ_2 is illustrated for a specific gas atom concentration $n = 10^{14} \text{ atoms cm.}^3$ in Fig. 3. The experimental points corresponding to $T > 500^\circ\text{K.}$ and $T < 120^\circ\text{K.}$ are calculated from eq. 11 using measured values of k_2 (Table II); in the temperature range from 120 to 500°K. the reaction is first order and γ_1 therefore is independent of gas atom concentration (eq. 10).

The work of other investigators has been examined on the basis of this model (Fig. 1). Smith's^{2a} experiments indicate that the efficiency of glass for hydrogen atom recombination exhibits a minimum at low temperatures, but the validity of his measurements may be questioned because of the presence of water vapor; also he ignored the effect of the probe on the atom concentration gradient in his tube. It is questionable whether at the lowest temperature employed by him (100°K.) an interpretation of the data on the basis of first-order analysis is applicable. We have re-evaluated his data obtained in the temperature range from 230 to 440°K. , by taking into account both radial and longitudinal diffusion of atoms in the tube¹² (*cf.* Fig. 3). Recently Tsu and Boudart^{2b} published the results of experiments in which they measured the hydrogen atom recombination coefficient of Pyrex glass in the tempera-

(12) Smith^{2a} appears to have made a computational error by attributing the length of his tube to be 300 cm. (see his Fig. 4). A tube of such length (nearly 10 ft.) is grossly unreasonable; a length of 300 mm. is more likely. Computing γ from his data on the basis of a 300 mm. tube gives values two orders of magnitude greater than those reported in his paper.

ture range from 190 to 440°K. These data are in substantial agreement with our measurements and our interpretation of the heterogeneous atom recombination process.

VISCOSITY BEHAVIOR OF THE SYSTEM POLYMETHYL ACRYLATE AND DIETHYL PHTHALATE OVER THE COMPLETE RANGE OF COMPOSITION

BY HIROSHI FUJITA¹ AND ETSUJI MAEKAWA

Physical Chemistry Laboratory, Department of Fisheries, Kyoto University, Maizuru, Japan

Received November 22, 1961

Viscosities, η , of solutions of a sample of polymethyl acrylate (PMA) in diethyl phthalate (DEP) were measured over the entire range of composition, *i.e.*, from 0 to 100% polymer, at a number of temperatures between about 20 and 110° by proper combination of capillary viscometers, a coaxial falling cylinder viscometer, and a tensile creep apparatus. The results conformed, in many respects, to those reported by previous investigators for other systems of amorphous polymer and organic diluent. Specifically, plots of $\log \eta$ against w_p , weight fraction of polymer, followed an S-shaped curve with its inflection point appearing, at all temperatures examined, in the region near $w_p = 0.6$. Neither the empirical relation $\log \eta \propto (w_p)^{1/2}$ nor $\eta \propto (w_p)^2$ was obeyed by the present data. It was found that the free volume equation for the viscosity of concentrated polymer solutions developed recently by Fujita and Kishimoto held over a fairly wide range of v_1 , volume fraction of DEP, at relatively low temperatures but over a very limited range ($v_1 < 0.1$) near $v_1 = 0$ at higher temperatures. Values of the parameters, $f(0, T)$, $\beta(T)$, and $\gamma(T)$, characterizing this viscosity equation were determined as functions of temperature, and their implication was discussed.

Introduction

Viscosity behavior of polymer solutions at high concentrations, especially in the region approaching the pure solid, has not yet been investigated extensively.² With the purpose of providing more experimental material to our knowledge on this subject we have determined, in this work, the viscosity of a sample of polymethyl acrylate in diethyl phthalate over the complete range of composition at a number of temperatures above the glass transition point of the polymer. The data obtained and their comparison with other systems are presented below. Recently, Fujita and Kishimoto³ have deduced a viscosity equation suited for concentrated solutions of long chain molecules by appropriate modification of the Doolittle free volume expression for the viscosity of simple liquids and illustrated its validity in terms of some available data on typical amorphous polymer-organic diluent systems. This viscosity equation will be subjected to further test with the present experimental data in order to obtain more information about its scope and limitation.

Experimental

Materials.—The polymethyl acrylate (designated as PMA) used in the present study was extracted from a commercial product, called Aron S-103, kindly furnished from the Toa Gosei Kagaku Co., Ltd. This contained about 40 wt. % of PMA in an unspecified solvent for industrial use. After it had been diluted with acetone to give about 2 wt. % concentration of PMA, the polymer was precipitated with the addition of water and then dried. The dry material again was dissolved in acetone, precipitated with water, and dried to a constant weight. No fractionation was effected because a great amount of material was needed to complete the entire viscosity measurement planned. The intrinsic viscosity of the purified polymer in acetone at 30°, measured in a viscometer of the Ubbelohde type with negligible kinetic energy correction, was 0.583 dl./g. (this yielded a value of 1.30×10^6 for the viscosity-average molecular weight when

use was made of the viscosity *vs.* molecular weight equation proposed by Takahashi, *et al.*, *Kogyo Kagaku Zasshi* (Japan), 60, 1059 (1957)). No reliable value was determined for the number-average molecular weight of the sample, since there occurred permeation of low-molecular-weight fractions through the semi-permeable membrane (du Pont cellophane 600) we used. The apparent specific volume V_p of the sample polymer, determined pycnometrically by using hexane as confining liquid over a range of temperature above 20°, followed the relation

$$V_p = 0.8165 + 5.60 \times 10^{-4} (\theta - 20) \quad (1)$$

where θ is the temperature.

The diethyl phthalate (designated as DEP) used as solvent or plasticizer was of technical grade and not purified further. Its apparent specific volume V_s , determined at a number of temperatures above 20°, was represented by the relation

$$V_s = 0.8932 + 6.75 \times 10^{-4} (\theta - 20) \quad (2)$$

When necessary, these relations for V_p and V_s were used to calculate the density of a given PMA-DEP mixture assuming no volume change on mixing. This assumption probably was good, because in this study we were concerned only with temperatures well above the glass transition point of the polymer in the dry state.

Preparation of Sample Solutions.—Viscosity measurements were made for 16 samples, which contained 0, 2.5, 5, 10, 20, 30, 40, 50, 60, 70, 75, 80, 85, 90, 95, and 100 % PMA by weight, respectively. Those containing less than 50 wt. % were prepared by sealing accurately weighed PMA and DEP in a flask and by heating the mixture mildly (at about 50–60°) until the polymer had dissolved completely. For relatively less viscous mixtures the magnetic stirrer device was effective to speed the dissolution of the polymer. The more concentrated solutions up to 95 wt. % were obtained first by mixing given amounts of PMA and DEP with acetone to give a PMA solution of about 10 wt. % and then by heating the mixture at about 50° to get acetone evaporated. It was assumed that when the shallow vat containing the mixture came to a constant weight the acetone had been removed completely. The samples of 95 and 100 wt. % were obtained in the form of a thin film for tensile creep measurements. A 5% acetone solution of PMA mixed with a required amount of DEP was cast on a mercury surface, followed by gradual evaporation of the casting solvent, leaching of the film in distilled water, and subsequent drying in an air oven at 60 to 70° for a long interval of time. This last process was important to remove all residual stresses in the film. It was assumed that during the preparation of these mixtures no loss of DEP occurred and thus each sample had a composition equal to that calculated in terms of the amounts of PMA and DEP weighed before mixing.

Viscometers.—Three different types of viscometer were

(1) Department of Polymer Science, Osaka University, Nakano-shima, Osaka, Japan.

(2) For a review of recent investigations in this field, see T. G. Fox, B. Gratch, and S. Loshaek, in "Rheology," edited by F. R. Eirich, Academic Press, Inc., New York, N. Y., 1956, Vol. I, Chap. 12.

(3) H. Fujita and A. Kishimoto, *J. Chem. Phys.*, 34, 393 (1961).

used; they were capillary viscometers, a coaxial falling cylinder viscometer, and a tensile creep apparatus. Except for the 95 wt. % solution, the measurement generally covered the range from about 20 to 110°.

For pure DEP and the 2.5 wt. % solution we employed a usual Ostwald viscometer, the instrument constant of which was determined by using water at 20° as the reference liquid.

In the range of viscosity from 10^{-1} to 10^6 poises, which, in the present system, covered PMA concentrations from 5 to 70% by weight, use was made of capillary viscometers of the pipet type and of the uniform bore type, depending upon the magnitude of viscosity to be measured. For the design, construction, and performance of the apparatus we mainly referred to the description of Fox, Gratch, and Loshak² and of Takayanagi.⁴ The liquid used to calibrate these viscometers was the 2.5 wt. % PMA solution for which absolute viscosities previously had been determined by the Ostwald viscometer in the manner described above. For both viscometers their instrument constants so determined agreed fairly well with the values computed according to Poiseuille's law from the accurately measured dimensions of the tubes. Argon was used to press up and down the sample liquid through the capillary tube. Before each determination of flow time, air bubbles contained in the sample solution were removed by evacuating the sample container for a sufficiently long interval of time at the temperature of the experiment concerned. This procedure was very essential for obtaining reproducible results. For less viscous solutions their viscosities were calculated from the times required to fill and empty the viscometer bulb under given pressures, by using the equation presented in Takayanagi's treatise.⁴ This equation needs no datum for the density of a given sample, but assumes that no drainage effect occurs when the liquid is pressed down through the capillary tube after the bulb has been filled. When this effect was rather appreciable, viscosities of the solutions were evaluated only from the times required to fill the bulb, with the necessary densities computed from eq. 1 and 2 subject to the assumption of no volume change on mixing. Of course, in this case, the viscometer was completely cleaned before each new determination. Shear-rate effects were negligible for solutions of viscosities less than 10^3 poises under the conditions of the present measurements. However, for more viscous samples the extrapolation of the measured viscosities to zero pressure difference was imperative to determine the "true" viscosity values. Unfortunately, such extrapolation requires a great amount of measurement to be performed. So, in this study, we were content with regarding viscosity values obtained at reasonably small pressure differences as being not significantly different from the values at zero shear rate. Furthermore, the measurements in the range above $10^{3.5}$ poises were not very reproducible. Thus the data obtained with the capillary viscometer (of the uniform bore type) for viscosities of the order of 10^7 to 10^6 poises doubtless are less reliable.

Samples having viscosities of the order of 10^5 to 10^9 poises were studied by means of a coaxial falling cylinder viscometer (made of stainless steel) of the type designed and used by Fox and Flory⁵ in their work on molten polystyrene and polyisobutylene fractions. It is stated that this instrument can be utilized to determine viscosities in the range of 10^6 to 10^{11} poises. In the present study, however, there were considerable difficulties in treating with this viscometer the samples which were either less viscous than 10^6 poises or more viscous than 10^9 poises. Samples having viscosities of the order of 10^5 poises were too soft to support their own weights in the annulus between the coaxial cylinders during the course of a particular measurement. On the other hand, for viscosities above 10^9 poises a very heavy weight had to be used in order to allow the inner cylinder to travel down for a measurable distance (in the traveling microscope of the accuracy we used) in a reasonable interval of time. There was a limit to the weights available to us. It should be remarked that such extremely viscous materials generally exhibit so pronounced a shear-rate effect that we should not employ a too heavy weight, if available, simply to speed the rate of falling of the inner cylinder. Although we did not check extensively, it is believed that the viscosity values

measured with the weights we employed would not differ appreciably from the values at zero shear rate.

Pure PMA and its 95 wt. % solution at temperatures below 60° were studied in an apparatus for tensile creep measurement; the sample film was suspended in a glass cylinder which had been sealed off at one end and immersed in a constant temperature bath. The lower end of the cylinder was filled with P_2O_5 to remove moisture from the film and to keep the inside of the cylinder at as low a humidity as possible during the particular measurement. In this connection we wish to remark that previous experiments on a sample of PMA by Fujita and Kishimoto^{6,7} indicated a pronounced influence of small amounts of water present in the sample upon the stress relaxation behavior of this polymer. The film was allowed to elongate downward by the weight of the lower clamp or, when necessary, plus the external load hung on it. Total weights were made as small as possible to ensure the deformation of the film within the region of linear viscoelasticity. When calculating the creep compliance $J(t)$ (where t is the time measured from the instant at which a load has been applied to the film) from measured elongations, corrections concerning the progressive change in sample cross section always were applied assuming that no volume change occurred on stretching.

Under the conditions in which measured plots of $\log J(t)$ against $\log t$ approached closely a straight line of unit slope, the data were treated according to the procedure suggested by Ninomiya⁸ to determine the required viscosity values. In this procedure, values of $dJ(t)/dt$ are plotted against $1/t$ and extrapolated graphically to $1/t = 0$; the ordinate intercept yields the inverse of the viscosity required. The data for pure PMA at 55 and 45° and those for the 95 wt. % solution at 50 and 40° were successfully treated in terms of this extrapolation procedure. For both samples the viscosities at temperatures lower than 40° were indirectly evaluated from the temperature shift factors, a_T , required to construct a master creep curve by sliding creep curves at different temperatures along the horizontal axis to that at 45° for pure PMA and to that at 40° for the 95 wt. % solution. The viscosity values thus determined from tensile creep measurements were taken as three times the shear viscosities, assuming that the Poisson ratios of these samples were 1/2 independent of temperature.

Results

Figure 1 shows viscosity values at fixed polymer concentrations as a function of $1/T$, where η is the shear viscosity in poises and T is the absolute temperature.⁹ The data obtained with different viscometers are distinguished by different marks. The general trend of this family of curves is similar to that found in previous data for other amorphous polymer-organic diluent systems.^{1,10-12} It is worth noticing that the curve for pure solvent is not linear but has an upward curvature in this rather wide range of temperature. This indicates that the apparent activation energy for viscous flow of DEP is not constant but increases, though not appreciably, with decreasing temperature. Until about 30 wt. % polymer is added, the value of this energy for the solution is nearly the same as that for the solvent. Beyond this limit the slope and curvature of $\log \eta$ vs. $1/T$ increase rather sharply with polymer concentration, yielding activation

(6) H. Fujita and A. Kishimoto, *J. Polymer Sci.*, **28**, 547 (1958).

(7) A. Kishimoto and H. Fujita, *ibid.*, **28**, 569 (1958).

(8) K. Ninomiya, Thesis, Kyoto University, 1951.

(9) The detailed numerical values have been deposited as Document number 7070 with the ADI Auxiliary Publications Project, Photoduplication Service, Library of Congress, Washington 25, D. C. A copy may be secured by citing the document number and by remitting in advance \$1.25 for photoprints or \$1.25 for 35-mm. microfilm payable to: Chief, Photoduplication Service, Library of Congress.

(10) F. Bueche, *J. Appl. Phys.*, **24**, 423 (1953).

(11) F. Bueche, *ibid.*, **26**, 738 (1955).

(12) J. D. Ferry, L. D. Grandine, Jr., and D. C. Udy, *J. Colloid Sci.*, **8**, 529 (1953).

(4) M. Takayanagi, in "Kobunshi Zikkengaku Koza" (Treatise on Experimental Methods in Polymer Research), Kyoritsu Publ. Co., Tokyo, 1958, Vol. III, pp. 46-73.

(5) T. G. Fox and P. J. Flory, *J. Am. Chem. Soc.*, **70**, 2384 (1948).

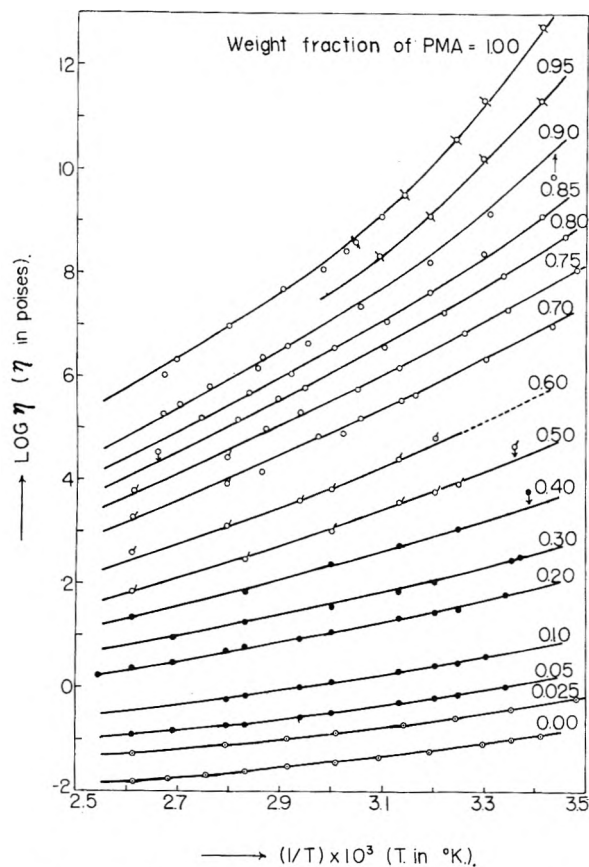


Fig. 1.—Logarithm of viscosity (η) plotted against reciprocal absolute temperature for the system polymethyl acrylate + diethyl phthalate as a function of weight fraction of polymer: \circ , by Ostwald viscometer; \bullet , by pipet type viscometer; \square , by uniform bore capillary viscometer; \bigcirc , by coaxial falling cylinder viscometer; \square , by tensile creep apparatus.

energies which are enormously large in magnitude and quite sensitive to temperature in the region approaching the pure polymer.

Recent work¹³ has demonstrated for a number of polymers (essentially of amorphous nature) in the dry state that their viscosity vs. temperature relations are represented quite accurately by a simple expression, known as the WLF equation, over a range of 100° above the glass transition temperatures of respective polymers, provided the parameter T_s , called the reference temperature, involved in the equation is adequately chosen for the given sample. From both dynamic mechanical and electrical measurements Williams and Ferry¹⁴ have deduced a value of 51° as the T_s relevant to PMA. It was found, however, that our viscosity data for pure PMA followed better the WLF equation if T_s was chosen to be 49.5° in place of 51°. Figure 2 shows this fit, where a_T is defined by $a_T = \eta(T)/\eta(49.5^\circ)$ by ignoring the slightly temperature-dependent terms which are to be included in the exact definition for a_T proposed by Ferry.¹⁵ It is seen that the WLF equation with $T_s = 49.5^\circ$ deviates slightly from experiment at temperatures

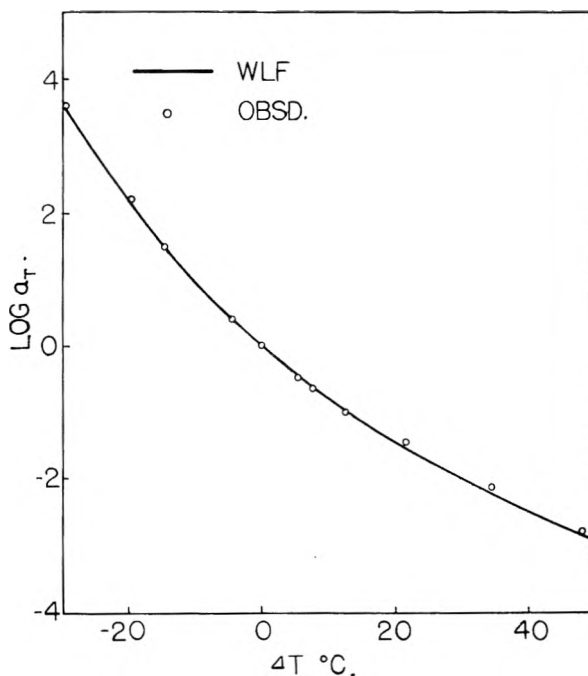


Fig. 2.—Fit of the Williams-Landel-Ferry equation (with $T_s = 49.5^\circ$) to the viscosity data for pure polymethyl acrylate: $\Delta T = T - T_s$; $a_T = \eta(T)/\eta(49.5^\circ)$.

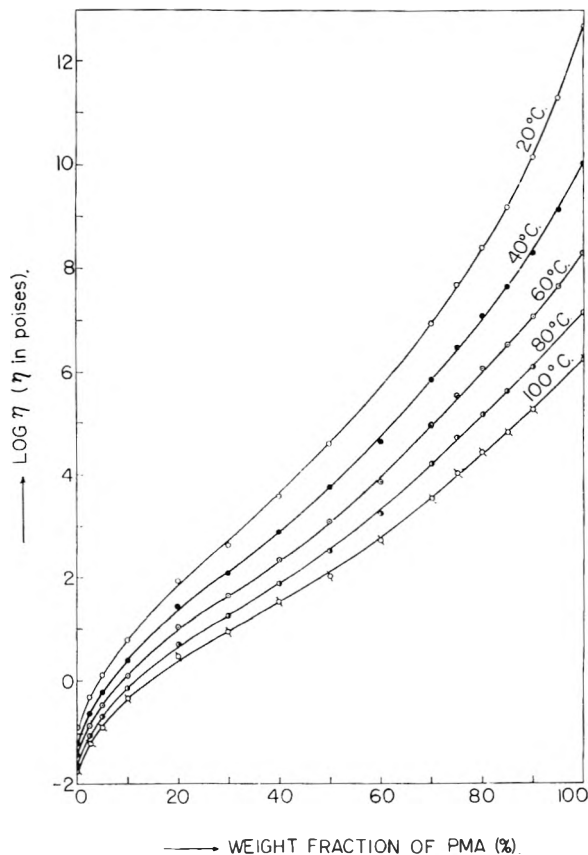


Fig. 3.—Plots for $\log \eta$ vs. weight fraction of polymer on the system polymethyl acrylate + diethyl phthalate as a function of temperature.

(13) M. L. Williams, R. F. Landel, and J. D. Ferry, *J. Am. Chem. Soc.*, **77**, 3701 (1955).

(14) M. L. Williams and J. D. Ferry, *J. Colloid Sci.*, **10**, 474 (1955).

(15) J. D. Ferry, *J. Am. Chem. Soc.*, **72**, 3746 (1950); see also ref. 13.

above 70°, but it is not certain whether this small deviation is really significant or not.

The variation of η with polymer concentration at

a fixed temperature is illustrated in Fig. 3 for 20, 40, 60, 80, and 100°. The points shown are not the values actually measured but are taken from the smooth curves drawn in Fig. 1. For all the temperatures indicated the curves exhibit an essentially similar feature. They are concave in the region of low w_p (the weight fraction of PMA in the mixture) and convex in the region of high w_p , against the abscissa axis. Thus they are S-shaped, with their inflection points appearing in the region of w_p near 0.6. The S-shaped character becomes more noticeable as the temperature is lowered. These features of the concentration dependence of η are substantially similar to those found in pertinent previous publications^{2,10,11} dealing with amorphous polymer-organic diluent systems over wide ranges of composition, and therefore may be regarded, at least for the moment, as being characteristic of polymer species that are essentially amorphous.

It is reported^{16,17} that some polymer-diluent systems followed the relation $\log \eta = a + b(w_p)^{1/2}$ (where a and b are constants independent of w_p) up to moderately high concentrations of polymer. The present data, however, do not follow this relation, the plots for $\log \eta$ vs. $(w_p)^{1/2}$ exhibiting upward curvature over the entire concentration range. In this respect, our system resembles polyvinyl acetate and polystyrene in various organic solvents investigated by Ferry and associates.^{12,18} Several investigators,¹⁹⁻²¹ notably Ferry and associates, demonstrated that the viscosities of some polymer-diluent systems increased in proportion to the fifth power of w_p . This implies that when the data on these systems were plotted in the form of $\log \eta$ vs. $\log w_p$, there appeared a concentration region in which the plots gave a straight line with slope of 5. With the data for the present system, however, no such linear region is obtained, but the plots give a smooth curve concave upward everywhere in the entire concentration region from 0 to 100% polymer. The extensive data of Fox, Gratch, and Loshaek² on polystyrene in dibenzyl ether also show a behavior quite similar to this. Thus, although any definite statement must be reserved, it appears that the law $\eta \propto w_p^5$ is applicable only within a very limited concentration range.

Discussion

When the pure polymer is chosen as reference, the viscosity equation proposed by Fujita and Kishimoto³ for concentrated solutions of a polymeric material reads

$$\frac{1}{\ln a_c} = f(0, T) + \frac{[f(0, T)]^2}{\beta(T)} \frac{1}{v_1} \quad (3)$$

where a_c is defined by

$$a_c = (1 - v_1)[\eta(0, T)/\eta(v_1, T)] \quad (4)$$

In these equations, $f(v_1, T)$ is the average fractional free volume in the mixture in which the volume

fraction of diluent is v_1 and the temperature is T , $\eta(v_1, T)$ is the viscosity of that mixture, and $\beta(T)$ is a temperature-dependent parameter defined by

$$\beta(T) = \gamma(T) - f(0, T) \quad (5)$$

where $\gamma(T)$ is another temperature-dependent parameter appearing when it is assumed that the free volume newly produced in a polymeric solid by the addition of a low-molecular-weight diluent is proportional to the volume of the diluent added. In passing, we wish to remark that in the previous article of Fujita and Kishimoto the notations $f(T, v_1)$, $\eta(T, v_1)$, and $\beta'(T)$ were adopted for the present $f(v_1, T)$, $\eta(v_1, T)$, and $\beta(T)$, and the reciprocal of the present a_c was denoted as a_c . These changes of the notations have no particular advantage but are just a matter of convenience.

Equation 3 predicts that there appears a linear region in the plot for $1/\ln a_c$ against $1/v_1$ and the intercept at $1/v_1 = 0$ and the slope of the straight line placed on that region allow determination of the quantities $f(0, T)$ (the fractional free volume in the pure polymer at temperature T) and $\beta(T)$. Substitution of these values into eq. 5 then permits evaluation of $\gamma(T)$. Figure 4 shows $1/\ln a_c$ plotted against $1/v_1$ corresponding to the data of Fig. 3. The values of v_1 needed were calculated by using eq. 1 and 2 for the apparent specific volumes of PMA and DEP with the assumption that no volume change occurs on mixing of the two components. It is seen that the data for relatively low temperatures obey eq. 3 over fairly wide ranges of DEP concentration and make reliable determination of $f(0, T)$ and $\beta(T)$ possible. However, as the temperature is raised, the region in which the plot appears linear is progressively restricted to higher values of $1/v_1$, i.e., eq. 3 is obeyed only for a narrower region of diluent concentration near the pure polymer. This situation leads to an increasing ambiguity in the determination of $f(0, T)$ and $\beta(T)$ for high temperatures. To minimize this difficulty the viscosity data must be determined at more numerous points in the region close to the pure polymer. It also should be remarked that values of $1/\ln a_c$ for small diluent concentrations are quite sensitive to the viscosity values for the pure solid. A slight alternation of $\eta(0, T)$ results in an appreciable change in $1/\ln a_c$, especially when the variation of viscosity with diluent concentration is less pronounced. In such circumstances, even if a good and long enough linear region is obtained for $1/\ln a_c$ against $1/v_1$, the derived values of $f(0, T)$ and $\beta(T)$ should be accepted with some reservation. This is because if the measured $\eta(0, T)$ were slightly erroneous, such a "good" linear region should be only illusory. We cannot claim that our data for the pure polymer as well as for the solutions having PMA concentrations higher than 85% by weight are sufficiently accurate, since, besides the considerable difficulties in manipulating the viscometers with these extremely viscous samples, no correction for the shear-rate effect was applied to them.

The plots of Fig. 4 all show downward curvature in the region of lower $1/v_1$; the value of $1/v_1$ at which this curvature becomes apparent varies with temperature. This trend is similar to that noticed previously³ for other systems such as polystyrene-

(16) P. J. Flory, *J. Phys. Chem.*, **46**, 870 (1942).

(17) R. S. Spencer and J. L. Williams, *J. Colloid Sci.*, **2**, 117 (1947).

(18) J. D. Ferry, E. L. Foster, G. V. Browning, and W. M. Sawyer, *ibid.*, **6**, 377 (1951).

(19) R. F. Landel, J. W. Berge, and J. D. Ferry, *ibid.*, **12**, 400 (1957).

(20) S. Onogi, Y. Kojima, and Y. Taniguchi, *J. J. S. T. M.*, **10**, 357 (1961).

(21) Y. Ohyanagi, *J. Colloid Sci.*, in press.

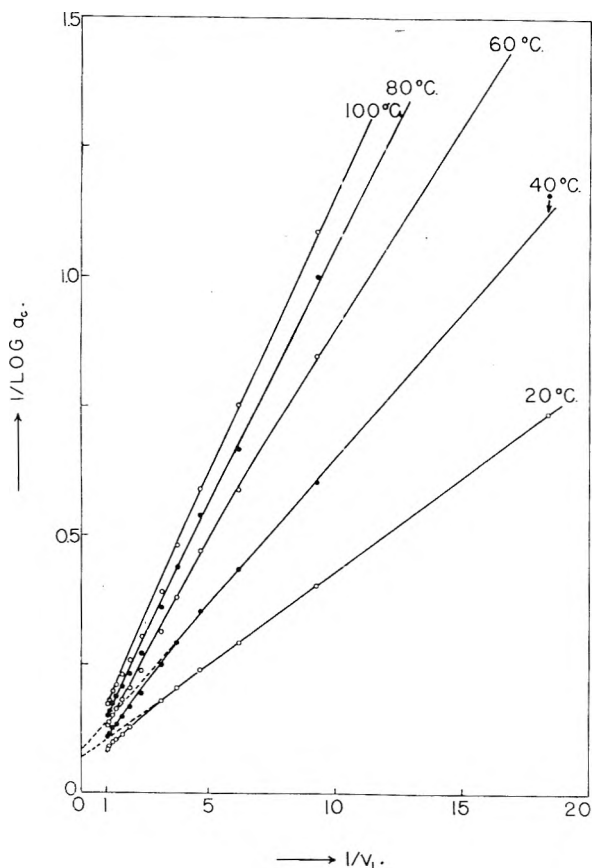


Fig. 4.—Plots for $1/\log a_c$ vs. $1/v_1$ on the system polymethyl acrylate + diethyl phthalate at different temperatures: $a_c = (1 - v_1)\eta(0, T)/\eta(v_1, T)$; v_1 = volume fraction of diethyl phthalate.

diethylbenzene, polystyrene-decalin, and polymethyl methacrylate-diethyl phthalate, although in these systems the downward deviations of the plots from linearity occurred at much higher diluent concentrations than in the present system. In this respect, the system polystyrene-dibenzyl ether investigated by Fox, Gratch, and Loshaek² appears to be rather exceptional; as was shown previously,³ the plots for $1/\ln a_c$ on this system do not exhibit any significant deviation from linearity up to as high diluent concentrations as $v_1 = 0.8$ or more at all temperatures in the range from 0 to 217°.

Equation 3 may be rewritten in the form

$$\frac{v_1}{\ln a_c} = \frac{[f(0, T)]^2}{\beta(T)} + f(0, T)v_1 \quad (6)$$

This indicates $v_1/\ln a_c$ to vary linearly with v_1 in the range in which $1/\ln a_c$ is a linear function of $1/v_1$. The values of $f(0, T)$ and $\beta(T)$ can be determined from the intercept and initial slope of the resulting curve. For a rigorous test of the free volume theory concerned here this plot is more adequate, because it brings to focus the details of experimental data for small values of v_1 ; as one may understand from the theoretical development of Fujita and Kishimoto³ eq. 3 or 6 originally should be effective only for solutions sufficiently concentrated in polymer component. Figure 5 shows $v_1/\ln a_c$ vs. v_1 corresponding to Fig. 4. In terms of this representation it is more apparent, than with Fig. 4, that at high temperatures the theory applies only for very

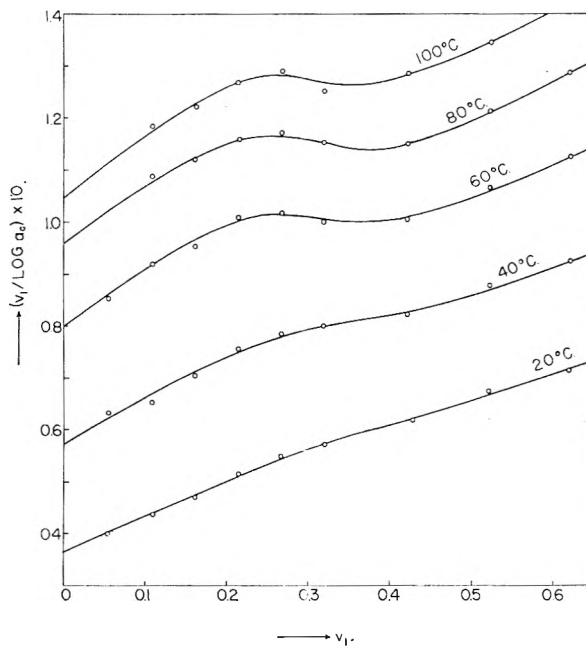


Fig. 5.—Plots for $v_1/\log a_c$ vs. v_1 on the system polymethyl acrylate + diethyl phthalate at different temperatures.

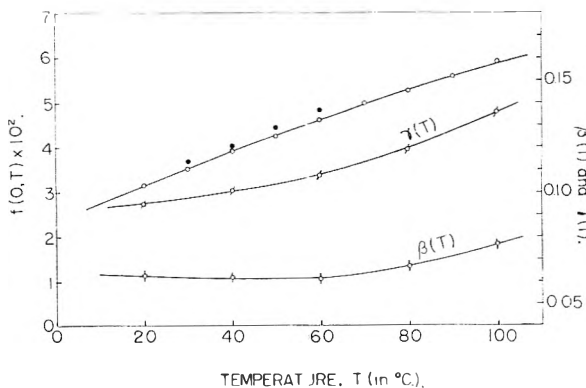


Fig. 6.—O, $f(0, T)$ values derived from the present viscosity data; ●, $f(0, T)$ values derived from sorption experiments for benzene in polymethyl acrylate (unpublished data of Kishimoto and Enda); ◊, $\beta(T)$ for the system polymethyl acrylate + diethyl phthalate; ◻, $\gamma(T)$ for diethyl phthalate in polymethyl acrylate.

narrow ranges near $v_1 = 0$, but the data for 20° obey it over a fairly wide range and permit accurate determination of $f(0, 20^\circ)$ and $\beta(20^\circ)$.

It has been shown³ that the viscosity of a pure polymer at temperature T relative to its value at a reference temperature T^* , i.e., $\eta(0, T)/\eta(0, T^*)$, is related to $f(0, T)$ by the equation

$$\ln [\eta(0, T)/\eta(0, T^*)] = 1/f(0, T) - 1/f(0, T^*) \quad (7)$$

With the $f(0, 20^\circ)$ value determined above as $f(0, T^*)$ it is possible to calculate $f(0, T)$ for other temperatures by substituting into this equation the viscosity values for the pure polymer taken from Fig. 1. The results of this operation appear plotted in Fig. 6. Here are included for comparison the $f(0, T)$ values derived by Kishimoto and Enda²² from their diffusion coefficient data for benzene in PMA by using the procedure described else-

(22) A. Kishimoto and Y. Enda, unpublished data.

where.^{23,24} The reasonable agreement of the two sets of $f(0, T)$ data indicates the internal consistency of the free volume interpretations for viscosity and diffusion on concentrated polymer solutions developed recently by Fujita and associates. It is seen that the $f(0, T)$ values so obtained increase almost linearly with increasing T in the range indicated; in this connection we may remark that the accepted glass transition point of PMA is in the vicinity of 3° . The average slope of $f(0, T)$ in the range $T < 50^\circ$ is $4.0 \times 10^{-4} \text{ deg.}^{-1}$. This is somewhat smaller than the value $4.5 \times 10^{-4} \text{ deg.}^{-1}$ found previously³ for polystyrene in the range above its glass transition temperature and the value $4.8 \times 10^{-4} \text{ deg.}^{-1}$ deduced from the free volume interpretation^{13,24} of the WLF equation for the temperature dependence of the viscosities of pure polymers.

Evaluation of the parameter $\beta(T)$ in terms of eq. 6 requires the determination of the intercept at $v_1 = 0$ of the plot for $v_1/\ln ac$ vs. v_1 . Except for those at 20° , the data in Fig. 5 show considerable scatter in the region of small v_1 and thus make their extrapolation to $v_1 = 0$ quite uncertain. However, this difficulty is to a great extent reduced by the requirement that the initial tangent of the plot should be equal to $f(0, T)$. Thus the solid lines in Fig. 5 have been drawn in such a manner that their initial slopes may yield the $f(0, T)$ values interpolated from the smooth curve for $f(0, T)$ shown in Fig. 6. Values of $\beta(T)$ and also of $\gamma(T)$ have been calculated from the intercepts so determined, and appear plotted in Fig. 6 as functions of temperature. One can see that $\beta(T)$ is nearly independent of T over the temperature range indicated, while $\gamma(T)$ increases steadily with increasing temperature.

(23) H. Fujita, A. Kishimoto, and K. Matsumoto, *Trans. Faraday Soc.*, **56**, 424 (1960).

(24) H. Fujita, *Fortschr. Hochpolym. Forsch.*, **3**, 1 (1961).

These trends of $\beta(T)$ and $\gamma(T)$ for PMA-DEP are different from those found previously³ for polystyrene-dibenzyl ether and polymethyl methacrylate-DEP, where the values of $\beta(T)$ decreased slightly with T and those of $\gamma(T)$ were almost constant over ranges of temperature above the glass transition points of respective polymers. This difference, however, should not be taken seriously, because the evaluation of these parameters is subject to considerable uncertainty, as has been noted in a previous article.³ Upon assuming that the glass transition temperature of PMA is in the vicinity of 3° , Fig. 6 gives a value of about 0.065 for $\beta(T)$ at this temperature. Fujita and Kishimoto have shown that the values of $\beta(T)$ for polymethyl methacrylate-DEP³ and poly-*n*-butyl methacrylate-DEP²⁵ at the glass transition temperatures of the respective polymers were nearly 0.050. These results lead to an interesting inference that when comparison is made at the glass transition temperature of each polymer, the value of the parameter $\beta(T)$ is roughly independent of polymer species and characteristic of a particular diluent. This also would be true of the parameter $\gamma(T)$, since, as is now widely accepted, the value of $f(0, T)$ at the glass transition temperature is nearly constant for a wide variety of polymers.²⁶

Acknowledgments.—This work was supported in part by a fund from the Japan Synthetic Rubber Company, Ltd., to which grateful acknowledgment is made. We are much indebted to Dr. Akira Kishimoto of this Laboratory for help with the design of the various viscometers used, and also to Miss Nobuko Noda and Miss Yoshiko Miki for their technical assistance.

(25) H. Fujita and A. Kishimoto, *Bull. Chem. Soc. Japan*, **33**, 274 (1960).

(26) For example, J. D. Ferry and R. F. Landel, *Kolloid-Z.*, **148**, 1 (1956).

SOME CONDITIONS FOR VALIDITY OF STATISTICAL THERMODYNAMIC TREATMENTS OF REACTION KINETICS

BY RICHARD M. NOYES

Department of Chemistry of the University of Oregon, Eugene, Oregon

Received November 28, 1960

In macroscopic systems undergoing net chemical change, theoretical treatments based on statistical methods are less satisfactory the more the reaction perturbs the population distribution among the allowable internal modes of motion of individual molecules. The perturbation is least if molecules interact frequently with their surroundings during any time necessary for significant motion along a reaction coordinate, but this restriction is not satisfied except perhaps in liquid phase. For infrequent interactions, as in gas phase reactions, statistical methods may still be valid if the other internal modes of motion are independently separable from motion along the reaction coordinate. Such separability is often a very poor approximation for displacements of the magnitude associated with chemical reaction. For the special case in which molecules are activated by collision and subsequently dissociate, the internal modes of motion not associated with the reaction coordinate will tend to have less energy at the moment of dissociation than would have been predicted from the temperature of the macroscopic system.

Introduction

Statistical thermodynamics was developed for the consideration of systems at equilibrium, and it is concerned with the instantaneous population distribution among accessible states in an ensemble of systems. Although it recognizes that individual molecules are constantly changing their states, even

classical non-quantum statistical mechanics is uninterested either in the frequency of this change or in the states occupied by specific molecules at times prior or subsequent to the time for which the population distribution is determined.

Chemical kinetics of necessity considers processes in non-equilibrium systems. Although treatments

of the subject attempt to retain the concept of a population distribution of molecular states, they must recognize that this distribution in a reacting system is perturbed from that in a similar system at equilibrium.

An individual molecular system retains a constant energy unless it interacts with its surroundings either through the action of intermolecular forces or by the emission or absorption of radiation. These interactions will cause a non-equilibrium distribution of state populations to relax to the equilibrium one, and the relaxation will be faster the more frequent the interactions. Thus, if an ensemble of interacting but non-reacting molecular systems has existed for a time long compared to the probable interval between interactions of an individual system, the population distribution will approximate closely to the equilibrium one regardless of what the initial distribution was. However, if the time period of interest is much shorter than the usual interval between interactions, the energies of states at the end of the period will be distributed very similarly to the energy distribution at the start of the period, and the individual molecules having certain energies at the end of the period will tend to be the same molecules as had these energies at the start of it.

If the existence of a chemical reaction perturbs the population of translational, rotational, and vibrational energy levels in a system, the extent of perturbation will be greater the less frequently molecules interact with each other. Also, the less the frequency of interaction, the more the subsequent behavior of a molecular system will be influenced by and predictable from its previous history.

All of the above observations are well recognized, and several authors¹⁻⁵ have recently addressed themselves to the difficult task of treating reaction in systems where equilibrium distributions are not maintained. The present paper is less ambitious and much more qualitative, but it attempts to make two points that do not appear to have been made in the previous discussions. One point is that the more nearly internal modes of motion are independently separable, the less are the perturbations in population distributions. The other point is that for the special case of a unimolecular dissociation in a gas at low pressure, at the moment of dissociation the modes of motion not associated with the reaction coordinate will have smaller energies than would be predicted from the temperature of the system.

Formulation of Problem

For generality, let a process in a microscopic molecular system be represented by



where R and P each represent one or more individual molecules that react or are produced and where the equation is balanced for all elements and charges. The state of the macroscopic system

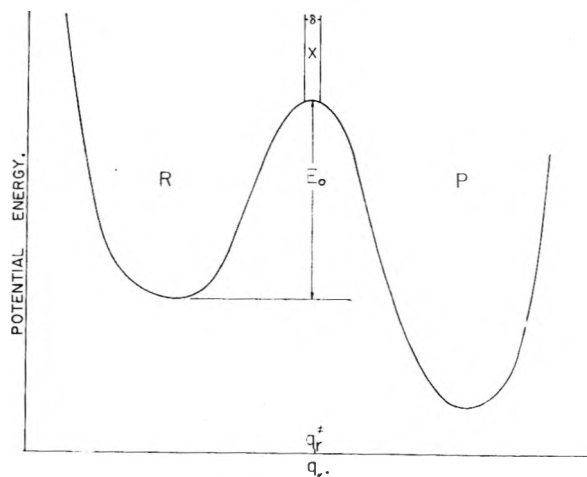


Fig. 1.—Reaction coordinate representation of chemical reaction.

should be describable satisfactorily as a sum of microscopic states involving small numbers of molecules, and eq. 1 should represent the only process contributing significantly to irreversible change in the macroscopic system.

Let there be j atomic nuclei in the microscopic system undergoing this process. If electronic distributions are established rapidly compared to the motions of the heavier nuclei, then the state of the microscopic system can be described at any stage of its reaction in terms of values for $3j$ coordinates and $3j$ momenta. Of these, 3 coordinates and 3 momenta involve motion of the center of mass of the system; they are independently separable and are of no chemical interest. The remaining coordinates and momenta involve rotational and vibrational modes that are also often assumed to be independent. The assumption is usually a good approximation when only low quantum excitations are involved, but the approximation becomes poor for the large molecular deformations associated with chemical reaction.

It is also often assumed that the distance a microscopic system has gone toward reaction can be described in terms of a single "reaction coordinate," q_r , which may be the extension of a normal mode of R or P. Motion along the reaction coordinate in at least one direction is restricted by a potential energy barrier. The situation under discussion is illustrated in Fig. 1.

A particular microscopic system is usually assigned state R or state P according to the value of q_r . A microscopic system is said to be in a transition state X if q_r is within a region of length δ on the top of the potential barrier; the symbol q_r^\ddagger is used for the reaction coordinate of a system in a transition state. Such a representation classifies a microscopic system on the basis of this single coordinate without considering the values of the $3j$ momenta or of the other $3j - 1$ coordinates.

If the macroscopic system is in a state of thermodynamic equilibrium, and if the interatomic forces in the microscopic system are sufficiently understood, it is possible in principle to calculate the number of microscopic states having any specified value of q_r . For states having this value of q_r , it is

- (1) E. E. Nikitin and N. Sokolov, *J. Chem. Phys.*, **31**, 1371 (1959).
- (2) K. E. Shuler, *ibid.*, **31**, 1375 (1959).
- (3) B. Widom, *ibid.*, **31**, 1387 (1959); **34**, 2050 (1961).
- (4) F. P. Buff and D. J. Wilson, *ibid.*, **32**, 677 (1960).
- (5) J. Ross and P. Mazur, *ibid.*, **35**, 19 (1961).

also possible to calculate the population distribution for all allowable combinations of values for the other $3j - 1$ coordinates and $3j$ momenta.

If the macroscopic system is not at equilibrium with respect to process 1, the populations in these states will differ from those calculated by equilibrium statistics. However, it is still possible to make at least qualitative estimates of the directions in which some of these populations differ from the equilibrium values.

Effects of Interaction Frequency and of Separability

Systems with Frequent Interactions.—As was indicated in the Introduction, if a microscopic system undergoes sufficiently frequent interactions with its surroundings, state populations for internal modes of motion will not differ significantly from the predictions of equilibrium statistics. By applying these equilibrium principles, Glasstone, Laidler, and Eyring⁶ derived the familiar equation

$$k = \kappa \frac{kT}{h} \frac{F^\ddagger}{F_R} e^{-E_0/RT} \quad (2)$$

where k is the rate constant for process 1, k is the Boltzmann constant, κ is the so-called transmission coefficient, and E_0 is the total difference in energies for microscopic systems in the lowest possible energy levels for states R and X. The partition function F_R is computed for all $3j$ modes of motion of the microscopic system, while F^\ddagger involves the $3j - 1$ modes for motions other than along the reaction coordinate.

The partition function F^\ddagger is calculated when the value of q_r is q_r^\ddagger , so that in an ensemble of transition states the other $3j - 1$ modes all have the degree of excitation appropriate to the temperature of the macroscopic system. If interactions are frequent during the time necessary for motion along the reaction coordinate in Fig. 1, such a treatment is valid if motion along the reaction coordinate is separable from the other modes of motion over a small region near the potential maximum. This separability need not be in terms of the normal modes for small vibrations of R, and the separability need not be valid for significant displacements from the potential maximum.⁷ To the extent that motion along the reaction coordinate is independent of the other modes of motion in a microscopic system, the partition function F^\ddagger will be applicable to systems in state X of Fig. 1 even if interactions are less frequent than was implied in the above discussion.

Since the time necessary to traverse the reaction coordinate from R to P is often of the order of the time of a molecular vibration (about 10^{-13} second), the frequency of interaction required for this discussion is scarcely attainable except perhaps in liquid phase. Equation 2 is not rigorously applicable to gas reactions unless motion along the reaction coordinate is separable from other motions even for large displacements.

A microscopic system with sufficient energy to react will usually lose energy during an interaction with its surroundings. If interactions are frequent,

a system that has passed through state X of Fig. 1 will almost certainly lose energy before q_r has time to attain the value q_r^\ddagger again. Hence the system will be stabilized on the side of the barrier on which it left X, and the transmission coefficient, κ , will be very close to unity.

Systems with Infrequent Interactions.—If interactions are infrequent compared to the time necessary for passage along the reaction coordinate, a model for treatment is suggested by Eyring, Walter, and Kimball.⁸ They applied quantum mechanics to a one-dimensional plane wave moving along the reaction coordinate in a constant energy system and derived an expression formally identical with eq. 2. The derivation requires that the reaction coordinate be truly separable from the other modes of motion so that F^\ddagger in eq. 2 can assume that the temperatures of the other modes are the same as the temperature of the macroscopic system. However, if the motions are not separable, the energies of the other $3j - 4$ modes of chemical interest presumably corresponded to the macroscopic temperature at the time of the last interaction but do not necessarily do so when q_r attains the value q_r^\ddagger .

The modes are not in fact separable for large displacements. Probably the simplest example is the dissociation of a diatomic molecule where q_r is the length of the bond that is breaking. As this bond stretches in a constant energy system, the moment of inertia increases, and the angular velocity and kinetic energy of rotation decrease. For an ensemble of microscopic systems that undergo dissociation, if their rotational temperature at the time of activation is the same as the temperature of the macroscopic system, then their rotational temperature at the time of dissociation is less than that of the macroscopic system. In short, when $q_r = q_r^\ddagger$, the rotational partition function does not correspond to the value predicted by the Glasstone, Laidler, and Eyring⁶ assumption.

Significantly, Eliason and Hirschfelder⁹ could not derive eq. 2 from collisional postulates unless they assumed constancy of rotational quantum numbers during reaction; such an assumption can be regarded as a conservation of angular momentum and does not permit rotational temperature also to remain constant.

Although Slater¹⁰ has treated this type of problem in terms of independent normal modes, the treatment then becomes a matter of phasing so that the "reaction coordinate" of the above discussion becomes a superposition of several modes. Recent work by Schlag and Rabinovitch¹¹ indicates that at least for cyclopropane isomerization a model based on non-separable modes is probably preferable to the Slater model.

In summary, statistical thermodynamic relations are applicable to internal modes of motion if inter-

(8) H. Eyring, J. Walter, and G. E. Kimball, "Quantum Chemistry," John Wiley and Sons, New York, N. Y., 1944, p. 305 ff.

(9) M. A. Eliason and J. O. Hirschfelder, *J. Chem. Phys.*, **30**, 1426 (1959).

(10) N. B. Slater, "Theory of Unimolecular Reactions," Cornell University Press, Ithaca, N. Y., 1959.

(11) E. W. Schlag and B. S. Rabinovitch, *J. Am. Chem. Soc.*, **82**, 5996 (1960).

(6) S. Glasstone, K. J. Laidler, and H. Eyring, "The Theory of Rate Processes," McGraw-Hill Book Co., New York, N. Y., 1941, p. 185 ff.

(7) I am indebted to a referee for these observations.

actions of microscopic systems are sufficiently frequent. If interactions are infrequent, statistical thermodynamic relations are still applicable provided the modes of motion are independently separable even for the large displacements associated with reaction. If interactions are infrequent and if the modes of motion are not separable, rigorous treatment will be very complex if it is attempted within the framework of statistical thermodynamics.

Classification of Transition States

Classification in Equilibrium Systems.—Transition states can be classified in principle according to their past histories and future fates. If interactions are infrequent, and if modes of motion are not separable, such classification permits some interesting predictions about energy distributions in microscopic systems during chemical reaction.

Let us postulate a macroscopic system in equilibrium for all processes including eq. 1, and let the system be a sufficiently dilute gas that interactions are infrequent in the time necessary for a microscopic system to traverse a significant section of the reaction coordinate including the potential maximum.

At any instant, each of the transition state species present in the macroscopic system can be assigned to one of four classes: (1) Those microscopic systems that underwent their last interaction on side R and that are destined to undergo their next one on side P. (2) Those systems that underwent their last interaction on side P and that are destined to undergo their next one on side R. (3) Those systems that underwent their last interaction on side R and that are destined to undergo their next one also on side R even though they may spend some of the intervening time on side P. (4) Those systems that underwent their last interaction on side P and that are destined to undergo their next one also on side P.

Only classes 1 and 2 contribute to net chemical change; their concentrations must be equal and they must be formed at equal rates in this equilibrium system. Also, microscopic reversibility requires that ensembles of systems in classes 1 and 2 will have the same population distributions for the other $3j - 1$ modes of motion.

As has been indicated above, classes 3 and 4 will be of negligible importance if microscopic systems undergo frequent interactions. However, for a system with infrequent interactions, these classes may contribute significantly to the total concentration of transition states. Even though classes 1 and 2 must form at equal rates in an equilibrium system, transition states of classes 3 and 4 may form at rates that are not simply related to each other or to the rate of formation of systems leading to net reaction.

If the numbers of species in classes 3 and 4 differ significantly, then even in the equilibrium system transition states formed after an interaction on side R (classes 1 and 3) will manifest a different transmission coefficient, κ , than will transition states formed after an interaction on side P (classes 2 and 4).

Since the macroscopic system is at equilibrium, the partition function for the ensemble of *all* transition states present at any instant must correspond

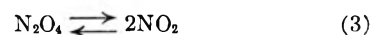
to the F^\ddagger predicted by the Glasstone, Laidler, and Eyring⁶ treatment. However, there is no requirement that this condition be satisfied for the transition states in any of the individual classes. Since classes 1 and 2 are the only ones that contribute to net chemical change, significant numbers of transition states in classes 3 or 4 can seriously disrupt the predictions of eq. 2 provided the energy distributions of these classes are different.

Extension to Non-equilibrium Systems.—Let us now postulate a similar macroscopic system with the same concentration of R as the equilibrium system considered in the previous section but with less P. This system will undergo chemical change. It is generally assumed that transition states in classes 1 and 3 will form at the same rate as they did in the equilibrium system, although the recent work of Widom³ casts some doubt on the exact validity of this assumption.

We have already seen that classes 1 and 2 can be described by the same partition function in the equilibrium system, that F^\ddagger is the partition function applicable to the total of all transition states in the equilibrium system, and that classes 3 and 4 make negligible contributions to the total population if interactions are frequent. Then for the situation of frequent interactions, F^\ddagger will also be a satisfactory partition function for the transition states of class 1 forming in the non-equilibrium system, and eq. 2 will be valid.

However, if interactions are infrequent, transition states of class 4 may contribute to the transition state population in the equilibrium system but will make less contribution in the reacting system. If the energy distribution of internal modes in class 4 differs from that in classes 1 and 2 and is also different from class 3, eq. 2 will no longer be applicable to the reacting system.

Application to Dissociations.—The above discussion can be illustrated by a unimolecular dissociation such as that of N_2O_4 .



A gas containing these species will also contain a number of excited molecular species of empirical formula N_2O_4 that contain enough internal energy to dissociate if they go a sufficient period without any collision. These excited molecules are not transition states, but they can be classified in the same way as the transition states above. Molecules in class 1' were formed by excitation of N_2O_4 and will dissociate before they lose their excitation. Those in class 2' were formed by collision of two NO_2 molecules and will be stabilized by collision with another molecule. Those in class 3' were formed by excitation of N_2O_4 and will be stabilized by collision without dissociation. Those in class 4' were formed by collision of two NO_2 molecules and will dissociate without stabilization.

In an equilibrium mixture, the average internal energy of all excited molecules is calculable by equilibrium statistics, but molecules in different classes have different average internal energies. Since it is well established that the rate constant for dissociation of an excited molecule increases with the energy content of such a molecule, those

molecules that are destined to dissociate (classes 1' and 4') will have more average energy than will those that are destined to be stabilized (classes 2' and 3').

In an equilibrium mixture, classes 1' and 2' will be present in equal concentration regardless of pressure and will have the same average energies. If the system is not at chemical equilibrium, the concentrations of these classes will be different but they should still have very nearly the same average internal energies.

Lowering the pressure will increase the concentration of class 4' and decrease that of class 3'. If the pressure is sufficiently low, most excited molecules will be in class 4'.

If a low pressure reacting system containing an excess of N_2O_4 is compared with a similar equilibrium system having the same pressure of N_2O_4 but more NO_2 , the reacting and equilibrium systems will have very nearly the same concentrations of excited molecules in classes 1' and 3', but the reacting system will have fewer in classes 2' and 4'. The above arguments then indicate that the excited molecules in the reacting system will have lower average internal energy than those in the equilibrium system and that the difference will be greater the lower the pressure and the greater the contribution of class 4' to the equilibrium system.

These predictions are in accord with the experimental observations of Carrington and Davidson.¹² At pressures below about one atmosphere, the kinetics indicate that the rate of reaction 3 is determined by collisional activation and that virtually all of the activated molecules decompose before subsequent collisions. The temperature dependence of the rate indicates that during collisions in which N_2O_4 molecules are activated the colliding molecules contain 11.0 kcal./mole more than the average energy of the same chemical species at that temperature. On the other hand, thermodynamic arguments indicate that a pair of thermally equilibrated NO_2 molecules contains 13.1 kcal./mole more energy than N_2O_4 .

At the "high pressure limit" where the Glasstone, Laidler, and Eyring⁶ derivation would be applicable, it is hard to see how the activation energy could be less than 13.1 kcal./mole. It has been known for some time that the activation energy of a unimolecular dissociation may decrease as the pressure is lowered, but the N_2O_4 reaction seems to be the best authenticated case in which the low pressure value actually goes below the ΔH^0 of the equilibrium reaction. The Carrington and Davidson data seem to require that in a dissociating N_2O_4 molecule in the transition state the modes of motion not associated with the reaction coordinate actually have less average energy than would be predicted from the temperature of the system, and the NO_2 molecules just formed by a dissociation must be less excited than thermally equilibrated molecules.

This apparent violation of statistical distributions does not exist in an equilibrium system be-

cause such a system contains "collision complexes" of pairs of NO_2 molecules that remain associated for periods short compared to the time required for collision with other molecules, and these species contain greater average internal energy than the equilibrium value computed from the temperature of the system. Rice¹³ has recently commented about such species and their different concentrations in equilibrium and non-equilibrium systems, but he does not make the present point about different average internal energies.

Summarizing Discussion

Because statistical thermodynamics is a well developed discipline, people developing theories of irreversible processes are tempted to use the language of population distributions for as many as possible of the modes of motion in a reacting system. The permissibility of such a procedure must be established for any specific case by considering the rate of chemical change, the frequency of interactions between microscopic systems, and the separability of internal modes of motion.

For reactions in liquid phase, the criteria can be clearly established. Frequent molecular interactions maintain equilibrium population distributions for internal modes of motion, but transport of molecules is sufficiently slow that non-equilibrium spatial distributions may develop in an apparently homogeneous reacting system. The importance of these effects can be assessed unequivocally if the rate constant has been measured and if the diffusion coefficients of the reactive species are known or estimable.¹⁴

In gas phase, transport processes are so rapid that no chemical reaction in an initially homogeneous system could appreciably perturb the equilibrium distribution of positions and momenta of the centers of mass of remaining unreacted species. However, collisional interactions in gas phase are not frequent during times necessary for significant motion along a reaction coordinate. Any attempt to use equilibrium population distributions is affected by the extent to which motion along this reaction coordinate is separable from other internal modes of motion. Decisions about separability are not made easily, but they are of concern not only for the unimolecular processes discussed above but also for bimolecular reactions like abstraction that seem to go during a single collision.

Equilibrium properties have been of great assistance as theories of chemical kinetics have developed. As our treatment of kinetic phenomena gets more detailed and sophisticated, the break with equilibrium theory becomes more and more complete. Each stage of the break is fraught with difficulty, and the present paper suggests a direction in which breaks may develop but provides little insight into their nature.

Acknowledgment.—The subject of this paper is part of the basic objective set in an application to the John Simon Guggenheim Foundation that led to a fellowship for the year 1955–1956. The clarification of the ideas has been proceeding slowly since then.

(12) T. Carrington and N. Davidson, *J. Phys. Chem.*, **57**, 418 (1953).

(13) O. K. Rice, *ibid.*, **65**, 1972 (1961).

(14) R. M. Noyes, *Progr. Reaction Kinetics*, **1**, 129 (1961).

The development of the approach used here was instigated by Dr. J. Halpern of the University of British Columbia when he pointed out the alternative derivations of eq. 2 during a convivial evening in the Munich Ratskeller. The trip during which that event took place was supported in part by the National Science Foundation.

Comments by referees have clarified numerous points and have led to three complete draftings of the manuscript. I accept responsibility for erroneous and unclear passages that remain. This working over of ideas has been supported in part by the U. S. Atomic Energy Commission under Contract AT(45-1)-1310.


THE STABILITY CONSTANTS OF THE MONO- AND DIPYRAZINESILVER COMPLEXES¹

BY JOHN G. SCHMIDT AND R. F. TRIMBLE

Department of Chemistry, Southern Illinois University, Carbondale, Illinois

Received November 30, 1961

The stepwise stability constant of $[\text{Ag}(\text{C}_4\text{H}_4\text{N}_2)]^+$ is 32.3 and of $[\text{Ag}(\text{C}_4\text{H}_4\text{N}_2)_2]^+$, 4.2. These values are calculated from the solubilities of Ag_2SO_4 and $[\text{Ag}(\text{C}_4\text{H}_4\text{N}_2)]\text{NO}_3$ in aqueous pyrazine. The solubility product of $[\text{Ag}(\text{C}_4\text{H}_4\text{N}_2)]\text{NO}_3$ is 2.3×10^{-4} .

A number of metal salt adducts with pyrazine  or its C-methyl derivatives have been reported² but no studies have been made of the equilibria involved. This paper describes a determination of the stability constants of $[\text{Ag}(\text{C}_4\text{H}_4\text{N}_2)]^+$ and $[\text{Ag}(\text{C}_4\text{H}_4\text{N}_2)_2]^+$ from solubility data.

When an aqueous solution of pyrazine is added to an excess of silver nitrate solution a precipitate of shiny white platelets forms immediately. If the order of addition is reversed, however, and silver nitrate is added to an excess of pyrazine, the precipitate is formed only very slowly and after cooling. In each case the precipitate is $[\text{Ag}(\text{C}_4\text{H}_4\text{N}_2)]\text{NO}_3$. There is no detectable odor of pyrazine over the dried salt.

Attempts to carry out conductometric titrations of silver nitrate with pyrazine or *vice versa* were unsuccessful. Breaks in the conductance curves did not occur at reasonable stoichiometric ratios nor were they reproducible. We believe that the shape of the curves depends on solubility and complex formation equilibria which are established only slowly. This led us to measure the solubility of silver sulfate and pyrazinesilver nitrate in pyrazine solutions. Stability constants for the two complexes were calculated from these data.

Experimental

Reagents.—The pyrazine was a research sample supplied by Wyandotte Chemicals Corp. Recrystallization was found to have no effect on the melting point or the ultraviolet absorption spectrum of the compound nor on the pH of its aqueous solutions. The material used in this study was not recrystallized. Stock solutions of pyrazine were made with distilled water and weighed amounts of the solid. The pyrazine solutions used in the solubility measurements were made by suitably diluting the stock solution. The other reagents used were all of analytical grade and used without further purification.

(1) From the M.A. Thesis of John G. Schmidt, Southern Illinois University, August 1961. A preliminary report was given at the 54th meeting of the Illinois State Academy of Science, April 28, 1961.

(2) (a) C. Stoehr, *J. prakt. Chem.*, [2] **47**, 453, 460, 470 (1893); **48**, 21 (1893); **49**, 402 (1894); **51**, 456, 459 (1895); (b) the most recent work is A. B. P. Lever, J. Lewis, and R. S. Nyholm, *Nature*, **189**, 58 (1961).

Pyrazinesilver Nitrate.—The addition of hot 0.01 *M* pyrazine to an equal volume of hot 0.03 *M* AgNO_3 immediately produced a large quantity of precipitate. When hot 0.01 *M* AgNO_3 was added to an equal volume of hot 0.03 *M* pyrazine no precipitate was obtained until after the solution had been cooled in ice. Both preparations were collected by filtration, washed with several portions of cold water, and dried at room temperature. When washed free of excess AgNO_3 the material was stable toward light. Silver was determined by the Volhard method.

Sample 1 (made with excess AgNO_3)	42.94% Ag
Sample 2 (made with excess $\text{C}_4\text{H}_4\text{N}_2$)	42.95% Ag
Calcd. for $[\text{Ag}(\text{C}_4\text{H}_4\text{N}_2)]\text{NO}_3$	43.16%

In sealed capillary tubes both samples decomposed at 239° without prior discoloration. Stoehr² reported the compound to become discolored at about 200° and to decompose at 253°.

The Solubility of Ag_2SO_4 .—Solid Ag_2SO_4 was added to 50 ml. of pyrazine solution in 28-ml. glass stoppered bottles, which were agitated in a constant temperature bath at $30.0 \pm 0.01^\circ$ for an hour. No increase in solubility was observed for longer equilibration times. The solutions then were filtered and the total dissolved silver determined by the Volhard method. The pyrazine concentrations ranged from 0 to 0.2 *M*. The solubility measured in pure water (0.0283 *M*) falls almost exactly on a line plotted through the points obtained by Simons and Ricci.^{3a} During the titrations there was occasionally some solid pyrazinesilver nitrate present but this was rapidly converted to the much less soluble AgSCN and did not interfere with the analysis.

The Stability Constant of $[\text{Ag}(\text{C}_4\text{H}_4\text{N}_2)]^+$.—The solubility of Ag_2SO_4 in water, 0.0283 *M*, and the corresponding ionic strength, 0.0850, were substituted into the equation derived by Vosburgh and McClure^{3b} for the solubility of Ag_2SO_4 as a function of ionic strength at 25°. This gives the equation

$$2 \log[\text{Ag}^+] + \log[\text{SO}_4^{2-}] - (3\sqrt{\mu})/(1 + \sqrt{\mu}) = 0.360 \mu - 4.749 \quad (1)$$

where -4.749 is the logarithm of the solubility product at zero ionic strength and 30°.

The measured solubility in pyrazine solution gives the sulfate ion concentration and ionic strength from which the free silver ion concentration can be calculated by means of eq. 1. The concentration of complexed silver is the difference between this free silver concentration and the total silver concentration measured by the solubility. With the assumption that, to a first approximation, there is no dipyrazinesilver formed in these solutions, the stability constant, $K_1 = [\text{AgPz}^+]/[\text{Ag}^+][\text{Pz}]$, can be calculated from the equation: $K_1 = (C_{\text{Ag}} - [\text{Ag}^+])/[\text{Ag}^+][\text{Pz}] - C_{\text{Ag}} + [\text{Ag}^+]$ where

(3) (a) E. L. Simons and J. E. Ricci, *J. Am. Chem. Soc.*, **68**, 2194 (1946); (b) W. C. Vosburgh and R. S. McClure, *ibid.*, **65**, 1060 (1943).

C_{Pz} and C_{Ag} are the total pyrazine and total silver concentrations. The results are shown in Table I.

TABLE I: K_1 CALCULATED FROM THE SOLUBILITY OF Ag_2SO_4 IN PYRAZINE

C_{Ag}, M	C_{Pz}, M	$[Ag^+], M$	K_1
0.0566	0	0.0566	..
.0598	0.005	.0564	37.7
.0623	.010	.0560	30.4
.0656	.015	.0556	36.0
.0672	.020	.0552	27.2
.0791	.040	.0541	30.9
.0897	.060	.0533	28.9
.1358	.140	.0516	29.2
.1296 ^a	.180		
.1194 ^a	.200		

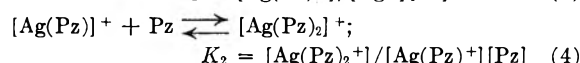
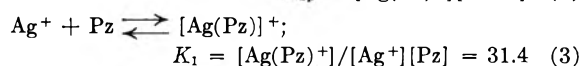
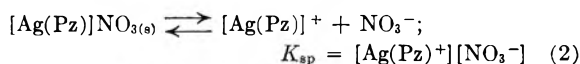
31.4 ± 3.6

^a The solid phase was yellow instead of white.

The values at 0.18 and 0.20 M pyrazine cannot be used because of the change in the nature of the solid phase. The values of K_1 do not show a trend to lower values at higher pyrazine concentrations and this, together with their approximate constancy, justifies the initial assumption that the dipyrazinesilver concentration is negligible. The average value of K_1 is 31.4 with a standard deviation of 3.6.

The Instability Constant of $[Ag(C_4H_4N_2)_2]^+$.—Varying amounts of stock pyrazine and $AgNO_3$ solutions were run into 2-oz. bottles from burets and the total volume brought to 50 ml. with distilled water. The bottles were agitated at $30.0 \pm 0.1^\circ$ for an hour. Our experience in carrying out conductimetric titrations of $AgNO_3$ with pyrazine indicated that equilibrium was reached in this time. The solutions were filtered and the total dissolved silver determined by the Volhard method.

In a saturated solution of pyrazinesilver nitrate in pyrazine the following equilibria exist



If at low pyrazine concentrations we can neglect the dipyrazinesilver concentration, we have the relations

$$C_{Ag} = [Ag^+] + [Ag(Pz)^+]$$

$$C_{Pz} = [Pz] + [Ag(Pz)^+]$$

$$[NO_3^-] = C_{Ag}, \text{ and}$$

$$K_{sp} = (C_{Ag})(X - \sqrt{X^2 - Y})/2 \text{ where } X = C_{Ag} + C_{Pz} + 31.4 \text{ and } Y = 4(C_{Ag})(C_{Pz})$$

The positive root of $\sqrt{X^2 - Y}$ gives a $[Ag(Pz)]^+$ concentration greater than C_{Ag} and so is discarded. The solubilities (equal to C_{Ag}) of $[Ag(Pz)]NO_3$ in pyrazine solutions are given in Table II together with the calculated K_{sp} values.

The solid complex was made *in situ* by adding silver nitrate to aqueous pyrazine. The first three entries in the table are for solutions made up with an excess of silver nitrate and thus correspond to the determination of the solubility of $[Ag(Pz)_2]NO_3$ in $AgNO_3$ solution rather than in pyrazine solution.

It can be seen from Table II that the calculated value of K_{sp} remains fairly constant up to a point that corresponds to a solution of $[Ag(Pz)]NO_3$ in 0.060 M pyrazine. The average value of the first eight determinations is 2.28×10^{-4} with a standard deviation of 0.10×10^{-4} . At higher pyrazine concentrations the calculated K_{sp} increases. This indicates the failure of the assumption that no $[Ag(Pz)_2]^+$ is formed.

Knowing K_1 and the K_{sp} of $[Ag(Pz)]NO_3$ we can calculate K_2 from the data at high pyrazine concentrations. In these solutions we have

$$C_{Ag} = [Ag^+] + [AgPz^+] + [AgPz_2^+]$$

$$C_{Pz} = [Pz] + [AgPz^+] + 2[AgPz_2^+]$$

$$[AgPz^+] = K_{sp}/C_{Ag} \text{ and}$$

$$[Ag^+] = K_{sp}/K_1[Pz]C_{Ag} \text{ whence}$$

$$[Pz]^2 + (2C_{Ag} - C_{Pz} - K_{sp}/C_{Ag})[Pz] - 2K_{sp}/K_1C_{Ag} = 0$$

After solving this equation for the free pyrazine concentration one can find the concentrations of free silver and of dipyrazinesilver and then calculate K_2 . The results of these calculations are shown in Table III. These figures correspond to the last seven entries in Table II. The values of K_2 seem to approach a value of about 4.5 as the pyrazine concentration increases. The average of the last 5 values of K_2 is 4.2 with a standard deviation of 0.5.

TABLE II

SOLUBILITY PRODUCT OF $[Ag(Pz)]NO_3$

C_{Ag}, M	C_{Pz}, M	K_{sp}	
0.0566	0.0066	2.32×10^{-4}	
.0343	.0143	2.26×10^{-4}	
.0266	.0226	2.18×10^{-4}	
.0236	.0316	2.27×10^{-4}	
.0208	.0448	2.23×10^{-4}	
.0196	.0556	2.22×10^{-4}	Av. value
.0193	.0593	2.24×10^{-4}	(2.28 ± 0.10)
.0192	.0792	2.49×10^{-4}	× 10 ⁻⁴
.0193	.1193	2.71×10^{-4}	
.0197	.1397	3.08×10^{-4}	
.0204	.1604	3.40×10^{-4}	
.0204	.1704	3.44×10^{-4}	
.0205	.1804	3.55×10^{-4}	

TABLE III

VALUE OF K_2 CALCULATED FROM THE SOLUBILITY OF $[Ag(Pz)NO_3]$ IN PYRAZINE

C_{Ag}, M	C_{Pz}, M	$[Ag^+], M$	$[Pz], M$	$[Ag^+Pz^+], M$	$[Ag^+Pz_2^+], M$	K_2
0.0193	0.0573	0.0078	0.0478	0.0115	0	..
.0192	.0792	.0059	.064	.0116	0.0017	(2.5)
.0193	.01192	.0037	.0996	.0115	.0041	3.6
.0197	.1397	.0031	.1178	.0113	.0053	4.0
.0204	.1604	.0026	.1357	.0109	.0069	4.8
.0204	.1704	.0024	.1454	.0109	.0071	4.5
.0205	.1804	.0023	.1548	.0109	.0073	4.3

4.2 ± 0.5

With a value for K_2 one can recalculate the value of K_1 from the solubility of silver sulfate in pyrazine without assuming the absence of dipyrazinesilver.

The average initial and corrected values of K_1 are 31.4 ± 3.6 and 32.3 ± 3.5 , respectively. Because the correction is small compared to the standard deviation of K_1 the corrected value was not used to obtain a corrected value of K_2 .

Discussion

In our calculations we have ignored the possible formation of species such as $[Ag_2(Pz)]^{++}$ and $[AgH(Pz)]^{++}$. Our justification for this is the very low basicity of the second nitrogen: $pK_{HI,+} = 0.65$, $pK_{H_2L,+} = -5.78$.⁴ The geometry of the ligand precludes chelation. Aliphatic diamines form a complex of the type $[Ag_2(\text{amine})_2]^{++}$, as does the only aromatic heterocyclic diamine previously studied, 2,2'-bipyridine.⁵ Although solubility data such as ours is inadequate for the study of polynuclear complexes it seems probable that this dimeric species can be ruled out on the basis of ligand geometry and the low $pK_{HI,+}$.

(4) A. S. C. Chia and R. F. Trimble, *J. Phys. Chem.*, **65**, 863 (1961).

(5) E. Scrocco and O. Salvetti, *Boll. sci. fac. chim. ind. Bologna*, **12**, 98 (1954).

Peard and Pflaum⁶ prepared a number of solid complexes of silver with aromatic heterocyclic amines. Only 4,8-dimethylquinoline and 4,4'-bipyridine gave 1:1 complexes instead of $[\text{Ag}(\text{amine})_2]^+$. The 1:2 complexes all melted without decomposition at temperatures below 160°. The bipyridine complex, like our pyrazine complex, had a very high melting point (250°) which led the authors to suggest a polymeric structure. In solid $[\text{Ag}(\text{Pz})\text{NO}_3]$ there may be polymeric chains in which pyrazine acts as a bidentate bridging group. A similar structure has been suggested for solid nickel pyrazine complexes.^{2b}

A value of K_2 less than K_1 is very unusual for monodentate ligands. Of the 17 complexes of silver with aromatic heterocyclic amines listed in "Stability Constants"⁷ $\log K_1$ and $\log K_2$ values are given for 10 (Table nos. 113, 117-9, 166-8, 202-3, 246), of which only 4-methoxypyridine forms complexes with $K_2 < K_1$. The ratio $\log K_2/\log K_1$ ranges from 0.95 to 1.32 for these complexes. For pyrazinesilver the value is 0.62/1.51 or 0.41. Weimer and Fernelius⁸ data on the silver complex of 6-methyl-2-picolyamine give $\log K_2/\log K_1 = 0.87$. It is

(6) W. J. Peard and R. T. Pflaum, *J. Am. Chem. Soc.*, **80**, 1593 (1958).

(7) J. Bjerrum, G. Schwarzenbach, and L. G. Sillén, "Stability Constants of Metal-Ion Complexes," Part I, The Chemical Society, London, 1957.

(8) H. R. Weimer and W. C. Fernelius, *J. Phys. Chem.*, **64**, 1951 (1960).

thought that the coordination is through the primary amine rather than the ring N so it cannot be compared with the aromatic heterocyclic amine complexes considered above.

Pyrazinesilver complex is atypical in yet another way. The ratio $\log K_1/pK_a$ is approximately constant for silver complexes with a given type of amine.⁹ For aliphatic amines the ratio varies from 0.25 for primary amines to 0.32 for tertiary amines. For aromatic heterocyclic amines the value ranges from 0.31 to 0.43 with an average of 0.36. The fractional value is to be expected since the proton has a tremendously greater ionic potential than a metal ion. For pyrazinesilver, however, $\log K_1/pK_a$ is 2.3. The stability is some hundred-fold greater than we would expect from the basicity of pyrazine alone. We do not know the source of this extra stability. If pi bonding were involved we would expect extra stability to appear with other aromatic heterocyclic amine complexes. Furthermore, there is evidence that pi bonding does not occur in solid cobalt, nickel, or manganese complexes with pyrazine.^{2b}

Acknowledgments.—This work was supported by the Graduate Council of Southern Illinois University. We also are indebted to the Wyandotte Chemicals Corporation for a generous sample of pyrazine.

(9) G. Schwarzenbach, *Helv. Chim. Acta*, **36**, 23 (1953).

EFFECTS OF SOLUTION COMPOSITION ON THE POTENTIALS OF THE COUPLES: Np(V-VI), Fe(II-III), Hg(0-I), AND Hg(I-II)¹

BY A. J. ZIELEN AND J. C. SULLIVAN

Argonne National Laboratory, Argonne, Illinois

Received December 4, 1961

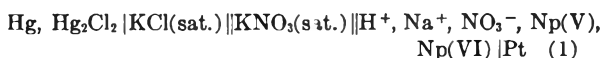
A linear variation with hydrogen ion concentration was found for the formal potential of the Np(V-VI) couple at 25° in perchloric acid-sodium or lithium perchlorate solutions of ionic strength 2. The major portion and very probably all of this acid dependence is shown to be caused by activity coefficient changes, reaffirming NpO_2^+ and NpO_2^{2+} as the only Np(V) and Np(VI) species of consequence in acid solutions. Similar measurements in sodium perchlorate solutions were made of the Fe(II-III), Hg(0-I), and Hg(I-II) couples. Equations for the formal potentials as a function of hydrogen ion concentration are given, and activity coefficient effects produced by the substitution of Na^+ or Li^+ for H^+ at constant ionic strength are discussed.

Introduction

The assignment of the general formulas MO_2^+ and MO_2^{2+} as the dominant species in acid solution for the (V) and (VI) oxidation states of U, Np, Pu, and Am is based on a variety of evidence.² Earlier this assignment was largely based on the reversibility and acid independence of the actinide (V-VI) couples, but at present the infrared measurements of Jones and Penneman³ probably represent the single, most compelling proof. However, the hydrogen ion dependence of these oxidation-reduction couples remains the most direct test of the species

involved, especially if only minor amounts of other forms are present.

In the only reported study of the Np(V-VI) couple as a function of acidity, a definite though minor hydrogen ion dependence was observed. Magnusson, Hindman, and LaChapelle⁴ studied the cell



Holding the nitrate concentration constant at 1.02 M, the hydrogen ion was varied from 0.12 to 1.02 M. This resulted in a 20 mv. variation in the observed e.m.f. compared to a 55 mv. predicted change if the (V-VI) couple possessed a first power

(1) Based on work performed under the auspices of the U. S. Atomic Energy Commission.

(2) J. J. Katz and G. T. Seaborg, "The Chemistry of the Actinide Elements," Methuen and Co., Ltd., London, 1957, pp. 176-179, 220-223, 292-297, 366-370.

(3) L. H. Jones and R. A. Penneman, *J. Chem. Phys.*, **21**, 542 (1953).

(4) L. B. Magnusson, J. C. Hindman, and T. J. LaChapelle, Paper 15.4, "The Transuranium Elements," National Nuclear Energy Series, IV, McGraw-Hill Book Co., Inc., New York, N. Y., 1949, Vol. 14B, Part II, p. 1059.

hydrogen ion dependence. However, independent experiments indicated that at least 10 mv. and perhaps all of this change was due to the junction potential of the saturated potassium nitrate bridge. Thus, although a small hydrogen ion effect appeared very probable, the authors concluded the Np(V-VI) couple to be mainly acid independent.

In a recent communication we have described procedures for precise measurements of the Np(V-VI) couple without liquid junction potential, using the glass electrode as an intermediate for the standard hydrogen electrode.⁵ Determination of formal potentials by this method allowed a critical test of any hydrogen ion dependence of the Np(V-VI) couple. In order to investigate possible changes in activity coefficients, similar measurements also were made of the formal potentials of the couples: Fe(II-III), Hg(0-I), and Hg(I-II).

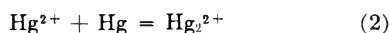
Experimental

Reagents and Analytical Procedures.—An approximately 1:1 ferrous-ferric perchlorate stock solution was prepared by dissolving the reagent grade sulfates in water followed by titration with barium perchlorate. The barium sulfate precipitate was removed by centrifugation and passage through a fine sintered glass filter. After standing several days, the filtration was repeated and the solution diluted to final volume with a known amount of dilute perchloric acid. It was estimated that the slight excess of barium perchlorate used amounted to $ca. 3 \times 10^{-4} M$ in the final cell solutions.

The equilibrium ferrous concentrations were determined by direct micro titrations of cell solution samples at the end of each potential run, using standard ceric sulfate and ferroin indicator. A comparison check of the micro titration procedure with macro scale results agreed within 0.1%. Ferric content was taken as the difference from the calculated total iron concentration obtained by a Zimmermann-Reinhardt process standardization of the ferrous-ferric stock.

A mercurous perchlorate and a mixed mercurous-mercuric perchlorate stock were prepared by dissolution of a weighed amount of HgO (yellow, Mallinckrodt, analytical reagent) in a known excess of perchloric acid. A portion of this solution was stored over metallic mercury with frequent and vigorous shaking. After several days equal aliquots of the resulting Hg(I) solution and the original Hg(II) solution were combined to form the mixed Hg(I-II) stock. All metallic mercury was triple distilled and filtered before use.

The mercury(I) and (II) concentrations in the cell solutions all were calculated quantities based on the original weight of HgO used plus appropriate minor corrections for the equilibrium⁶



Primarily this assumed stability of the Hg(I-II) stock. This was checked by analysis for Hg(I) in the mixed stock at the end of the cell measurements (a three-week period) by the method of Willard and Young.⁷ The calculated and found concentration agreed within 0.2%.

Details of the neptunium(V) and (VI) preparation and all other reagents employed have been summarized previously.⁸ Two independent stock solutions, A and B, of mixed neptunium(V-VI) perchlorates were used. In the final cell solutions stocks A and B, respectively, gave total neptunium concentrations of 2.167 and $1.005 \times 10^{-2} M$ and approximate Np(V)/Np(VI) ratios of 1.04 and 1.22. As before⁵ the actual Np(V)/Np(VI) ratio was determined directly by multiple spectrophotometric analyses of the cell solutions at the end of each potential run. The hydrogen ion concentrations of the cell solutions from stock A were determined by direct micro titration with standard base after reduction of all neptunium to the (V) state with excess sodium nitrite.

(5) J. C. Sullivan, J. C. Hindman, and A. J. Zielen, *J. Am. Chem. Soc.*, **83**, 3373 (1961).

(6) S. Hietanen and L. G. Sillén, *Arkiv Kemi*, **10**, 103 (1956).

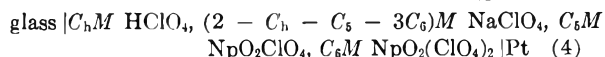
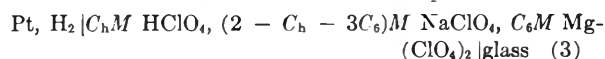
(7) H. H. Willard and P. Young, *J. Am. Chem. Soc.*, **62**, 557 (1930).

(8) J. C. Sullivan, A. J. Zielen, and J. C. Hindman, *ibid.*, **82**, 5288 (1960).

This is a satisfactory procedure only at relatively high acid and low neptunium concentrations. To extend our measurements below 0.2 *M* hydrogen ion, stock B was prepared with a low free acid concentration ($ca. 10^{-2} M$); and the pH of the stock solution was measured after a tenfold dilution with a Beckman Model G pH Meter. Conversion to moles/l. of hydrogen ion was done by calibration with solutions of known acidity and similar ionic strength. The $[\text{H}^+]$ of the cell solutions then was calculated from make-up with a minimum of 97% of the total acid obtained from the addition of a pure perchloric acid stock.

The hydrogen ion concentrations of the iron and mercury cells also were obtained by calculation. However, the free acid contents of these stocks were accurately known, and their maximum contribution to the total hydrogen ion was only about 10%.

Potentiometric Measurements.—Illustrating with the Np(V-VI) couple, potentials as a function of hydrogen ion concentration or C_h were made on the cell pairs



With C_5 and C_6 —the Np(V) and Np(VI) concentrations—relatively small ($ca. 5 \times 10^{-3}$ or 10^{-2}), the hydrogen ion response of the glass electrode is assumed the same in the similar solutions of cells 3 and 4. Addition of the two potentials gives the junction-free e.m.f. of the reaction



Details of the apparatus and procedure have been described.⁵ However, it should be noted that in cells of type 3 there is a cancellation of hydrogen ion activity and hence no need to match precisely the acidities of cells 3 and 4. At one atmosphere of hydrogen the e.m.f. of (3) supplies the "standard potential" of the glass electrode with possible changes in the asymmetry potential of the glass as the only variable. Thus our basic assumption of identical glass electrode response in two different but similar solutions requires only matching of the asymmetry potentials. This has been verified under much more drastic conditions than encountered here and will be discussed in a subsequent manuscript.

Cell pairs similar to (3) and (4) were used for the Hg(I-II) and Fe(II-III) couples, using Y^{3+} as an inert substitute for Fe^{3+} . The shiny platinum electrode of (4) was replaced by a mercury pool contacted by a platinum needle for the Hg(0-I) couple. Two types of Beckman glass electrodes were employed: the now obsolete 290-7 and the current 39177. The stability performance of the latter type was much superior, probably because of the improved shielding which extends well into the body of the electrode. The 39177 electrode was used only in cells prepared from mixed neptunium stock B.

All measurements were carried out at $25.00 \pm 0.02^\circ$ in solutions of ionic strength 2.00 with substitution of sodium or lithium perchlorate for perchloric acid. The moles/l. concentration scale was used throughout and the potentials are given in absolute volts. The signs of cells and relative electrode potentials conform to the Stockholm Convention.⁹ Hydrogen electrode potentials were converted to the standard one atmosphere by conventional barometric, hydrostatic, and water vapor pressure corrections. Cell solution vapor pressures were calculated by linear interpolation from osmotic coefficient data of pure 2 *M* perchloric acid and sodium or lithium perchlorate.¹⁰

Results

The results for each couple are presented in terms of the formal potential E' . The following equations summarize first the method of calculating E' from the observed e.m.f. E and second the relationship of E' to the standard potential E^0 and the pertinent activity coefficient terms. Concentrations in moles/l. are indicated by brackets and mean molar activity coefficients by γ . The γ sub-

(9) J. A. Christiansen, *ibid.*, **82**, 5517 (1960).

(10) R. A. Robinson and R. H. Stokes, "Electrolyte Solutions," Academic Press, Inc., New York, N. Y., 1959, p. 483.

scripts h, 5, 6, 2, 3, 1, and 2' refer, respectively, to y_{\pm} of HClO_4 , NpO_2ClO_4 , $\text{NpO}_2(\text{ClO}_4)_2$, $\text{Fe}(\text{ClO}_4)_2$, $\text{Fe}(\text{ClO}_4)_3$, $\text{Hg}_2(\text{ClO}_4)_2$, and $\text{Hg}(\text{ClO}_4)_2$. Throughout we have abbreviated the familiar $2.30258 RT/F$ term by k , and at 25° the value of k used was 0.059156 abs. v.

Np(V)-Np(VI)

$$E' = E + k \log [\text{H}^+][\text{Np(V)}]/[\text{Np(VI)}] \quad (6a)$$

$$E' = E^0_{\text{Np(V-VI)}} - k \log y_h^2 y_5^2 / y_6^3 \quad (6b)$$

 $\text{Fe}^{2+}-\text{Fe}^{3+}$

$$E' = E + k \log [\text{H}^+][\text{Fe}^{2+}]/[\text{Fe(III)}] + E_{\text{hydr}} \quad (7a)$$

$$E' = E^0_{\text{Fe(II-III)}} - k \log y_h^2 y_2^2 / y_3^4 \quad (7b)$$

$$E_{\text{hydr}} = k \log (1 + 1.5 \times 10^{-3} / [\text{H}^+] + 5.2 \times 10^{-3} [\text{Fe}^{3+}] / [\text{H}^+]^2) \quad (7c)$$

Hg-Hg₂²⁺

$$E' = E + 0.5 k \log [\text{H}^+]^2 / [\text{Hg}_2^{2+}] \quad (8a)$$

$$E' = E^0_{\text{Hg(0-1)}} - 0.5 k \log y_h^4 / y_1^3 \quad (8b)$$

 $\text{Hg}_2^{2+}-\text{Hg}^{2+}$

$$E' = E + 0.5 k \log [\text{H}^+]^2 [\text{Hg}_2^{2+}] / [\text{Hg(II)}]^2 + E_{\text{hydr}} \quad (9a)$$

$$E' = E^0_{\text{Hg(I-II)}} - 0.5 k \log y_h^4 y_3^3 / y_2^6 \quad (9b)$$

$$E_{\text{hydr}} = k \log (1 + 2 \times 10^{-4} / [\text{H}^+]) \quad (9c)$$

The quantity E_{hydr} included in eq. 7 and 9 represents minor corrections applied to E' for the known hydrolysis reactions of Fe^{3+} and Hg^{2+} . The constants of Milburn and Vosburgh¹¹ at 25° and $\mu = 2$ for the formation of FeOH^{2+} and $\text{Fe}_2(\text{OH})_2^{4+}$ furnished the parameter values for (7c), and the results of Hietanen and Sillén¹² at 25° and $\mu = 0.5$ were used despite the difference in ionic strength for (9c). The maximum E_{hydr} values were 0.29 mv. for the iron cells and 0.03 mv. for the Hg(I-II) couple. Hydrolysis corrections involving Fe(II) and Hg(I) can be safely assumed negligible at the $[\text{H}^+]$ values employed here.^{3,14}

The observed effects on E' produced by the substitution of Na^+ or Li^+ for H^+ at constant ionic strength are presented in Fig. 1 and Table I. In each case the data can be represented within experimental uncertainty by the empirical equation

$$E' = a + b[\text{H}^+] \quad (10)$$

The actual data points are illustrated in Fig. 1 as the change in E' with increasing acid concentration, i.e., $\Delta E' = E' - a$. For clarity each of the ordinate intercepts has been successively increased by 0.5 mv. Table I lists the a and b parameter values found for each couple by least squares analyses of the data with an IBM 704 computer. Within the $[\text{H}^+]$ limits listed, these values and eq. 10 provide a compact summary of the acid dependence of the formal potentials. The column headed σ contains the least squares standard deviations of E' and indicates the experimental precision attained for each couple.¹⁵ The metal ion concentrations for each couple are summarized in the legend of Fig. 1.

(11) R. M. Milburn and W. C. Vosburgh, *J. Am. Chem. Soc.*, **77**, 1352 (1955).

(12) S. Hietanen and L. G. Sillén, *Acta Chem. Scand.*, **6**, 747 (1952).

(13) B. O. A. Hedström, *Arkiv Kemi*, **5**, 457 (1953).

(14) W. Forsling, S. Hietanen, and L. G. Sillén, *Acta Chem. Scand.*, **6**, 901 (1952).

(15) Note that the low σ of the Fe(II-III) couple corresponds to the only case where a really precise measure of cell component concentrations could be made, and thus it gives the best indication of the precision of our technique with the glass electrode.

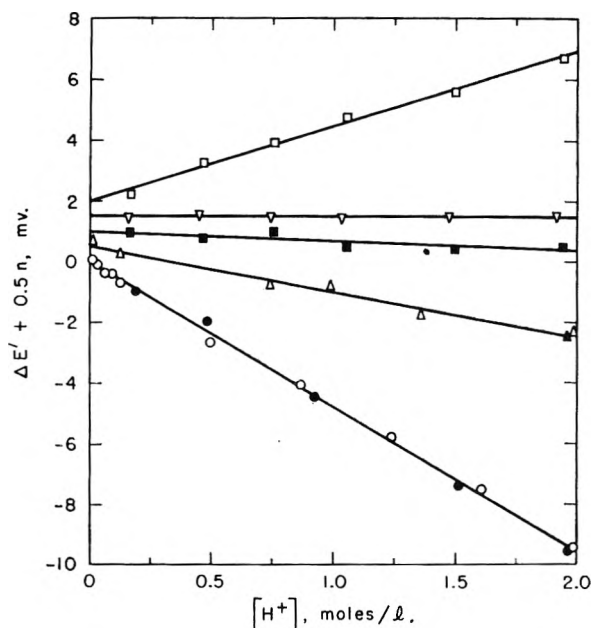


Fig. 1.—Formal potential changes with the replacement of Na^+ or Li^+ by H^+ at $\mu = 2$. Ordinate displacement for clarity indicated by n value. Np(V-VI) couple: ● and ○, stocks A and B in NaClO_4 , $n = 0$; ▲ and △, stocks A and B in LiClO_4 , $n = 1$; see text (exp. section) for details of Np stocks A and B. Hg(0-I) couple: ■, $[\text{Hg}_2^{2+}] = 0.01981 M$, $n = 2$; Fe(II-III) couple: ▽, $\Sigma \text{Fe} = 0.01930 M$, $[\text{Fe}^{2+}] \cong 0.0106 M$, $n = 3$; Hg(I-II) couple: □, $[\text{Hg}_2^{2+}] = 0.00986 M$, $[\text{Hg(II)}] = 0.01002 M$, $n = 4$.

TABLE I

VARIATION OF FORMAL POTENTIALS WITH $[\text{H}^+]$ AT 25° AND $\mu = 2.00$

Couple	$[\text{H}^+]$ Range, moles/l.	$E' = a + b[\text{H}^+]$		
		a , abs. v.	$b \times 10^4$, mv. l./mole	σ , mv.
Np(V-VI) ^a	0.0113-1.985	1.12940	-1.51	0.19
Np(V-VI)	0.128-1.985	1.13599	-4.78	.18
Fe(II-III)	.1593-1.916	0.73748	0.00	.08
Hg(0-I)	.1658-1.941	.77094	-0.31	.17
Hg(I-II)	.1658-1.941	.91544	2.46	.16

^a In LiClO_4 solutions, all others in NaClO_4 .

The observed variation in E' of the Np(V-VI) couple is in the same direction though not as large as the earlier results.⁴ Respective 25° values of 1.1364 and 1.1268 abs. v. for the formal potential in 1 M HClO_4 and in 1 M $\text{Mg}(\text{ClO}_4)_2 + 0.1 M$ HClO_4 have been previously determined⁵ and indicate the sensitivity to medium of this neptunium couple.

For the Fe(II-III) couple at 25° a formal potential of 0.7394 v. in 0.5 M HClO_4 has been determined by Connick and McVey,¹⁶ and Magnusson and Huizenga¹⁷ report 0.738 ± 0.001 v. for solutions 0.25 to 1 M in HClO_4 with NaClO_4 added to maintain an ionic strength of one. These values and our result at $\mu = 2$ are in accord with the slow decrease in E' with increasing ionic strength indicated by the data of Schumb, Sherrill, and Sweetser.¹³

No comparable formal potential values for the individual mercury couples could be found in the

(16) R. E. Connick and W. H. McVey, *J. Am. Chem. Soc.*, **73**, 1798 (1951).

(17) L. B. Magnusson and J. R. Huizenga, *ibid.*, **75**, 2242 (1953).

(18) W. C. Schumb, M. S. Sherrill, and S. B. Sweetser, *ibid.*, **59**, 2360 (1937).

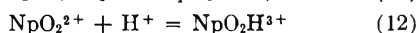
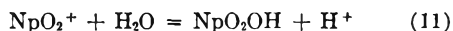
literature. However, the difference $E'_{I-II} - E'_{0-I}$, which equals $k \log K_2$ where K_2 is the concentration equilibrium quotient of reaction 2, can be compared against the results of Hietanen and Sillén.⁶ Using the mean of their tabulated values in 0.01 M $HClO_4$ and $\mu = 2(NaClO_4)$ and their estimated $Hg(II)$ hydrolysis correction, we calculate: $134.1 + 9.8 + 0.6 = 144.5 \pm 0.5$ mv. for the formal potential difference. At the same acidity the parameters of Table I give the excellent check 144.53 mv. even though this represents a significant extrapolation from our lowest observed hydrogen ion concentration (*ca.* 0.17 M).

Discussion

Numerous investigations of mixed electrolyte systems at constant ionic strength have indicated that appreciable activity coefficient changes commonly occur. Generally Harned's rule is closely followed. That is the logarithms of the individual mean activity coefficients are linear functions of medium changes.¹⁹ Hence the linear dependencies of $\Delta E'$ (or E') in Fig. 1 are readily rationalized. However, for the case of the $Np(V-VI)$ couple it is also necessary to consider the possibility of multiple $Np(V)$ or $Np(VI)$ species in hydrogen ion dependent equilibria.

$Np(V)$ and $Np(VI)$ Species.—The maximum observed change in E' amounted to 9.4 mv. compared to *ca.* 130 mv. expected if the $Np(V-VI)$ couple has a first power $[H^+]$ dependence. Clearly this indicates the primary neptunium species to be similarly oxygenated, or NpO_2^+ and NpO_2^{2+} on the firm basis established for the $Np(VI)$ structure.³

Since Fig. 1 indicates no effect on doubling the neptunium concentration, polynuclear species cannot be important. The direction of change in E' does indicate the possibility of either or both the reactions



And quantitatively their effect on E' can be expressed as

$$E' = E^0 - E_y + k \log ([H^+] + K_{11})/[H^+] \quad (13)$$

$$E' = E^0 - E_y - k \log (1 + K_{12}[H^+]) \quad (14)$$

where K_{11} and K_{12} are the concentration equilibrium quotients of (11) and (12) and E_y abbreviates the activity coefficient contribution of eq. 6b.

Neither (13) nor (14) predict the observed linear variation of E' with $[H^+]$. In fact this allows elimination of reaction 11 as important since it would require a marked upward curvature of the formal potential as $[H^+]$ approaches zero. This is in accord with the negligibly small pK_{11} of 8.9 estimated by Kraus.²⁰

The possible effect of reaction 12 is more subtle. Assuming constant activity coefficients, a reasonably good fit to the data can be made with eq. 14. A

(19) See for example, H. S. Harned and B. B. Owen, "The Physical Chemistry of Electrolytic Solutions," Reinhold Publ. Corp., New York, N. Y., 3rd ed., 1958, Chap. 14. However, here we intend a more general statement than the usual ternary system of H_2O and two mixed salts.

(20) K. A. Kraus, Paper P/731, "Proceedings of the International Conference on the Peaceful Uses of Atomic Energy," United Nations, New York, N. Y., 1956, Vol. 7, p. 245.

general least squares analysis with the IBM 704 gave respectively in sodium and lithium perchlorates: $K_{12} = 0.222$ and 0.063 l./mole and E' standard deviations of 0.25 and 0.18 mv. The 3.5-fold change of K_{12} with medium is impossibly large and obviously contradicts the assumption of constant activity coefficients.

Thus although the present data do not allow the occurrence of reaction 12 to be entirely dismissed, very plausibly all and certainly most of the acid dependence of E' in sodium perchlorate solutions must be caused by changes in activity coefficients. The non-existence of any appreciable amount of NpO_2H^{3+} also is indicated by the hydrogen ion dependencies observed in all oxidation-reduction kinetic studies made to date with $Np(VI)$.^{8,21} The isotopic exchange kinetics of $Np(V)$ and $Np(VI)$ presents a special case where a hydrogen ion dependent path was observed that does require either NpO_2H^{3+} or the more probable NpO_2H^{2+} as an intermediate.²² However, over a perchloric acid range of 0.1 to 3 M the form of the observed rate law would require $K_{12}[H^+] \ll 1$ (or the equivalent K for NpO_2H^{2+}).

Activity Coefficient Effects.—Assuming Harned's rule behavior, each of the activity coefficient terms of eq. 6b through 9b can be expressed as

$$\log y_j = \log y_{(0)j} + \alpha_j [H^+] \quad (15)$$

where $y_{(0)j}$ indicates the mean molar activity coefficient of component j at infinite dilution in 2 M sodium (or lithium) perchlorate and α_j is a parameter. Illustrating with the $Np(V-VI)$ couple, eq. 6b then can be written as

$$E' = E^0_{Np(V-VI)} - E_{(0)y} - 2k(\alpha_h + \alpha'_5 - 1.5\alpha'_6)[H^+] \quad (16)$$

$$E_{(0)y} = k \log (y_{(0)h} y_{(0)5}^2 / (y_{(0)6})^3) \quad (17)$$

The α_h parameter is the same as the α_{12} used by Harned and Owen for acid-salt mixtures.¹⁹ However, the primes on α'_5 and α'_6 indicate a different but related type of parameter expressing the activity coefficient change of a species at infinite dilution as the constant ionic strength medium is changed from pure salt to pure acid.

Equations similar to (16) are readily derived for each of the couples and predict the linear relationship of E' and $[H^+]$. Representing in each case the combined α terms by $f(\alpha)$, it follows that $f(\alpha) = -b/2k$, where the b parameters are as listed in Table I. This assumes a negligibly small change in E' and hence b as the relatively low metal ion concentrations of each couple are reduced to zero. The form and values obtained for each couple are presented in Table II. Subscripts are as defined for eq. 6 through 9.

Considering the wide usage of perchloric acid and sodium or lithium perchlorates as constant ionic strength media, it is remarkable that no activity coefficient data are available for these acid-salt mixtures. However, the order of magnitude of α_h can be obtained by estimating the activity coeffi-

(21) (a) A. J. Zielen, J. C. Sullivan, D. Cohen, and J. C. Hindman, *J. Am. Chem. Soc.*, **80**, 5632 (1958); (b) J. C. Hindman, J. C. Sullivan, and D. Cohen, *ibid.*, **81**, 2316 (1959); **79**, 4029 (1957); **76**, 3278 (1954).

(22) J. C. Sullivan, D. Cohen, and J. C. Hindman, *ibid.*, **79**, 3672 (1957).

TABLE II

HARNED'S RULE PARAMETERS AT 25° AND $\mu = 2.00$

Couple	$f(\alpha)$	$-b/2k, l./mole$
Np(V-VI)	$\alpha_h + \alpha'_6 - 1.5\alpha'_6$	0.0128 ^a .0404
Fe(II-III)	$\alpha_h + 1.5\alpha'_2 - 2\alpha'_3$.0000
Hg(0-I)	$\alpha_h - 0.75\alpha'_1$.0026
Hg(I-II)	$\alpha_h + 0.75\alpha'_1 - 1.5\alpha'_2'$	-.0208

^a In LiClO₄ solutions, all others in NaClO₄.

cient of the infinitely dilute acid in the pure salt solution as the geometric mean of the pure component activity coefficients. Thus in 2 molal solutions the γ_{\pm} values of HClO₄, NaClO₄, and LiClO₄ at 25° are, respectively: 1.055, 0.609, and 1.158²³; and neglecting molal-molar differences, we obtain α_h estimates of 0.06 and -0.01 in sodium and lithium perchlorate solutions. This is at least sufficient to indicate the reasonableness of the $f(\alpha)$ values in Table II.

Definite statements concerning the α' terms must await more accurate values of α_h . Nevertheless, since at least in sodium perchlorate medium the activity coefficient of HClO₄ must vary over a considerable range, the diverse results obtained for the various couples amply signifies that the activity coefficients of the other species also are changing. As discussed by Harned and Owen,²⁴ the changes in solubility of sparingly soluble salts presents another striking example of activity coefficient changes of species at low concentration in relatively high, constant ionic strength media.

At present some activity coefficient evaluations can be made in 2 M perchloric acid solutions, and the results for the various species are summarized in Table III. In each case the formal potential at the highest acid concentration listed in Table I (no added NaClO₄) was used with the best available value of the standard potentials and y_h for pure 2 M perchloric acid. Using the 25° density data of Markham,²⁵ 2 M equals 2.201 molal HClO₄. Interpolation gave a mean molal γ_h of 1.119²³; and converting to the molar scale, $y_h = 1.228$ for 2 M HClO₄. The E^0 values for the Fe(II-III) and Hg(0-I) couples were taken from Schumb, Sherrill, and Sweetser¹⁸ and El Wakkad and Salem.²⁶ Since there appears to be a considerable uncertainty in

E^0 for the Hg(I-II) couple,²⁷ the difference between the two mercury couples was used with the corresponding E^0 .⁶ Where necessary E^0 values were converted to absolute volts and the molar scale. No results can be given for the Np(V-VI) couple because a standard potential has never been determined.

TABLE III

ACTIVITY COEFFICIENTS AT 25° IN 2 M HClO₄

Couple	$y_{\text{HClO}_4} = 1.228 \pm 0.005$	
	$E^0, \text{ abs. mv.}$	y_{\pm}
Hg(0-I)	797.1 \pm 0.4	$y_{\text{Hg}_2(\text{ClO}_4)_2} = 0.657 \pm 0.008$
Hg(I-II)-Hg(0-I)	115.0 \pm 1.0	$y_{\text{Hg}(\text{ClO}_4)_2} = 1.034 \pm 0.02$
Fe(II-III)	770.3 \pm 0.2	$\frac{[y_{\text{Fe}(\text{ClO}_4)_2}]^3}{[y_{\text{Fe}(\text{ClO}_4)_3}]^4} = 2.38 \pm 0.03$

In conclusion our results demonstrate that the much abused principle of constant ionic strength cannot be used with any certainty when major medium changes occur. In a pithy discussion of this problem Young and Jones²⁸ express doubts of the significance of a major portion of the complex ion association "constants" reported in the voluminous literature of this field. Moreover, Pitzer and Brewer²⁹ have pointed out that the use of very high ionic strengths in order to minimize per cent. substitution changes in medium is not an effective procedure. This is based on the fact that the α parameters of Harned's rule are relatively independent of total concentration, and thus approximately the same percentage change in activity coefficients will occur for a fixed amount of substitution regardless if $\mu = 0.1$ or 3.

If substitution for H⁺ must be made in perchlorate medium, then the individual activity coefficients clearly indicate the superiority of Li⁺ over Na⁺. Using sodium perchlorate, the extreme effects we have observed on the formal potentials correspond to net activity coefficient changes of -45% and +21% for Np(V-VI) and Hg(I-II) couples. Also a fortuitous cancellation of changes probably occurs frequently as indicated by the Fe(II-III) and Hg(0-I) couples. However, no *a priori* prediction can as yet be made for any given reaction.

(27) D. J. G. Ives and G. J. Janz, "Reference Electrodes," Academic Press, New York, N. Y., 1961, p. 147.

(28) T. F. Young and A. C. Jones, "Annual Review of Physical Chemistry," Annual Reviews, Inc., Stanford, Calif., Vol. 3, 1952, pp. 285-287.

(29) G. N. Lewis and M. Randall (revised by K. S. Pitzer and L. Brewer), "Thermodynamics," McGraw-Hill Book Co., Inc., New York, N. Y., 2nd ed., 1961, p. 580.

(23) Reference 10, pp. 491-492.

(24) Reference 19, pp. 613-615.

(25) A. E. Markham, *J. Am. Chem. Soc.*, **63**, 874 (1941).(26) S. E. S. El Wakkad and T. M. Salem, *J. Phys. Chem.*, **54**, 1371 (1950).

COACERVATION OF SALTS OF POLYVINYLSULFONIC ACID AS INDUCED BY HEAVY METAL IONS¹

BY FRANK MILLICH² AND MELVIN CALVIN

Departments of Chemistry of the Universities of Kansas City, Missouri, and California at Berkeley, Berkeley, Calif.

Received December 6, 1961

Investigation has been conducted to establish a preliminary profile of experimental conditions which affect the interaction of heavy metal ions with salts of polyvinylsulfonic acid samples (PVSA) of different average molecular weight. The qualitative effects of cationic dyes also are mentioned. Phase diagrams of incipient separation of coacervate phase and resolution thereof are given as a function of PVSA and metal ion concentration for salts of silver, cupric, and ferric ions. These results are contrasted with those of alkali metal salts, and silver is in contrast to cupric and ferric cations. The drastic effect of the change in value of the temperature coefficient of phase separation with change in ionic strength is noted, and the effects of acidity of the media and average molecular weight of PVSA upon degree of phase separation also are discussed.

Introduction

The importance of heavy metal ions in the chemical mechanisms of biological reactions is readily acknowledged. The catalytic activities of at least eight metals, *i.e.*, Fe, Co, Mg, Ca, Zn, Mn, Cu, and K, have been identified with enzyme systems.³ The need exists, however, for detailed knowledge of metal ion interaction with polyelectrolytes. Detailed "proposed mechanisms" for enzyme-coenzyme substrate interplay are plentiful in the literature,⁴ yet definitive quantitative treatment of electrolyte-polyelectrolyte interactions are contrastingly meager, especially in concentrated systems. It is reasonable that such systems of high concentration of interacting groups are capable of high kinetic rates without the necessity of having reactive sites positioned by primary bonds. Such systems profit from the advantages of numerous associative forces, entropy factors, and high encounter frequencies.

Current studies that are pertinent to the subject of enzyme action are those covering the physics of colloid systems; studies of ion binding of polyelectrolytes and their properties; and "super-rate" kinetics of intramolecularly reacting chemical groups, usually vicinally located to one another in a molecule, or separated by four carbon bond lengths. It remains to be demonstrated in exactly what way concentrated media provide highly beneficial conditions for interaction of diffusible reactants. This, however, is precluded by the present lack of knowledge and difficulties of precise definition of physical factors. Most theories, such as that of ionic strength, quantitatively describe only relatively dilute solutions, even in the absence of polymeric species. A discussion of unsuccessful attempts at the application of various theoretical approaches to a quantitative description of bolaform electrolytes is given by Rice and Harris.⁵

The present study seeks to give a preliminary profile of experimental conditions affecting the interaction of heavy metal ions with salts of polyvinyl-

sulfonic acid (PVSA), a polymer which is known to yield aqueous complex-coacervate solutions.⁶

Experimental

Materials.—Three polymer samples of polyvinylsulfonic acid were used. One polymer, sample M, was polymerized by irradiation of a 70% aqueous solution at room temperature for 12 hr. with ultraviolet light from a 1000-watt G.E. AH-6 lamp at a distance of 6 in. The monomer (b.p. 128° at 2 mm., n_D^{25} 1.4500) and the polymerization mixture were made up in a quartz reaction vessel by distilling, in turn, monomer, under reduced pressure, and water, directly into a quartz reaction vessel before sealing, to exclude oxygen. The two other samples, H and D, were obtained through the courtesy of Dr. D. S. Breslow of the Hercules Powder Company, Wilmington, Delaware. Samples H and D originated from spontaneous polymerization of concentrated aqueous solutions of sodium ethylenesulfonate.

All three polymer samples were filtered as aqueous solutions of their sodium salts through fine porosity sintered glass filters. Polymers M and D, after treatment with Nuchar decolorizing charcoal, were precipitated two times by adding 20 ml. of saturated sodium chloride to an otherwise stable milky suspension which is produced when 700 ml. of methanol is added, with stirring, to a solution of 20 g. of polymer in 300 ml. of water. In this way 95% of the original material is recovered, and only unreacted monomer and low molecular weight oligomers are separated out. Dialysis through cellulose tubing (Visking Co.) of 24 Å. pore size removed contaminants capable of reducing neutral or acidic permanganate solution, as evaluated by iodimetry.

Methods.—Sedimentation velocity analyses of sodium salts of the polymer samples at 1.5% concentration in 0.5 M NaCl were conducted in a Spinco Model E ultracentrifuge at 52,640 r.p.m. for 1 to 2 hr. at 26°. The sedimentation constant for sample D also was determined in 0.5 M NaCl at three different concentrations: 0.94, 1.56, and 2.60 weight %. One determination of the sedimentation constant in 0.1 M Na₂SO₄ was made on a 1.50% solution of sample D.

Viscosities of samples of sodium polyvinylsulfonic acid (Na-PVSA) in solutions of two different salts were determined in an Ostwald viscometer at 24.82 ± 0.01°. Refractive indices were determined in a Bausch and Lomb six decimal place refractometer at 26.0 ± 0.1, with monochromatic light (Na D-line).

The qualitative screening of distribution of colored ionic species between phases of a coacervate solution was performed by visual observation at 0° of the color resulting from one or more drops of a concentrated solution of each ion, *e.g.*, ~2 M with respect to metal ion, millimolar with dye ion added, to 1 ml. of Na-PVSA sample M (0.3 eq. in 1.5 M NaCl solution). The latter solution is monophasic at room temperature, but yields two phases at 0°.

Phase diagrams at 24.82 ± 0.01° were obtained by titration of decimilliliter volumes of polymer solution, with solutions of metal ion. In one series (Fig. 1) a variety of concentrations of a simple electrolyte also was included in the polymer solution. Polymer solutions were metered with micropipets, the titrant with a microburet (L.S. Starrett Co., Athol, Mass.) which was graduated to 0.1 λ , though only droplets of 2 λ or larger were transferred.

(1) This investigation was aided by a postdoctoral fellowship (PF-41 A) from the American Cancer Society.

(2) To whom inquiries should be directed: University of Kansas City, 5100 Rockhill Road, Kansas City 10, Missouri.

(3) V. A. Najjar in symposium on "Phosphorus Metabolism," Vol. I, ed. by W. D. McElroy and B. Glass, Johns Hopkins University Press, Baltimore, Md., 1951, p. 500.

(4) M. Dixon and E. C. Webb, in "The Enzymes," Academic Press, Inc., New York, N. Y., 1958, Chap. VII.

(5) S. A. Rice and F. E. Harris, *J. Phys. Chem.*, **58**, 725, 733 (1954).

(6) H. Eisenberg and G. Ram Mohan, *ibid.*, 671 (1959).

TABLE I
PHYSICAL PROPERTIES OF POLYVINYL SULFONIC ACID SAMPLES

Sample	$[\eta]$, ^c dl./g.	\bar{M}_n^a	\bar{M}_w^a	$[\eta]$, ^d dl./g.	\bar{M}_w^b	$\frac{26.0}{dn_D/dc^d}$ dl./g.	η_{sp}/c^e	$S_{20,w}$ $\times 10^{13}$, sec. ⁻¹
Na-PVSA, H	0.290; .27 ^e	40,000	85,000	0.183	30,000	0.125	1.25	4.01 ^d
Na-PVSA, M	.214	27,000	60,000	.150	21,900	.130	...	3.67 ^d
Na-PVSA, D	.144	18,000	40,000	.094	11,000	...	0.44	2.06 ^c 2.50 ^d

^a Molecular weights were evaluated from the graphs of Breslow and Kutner,⁸ which correlate viscosity in 0.1 *M* Na₂SO₄ with light scattering. ^b Molecular weights were evaluated from the data of Dialer and Kerber,⁷ which correlate viscosity in 0.5 *M* NaCl with ultracentrifuge sedimentation velocity. ^c Intrinsic viscosities; solvent, 0.1 *M* Na₂SO₄. ^d Intrinsic viscosities; solvent, 0.5 *M* NaCl. ^e Data of D. S. Breslow (private communication): viscosities of 1% solutions in 0.1 *N* Na₂SO₄.

Points shown in the phase diagrams indicate the very first and last indication of opacity of solutions.

Results and Discussion

A. Molecular Weights of Samples.—Sedimentation velocity analysis showed dc/dx distribution patterns which cannot be distinguished from gaussian distribution within the precision of the determination. There seems to be little or no dependence of the sedimentation constant on concentration in the range investigated. Table I summarizes some of the properties which have been determined for the three samples. Sedimentation velocity data were obtained for our samples in 0.5 *M* NaCl solution, as well as viscosity data in the same solvent, to check the correspondence of physical properties reported by Dialer and Kerber.⁷ However, lower values of calculated molecular weights result when compared to the data of viscosity-molecular weight correlation in a different salt solution made by Breslow and Kutner⁸ with data from osmometry and light scattering.

Referring viscosity measurements in 0.1 *M* Na₂SO₄ for samples H, M, and D to the data of the latter authors, we obtain indication of both number and weight-average molecular weights which are numerically larger (the latter by 300%) than that indicated by the ultracentrifuge average molecular weights. Viscosity data would undoubtedly show a limited dependence on rate of shear, but the magnitude of the discrepancy found above points to the probable need of closer scrutiny of the influence of solvent on polymers which are capable of coacervation. The large dependence of intrinsic viscosity on sodium sulfate concentration shown by Breslow and Kutner⁸ accentuates this point. It has been stated that the comparison of intrinsic viscosity with ultracentrifuge molecular weights and perhaps with light scattering is valid only if the exponent in the Staudinger equation is close to unity; this is not the case with Na-PVSA. For present purposes, it only is necessary to establish the relative order of molecular weights for the three samples in order to demonstrate if molecular weight differences are significant in coacervation. For the present, the samples H, M, and D, listed in order of decreasing molecular weight, remain characterized by viscosity data in two different solvents and sedimentation constants.

B. Distribution of Ions between Coacervate and Equilibrium Phases.—The results of a qualita-

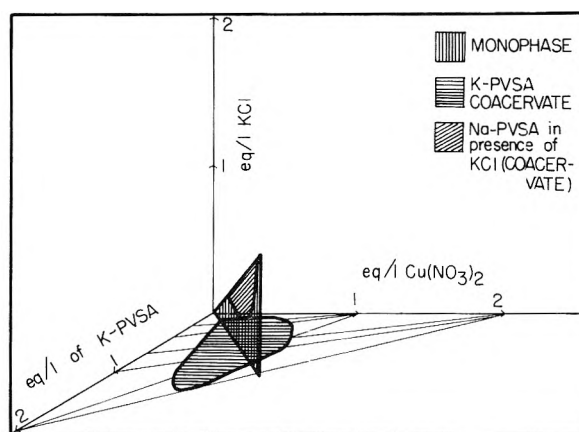


Fig. 1.—Phase diagram of coacervation of potassium polyvinylsulfonate by cupric nitrate in the presence of simple electrolyte at 24.82°. Equivalence per liter of PVSA = gram equivalent per liter of segment unit, $-\text{CH}_2\text{CH}(\text{SO}_3^-)$.

tive screening of the distribution of colored ions between the heavier, coacervate phase and the more polymer-dilute equilibrium phase are as follows: the anions, *i.e.*, dichromate, fluorescein, Rose Bengal, and ferricyanide, became localized in the equilibrium phase, as did Nile blue monocation; the cations, *i.e.*, cerium(IV), iron(III), copper(II), nickel(II), manganese(II), silver(I), and the monoprotonated Proflavin, became localized in the coacervate phase; while ionic forms of acridine orange, thionine, safranin, and congo red were insoluble and salted out of solution. Of the cations, those of the heavy metals induced coacervation at room temperature without the need for cooling.

The generalization arises that the distribution is determined largely by the sign of the charge of each ion—cations of added simple electrolyte being localized in the polyanionic coacervate phase and anions being repelled from this phase. Only one exception to this rule was found: Nile blue hydrochloride became a solute of the equilibrium phase and was repelled completely by the high ionic strength of the medium of the coacervate phase. Since several dyes salt out of this medium it is not surprising that the ionic strength effect on aromatic dyes may predominate in certain cases. A wider spectrum of the influence of ionic strength on distribution of proteins, for instance between two neutral coacervate phases may be appreciated by reference to the data of Albertsson and Nyns.⁹

(7) K. Dialer and R. Kerber, *Makromol. Chem.*, **17**, 56 (1956).

(8) D. S. Breslow and A. Kutner, *J. Polymer Sci.*, **27**, 295 (1958).

(9) P. Albertsson and E. J. Nyns, *Nature*, **184**, 1466 (1959).

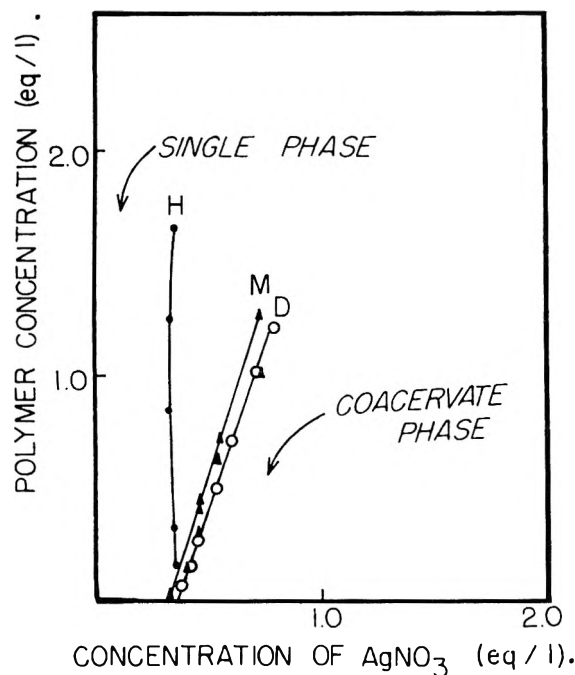


Fig. 2.—Phase diagram of the coacervation of potassium polyvinylsulfonate by silver nitrate, as a function of samples of different average molecular weight (see Table I).

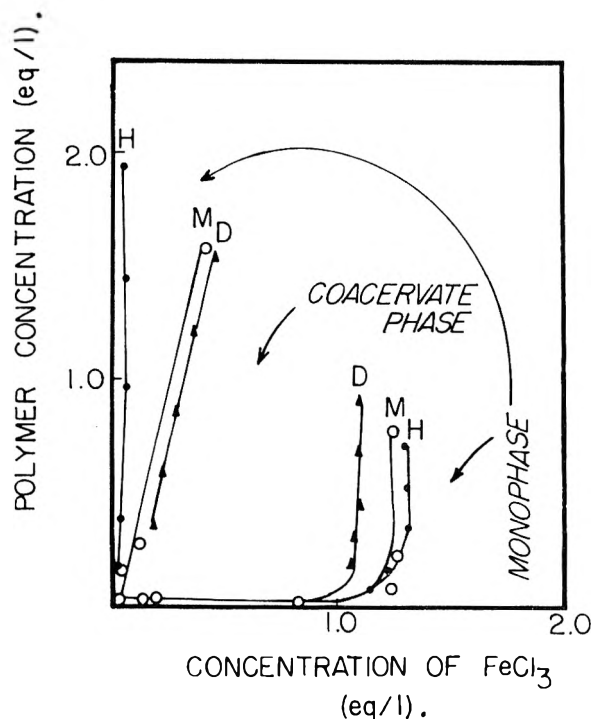


Fig. 4.—Phase diagram of coacervation of potassium polyvinylsulfonate by ferric chloride, as a function of samples of different average molecular weight (see Table I).

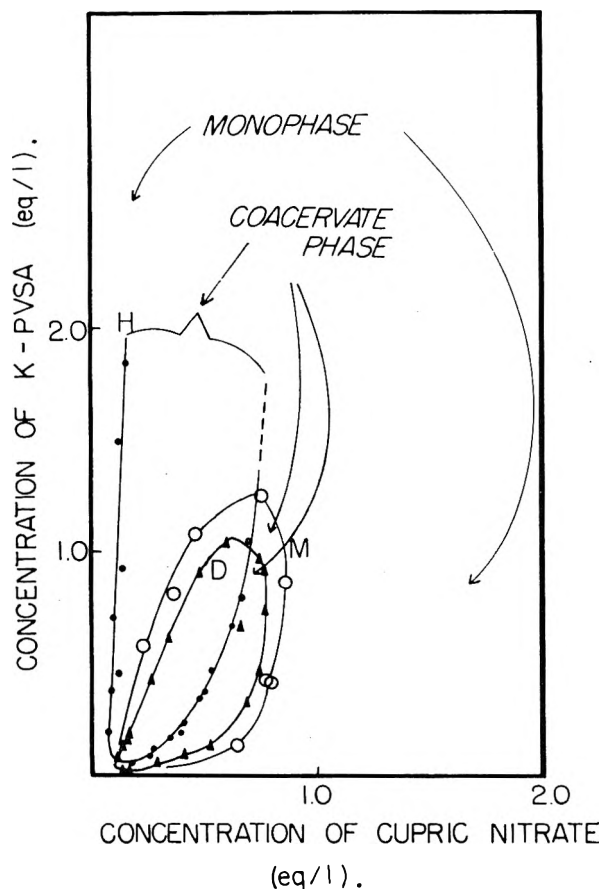


Fig. 3.—Phase diagram of coacervation of potassium polyvinylsulfonate by cupric nitrate, as a function of samples of different average molecular weight (see Table I).

Quantitatively, in contrast with the anionic dyes which showed strong differentiation between the two phases of the system, the chromate ion phase preference was poor and could be noticeably demonstrated only at low chromate concentration. This observation also reflects upon the higher sensitivity to ionic strength imparted to the character of ionic dyes by their partial lyophilic nature.

C. Coacervation Induced by Heavy Metals.—Following the observation that when heavy metal ions were employed in the above experiments they induced formation of coacervate phases without the need for cooling, quantitative studies were designed to reveal the extent of these effects. The three samples of PVSA, differing in molecular weight, were employed in the form of their sodium and potassium salts. The results are summarized in Fig. 1 to 4. Several conclusions about the factors affecting the degree of phase separation may be drawn from inspection of these diagrams.

1. Molecular Weight of the Polyanion.—In each case, *i.e.*, with silver ion, Fig. 2; with cupric ion, Fig. 3, and with ferric ion, Fig. 4, the tendency to develop a second phase is greatest with the PVSA sample of highest molecular weight, and *vice versa*, when equivalent concentrations in gram ionic weight per liter of metal and poly-ion are compared.

2. Sensitivity of Coacervate to Ionic Strength of the Medium.—From the slopes of the curves in Fig. 2, depicting an inverse dependence of coacervate formation on the concentration of interacting constituents, and thus on ionic strength, it is apparent that with the samples of higher molecular weight the dependency is less, being almost nil for sample H, which shows a slope of 90°. The abscissa

intercept, however, apparently is the same for all three samples. Calculation of the ionic strength of the metal titrant for the extrapolated abscissa value of zero concentration of polymer (sample H, Fig. 2-4) along the slope of incipient phase separation gives the values: silver nitrate, 0.34; cupric nitrate, 0.10; ferric chloride, 0.06.

3. Resolubilization by High Concentration of Metal Ion.—The phase diagrams of the interaction of cupric and of ferric ion with K-PVSA contrast with those of silver (Fig. 3 and 4 *vs.* Fig. 2) by showing an area of high concentration of metal ion at which the coacervate redissolves. One factor which undoubtedly plays a role is the acidity developed in solution by solvolysis of cupric and ferric ions, as distinct from the properties of silver ion in aqueous solution. The solubilizing effect of adding HCl to the above systems can be demonstrated. Alternatively, polyvalency of metals can afford ampholyte character to the polymer-metal complex. The phenomenon of redissolution is not new, having been reported as occurring with polyphosphates.¹⁰ The phenomenon has an apparent analogy with the solubility properties of antibody-antigen complexes.

4. Temperature Dependence of Coacervate Phase Separation.—The amount of coacervate separating out increases with decrease in temperature. Gross difference in temperature dependence was visibly apparent upon dilution of the coacervate mixture. It is possible to induce phase separation for some one concentrated solution of metal and polymer simply by titrating with water. The copious coacervate solutions initially formed can be redissolved merely by raising the temperature of the mixture by 5 or 10 degrees. However, as addition of water progresses, this temperature dependence diminishes until, for instance, a coacervate mixture produced by equivalent volumes of 0.1 *N* ferric chloride and 0.1 *N* K-PVSA can be boiled without dissolution. The apparent color of this latter, presumably ionically, tightly cross-linked material is an appreciably more intense red. An X-ray crystallographic analysis failed to show any pattern of regularity for this latter material. Van Wazer distinguishes types of association between metal ions and polyphosphates which can be differentiated experimentally.¹¹

5. Specific Ion Association.—As previously reported⁶ there appears to be a selective association between PVSA and potassium ion as compared to ammonium, hydrogen, lithium, cesium, rubidium, and sodium ions, as shown by the ease of coacervate

formation (*i.e.*, the concentration and temperature ranges over which formation occurs); although sodium and rubidium show the coacervation phenomenon to a lesser degree in the temperature range which practically is attainable with aqueous solutions. This is somewhat curious since Dowex 50, sulfonate polystyrene, associates ions by order of valency and ratio of hydrated ion.^{12,13}

The difference for the contrasting property of PVSA probably lies not in the density of charge difference between an aliphatic and aromatic sulfonate group, since that would not explain a maximum effect for potassium. To say that aqueous KCl solution is a poorer solvent than, for example, aqueous NaCl is begging the question, though some solvent effect is probable, as seen in the differential effect among KCl, KBr, and KI solutions upon the coacervation of K-PVSA.⁶ The nature of the specificity seems to lie in the steric pliability of PVSA when contrasted to the rigid ion-exchange resin, which enables it to group anionic sites about a cation. Consideration of the dominant role which flexibility of polymer chains plays in ability to complex is indicated in studies such as those of Bradley¹⁴ and Rice and Harris.⁵

Figure 1 supports the fact that the case of coacervation which is induced by a heavy metal, as in the case of cupric ion, is strongly dependent upon whether the counterion of PVSA is K⁺ or Na⁺. As seen, the copper coacervate could not be formed from the sodium salt of PVSA at room temperature, as was possible with the K-PVSA, without the addition of monovalent electrolyte (KCl).

Data has been gathered for the quantitative evaluation of the dissociation constant of ferric ion with Na-PVSA and with sodium propane-2-sulfonate, a monomeric analog of the polyelectrolyte. Further work is planned for the extension of this preliminary survey to alkaline earth and lanthanum metal ions.

Acknowledgment.—Our thanks are given to Dr. D. S. Breslow, Hercules Powder Co., for some samples of Na-PVSA; to Miss H. Rubin, University of California, for X-ray crystallographic determinations; to Mr. Robert Wills, University of California Radiation Laboratory, for obtaining ultracentrifuge sedimentation data; and to the American Cancer Society for its financial support of this research.

(12) "Dowex Ion Exchange," Dow Chemical Co., Midland, Michigan (1959), p. 9. The series given for monovalent ions is, in the order of decreasing associative ability: Ag, Tl, Cs, Rb, NH₄, K, Na, H, Li.

(13) J. Kielland, *J. Am. Chem. Soc.*, **59**, 1675 (1937), gives values for hydrated ionic radii. Neither ionic nor covalent radii offer a uniform correlation.

(14) D. F. Bradley and M. K. Wolf, *Proc. Natl. Acad. Sci. U. S.*, **45**, 944 (1959).

(10) Persoz, *Ann.*, **65**, 163 (1848).

(11) J. R. Van Wazer, discussion, reference 3.

CARBON DISULFIDE AS A REFERENCE SUBSTANCE FOR VAPOR-FLOW CALORIMETRY; THE CHEMICAL THERMODYNAMIC PROPERTIES

BY GUY WADDINGTON, J. C. SMITH, K. D. WILLIAMSON, AND D. W. SCOTT

Contribution No. 110 from the Thermodynamics Laboratory of the Bartlesville Petroleum Research Center, Bureau of Mines, U. S. Department of the Interior, Bartlesville, Oklahoma

Received December 7, 1961

Calorimetric values of vapor heat capacity for carbon disulfide were compared with values accurately calculated from the molecular spectra. Carbon disulfide was found to be a suitable liquid substance for testing the accuracy of vapor-flow calorimeters. Values of enthalpy of vaporization, vapor pressure, and parameters of the equation of state also were determined. The chemical thermodynamic properties were calculated for temperatures between 0 and 1500°K.

In developing the techniques of vapor-flow calorimetry now used in this Laboratory, the need for a reference substance was recognized. The requirements for a suitable reference substance are: (a) it must be a liquid of at least moderate volatility; (b) it must be available readily in a state of high purity; (c) it must be chemically stable, non-hygroscopic, and unreactive with the usual materials of construction of vapor-flow calorimeters; and (d) most important, it must have a simple enough molecular structure that the vapor heat capacity can be calculated accurately, *a priori*, from spectroscopic data. Carbon disulfide seemed a likely candidate, and vapor-flow calorimetry was done for that compound. However, at the time, the vapor heat capacity could not be calculated with the desired accuracy because some needed spectroscopic data were lacking. In the ensuing years, the needed spectroscopic data were reported, and a comparison of the experimental and calculated values can be made now.

This paper reports the vapor-flow calorimetry with carbon disulfide and supporting experimental studies, the calculation of the heat capacity and other thermodynamic functions from spectroscopic data, a tabulation of the chemical thermodynamic properties, and an appraisal of carbon disulfide as a reference substance for vapor-flow calorimetry.

The reported values are based on a molecular weight of 76.142 g. mole⁻¹ (1951 International Atomic Weights¹), the 1951 values of fundamental physical constants,² and the relations: 0° = 273.15°K. and 1 cal. = 4.184 joules (exactly).

Experimental

The Material.—C.P. carbon disulfide was distilled in an efficient fractionating column by H. J. Coleman of this Center. The purity of the distilled sample, determined by the time-temperature freezing point method, was 99.98 mole %. In ebulliometric studies, the difference between the boiling and condensation temperatures of the sample was found to be only 0.001° at 1 atm. pressure.

Vapor-Flow Calorimetry.—The vapor-flow calorimetry was done in 1948 with the apparatus described by Waddington, Todd, and Huffman,³ except that a metal cycling vaporizer replaced the glass vaporizer. The metal vaporizer has been replaced in turn by a glass vaporizer of similar design.⁴ The metal vaporizer was constructed primarily to

obtain more rapid thermal equilibration, but it could not be used with corrosive substances and was abandoned when the improved glass vessel⁴ was found to be as satisfactory calorimetrically.

Some metal parts of the apparatus were not completely inert to carbon disulfide. In particular, a nichrome-to-copper, silver-soldered joint in the heater of the calorimeter vessel definitely was corroded, and repairs were necessary before heat capacity determinations at the highest temperature could be completed. The small amount of reaction that occurred presumably had an insignificant effect on the accuracy of the results.

Corrections for heat losses in the calorimeter are made by determining the apparent heat capacity at several rates of flow. The apparent heat capacity values, $C_p(\text{app})$, are plotted against the reciprocal of flow rate, $1/F$, and the results are extrapolated to zero value of $1/F$. This treatment is based on the equation

$$C_p(\text{app}) = C_p + k/F \quad (1)$$

which implies that the absolute heat loss by radiation (no other types of heat loss are significant in a well designed calorimeter) is independent of the flow rate. However, for vapors of low specific heat, it is necessary to account for a small dependence of total heat loss on flow rate. The origin of a heat-loss term inversely proportional to F can be seen from Fig. 1, which is a schematic representation of the temperature profile in the calorimeter. The temperature of the entering vapor is measured by a platinum-resistance thermometer at position A; electrical energy is supplied by a heating element between points B and C (F); and the temperature is measured at points D and E (G) before the vapor leaves the calorimeter. Equation 1 applies strictly only when the temperature increment and profile at all flow rates is that given by the solid line ABCDE. For this condition, the total heat loss up to the thermometer at D is proportional to the area of BCDH, which usually is assumed to be independent of flow rate if ΔT is held constant. Actually, the heat losses that occur in the calorimeter will cause the temperature of the vapor to fall after it passes the heater, as shown on a much exaggerated scale by the dashed profile BFDG. Therefore, the heat loss up to point D is proportional to the area BFDH, the area of BFDC being inversely proportional to the flow rate. An energy balance on the calorimeter up to point D then gives

$$Q(\text{input}) = C_p(\text{app})F\Delta T = C_pF\Delta T + k_1\Delta T + (k_2/F)\Delta T \quad (2)$$

In this equation, $k_1\Delta T$ is related to the area BCDH and $(k_2/F)\Delta T$ is related to the area BFDC. In the experiments, the slope of the line FDG is determined from the temperatures measured at points D and G, and the profile BFD is established from the results. The equation for $C_p(\text{app})$ including the flow-dependent term for heat loss is

$$C_p(\text{app}) = C_p + k_1/F + k_2/F^2 \quad (3)$$

In applying eq. 3, $C_p(\text{app}) - C_p$ is evaluated approximately by eq. 1, and k_2/F^2 is calculated as [area BFDC/area AFDH] [$C_p(\text{app}) - C_p$], the ratio of areas being calculated from the known temperature profile. A plot of $C_p(\text{app}) - k_2/F^2$ vs. $1/F$ then is used to evaluate C_p at $1/F = 0$. Actually the k_2/F^2 term is negligible for most organic vapors, but verges on significance for carbon disulfide vapor because of its unusually low *specific heat*. Neglect of the term would have introduced an error of 0.025 cal. deg.⁻¹ mole⁻¹ in the value of C_p° for carbon disulfide at 502.25°K.,

(1) E. Wichers, *J. Am. Chem. Soc.*, **74**, 2447 (1952). No values would be changed significantly by use of the new atomic weight scale [*Chem. Eng. News*, Nov. 20, 43 (1961)].

(2) F. D. Rossini, F. T. Gucker, Jr., H. L. Johnston, L. Pauling, and G. W. Vinal, *J. Am. Chem. Soc.*, **74**, 2699 (1952).

(3) G. Waddington, S. S. Todd, and H. M. Huffman, *ibid.*, **69**, 22 (1947).

(4) J. P. McCullough, D. W. Scott, H. L. Finke, W. N. Hubbard, M. E. Gross, C. Katz, R. E. Pennington, J. F. Messerly, and G. Waddington, *ibid.*, **75**, 1818 (1953).

a smaller error at 453.35°K., and entirely negligible errors at the lower temperatures.

The experimental values of enthalpy of vaporization and vapor heat capacity are given in Tables I and II. The enthalpy of vaporization may be represented by the empirical equation

$$\Delta H_v = 7868 - 0.096T - 1.419 \times 10^{-2}T^2 \text{ cal. mole}^{-1} \quad (4)$$

(280–320°K.)

Comparative Ebulliometry.—The vapor pressure of carbon disulfide was determined with the twin ebulliometer system described previously.⁵ The results are listed in Table III.

TABLE I
THE MOLAL ENTHALPY OF VAPORIZATION AND SECOND VIRIAL COEFFICIENT OF CARBON DISULFIDE

T, °K.	P, atm.	ΔH_v , cal.	B(obsd.), cc.	B(calcd.), cc. ^b
281.94	0.2470	6713 ± 3 ^a	-923	-915
298.15	.4749	6578 ± 3	-802	-808
319.37	1.0000	6390 ± 2	-696	-699

^a Maximum deviation from the mean of three or more determinations. ^b Calculated from eq. 7.

TABLE II
THE MOLAL VAPOR HEAT CAPACITY OF CARBON DISULFIDE
IN CAL. DEG. ⁻¹

T, °K.	→	325.65	367.65	407.10	453.35	502.25
C_p (1.000 atm.)		11.578	11.807	12.027	12.330	12.561
C_p (0.475 atm.)		11.359				
C_p (0.247 atm.)		11.271	11.626	11.915	12.245	12.503
C_p^o		11.175	11.568	11.890	12.218	12.484
$-T(d^2B/dT^2)$, obsd. ^a		0.383	0.230	0.143	0.110	0.076
$-T(d^2B/dT^2)$, calcd. ^b		0.377	0.231	0.156	0.105	0.073

^a Units: cal. deg. ⁻¹ mole⁻¹ atm.⁻¹. ^b Calculated from eq. 7.

TABLE III
THE VAPOR PRESSURE OF CARBON DISULFIDE

Boiling point, °C.	Carbon disulfide	p (obsd.), ^a mm.	p (obsd.) - p (calcd.), mm. Antoine eq. 5	Cox eq. 6
Water				
60.000	3.588	149.41	-0.02	0.00
65	8.772	187.57	.00	+ .01
70	13.999	233.72	-.02	+ .02
75	19.269	289.13	+.01	.00
80	24.582	355.22	-.03	-.05
85	29.927	433.56	-.05	+.02
90	35.318	525.86	+.05	+.03
95	40.751	633.99	+.02	.00
100	46.225	760.00	-.01	.00
105	51.744	906.06	-.19	-.13
110	57.295	1074.6	-.1	+.1
115	62.885	1268.0	+.1	+.3
120	68.531	1489.1	-.2	-.2
125	74.210	1740.8	-.1	.0
130	79.927	2026.0	-.2	.0

^a From vapor-pressure data for water given by N. S. Osborne, H. F. Stimson, and D. C. Ginnings, *J. Research Natl. Bur. Standards*, **23**, 261 (1939).

The Antoine and Cox equations selected to represent the results are

$$\log p = 6.94194 - 1168.623/(t + 241.534) \quad (5)$$

and

$$\log(p/760) = A(1 - 319.375/T) \quad (6)$$

$$\log A = 0.765175 - 5.4695 \times 10^{-4}T + 6.2076 \times 10^{-7}T^2$$

(5) G. Waddington, J. W. Knowlton, D. W. Scott, G. D. Oliver, S. S. Todd, W. N. Hubbard, J. C. Smith, and H. M. Huffman, *J. Am. Chem. Soc.*, **71**, 797 (1949).

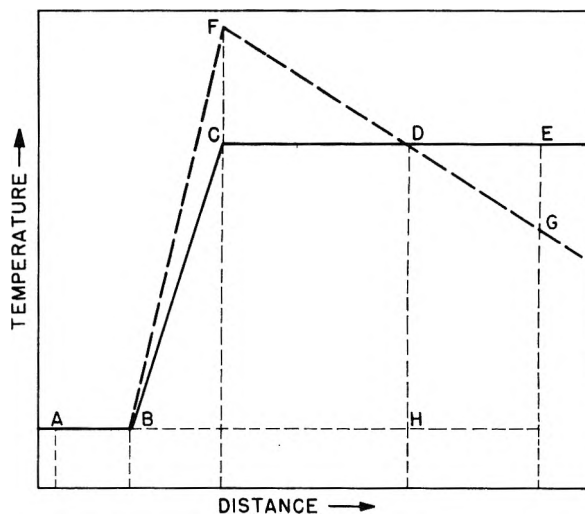


Fig. 1.—Schematic representation of the temperature profile in a vapor flow calorimeter.

In these equations, p is in mm., t is in °C., and T is in °K. The observed and calculated vapor pressure for both Antoine and Cox equations are compared in Table III. The normal boiling point is 46.22° (319.37°K.).

Effects of Gas Imperfection.—The effects of gas imperfection were correlated by the procedure described in an earlier paper.⁶ The empirical equation for B , the second virial coefficient in the equation of state, $PV = RT(1 + B/V)$, is

$$B = 143 - 150.4 \exp(550/T), \text{ cc. mole}^{-1} (208-500^\circ\text{K.}) \quad (7)$$

“Observed” values of B and $-T(d^2B/dT^2) = \lim_{P \rightarrow 0} (\partial C_p / \partial P)_T$

and those calculated from eq. 7 are compared in Tables I and II.

Bottomley and co-workers⁷ have made direct determinations of the second virial coefficient of carbon disulfide by both a differential compressibility method and a density balance method, with somewhat discordant results. The values obtained by differential compressibility agree moderately well with the results of this research but have a significantly different temperature dependence.

In addition to the second virial coefficient, all the other thermodynamic properties of carbon disulfide studied in this work have been the subject of earlier investigations reported in the literature. As the present results for the other properties were obtained by methods more accurate than the ones available to the earlier workers, a detailed comparison with the literature data is omitted.

Statistical Thermodynamic Calculations

Heat Capacity and Other Thermodynamic Functions from Spectral Data.—The thermodynamic functions for carbon disulfide were calculated from spectral data mainly so the calorimetric values of heat capacity could be compared with the theoretical ones. Account was taken of centrifugal stretching, rotation-vibration interaction, vibrational anharmonicity, and effects of isotopic composition.

The corrections to the rigid-rotator, harmonic-oscillator functions were calculated only for the most abundant isotopic species, C¹²S₂³², because the required spectral data were available for only that species. However, these small corrections would not be affected significantly by the isotopic composition. The vibrational constants adopted for

(6) J. P. McCullough, H. L. Finke, J. F. Messerly, R. E. Pennington, I. A. Hossenlopp, and G. Waddington, *ibid.*, **77**, 6119 (1955).

(7) G. A. Bottomley and C. G. Reeves, *J. Chem. Soc.*, 3794 (1958); G. A. Bottomley and T. A. Remington, *ibid.*, 3800 (1958).

TABLE IV
THE MOLAL CHEMICAL THERMODYNAMIC PROPERTIES OF CARBON DISULFIDE IN THE IDEAL GAS STATE^a

T, °K.	(F° - H°)/T, cal. deg. ⁻¹	(H° - H°₀)/T, cal. deg. ⁻¹	H° - H°₀, kcal.	S°, cal. deg. ⁻¹	C _p °, cal. deg. ⁻¹	ΔHf° ^b , kcal.	ΔFf° ^b , kcal.	log K/f ^b
0	0	0	0	0	0	-3.02	-3.02	Infinite
200	-45.043	7.731	1.546	52.774	9.450
273.15	-47.545	8.351	2.281	55.896	10.575	-2.87	-3.13	2.50
298.15	-48.285	8.551	2.549	56.836	10.876	-2.86	-3.15	2.31
300	-48.338	8.565	2.569	56.903	10.897	-2.86	-3.15	2.30
400	-50.902	9.272	3.709	60.174	11.828	-2.76	-3.26	1.78
500	-53.035	9.853	4.926	62.888	12.496	-2.69	-3.40	1.48
600	-54.876	10.337	6.202	65.213	12.998	-2.64	-3.54	1.29
700	-56.501	10.746	7.522	67.247	13.380	-2.60	-3.70	1.15
800	-57.959	11.094	8.876	69.053	13.675	-2.58	-3.85	1.05
900	-59.284	11.394	10.255	70.678	13.906	-2.57	-4.01	0.97
1000	-60.498	11.655	11.655	72.153	14.087	-2.55	-4.17	.91
1100	-61.620	11.883	13.071	73.503	14.233	-2.54	-4.34	.86
1200	-62.662	12.084	14.501	74.746	14.352	-2.53	-4.50	.82
1300	-63.637	12.262	15.941	75.899	14.450	-2.53	-4.67	.78
1400	-64.551	12.422	17.390	76.973	14.533	-2.54	-4.83	.75
1500	-65.413	12.565	18.847	77.978	14.602	-2.55	-4.98	.73

^a To retain internal consistency, some values are given to one more decimal place than is justified by the absolute accuracy.

^b The enthalpy, free energy, and common logarithm of equilibrium constant of formation for the reaction: C(c, graphite) + S₂(g) = CS₂(g).

C¹²S₂³², in the symbolism of Herzberg,⁸ are, in cm.⁻¹:

$$\begin{aligned} \omega_1^0 &= 659.2 & x_{11}^0 &= -1.2 & x_{12}^0 &= -7.8 & \nu_1 &= 658.0 \\ \omega_1^0 &= 396.5 & x_{22}^0 &= 2.3 & x_{23}^0 &= -6.4 & \nu_2 &= 396.7 \\ \omega_3^0 &= 1542.3 & x_{33}^0 &= -6.7 & x_{13}^0 &= -8.1 & \nu_3 &= 1535.6 \\ & & & & g_{22} &= -2.1 & & \end{aligned}$$

The foregoing vibrational constants are similar to those listed by Stoicheff⁹ (for Fermi resonance neglected), based on his high resolution Raman studies and earlier infrared work cited in his paper. However, the vibrational constants are revised to take account of Wentink's¹⁰ value of $\nu_3 - \nu_1$. Fermi resonance was not considered explicitly, as no general method exists for including the effect of Fermi resonance on the thermodynamic functions.

The rotational constants, determined in the high resolution infrared study of Guenther, Wiggins, and Rank,¹¹ and partly confirmed by Stoicheff's Raman study,⁹ are, in cm.⁻¹

$$\begin{aligned} B_{000} &= 0.10910 (I_0 = 256.49 \times 10^{-40} \text{ g. cm.}^2) & D &= 1 \times 10^{-8} \\ \alpha_1 &= 0.000155 & \alpha_2 &= -0.000256 (\text{av.}) & \alpha_3 &= 0.00071 \end{aligned}$$

The corrections to the rigid-rotator, harmonic-oscillator functions were calculated by use of the formulas and tables of Pennington and Kobe.¹²

Effects of isotopic composition were taken into account by calculating the moments of inertia and fundamental vibrational frequencies (assumed harmonic) for the other isotopic species. The rigid-rotator, harmonic-oscillator contributions were calculated separately for each species and then weighted according to the isotopic composition, taken to be 89.6% C¹²S₂³², 1.4% C¹²S³²S³³, 7.9% C¹²S³²S³⁴, and 1.1% C¹³S₂³².

(8) G. Herzberg, "Infrared and Raman Spectra of Polyatomic Molecules," D. Van Nostrand Co., Inc., New York, N. Y., 1945.

(9) B. P. Stoicheff, *Can. J. Phys.*, **36**, 218 (1958).

(10) T. Wentink, Jr., *J. Chem. Phys.*, **29**, 188 (1958).

(11) A. H. Guenther, T. A. Wiggins, and D. H. Rank, *ibid.*, **28**, 682 (1958).

(12) R. E. Pennington and K. A. Kobe, *ibid.*, **22**, 1442 (1954). A misprint occurs in eq. 23 of this paper; ν_3 should appear instead of ν_2 .

The calculated values of the thermodynamic functions, for selected temperatures up to 1500°K., are listed in columns 2-6 of Table IV.

NOTE ADDED IN PROOF.—Two recent articles report calculated thermodynamic functions for carbon disulfide. The values in one [J. S. Gordon, *J. Chem. Eng. Data*, **6**, 390 (1961)] agree well with those given here, but the values in the other [B. J. McBride and S. Gordon, *J. Chem. Phys.*, **35**, 2198 (1961)] agree less well. The calculated values of C_p⁰ in the latter differ from the experimental values as much as 0.5%.

Enthalpy, Free Energy, and Equilibrium Constant of Formation.—The calculated values of the thermodynamic functions were used with the calorimetric value of the enthalpy of formation at 298.15°K. determined by Good, Lacina, and McCullough¹³ in computing values of ΔHf°, ΔFf°, and log Kf. Literature values were taken for the thermodynamic functions of C(c, graphite)¹⁴ and S₂(g).¹⁵ The results are listed in columns 7-9 of Table IV.

Appraisal of Carbon Disulfide as a Reference Substance.—The observed values of heat capacity determined by vapor-flow calorimetry are compared with the theoretical values in Table V. The comparison shows that the observed values have an accuracy within the ±0.2% expected of the calorimetric method. In general, carbon disulfide meets the requirements for a suitable reference substance listed at the beginning of this paper. Its volatility is somewhat higher than ideal, and commercially available material requires final purification in the investigators' laboratory. As observed in this work, carbon disulfide does corrode certain metals and alloys that may be used in a vapor-flow calorimeter system; however, systems can be constructed from materials inert to carbon disulfide. The low *specific heat* makes carbon disulfide vapor

(13) W. D. Good, J. L. Lacina, and J. P. McCullough, *J. Phys. Chem.*, **65**, 2229 (1961).

(14) D. D. Wagman, J. E. Kilpatrick, W. J. Taylor, K. S. Pitzer, and F. D. Rossini, *J. Research Natl. Bur. Standards*, **34**, 143 (1945).

(15) W. H. Evans and D. D. Wagman, *ibid.*, **49**, 141 (1953).

TABLE V
COMPARISON OF OBSERVED AND CALCULATED VAPOR HEAT
CAPACITY OF CARBON DISULFIDE

T, °K.	C _p , cal. deg. ⁻¹ mole ⁻¹		Diff.
	Obsd.	Theor. ^a	
325.65	11.175	11.172	+0.003
367.65	11.568	11.565	+ .003
407.10	11.880	11.883	- .003
453.35	12.218	12.209	+ .009
502.25	12.484	12.509	- .025

^a Five point Lagrangian interpolation of the values at even temperatures in Table IV.

somewhat atypical of the usual organic vapors studied by vapor-flow calorimetry, but that property may well be an advantage instead of a disadvantage for a reference substance. The low *specific heat* magnifies the k_2/F^2 term in eq. 3 that is necessary because of the temperature profile within the calorimeter. If accurate results are obtained with carbon disulfide, for which the term is magnified, more confidence can be placed in results obtained with typical organic vapors for which the term is small or negligible.

Water is the only other liquid for which the vapor

heat capacity can be calculated accurately from spectroscopic data. Although water does meet the requirements for a suitable reference substance for vapor-flow calorimetry, and has been studied successfully,¹⁶ it has two disadvantages. First, the heat capacity of water vapor varies rapidly and non-linearly with pressure in the temperature range of interest because of association through hydrogen bonding. Second, water has somewhat unfavorable boiling and condensation behavior related to the high surface tension, which makes it difficult to handle in a flow calorimeter. These two disadvantages make water less suitable as a reference substance than carbon disulfide, which is a normal unassociated compound.

Benzene is another useful substance for testing the accuracy of vapor-flow calorimeters.¹⁷ It is more convenient to work with than either carbon disulfide or water, but the heat capacity of benzene cannot be calculated from spectroscopic data with as high accuracy as for the two simpler molecules.

(16) J. P. McCullough, R. E. Pennington, and G. Waddington, *J. Am. Chem. Soc.*, **74**, 4439 (1952).

(17) D. W. Scott, G. Waddington, J. C. Smith, and H. M. Huffman, *J. Chem. Phys.*, **15**, 565 (1947).

ON THE DETERMINATION OF LONDON-VAN DER WAALS CONSTANTS FROM SUSPENSION AND EMULSION VISCOSITY AND SURFACE ENERGY DATA

By THOMAS GILLESPIE AND RALPH M. WILEY

Physical Research Laboratory, The Dow Chemical Company, Midland, Michigan

Received December 7, 1961

A method has been developed for determining the London-van der Waals constant and the minimum distance of separation between emulsion drops and suspension particles from rheological and surface energy data. Data of Albers and Overbeek for W/O emulsions and new data for nearly spherical and irregular solid particles in oil have been treated by this method with results which are directly opposite to the conclusions of Albers and Overbeek. The alternative theory suggests that the London-van der Waals constants are of the same order as commonly used in aqueous media, emulsifier layers enter in, and the minimum distance of separation is small and that even with "spherical" particles there can be a finite area of contact.

I. Introduction

The forces between suspension particles and between emulsion drops usually are a complex function of electric double layer repulsion, Born repulsion, London-van der Waals attraction, and short range attraction such as hydrogen bonding. When oil is the continuous phase there is reason to believe that in some cases the force is due largely to London-van der Waals attraction and Born repulsion.^{1,2} In such simple cases one might hope to measure these forces by appropriate rheological measurements and in this way obtain a check on various theories for the non-Newtonian flow of suspensions and emulsions as well as data of intrinsic fundamental interest.

In what follows, it is shown that there are two cases. In one of these the particles or drops may be considered to be in "point contact" and we have developed a method of determining the London-van

der Waals constant and the minimum distance of separation for this type of system. In the other case, there is a finite area of contact and this complication prevents the separate determination of these quantities and they can only be estimated approximately.

II. Theoretical Considerations

We have been estimating for some time the energy of interaction between colloid particles in shear-thinning systems using a rheological theory based on the arguments of Goodeve.³⁻⁵ In this theory the work done in shearing a suspension is considered to be due to the sum of hydrodynamic effects (such as that due to the disturbance of flow caused by the presence of suspended material) and the work necessary to rupture links which are continually re-forming under shear. When the shear rate is large this theory leads to the relation³⁻⁵

(1) W. Albers and J. Th. G. Overbeek, *J. Colloid Sci.*, **14**, 510 (1959).

(2) W. Albers and J. Th. G. Overbeek, *ibid.*, **15**, 589 (1960).

(3) C. F. Goodeve, *Trans. Faraday Soc.*, **35**, 342 (1939).

(4) T. Gillespie, *J. Colloid Sci.*, **15**, 219 (1960).

(5) T. Gillespie, *J. Polymer Sci.*, **46**, 383 (1960).

$$S = \mu^*G + C_1 \quad (1)$$

where S and G are the shear stress and shear rate, respectively, μ^* is the "Newtonian viscosity," and C_1 is the ultimate dynamic yield value.

The suspensions examined in the present work were Newtonian up to a critical concentration at which they became non-Newtonian. We assumed all links were effective and from previous work³⁻⁵ this leads to

$$C_1 = \frac{E_A K_1}{2} N(N - N_c) \quad (2)$$

where E_A is the energy of interaction and K_1 is the rate constant for collisions at unit shear rate in the absence of Brownian movement. N is the number of particles per cc. and N_c is the number of particles per cc. at the critical concentration.

In the interests of clarity, we may take K_1 equal to its value for a suspension of uniform particles, *i.e.*

$$K_1 = \frac{32}{3} a^3 \quad (3)$$

where a is the particle radius.⁶

By measuring the ultimate dynamic yield value, C_1 , at various concentrations the energy of interaction E_A can be determined using eq. 2 and 3.

From Bradley's early work⁷ and subsequent work by Hamaker⁸ we may write as an approximation for identical spheres in point contact

$$E_A = \frac{Aa}{12h_m} \quad (4)$$

A is the effective London-van der Waals constant and h_m is the distance corresponding to the maximum energy which commonly is called "the distance of minimum separation."

From the work of Bradley⁷ and Hamaker⁸ it can be shown quite easily that

$$A = 96\pi h_m^2(\gamma_{11} + \gamma_{22} - 2\gamma_{12}) \quad (5)$$

where γ_{11} and γ_{22} are the surface energy of the dispersed phase and the continuous phase, respectively. γ_{12} is the surface energy descriptive of the interface between the dispersed and continuous phases. These surface energies may be measured directly or with the help of the relation

$$\gamma_{11} = \gamma_{12} + \gamma_{22} \cos \theta \quad (6)$$

where θ is the contact angle.

Combining eq. 4 and 5

$$h_m = \frac{E_A}{8\pi a \delta} \quad (7)$$

$$A = \frac{3}{4\pi \delta} \left(\frac{E_A}{a} \right)^2 \quad (8)$$

where

$$\delta = \gamma_{11} + \gamma_{22} - 2\gamma_{12} \quad (9)$$

Using eq. 7 and 8, the effective London-van der Waals constant and h_m can be determined from the value of E_A determined from flow measurements and the value of δ from surface measurements.

If there is a finite area of contact between particles eq. 4 would have to be modified. As an approxi-

mation, we may use the corresponding expression for flat parallel plates

$$E_A = \frac{A\sigma}{48\pi h_m^2} \quad (10)$$

where σ is the area of contact.

We cannot solve for A and h_m as we did in the simpler case by making use of eq. 5. However, we can solve for σ . The result is

$$\sigma = \frac{E_A}{2\delta} \quad (11)$$

The value of σ determined from eq. 11 using flow and surface measurements can be compared with direct microscopic observations.

III. Experimental

Two types of solid particles were chosen for suspension viscosity measurements. One of these was Neo-Novacite silica obtained from Malvin Minerals Company, Hot Springs, Arkansas. The particles were typical of silica, being like small pieces of ground glass, *i.e.*, roughly spherical with flat portions. By microscopic examination we found the number average particle radius was 3 μ , the average axial ratio was 1.27, and the average length of the apparent line of contact of particles at rest was 3.2 μ . The second suspension contained crosslinked polystyrene beads (X.P. S.). They were made by polymerizing an emulsion of styrene with 8% divinylbenzene in water using a very small particle size silica as emulsifier. The number average radius was 1.5 μ . The beads had a considerably narrower size distribution than the Neo-Novacite silica and, although they were not perfect spheres, the axial ratio was small for most of them.

To make the suspensions, the particles were dispersed in dioctyl phthalate using a high speed laboratory mill. No emulsifiers were used. The flow properties were assessed with a Ferranti-Shirley cone and plate viscosimeter at 25°. In each test the instrument was run at a shear rate of 670 sec.⁻¹ for half an hour before taking measurements. Typical shear rate-shear stress curves are shown in Fig. 1 and 2.

The surface properties of emulsion IV of Albers and Overbeek² were assessed with a du Nouy ring balance. The emulsion contained 1% sorbitan monostearate and 20% water dispersed in a mixture of carbon tetrachloride in benzene of the same density as water at 25°.

IV. Discussion

Table I summarizes the data obtained with the suspensions and Emulsion IV of Albers and Overbeek. For their other emulsions there were not enough data to determine the ultimate dynamic yield value with confidence. In Table I, a refers to the most frequent particle or drop radius. E_A was determined from yield value measurements and eq. 2 and 3. For the emulsion data N_c was taken to be zero.⁴ For the silica the surface energy value was obtained from Bradley⁷ while for the polymer beads it was obtained from measurements of the surface tension of the monomer mixture.

The London-van der Waals constant and h_m in the case of the emulsion were determined by using eq. 7 and 8 which assume "point contact." When these equations were applied to the suspension data the calculated values of h_m were of the order of 1200 Å., which is very large, hence we calculated the area of contact from eq. 11. Using eq. 10, we calculated the value of h_m for values of A in the range 10⁻¹³ to 10⁻¹¹ erg as suggested by quantum theory.

The figures in the last row in Table I indicate that the area of contact is relatively small. Assuming that the contact area was circular, we calculated the apparent area of contact from the value of 3.2 μ

(6) M. von Smoluchowski, *Z. physik. Chem.* (Leipzig), **92**, 129 (1917).

(7) R. S. Bradley, *Phil. Mag.*, **13**, 853 (1932).

(8) H. C. Hamaker, *Physica*, **4**, 1058 (1937).

for the average apparent length of the line of contact. On this basis the contact area was estimated to be about twice the figure given in Table I.

TABLE I
SUMMARY OF THE EXPERIMENTAL AND DERIVED DATA

	Emul- sion IV (ref. 2)	Silica D.O.P.	X.P.S. D.O.P.
$a(\mu)$	3.5	3	1.5
$E_A \times 10^9$ (ergs)	10	3160	400
γ_{11} (ergs/cm. ²)	31.4 ^a	33.8	32
γ_{22} (ergs/cm. ²)	27.1	30.4	30.4
γ_{12} (ergs/cm. ²)	4.3	3.4 ^a	1.6 ^a
δ (ergs/cm. ²)	50	57.4	59.2
$\sigma \times 10^8$ (cm. ²)	0	2.75	0.34
A (ergs)	3.9×10^{-12}	10^{-12} - 10^{-11}	10^{-12} - 10^{-11}
$h_m, \text{Å.}$	2.3	0.8-2.4	0.8-2.4
<u>Area of contact</u>			
Area of av. particle	0	0.024	0.012

^a Obtained from eq. 6 using $\cos \theta$ equal to 1.

The results we have obtained are realistic and suggest that the technique outlined above should be of considerable value, particularly for systems in which there is no complication due to an area of contact. For more precise work, one would have to work with systems with a much narrower size distribution or modify the equations to take into account known effects of size distribution on particle adhesion⁷ and possible effects on the rheological kinetics.⁶

It should be emphasized that the arguments presented above cannot be used without serious modification when electric double layer repulsion, etc., are not negligible.

Finally, we believe that the present analysis is preferable to the treatment of emulsion viscosity data presented by Albers and Overbeek.² They outlined a method of determining A/h_m^2 by equating the force to pull a doublet apart to the Stokes drag of the continuous phase at the point when the S vs. G plot becomes linear. Their values of A/h_m^2 are much smaller than those calculated from eq. 5. When applied to our data their technique leads to the same conclusions as for W/O emulsions, namely, that the London-van der Waals constants are very small or h_m is larger than we realize. As an explanation for their results they took A to be $4 \times$

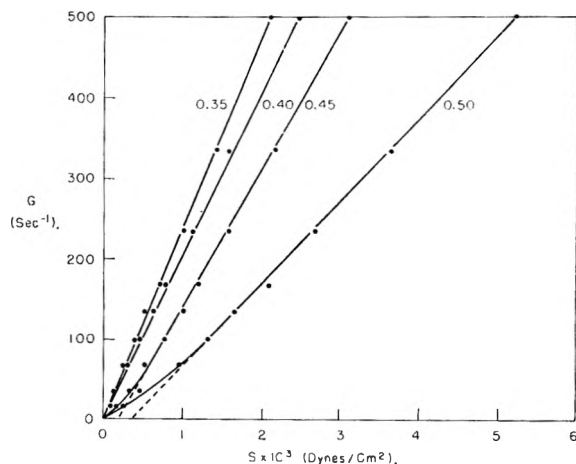


Fig. 1.—The relation between shear stress and shear rate for silica dispersions in dioctyl phthalate. The numbers refer to the fractional solids volume.

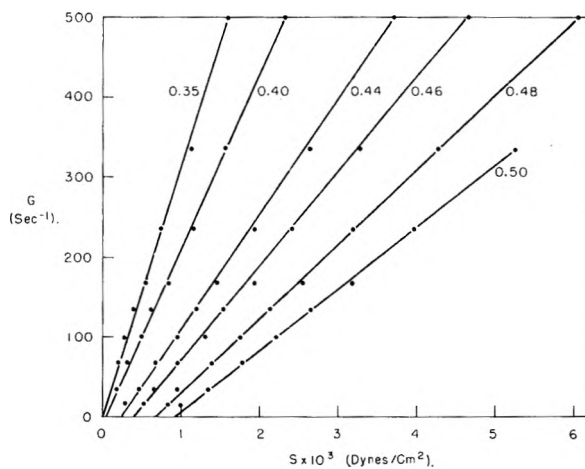


Fig. 2.—The relation between shear stress and shear rate for crosslinked polystyrene beads in dioctyl phthalate. The numbers refer to the fractional solids volume.

10^{-15} erg, regardless of the emulsifier, and h_m of the order of 40 Å., i.e., about twice the length of an emulsifier molecule. The present work would suggest that the emulsion drop plus its emulsifier layer acts as an entity and h_m is the distance between the outer portions of the emulsifier layer.

THE DENSITY OF LIQUID COPPER FROM ITS MELTING POINT (1356°K.) TO 2500°K. AND AN ESTIMATE OF ITS CRITICAL CONSTANTS^{1,2}

By J. A. CAHILL AND A. D. KIRSHENBAUM

Research Institute of Temple University, Philadelphia 44, Pa.

Received December 8, 1961

The density of liquid copper was determined in an argon atmosphere by the immersed sinker method from 1356 to 2500°K. Zirconium dioxide coated molybdenum sinkers with aluminum oxide and zirconium oxide crucibles were employed below 2100°K., while graphite sinkers and crucibles were used to 2500°K. The density, with respect to temperature, is best expressed by the equation $D \text{ g./cm.}^3 = 9.077 - 8.006 \times 10^{-4} T^\circ\text{K.}$ The liquid density at the melting point (1356°K.) is 7.992 g./cm.³ and 6.792 g./cm.³ at the normal boiling point (2855°K.). The molar volumes and thermal coefficients of expansion of liquid copper were calculated. Copper upon melting was found to expand 4.51% of its solid volume. The critical constants of copper were estimated to be: $T_{\text{crit.}} = 8900 \pm 900^\circ\text{K.}$; $D_{\text{crit.}} = 1.04 \pm 0.2 \text{ g./cm.}^3$; $V_{\text{Mcrit.}} = 61 \pm 10 \text{ cm.}^3/\text{mole.}$

Introduction

A knowledge of the density of liquid metals which melt at temperatures exceeding 1000°K. has become extremely important to many branches of scientific investigation. It has been noted, however, that many of these data for even our most abundant metallic elements have not been measured over a temperature range which is concurrent with the temperature spread existing between their melting points and normal boiling points. Copper, which ranks high in importance and abundance among the common metals, is in this category. It is a liquid at atmospheric pressure over a temperature range of 1500°K. (m.p. = 1356°K., n.b.p. = 2855°K.).³

A literature search showed that the only measurements made over a range of temperature were those made by Bornemann and Sauerwald⁴ and Widawski and Sauerwald.⁵ They determined the density by measuring the loss in weight of an immersed quartz sinker from the melting point to only 1873°K. Their data were reproducible to $\pm 0.04 \text{ g./cm.}^3$ and only covered a 400° range.

The authors have measured the density of liquid copper from its melting point (1356°K.) to 2500°K. (an 1150° range).⁶

Experimental

Apparatus.—The temperature source used in these measurements was the carbon tube resistance furnace described previously⁷ operated in an argon atmosphere. For temperatures to 2100°K., molybdenum sinkers coated with zirconium oxide were used in conjunction with aluminum oxide and zirconium oxide crucibles. At the higher temperatures (2100 to 2500°K.) graphite crucibles and sinkers were employed.⁸ Both the zirconium oxide coated molybdenum and graphite sinkers were 2 cm. long and were 1.3 cm. in diameter and tapered into a stem 0.20 cm. in diameter and 3 cm. long. A steel counterweight was incorporated as part

of the upper section of the molybdenum and graphite suspension rods to maintain a stable immersion of the sinkers in the buoyant liquid copper.

Procedure.—The density of liquid copper was determined by the immersed sinker method. The procedure, as described previously,⁹ consisted in measuring the weight loss of a sinker in the liquid copper while simultaneously measuring the temperature of the copper with a calibrated optical pyrometer. The temperature measurements were made under black body conditions. The accuracy of the pyrometer was found to be $\pm 0.2\%$.

The volume of the sinker at 20° was determined by the loss in weight of the sinker when immersed in mercury, corrected for surface tension. The volumes of the sinkers always were corrected to the operating temperature. For the graphite sinkers the thermal expansion data reported by Goldstein, *et al.*,¹⁰ were used together with data known for the graphite used¹¹; while the coefficient of expansion values reported by Bockris, *et al.*,¹² were used for the ZrO₂-coated molybdenum sinkers. The volume of the sinker depended upon its depth of immersion in the liquid copper. This was determined by the difference between the depth of the liquid copper and the distance of the sinker from the crucible base.⁸

The losses in weights were corrected for surface tension using the values of Allen and Kingery¹³ (1270 dynes/cm. at 1373°K. and 1160 dynes/cm. at 1723°K.) extrapolated to 2500°K. with a contact angle of 170°. The correction varied from 0.600 to 0.800 g. The corrected density was calculated from the equation

$$\frac{W_A - W_m - \pi d \gamma \cos \alpha}{V_T} = D$$

where W_A and W_m is the weight of the sinker in air and melt, respectively, d is the diameter of the stem of the sinker, γ the surface tension, and α the contact angle between the stem and the liquid copper.

Materials Used.—The samples used in these studies were electrolytic copper with a purity of 99.97% metallic copper. Analysis of the copper after use in a graphite crucible up to 2500°K. showed a carbon content of 0.021% carbon. This is in good agreement with that reported by Ruff and Bergdahl¹⁴ (0.024% at 2488°K.). This required a correction of only $+0.001 \text{ g./cm.}^3$ at 2495°K.

Results

Using the apparatus and procedure described above, the density of liquid copper was determined

(1) Presented before the Physical and Inorganic Division of the 4th Delaware Valley Regional Meeting of the A.C.S., Jan. 25, 1962.

(2) This work was sponsored by the National Science Foundation under Grants 6278 and 15540.

(3) D. R. Stull and G. C. Sinke, "Thermodynamic Properties of the Elements," A.C.S. Series No. 18 (1956), p. 82.

(4) K. Bornemann and F. Sauerwald, *Metallkunde*, **14**, 145 (1922).

(5) E. Widawski and F. Sauerwald, *Z. anorg. u. allgem. Chem.*, **192**, 145 (1930).

(6) A. D. Kirshenbaum, "Second Annual Report on High Temperature Inorganic Chemistry," under Research Grant NSF-G 6278, Research Institute of Temple University, December 15, 1960.

(7) A. D. Kirshenbaum and J. A. Cahill, *J. Inorg. & Nuclear Chem.*, **14**, 283 (1960).

(8) A. D. Kirshenbaum, J. A. Cahill, and A. V. Grosse, *ibid.*, **22**, 33 (1961).

(9) A. D. Kirshenbaum, J. A. Cahill, and C. S. Stokes, *ibid.*, **15**, 297 (1960).

(10) A. Goldstein, T. E. Waterman, and H. J. Hirschhorn, "Thermophysical Properties of Solid Materials," Vol. I, WADC Technical Report 58-476, Aug., 1960, pp. 59-158.

(11) Dixon E-821, fine grain petroleum coke base stock with a transverse linear coefficient of expansion from 100-600° of 35×10^{-7} and a parallel expansion of 20.8×10^{-7} .

(12) J. O'M. Bockris, J. L. White, and J. D. Mackenzie, "Physico-Chemical Measurements at High Temperatures," Academic Press, New York, N. Y., 1959, p. 347.

(13) B. C. Allen and W. D. Kingery, *Trans. Metal. Soc. AIME*, **215**, 30 (1959).

(14) O. Ruff and B. Bergdahl, *Z. anorg. u. allgem. Chem.*, **106**, 91 (1919).

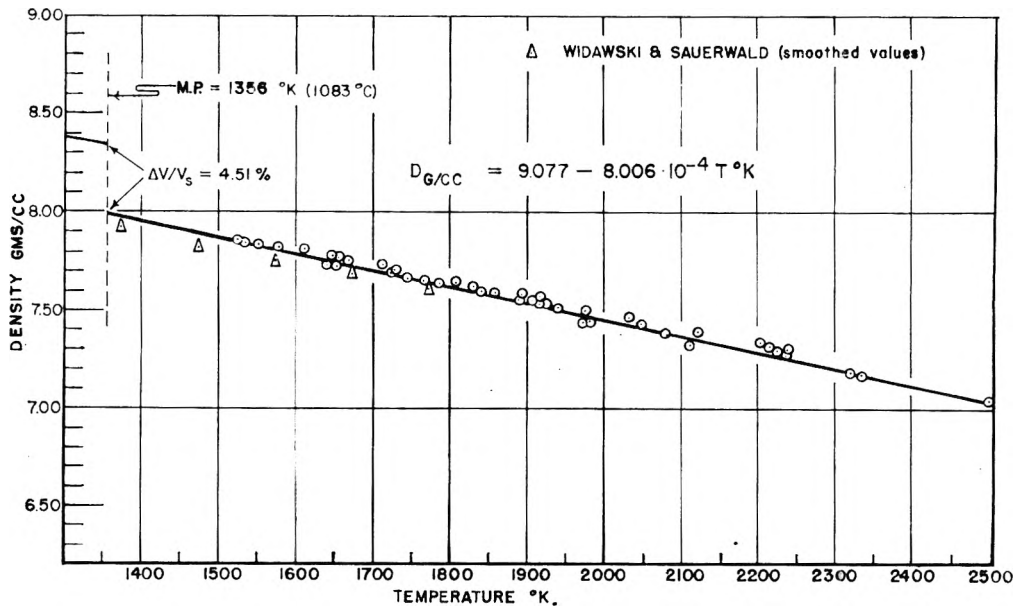


Fig. 1.—Density of liquid copper.

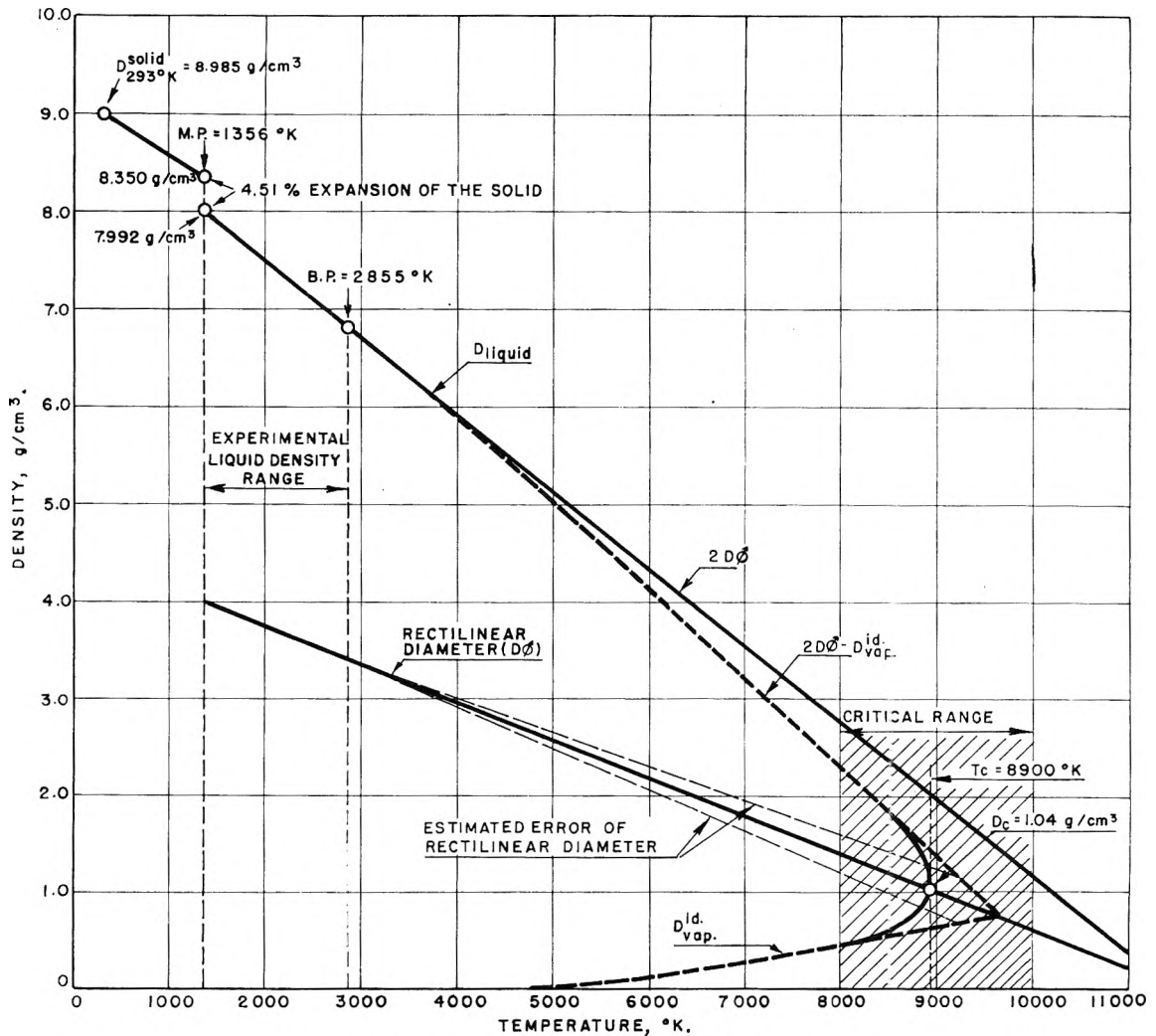


Fig. 2.—The liquid range diagram for copper.

from its melting point (1356°K.) to 2500°K. The results obtained fall on a straight line as shown in

Fig. 1 when density is plotted against temperature. The equation of this line as determined by the

method of least mean squares is

$$D \text{ g./cc.} = 9.077 - 8.006 \times 10^{-4} T^{\circ}\text{K.} \pm 0.011$$

Thus, the liquid density is 7.992 g./cm.³ at the melting point (1356°K.) and 6.792 g./cm.³ at the boiling point (2855°K.). This is equivalent to a change in liquid density with temperature (dD/dt) of -8.006×10^{-4} . Extrapolation of the solid density reported by Sauerwald^{4,5} gives a solid density of 8.350 g./cc. at the melting point. Therefore, the volumetric expansion on melting, $\Delta V/V_s$, is 4.51%. The atomic volumes were calculated for various temperatures from the smoothed density values obtained from the liquid copper density equation. They are summarized in Table I together with the cubical coefficient of expansion values calculated from the equation

$$-\frac{dD}{dt} = \beta D_t$$

where dD/dt is the change in density with temperature, β is cubical coefficient of expansion, and D_t is the density at temperature t .

Estimate of the Critical Constants.—A method of estimating the critical constants of metals has been described lately by Grosse.¹⁵

From this method, the critical temperature was calculated to be $8900 \pm 900^{\circ}\text{K.}$ while the critical density and atomic volume are $1.04 \pm 0.2 \text{ g./cm.}^3$ and $61 \pm 10 \text{ cm.}^3/\text{mole}$, respectively. The rectilinear diameter $D_{\theta} = 4.538 - 4.003 \times 10^{-4} T^{\circ}\text{K.}$ in g./cm.^3 .

(15) A. V. Grosse, *J. Inorg. & Nuclear Chem.*, **22**, 23 (1961).

TABLE I

ATOMIC VOLUMES AND EXPANSION COEFFICIENTS OF LIQUID COPPER

Temp., °K.	Density, g./cm. ³ (smoothed values)	Atomic volume, cm. ³ /mole	Cubical expansion coefficient $\beta \times 10^6$, °K. ⁻¹
1356 (m.p.)	7.992	7.952	100.2
1400	7.956	7.990	100.6
1600	7.797	8.152	102.7
1800	7.636	8.324	104.8
2000	7.476	8.503	107.1
2200	7.316	8.688	109.4
2400	7.156	8.883	111.9
2855 (b.p.)	6.792	9.359	117.9

Figure 2 shows the whole liquid range diagram from melting point to critical temperature. The densities of the liquid copper above the normal boiling point are presented in Table II.

TABLE II

THE LIQUID DENSITY OF COPPER ABOVE ITS NORMAL BOILING POINT

Temp., °K.	Liquid density, g./cm. ³
3000	6.675
4000	5.87
5000	5.03
6000	4.16
7000	3.2

Acknowledgment.—We wish to thank Dr. A. V. Grosse for his helpful advice and Lucia Streng for the analytical determinations.

IDEALITY OF *n*-BUTANE:ISOBUTANE SOLUTIONS

BY J. F. CONNOLLY

Research and Development Department, American Oil Company, Whiting, Indiana

Received December 9, 1961

Gas compressibilities were measured for the isobutane:*i*-butane system up to the saturation pressures, in the temperature range 70 to 170°, and 2nd and 3rd virial coefficients were derived. Mixed 2nd virial coefficients calculated on the basis of Amagat's law agreed with the experimental values to 1 cc./mole on the average. Phase boundaries were measured for the same system from 70° to the critical temperature of *i*-butane. The phase-boundary pressures computed using the ideal-solution laws and the virial coefficients agreed with the observed values within 0.2%.

Introduction

Solutions of compounds as closely related to one another as *n*-butane and *i*-butane might well be expected to form nearly ideal solutions as long as the critical region is not approached too closely. Redlich's vapor-liquid equilibrium measurements, made near atmospheric pressure, have shown that a number of isomers come close to forming ideal solutions¹ below a reduced temperature of 0.7. Because of the higher saturation pressures at temperatures nearer the critical, an accurate knowledge of gas compressibilities would be a necessary addition to vapor-liquid equilibrium data in testing the ideal solution laws.

The present work was done in the reduced temperature range from 0.8 to near 1 in order to ascertain whether or not ideality continued to hold at higher temperatures. Phase-boundary pressures

were measured for both compounds and three mixtures in the temperature range 70° to near the critical temperature of *i*-butane. Gas compressibilities were measured from 4 atm. to close to the saturation pressures for both compounds and a 50:50 mixture in the temperature range 70 to 170°.

Experimental

The *n*-butane and *i*-butane were Phillips research grade materials with stated purities of 99.99 and 99.96 mole %. They were not purified further except to remove the air present by distillation *in vacuo*. The purities of the resulting products were confirmed by the small pressure rises, 0.01 atm., observed between the two phase boundaries, *i.e.*, between the dew (first trace of liquid) point and the visual bubble (last trace of gas) point.

In the experimental method,² a sample was confined above mercury in a calibrated glass capillary and stirred with a magnetically driven steel ball. Volumes were determined by measuring lengths with a cathetometer. Pressures were measured with a dead weight gage; temperatures with a

(1) O. Redlich and A. T. Kister, *J. Am. Chem. Soc.*, **71**, 505 (1949).

(2) J. F. Connolly and G. A. Kandalic, *Phys. Fluids*, **3**, 463 (1960).

platinum-resistance thermometer. Critical points were determined visually. Dew points were determined by noting the discontinuity in the pressure-volume isotherm. Bubble points were determined both from the discontinuity in the pressure-volume isotherm and by visual observation of the disappearance of the last trace of vapor.

The bubble and dew point determinations are illustrated in Fig. 1 for the 160°F. isotherm of the 50-50 *n*-butane:*i*-butane mixture. The pressure usually rose sharply by about 0.01 atm. as the last trace of vapor disappeared. Because this rise occurred with the pure substances also, it presumably was due to traces of volatile impurities. The true bubble point was taken as the discontinuity defined by a short linear extrapolation of the isotherm.

The observed vapor pressures of *n*-butane and *i*-butane are listed in Table I. The dew and bubble points of the three mixtures are listed in Table II.

TABLE I
VAPOR PRESSURE OF *n*-BUTANE AND *i*-BUTANE (ATM.)

Temp., °C.	<i>n</i> -Butane ^a	<i>i</i> -Butane ^a
71.11	8.20	11.00
87.78	11.79	15.52
104.44	16.42	21.29
121.11	22.28	28.56
133.72	27.67	35.32
134.62	...	35.85 ^b
137.78	29.62
151.97	37.35 ^b

^a The vapor pressures of both compounds agree with Sage and Lacey's values^{3,4} to about 0.1%. ^b Critical state. Comparing these critical constants with the values selected by Kobe⁵ shows them to be lower by 3.0° and 0.1 atm. for *n*-butane and 0.3° and 0.2 atm. for *i*-butane.

Liquid and Vapor Compositions.—In order to obtain both liquid and vapor compositions at the same temperature and pressure, interpolation with respect to composition is necessary. Because the variations of the bubble and dew point pressures with composition were not far from linear, they were represented within experimental error by quadratic equations such as

$$p = a + by_2 + cy_2^2 \quad (1)$$

for dew points and

$$p = a' + b'x_2 + c'x_2^2 \quad (2)$$

for bubble points; where p is the pressure in atm., and y_2 and x_2 are mole fractions of *i*-butane in the vapor and liquid phases. The constants in eq. 1 and 2 along with closeness of fit to the data are given in Table III. Values of x_2 at each dew pressure and of y_2 at each bubble pressure were calculated from these equations. They are listed in Table II.

The critical temperatures of the mixtures were represented with a maximum deviation of 0.02° by

$$t_c(°C.) = 151.97 - 16.58y_2 - 0.76y_2^2$$

and the critical pressures with a maximum deviation of 0.01 atm. by

$$p_c(\text{atm.}) = 37.35 - 1.03y_2 - 0.46y_2^2$$

Virial Coefficients.—To represent the gas compressibilities in the density range of this work the virial equation of state, terminated after the 3rd virial term, is sufficient. The equation is

(3) R. H. Olds, H. H. Reamer, B. H. Sage, and W. N. Lacey, *Ind. Eng. Chem.*, **36**, 282 (1944).

(4) W. M. Morris, B. H. Sage, and W. N. Lacey, *Trans. Am. Inst. Mining Met. Engrs.*, **136**, 158 (1940).

(5) K. A. Kobe and R. E. Lynn, Jr., *Chem. Rev.*, **52**, 117 (1953).

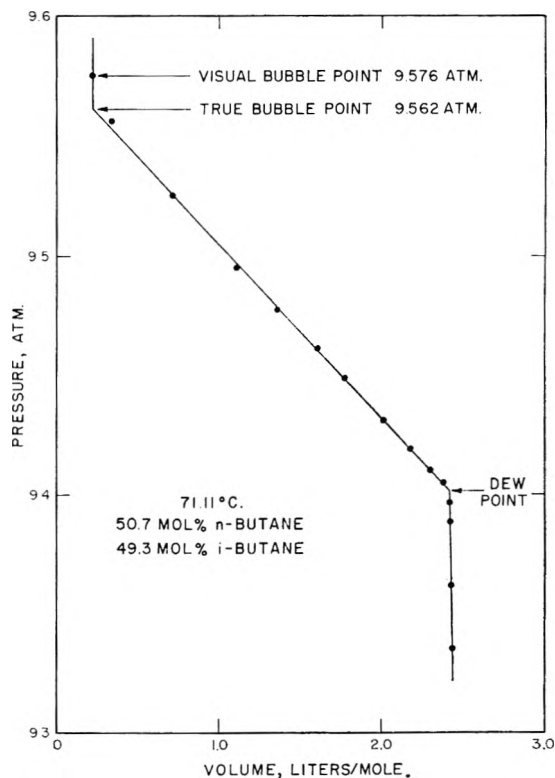


Fig. 1.—Pressure-volume isotherm in the two-phase region.

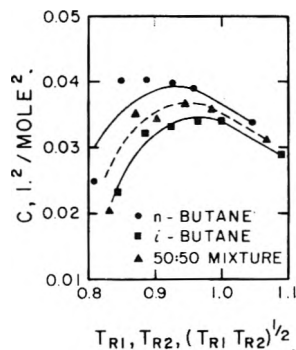


Fig. 2.—Third virial coefficients.

$$\frac{pv}{RT} = 1 + \frac{B}{v} + \frac{C}{v^2} \quad (3)$$

where v is molal volume, and B and C are the 2nd and 3rd virial coefficients of the mixtures

$$B = y_1^2 B_{11} + 2y_1 y_2 B_{12} + y_2^2 B_{22} \quad (4)$$

$$C = y_1^3 C_{111} + 3y_1^2 y_2 C_{112} + 3y_1 y_2^2 C_{122} + y_2^3 C_{222} \quad (5)$$

B_{11} and C_{111} being the virial coefficients of *n*-butane; B_{22} and C_{222} the virial coefficients of *i*-butane; and B_{12} , C_{112} , and C_{122} "mixed" virial coefficients that depend on the forces between unlike molecules.

To obtain C , eq. 3 was fitted to the experimental data by least squares. In Fig. 2 the values for *n*-butane, *i*-butane, and the 50:50 mixture are plotted against the reduced temperatures of *n*-butane and *i*-butane, and the geometric mean of the reduced temperatures. The points scatter below a reduced temperature of 0.9. Such scatter is to be expected because the density that may be reached without exceeding the saturation pressure is small at the lower temperatures. Because this makes the measured deviations from ideality very small, the

TABLE II
COMPARISON OF OBSERVED PHASE-BOUNDARY PRESSURES WITH THOSE CALCULATED ON THE BASIS OF IDEAL SOLUTIONS
Dew points

Temp., °C.	y_2	p (atm.)	x_2^a	ϕ_1^0/ϕ_1	ϕ_2^0/ϕ_2	I_1	I_2	$100(p - p_{ideal})/p$ %
71.11	0.246	8.76	0.202	1.012	0.955	1.002	0.990	0.1
	.493	9.40	.435	1.026	.968	1.005	.993	.2
	.750	10.17	.706	1.043	.983	1.008	.996	.2
87.78	.246	12.54	.207	1.015	.948	1.003	.987	.1
	.493	13.41	.442	1.032	.962	1.006	.991	.2
	.750	14.42	.712	1.054	.980	1.010	.995	.2
104.44	.246	17.44	.213	1.018	.939	1.004	.983	.2
	.493	18.56	.450	1.040	.956	1.009	.988	.1
	.750	19.88	.719	1.067	.977	1.014	.993	.2
121.11	.246	23.60	.221	1.023	.927	1.006	.976	.1
	.493	25.06	.461	1.050	.947	1.012	.984	.1
	.750	26.76	.726	1.083	.971	1.020	.992	.1
133.72 ^b	.246	29.31	.230	1.027		1.007		.2
	.493	31.07	.472	1.061		1.015		.2
	.750	33.16	.735	1.107		1.025		-.2

Bubble points

	x_2	p (atm.)	y_2^a	ϕ_1^0/ϕ_1	ϕ_2^0/ϕ_2	I_1	I_2	$100(p - p_{ideal})/p$ %
71.11	0.246	8.88	0.296	1.015	0.957	1.003	0.991	0.2
	.493	9.56	.551	1.030	.971	1.006	.994	.1
	.750	10.29	.788	1.046	.985	1.009	.997	.1
87.78	.246	12.68	.289	1.018	.950	1.004	.988	.1
	.493	13.60	.544	1.036	.966	1.007	.992	.2
	.750	14.56	.784	1.057	.983	1.011	.996	.1
104.44	.246	17.59	.282	1.021	.942	1.005	.984	.1
	.493	18.77	.536	1.044	.959	1.010	.989	.1
	.750	20.04	.779	1.071	.979	1.015	.994	.2
121.11	.246	23.76	.273	1.025	.929	1.007	.977	.2
	.493	25.26	.526	1.054	.950	1.013	.985	.1
	.750	26.91	.772	1.087	.974	1.021	.993	.1
133.72 ^b	.246	29.39	.264	1.029		1.008		.0
	.493	31.25	.514	1.065		1.016		.0
	.750	33.26	.764	1.110		1.026		-.4

^a From eq. 1 and 2. ^b This temperature is too close to the critical temperature of *i*-butane to permit the calculation of ϕ_2^0 and I_2 . Therefore, p was calculated from: $p = \frac{p_1^0 \phi_1^0 I_1}{\phi_1} \left(\frac{x_1}{y_1} \right)_{\text{exptl.}}$

TABLE III
CONSTANTS FOR EQUATIONS 1 AND 2

Temp., °C.	Dew points				Bubble points			
	a	b	c	Max. dev., atm.	a'	b'	c'	Max. dev., atm.
71.11	8.200	2.088	0.714	0.00	8.200	2.729	0.073	0.00
87.78	11.792	2.833	0.906	.00	11.792	3.587	.142	.00
104.44	16.421	3.845	1.025	.01	16.420	4.679	.193	.01
121.11	22.285	5.027	1.248	.01	22.286	5.838	.434	.01
133.72	27.675	6.236	1.407	.01	27.676	6.880	.760	.01

values of B and C , particularly C , will be more uncertain at these temperatures. The uncertainty in the low temperature C 's has very little effect on the calculation of fugacities because of the low saturation pressures at these temperatures.

Values of B , as well as C , were obtained in the course of fitting eq. 3. However, in order to obtain slightly better values of B at the lower temperatures, the values of C from eq. 3 were smoothed graphically (Fig. 2) and the least squares process was repeated using the equation

$$\frac{pv}{RT} - 1 = \frac{C(\text{smoothed})}{v^2} = \frac{B}{v} \quad (6)$$

Equation 6 reproduced the experimental compressi-

bility factors with a standard deviation of about 0.05%. It gave values of B which were the same as those from eq. 2 at high temperatures, and differed by only 2 or 3 cc. per mole at the lower temperatures.

Values of B from equation 6 are plotted in Fig. 3 and listed in Table IV. Values of the mixed 2nd virial coefficient, calculated by means of eq. 4 from B for the 50:50 mixture, also are listed in Table IV under B_{12} .

Amagat's law⁶ would require a B_{12} for which

$$B_{12} = \frac{B_{11} + B_{22}}{2}$$

The experimental values agreed with this equation

TABLE IV
 VIRIAL COEFFICIENTS

Temp., °C.	<i>n</i> -Butane ^a			<i>i</i> -Butane ^a			0.507 <i>n</i> -Butane 0.493 <i>i</i> -Butane			
	- <i>B</i> ₁₁ , cc./mole	<i>C</i> ₁₁₁ , l. ² /mole ²	Max. ^c density, mole/l.	- <i>B</i> ₂₂ , cc./mole	<i>C</i> ₂₂₂ , l. ² /mole ²	Max. ^c density, mole/l.	- <i>B</i> ₁ , cc./mole	<i>C</i> ₁ , l. ² /mole ²	Max. ^c density, mole/l.	- <i>B</i> ₁₂ , cc./mole
71.11	517.0	(0.0300) ^b	0.35	457.2	(0.0240)	0.50	485.8	(0.0270)	0.41	483.7
87.78	464.7	(.0355)	.52	412.7	(.0305)	0.73	438.6	(.0325)	.60	437.9
104.44	418.6	(.0380)	.75	374.0	.0335	1.08	396.9	.0360	.87	396.9
121.11	381.3	.0395	1.08	341.1	.0345	1.68	361.7	.0370	1.29	361.7
133.72	356.1	.0390	1.46	318.3	.0340	1.70	337.8	.0365	1.84	338.1
137.78	348.6	.0385	1.65	311.5	.0335	1.70	330.0	.0360	1.72	329.5
171.11	289.8	.0340	1.58	259.6	.0290	1.70	274.1	.0310	1.82	273.1

^a Virial coefficients of *n*-butane and *i*-butane, in the ranges 0 to 300° and 140 to 300°, respectively, have been reviewed.⁷
^b Values in parentheses are uncertain. ^c Maximum density used in fitting eq. 6.

to 1 cc./mole on the average and 3 cc./mole at the maximum. Such agreement is within experimental error.

Ideality of the Liquid Phase.—A concentrated solution is said to be ideal when its activity coefficients, as defined by a particular choice of reference states, are unity. Except near atmospheric pressure, it is not possible to choose the same liquid reference states for both components, unless one is willing to countenance hypothetical states with somewhat indeterminate properties. Therefore, the reference state for *n*-butane was taken as pure *n*-butane and that for *i*-butane as an infinitely dilute solution of *i*-butane in *n*-butane. The chemical potentials in the liquid phase then are given by

$$\begin{aligned}\mu_1^L &= \mu_1^s(p, T) + RT \ln \gamma_1 x_1 \\ \mu_2^L &= \mu_2^s(p, T) + RT \ln \gamma_2 x_2\end{aligned}$$

where γ_1 and γ_2 are activity coefficients of *n*-butane and *i*-butane, for which $\lim_{x_1 \rightarrow 1} \gamma_1 = \lim_{x_2 \rightarrow 1} \gamma_2 = 1$. Therefore, the chemical potential of pure *n*-butane is equal to μ_1^s whereas the chemical potential of *i*-butane in its standard state is given by

$$\mu_2^s(p, T) = \lim_{x_2 \rightarrow 0} [\mu_2^L - RT \ln x_2]$$

For the gas phase we have

$$\mu_i^G = F_i(T) + RT \ln f_i^G \quad (7)$$

where f is a fugacity and $F(T)$ is the chemical potential of the pure gas in the ideal gas state at 1 atm.

By equating chemical potentials for each species in the two phases at equilibrium, and making use of the expressions

$$V_1 = \left(\frac{\partial \mu_1^s}{\partial p} \right)_T \text{ and } \bar{V}_2^* = \left(\frac{\partial \mu_2^s}{\partial p} \right)_T \quad (8)$$

we obtain

$$f_1^G = f_1^L = \gamma_1 x_1 f_1^0 \exp \left[\frac{1}{RT} \int_{p_1^0}^p V_1 dp \right] \quad (9)$$

for *n*-butane, and

$$f_2^G = f_2^L = (\gamma_2 / \gamma_2^0) x_2 f_2^0 \exp \left[\frac{1}{RT} \int_{p_2^0}^p \bar{V}_2^* dp \right] \quad (10)$$

for *i*-butane; where V_1 is the liquid molal volume of

(6) J. A. Beattie, "Thermodynamics and Physics of Matter," F. D. Rossini, Ed., Princeton University Press, Princeton, N. J., 1955, p. 305.

(7) H. G. David and S. D. Hamann, "Proc. Joint Conf. Thermodynamic and Transport Properties of Fluids," Inst. Mech. Engrs., London, 1957, pp. 74-78.

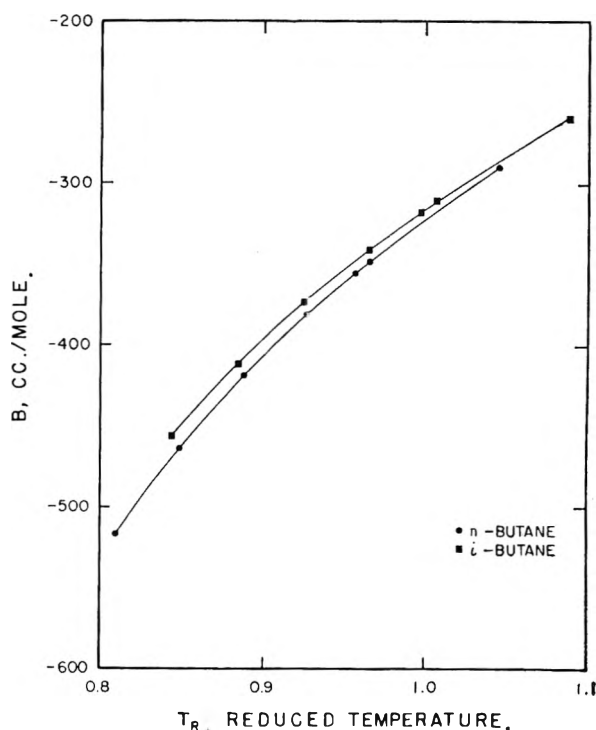


Fig. 3.—Second virial coefficients of *n*-butane and *i*-butane.

pure 1 (*n*-butane), \bar{V}_2^* is the partial molal volume of *i*-butane at infinite dilution ($x_2 = 0$) in 1, and the superscript 0 denotes the value of the property for the pure substance at its vapor pressure. For ideal solutions $\gamma_1 = \gamma_2 = 1$ over the whole composition range and we have

$$f_i^G = x_i f_i^0 I_i$$

or

$$y_i p \phi_i = x_i p_1^0 \phi_i^0 I_i \quad (11)$$

where

$$I_1 = \exp \left[\frac{1}{RT} \int_{p_1^0}^p V_1 dp \right], I_2 = \exp \left[\frac{1}{RT} \int_{p_2^0}^p \bar{V}_2^* dp \right]$$

and ϕ is a gaseous fugacity coefficient.

Before eq. 11 can be applied to the calculation of phase boundary pressures at a particular temperature, liquid volumes must be known as a function of pressure, and ϕ_i must be known as a function of pressure and composition. Values of V_1 and \bar{V}_2^* ⁸

(8) For ideal solutions $\bar{V}_2^* = V_2$ only when $p \geq p_2^0$, and in the present case $p < p_2^0$. However, the p -pressure is short enough so that \bar{V}_2^* at p_2^0 can be used from p_2^0 to p .

are available⁸ and the virial equation of state in combination with eq. 7 gives⁶ an expression for ϕ_i

$$\phi_i = \frac{f_i}{y_i p} = \frac{RT}{pv} \exp \left[\frac{2}{v} (y_i B_{ii} + y_i B_{ij} + \frac{3}{2v^2} (y_i^2 C_{iii} + 2y_i y_j C_{ijj} + y_j^2 C_{ijj})) \right] \quad (12)$$

Table IV gives all of the virial coefficients needed in eq. 12 except the mixed 3rd virial coefficients C_{112} and C_{122} . However, C_{111} and C_{222} are so close together that it makes little difference what combining rule is used to obtain these mixed virial coefficients. Therefore, it was assumed that

$$C_{112} = \frac{2C_{111} + C_{222}}{3}, \quad C_{122} = \frac{C_{111} + 2C_{222}}{3} \quad (13)$$

Equations 13 in combination with eq. 5 predict exactly the values of C for the 50:50 mixture listed in Table IV.

To calculate ideal dew point pressures, equations 3, 11, and 12 were solved simultaneously by iteration at each dew point composition and temperature. Analogously for the bubble points, bubble point pressures were calculated. The ideal pressures agreed with the experimental ones within 0.15% on the average. A detailed comparison is made in Table II.

It is pertinent to ask what the differences between observed and ideal phase-boundary pressures mean in terms of the activity coefficients γ_1 and γ_2 . An approximate expression relating deviations in

(9) B. H. Sage and W. N. Lacey, "Thermodynamic Properties of the Lighter Paraffin Hydrocarbons and Nitrogen," Am. Pet. Inst., New York, N. Y., 1955.

activity coefficients with deviations in boundary pressures may be obtained for a 50:50 mixture ($x_1 = 0.5$) as follows: Because the ratio $I_1\phi_2/I_2\phi_1$ varies very slowly with pressure and vapor composition, which in turn are close to the ideal values, we may use eq. 9 and 10 to write

$$\frac{y_1}{y_2} = \frac{\gamma_1 \gamma_2^0 x_1 f_1^0}{\gamma_2 x_2 f_2^0} \left(\frac{I_1 \phi_2}{I_2 \phi_1} \right)_{ideal}$$

If the deviations from ideality are "regular"¹⁰ and independent of pressure, then $\ln \gamma_1 = Ax_1^2$ and $\ln(\gamma_2/\gamma_2^0) = Ax_2^2$, yielding $\gamma_1 \gamma_2^0/\gamma_2 = 1$ for a 50:50 mixture. Therefore, for a 50:50 mixture, $(y_1/y_2) = (y_1/y_2)_{ideal}$ and eq. 9 gives

$$\frac{p - p(ideal)}{p} = \frac{\gamma_1 - (I_1/\phi_1)_{ideal}/(I_1/\phi_1)}{\gamma_1} \quad (14)$$

Although ϕ_1 is more sensitive to pressure than ϕ_1/ϕ_2 , the variation is slow enough and p is close enough to $p(ideal)$ that the approximate equation of state $pv = RT + Bp$ may be applied to eq. 14. Then

$$\gamma_1 - 1 = \alpha \frac{p - p(ideal)}{p}$$

where $\alpha \cong 1 - p(V_1 - B_{11})/RT$, which varies from 0.8 to 0.5 for this system in the temperature range 70 to 130°. Thus the activity coefficients of the 50:50 mixture are ideal to roughly the same degree as the phase boundary pressures.

Acknowledgments.—The author thanks G. A. Kandalic for his aid in making the measurements and W. A. Junk for his advice.

(10) J. H. Hildebrand and R. L. Scott, "The Solubility of Nonelectrolytes," Reinhold Publ. Corp., New York, N. Y., 1950, p. 35, 131.

THE DIELECTRIC BEHAVIOR OF VAPORS ADSORBED ON POROUS SOLIDS

By J. M. THORP

Chemistry Department, University of Auckland, Auckland, New Zealand

Received December 11, 1961

An investigation has been made of the dielectric behavior (at a frequency of 0.5 Mc./sec.) of water adsorbed on alumina, and of benzene adsorbed on both alumina and silica gel, at 25°. Isosteric heats of sorption, and data relating to pore size distribution, were obtained from the determination of sorption isothermals. For water adsorbed on alumina, the plot of capacitance increment against the amount adsorbed was found to be reversible, for both adsorption and desorption, throughout the entire sorption range. The absence of dielectric hysteresis was considered to be due to strong adsorbate-adsorbate interaction. Evidence was obtained for the physical adsorption of a layer of orientated water molecules onto an alumina surface modified by initial chemisorption. The evaluated dielectric constant, ϵ_2 , for benzene adsorbed entirely in the capillary condensed state, on both alumina and silica gel, compared well with ϵ_{liq} , the literature value for the normal liquid. In an adsorbed benzene monolayer, ϵ_1 was lower than ϵ_{liq} on silica gel, but higher (and equal to ϵ_{solid}) on alumina. The former was considered to be due to the interaction of the π -electrons in the benzene monolayer with the silica hydroxyl groups. It was assumed that this interaction was absent with alumina, the higher value of ϵ_1 observed with the latter being due to close-packing of the benzene molecules on the surface. Dielectric hysteresis was observed for benzene on alumina, but not on silica gel. An explanation has been given in terms of the uneven electron density in the benzene molecule, together with the different polarizing influences of the two adsorbent surfaces.

A previous paper¹ reported an investigation of the dielectric behavior of water, methyl alcohol, and ethyl alcohol sorbed on three porous powdered adsorbents: silica gel, alumina, and a mixed silica-ferrous oxide gel. These systems were chosen primarily with the object of investigating whether the hysteresis phenomena observed in the sorption isotherms also occurred in the plots of incremental

electrical capacitance against the amount adsorbed. Such a hysteresis loop was in fact observed, the start coinciding with that of the corresponding loop in the isotherm, indicating the onset of capillary condensation. The hysteresis in the capacitance plot was attributed to the different electrical properties of the polar molecules adsorbed in orientated multilayers, built up simultaneously with capillary condensation during adsorption, from those in the

(1) J. M. Thorp, *Trans. Faraday Soc.*, **55**, 442 (1959).

entirely capillary condensed state during desorption.

With alumina and a mixed silica-ferric oxide gel, both of which exhibited isotherms of similar shape, indicating a wide variation in pore size, it was observed that the desorption branch of each loop had higher values of capacitance than the corresponding adsorption points. On the other hand, with a more uniform narrow-pore silica gel, the converse was found, the adsorption points having the higher capacitances. Further, with the silica gel the capacitance loops showed a decrease in size for water, methyl alcohol, and ethyl alcohol, in that order, that for ethyl alcohol barely being discernible. With the other two adsorbents, however, the loops investigated showed the converse, ethyl alcohol now exhibiting the largest loop. Data for the system alumina-water, which then had not been investigated, are presented now. Results conform to previous observation in that the capacitance hysteresis for this system, if any, is so small that no loop is detectable within the limits of experimental error ($\pm 0.08 \mu\text{mf.}$), the capacitance plot being reversible throughout the entire desorption range up to saturation, for both adsorption and desorption.

Recent investigation² has shown that adsorbed water can exist in a highly ordered state. Methyl alcohol and, to a smaller extent, ethyl alcohol also exhibit molecular association by hydrogen bonding. Consequently in narrow pores (which predominate in the silica gel) less freedom of dipole orientation could be expected in a three-dimensional network of hydrogen-bonded molecules in the capillary condensed state than in adsorbed multilayers. The greater restriction was indicated by the lower capacitances in the desorption branch of the loop. It followed that the size of the hysteresis loop would increase from ethyl alcohol to water, as observed, since the greater the hydrogen bonding between sorbate molecules, the greater the molecular restriction during desorption.

The other two adsorbents, however, have a greater proportion of larger pores, and it was considered that the existence of these macropores caused the "inversion" of the capacitance hysteresis. The behavior of capillary condensed sorbate was considered to approach that of the normal liquid in large pores, so that molecular orientation then was less restricted than in the adsorbed multilayers.

The main part of this paper is concerned with the sorption of a non-polar sorbate, benzene, on the silica gel and alumina. These two commercial adsorbents were chosen for further investigation owing to their contrasting behavior with regard to capacitance hysteresis. If this hysteresis can be attributed solely to the restriction of the orientation of dipoles present in different sorbed states, then a non-polar adsorbate would not be expected to exhibit any electrical hysteresis.

Experimental

Powdered adsorbent (between 50 and 70 mesh) was evacuated at 150° for about 8 hr. and then saturated with sorbate vapor, desorption being investigated first in each

system. The silica gel was supplied by British Drug Houses Ltd. and the alumina was "type A" from Peter Spence Ltd. The apparent density, or granule density, was determined by mercury displacement, being 0.89 and 0.80 g. cm.⁻³, respectively. Water was purified by passing through a resin column. Analar benzene was dried with 5A Linde Sieve Zeolite, and then was fractionally recrystallized. The purified benzene sample of m.p. 5.52° was stored in a flask containing fresh zeolite pellets. Saturated vapor pressures of sorbed water and benzene at 25 ± 0.05° were found to be 23.75 ± 0.10 and 94.4 ± 0.4 mm. (literature values being 23.76³ and 94.0⁴ mm., respectively).

Sorption isotherms and capacitance measurements were determined separately and have been described in more detail elsewhere.¹ In sorption measurements, the amount adsorbed was determined directly by weighing the adsorbent container, which could be detached from a mercury manometer by means of a waxed joint. Both the container and manometer were immersed in a thermostat for the measurement of the equilibrium pressure, the latter being determined by means of a cathetometer.

For measurements of capacitance the adsorbent container was replaced by the dielectric cell, consisting of two stainless steel coaxial cylinders contained in a glass vessel, which could be attached to the manometer by means of the same waxed joint. The capacitance of the empty cell was about 25 $\mu\text{mf.}$ The space between the cylinders (about 11 ml.) was packed with the powdered adsorbent. After evacuation at 150°, the dielectric cell was attached to the manometer and the initial capacitance measurement was made. Capacitance changes for the addition (or removal) of vapor were determined by means of a voltage resonance method at a frequency of 1/2 Mc./sec., the precision condenser being accurate to within $\pm 0.08 \mu\text{mf.}$ The capacitance increment, $\Delta C(\mu\text{mf.})$, was plotted against the amount adsorbed (mg./g.), the latter being obtained for each pressure reading from the isotherm initially determined. In the determination of both sorption isotherms and capacitance curves, several desorption and adsorption runs were made for each system in order to check that the curves were reproducible.

Results

1. **Sorption Isotherms.**—The sorption isotherms at 25° for benzene on both silica gel and alumina are shown in Fig. 1, together with additional desorption curves determined at 35°, so that isosteric heats of sorption could be calculated for each system by means of the Clausius-Clapeyron equation.

The sorption isotherm for water on alumina at 25° also was determined to complete the data obtained previously. These results are plotted (Fig. 2) as volume adsorbed/g. adsorbent against relative pressure to allow comparison with those for benzene on the same adsorbent. (The curves determined at higher temperatures are omitted to preserve clarity.) As might be expected, chemisorption of water on alumina is clearly indicated, the curve approaching a volume of 0.065 ml./g. at zero pressure, whereas that for benzene approaches the origin. This also explains why the hysteresis loop for water starts almost immediately, whereas that for benzene does not start until a relative pressure of 0.175 is exceeded. With benzene the initial reversible curve represents the adsorption or desorption of a monolayer, whereas for water this represents physical adsorption toward the end of a monolayer, and the start of a second layer.

With benzene, both adsorbents exhibit hysteresis, indicating capillary condensation, and conse-

(2) S. M. Nelson, *Ann. Repts. on Progr. Chem.* (Chem. Soc. London), **54**, 83 (1957).

(3) "International Critical Tables," McGraw-Hill Book Co., New York, N. Y.

(4) C. K. Ingold, C. G. Raisin, and C. L. Wilson *J. Chem. Soc.*, 915 (1936).

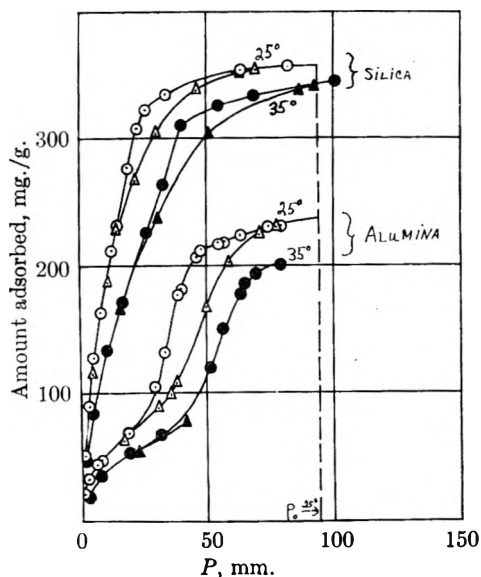


Fig. 1.—Sorption isotherms for benzene on silica gel and alumina at 25 and 35°: at 25°, ○ desorption, △ adsorption; at 35°, ● desorption, ▲ adsorption.

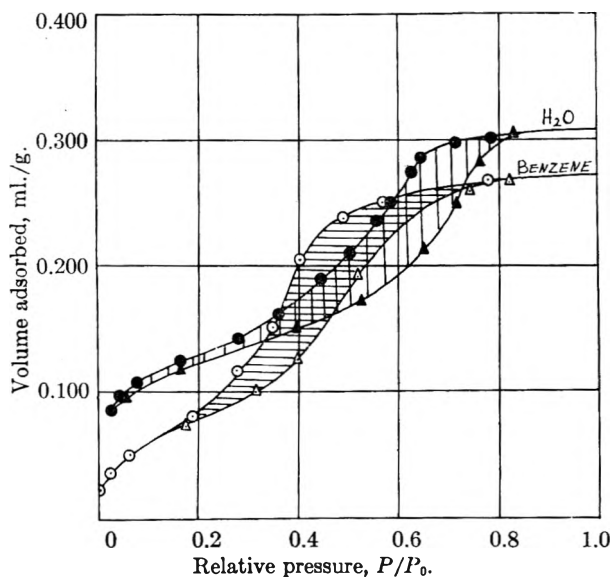


Fig. 2.—Sorption isotherms for water and benzene on alumina at 25°: H₂O, ● desorption, ▲ adsorption; benzene, ○ desorption, △ adsorption.

quently the Kelvin equation can be applied to the desorption branch of each loop. This enables calculation of the "Kelvin radius," r_k , of the pores which are filled at vapor pressure p , and at temperature $T^\circ\text{K.}$, by the relation $\log_e p_0/p = 2M\gamma/d r_k RT$, where M , γ , and d are, respectively, the molecular weight, surface tension, and liquid density of the adsorbate. If the Kelvin radius is plotted against the volume of adsorbate, then the distribution curve (dv/dr against r_k) can be obtained. The latter plot (Fig. 3) gives the distribution of the volume condensed in the pores according to the pore radius. The uniform pore structure of the silica gel, with its tall narrow peak at 12.5 Å., is apparent immediately in contrast to the lower and wider "peak" for alumina, the most frequently occurring pore radius (about 21 Å.) being nearly double. Before capillary condensation starts, one or two layers of adsorbate

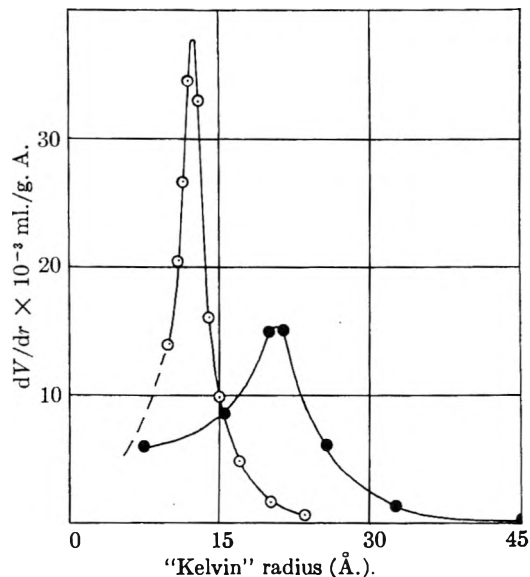


Fig. 3.—Distribution of volume according to pore radius, for benzene on silica gel (○) and alumina (●).

molecules are adsorbed initially, and this adsorbed layer thickness must be added to the mean Kelvin radius in order to obtain the true mean pore radius. It is assumed that benzene molecules are adsorbed flat on the surface and the van der Waals thickness has been taken as 3.7 Å. Calculated values of the true mean pore radius for both the silica gel and alumina are shown in Table I. The number of layers adsorbed (n) before capillary condensation occurs has been estimated by comparison of the amount adsorbed at the beginning of the loop with that held in the monolayer (the latter being obtained from the capacitance curve). The average pore radius also has been calculated from $r_0 = 2V_s/S$, where V_s is the saturation volume and S is the surface area, assuming that the adsorbent consists of uniform cylindrical capillaries. Although the latter is only a rough approximation, agreement is surprisingly good.

TABLE I
DATA WITH BENZENE AS ADSORBATE

	Silica gel	Alumina
Amount in monolayer (mg./g.)		
(from capacitance measurements)	120	70
(from differential heat curve)	130	70
Surface area ($\times 10^6$ cm. ² /g.)	4.06	2.27
Saturation volume, V_s (ml./g.)	0.412	0.273
Approximate amount adsorbed at start of hysteresis loop in isotherm (mg./g.)	230	70
Number of adsorbed layers before capillary condensation, n	2	1
Mean Kelvin radius, r_k (Å.)	12.5	21.0
Mean true pore radius (Å.)	19.9	24.7
($r_0 = r_k + n\sigma$)		
(Approx. check) $r_0 = 2V_s/A$ (Å.)	20.3	24.0

Isosteric Heats of Sorption.—The relation between the amount of sorbed benzene and the isosteric heat of sorption (calculated from the isotherms at 25 and 35°) is shown in Fig. 4 for both silica gel and alumina.

Sorption initially occurs on those parts of the surface which exhibit the highest adsorption potentials. This is indicated by high initial heats of sorption which drop fairly sharply, at a higher surface coverage, to a value characteristic of the adsorption on the more homogeneous part of the surface. For silica gel, this latter region extends over as much as half the surface, a steady value of 13.0 ± 0.5 kcal./mole being observed up to the completion of a monolayer. The equivalent value for alumina is in the region of 11.0 kcal./mole. It seems reasonable that the point at which the heat curve begins to decrease (toward the value for the heat of condensation) indicates the beginning of multilayer adsorption, and thus can be taken as the completion of the monolayer, as also suggested by Hayakawa.⁵ If the adsorbate molecules interact with each other on the surface, the curve may rise to a maximum at the completion of a monolayer. Isirikyan and Kiselev⁶ observed such a maximum with hexane on a graphitized surface, whereas with benzene they found the heat of adsorption remained nearly constant during the filling of the monolayer, the latter being in agreement with the present observation for benzene on silica gel. They suggested that the weak (dispersion) attraction between the adsorbed benzene molecules must have balanced the weak electrostatic repulsion of the CH dipoles, and quadrupoles formed by the π -electron clouds. In the case of a polar adsorbent, as silica gel, the benzene molecules would be strongly polarized and induced dipoles would reduce the adsorbate-adsorbate interaction still further. Alumina, on the other hand, seems to exhibit a maximum, although of such small range that little significance can be safely attached. (Nevertheless, a maximum would be in agreement with smaller polarization of the benzene by the alumina surface, as indicated by the capacitance measurements discussed later.) Monolayer values estimated thus, from the heat curves, agree well with those values at which a change in slope occurred in the capacitance curves.

For water on alumina (Fig. 5) isosteric heats of sorption were calculated from isotherms determined at 25 and 30°. At the lowest reproducible surface coverage, heats of sorption were found to be lower than the heat of condensation of water, and must represent, therefore, the physical adsorption of a layer of molecules on a fully hydrated surface. At the start of a second physically adsorbed layer, the curve rises toward the heat of condensation, and thus, in this case, the minimum represents the completion of a physically adsorbed monolayer. This value agrees well with those estimated from both the capacitance curve and the B.E.T. plot. The latter was the only successful application of the B.E.T. theory, and must be due to the more homogeneous surface presented by the hydrated alumina, since the plot for benzene on alumina did not prove linear.

2. Capacitance Measurements. (i) **Alumina- H_2O .**—For water on alumina, the relation between the capacitance increment and the amount adsorbed

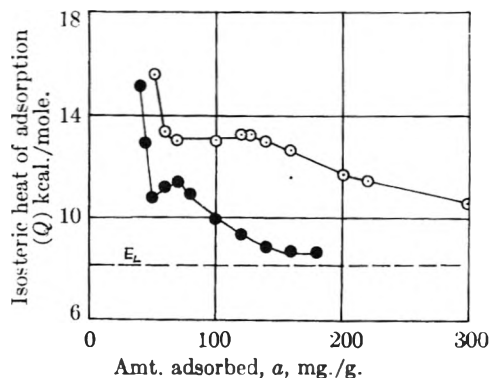


Fig. 4.—Isosteric heats of sorption for benzene on silica gel (O) and alumina (●).

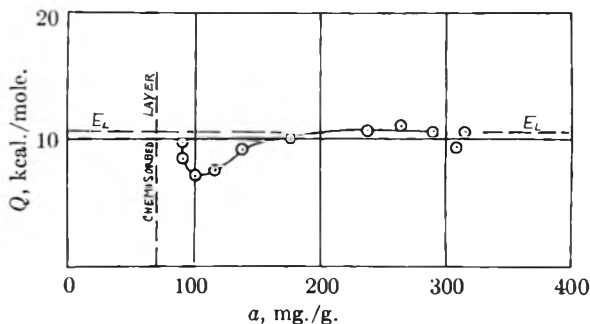


Fig. 5.—Isosteric heats of sorption for water on alumina.

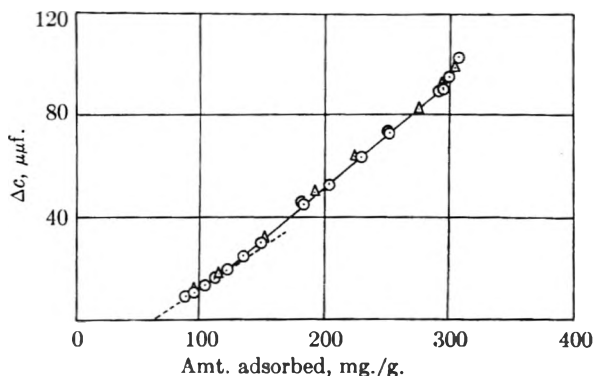


Fig. 6.—Capacitance increment plotted against the amount adsorbed, for water on alumina at 25°: O, desorption; Δ, adsorption.

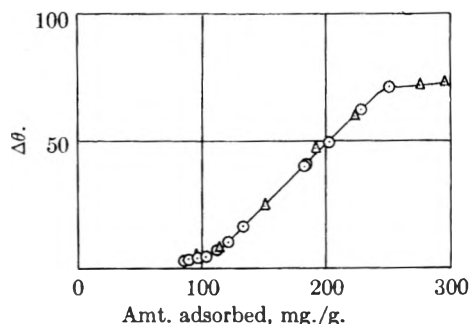


Fig. 7.—Amount adsorbed plotted against $\Delta\theta$ (\propto conductivity) for water on alumina at 25°: O, desorption; Δ, adsorption.

is shown in Fig. 6. The plot is reversible, with respect to both adsorption and desorption, over the entire range up to saturation. A small but definite change in slope of the initial linear region is observed at about 112 mg./g. (the B.E.T. value

(5) T. Hayakawa, *Bull. Chem. Soc. Japan*, **30**, 243 (1957).

(6) A. A. Isirikyan and A. V. Kiselev, *J. Phys. Chem.*, **65**, 601 (1961).

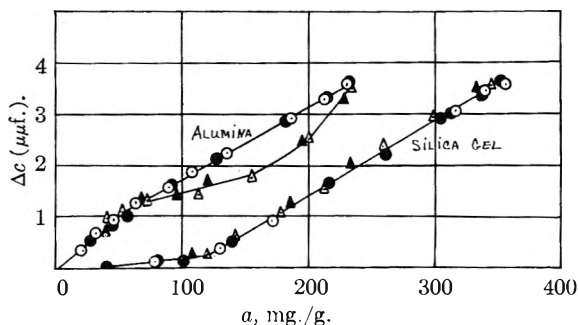


Fig. 8.—Capacitance increment plotted against the amount adsorbed, for benzene on silica gel and alumina at 25°C: O, 1st desorption; ●, 2nd desorption; Δ, 1st adsorption; ▲, 2nd adsorption.

being 106 mg./g.). This is confirmed by the more decisive change in slope, which occurs at 110 mg./g., in the plot (Fig. 7) of the amount adsorbed against the width of the resonance peak (at 0.707 of the maximum deflection), the latter being proportional to the conductance. The isotherm indicates the occurrence of chemisorption (approximately 65 mg./g.), consequently the B.E.T. value and the change in the slope of both the capacitance and conductance plots must denote the completion of a physically adsorbed "monolayer" after an initial chemisorbed layer has hydrated the original alumina surface. In both Fig. 6 and 7, the first linear region intercepts the axis at about 60 mg./g., in near agreement with that estimated from the isotherm. The surface area calculated on the basis of this chemisorbed layer is 2.28×10^6 cm.²/g. ($a_m = 65$ mg./g.), which compares well with that calculated with benzene, 2.27×10^6 cm.²/g. Further, in the low sorption region, the heats of sorption confirm this, being lower than E_L , the heat of condensation of water, and reaching a minimum at 108 mg./g., before increasing to the value of E_L at higher sorption. It seems reasonable to conclude, therefore, that the initial linear region in the capacitance plot is due to an orientated layer of water molecules adsorbed on a fully hydrated alumina surface. At such high surface hydroxyl concentration, the adsorption of each water molecule may lead to the formation of two hydrogen bonds with two adjacent OH groups on the surface. Consequently the conductance of such a layer would be small, the dielectric constant would be low ($\epsilon_1 = 18$), and the heat of sorption would be reduced by the repulsion of the adjacent parallel dipoles; all indeed observed. The relatively small change in slope to another linear region ($\epsilon_2 = 22$) represents the adsorption of additional layers of water molecules, in which the hydrogen bonding presumably would be nearer that in ice, with the dipoles no longer parallel. Thus the heat of adsorption would increase, the conductance would increase, while the dielectric constant, although increased, still would be expected to be well below that of the normal liquid.

(ii). **Capacitance Measurements with Benzene as Adsorbate.**—Figure 8 shows the incremental capacitance data for benzene on both alumina and silica gel. The maximum change at near saturation, with either adsorbent, is only 3.5 $\mu\mu\text{f.}$, and

consequently the scale is $\times 20$ compared with that for water, where the maximum value was of the order of 100 $\mu\mu\text{f.}$ Points obtained in two different runs are indicated in order to show the measure of the reproducibility obtained. With alumina a loop is obtained (clearly outside the limits of experimental error) whereas with the silica gel the plot is reversible. For both adsorption and desorption, each adsorbent exhibits two linear regions which intersect at the completion of a monolayer. These values are shown in Table I together with those estimated from the heat curves.

The dielectric constant of the adsorbate has been calculated using the simple equation used by Higuti and others⁷

$$\epsilon_{\text{app}} = \epsilon_{\text{adsorbent}} + V(\epsilon_{\text{adsorbate}} - \epsilon_{\text{adsorbent}}) \quad (1)$$

where ϵ_{app} is the apparent dielectric constant of the adsorbent and adsorbate system $\epsilon_{\text{app}} - 1 = \Delta C/C_0$, $\epsilon_{\text{adsorbent}}$ is the dielectric constant of the evacuated adsorbent, $\epsilon_{\text{adsorbate}}$ is the dielectric constant of the adsorbate, and V is the volume fraction of condensed adsorbate in the adsorbent. The latter was calculated from $V = a\rho_1/\rho_2$, where ρ_1 is the density of the adsorbent, ρ_2 is the density of the adsorbate, and a is the amount adsorbed in mg./g. The dielectric constants of the silica gel and alumina were found to be 1.70 and 1.73, respectively. Table II gives the dielectric constant of benzene when adsorbed in a monolayer (ϵ_1), and in the capillary condensed state (ϵ_2), both being calculated from the appropriate linear regions in the capacitance plots.

TABLE II
DIELECTRIC CONSTANTS OF BENZENE, ADSORBED IN A MONOLAYER AND IN THE CAPILLARY CONDENSED STATE, AT 25°

Adsorbent	(Mono-layer) ϵ_1	(Capillary condensed) ϵ_2	(Lit.) ϵ_{liq}
Silica gel	1.85	2.23	2.27
Alumina	2.45	2.24	2.27

For both adsorbents, the dielectric constant of capillary condensed benzene compares well with the liquid value. In the monolayer, the polarizing influences of the silica and alumina surfaces are seen to be very different, ϵ_1 being lower than the liquid value with silica gel, but being greater than the liquid value, approximating to that of the solid (2.46 at 5°) with alumina.

3. Comparison of Adsorbents. "Reduced" Sorption Isotherms.—In order to compare the adsorptive properties of the silica gel and alumina, the results have been recalculated in terms of the amount adsorbed per unit surface area instead of per unit weight of adsorbent. This involves the calculation of the surface area/g. adsorbent, which may be influenced both by pore size and the diameter of the adsorbate molecule, and also depends on whether the molecules are close-packed on the surface or are adsorbed on specific sites. The surface area calculated with benzene as adsorbate (using 42.0 Å.² as the area of the benzene molecule adsorbed flat on the surface), is shown in Table III, together with values obtained with the polar ad-

(7) I. Higuti, *Bull. Inst. Phys. Chem. Research (Tokyo)*, **20**, 489 (1941); S. Kurosaki, *J. Phys. Chem.*, **58**, 320 (1954).

TABLE III
SPECIFIC SURFACE OF ADSORBENT

Adsorbent	Sorbate	Molecular area (Å. ²)	Monolayer value, a_m		Surface area $\times 10^6$, cm. ² /g.
			mg./g.	mmoles/g.	
Alumina	H ₂ O	10.5	65 (chemisorbed)	3.61	2.28
	MeOH ^a	18.1	67	2.10	2.28
	EtOH ^c	23.1	75	1.63	2.27
	C ₆ H ₆	42.0	70	0.90	2.27
Silica gel	H ₂ O ^a	10.5	85	4.72	3.00
	MeOH ^a	18.1	125	3.91	4.26
	EtOH ^c	23.1	135	2.93	4.08
	C ₆ H ₆	42.0	125	1.60	4.05

^a Previous work.

sorbates used previously. Assuming the latter to be spherical molecules with hexagonal close packing on the surface, the area per molecule has been calculated from $A = 1.091(M/N\rho)^{2/3}$, where N is the Avogadro number, ρ is the liquid density, and M is the molecular weight.

The apparent discrepancy in the surface area of silica gel calculated with water as sorbate must be due to the adsorption sites being wider apart than the diameter of the water molecule, so that spaces are left between adsorbed molecules. The other data confirm that the adsorbed molecules must be close-packed on the surface in both adsorbents, the number of molecules adsorbed per unit area being independent of the nature of the underlying surface.

The surface areas of silica gel and alumina were taken as 4.05×10^6 and 2.27×10^6 cm.²/g., respectively, and the "reduced" sorption isotherms in which the amount adsorbed is reduced to μ moles per m.² are shown in Fig. 9. Similarly, a true comparison of the heat of sorption curves exhibited by the two adsorbents is shown in Fig. 10.

The relation between ΔC and a (Fig. 8), on the other hand, is of more interest with a , the amount adsorbed, in mg./g. (and not in μ moles/m.²), since the volume adsorbed is the more important factor. From eq. 1 it can be seen that $\partial(\Delta C)/\partial V$ will be proportional to $\epsilon_{\text{sorbate}} - \epsilon_{\text{adsorbent}}$, and since $\epsilon_{\text{adsorbent}}$ is almost identical for both alumina and silica gel, and the densities of the two adsorbents are within 10%, then as an approximation, $\partial(\Delta C)/\partial a \propto (\epsilon_{\text{sorbate}} - 1.71)$ for both silica gel and alumina. The parallel linear regions exhibited by the two adsorbents for benzene in the capillary condensed state clearly illustrate that $\epsilon_{\text{sorbate}}$ is the same in both adsorbents (Table I). The initial linear regions during monolayer sorption show contrasting behavior, with the slopes (and thus $\epsilon_{\text{sorbate}}$) given by alumina and silica gel being greater and smaller, respectively, than that for capillary condensed benzene.

Discussion

Figures 9 and 10 show that the silica surface exhibits a higher adsorption potential than the alumina. Both the narrower pore structure and the different ionic nature of the surface contribute to increase the forces with which benzene is adsorbed. Further, Kiselev and his co-workers⁸ have shown that the π -electrons of benzene mole-

(8) A. V. Kiselev, "The Structure and Properties of Porous Materials," edited by D. H. Everett and F. S. Stone, Butterworths Publications, London, 1958, p. 195.

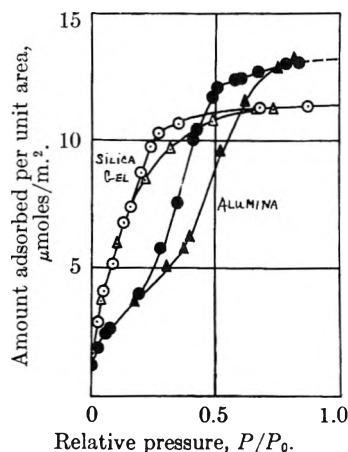


Fig. 9.—"Reduced" isotherms for benzene on silica gel and alumina at 25° (relative pressure plotted against the amount adsorbed per unit area): silica gel, O desorption, Δ adsorption; alumina, ● desorption, ▲ adsorption.

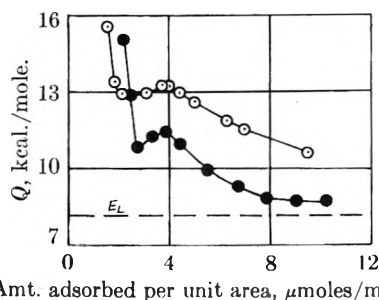


Fig. 10.—Isosteric heat of adsorption plotted against the amount adsorbed per unit area, for benzene on silica gel (O) and alumina (●).

cules are able to interact with hydroxyl dipoles in a silica gel surface to form weak hydrogen bonds, the energy of interaction being of the order 4-6 kcal./mole.⁹ In agreement with this, the dielectric constant of a monolayer of benzene is 25% lower when adsorbed on silica gel than on alumina, the latter value being in close agreement with that for the solid. Since the sorption data indicate that adsorbed benzene molecules are close-packed on both adsorbent surfaces, then the difference must be due solely to the much stronger (electron) polarization of the benzene monolayer by the silica surface, which could be partly explained by the hydrogen bond mechanism postulated by Kiselev. It seems reasonable to assume that the packing of the benzene molecules in the monolayer would be

(9) A. V. Kiselev and D. P. Poshkus, *Doklady Akad. Nauk S.S.S.R.*, 120, 834 (1958).

similar to that in the parallel planes in the solid. Thus, unless the adsorbent surface polarized the monolayer to any great extent, the value of ϵ_1 would be expected to equal that of the solid, as observed with alumina. It seems, therefore, that benzene molecules are not able to hydrogen bond with OH groups in the alumina surface, which is confirmed by the lower heats of adsorption observed (13.0 and 11.0 kcal. for silica gel and alumina, respectively), although other factors, such as pore size and the different ionic natures of the surfaces, also contribute.

After the completion of a monolayer on the silica gel, additional adsorbed layers and capillary condensed benzene both behave as normal liquid, the capacitance plot being linear and reversible, with respect to both adsorption and desorption, from the start of the second layer up to saturation. The calculated dielectric constant (2.23) agrees well with that for liquid benzene at 25° (2.27).

Normal liquid behavior is observed, likewise, during desorption for capillary condensed benzene on alumina. During adsorption, however, the curve branches out underneath that for desorption, the dielectric constant initially being lower, although gradually increasing with increase in slope of the curve until the loop finally closes at the saturation point. It appears, therefore, that the presence of adsorbed multilayers of benzene molecules must cause a decrease in the over-all dielectric constant of the alumina-benzene system. An explanation

can be suggested in terms of the quadrupole nature of the benzene molecule due to the uneven electron density distribution. Part of the van der Waals attractive forces between adsorbed benzene multilayers is the mutual interaction between benzene quadrupoles and the dipoles they induce in adjacent layers. The benzene molecules adsorbed directly onto the surface will have, therefore, in addition to any dipoles induced by surface ions, dipoles induced by the benzene layer above. Thus the polarization of the first layer will be increased by the adsorption of the second layer. This will be of little significance when the first layer already is considerably polarized by the surface, as with benzene on silica gel, but with alumina the effect must be sufficient to cause the hysteresis loop observed. During desorption, multilayers are absent, and except for a monolayer, the pores are either empty or full, according to the conditions related by the Kelvin equation. In full capillaries, the benzene molecules will have lost, to a large extent, the ordered layer orientation found in the adsorbed multilayers, and thus the magnitude of the induced dipole effect would be diminished. This explanation could be tested by the use of a non-polar adsorbate of even electron distribution, and work on these lines is being considered.

Acknowledgment.—The author gratefully acknowledges a grant from the University of New Zealand Grants Committee in support of this research.

THE THERMAL DECOMPOSITION OF PERCHLORIC ACID VAPOR^{1,2}

BY JOSEPH B. LEVY

Kinetics and Combustion Division of Atlantic Research Corporation, Alexandria, Va.

Received December 11, 1961

The thermal decomposition of perchloric acid vapor has been studied from 200 to 439°. The reaction products over this temperature range have been found to be chlorine, water, and oxygen. From 200 to 350° the kinetics of the decomposition reaction have been studied by determining the rate of chlorine formation colorimetrically; from 350 to 439° the kinetics were determined by a flow system technique. The results of the kinetic measurements are interpreted in terms of a heterogeneous reaction at the lower temperatures and a homogeneous one at the higher temperatures. A mechanism for the homogeneous reaction is proposed.

Introduction

The deflagration of pure ammonium perchlorate has been under study in this Laboratory for some time.³ A plausible mechanism for this process involves the vaporization of ammonia and perchloric acid vapors from the solid surface followed by exothermic gas-phase reactions in a zone very close to the surface. In order to get a better understanding of these gas-phase reactions, it seemed desirable to study the thermal decomposition of per-

chloric acid vapor. The results of this study are reported here.

Experimental Part

Chemicals.—Anhydrous perchloric acid was prepared from the commercial 70–72% aqueous acid⁴ and 20% fuming sulfuric acid.⁵ The infrared spectrum of the vapor of this material indicated the presence in it of chlorine heptoxide. In the colorimeter runs, the procedure adopted was, therefore, to convert the anhydrous perchloric acid to the monohydrate by the addition of an appropriate amount of the 70–72% perchloric acid and to distill anhydrous perchloric acid from the molten monohydrate. It is reported that this procedure produces pure anhydrous acid until the liquid reaches the dihydrate composition⁶; no more than

(1) This research was supported by the Propulsion Research Division, Air Force Office of Scientific Research, Office of Aerospace Research, United States Air Force, Washington 25, D. C., under Contract Number AF 49(638)-813. Reproduction in whole or in part is permitted for any purpose of the United States Government.

(2) A part of this material was presented at the 140th National Meeting of the American Chemical Society, Chicago, Illinois, September, 1961.

(3) J. B. Levy and R. Friedman, "Eighth Symposium (International) on Combustion," Williams and Wilkins, Baltimore, 1962, pp. and earlier papers referred here.

(4) Baker and Adams reagent grade 70–72% perchloric acid was used in this work. Although analysis showed that, at least in some cases, the acid was more dilute than the label indicated, the term 70–72% perchloric acid as received will be used here to designate this product as taken directly from the bottle.

(5) G. F. Smith, *J. Am. Chem. Soc.*, **75**, 184 (1953).

(6) (a) G. D. Parkes and J. W. Mellor, "Mellor's Modern Inorganic Chemistry," Longmans, Green and Co., New York, N. Y., 1946,

1% of any monohydrate sample was used, the rest being discarded. The infrared spectrum of the vapor so obtained gave no evidence of the presence of chlorine heptoxide.

In the flow system experiments, the 70–72% acid as received was used initially. Analyses of one lot showed the acid content to be 63% and in subsequent runs the acid first was concentrated to approximately the azeotropic composition (73.6% acid) by passage of nitrogen through it.

Analyses.—It was necessary to analyze solutions for acidity, chloride ion, and hypochlorite ion. These analyses were performed on different aliquots. For the acidity and chloride determinations, the hypochlorite was reduced to chloride ion with neutral sodium nitrite solution. Chloride ion was determined by the Volhard method. Hypochlorite was determined iodometrically.

The Colorimeter Experiments

Apparatus.—The kinetics of the thermal decomposition of perchloric acid over the range 200–350° were determined by observing the rate of chlorine formation colorimetrically. The colorimeter was constructed from the instructions of Hawes, *et al.*,⁷ and was calibrated with chlorine at 25°. Beer's law was obeyed in the pressure range 0–100 mm., some negative deviation from linearity being observed above that pressure. All the experiments reported here were performed at pressures within the linear range. The absorbance was unaffected by temperature up to 400° or by pressure of inert gas up to one atmosphere. As a final check on the method, experiments were carried out wherein weighed amounts of the 70–72% perchloric acid, as received, were introduced into the cell, thermally decomposed, and the number of moles of chlorine, determined colorimetrically, compared to that calculated from the weight of perchloric acid introduced. The two values agreed to within ±3%.

The reaction vessels used in the kinetic experiments were cylindrical photometric cells 100 mm. long and 22 mm. in diameter. These were constructed of Pyrex glass for most of the runs; a few runs were made with a quartz cell. The cell was housed in an aluminum block furnace inserted in the light path of the colorimeter. The furnace was a cylindrical block of aluminum 75 mm. in diameter and 150 mm. long with an axial hole just big enough to allow the insertion of the cell. The block was heated electrically and the temperature controlled by a Fenwal thermostat inserted in an axial hole to one side of the central hole. Control was excellent, the variation being ±0.5° over the temperature range studied (200–350°) and the temperature being uniform along that part of the block housing the cell.

To determine the temperature of the cell for various block temperatures, a glass tube having the same dimensions as the cell was filled with air at a pressure of about 50 mm. A thermocouple was inserted in a well that ran the length of the tube along the axis. It was found in this fashion that at 300 and 350° the cell temperature was 2° below the block temperature. The temperatures for the kinetic runs therefore have been taken as 2° below block temperature and have been assigned an accuracy of ±1°, which is felt to allow satisfactorily for any deviations.

Procedure.—The photometric cells were fitted with capillary side arms that extended so that they were exterior to the furnace and could be cooled in Dry Ice–acetone baths. These cells were sealed to a vacuum line. Gaseous perchloric acid was generated from the monohydrate and condensed in the side arm, the liquid volume serving as a rough measure of the amount. The cell was sealed off with a torch and inserted in the furnace to attain thermal equilibrium. The side arm, which was wrapped with nichrome wire, then was heated to vaporize the perchloric acid, a process requiring less than a minute, and time and readings begun. The infinity reading of the colorimeter was used to calculate the initial perchloric acid pressure. Rate data were plotted for a first order reaction as $\log [D_{\infty}/(D_{\infty} - D_t)]$ where $D_t = \log (I_0/I_t)$.

The Flow System Experiments

Nitrogen was passed at a known flow rate through a saturator containing perchloric acid, thence to a reaction

vessel, and finally to gas-washing bottles where the unreacted acid and the products were absorbed. The nitrogen flow rate was controlled by use of critical flow orifices.⁸ By suitable choice of orifices and driving pressures, flow rates varying from 2.88×10^{-4} to 1.70×10^{-3} mole/sec. could be achieved with an accuracy of ±0.5%. The nitrogen passed through a copper preheat coil to a gas-washing bottle containing perchloric acid. The bottle and coil were immersed in a bath of boiling water. The reaction vessel was a U-tube of about 130 cc. capacity. Before the nitrogen–acid stream entered the reaction vessel, it passed through a preheat coil. Both coil and U-tube were immersed in a constant temperature bath consisting of a molten mixture of sodium and potassium nitrates and sodium nitrite. The reaction products were absorbed in a train of two gas-washing bottles containing standard sodium hydroxide. Tests with litmus and starch iodide paper showed that no acid or chlorine passed through these bottles. Except for the copper preheat coil the apparatus was made of Pyrex glass. The tubing between the two baths and between the U-tube and the absorption train was electrically heated to prevent condensation.

Procedure.—The duration of the experiments was one hour. After it had been found that the acid as received was considerably more dilute than the azeotropic composition, the procedure was to bubble nitrogen through the acid until the effluent composition showed that the liquid composition was close to that of the azeotrope.

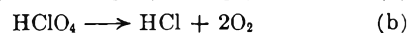
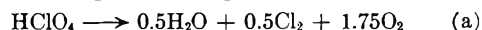
The nitrogen was Southern Oxygen Company oil-free nitrogen, rated 99.9% pure, and was taken directly from the cylinder without further purification. A run made with the reaction vessel at 100° showed no reaction; from this it was concluded that there were no impurities in the nitrogen that would interfere with the experiments. No other carrier gas was used.

The fraction of reaction was taken as the ratio of moles of chloride ion, as determined by the Volhard method, to the moles of total acid passed. The residence time was calculated from the flow rate, the reaction vessel volume, the temperature, and the pressure in the reaction vessel. The last was above atmospheric pressure because of the resistance to flow of the sintered disks in the gas-washing bottles. The extent of this back pressure was measured with a mercury barometer for nitrogen flowing alone through the reaction vessel under experimental conditions.

Probing experiments with thermocouples demonstrated that the temperature downstream of the U-tube fell so rapidly that reaction downstream of the U-tube could be neglected. To test whether reaction occurred in the preheat coil, (which was found to be long enough, 90 cm., to bring the gas to bath temperature) experiments were performed, over the temperature range of the kinetic measurements, in which the products emerging from the preheat coil were taken directly to the gas-washing bottles. It was found that the amount of reaction occurring was that expected if the gas stream was brought to temperature in a very small part of the preheat coil. The procedure therefore was adopted of calculating residence times on the basis of a reaction volume equal to that of the coil plus the U-tube. All the constants reported here were calculated in this way.

Results

The Products of the Reaction.—The two possible modes of decomposition of perchloric acid are



Prior to performing the colorimeter experiments, samples of perchloric acid were carried to complete decomposition at what were expected to be the temperature limits of the kinetic studies, *i.e.*, 210 and 400°. Chloride analyses by the Volhard and iodometric methods were performed and the results obtained by the two methods agreed, showing that route (a) represents the sole stoichiometry of the reaction from 210 to 400°. When it became necessary to extend the temperature range upward,

p. 516; (b) P. C. L. Thorne and E. R. Roberts, "Inorganic Chemistry," (F. Ephraim) Interscience Publishers, Inc., New York, N. Y., 1943, 4th ed., p. 379.

(7) R. C. Hawes, R. R. Davis, H. Cary, and A. E. Beckman, *Anal. Chem.*, **23**, 503 (1951).

(8) J. W. Andersen and R. Friedman, *Rev. Sci. Instr.*, **20**, 61 (1949).

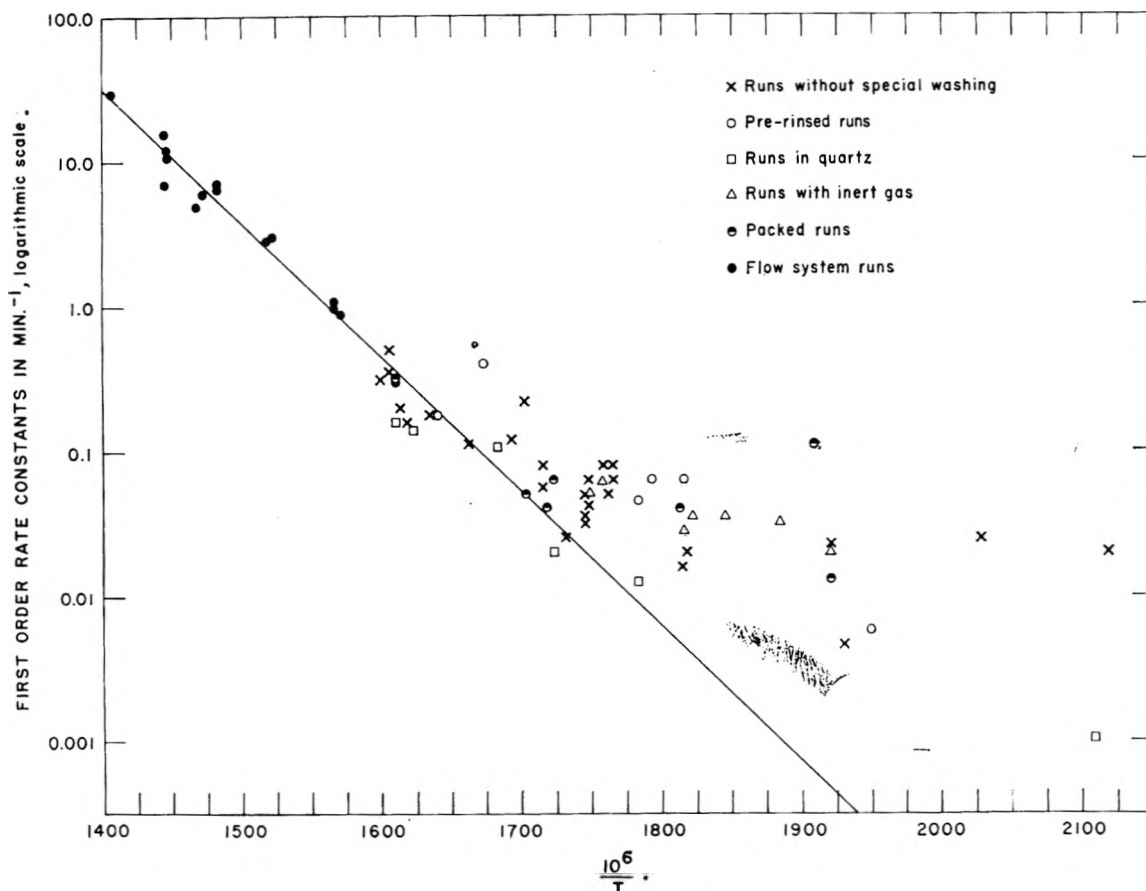


Fig. 1.—Temperature dependence of the rate of decomposition of gaseous perchloric acid.

similar analyses were performed for the flow run products and these indicated that route (b) represented the stoichiometry up to 439°.

The Kinetics of the Colorimeter Experiments

These measurements covered the temperature range of 201–350°. Above the latter temperature the rates were too rapid to allow the use of this technique.

The Order of the Reaction.—When the data from the experiments were plotted for a first-order reaction the resultant curves were linear for the first 50–90% of reaction, falling off thereafter.⁹ The practice followed was to calculate rate constants from the initial portion of the curve. Data obtained in this way for various conditions are plotted in Fig. 1.

To test the first-order nature of the reaction the initial pressure of perchloric acid was varied to the extent allowable by the sensitivity range of the colorimeter. The rates are shown in Table I (see also Fig. 1). The initial pressures have been varied by a factor of ten while the rate variation is only about 50%. Since, as Fig. 1 shows, there was scat-

(9) Evidence was presented in the Experimental part for the absence of chlorine heptoxide from the perchloric acid. The form of the rate curves obtained supports this evidence. Since the half-life for chlorine heptoxide, even at the lowest temperature in these studies, 200°, would be only a few tenths of a second,¹⁰ the presence of this compound would be indicated by a steep initial rise in the rate curves. Such rises were not observed.

(10) R. V. Figini, E. Colocchia, and H. J. Schumacher, *Z. physik. Chem. (Frankfurt)*, **14**, 32 (1958).

TABLE I

THE EFFECT OF INITIAL PERCHLORIC ACID PRESSURE ON THE RATE OF THERMAL DECOMPOSITION AT 300° ($10^6/T = 1745$)

P_0^a HClO ₄ , mm.	First-order rate constant, min. ⁻¹
17.6	0.032
53.6	.036
137.2	.043
181.0	.049

^a Calculated from the final colorimeter reading as the pressure reduced to 25°.

ter in the data as great as the variation shown in Table I, the assumption of first-order behavior appears well-founded.

The Effect of Light.—The effect of the light from the colorimeter light source on the rate was checked by inserting a shutter between the light and the reaction cell that shielded the cell from the light, except for the brief exposures required for taking data points. Experiments at 272, 298, and 345° indicated a somewhat lower rate in the dark than in the light and the data reported here all were taken with the shutter technique.

The Effect of Pressure.—The data of Table I suggest that the kinetics may be showing pressure dependence. In general the pressures of perchloric acid were chosen to give the best accuracy on the colorimeter and therefore were of the order of 20–60 mm. Experiments were run at 248, 278, and 300° in which the total initial pressure was brought

to one atmosphere with nitrogen or helium. The results are plotted in Fig. 1 and fall in well with the other "runs without special washing" (see section on the effect of surface). It was, therefore, concluded that the kinetics were not in a pressure-dependent range and further experiments with inert gases added were not performed.

The Effect of Surface.—The effect of surface first was tested by packing the reaction cells with short lengths of Pyrex tubing. A 3.5-fold increase in surface area to volume ratio was achieved in this way. The data for the packed runs are included in Fig. 1. Only one point, at 251°, $10^6/T = 1908$, indicated any acceleration and since it could not be reproduced, it was concluded that there was no surface effect.

Subsequently, it was observed that the treatment of the surface of the unpacked cell did affect the rate, the effect being most pronounced at the lower temperature. Thus at 201° when the reaction cell was rinsed with distilled water prior to the run, dried, and flamed while evacuated to 3 μ pressure, the resultant rate was significantly lower than that observed when one or more runs had been made in the cell without an intervening rinse. Points taken under the latter conditions are shown in Fig. 1 as "runs without special washing." (Since the earlier experiments had not revealed any surface effects and since all the products were volatile, the usual practice was to evacuate and flame the cells between runs rather than washing them. Thus the bulk of the points are "runs without special washing.") Points taken under the former conditions are referred to in Fig. 1 as "pre-rinsed runs." Points that were taken in a quartz cell are labeled as "runs in quartz." Figure 1 shows that the effects of rinsing the Pyrex cell or of replacing it by the quartz cell were quite similar and were pronounced near 200°, fairly strong at 240°, but not very noticeable above about 310°.

It thus appears that the nature of the reaction cell surface was very important from 200 to about 310° but did not affect the results very much above the latter temperature.

The Effect of the Reaction Products.—The reaction products are oxygen, water, and chlorine. The effect of added chlorine or oxygen on the reaction was not investigated but a few experiments were performed on the effect of initially-added water (see Table II). These indicate a moderate inhibiting effect of water. It may be noted that the inhibition is not very powerful, so that the presence of small amounts of water in the perchloric acid should not affect the kinetics significantly.

TABLE II

THE EFFECT OF WATER ON THE RATE OF THERMAL DECOMPOSITION OF PERCHLORIC ACID VAPOR AT 294°

Moles water/mole perchloric acid present originally	First-order rate constant k , min. ⁻¹
0	0.062 ± 0.008 ^a
2.53	0.038
5.0	0.017

^a Average of the four runs at this temperature.

The Kinetics of the Flow Experiments

These experiments covered the range 347–439°. Rate constants were calculated on a first-order basis. The fraction of reaction was set equal to the ratio of the moles of chloride ion to the moles of acid passed. For a number of runs, including one at 439°, the upper temperature of these studies, chloride was determined both argentometrically by the Volhard method and iodometrically, and it was found that the results obtained by these two methods were in agreement. The rate constants used have been those of the Volhard determinations since those were performed for all the experiments.

The Order of the Reaction.—The first-order treatment of the kinetics is supported by the data in Table III.

TABLE III

THE EFFECT OF PERCHLORIC ACID PRESSURE AND PER CENT REACTION ON THE FLOW SYSTEM KINETICS

Run	Temp., °C.	Mole fraction of perchloric acid	Res. time, sec.	% Reaction	k , min. ⁻¹
1	367	0.00038	8.48	16.2	1.12
2	367	.0017	8.64	18.0	1.23
3	367	.0023	2.92	5.88	1.09
4	403	.00063	1.91	24.9	7.95
5	403	.0020	1.38	17.7	7.50

Runs 1 and 3 show that the reaction rate was not affected by a 6-fold variation in the mole fraction of perchloric acid at 367°; runs 4 and 5 illustrate the same point for a 3-fold variation in mole fraction at 403°. Runs 1–3 show that the first-order rate constant was independent of per cent. reaction for 5.88–18.0%.

The Effects of Other Parameters.—In the flow experiments the effects of reaction products and of light were not investigated. It may be noted that the reaction vessel was well shielded from light since it was beneath the surface of the bath liquid and the bath container was opaque. Since the experiments all were near atmospheric pressure, there was no need to investigate pressure effects.

Although it seemed clear that, in the temperature range of the flow experiments, surface effects could be neglected (see Discussion) experiments were performed at 386 and 439° wherein the U-tube was packed with short pieces of 5-mm. Pyrex tubing. The ratio of area to volume was increased by a factor of ten. In each case the packed vessels gave an increase in the rate of 11–12%. This suggested the possibility that there was a small surface contribution to the over-all rate, of the order of 1–2%. In view of the experimental scatter of the data (see Table III) this effect was not considered further.

Discussion

The Nature of Perchloric Acid.—There are statements in the literature^{6b,11} that 100% perchloric acid or even highly concentrated perchloric acid is actually a mixture of the acid, chlorine heptoxide, and water. The apparent absence of significant amounts of chlorine heptoxide in the product generated from the monohydrate (as

(11) A. E. Missan and A. M. Sukhotin, *Zhur. Neorg. Khim.*, **4**, 606 (1959).

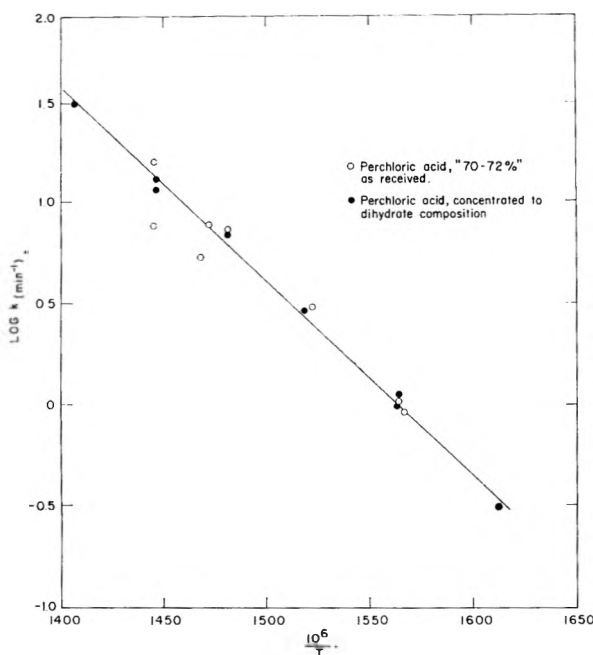


Fig. 2.—Arrhenius plot for flow decomposition of perchloric acid dihydrate vapor: $k = 5.8 \times 10^{13} \exp(-45,100/RT) \text{ sec.}^{-1}$.

indicated by the infrared spectrum and the kinetic curves) indicates that perchloric acid in the liquid state can exist as such. The procedure here was such that the acid was condensed and kept cold (-80°) as soon as it was formed. It is possible that for longer times at higher temperatures an equilibrium dissociation does occur, but it clearly did not under the conditions of these experiments.

The General Form of the Rate-Temperature Curve.—The Arrhenius plot of the data in Fig. 1 is clearly not a straight line but rather appears to have two lines of different slopes. A good straight line can be drawn through the flow rate data and this line has been drawn in Fig. 1. It is clear that the colorimeter data above about 315 to 327° ($10^6/T = 1700$ to 1660) fall fairly well around this line, and indeed at the one temperature where the two methods overlap, 347° , ($10^6/T = 1613$), the data agree very well. Below 315° the colorimeter data fall above this line and indeed the points for "runs without special washing" despite their scatter would cluster around a line of much lower slope than that of the flow rate data.

These considerations coupled with the surface effect results are interpreted to mean that the reaction is heterogeneous at temperatures below 315 to 327° and homogeneous above this range. Pre-rinsing the Pyrex cells or replacing them by quartz reduces the heterogeneous catalysis of the reaction but by no means eliminates it. Thus, the points for the "pre-rinsed runs" and for the "runs in quartz" still fell well above the extrapolation of the higher temperature line. The convergence of the data for the "runs without special washing" with the "pre-rinsed runs" and the "runs in quartz" at the higher temperatures is in line with this interpretation.

Surface effects also may be the cause of the inhibiting effect of water observed at 294° (Table II).

The agreement of the flow rate data and the colorimeter data, noted above, rules out any effect of water on the homogeneous reaction and it may be that the added water performs the same function as was accomplished by the pre-rinsing techniques.

No attempt has been made to draw a line through the lower temperature (200 – 315°) data, although it is clear that such a line (through the points for "runs without special washing") would correspond to an activation energy of the order of 10 kcal./mole . The data for the flow rate runs are plotted separately as the Arrhenius plot in Fig. 2. Least square treatment of these data yields the expression

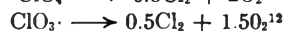
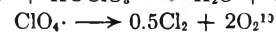
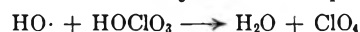
$$k = 5.8 \times 10^{13} \exp(-45,100/RT \text{ sec.}^{-1})$$

The Mechanism of the Reaction.—Since it is the homogeneous reaction which is of interest and since heterogeneous reactions are very difficult to interpret, only the mechanism for the former reaction will be considered.

The first-order nature of the reaction and the magnitude of the activation energy point strongly to the following step as being rate-determining.



This would be followed by the fast steps



The energy of reaction of the rate-determining step may be calculated from the heats of formation, $\text{HOClO}_3(\text{g}) -2.3 \text{ kcal./mole}$,¹³ $\text{HO}\cdot(\text{g}) 8.96 \text{ kcal./mole}$,¹⁴ and $\text{ClO}_3\cdot(\text{g}) 37 \text{ kcal./mole}$.¹⁵ These yield the figure 48.3 kcal./mole .¹⁶ This is somewhat higher than the observed figure. However, the experimental activation energy E_a , which is $d \ln k/d(1/T)$, is related to the true activation energy E , which is the difference in energy between the ground and activated states, by

$$E = E_a + (f - 1)RT^{19}$$

where f is the number of square terms, *i.e.*, the number of degrees of freedom of the molecule whereby energy can be stored and which can contribute toward activation. For perchloric acid, f can be as high as 13 so that $(f-1)RT$ can be as great as about 14 kcal . The discrepancy between the value of E_a of 45 and E of 48 may be due to this cause or to inaccuracies in the heat of formation data. In any event, the values are close enough to render the above mechanism very plausible.

(12) H. J. Schumacher and G. Stieger, *Z. anorg. u. allgem. Chem.*, **184**, 272 (1929).

(13) R. D. Schultz and A. O. Dekker, "Sixth Symposium (International) on Combustion," Reinhold Publ. Corp., New York, N. Y., 1957, p. 618.

(14) R. Barrow, *Arkiv Fysik*, **11**, 291 (1956).

(15) C. F. Goodeve and A. E. L. Marsh, *Trans. Faraday Soc.*, **32**, 8790 (1936).

(16) The experimental activation energy found for the homogeneous thermal decomposition of chlorine heptoxide was 32.9 kcal./mole ¹⁰ but the critical dissociation energy which corresponds to the energy required to cleave the O-Cl bond was 48.2 kcal./mole . The values usually assigned to the O-Cl bond are of the order of 50 kcal./mole .^{17,18}

(17) T. L. Cottrell, "The Strengths of Chemical Bonds," Butterworths Scientific Publications, London, 1958, 2nd ed., p. 280.

(18) L. Pauling, "Nature of the Chemical Bond," Cornell University Press, Ithaca, N. Y., 1960, 3rd ed., p. 85.

(19) A. A. Frost and R. G. Pearson, "Kinetics and Mechanism," John Wiley and Sons, Inc., New York, N. Y., 1953, p. 24.

Finally, the difference between the behavior of perchloric acid in the gas phase and that in the liquid phase may be noted. It has been known since the discovery of perchloric acid that the anhydrous liquid was quite unstable even at room temperature. Recently Zinov'ev and Tsentsiper²⁰

have studied the thermal decomposition of the liquid at 40–96° and reported an activation energy of 22.2 kcal. mole⁻¹. The decompositions in the two phases clearly proceed by different mechanisms.

(20) A. A. Zinov'ev and A. B. Tsentsiper, *Russian J. Inorg. Chem.*, **4**, 329 (1959).

THE EFFECT OF HYDROGEN IODIDE ON THE RADIOLYSIS OF CYCLOHEXANE- d_{12} ¹

BY JAMES R. NASH AND WILLIAM H. HAMILL

Department of Chemistry and the Radiation Laboratory, University of Notre Dame, Notre Dame, Indiana

Received December 12, 1961

The γ -radiolysis of dilute solutions of hydrogen iodide in cyclohexane- d_{12} leads to $G(\text{D-atom}) \cong 1.7$. There is a remarkably large $G(\text{H}_2)$, amounting to 2.2 molecules/100 e.v. at 0.7 mole % HI. This effect, attributed to dissociative electron attachment, seriously complicates using halogens or halides as H-atom and free radical scavengers.

Introduction

The effects of solutes at small concentrations upon $G(\text{H}_2)$ from γ -irradiated liquid cyclohexane have been attributed variously to electron attachment,^{2,3a} to H-atom scavenging,^{3b} to energy transfer,⁴ and to "quenching."⁵

Our recent report⁶ on the photolysis of solutions of hydrogen iodide in deuterated hexane has suggested, because of the ease with which the sources of hydrogen produced are differentiated, that a similar study in the radiolysis of hydrocarbon solutions might distinguish between atomic and molecular hydrogen. Hydrogen iodide has been used previously^{2,3} in γ -irradiated cyclohexane and it was found that $\Delta G(\text{H}_2) = 1.0$ in 0.1 M solution, the increase being attributed to energy transfer from solvent to solute.

Experimental

Cyclohexane- d_{12} of 99.6% isotopic purity was obtained from Merck and Co. The small amount of benzene initially present was removed by percolating through a small silica gel column. Hydrogen iodide was prepared as previously described.^{3b}

The dose rate, based upon Fricke dosimetry, was 1.4×10^{20} e.v. l.⁻¹ min.⁻¹. For a single run with (light) cyclohexane, $G(\text{H}_2) = 5.35$.

Solutions were prepared by distilling one ml. of cyclohexane- d_{12} into a graduated volume in a greaseless vacuum system. Following volume determination, the solvent was distilled into the radiolysis cell which already contained the previously measured hydrogen iodide. After radiolysis, the products volatile at -196° were collected and analyzed as previously described.^{3b} Solvent was recovered by distilling the solution into a cell containing copper wire and, after hydrogen evolution, adding bromine and passing through a capillary column of silica gel. Recovered solvent showed

essentially no ultraviolet absorption and no cyclohexene was detected by infrared absorption.⁷

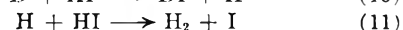
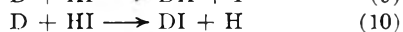
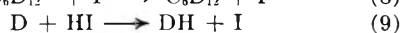
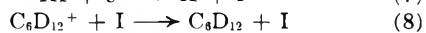
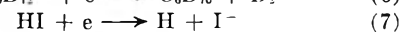
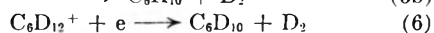
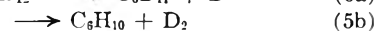
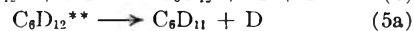
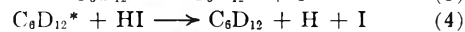
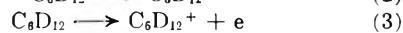
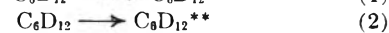
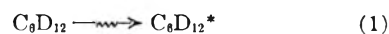
Results

Yields of hydrogen and the isotopic distributions appear in Table I where $G(h)$ represents the total yield of hydrogen and $G(d)$ represents the combined $G(\text{HD}) + G(\text{D}_2)$. In all experiments except that with the lowest hydrogen iodide concentration, the hydrogen produced corresponded to a small fraction of the initial amount of solute. The experiment with equal concentrations of iodine and of hydrogen iodide shows that iodine produced during a run cannot interfere significantly. Results with iodine only measure "molecular" products.

The reduced yield of hydrogen in cyclohexane- d_{12} compared to cyclohexane has been reported previously.⁴ We have confirmed the result in Table I for cyclohexane- d_{12} without solute by two additional runs at the same dose using 1 Mev. Van de Graaf generator electrons, at 0.5 μamp . It should be observed that $G(h)$ increases smoothly with increasing hydrogen iodide without evidence of approaching a limit. Also, $G(\text{H}_2)$ is remarkably large and still increasing. There is a disproportionately large yield of HD from isotopic impurity, which has been remarked previously.⁴

Discussion

We shall have occasion to refer to the reactions



We attribute the yields of HD in the presence of hydrogen iodide mainly to the scavenging of D

(7) H. A. Dewhurst, *J. Phys. Chem.*, **63**, 813 (1959).

(1) The radiation laboratory is operated under Atomic Energy Commission contract At (11-1)-38.

(2) R. H. Schuler, *J. Phys. Chem.*, **61**, 1472 (1957).

(3) (a) R. R. Williams, Jr., and W. H. Hamill, *Radiation Research*, **1**, 158 (1954); (b) L. J. Forrestal and W. H. Hamill, *J. Am. Chem. Soc.*, **83**, 1535 (1961).

(4) (a) J. Chang and M. Burton, paper presented at the 137th National Meeting of the Am. Chem. Soc., Cleveland, April, 1958.

(b) J. Y. Chang, Ph.D. thesis, Univ. of Notre Dame, 1958.

(5) P. J. Dyne and W. M. Jenkinson, *Can. J. Chem.*, **39**, 2163 (1961).

(6) J. R. Nash, R. R. Williams, and W. H. Hamill, *J. Am. Chem. Soc.*, **82**, 5974 (1960).

TABLE I
 YIELDS OF HYDROGEN FROM IRRADIATED HI SOLUTIONS IN C₆D₁₂

Solute mole %	0	0	0 ^a	0.05HI ^a	0.1HI	0.34HI	0.7HI	0.34I ₂ ^a	0.34HI ^a
Time, min.	76	100	150	62	90	120	185	120	120
G(h)	4.15	4.13	4.18	4.42	4.62	5.16	5.55	2.00	3.80
G(H ₂)	0.05	0.03	0.03	0.72	1.00	1.90	2.35	0.01	1.26
G(HD)	0.37	0.28	0.35	1.13	1.36	1.50	1.57	0.06	0.83
G(D ₂)	3.73	3.82	3.80	2.56	2.26	1.75	1.63	1.92	1.68
G(d)	4.10	4.10	4.15	3.69	3.62	3.25	3.20		

^a Recovered solvent used in these experiments.

atoms, reaction 9. The values of $G(\text{HD})$ at higher concentrations appear to reach a plateau at $G(\text{HD}) \cong 1.7$ and are consistent with a ratio of rate constants for reaction with hydrogen iodide relative to reaction with solvent^{3b} of the order of 5×10^3 . If D-atom scavenging alone were involved, $G(\text{d})$ would remain constant, rather than decrease. Similarly $G(\text{h})$ would be constant, rather than increase.

To consider this point further we must interpret $G(\text{HD})$ for runs with no added hydrogen iodide. The effect of iodine shows HD to be mostly of atomic origin, as is H₂, while the ratio H₂/HD indicates the atoms to be about one-half H. With this approximation, which is not critical, we estimate the corrected yields of hydrogen for isotopically pure C₆D₁₂ which appear in Table IIA.

TABLE II

A. YIELDS CORRECTED FOR ISOTOPIC IMPURITY						
Solute mole %	0	0.05HI	0.10HI	0.34HI	0.70HI	0.34I ₂
G(h)	4.15	4.42	4.62	5.16	5.55	2.00
G(H ₂)		0.55	0.83	1.73	2.18	
G(HD)		1.25	1.48	1.62	1.69	
G(D ₂)	4.15	2.66	2.36	1.85	1.73	2.00
G(d)	4.15	3.91	3.84	3.47	3.42	
B. INCREMENTS OF YIELDS						
$\Delta G(\text{H}_2)$		0.55	0.83	1.73	2.18	
$\Delta G(\text{d})$		0.24	0.31	0.68	0.73	
Ratio		2.3	2.7	2.5	3.0	

The increase in $G(\text{h})$ due to solute hydrogen iodide is matched by comparable effects in cyclohexane with other solutes, iodine excepted. Thus, over a wide concentration range of methyl iodide together with $10^{-2} M$ hydrogen iodide, $G(\text{H}_2) + G(\text{CH}_4) = 6.5$, while $G(\text{H}_2) = 5.85$ in pure cyclohexane.^{3b,8} With added iodine alone in cyclohexane, $G(\text{H}_2) + G(\text{HI}) \cong 5.8$. This indicates that the effect of solutes to increase the total yield of products is not due to scavenging of H-atoms otherwise lost by addition to unsaturates.

The complementary relation of the yields, except for the increase in combined product achieved below $\sim 1\%$ of solute, shows that the two products arise from competitive processes. Whereas these seem to occur with equal efficiencies in the systems studied previously,^{3b} the constant ratio $\Delta G(\text{H}_2)/\Delta G(\text{d}) = 2.5$ in Table IIB indicates that the competitive processes may occur with rather different efficiencies. This difference may depend, at least in part, upon the nearly complete absence of the

cage effect for dissociations producing a hydrogen atom.⁶

The large values of $G(\text{H}_2)$ in Table II also might be attributed to reaction steps 4 or 10. Since $G(\text{H}_2)$ does not show the concentration dependence of $G(\text{HD})$, step 10 must be unimportant. If the formation of D-atoms is not diminished by solute, by comparison with the results for $G(\text{HI})$ in cyclohexane with added methyl iodide,^{3b} then the decrease in $G(\text{d})$ is to be attributed to "molecular" D₂. This conclusion is inconsistent with our earlier interpretation, based on more limited facts, that the effect of hydrogen iodide in cyclohexane to increase $G(\text{H}_2)$ involved energy transfer from an excited state, C₆H₁₂^{*}, which did not otherwise liberate hydrogen (*viz.*, step 4). It appears now that we are dealing with two competitive processes, each of which liberates hydrogen, one of which is more efficient than the other. Also, in the present case, $\Delta G(\text{H}_2)$ from energy transfer (or any other process) would be ~ 2.5 times as efficient as decomposition of C₆D₁₂ yielding D. Such efficient processes of energy transfer in γ -irradiated organic liquids often have been postulated but have not yet been demonstrated. In fact, scintillator efficiency is only $\sim 1\%$.⁹

We propose a mechanism including steps 2, 3, 5-9, and 11. The competition mentioned above is considered to involve steps 6 and 7, which receives strong support from recent observations that addition of naphthalene to γ -irradiated organic glasses produces the well known absorption spectrum of the corresponding anion C₁₀H₈⁻ with yields approximating $G(\text{H}_2)$ in this work at similar concentrations of solute.¹⁰

It was not possible in earlier work^{3b} to assess reliably the relative contributions of solutes to scavenging and to other protective mechanisms. Thus, for methyl iodide in cyclohexane, the C-I bond may be ruptured by H-atoms, by electron attachment, or by excitation. In each case one expects $G(\text{H}_2)$ to be depressed and $G(\text{CH}_4)$ to be increased correspondingly. In the present instance, some further resolution of the effect of solute is possible. It is now quite clear from Table I that the solute intervenes extensively, whether by electron attachment or by energy transfer, even at low concentrations for which the observed effect generally has been attributed to H-atom scavenging exclusively. We find, from an empirical linear graph of $G(\text{CH}_4)$ vs. $\log(\% \text{CH}_3\text{I})$ in cyclohexane,^{3b} the same slope as for $G(\text{H}_2)$ vs. $\log(\% \text{HI})$ in this work. This is consistent with our proposed mecha-

(9) S. Lipsky and M. Burton, *J. Chem. Phys.*, **31**, 1221 (1959).

(10) J. R. Nash, P. S. Rao, J. Guarino, M. Reayne, and W. H. Hamill, *J. Am. Chem. Soc.*, **84**, 500 (1962).

(8) It appears now that $G(\text{H}_2) = 5.4$ is more nearly correct for cyclohexane.

nism, and suggests that one electron breaks one C-I bond or one H-I bond, in either medium.

The results of Tables I and II indicate that even at 0.02 *M* iodine, by analogy with the results for hydrogen iodide, $G(D_2)$ resulting from I^- formation may approximate 0.5 molecule/100 e.v. In apparent contradiction, $\Delta G(H_2) = 2.0$ and $G(HI) = 1.9$ in ordinary cyclohexane. This difficulty is removed by a recent observation that addition of iodine to cyclohexane *after* irradiation results in liberation of hydrogen iodide, with $G(HI) \sim 0.5$ based on a single run.¹¹

Finally it should be noted that our previous work indicated a quite restricted domain for the electron,

not exceeding the second coordination layer and rendering implausible any notion of ionization in liquids. The present interpretation indicates that the average electron encounters some 10^3 molecules or more, thus approximating the description of Samuel and Magee.¹²

Acknowledgment.—We are grateful to Dr. Harold A. Dewhurst for examining and commenting upon the manuscript.

(11) J. Roberts, this Laboratory. This result suggests the presence of cyclohexadiene since T. Gaumann, *Helv. Chim. Acta*, **44**, 1337 (1961), reports the corresponding reaction for phenylcyclohexadiene.

(12) A. H. Samuel and J. L. Magee, *J. Chem. Phys.*, **21**, 1080 (1953).

THE IODINE COMPLEXES OF SOME SATURATED CYCLIC SULFIDES*

BY MILTON TAMRES AND SCOTT SEARLES, JR.

Chemical Laboratories of The University of Michigan, Ann Arbor, Michigan, and of Kansas State University, Manhattan, Kansas

Received December 13, 1961

A spectrophotometric method has been used to obtain thermodynamic data for the iodine complexes with small ring saturated cyclic sulfides and with diethyl sulfide in *n*-heptane. The results for both the charge-transfer and blue-shift spectra give a stability order of 5- > 6- > 4- > 3-membered ring, with the diethyl sulfide-iodine stability lying between that of the 5- and the 6-membered ring. This order contrasts sharply with that found for the analogous cyclic ether-iodine complexes, which is 4- > 5- > 6- > 3-membered ring. Thus it is apparent that the heteroatom itself plays a large role in determining the electron distribution in different sized rings, even for heteroatoms in the same family of the periodic table.

Introduction

It has been established through investigations of hydrogen bonding¹ and of iodine complex formation^{2,3} that the variation of electron donor ability with ring size for the cyclic ethers is in the order 4- > 5- > 6- > 3-membered ring. Additional support for this order comes from n.r.r. studies⁴ and, for the 5- and 6-membered ring, from measurements of pK_a 's⁵ and of the stabilities of BF_3 addition compounds.⁶ These studies make clear the fact that this variation in basicity is an *intrinsic* property of the cyclic ethers which must be associated with the electronic redistribution of charge about the atoms in the ring as a result of the change in geometry of the atomic arrangement.

A short time ago McCullough and Mulvey⁷ reported that the stability constants at 25° for the iodine complexes of thiacyclobutane, thiacyclopentane, and thiacyclohexane are in the order 5- > 6- > 4-membered ring, which is different from that of the oxygen case. Since the oxygen series had been studied so thoroughly, it was felt that a more detailed thermodynamic study of the cyclic sulfide-iodine system was desirable. As in the oxygen case, the iodine complexes with the cyclic sulfides

can be studied in both the visible and the ultraviolet regions, thereby giving independent checks on the basicity sequence. Because the complex has a much larger molar absorptivity index in the latter region, more dilute solutions of iodine can be employed and this minimizes the onset of side reactions such as those observed by McCullough and Mulvey for the thiacyclobutane-iodine complex. Similar side reactions occur with ethylene sulfide, which is unsubstituted like the other cyclic sulfides, and with propylene sulfide. The effects are less with *trans*-2,3-butylene sulfide and, hence, this compound was used to study the 3-membered ring.

Experimental

Apparatus.—The same apparatus was used as has been described previously.^{2,3} The photometric scale of the Beckman instrument was checked by using a standard potassium dichromate solution.⁸ A further check in the ultraviolet region was made using dilute benzene solution.

Procedure.—The general techniques utilized to control the temperature, to eliminate fogging of the cells at the lower temperatures, to minimize side reactions through use of compartmentalized flasks, and to make up the solutions are the same as those already described.² The data for several temperatures, obtained at the wave length of maximum absorption in both spectral regions, are given in Table I. As was done previously,² calculations of the change in concentration with temperature were made by assuming the densities of the solutions at the different temperatures would be essentially the same as those for the pure solvent, the values for which were taken from Timmermans.⁹ All measurements were made using 1.000-cm. matched cells.

Materials.—The source of iodine and of *n*-heptane and

* Presented before the Division of Physical Chemistry at the 140th National Meeting of the American Chemical Society, Chicago, Ill., September 3-8, 1961.

(1) S. Searles and M. Tamres, *J. Am. Chem. Soc.*, **73**, 3704 (1951).

(2) Sister M. Brandon, M. Tamres, and S. Searles, *ibid.*, **82**, 2129 (1960).

(3) M. Tamres and Sister M. Brandon *ibid.*, **82**, 2134 (1960).

(4) H. S. Gutowsky, R. L. Rutledge, M. Tamres, and S. Searles *ibid.*, **76**, 4242 (1954).

(5) E. M. Arnett and C. Y. Wu, *ibid.*, **82**, 4999 (1960).

(6) D. E. McLaughlin, M. Tamres, and S. Searles, *ibid.*, **82**, 5621 (1960).

(7) J. D. McCullough and D. Mulvey, *ibid.*, **81**, 1291 (1959).

(8) Spectrophotometry, National Bureau of Standards Circular 484, U. S. Government Printing Office, Washington 25, D. C., 1949.

(9) J. Timmermans, "Physico-chemical Constants of Pure Organic Compounds," Elsevier Publishing Co., New York, N. Y., 1950, p. 60 and p. 224.

TABLE I

SULFIDE-IODINE COMPLEXES^{a,b}

[S] × 10 ³ , mole/l.	[I ₂] × 10 ³ , mole/l.	Absorbance				
		5.6°	14.7°	19.8°	25.0°	40.2°
Diethyl sulfide in <i>n</i> -heptane						
Visible		λ = 437 mμ				
3.099	61.61	0.708	0.537	0.392	0.228	
6.162	61.54	.915	.749	.592	.378	
3.095	46.01	.534	.405	.292	.168	
6.160	46.07	.687	.566	.442	.282	
9.267	45.92	.754	.644	.529	.359	
6.679	24.04	.365	.304	.240	.156	
13.35	24.01	.412	.365	.312	.227	
16.59	24.04	.429	.385	.334	.250	
Ultraviolet		λ = 303 mμ				
10.51	2.382	0.596	0.518	0.442	0.314	
17.45	2.387	.609	.546	.501	.367	
7.036	2.380	.543	.454	.364	.238	
3.520	3.555	.680	.525	.388	.228	
13.40	1.155	.282	.244	.220	.152	
3.348	3.467	.621	.475	.349	.199	
10.03	2.310	.553	.474	.409	.276	
<i>trans</i> -2,3-Butylene sulfide in <i>n</i> -heptane						
Visible		λ = 446 mμ				
4.241	128.5	0.450	0.334	0.278	0.233	
8.452	128.4	.732	.564	.470	.413	
12.67	128.4	.948	.747	.647	.563	
Ultraviolet		λ = 300 mμ				
4.239	12.68	0.809	0.583	0.480	0.408	0.227
8.470	12.61	1.265	0.975	0.824	.717	.424
1.268	12.68	1.600	1.295	1.105	.968	.590
3.014	9.05	0.431	0.329	0.260	.217	..
6.018	9.09	.716	.540	.451	.384	.225
9.053	9.07	.960	.740	.629	.533	.319
Trimethylene sulfide in <i>n</i> -heptane						
Visible		λ = 442 mμ				
4.740	54.46	0.492	0.370	0.269	0.162	
14.26	54.42	.733	.621	.508	.343	
23.79	54.34	.825	.730	.624	.458	
9.514	43.74	.534	.441	.335	.216	
18.99	43.70	.632	.553	.455	.323	
28.50	43.62	.681	.612	.525	.395	
Ultraviolet		λ = 306 mμ				
18.97	2.616	0.551	0.474	0.396	0.279	
14.16	2.623	.528	.446	.358	.242	
4.737	5.240	.729	.558	.400	.231	
9.534	3.895	.711	.571	.447	..	
23.69	2.621	.569	.491	.422	.308	
Trimethylene sulfide in CCl ₄						
Visible		λ = 436 mμ				
4.814	59.12	0.608	0.452	0.327	0.201	
14.49	59.16	0.950	.797	.645	.452	
24.21	59.12	1.074	.944	.793	.600	
9.649	47.54	0.686	.547	.421	.277	
19.35	47.50	.830	.705	.590	.424	
28.99	47.52	.896	.793	.681	.523	
Ultraviolet		λ = 310 mμ				
16.46	2.764	0.627	0.535	0.439	0.298	
8.256	4.119	.739	.592	.452	.278	
4.080	5.533	.723	.534	.387	.224	
20.46	2.783	.680	.580	.489	.345	

Thiacyclopentane in *n*-heptane

Visible		λ = 438 mμ				
4.488	28.84	0.409 ^c	0.351	0.309	0.265	0.166
8.992	28.79	.477 ^c	.437	.400	.360	.255
13.49	28.76	.509 ^c	.472	.440	.409	.306
2.239	28.77	.314 ^c	.249	.208	.174	.100
6.723	28.80	.461 ^c	.408	.367	.325	.221
11.23	28.79	.511 ^c	.465	.430	.395	..
Ultraviolet		λ = 306 mμ				
1.686	3.269	0.476 ^c	0.371	0.260	0.144	
3.374	3.266	.623 ^c	.523	.401	.244	
5.057	3.262	.698 ^c	.608	.490	.317	
0.841	3.270	.318 ^c	.234	.153	.081	
2.528	3.260	.555 ^c	.456	.337	.198	
Thiacyclohexane in <i>n</i> -heptane						
Visible		λ = 436 mμ				
2.142	30.89	0.279 ^c	0.210	0.145	0.083	
6.478	30.91	.451 ^c	.379	.293	.190	
10.82	30.88	.513 ^c	.453	.372	.263	
4.319	30.74	.390 ^c	.315	.233	.142	
8.654	30.72	.483 ^c	.419	.336	.227	
12.97	30.90	.532 ^c	.473	.396	.286	
Ultraviolet		λ = 302 mμ				
2.174	2.060	0.287 ^c	0.219	0.153	0.090	
6.504	2.053	.457 ^c	.390	.306	.204	
10.85	2.055	.520 ^c	.461	.383	.276	
4.321	2.164	.410 ^c	.340	.256	.159	
8.656	2.164	.507 ^c	.449	.366	.250	
12.99	2.172	.561 ^c	.506	.427	.309	

^a Concentrations at 25°. ^b Cell lengths = 1.000 cm. ^c Temperature at 6.7°.

their purification has been given.² Carbon tetrachloride was purified in the manner described by Fieser.¹⁰

trans-2,3-Butylene sulfide was synthesized by the reaction of *trans*-2,3-epoxybutane with potassium thiocyanate, as described previously.¹¹ It had b.p. 43° (140 mm.) and *n*_D²⁰ 1.4602 (reported b.p. 43–43.2° (140 mm.) and *n*_D²⁰ 1.46024). Its infrared spectrum agreed with that in the literature.

The diethyl sulfide used was a center cut from a fractional distillation of the commercial product obtained from the Eastman Kodak Co. Thiacyclopentane and thiacyclohexane were prepared by the methods described by Whitehead, *et al.*¹² Thiacyclobutane was prepared by the reaction of 3-bromo-1-chloropropane with thiourea, followed by treatment with hot NaOH. The product was steam distilled, dried over Na₂SO₄, and fractionated. Refractive indices of these sulfides checked with those reported in the literature, and analysis of the sulfides by vapor phase chromatography showed the absence of impurities.

Discussion

The usual method of analyzing spectral results to determine the equilibrium (association) constant, *K*_c, and molar absorptivity index, *a*_c, of a complex is to use the Benesi-Hildebrand¹³ equation, or some modification of it such as that employed by Ketelaar, *et al.*,¹⁴ by Scott,¹⁵ and by Brandon, Tamres, and Searles.² Each of these equations contains an approximation which neglects some of the concentration terms, thereby reducing the original

(10) L. F. Fieser, "Experiments in Organic Chemistry," second ed., D. C. Heath, Boston, Mass., 1941, p. 365.

(11) N. P. Neureiter and F. G. Bordwell, *J. Am. Chem. Soc.*, **81**, 578 (1959).

(12) E. V. Whitehead, R. A. Dean, and F. A. Fidler, *ibid.*, **73**, 3632 (1951).

(13) H. A. Benesi and J. H. Hildebrand, *ibid.*, **71**, 2703 (1949); **70**, 2832 (1948).

(14) J. A. A. Ketelaar, C. van de Stolpe, A. Goudsmit, and W. Dzubas, *Rec. trav. chim.*, **71**, 1104 (1952).

(15) R. L. Scott, *ibid.*, **76**, 787 (1956).

TABLE II
 SPECTROPHOTOMETRIC DATA IN THE VISIBLE REGION FOR THE FORMATION OF SULFIDE-IODINE COMPLEXES^a

Sulfide	Solvent	λ_{\max} , m μ	t_c , °C.	K_c, b, c l./mole	$(a_c - a_x)^b$	K_c, d l./mole	$(a_c - a_x)^d$
<i>trans</i> -2,3-Butylene sulfide	<i>n</i> -Heptane ^{e,f}	446	5.6	65.7 ± 3.7	1.32	67.8	1573
			14.7	49.7 ± 2.3	1.29	51.2	1479
			19.8	38.4 ± 5.7	1.59	39.5	1514
			25.0	33.0 ± 1.1	1.28	33.9	1488
Thiacyclobutane	<i>n</i> -Heptane ^{e,f}	442	5.6	226.0 ± 5.2	1776	214.2	1766
			14.7	141.3 ± 3.1	1744	138.3	1733
			25.0	90.7 ± 1.8	1.90	90.3	1677
			40.2	51.8 ± 1.2	1.73	51.9	1561
	CCl ₄ ^{e,f}	436	5.6	194.5 ± 3.1	2188	185.9	2173
			14.7	120.4 ± 1.8	2142	118.5	2125
			25.0	79.5 ± 0.5	2.77	79.2	2061
			40.2	45.0 ± 0.6	2.14	45.2	1998
CCl ₄ ^{g,h,i}	437	25			87	1950	
Thiacyclopentane	<i>n</i> -Heptane ^{e,f}	438	6.7	593.1 ± 42.8	1.92	546.4	1976
			14.7	376.8 ± 12.4	1.87	363.4	1968
			19.8	282.4 ± 7.8	1.66	277.3	1946
			25.0	210.7 ± 4.8	1.63	209.3	1943
	CCl ₄ ^{g,h,i}	438	40.2	111.9 ± 2.8	1.843	112.5	1824
			25			186	2500
Thiacyclohexane	<i>n</i> -Heptane ^{e,f}	436	6.7	387.5 ± 3.0	2.48	372.3	2026
			14.7	249.0 ± 1.9	2.12	246.0	1989
			25.0	153.3 ± 1.1	1.58	153.7	1935
			40.2	82.9 ± 1.6	1.60	83.5	1841
	CCl ₄ ^{g,h,i}	431	25			110 ^j	2830
Diethyl sulfide	<i>n</i> -Heptane ^{e,f}	437	5.6	603.3 ± 33.2	1.33	487.0	1949
			14.7	319.4 ± 8.1	1.85	290.4	1904
			25.0	187.1 ± 3.4	1.856	179.5	1858
			40.2	92.9 ± 1.1	1.778	91.9	1775
Dimethyl sulfide	CCl ₄ ^{k,i}	437	23			71	2050

^a The data are reliable to only 3 significant figures. More figures are listed, however, to better compare the results from the two methods of calculation. ^b Based on the approximate equation 3. ^c Error limits calculated by the Fieller¹⁹ method for the 50% confidence interval. The K_c values obtained in the error analysis were essentially identical with those obtained by the least squares treatment of eq. 3, the small differences which arose were in the fourth figure. ^d Based on the full equation 1. ^e Iodine-solvent blank. ^f This work. ^g Pure solvent blank. ^h Reference 7. ⁱ Based on iterative method. ^j Revised value is 148. J. D. McCullough, private communication. ^k Reference 38.

equation from a quadratic to a linear form. While this has the advantage of simplifying the calculations for K_c and a_c , it was pointed out^{16,17} that, in some cases, these approximations can lead to appreciable error which might be of the order of 10% of K_c . In a recent detailed analysis¹⁸ of the error introduced when using approximations to evaluate K_c , it was shown that these errors are pronounced only in the case of the formation of strong complexes and, even here, the errors are expected to be small if the molar absorptivity index of the complex is very large. Thus for iodine complexes, where the molar absorptivity index in the ultraviolet region is several times that in the visible region (by about a factor of 10 in the case of sulfide complexes), there is an advantage from the analytical standpoint to working in the former region in addition to the advantage of minimizing the occurrence of side reactions.

The full equation¹⁸ which was used to determine K_c and a_c is

$$\frac{C_B b C_Z}{A} = \frac{C_B + C_Z}{(a_c - a_x)} + \frac{1}{K_c(a_c - a_x)} - \frac{A}{b(a_c - a_x)^2} \quad (1)$$

(16) N. J. Rose and R. S. Drago, *J. Am. Chem. Soc.*, **81**, 6138 (1959).

(17) R. S. Drago and N. J. Rose, *ibid.*, **31**, 6141 (1959).

(18) M. Tamres, *J. Phys. Chem.*, **65**, 654 (1961).

where K_c and a_c have been defined previously, C_B and C_Z are the molar concentrations of base and of acid, respectively, a_x is the molar absorptivity index of the free acid, A is the absorbance, and b is the length of the cell. This equation, applicable to the case where an iodine-solvent solution is used as the blank,² is of the form

$$Y = sX + i^* - s^2W \quad (2)$$

where the terms can be compared with those given in a previous paper.¹⁸

For comparison, the modified equation, obtained by neglecting the last term in eq. 1, is

$$\frac{C_B b C_Z}{A} = \frac{C_B + C_Z}{(a_c - a_x)} + \frac{1}{K_c(a_c - a_x)} \quad (3)$$

which is of the linear form

$$Y = sX + i \quad (4)$$

It has been recommended¹⁸ that a least squares treatment of eq. 1 is to be preferred to that based on taking sets of individual points two at a time, as proposed by Rose and Drago.¹⁶ Consequently, the results for K_c and a_c in the tables which follow were obtained by this method.

In order to minimize the computational time in-

(19) E. C. Fieller, *Appendix Suppl. J. Roy. Stat. Soc.*, **7**, 1 (1940).

TABLE III
SPECTROPHOTOMETRIC DATA IN THE ULTRAVIOLET REGION FOR THE FORMATION OF SULFIDE-IODINE COMPLEXES^a

Sulfide	Solvent	λ_{max} , m μ	t , °C.	K_c, b, c l./mole	$(a_c - a_2)^b$	K_c, d l./mole	$(a_c - a_2)^d$	
<i>trans</i> -2,3-Butylene sulfide	<i>n</i> -Heptane ^e	300	5.6	73.6 ± 2.6	25336	73.9	25227	
			14.7	54.9 ± 3.3	24179	55.1	24087	
			19.8	43.0 ± 1.7	24419	43.1	24339	
			25.0	36.1 ± 1.7	24215	36.2	24139	
			40.0	20.0 ± 0.8	23954	20.0	23907	
Thiacyclobutane	<i>n</i> -Heptane ^f	306 ^g	5.6	267.8 ± 7.8	24545	265.5	24555	
			14.7	181.8 ± 6.6	22937	180.9	22942	
			25.0	111.7 ± 0.9	22257	111.4	22257	
			40.2	60.8 ± 0.4	20495	60.8	20490	
		CCl ₄	310 ^g	5.6	168.5 ± 9.6	30340	167.8	30344
				14.7	117.6 ± 2.4	28986	117.4	28985
				25.0	79.1 ± 2.7	28274	79.0	28270
				40.2	45.4 ± 2.7	26209	45.4	26202
Thiacyclopentane	<i>n</i> -Heptane ^h	306	6.7	625.2 ± 11.5	27416	622.8	27333	
			14.7	418.0 ± 4.0	27060	417.9	26976	
			25.0	251.1 ± 1.9	26902	251.5	26823	
			40.2	140.4 ± 3.2	24113	140.7	24057	
Thiacyclohexane	<i>n</i> -Heptane ^h	302	6.7	354.8 ± 12.6	30720	353.9	30697	
			14.7	241.5 ± 3.3	30371	241.3	30347	
			25.0	155.3 ± 1.5	29565	155.4	29542	
			40.2	90.9 ± 2.8	27332	90.9	27312	
Diethyl sulfide	<i>n</i> -Heptane ^f	303	5.6	597.6 ± 57.6	27290	589.1	27299	
			14.7	348.4 ± 29.8	26151	346.1	26152	
			25.0	180.4 ± 7.3	27561	180.1	27556	
			40.2	102.1 ± 7.3	24525	102.1	24515	

^a The data are reliable to only 3 significant figures. More figures are listed, however, to better compare the results from the two methods of calculation. ^b Based on the approximate equation 3. ^c Error limits calculated by the Fieller¹⁹ method for the 50% confidence interval. The K_c values obtained in the error analysis were essentially identical with those obtained by the least squares treatment of eq. 3, the small differences which arose were in the fourth figure. ^d Based on the full equation 1. ^e Iodine-solvent blank. ^f Sulfide-solvent blank. ^g For the concentrations used, the free sulfide contributes to the absorbance. ^h Pure solvent blank.

volved, a program was worked out for the IBM 709 which automatically (a) solved for K_c and for $a_c - a_2$ in eq. 3, (b) computed the error limits of K_c for the linear equation, based on the method of Fieller,¹⁹ and (c) solved for K_c and for $a_c - a_2$ in eq. 1. Results for the sulfide-iodine complexes obtained in the visible region are given in Table II. Columns 5 and 6 give K_c and $a_c - a_2$, respectively, which were obtained by using the linear equation 3. The next two columns list the results obtained by using the complete equation 1. In accordance with the remarks made above and in a previous discussion,¹⁸ the differences are quite pronounced for the stronger complexes at the lowest temperatures. As an indication of the precision of the data, the results of the error analysis¹⁹ for the 50% confidence interval are included in column 5. The equilibrium constants at 25° in Table II compare quite favorably with those reported for thiacyclobutane, thiacyclopentane, and thiacyclohexane by McCullough and Mulvey,⁷ although these authors used carbon tetrachloride as the solvent.

Further verification for the stability of the sulfide-iodine complexes is given in Table III, which lists the results of the study in the ultraviolet region. For this region, because lower iodine concentrations were employed due to the much larger molar absorptivity index of the complex, the more convenient approximate eq. 3 is found to give results which are practically the same as those obtained with the more complete eq. 1, as expected.¹⁸ Again, an

error analysis for the 50% confidence interval is included.

The thermodynamic data for the sulfide-iodine complexes are given in Table IV. The least precise measurements, and also the first ones made in this series, were obtained for the charge-transfer study of the diethyl sulfide-iodine complex. Here, the value determined for the molar absorptivity index of the complex did not vary systematically with temperature, in contrast to expectation, and this leads to greater error in the thermodynamic functions. The ΔH found seems somewhat high in comparison to that obtained in the blue-shift study and to those obtained by other investigators.^{20,21} The other results are self-consistent and are in fair agreement also with recent work of McCullough²² and co-workers on thiacyclopentane and thiacyclohexane.

Studies on thiacyclobutanes show that α -methyl substitution results in an increase in basicity.²³ If the inductive effects are bigger than the steric effects in the 4-membered ring sulfides, it would be expected that they would be still more dominant in the 3-membered analogs. Hence, it would be anticipated that the unsubstituted 3-membered ring

(20) H. Tsubomura and R. P. Lang, *J. Am. Chem. Soc.*, **83**, 2085 (1961).

(21) S. P. McGlynn, *Radiation Research Suppl.*, **2**, 300 (1960).

(22) J. D. McCullough, private communication. We are grateful to Prof. McCullough for making his results available to us.

(23) H. R. Hays, S. Searles, and M. Tamres, unpublished observations.

sulfide, *i.e.*, ethylene sulfide, is an even weaker electron donor toward iodine than is *trans*-2,3-butylene sulfide.

TABLE IV

THERMODYNAMIC DATA FOR THE FORMATION OF SULFIDE-IODINE COMPLEXES^a

Sulfide	Solvent	Spectral region	$-\Delta H^0$, kcal./mole	$-\Delta F_c^0$, kcal./mole	ΔS_c^0 , e.u.
<i>trans</i> -2,3-Butylene sulfide	<i>n</i> -Heptane	Vis	6.04 ± 0.47	2.09	13.2 ± 1.6
		U.V.	6.63 ± .27	2.11	15.2 ± 0.9
Thiacyclobutane	<i>n</i> -Heptane	Vis	7.09 ± .15	2.68	14.8 ± .5
		U.V.	7.46 ± .15	2.80	15.6 ± .5
	CCl ₄	Vis	7.03 ± .17	2.59	14.9 ± .6
Thiacyclopentane	<i>n</i> -Heptane	U.V.	6.57 ± .08	2.58	13.4 ± .3
		Vis	8.28 ± .18	3.19	17.1 ± .6
	CCl ₄ ^b	U.V.	7.77 ± .21	3.30	15.0 ± .7
Thiacyclohexane	<i>n</i> -Heptane	Vis	8.7 ± .4	3.10	18.7 ± 1.4
		U.V.	7.75 ± .13	2.99	16.0 ± 0.4
	CCl ₄ ^b	U.V.	7.06 ± .19	3.00	13.6 ± 0.6
Diethyl sulfide	<i>n</i> -Heptane	Vis	7.1 ± .3	2.92	14.1 ± 1.0
		U.V.	8.31 ± .15	3.08	17.6 ± 0.5
	U.V. ^c	8.90 ± .60	3.14	19.4 ± 2.0	
		U.V. ^d	7.82 ± .02 ^d	3.08	15.9

^a Errors given are standard errors as obtained from the slope and intercept of a least squares calculation. ^b Ref. 22. ^c Ref. 20. ^d Ref. 21.

Usually any of the thermodynamic properties, ΔH^0 , ΔF^0 , and ΔS^0 , serve as a measure of basicity.²⁴ In our study, the variation between the ΔH^0 found in the ultraviolet and in the visible region makes this function less reliable as a criterion, and we shall use ΔF_c^0 instead. It should be pointed out however, that the average of the ΔH^0 's of the cyclic sulfide complexes in the two regions do parallel the ΔF_c^0 order. It seems definite, then, that the basicity of the cyclic sulfides toward iodine varies with ring size in the order 5- > 6- > 4- > 3-membered ring. This is in contrast to the order found for the cyclic ethers, namely, 4- > 5- > 6- > 3-membered ring.^{2,3} Thus, it seems further established that the ring size effect differs for heteroatoms even if they both belong to the same family in the periodic table.

The basicity order for the cyclic ethers had been found to apply to hydrogen bonding interaction¹ as well as to iodine complex formation. There is evidence that a similar correlation applies to the cyclic sulfides.²⁵ Other support for the above basicity order is found in the work of Cerniani, Modena, and Todesco²⁶ on the rate of oxidation of cyclic sulfides with hydrogen peroxide; the observed order being 5- > 6- > 4-membered ring.

In a previous preliminary report on a condensed phase study of the cyclic sulfide-boron trifluoride addition compounds,²⁷ data were presented which indicated that thiacyclobutane-boron trifluoride formed the strongest adduct. A reinvestigation of

(24) (a) R. M. Keefer and L. J. Andrews, *J. Am. Chem. Soc.*, **77**, 2164 (1955); (b) N. Ogimachi, L. J. Andrews, and R. M. Keefer, *ibid.*, **77**, 4202 (1955).

(25) Data obtained by Dr. Paul von R. Schleyer and co-workers, who have found that the hydrogen bonding interaction of the cyclic sulfides toward phenol is in the order 5- > 6- > 4- > 3-membered ring. We thank Dr. Schleyer for making his results available to us.

(26) A. Cerniani, G. Modena, and P. E. Todesco, *Gazz. chim. ital.*, **90**, 382 (1960).

(27) M. Tamres, S. Searles, and R. F. Vance, Abstracts, 123rd National Meeting of the Am. Chem. Soc., Los Angeles, Calif., March, 1953, p. 25-M.

this problem makes it now appear that this result could be accounted for on the basis of polymerization of thiacyclobutane in the presence of boron trifluoride.²⁸ At present, then, there exists no contradiction to the basicity order of the cyclic sulfides toward any electron acceptor.

Correlations with basicity often have been attempted by measuring fundamental physical properties of the electron donors themselves, and Table V lists data for several properties of the cyclic sulfides. There is, however, no indication of any apparent relation between these experimental values and the basicity order.

TABLE V

SOME PHYSICAL CHARACTERISTICS OF CYCLIC SULFIDES

Sulfide	N.m.r. shifts ^{a, c} , α -CH ₂	β -CH ₂	I_p , ^e e.v.	Ultra-violet spectra ^d
Ethylene sulfide	-0.24	...	8.87 ^a ± 0.15	~245 ^e
Thiacyclobutane	-.18	-0.18	8.64	~265 ^e
Thiacyclopentane	-.24	-.28	8.48	~230 ^f
Thiacyclohexane	-.25	-.32	8.36	~215 ^f

^a Shift = $(H_r - H_a) \times 10^5 / H_r$; R. L. Rutledge, Ph.D. thesis, University of Illinois, 1958. These data are slightly different from those reported in ref. 4. ^b Work in our Laboratories (unpublished) indicates that the same data are obtained even when the sulfides have been diluted with as much as 70% CCl₄. Our value for the α -CH₂ of thiacyclopentane is -0.20, which is somewhat lower than that obtained by Rutledge. ^c L. D. Isaacs, W. C. Price, and R. G. Ridley, "Vacuum Ultraviolet Spectra and Molecular Ionization Potentials," in "The Threshold of Space," ed. by M. Zelikoff, Pergamon Press, Ltd., London, 1957, pp. 143-150. ^d Reference 34. ^e Weak band, region of maximum. ^f Weak band, region of inflection. ^g E. Gallegos and R. W. Kiser, *J. Phys. Chem.*, **65**, 1177 (1961).

(1) A high electron density on the heteroatom would be expected to result in a diminished electron density around other atoms in the molecule. In the cyclic ethers, the range of n.m.r. shifts of the α -CH₂ groups is large, and there is found a satisfactory correlation between these shifts and the electron donor ability of the oxygen atom.⁴ The n.m.r. shifts for the cyclic sulfides fall within a much more limited range, and most are within experimental error of each other. The shielding of the protons in the α -CH₂ groups of thiacyclobutane does not coincide with that anticipated from the basicity order. This compound, unlike trimethylene oxide, has a rather unusual spectrum in that a single peak is observed for the protons in both the α - and β -methylenes.

(2) According to the Mulliken charge-transfer theory,²⁹ $h\nu = W_E - W_N \approx I_p - E_a - e^2/r$, where W_E and W_N are the energies of the excited and the ground state of the system, respectively, E_a is the electron affinity of the iodine molecule, and e^2/r is the coulombic energy of attraction of the oppositely charged species at the internuclear distance r . For a given electron acceptor, such as iodine, several correlations of I_p vs. $h\nu$ have been proposed.³⁰ Instances of a lack of correlation have

(28) These Laboratories, unpublished work.

(29) R. S. Mulliken, *J. Am. Chem. Soc.*, **74**, 811 (1952).

(30) (a) S. H. Hastings, J. L. Franklin, J. Schiller, and F. A. Matsen, *ibid.*, **75**, 2900 (1953); (b) C. van de Stolpe, Ph.D. thesis, Amsterdam, 1953; (c) H. McConnell, J. S. Ham, and J. R. Platt, *J. Chem. Phys.*, **21**, 66 (1953).

been noted,³¹ these generally being for the case involving quite strong interaction, *e.g.*, triethylamine-iodine. The sulfide-iodine complexes also are rather strong, and they too do not fall on the general plot of I_p vs. $h\nu$.³² The I_p 's are most likely those for the adiabatic process because of the stabilization by the ring of the geometric structure in both the molecule and the ion.^{31c} For the cyclic sulfides, the factors which could complicate the correlation should cancel. Yet, no apparent relation exists between I_p and $h\nu$ for this series. The experimental differences are too small, however, to permit a definitive conclusion.³³

(3) Davis⁵⁴ noted a correlation between the ultraviolet absorption spectra of the cyclic sulfides with the previously reported basicity order.²⁷ In view of the present results, this interpretation would have to be modified.

The effect of the ring on a sulfur atom is different from the effect on a carbon atom. In the case of cyclic sulfoxides,³⁵ the frequency of the sulfoxyl group is in the order 5- < 6- < 4- membered ring,³⁶ and the hydrogen bonding ability order is 6- \sim 5- > 4-membered ring, a clear resolution between the electron donor ability of tetramethylene sulfoxide and pentamethylene sulfoxide not being possible by the technique used. The result for the cyclic ketones is different, the hydrogen bonding order is clearly 7- > 6- > 5- > 4-membered ring, and the carbonyl frequency increases systematically from the 7- to the 4-membered ring.³⁵

Sulfur and oxygen not only show a difference in basicity order in their ring size effects, but they also show a reversal in their strength of interaction toward various electron acceptors, *e.g.*, the proton and iodine. The ethers interact more strongly in forming hydrogen bonds than do the sulfides, and the reverse is true in their interaction with iodine.

Two factors apparently are involved in these electron donor-acceptor interactions: (1) The smaller oxygen atom has a higher electron charge density than does the larger sulfur atom, and this condition should be more favorable for interaction with a proton. (2) The larger sulfur atom is more polarizable than the oxygen atom, which could result in a stronger interaction with the large iodine molecule because of favorable mutual polarization. Such factors have been noted to be of importance in the rates of nucleophilic displacement by nucleophilic reagents.³⁷ Table VI lists some dipole moment (μ) and polarization data (p = total polarization, R_D = molar refraction for the sodium

d-line) for cyclic sulfides and cyclic ethers. The largest dipole moment in the sulfide series is that of the 5-membered ring, while for the cyclic ethers it is the 4-membered ring, which may account partially for the differences observed in the basicity order of the two series. Furthermore, in the case of the cyclic ethers, the total polarization and dipole moments are in the same order; and for the 4-, 5-, and 6-membered ring they also follow the observed basicity order. For the cyclic sulfides, the total polarizations do not follow the same sequence as do the dipole moments, and it is the former rather than the latter which gives the better correlation with basicity. Only in the case of the 3-membered ring compounds, particularly ethylene oxide, does the correlation with basicity seem poor. This may be due in part to the fact that dipole moment and polarization are molecular properties whereas electron donor-acceptor interaction depends primarily on the local electron distribution at the bonding site.

TABLE VI
DIPOLE MOMENT DATA FOR CYCLIC SULFIDES AND CYCLIC ETHERS^a

Compound	R_D , cm. ³	μ , D.	P , cm. ³
Ethylene oxide	12.9 ^b	1.91 ^b 1.88 ^d	(87.5) ^c
Oxetane	15.65	1.92	91.20
Tetrahydrofuran	20.00	1.75	82.55
Tetrahydropyran	24.87	1.55	74.22
Ethylene sulfide	(16.9) ^e	1.84 ^d	(86.1) ^c
Thiacyclobutane	21.51	1.78	86.21
Thiacyclopentane	26.09	1.90	99.98
Thiacyclohexane	30.83	1.71	90.86

^a Data from C. W. N. Cumper and A. I. Vogel, *J. Chem. Soc.*, 3521 (1959), in benzene solution, unless otherwise stated. ^b W. L. G. Gent, *ibid.*, 58 (1957). The value of 1.91 is for the vapor; a value of 1.82 is reported in benzene solution. ^c Calculated. ^d G. L. Cunningham, Jr., A. W. Boyd, R. J. Meyers, W. D. Gwinn, and W. I. Le Van, *J. Chem. Phys.*, 19, 676 (1951). ^e Estimated using the value of 4.6 cm.³ as the molar refraction per methylene group.

Comparing the complexing abilities of diethyl and dimethyl³⁸ sulfides with those of the cyclic sulfides shows rather conclusively that the basicity order toward iodine is $(CH_2)_4S > (C_2H_5)_2S > (CH_2)_5S > (CH_2)_3S > (CH_3)_2S > trans-(CH_3CH)_2S$. It is interesting to note but difficult to explain the report that the order of coordination toward borane, and possibly toward boron trifluoride, is $(CH_3)_2 \approx (C_2H_5)_2S > (CH_2)_4S$.³⁹ It should be pointed out, however, that precise experimental data for the sulfides, particularly in their association with boron trifluoride, are difficult to obtain.

Acknowledgment.—This research was supported in part by a grant from the Petroleum Research Fund administered by the American Chemical Society. Grateful acknowledgment is hereby made to the donors of this fund. The authors wish to acknowledge also the capable assistance of Mrs.

(38) N. W. Tideswell and J. D. McCullough, *J. Am. Chem. Soc.*, **79**, 1031 (1957).

(39) T. D. Coyle, H. D. Kaesz, and F. G. A. Stone, *ibid.*, **81**, 2989 (1959).

(31) (a) S. Nagakura, *J. Am. Chem. Soc.*, **80**, 520 (1958); (b) G. Briegleb and J. Czokalla, *Z. Elektrochem.*, **63**, 6 (1959); (c) J. Collin, *ibid.*, **64**, 936 (1960).

(32) See Fig. 4 of reference 31b.

(33) Dr. R. W. Kiser has redetermined the I_p 's of the 4-, 5-, and 6-membered ring sulfides (private communication). Thiacyclobutane and ethylene sulfide have I_p 's which are nearly the same, within experimental error, and which are slightly higher than those of thiacyclopentane and thiacyclohexane, the latter two also being within the limits of error.

(34) R. E. Davis, *J. Org. Chem.*, **23**, 1380 (1958).

(35) M. Tamres and S. Searles, *J. Am. Chem. Soc.*, **81**, 2100 (1959).

(36) A similar finding has been reported by C. A. Meyers, Abstracts, 140th National Meeting of the Am. Chem. Soc., Chicago, Ill., September, 1961, p. 5-T.

(37) J. Hine, "Physical Organic Chemistry," McGraw-Hill Book Co., New York, N. Y., 1956, pp. 138-142.

Lila M. Hall for the spectral measurements with diethyl sulfide and with thiacyclobutane. M. T. wishes to thank the Horace H. Rackham School of

Graduate Studies at The University of Michigan for a grant which made possible the purchase of a Beckman DU spectrophotometer.

MICROWAVE ABSORPTION AND MOLECULAR STRUCTURE IN LIQUIDS. XLVII. THE DIELECTRIC RELAXATION OF QUINOLINE, ISOQUINOLINE, AND SEVERAL MONOSUBSTITUTED BIPHENYLS IN A VERY VISCOUS SOLVENT^{1,2}

BY ERNEST N. DICARLO³ AND CHARLES P. SMYTH

Frick Chemical Laboratory, Princeton University, Princeton, N. J.

Received December 18, 1961

The dielectric constants and losses at wave lengths of 1.25, 3.22, 10, 25, and 50 cm. have been measured for isoquinoline and quinoline in Nujol solution at 20, 40, and 60°. Measurements also have been made at wave lengths of 10, 25, and 50 cm. on Nujol solutions of 4-iodobiphenyl, 2-iodobiphenyl, 2-bromobiphenyl, and 2-methoxybiphenyl at the above temperatures. Measurements of dielectric constant alone have been made at a wave length of 575 m. and refractive indices were determined for the sodium-D line. The Cole-Cole arc plots have been used to calculate the most probable dielectric relaxation times and the distribution parameters for the solutions. The free energies and heats of activation for the dielectric relaxation processes also have been calculated. The effect of difference in dipole location is too small to detect in quinoline and isoquinoline. The effect is very large in the biphenyls, 4-iodobiphenyl having relaxation times about six times those of 2-iodobiphenyl. The relaxation times show that the relaxation of 4-iodobiphenyl occurs by rotation of the molecule around its two short axes, while relaxation of the 2-substituted biphenyls occurs predominantly by rotation around the long axis. No separation of relaxation times could be effected for any of the molecules. In the case of 2-methoxybiphenyl, this shows that rotation of the methoxy group is prevented by steric hindrance. The large difference between the slope of the optical dielectric constant and that of the square of the refractive index for this molecule points to libration of the methoxy group. The energies of activation are consistent with the observed relaxation times. The observed distribution parameters were large for all the molecules indicating that they were determined, for the most part, by the nature of the solvent used.

Previous papers of this series have reported dielectric measurements carried out upon solutions of polar molecules in solvents of different viscosities in order to investigate the relation between dielectric relaxation time, viscosity, and location of the molecular dipole within the molecule.⁴ Recent investigations have employed the very viscous mixture of hydrocarbons, Nujol.^{5,6} The present study was made to extend our knowledge by investigating large solute molecules of known size, shape, and dipole location in Nujol. When there is a possibility of more than one relaxation time for a molecule, the highly viscous solvent tends to effect a separation of the times,⁷ provided that the mechanisms corresponding to the individual relaxation times involve significantly different rotations. Also, the use of Nujol in conjunction with very large solute molecules has been found to lower the frequencies of the dispersion region to such an extent that it is possible to observe directly the region in which the dielectric constant values may be near that of the optical dielectric constant.⁵

(1) This research was supported by the U. S. Army Research Office—Durham. Reproduction, translation, publication, use, or disposal in whole or in part by or for the United States Government is permitted.

(2) This paper represents part of the work submitted by E. N. DiCarlo to the Graduate School of Princeton University in partial fulfillment of the requirements for the degree of Doctor of Philosophy.

(3) Esso Foundation Fellow, 1960–1961; National Science Foundation Summer Fellow, 1961.

(4) C. P. Smyth, *Proc. Natl. Acad. Sci. U. S. A.*, **42**, 234 (1956).

(5) O. F. Kalman and C. P. Smyth, *J. Am. Chem. Soc.*, **82**, 783 (1960).

(6) E. L. Grubb and C. P. Smyth, *ibid.*, **83**, 4122 (1961).

(7) E. L. Grubb and C. P. Smyth, *ibid.*, **83**, 4873 (1961).

Experimental Methods

Apparatus.—The apparatus and the various methods of measurement have been described in previous papers.^{8–10}

Purification of Materials.—The substances investigated were obtained from (A) The Eastman Kodak Company, (B) Monsanto Chemical Company, (C) Matheson Coleman & Bell. The source of each compound, method of purification, refractive index, and boiling or melting point are listed in Table I.

TABLE I
SOURCES, METHODS OF PURIFICATION, REFRACTIVE INDICES,
BOILING POINT, OR MELTING POINT

	n_D^{25}		M.p., °C.
2-Iodobiphenyl ^a (A)	1.65878	4-Iodobi- phenyl ^d (A)	113.7–114.3
Isoquinoline ^b (A)	1.62236 (25.1°)		
2-Bromobi- phenyl ^c (A)	1.62616	Quinoline ^e (C)	109–110 (13 mm.)
2-Methoxybi- phenyl ^a (B)	1.60656		

^a Used as received. ^b Refluxed over barium oxide for 15 hr. and fractionally distilled under reduced pressure.

^c Fractionally distilled under reduced pressure and stored over Drierite. ^d Recrystallized from a mixture of absolute ethanol and benzene and dried under vacuum over phosphorus pentoxide in an Abderhalden pistol. ^e Refluxed over barium oxide for 24 hr. and fractionally distilled under reduced pressure.

Nujol was purchased from a local drug store and treated as previously described.¹¹

(8) H. L. Laquer and C. P. Smyth, *ibid.*, **70**, 4097 (1948).

(9) W. M. Heston, Jr., A. D. Franklin, E. J. Hennelly, and C. P. Smyth, *ibid.*, **72**, 3443 (1950).

(10) D. A. Pitt and C. P. Smyth, *J. Phys. Chem.*, **63**, 582 (1959).

(11) A. J. Curtis, P. L. McGeer, G. B. Rathmann, and C. P. Smyth, *J. Am. Chem. Soc.*, **74**, 644 (1952).

Experimental Results

The experimental results were treated in the manner previously described,¹² except that the values of the dielectric constant ϵ' , the loss ϵ'' , and the square of the refractive index for the sodium D line were plotted against the weight fraction of solute in the solution, instead of the mole fraction, because of the assortment of molecular weights in the solvent. The slopes of the straight lines thus obtained, a' , corresponding to ϵ' , and a'' , corresponding to ϵ'' , were plotted in Cole-Cole arcs¹³ in the usual fashion¹² to obtain the critical wave lengths, λ_m , the corresponding relaxation times, τ , the distribution coefficients, α , and the arc intercepts at infinite frequency, a_∞ . The values of these quantities are given in Tables II and III. The concentration range is given in parentheses for each set of solutions in Table II. The viscosity of the Nujol, as measured by J. E. Anderson in this Laboratory, was 226.1 c.p.s. at 20°, 65.3 c.p.s. at

TABLE II

SLOPES FOR THE DEPENDENCE OF THE DIELECTRIC CONSTANT AND LOSS OF SOLUTIONS ON WEIGHT FRACTION OF SOLUTE

Wave length (cm.)	20°		40°		60°	
	a'	a''	a'	a''	a'	a''
Quinoline-Nujol (0-0.031)						
1.25	0.71	0.25	0.79	0.44	0.68	0.47
3.22	1.22	.77	1.46	.94	1.78	1.00
10	2.07	.85	2.52	.83	2.63	0.68
25	2.99	.73	3.08	.62	3.00	.35
50	3.36	.63	3.30	.39	3.15	.21
57500	3.76		3.50		3.16	
Isoquinoline-Nujol (0-0.030)						
1.25	0.907	0.800	1.23	0.952	1.52	1.09
3.22	1.85	1.30	2.21	1.36	2.38	1.33
10	3.19	1.31	3.60	1.16	3.84	0.923
25	4.66	1.20	4.58	0.765	4.32	.505
50	5.19	0.825	4.85	0.425	4.48	.270
57500	5.42		4.87		4.54	
2-Bromobiphenyl-Nujol (0-0.064)						
10	0.38	0.08	0.41	0.14	0.48	0.19
25	.41	.15	.59	.24	.75	.26
50	.60	.22	.83	.24	.95	.16
57500	1.10		1.04		.97	
2-Methoxybiphenyl-Nujol (0-0.060)						
10	0.566	0.061	0.619	0.108	0.648	0.155
25	.580	.121	.731	.192	0.848	.249
50	.820	.258	.985	.252	1.10	.214
57500	1.40		1.30		1.21	
2-Iodobiphenyl-Nujol (0-0.060)						
10	0.340	0.052	0.371	0.066	0.442	0.136
25	.379	.076	.433	.140	.522	.175
50	.462	.143	.567	.179	.709	.135
57500	.895		.840		.790	
4-Iodobiphenyl-Nujol (0-0.056)						
10	0.370	0.019	0.384	0.038	0.400	0.081
25	.377	.044	.425	.098	.436	.130
50	.410	.072	.435	.134	.553	.210
57500	1.28		1.18		1.06	

(12) A. D. Franklin, W. M. Heston, Jr., E. J. Hennelly, and C. P. Smyth, *J. Am. Chem. Soc.*, **72**, 3447 (1950).

(13) K. S. Cole and R. H. Cole, *J. Chem. Phys.*, **9**, 341 (1941).

TABLE III

SLOPES a_D FOR THE DEPENDENCE OF SQUARE OF REFRACTIVE INDEX ON WEIGHT FRACTION, WITH INFINITE FREQUENCY INTERCEPTS a_∞ , CRITICAL WAVE LENGTHS λ_m , RELAXATION TIMES τ , AND DISTRIBUTION PARAMETERS α

t , °C.	a_D	a_∞	λ_m (cm.)	τ (10^{-12} sec.)	α
Quinoline-Nujol					
20	0.300	0.37	8.84	46.9	0.33
40		.39	5.01	26.6	.25
60		.44	3.35	17.8	.20
Isoquinoline-Nujol					
20		0.48	8.47	45.0	0.29
40		.56	4.73	25.1	.24
60	0.300	.56	3.28	17.4	.23
2-Bromobiphenyl-Nujol					
20		0.330	76.7	407.3	0.25
40	0.260	.345	33.5	177.8	.17
60		.360	19.7	104.7	.07
2-Methoxybiphenyl-Nujol					
20	0.281	0.535	110.2	584.8	0.26
40		.556	47.0	249.4	.24
60		.575	27.2	144.6	.10
2-Iodobiphenyl-Nujol					
20	0.275	0.322	112.2	595.6	0.29
40		.322	53.1	281.8	.24
60		.328	27.7	147.1	.19
4-Iodobiphenyl-Nujol					
20		0.364	631	3349	0.23
40	0.307	.363	240	1276	.23
60		.359	116	616.5	.22

40°, and 25.3 c.p.s. at 60°. The density of the Nujol, as measured by E. Forest in this Laboratory, was 0.8790 at 20°, 0.8678 at 40°, and 0.8560 at 60°.

Discussion of Results

For each set of solutions the Cole-Cole arc plots were used to represent the distribution of relaxation times since the points were so well distributed over the arcs or so well grouped at one end as to establish the arcs as good representations of the data. Because of this favorable distribution of points along the curves, the high frequency intercepts, a_∞ , of the arcs with the abscissa axis, corresponding to the optical dielectric constant, appear to be unusually accurate for all the molecules considered in this study with the possible exception of isoquinoline for which a longer extrapolation was required. For quinoline and the biphenyl molecules, excluding 2-methoxybiphenyl, the high frequency intercepts are close to the a_D values and are indicative of normal atomic polarization values for these molecules.

Previous data obtained from measurements on solutions of isoquinoline in Nujol,⁵ although representable by a Cole-Cole arc, seemed to indicate the presence of two maxima in the dielectric loss-frequency curve at 20° merging to one wide maximum at 60°. As the differences in the axial lengths of the molecule appeared to be much too small to give relaxation times sufficiently different to cause two distinct maxima in the curve, further measurements evidently were needed for clarification. The

present measurements on quinoline and isoquinoline consequently have been made. The redetermination of the critical wave lengths and corresponding relaxation times of isoquinoline gave results in good agreement with the earlier measurements.⁵ However, the dielectric loss-frequency curve at 20° shows the presence of only one maximum, confirming the expectation that the asymmetry of the molecule is not sufficiently great to make its effect evident in two distinguishable relaxation times. If isoquinoline oriented by rotation around the axis in the carbon-carbon bond held in common by the two rings (an orientation practically absent in quinoline, where the molecular dipole is almost parallel to this axis) its relaxation time would be expected to be longer than that of quinoline, since rotational orientation around this particular axis should occur with slightly greater difficulty than that around the other two axes. 2-Substituted naphthalenes have slightly longer relaxation times than the corresponding 1-substituted compounds,⁶ but, in this case, the substituent in the 2-position adds to the length of the molecule, thus further increasing the relaxation time. The relaxation times in Table III for quinoline are practically identical with those for isoquinoline, showing that only small differences exist in the frictional resistances to rotation around the different molecular axes. This is consistent with the small distribution parameters, 0.07 to 0.14, found for the two substances as pure liquids¹⁴ and in solution in molten naphthalene.¹⁵ The large and nearly identical distribution parameters for the two substances in Nujol solution presumably result from the variety of molecular environments produced by the mixed hydrocarbons of the solvent. Large distributions of relaxation times have also been found in Nujol solution¹¹ for even more symmetrical molecules, including the nearly spherical molecule of *t*-butyl chloride, which shows no distribution in the pure liquid state and in carbon tetrachloride solution.¹¹

As seen from Table III, the relaxation time of 4-iodobiphenyl at a given temperature is much larger than the corresponding relaxation times of the 2-biphenyls investigated. This is to be expected since the dipole moment in 4-iodobiphenyl is directed along its long axis, while the principal component of the dipole in a 2-biphenyl lies along a short axis of the molecule. Therefore, relaxation of 4-iodobiphenyl will occur by rotations about the short axes of the molecule, the latter requiring far more displacement of the surrounding solvent molecules than rotation about the long axis, the principal orientational mechanism involved in the relaxation of the 2-biphenyls. For the same reason, the variation of relaxation time with temperature is more pronounced for 4-iodobiphenyl than for the 2-biphenyl molecules. Also, the relaxation time at a given temperature is longer for 2-iodobiphenyl than for 2-bromodiphenyl, this effect being due to the larger size and polarizability of the iodine atom as compared to the bromine atom.

(14) R. S. Holland and C. P. Smyth, *J. Phys. Chem.*, **59**, 1088 (1955).

(15) R. C. Miller and C. P. Smyth, *J. Am. Chem. Soc.*, **79**, 308 (1957).

As seen from Table III, the relaxation times and distribution parameters for 2-iodobiphenyl are close to those obtained for 2-methoxybiphenyl, which would be the case if the latter molecule relaxed only by over-all molecular rotation since the methoxy group and the iodine atom are similar in size. It is concluded, therefore, that in 2-methoxybiphenyl there is very little, if any, contribution to the dipole orientational mechanism by internal rotation of the methoxy group. As a further check of the above interpretation, dielectric absorption measurements were made on solutions of this compound at 3.22 cm., a wave length at which internal rotations should contribute considerably to the loss. No significant absorption was observed at this frequency, showing that methoxy group rotation is not contributing to the relaxation process, which evidently consists wholly of molecular rotation. This is in marked contrast to the result obtained in Nujol solution for 4-methoxybiphenyl,⁷ where it was found that methoxy group rotation contributes approximately 60% to the relaxation of the molecule. As mentioned previously, the high frequency intercepts, a_{∞} , determined for 2-methoxybiphenyl from the Cole-Cole arc plots appear to be reliable. This is especially true at 20° due to the very favorable distribution of points along the arc at this temperature. The fact that the $a_{\infty}-a_D$ value is considerably larger for this molecule than for the other biphenyls studied indicates that 2-methoxybiphenyl possesses an additional polarization probably associated with a high-frequency librational motion of the hindered methoxy group.

As with quinoline and isoquinoline, large distribution parameters were found for the biphenyls and again this probably is due to the variety of environment provided by the solvent. The nearly symmetrical 4-iodobiphenyl molecule should show no distribution in the absence of an effect of solvent since it may rotate about two nearly equivalent axes. In fact, a negligible distribution of relaxation times has been found in heptane and hexadecane solutions for 4-bromobiphenyl,¹⁶ and a small distribution parameter, 0.08 to 0.03, even in Nujol.⁵ One would expect the distribution parameters of the 2-biphenyls to be much larger than those of 4-iodobiphenyl if rotations about the long axis and the two nearly equivalent short axes both contributed appreciably to the relaxation process. However, the distribution parameters for the 2-biphenyls are of the same size or smaller than those for 4-iodobiphenyl, indicating that the 2-biphenyls relax, for the most part, by one type of orientational motion, presumably turning about the long axis of the molecule. Dielectric measurements made on 2-bromobiphenyl in heptane and hexadecane solutions¹⁶ indicate only one relaxation time (*i.e.*, $\alpha = 0.02$) and, therefore, agree with the above interpretation.

The free energies, ΔF^* , and heats, ΔH^* , of activation for dielectric relaxation, calculated in the usual manner,¹⁷ are given in Table IV.

The similarity of the values for quinoline and iso-

(16) Measured by B. B. Howard in this Laboratory.

(17) E. J. Hennelly, W. M. Heston, Jr., and C. P. Smyth, *J. Am. Chem. Soc.*, **70**, 4102 (1948).

TABLE IV
FREE ENERGIES AND HEATS OF ACTIVATION (KCAL./MOLE)
FOR DIELECTRIC RELAXATION IN NUJOL SOLUTIONS

Solute	ΔF^*	ΔH^*
Quinoline	3.30	4.09
Isoquinoline	3.27	3.97
2-Bromobiphenyl	4.55	5.91
2-Methoxybiphenyl	4.77	6.12
2-Iodobiphenyl	4.78	6.18
4-Iodobiphenyl	5.78	7.60

quinoline is to be expected from the similarity of

their relaxation mechanisms indicated by their relaxation times. The larger values for the biphenyls result from the greater lengths of their molecules. The virtual identity of the values for 2-methoxybiphenyl with those for 2-iodobiphenyl give further confirmation of the similarity of the rotation mechanisms for these two molecules and, consequently, of the absence of contribution from methoxy group rotation. The larger values for 4-iodobiphenyl are, at least, qualitatively consistent with the longer relaxation time resulting from its rotation about the short molecular axes.

FARADAIC RECTIFICATION AND ELECTRODE PROCESSES. III. EXPERIMENTAL METHODS FOR HIGH FREQUENCIES AND APPLICATION TO THE DISCHARGE OF MERCUROUS ION

BY HIDEO IMAI¹ AND PAUL DELAHAY

Coates Chemical Laboratory, Louisiana State University, Baton Rouge, Louisiana

Received December 21, 1961

Experimental methods are described for faradaic rectification studies up to 50 Mc. and are applied to the discharge of Hg(I) on mercury. Apparent exchange current densities up to 10 amp. cm.⁻² were measured which correspond to an apparent standard rate constant of $k_a^0 = 100$ cm. sec.⁻¹ for an electrode process involving both soluble oxidant and reductant of equal concentrations of $C = 5 \times 10^{-4}$ mole per liter ($n = 2$, $D_0 = D_R = 10^{-6}$ cm.² sec.⁻¹) or to $k_a^0 = 1000$ cm. sec.⁻¹ for $C = 5 \times 10^{-3}$ mole per liter. The following topics are covered: design of a cell for dropping mercury electrode with low inductance and very small stray capacity; measurement of the cell impedance; determination of rectification voltages; heating of electrolyte; measurement of non-faradaic rectification; and experimental errors. A method of interpretation is developed which does not require independent determination of the differential capacity of the double layer. The k_a^0 for discharge of Hg(I) on Hg at $24 \pm 2^\circ$ in 0.1, 0.2, and 1.1 M HClO₄ is 0.28, 0.35, and 1.3 cm. sec.⁻¹, respectively, and the transfer coefficient α is 0.28. These variations of k_a^0 are correlated with the double layer structure and are of the order predicted by approximate theory. The k_a^0 's and α also are compared with data obtained by the double pulse galvanostatic method. The much lower value of $k_a^0 = 0.047$ cm. sec.⁻¹ for 0.98 M HClO₄ for the latter method suggests the occurrence of a coupled chemical reaction.

Theoretical and experimental methods for the study of fast electrode processes by faradaic rectification, previously reported from this Laboratory,^{2,3} are applied in this paper to frequencies up to 50 Mc. Such high frequencies are necessary in the study of fast electrode processes, and the development of the appropriate experimental methods is of interest. Results are given for the discharge of mercurous ion on mercury in perchloric acid and are correlated with the double layer structure. The instrument previously described^{2b} was tested up to 51 Mc. but was not used extensively, and only frequencies up to 2 Mc. were utilized in previous work in this Laboratory.^{2a} Barker⁴ used frequencies from 100 Kc. to 1.6 Mc. and occasionally 6.4 Mc.

Experimental

Solutions.—Solutions were prepared from analytical grade reagents and water that had been bidistilled over KMnO₄. The stock solution of Hg(I) was kept over Hg and was standardized by electrogravimetry. Solutions were treated with purified activated charcoal according to Barker,⁴

and charcoal was removed by centrifugation. Complete removal of small charcoal particles was somewhat critical for the more dilute solutions of Hg(I) because of the instability of potential for improperly treated solutions. Oxygen was not removed from the solution as it did not seem to interfere.

Cell.—A cell with a mercury pool and a dropping mercury electrode was designed for high frequency studies. Conventional cells cannot be used above 1 Mc. (or even lower frequencies) because the stray capacity of the mercury reservoir and the inductance of the mercury column in the polarographic capillary are much too high. These unfavorable features are eliminated by the use of a short capillary with a constricted section and a small mercury reservoir connected to a manostat and a manometer (mercury column type). The constricted capillary in the cell of Fig. 1 was constructed from conventional polarographic capillary, and the drawn out capillary was cut to proper length after grinding of a circular groove. Heating of mercury in the constricted section caused interruption of the flow of mercury when a.c. pulses longer than 5–10 msec. were accidentally applied at the higher current densities. The capillary, however, could be reclaimed by application of pressure and gentle heating. Mercury was added in reservoir R₁ every 30 min. to maintain the level constant within 1 mm. This was done with the stopcock closed and by careful squeezing of the plastic bottle B. The cell of Fig. 1 was fitted with a saturated calomel microelectrode in the study of rectification by the double layer. No liquid bath was used for temperature control because of increase in stray capacity (with a conducting bath) and the relative uncertainty in temperature resulting from heating of the electrolyte at the higher frequencies (see Discussion).

The capillary characteristics were as follows for the 0.1, 0.2, and 1.1 M HClO₄ solutions: $m = 0.896, 0.133$, and 0.263 mg. sec.⁻¹; drop time at open circuit without hammer, 9.0, 44.0, and 21.0 sec.; head of mercury in manostat and

(1) Postdoctoral research associate 1960–1962; on leave from Minami College, Hiroshima University, Hiroshima.

(2) (a) P. Delahay, M. Senda, and C. H. Weis, *J. Am. Chem. Soc.*, **83**, 312 (1961); (b) M. Senda, H. Imai, and P. Delahay, *J. Phys. Chem.*, **65**, 1253 (1961); see ref. 2a for bibliography.

(3) See also the related papers: (a) M. Senda and P. Delahay, *J. Am. Chem. Soc.*, **83**, 3763 (1961); (b) M. Senda and P. Delahay, *J. Phys. Chem.*, **65**, 1580 (1961).

(4) G. C. Barker, "Transactions of the Symposium on Electrode Processes, Philadelphia, 1959," E. Yeager, ed., John Wiley and Sons New York, N. Y., 1961, pp. 325–365.

manometer connected to reservoir R_1 , 250, 325, and 370 mm.; drop time with hammer, 3.33, 3.33, and 5.00 sec.; time of application of a.c. pulse, 1.66, 2.88, and 1.32 sec.; area, 1.11×10^{-2} , 4.59×10^{-3} , and 4.21×10^{-3} cm.².

Cell Impedance.—The cell impedance, which must be known for the evaluation of the voltage amplitude across the electrode impedance, was measured with a General Radio radio-frequency bridge, type 1606-A (400 kc. to 60 Mc.). The bridge was connected to a Hewlett-Packard signal generator, type 606A, whose output was modulated by a Tektronix pulse generator, type 161. The latter was triggered via a Tektronix wave form generator, type 162, by the rotating disk with contacts which actuated the magnetic hammer of the d.m.e. The balance detector was a National receiver, type HRO-50TI, the output of which was displayed on a Tektronix cathode-ray oscilloscope, type 535.

Data in Table I show that the non-resistive part X of the cell impedance is essentially proportional to the frequency. Hence, X was purely inductive and the cell stray capacity was negligible, at least up to 50 Mc. The resistive component which depends on the electrolyte relaxation and the "skin" effect was nearly independent of frequency. Similar conclusions were reached for the other solutions in this work.

TABLE I

CELL IMPEDANCE ^a FOR 1.1 M HClO ₄			
f , Mc.	R , ohms	X , ^b ohms	Z , ^c ohms
1	45.5	0	45.5
3.5	43.6	1.1	43.6
7	43.4	2.5	43.5
14	44.4	5.6	44.8
21	44.6	3.6	45.4
28	45.0	11.8	45.4
50	45.2	22.2	50.2

^a D.m.e. characteristics: $m = 0.263$ mg. sec.⁻¹, t (magnetic hammer) 1.32 sec., $T = 26.0^\circ$. ^b Non-resistive component of impedance. ^c Total impedance.

Faradaic Rectification.—Rectification voltages were measured directly from cathode-ray oscilloscope display. The instrument was as previously described except for two changes. (a) The amplitude of the a.c. pulse applied to the cell was displayed on a Tektronix, model 585 with plug-in unit 80 and probe P80, in the higher frequencies range; this high frequency oscilloscope (up to 100 Mc.) was not available in our previous work. (b) The filter circuit was modified to improve its characteristics below 1 Mc.: a 0.5 millihenry choke was connected between the d.m.e. and the input of the low-pass filter previously used, and a 0.01 μ f. capacitor was connected across the input of the filter. The connection between the choke and the d.m.e. was short (5 cm.). The double pulse method previously described^{2b} was used at the higher frequencies to shorten application of the a.c. pulse to a few milliseconds and minimize heating of the supporting electrolyte (See Discussion).

Rectification by the Double Layer.—Non-faradaic rectification was studied with the same instrument^{2b} as above except that the mean potential of the d.m.e. was controlled against a saturated calomel electrode and the charge due to rectification was compensated by a square pulse of 10 μ sec. duration (Fig. 2). Compensation was ascertained with a Tektronix oscilloscope, type 535, which was fitted with a plug-in amplifier E and operated at the maximum sensitivity of 50 μ v. cm.⁻¹. A limitation of the equipment previously described^{2b} became apparent in this work, namely that the modulated a.c. signal from the two transmitters is not sufficiently free of transients to allow unambiguous detection of compensation. This limitation disappeared when the Hewlett-Packard signal generator, type 606A, was substituted for the transmitters but the limited output power of the generator prevented application above 7.5 Mc. The Hewlett-Packard 460AR which has rather poor transient characteristics also was eliminated from the instrument previously described.^{2b}

Analysis of Data

The general equation for the rectification voltage for control of the mean faradaic current to zero (cf. eq. 9 and 23 in ref. 2a) has the following form in

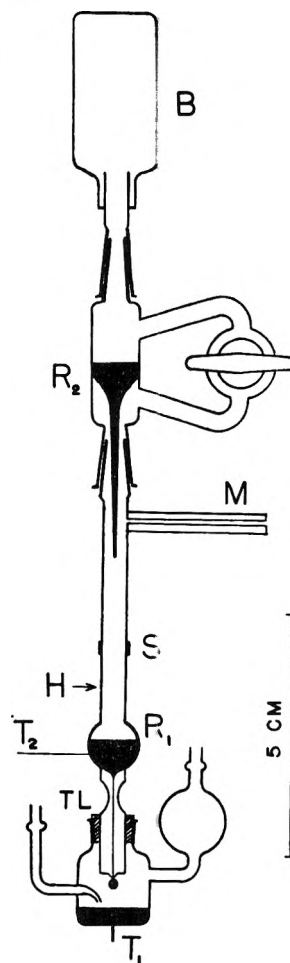


Fig. 1.—Cell for very high frequency measurements: B, plastic bottle; R_1 , R_2 , mercury reservoirs; M, connected to manometer and manostat; S, graded seal between Pyrex and soft glass (lower part with capillary); H, magnetic hammer; T_1 , Pt terminal, 18 gage; T_2 , Pt terminal, 22 gage; TL, Teflon stopper. A reference electrode (e.g., s.c.e.) can be inserted in the right-hand side bulb, if necessary.

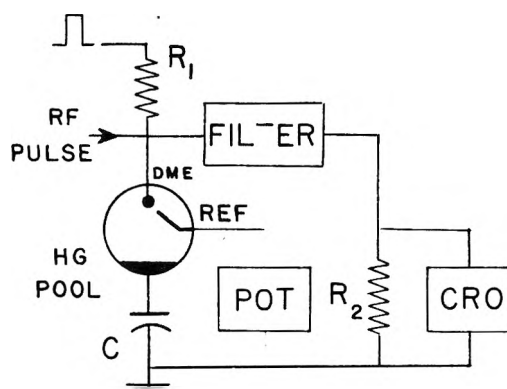


Fig. 2.—Cell circuit for study of rectification by the double layer: $R_1 = 5.5$ megohms; $R_2 = 3000$ ohms; $C = 1 \mu$ f.

the particular case of the discharge of Hg(I) on Hg

$$\frac{\Delta \bar{E}_\infty}{V_A^2} = \frac{nF}{RT} \left[\frac{2\alpha - 1}{4} - \frac{\alpha}{2} \frac{1 + \cot \theta_a}{1 + \cot^2 \theta_a} \right] \quad (1)$$

where $\Delta \bar{E}_\infty$ is the rectification voltage for $t \rightarrow \infty$; V_A the amplitude of the sinusoidal voltage across the faradaic impedance; α the transfer coefficient; θ_a the phase angle between the resistive and capaci-

tive components of the faradaic impedance; $n = 2$; and R , T , and F are as the usual. At sufficiently high frequencies (cf. eq. 27 in ref. 2a) one has

$$\frac{1 + \cot \theta_a}{1 + \cot^2 \theta_a} \approx \frac{1}{\cot \theta_a} = \frac{I_a^0}{2^{1/2} n F C D^{1/2} \omega^{1/2}} \quad (2)$$

where I_a^0 is the apparent exchange current density; C the bulk concentration of Hg(I); D the diffusion coefficient of Hg(I); and $\omega = 2\pi f$, f being the frequency.

When the faradaic impedance Z_f is very large in comparison with the double layer impedance $1/\omega c_1$ (c_1 differential capacity), one has $V_A \approx I_A/\omega c_1$ (I_A current amplitude), and there follows from eq. 1 and 2

$$\frac{\Delta \bar{E}_\omega \omega^2}{I_A^2} \approx \frac{1}{c_1^2} \frac{nF}{RT} \left\{ \frac{2\alpha - 1}{4} - \frac{\alpha I_A^0}{2^{1/2} n F C D^{1/2} \omega^{1/2}} \right\} \quad (3)$$

It will be assumed that (a) the differential capacity c_1 is not affected by variations of the Hg(I) concentration in the presence of a large excess of supporting electrolyte; (b) that c_1 is constant in the range of potentials corresponding to the variations in C ; and (c) that c_1 is frequency independent. The first two assumptions are realistic and the third one was verified experimentally. Further, it will be assumed that I_a^0 in this case is

$$I_a^0 = n F k_a^0 C^{1-\alpha} \quad (4)$$

where k_a^0 is the apparent standard rate constant.⁵ (The validity of this equation is discussed below.) It then follows from eq. 3 that the ratio of the slopes of the plot $\Delta \bar{E}_\omega \omega^2/I_A^2$ against $\omega^{-1/2}$ for two concentrations of Hg(I), C_1 and C_2 , is $(C_2/C_1)^\alpha$. The coefficient α thus can be evaluated from the directly measurable quantities $\Delta \bar{E}_\omega$, I_A , and ω without independent determination of the differential capacity c_1 . The latter now can be evaluated from the intercept of the line $\Delta \bar{E}_\omega \omega^2/I_A^2$ against $\omega^{-1/2}$ for $\omega^{-1/2} = 0$. Finally, I_a^0 is calculated from the slope of the line $\Delta \bar{E}_\omega \omega^2/I_A^2$ against $\omega^{-1/2}$.

Description and Discussion of Results

Determination of c_1 , α , I_a^0 , and k_a^0 .—Conditions for control of the voltage across the electrode impedance by the double layer capacity were determined from plots of $\log(|\Delta \bar{E}_\omega|/I_A^2)$ against $\log \omega$ (Fig. 3). When $Z_f \gg 1/\omega c_1$, $V_A = I_A/\omega c_1$, and $|\Delta \bar{E}_\omega|/I_A^2$ is inversely proportional to ω^2 for pure charge transfer control or inversely proportional to $\omega^{3/2}$ in the range of frequencies in which Z_f varies linearly with $\omega^{-1/2}$. Conversely, when $Z_f \ll 1/\omega c_1$, $V_A = I_A Z_f$, and $|\Delta \bar{E}_\omega|/I_A^2$ is inversely proportional to ω at frequencies at which Z_f varies linearly with $\omega^{-1/2}$. It is seen from Fig. 3 that the slope of $\log(|\Delta \bar{E}_\omega|/I_A^2)$ vs. $\log \omega$ increases in absolute value with ω . This slope is slightly smaller than -2 at the lower frequencies and somewhat larger than -2 at the higher frequencies. It is concluded that the condition $Z_f \gg 1/\omega c_1$ which is prescribed in the analysis of data above is fulfilled at the higher frequencies. This conclusion was confirmed by comparison of the values of Z_f and $1/\omega c_1$ deduced from experimental data.

Values of $\Delta \bar{E}_\omega \omega^2/I_A^2$ are plotted against $\omega^{-1/2}$ in Fig. 4, and kinetic data are listed in Table II.

(5) For a review, see, e.g., P. Delahay in Vol. 1, "Advances in Electrochemistry and Electrochemical Engineering," P. Delahay, ed., Interscience Publishers, Inc., New York, N. Y., 1961, pp. 233-318.

Similar results were obtained for 0.1 M HClO₄ but are not plotted for the sake of clarity. Note that the plots in Fig. 4 are linear in the upper frequencies range and that the intercept at $\omega^{-1/2} = 0$ is the same for all solutions (cf. eq. 3). The values of k_a^0 and I_a^0 in Table II correspond to a very fast electrode process, and Barker's observation⁴ that faradaic rectification is entirely diffusion controlled for $C = 0.05$ mM Hg(I) in 1 M HClO₄ up to 6.4 Mc. is in agreement with the present findings. The precision for α and k_a^0 , as estimated for oscillographic determinations and other measurements, corresponds to a relative error of $\pm 10\%$, or perhaps a higher error. The differential capacity for $E \approx 0.71$ to $E = 0.67$ v. vs. n.h.e. was 43 $\mu\text{f. cm.}^{-2}$. This value is of the order of the approximate value, $c_1 \approx 39 \mu\text{f. cm.}^{-2}$ at $E \approx 0.65$ v. vs. n.h.e., reported by Grahame⁶ for 1 M HClO₄. It also agrees well with $c_1 \approx 39 \mu\text{f. cm.}^{-2}$ as calculated by Matsuda⁷ from data reported by Matsuda, Oka, and Delahay⁸ in a study of Hg(I) discharge by the double pulse

TABLE II
KINETIC DATA^a FOR THE DISCHARGE OF Hg(I) ON Hg IN HClO₄

C_{HClO_4} , M l. ⁻¹	$C_{\text{Hg(I)}}$, mM l. ⁻¹	α	k_a^0 , cm. sec. ⁻¹	I_a^0 , amp. cm. ⁻²
0.1	0.058	0.25	0.26	0.32
	.12	.26	.28	.55
	.23	..	.28	.92
	.47	.28	.28	1.50
	Av.	.26	.28	
0.2	0.058	0.28	0.35	0.43
	.12	.28	.35	0.70
	.23	..	.35	1.15
	.47	.28	.36	1.9
	Av.	.28	.36	
1.1	0.067	0.26	1.3	1.7
	.35	.30	1.4	5.9
	.73	..	1.3	9.8
	Av.	.28	1.3	

^a Differential capacities: 43 $\mu\text{f. cm.}^{-2}$ for the three acid concentrations.

galvanostatic method. One readily verifies from the I_a^0 's in Table II that the electrode impedance was essentially controlled by the double layer at the higher frequencies whereas this was not the case at the lower frequencies. Thus, the charge transfer resistance $r_{ct} = (RT/2F)(1/I_a^0)$ is 1.3×10^{-3} ohm for the highest value of I_a^0 (9.8 amp. cm.⁻²) as compared to $1/\omega c_1 = 7.4 \times 10^{-5}$ ohm for the highest frequency (50 Mc.) and $c_1 = 43 \mu\text{f. cm.}^{-2}$. Conversely, $r_{ct} = 4 \times 10^{-2}$ ohm for the lowest value of I_a^0 (0.32 amp. cm.⁻²) and $1/\omega_1 = 1.9 \times 10^{-2}$ ohm for the lowest frequency (0.2 Mc.).

The rate constant, $k_a^0 = 1.3$ cm. sec.⁻¹ for 1.1 M HClO₄ in Table II, is much larger than the value $k_a^0 = 0.047$ cm. sec.⁻¹ for 0.98 M HClO₄ one deduces from data obtained by the double pulse gal-

(6) D. C. Grahame, *Chem. Revs.*, **41**, 441 (1947).

(7) H. Matsuda, doctoral dissertation, Faculty of Engineering, Tokyo University, 1961, p. 407.

(8) H. Matsuda, S. Oka, and P. Delahay, *J. Am. Chem. Soc.*, **81**, 5077 (1959).

vanostatic method.^{8,9} The transfer coefficient is essentially the same in both methods, *i.e.*, 0.28 (Table II) *vs.* 0.24. Barring experimental or calculation mistakes, which it is hoped are unlikely, one must account for this discrepancy. It is suggested that the lower value obtained by the galvanostatic method results from the over-all effect of charge transfer and a coupled chemical reaction. The higher value of k_a^0 obtained by faradaic rectification would correspond to conditions in which the influence of the coupled chemical reaction is eliminated or at least minimized. The galvanostatic results were obtained by extrapolation to time $t = 0$ of data for $t \geq 1 \mu\text{sec.}$, whereas extrapolation to $\omega^{-1/2} \rightarrow 0$ of data obtained up to 50 Mc. in faradaic rectification is equivalent to extrapolation to $t = 0$ for $t \geq 2 \times 10^{-8}$ sec. Hence, it is possible that the effect of the coupled chemical reaction is eliminated or greatly minimized in faradaic rectification, but is not in the galvanostatic method. Further, the overvoltage corresponding to the chemical reaction in the galvanostatic method would be constant¹⁰ for sufficiently long times, and consequently no distortion was noted in the extrapolation plot which might have led one to suspect a coupled chemical reaction.

The nature of the chemical reaction could not be ascertained although one reaction can be ruled out as being rate-controlling, namely dissociation of the ion pair HgClO_4^+ in the bulk of the solution. The formation constant for HgClO_4^+ at 25° is approximately¹¹ 0.9, and consequently the species Hg_2^{++} and HgClO_4^+ are present at about the same concentration in 1 M HClO_4 . The discrepancy in the k_a^0 therefore would be much smaller than observed. It is possible that the coupled reaction is $2\text{Hg}^+ = \text{Hg}_2^{++}$ but this is pure speculation as information on Hg^+ in aqueous solution is very meager.¹²

Influence of Double Layer Structure.—The variations of k_a^0 with HClO_4 concentration is interpreted as a double layer effect. No detailed quantitative study was made because it would have required the determination of specifically adsorbed ClO_4^- , but it will be shown that the variations of k_a^0 with HClO_4 concentration are of the order of magnitude one would expect. Both Hg_2^{++} and HgClO_4^+ must be considered¹³ in 1.1 M HClO_4 (see above) whereas Hg_2^{++} is markedly predominant in 0.1 and 0.2 M HClO_4 . We shall assume that k_a^0 must be corrected for variations of the potential ϕ_2 in the outer Helmholtz plane (with respect to the potential ϕ_s in solution) according to the Frumkin theory.¹⁴ This is only a fair approximation but one which is reasonable since Hg(I) is, in all likelihood, not specifically adsorbed. The potential ϕ_2 can be evaluated from the Gouy-Chapman theory, provided one makes allowance for the component of the charge on the electrode corresponding to specific adsorption of ClO_4^- . As a coarse approximation

(9) H. Gerischer and M. Krause, *Z. physik. Chem. (Frankfurt)*, **14**, 184 (1958). One calculates from their data, which were not corrected for mass transfer overvoltage, $k_a^0 = 0.025 \text{ cm. sec.}^{-1}$; also $\alpha = 0.30$.

(10) H. Matsuda, P. Delahay, and M. Kleinerman, *J. Am. Chem. Soc.*, **81**, 6379 (1959).

(11) J. Bjerrum, G. Schwarzenbach, and L. G. Sillén, "Stability Constants. Part II," The Chemical Society, London, 1958, p. 111.

(12) W. C. E. Higginson, *J. Chem. Soc.*, 1438 (1951), reported $(\text{Hg}^+)^2/(\text{Hg}_2^{++}) = 10^{-6}$ to 10^{-8} on the basis of ultraviolet absorption spectra of dilute mercurous perchlorate solutions. However, A. M. Armstrong, J. Halpern, and W. C. E. Higginson, *J. Phys. Chem.*, **60**, 1661 (1956), suggest that Higginson's results could be interpreted on the assumption of the dismutation $\text{Hg}_2^{++} = \text{Hg}^{++} + \text{Hg}$.

(13) The species Hg_2OH^+ can be neglected; *cf.* ref. 11, p. 18.

(14) For a review, *cf.*, *e.g.*, R. Parsons, in ref. 5, pp. 1-64.

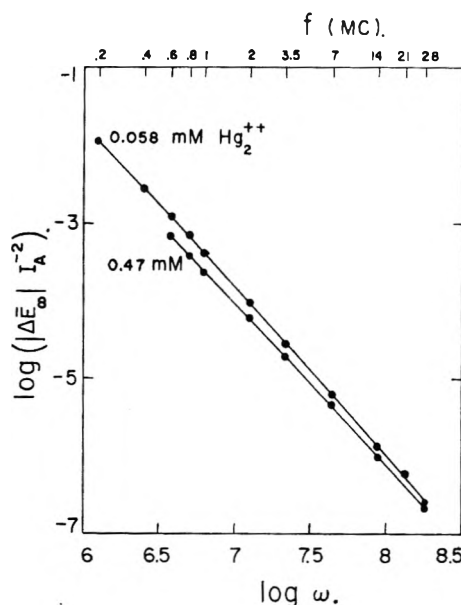


Fig. 3.—Plot of $\log(|\Delta E_\infty|/I_A^2)$ against $\log \omega$ for the discharge of Hg(I) in 0.2 M HClO_4 at $23.5 \pm 0.5^\circ$.

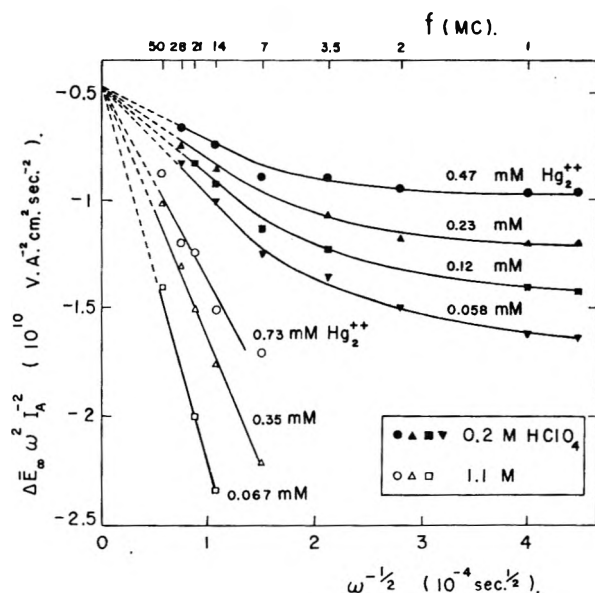


Fig. 4.—Plot of $\Delta E_\infty^2 \omega^2 / I_A^2$ against $\omega^{-1/2}$ for the discharge of Hg(I) in HClO_4 at $24 \pm 2^\circ$.

one has in the present case, *i.e.*, for potentials sufficiently different from the point of zero charge

$$\phi_2 - \phi_s = -\frac{RT}{F} \ln C_{\text{HClO}_4} + \text{constant} \quad (5)$$

Thus, $\phi_2 - \phi_s < 0$, and $\phi_2 - \phi_s$ decreases as C_{HClO_4} increases. Further

$$k_a^0 = k^0 \exp \left[\frac{\alpha n - z}{RT} F (\phi_2 - \phi_s) \right] \quad (6)$$

where k^0 is the standard rate constant; n the number of electrons in the rate-determining step; and z the ionic valence of Hg(I) . There follows from eq. 5 and 6 that k_a^0 should be proportional to $C_{\text{HClO}_4}^{z-\alpha n}$. Hence, k_a^0 should be proportional to $C_{\text{HClO}_4}^{1.44}$ for $z = 2$, $n = 2$, and $\alpha = 0.28$ and to $C_{\text{HClO}_4}^{0.44}$ for $z = 1$ and $n = 2$. The former correction should hold for 0.1 and 0.2 M HClO_4 for which Hg(I) is mostly Hg_2^{++} whereas the correction for 1.1 M HClO_4 is intermediate between $C_{\text{HClO}_4}^{1.44}$ and $C_{\text{HClO}_4}^{0.44}$. The ratio of the k_a^0 's for 1.1 M HClO_4 (Table II) is 4.6 as compared with the predicted ratio of 3.5 for $z = 1$ (using $C_{\text{HClO}_4}^{0.44}$).

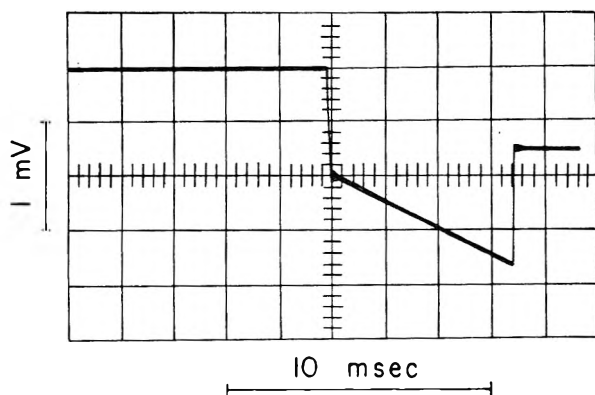


Fig. 5.—Oscillogram tracing showing drift of potential caused by heating of the electrolyte (0.1 M $HClO_4$) at 14 Mc. and $I_A = 31$ amp. $cm.^{-2}$. Rectification for 0.47 mM $Hg(I)$.

This calculation is very crude because eq. 5 is approximate, at any rate, and the approximation is made even poorer because specific adsorption of ClO_4^- was neglected. Further, k^0 is probably different for Hg_2^{++} and $HgClO_4^+$, and the double layer effect is complicated by the dissociation of $HgClO_4^+$ which is coupled with the charge transfer reaction and possibly by any other coupled reaction (see above).

The use of a Frumkin-type correction, even with rigorous calculation of $\phi_2 - \phi_a$, is approximate because of the uncertainty on the proper value of the potential in the double layer to be used and, moreover, the structure of the double layer was not considered in the solution of the boundary value problem in the derivation of the faradaic impedance. This simplification is entirely justified when the diffusion layer thickness ($\delta = [2D/\omega]^{1/2}$) is very large in comparison with the diffuse double layer thickness $1/\kappa$. The Frumkin correction for the double layer structure then can be made *a posteriori*. One has for 50 Mc. and $D \approx 10^{-5}$ $cm.^2$ $sec.^{-1}$, $\delta \approx 2.5 \times 10^{-7}$ $cm.$, whereas $1/\kappa \approx 10^{-7}$ $cm.$ for 0.1 M $HClO_4$ and $1/\kappa \approx 3 \times 10^{-8}$ $cm.$ for 1 M $HClO_4$. The above "non-Frumkin" correction therefore should not be entirely negligible. The quantitative analysis is difficult and equations published thus^{3b} far correspond to conditions which are not fulfilled here. It must be noted, however, that the dependence of I_A^0 on the concentration of $Hg(I)$ is more involved than that given by eq. 4 when the non-Frumkin correction is significant. Since a self-consistent interpretation of data on eq. 4 could be developed, it appears that the non-Frumkin correction is not too large.

Possibility of Frequency Dispersion of the Double Layer.—It was assumed above that the differential capacity of the double layer is frequency independent. This assumption was examined by study of non-faradaic rectification at the d.m.e. in 1.1 M $HClO_4$ up to 7.5 Mc. Higher frequencies could not be used because of instrumentation limitation (see Experimental). A fixed charge (passed in 10 $\mu sec.$) was supplied to the cell to compensate non-faradaic rectification, and the amplitude U of the alternating voltage across the cell was measured when compensation was achieved. Since^{3a,4}

$$\Delta q = \frac{V_A^2}{4} \frac{dc_1}{dE} \quad (7)$$

(V_A amplitude of a.c. signal across the double layer), the quantity U/fZ_c (Z_c impedance of the cell) should be frequency independent in the absence of double layer dispersion. This was the case for $E = -0.70, -0.38,$ and 0.18 v. vs. s.c.e. from 0.25 to 7.5 Mc. (partial data in Table III). This conclusion is in agreement with Barker⁴ who made a similar study for 1 M $HClO_4$ between 0.1 and 1.6 Mc. Frequency dispersion of the double layer—pri-

marily of the Helmholtz double layer since the contribution of the diffuse double layer is quite negligible for 1 M $HClO_4$ —need not be considered in this case up to 7.5 Mc. It was assumed that the same conclusion held up to 50 Mc. though no experimental evidence was available above 7.5 Mc. The interpretation based on this assumption was self-consistent.

TABLE III

NON-FARADAIC RECTIFICATION OF D.M.E. IN 1.1 M $HClO_4$ AT $E = 0.18$ v. vs. s.c.e.^a

q_1 $\mu\mu$ coulombs	f , Mc.	U , volts	U/fZ_c
36.4	0.25	0.54	3.4×10^{-8}
	.5	1.1	3.5
	.75	1.7	3.5
	1	2.2	3.4
	2.5	5.6	3.5
4.54	1	0.81	1.3×10^{-8}
	2	1.5	1.1
	4	3.3	1.2
	6	5.2	1.2
	7.5	7.1	1.3

^a Capillary characteristics: $m = 0.062$ $mg.$ $sec.^{-1}$; a.c. pulse applied at $t = 3.7$ sec.

Heating of the Electrolyte.—Heating of the electrolyte was appreciable at the higher frequencies and the lower concentrations of $HClO_4$. There resulted a shift in the equilibrium potential (Fig. 5) which did not exceed approximately 2 mv. in the most extreme conditions, namely 0.1 M $HClO_4$ and 28 Mc. The temperature coefficient of $Hg_2^{++} + 2e = 2Hg$ is¹⁵ approximately -0.045 mv. degree⁻¹ and consequently the increase in T for Fig. 5 is approximately 18° over 7 msec. Since rectification voltages could be measured within 200–300 $\mu sec.$ after application of the a.c. pulse, the increase in temperature actually affecting the measurement did not exceed 0.5 – 0.8° in this instance and 2° for the most extreme conditions of frequency and electrolyte concentration. The resulting error on the exchange current is rather small.

The measured increase in T has approximately the value one calculates on the assumption of no heat transfer to the electrode and the bulk of the solution. One then has^{2a} at the electrode surface $dT/dt = 0.24(I_A^2/2)(1/\kappa_e \delta_0 C_h)$, κ_e being the specific conductance of the electrolyte, C_h its specific heat, and δ_0 its density. One has approximately for Fig. 5 $\Delta T \approx 3I_A^2 \Delta t$, i.e., $\Delta T \approx 20^\circ$ over 7 msec. as compared to $\Delta T \approx 18^\circ$ from experiment. The experimental ΔT is a little smaller than the calculated ΔT because of heat transfer to the electrode and the bulk of the solution and experimental errors.

Conclusion

It would appear from this work that the kinetics of fast electrode processes can be studied by faradaic

(15) As evaluated from the e.m.f. of an H-cell with the arms at the temperatures T_1 and T_2 . The cell was filled with 1.46 mM Hg_2^{++} in 0.1 M $HClO_4$. The e.m.f. was measured with the Hewlett-Packard DC microvolt-ammeter, Model 425A. Exact interpretation of such a non-isothermal cell is difficult, but the order of magnitude of $\Delta E/\Delta T$ is obtained. The temperature coefficient could not be calculated because ΔS^0 for Hg_2^{++} could not be found in the literature.

rectification up to 50 Mc. (and possibly at higher frequencies with electrolytes of high conductivity). Apparent exchange current densities up to 10 amp. cm.⁻² were measured which correspond to an apparent standard rate constant of approximately 100 cm. sec.⁻¹ for an electrode process involving both soluble oxidant and reductant at equal concentrations of $5 \times 10^{-4} M$ ($n = 2$, $D_o = D_R = 10^{-5}$ cm. sec.⁻¹). Somewhat faster processes could even be studied with more dilute solutions. The

method should prove most useful in the study of a number of processes which are too rapid for other methods presently available. Moreover, the investigation of relatively slow electrode processes at high frequency may allow the detection and the study of coupled chemical reactions which are too rapid to be detected by other methods.

Acknowledgment.—The support of this work by the National Science Foundation is gladly acknowledged.

THE PHOTOCHEMICAL DECOMPOSITION OF BARIUM AZIDE

BY P. W. M. JACOBS, F. C. TOMPKINS, AND V. R. PAI VEFNEKER

Department of Chemistry, Imperial College, London, S.W. 7

Received December 21, 1961

The kinetics of nitrogen evolution from barium azide irradiated with ultraviolet light from low and high pressure mercury arcs has been investigated as a function of intensity, temperature, and time of irradiation. These results emphasize the important role played in the reaction by the barium product formed as a result of photolysis. Two mechanisms of the photo-decomposition which are consistent with these detailed kinetic results are proposed and discussed in the light of our present knowledge of the physical properties of azide crystals. The first of these, which occurs chiefly in fresh salt, is the formation of barium atoms (pre-nuclei); the second is the thermal production of positive holes by the transfer of electrons to barium pre-nuclei which have become ionized by photoemission of an electron into the conduction band. The significance of a purely thermal contribution to the photolytic rate also is assessed.

There have been several previous investigations of the effects of radiation on barium azide. Irradiation with soft X-rays¹ produces barium nitride and nitrogen. Pre-irradiation of barium azide with α -particles² or ultraviolet light³ accelerates the rate of subsequent thermal decomposition. Irradiation with ultraviolet light⁴ causes the evolution of nitrogen at a rate proportional to the square of the intensity and with a temperature-dependence corresponding to an energy of activation of 5 kcal./mole. Failure to detect photoconductivity⁵ was held to imply that the primary process was the formation of excitons⁴ rather than of free electrons and positive holes.⁶

Recent investigations,⁷ however, have shown that the mechanism of photolysis must be more complicated than the bimolecular decomposition of excitons at traps.⁴ In particular, the rate of photolysis under irradiation with a high pressure lamp at first decreased and then increased again, finally attaining a constant value. The intensity-dependence appeared to be complicated, the exponent n in the equation $R = CI^n$ varying from 0.5 to 2. This work, though valuable in pointing to the role of the metallic product in photochemical as well as thermal decomposition, was unsatisfactory in that the temperature dependence was not examined and also because insufficient account was taken of the effects of the "dark rate" in determining the value of n .

Consequently, the kinetics of nitrogen evolution under ultraviolet irradiation has been re-examined in some detail and the results of this investigation are recorded below.

Experimental

Barium azide was prepared by neutralization of an approximately 5% solution of hydrazoic acid with barium hydroxide of A.R. quality. The solution was maintained neutral to phenolphthalein during evaporation on a water bath to incipient crystallization and the azide then was precipitated by addition of absolute alcohol. The fine white precipitate was filtered, redissolved in the minimum amount of distilled water made slightly acidic with hydrazoic acid, and the barium azide obtained either by addition of absolute alcohol or by slow evaporation of the acidic solution. The former method yields a white amorphous powder, the latter a mass of tiny crystals. The azide was dehydrated over phosphorus pentoxide in a desiccator. The hydrazoic acid was obtained by two methods: (i) by dropping sulfuric acid onto a solution of sodium azide and sodium hydroxide and distilling off the hydrazoic acid into water and (ii) by passing a 10% solution of sodium azide through a cation exchanger in the hydrogen form. No differences were observed in the behavior of products obtained by these slight variations in technique.

The azide was contained in a transparent silica cell with a flat window, connected *via* a B.14 standard joint to the vacuum line. This consisted, in sequence, of a trap immersed in liquid nitrogen, a standard volume, a pirani gage (P_1), a cut off (C_1), a diffusion pump (D), a second trap, a second pirani gage (P_2), a McLeod gage, and a second cut off (C_2) which separated the line from the second diffusion pump (D_2) and the backing pump. This enabled the rate of nitrogen evolution to be measured either on P_1 with C_1 raised (the accumulatory method) or on P_2 with C_1 lowered and C_2 raised. In the accumulatory method the azide is in continual contact with the nitrogens evolved, which may reach a pressure of several microns. In the second method (referred to as "pumping") the diffusion pump D_1 maintains a pressure of $<10^{-5}$ mm. over the salt during photolysis. The volumes of the two measuring systems were determined by calibration with nitrogen and it also was confirmed that the effective volume of the second system was independent of the pressure in it (which of course backs the first diffusion pump D_1) up to the limit tested (20μ).

The temperature of the salt was measured with a cali-

(1) P. Gunther, L. Lepin, and K. Andreew, *Z. Elektrochem.*, **36**, 218 (1930).

(2) W. E. Garner and C. H. Moon, *Nature*, **131**, 513 (1933).

(3) W. E. Garner and J. Maggs, *Proc. Roy. Soc. (London)*, **A172**, 299 (1939).

(4) J. G. N. Thomas and F. C. Tompkins, *ibid.*, **A209**, 550 (1951); **A210**, 111 (1951).

(5) P. W. M. Jacobs and F. C. Tompkins, *ibid.*, **A215**, 254 (1952); **215**, 265 (1952).

(6) N. F. Mott, *ibid.*, **A172**, 325 (1933).

(7) P. W. M. Jacobs, F. C. Tompkins, and D. A. Young, *Discussions Faraday Soc.*, **28**, 234 (1959).

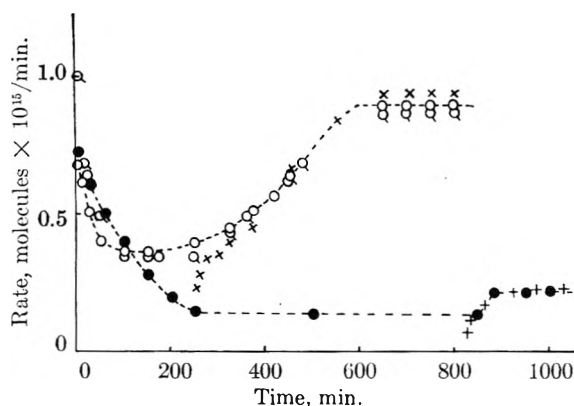


Fig. 1.—Rate of photolysis of barium azide, expressed in molecules $\times 10^{15}/\text{min.}$, as a function of time: (a) \circ , fresh salt, pumped; (b) \circ , fresh salt, accumulatory; (c) \bullet , fresh salt, pumped, at half the intensity used for (a); (d) \times , annealed azide, pumped, at same intensity as (a); (e) $+$, annealed azide, pumped, at same intensity as (c). Time scales for (d) and (e) have been adjusted to match the acceleratory periods of (a) and (c), respectively.

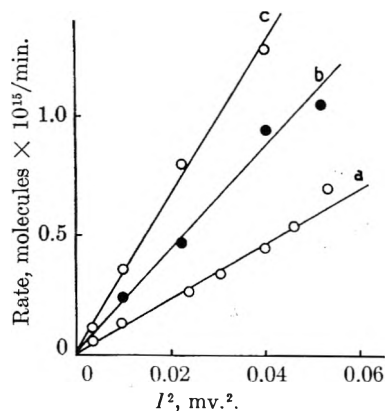


Fig. 2.—Dependence of the rate of photolysis on intensity of the low pressure arc (given in terms of the thermopile e.m.f.): (a) during the acceleratory period, after 60 min. irradiation; (b) in constant rate period, pumping; (c) in constant rate period, accumulatory.

brated copper-constantan thermocouple. The intensity of the irradiation from the low pressure arc was varied by controlling the voltage to the primary of the lamp transformer; because the intensity distribution of the high pressure arc varies with temperature, its intensity was varied by varying the distance of the lamp from the photolysis cell. Both lamps were calibrated by replacing the cell by a Kipp thermopile; intensities are recorded in terms of the e.m.f. registered by the thermopile as the intensity distribution for the high pressure arc is not accurately known and the number of quanta received by the azide therefore cannot be calculated. The emission spectra of the two arcs have been reproduced in another paper.⁷ A water filter always was used in conjunction with the high pressure arc to remove infrared components.

Results

The rate of nitrogen evolution from barium azide irradiated with the low pressure arc is shown in Fig. 1 as a function of time. For fresh salt (a,b,c) the rate at first decreases with time (for about 100 min. at the higher intensity) then remains more or less constant, then increases again and finally, after about 5 hr., attains a constant rate which is maintained over very long irradiations. If the shutter between the lamp and cell is replaced, the rate of evolution of gas decreases steadily until it becomes equal to the original outgassing rate of the system.

The rate of gas evolution after the shutter is replaced we term the "dark rate."

It is apparent from Fig. 1 that there is no difference in the behavior of the salt whether the accumulatory technique is used or whether it is pumped during irradiation (*cf.* a and b). The somewhat higher initial rate for b probably is not significant, for it could be due to other causes such as a difference in particle size or the distribution of material in the cell. When salt which has been irradiated for at least 5 hr. is left overnight connected to the pumps and then re-irradiated, the rate is at first slightly lower than the minimum found for that intensity using fresh salt (curve d) but it rapidly increases until it coincides with the value at the beginning of the acceleratory region, after which it follows precisely the behavior of the fresh salt. The changes which take place during the intervals between successive irradiations we refer to as "annealing." The same type of behavior is observed when irradiation of lower intensity (curves d, e) is used, the initial fall in rate to the minimum taking longer, the minimum being much flatter, and the acceleration to a final constant rate being longer delayed and smaller in magnitude. The previous experimental results⁴ with low pressure arcs were obtained using short irradiation times over which the variations found here during much longer irradiations would not normally be observed, although Thomas and Tompkins⁴ did note a decreasing rate on a long irradiation of fresh salt.

Salt irradiated with the high pressure arc behaves in precisely the same way as depicted in Fig. 1 and again there is no dependence on the pressure of nitrogen in the reaction vessel. The dependence of the final constant rate on intensity is shown by the data plotted in Fig. 2 to be $R \propto I^2$, a result that is independent of whether the reaction cell is pumped during photolysis or whether the accumulatory method is used. The dark rate is practically zero for fresh salt and increases steadily with the amount of decomposition, reaching a maximum in the constant rate period. The dark rate also depends on the intensity during irradiation, the relationship being $R_d \propto I^2$. This dependence of both the light and dark rates on the square of the intensity holds not only during the final constant rate period but also during the acceleratory period.

The temperature coefficient of the photolytic reaction was measured at various stages of the reaction and the corresponding activation energies calculated. These results are shown in Table I.

TABLE I

ACTIVATION ENERGY (IN KCAL./MOLE) FOR THE PHOTOCHEMICAL DECOMPOSITION OF BARIUM AZIDE AT VARIOUS STAGES OF THE REACTION, MEASURED IN THE RANGE FROM -25 TO $+25^\circ$

Source	Initial process	At the minimum	Constant rate period	"Dark" reaction
Low pressure arc	4.4	9.3	20.1	19.8
High pressure arc	4.7	11.5	19.4	20.2
High pressure arc + OX7 filter	19.3	..
High pressure arc + OY10 filter	5.1	19.7	37.4	..

The radiation from the low pressure arc is predominantly the 2537 Å. resonance line. That from the high pressure arc is more or less continuous, with the principal mercury lines superimposed. On interposing a Chance OY10 filter, radiation shorter than wave length of 3500 Å. is totally excluded (50% transmission at 3690 Å.). If a Chance OX7 filter is used, radiation between 2400 and 4200 Å. is passed, with >50% transmission between 2550 and 3890 Å. For brevity, we shall refer to the two wave length regions as "short" and "long."

There are three main differences in the photolytic behavior of short and long wave lengths. The high pressure lamp filtered by OX7 behaves like the low pressure lamp: the rate of photolysis goes through the same variations with time, it varies with the second power of the intensity of the radiation (Fig. 3) and the activation energy (Table I) shows the same variations. In contrast, with long wave lengths, the rate of photolysis of salt (pre-irradiated with the full arc into the constant rate period) varies as the first power of I (Fig. 3) and the activation energy is 37 kcal./mole. The dependence of photolysis rate on time for fresh salt is also quite different. Surprisingly, fresh salt does photolyze at a reasonable rate (2×10^{14} molecules/min.) but the rate decreases steadily to 1/5 of the initial value over a period of about 13 hr., after which it remains constant (Fig. 4) at a rate equal to about 1/20 of the constant rate obtained with the unfiltered arc.

It seems clear that the acceleratory period is due to the presence of barium formed during the photolysis. This was confirmed by two experiments. First irradiated salt was exposed to the atmosphere for several days. The brown salt gradually went white with this treatment and, on subsequent irradiation, showed the deceleratory period associated with fresh salt (Fig. 5). The initial rate was lower than for fresh salt and the minimum rate more rapidly attained as though the barium had been partly but not completely oxidized by this treatment. The effect of intensity on the rate *vs.* time curve again is clearly shown in Fig. 5.

In the second experiment fresh salt was decomposed *thermally* to various stages and the photolytic rate determined at each stage. The fractional decomposition α could be calculated from the amount of gas evolved and in Fig. 6, the photolytic rate is plotted against α . Also shown is the photolytic rate *vs.* α for a run in which the salt was decomposed entirely photochemically.

Figure 7 shows the rate-time curves for barium azide which has been irradiated until the constant rate is reached and then annealed. Curve 1 shows the normal behavior on irradiation after a 12 hr. anneal. The constant rate is attained after 4 hr. Curve 2 shows the photolytic rate after thermal decomposition (to the extent required to give the same constant rate) followed by a 5 min. anneal. Curve 3 shows the behavior in a similar experiment but after a 12 hr. anneal while for curve 4 (identical with 1) the annealing time was 24 hr. Thus, again, in the acceleratory period, the photolytic rate depends only on the extent of the previous decomposition and not on whether it is performed

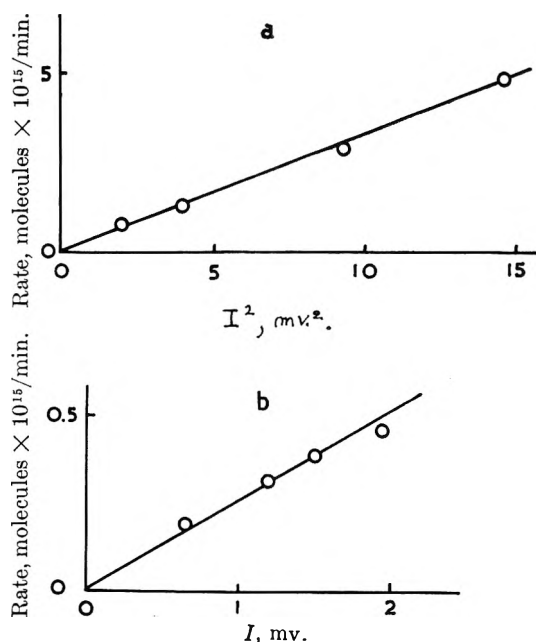


Fig. 3.—Dependence of the rate of photolysis on intensity of the high pressure arc: (a) filtered through OX7; (b) filtered through OY10.

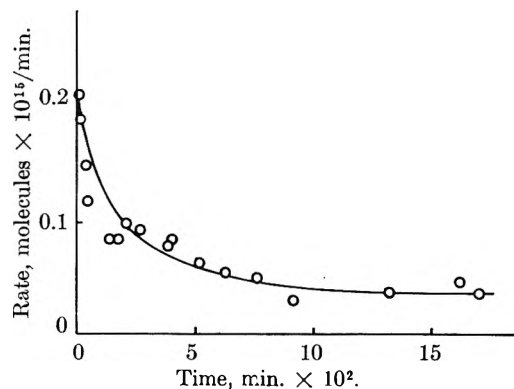


Fig. 4.—Dependence of the rate of photolysis of fresh barium azide on time when irradiated with the high pressure arc filtered through OY10.

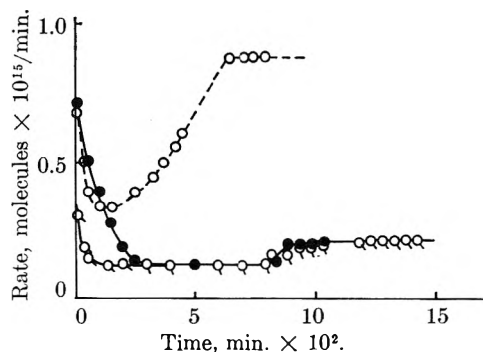


Fig. 5.—Effect of exposing annealed salt to the atmosphere: (a) \circ , fresh salt; (b) \bullet , fresh salt, at half the intensity used for (a); (c) \circ , salt used for (a) after exposure to the atmosphere, same intensity as (b) (compare Fig. 1).

thermally or photochemically, except that the annealing process is somewhat slower after thermal decomposition than after photochemical decomposition (*cf.* curves 3 and 1).

In an attempt to decide whether or not more than one mechanism for the production of nitrogen

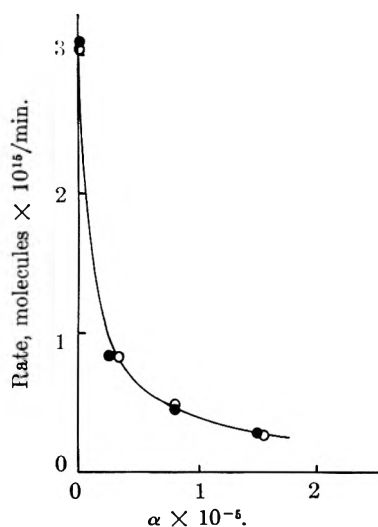


Fig. 6.—Rate of decomposition of fresh salt as a function of the fractional decomposition α : O, photolytic rate, after thermal decomposition; ●, photolytic rate after photochemical decomposition.

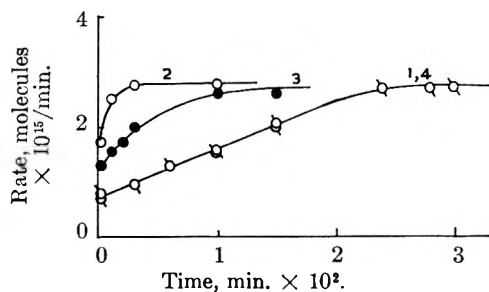


Fig. 7.—Rate of photochemical decomposition of barium azide after thermal decomposition and annealing. For details, see text.

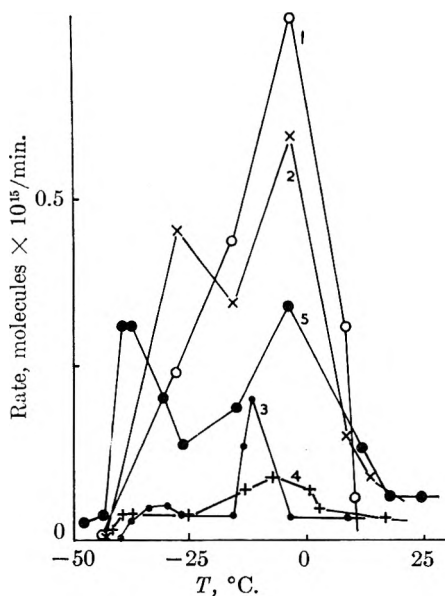


Fig. 8.—Rate of gas evolution as a function of temperature from barium azide irradiated at -70° : 1, 2, 3, 4 indicate successive irradiations of 0.5 hr. each. The time of irradiation for curve 5 was 3 hr.

exists, a fresh sample of BaN_6 was irradiated for 0.5 hr. at -70° , at which temperature the rate of nitrogen evolution is zero. The dewar then was lowered and the salt allowed to warm without

further irradiation and the temperature of the salt and gas pressure noted at suitable time intervals. The rate of gas evolution is plotted in Fig. 8 as a function of salt temperature. This experiment must be regarded as only a qualitative one, but in spite of this, certain conclusions can be drawn. Two peaks, centered at about -35 and -5° , are observed. (In the first run, the heating was carried out too rapidly so that the first peak is merged with the second one.) The peak heights decrease in successive runs, in agreement with the usual behavior in photolysis at higher temperatures, but possible variations in the rates of the peak heights could not be established.

Significant color changes were noticed during these experiments. When fresh salt is irradiated at -70° there is no color change but on warming to -35° the salt shows a violet coloration, which disappears at -5° , when the salt turns white again. This cycle of changes was repeated with the second irradiation, but on the third cycle, the salt appeared greenish after warming to -5° and thereafter turned gradually brown, the usual color observed on prolonged photolysis. Nevertheless the appearance of a violet color at -35° when the first gas evolution takes place was still observable. These observations imply the formation of some unstable intermediate (with the evolution of N_2) from the primary result of the irradiation, at -35° , and the decomposition of this intermediate at -5° with further nitrogen evolution.

Discussion

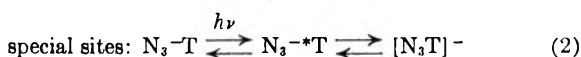
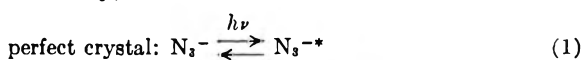
The experimental results reported in this paper indicate that there must be at least two photolytic mechanisms for the production of nitrogen when barium azide is irradiated with ultraviolet light. By considering the results for the dependence of the rate of photolysis on time (Fig. 1), temperature (Table I), and source (Fig. 4 and Table I) we may conclude that fresh salt is decomposed by ultraviolet light of wave length in the region of 2537 Å. at a rate which (i) decreases steadily with increasing amount of decomposition, (ii) varies as the square of the intensity of the radiation, and (iii) is associated with an activation energy of about 5 kcal./mole. These results, while more detailed, are in substantial agreement with the earlier investigation by Thomas and Tompkins.⁴ In contrast the rate of photolysis of fresh salt with light of long wave length (>3500 Å.) is about 1/5 as large, and an acceleratory period was not observed. We are, however, not inclined to regard this result as indicating a new mode of photolysis but believe rather that it simply reflects the reduced absorption coefficient for light of long wave length as compared with ultraviolet light. The whole scale of events therefore is altered (*cf.* the effect of intensity shown in Fig. 1).

When irradiation of fresh salt with the low or high pressure arc, or with the latter using an OX7 filter, is prolonged beyond about 300 min., an increase in the rate of photolysis is observed. This definitely indicates the onset of a new mechanism, for although the rates are throughout proportional to I^2 , the activation energy increases from 9–10 at the minimum to 20 kcal./mole during the constant rate

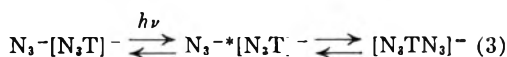
period. We interpret these results as indicating that the second mechanism, characterized by a thermal activation energy of around 20 kcal./mole, can only set in once substantial photolysis has occurred and that the apparent activation energy of 9–10 kcal. is due to both processes occurring concurrently.

We accordingly propose the following model for the decomposition of barium azide. Light of short wave length, *i.e.*, around 2537 Å., is absorbed within the tail of the first absorption band. Previously,⁷ this had been tentatively identified with an exciton transition: however, the remarkable constancy of the position of this band in sodium, potassium, rubidium, and cesium azides^{8–10} and the recent identification of exciton bands at much shorter wave lengths¹¹ makes it likely that the band in the 2400–2600 Å. region of the alkali azides corresponds to an internal transition¹¹ on the azide ion. This excitation then will be the primary photochemical process on irradiation and it seems reasonable to presume that this statement also is true of barium azide, the absorption edge of which has been placed by reflectance measurements⁶ at around 2600 Å.

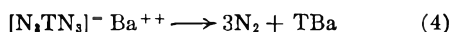
The decreasing rate of photolysis of fresh salt with time (Fig. 1) indicates that the reaction proceeds at centers which are gradually consumed. These centers seem likely to be either impurity ions or crystal imperfections, namely anion vacancies or jogs in dislocations. Each of these three species possesses the necessary property of being able to function as an electron acceptor. In perfect, pure crystal, the excited azide ion N_3^{-*} has no option but to decay to the normal ground state, N_3^- , after the appropriate lifetime, but adjacent to an electron acceptor, partial or total charge transfer of the excited electron to the "trap" T may occur. Formally, then



Repetition of 2 within the (relatively long) lifetime of $[N_3T]^-$ gives two adjacent excited azide ions



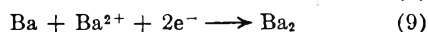
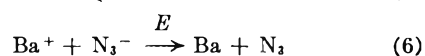
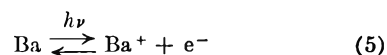
which can either revert to the ground state with the emission of phonons or undergo chemical decomposition



The latter process involves the transfer of the two excited electrons to an adjacent Ba^{++} ion and the evolution of nitrogen. As the reaction proceeds, the crystal clearly assumes different properties in the locality of T, and the rate of reaction thus decreases due to the falling number of sites which can function as traps. The possibility that T is an anion vacancy ought not to be excluded because the production of

anion vacancies by (4) would not regenerate the trap, since it would leave an aggregate of three vacancies in place of the original single one. It is noteworthy that the final steady rate of this process is not zero (*cf.* the low intensity runs in Fig. 1 and 5); possibly more than one type of trap is involved. Since the reaction involves two activated species, the rate will depend on the second power of the intensity, as observed. The low activation energy of 5 kcal. is associated with (4) since neither (2) nor (3) should require thermal energy. The much lower rates observed with long wave lengths are due to the very low absorption coefficient and consequently low rate of excitation of the internal transition.

In a previous paper,⁷ various mechanisms consistent with the experimental facts, as they then were known, were proposed. The above mechanism is essentially mechanism Ia of reference 7, except that a decrease in the number of traps with time is now proposed, since it is no longer necessary to invoke an obscuring effect by the product on the surface of the crystal. It also may be noted that a slight change in notation, from N_3Te^* to $[N_3T]^-$, has been adopted. The result of this first reaction is the production of barium atoms at kink sites or other special positions in the lattice. Since the first ionization potential of barium is 5 e.v. and the electron affinity of the crystal probably around 3 e.v. (see Fig. 9 later) these atoms can, under irradiation, emit electrons into the conduction band of the crystal. This does not give a normal lattice barium ion but a Ba^+ ion which is not part of the lattice, since two adjacent anions already have been lost and the Ba atom occupies essentially a trivacancy. An electron then is transferred thermally from an adjacent azide ion giving a positive hole. Simultaneously irradiation is producing excited azide ions and these react with each other (as in the first process) and with the positive holes. There also will be some bimolecular decomposition of holes but this is likely to be less probable than the reaction of holes and excited ions. The second process is then



with $R_7 > R_8$. This mechanism explains the increasing rate, since sites are produced by the first process and regenerated by the second one (eq. 9). The activation energy for (6) should be about 1 e.v., since this is the dominant thermal process of the above sequence of reactions. The apparent activation energies of 0.45 at the minimum and 0.9 e.v. in the constant rate period are "averages" of the two simultaneous photochemical processes, the second one becoming more important over the acceleratory period. This second process will continue in a self-propagatory manner as long as the barium produced can be regarded as "atomic," *i.e.*, single atoms or small groups of atoms. At some state which we

(8) J. Cunningham and F. C. Tompkins, *Proc. Roy. Soc. (London)*, **A251**, 27 (1959).

(9) H. G. Heal and J. P. S. Pringle, *J. Phys. Chem. Solids*, **15**, 261 (1960).

(10) H. A. Papazian, *ibid.*, **21**, 81 (1961).

(11) S. K. Deb, *J. Chem. Phys.*, in press.

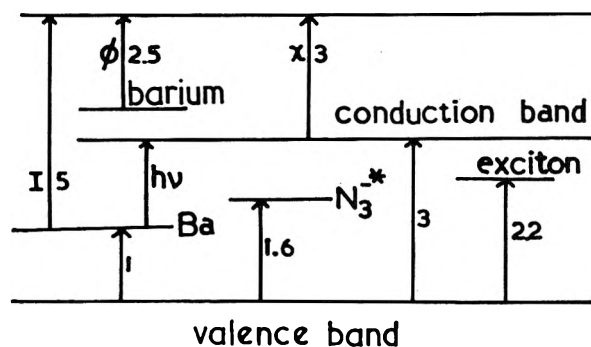
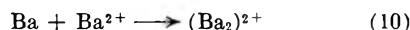


Fig. 9.—Approximate energy level diagram for barium azide. All energy values are thermal values, expressed in e.v. With the exception of I and ϕ these have been roughly estimated by analogy with other azides.

are not in a position to specify precisely, these pre-nuclei will become large enough to recrystallize and form metal specks. When they do so, their energy levels become those characteristic of bulk metal and can no longer participate in this reaction. An approximate energy level diagram is given in Fig. 9. This mechanism supersedes mechanism III of reference 7¹² in that atomic barium is now seen to be the most likely active catalyst (see Fig. 9 and following discussion of the dark rate).

On closer inspection, it appears that the second process, summarized in eq. 5-9, can proceed by a purely thermal mechanism. A barium atom traps an adjacent barium ion¹³



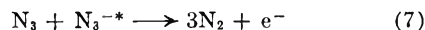
Electrons then are transferred from azide ions to the positively charged barium and the positive holes react together. This cycle of events can continue until the pre-nuclei all grow into large specks of barium. This mechanism is consistent with the known facts about the dark rate. With fresh salt the dark rate is zero, but it steadily increases up to a maximum in the constant rate period. The pre-nuclei are destroyed by this reaction so consequently the initial photo-rate is low (below the minimum) on recommencing irradiation. The anneal-

(12) A. Bardins, *Discussions Faraday Soc.*, **28**, 248 (1959).

(13) J. W. Mitchell, *Rept. Progr. Phys.*, **20**, 433 (1957).

ing process is thus the growth of barium atoms and pre-nuclei into metal specks by *thermal* decomposition of the azide.

With light of long wave length ($>3500 \text{ \AA}$.) the first process (bimolecular decomposition of excited azide ions) occurs but with low efficiency. Once some decomposition has occurred, *i.e.*, on the flat region of Fig. 4, the activation energy is 20 kcal./mole because the second process

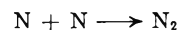
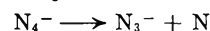


is dominant. However, if the salt is first decomposed into the constant rate period, so that more barium prenuclei are available, then positive holes are produced at a faster rate than excited ions because the photoionization of Ba is more efficient than excitation of the internal transition, with light of long wave length. The rate of supply of N_3^{*-} then becomes the limiting factor and the activation energy becomes that for the thermal value of this excitation. This can be estimated as roughly the optical value divided by the dielectric constant ratio (we take a value 3 for this ratio, in view of the known dielectric constants of other azides¹⁴), *i.e.*, 4.8/3 or 1.6 e.v. This is in accord with the experimental value. Moreover, the rate depends on the first power of the intensity, as it should since only the concentration of holes is proportional to the intensity.

Finally, the results of the "warm-up" experiments shown in Fig. 8 allow us to be a little more specific about the nitrogen evolution reaction. This apparently goes in two steps: a possible sequence is



at -35° , followed by



at -5° , since the species N_4^- has been identified in irradiated KN_3 by electron spin resonance.¹⁵

Acknowledgment.—We are indebted to the Corps of Engineers, U. S. Army, for financial support under contract DA-44-009 ENG. 4187.

(14) B. L. Evans, A. D. Yoffe, and P. Gray, *Chem. Rev.*, **59**, 515 (1959).

(15) A. J. Shuskus, C. G. Young, O. R. Gilliam, and P. W. Levy, *J. Chem. Phys.*, **33**, 622 (1960).

RADIATION CHEMISTRY OF OCTAMETHYLCYCLOTETRASILOXANE

BY CLARENCE J. WOLF* AND A. C. STEWART†

Parma Research Laboratory, Union Carbide Corporation, Parma 30, Ohio

Received December 22, 1961

The effects of dose, dose rate, temperature, and scavengers (iodine and oxygen) on the γ -ray induced gas and polymer formation from octamethylcyclotetrasiloxane were investigated. In the absence of scavengers, the hydrogen, methane, and ethane yields are 0.89, 2.08, and 0.29 molecules per 100 e.v., respectively. The hydrogen and ethane yields are independent of the scavenger concentration (between 2 and 11×10^{-3} molar) and of the dose: their yields are 0.57 and 0.29 molecule per 100 e.v., respectively. The methane yield is quite sensitive to both iodine concentration and dose. Two specific types of higher molecular weight products were found—cyclic dimers and linear polydimethylsiloxanes. The former are produced by a temperature independent process, while the latter are formed with an apparent activation energy of 7 kcal./mole.

Introduction

The radiolysis of silicones has received considerable attention in the last few years.¹⁻¹³ Monomers,^{4,5,9,10} polymeric fluids,^{1,2,7,11,12} rubbers, and elastomers have been investigated. Warrick,³ Kantor,⁴ and Lawton, *et al.*,⁵ have studied the radiation chemistry of cyclic dimethylsiloxanes. The cyclic trimer, hexamethylcyclotrisiloxane, undergoes rapid polymerization upon irradiation as a solid (m.p. 64°) but polymerizes slowly when irradiated as a liquid.⁵ The cyclic tetramer, octamethylcyclotetrasiloxane, does not exhibit this phase effect.⁴ Kantor found that the principal products of radiolysis of octamethylcyclotetrasiloxane were dimers, but we have found both dimeric products and linear polymers which result from siloxane bond rearrangement.

Dimethyl silicone oils cross-link when irradiated with high-energy radiation and yield hydrogen, methane, and ethane. The methane yield from most of the silicones studied^{1,4,7-9} is about twice the hydrogen yield. Radiolysis of dimethylsilicones produces ethane in lower yields than hydrogen or methane, but the ratio of ethane to total gas produced changes for the different silicones and is higher for radiolysis of polymeric fluids.

Experimental

Octamethylcyclotetrasiloxane (hereafter referred to as the octamethyl tetramer) was purified by distillation in an efficient column, then dried over calcium hydride prior to a

second fractional distillation at 175–176°. High temperature gas chromatography showed that the resulting material contained less than one part per ten thousand cyclic trimer or pentamer silicone impurity.

Solutions were degassed on the vacuum line by repeating a cycle of freezing, pumping, and thawing at least eight times; they then were condensed into glass ampoules at liquid nitrogen temperature. A single series for which reproducible results could be obtained consisted of ten or twenty ampoules filled simultaneously but irradiated for different time intervals.

Samples were irradiated in either an 1800 curie or 3500 curie cobalt-60 γ -ray source. The dose at a given irradiation position was determined by means of the Fricke dosimeter and all doses were corrected for the decay of the source and for the difference between the electron density of the sample and that of the dosimeter. The G (molecules changed per 100 e.v. energy absorbed) for the conversion of ferrous to ferric ions was taken to be 15.6.¹⁴ Gaseous products of irradiation were removed from the irradiated sample by means of a Toepler pump, passed through a -78° trap, measured, and then analyzed in a gas chromatograph. Argon carrier gas and a column of Linde 13X Molecular Sieve were used for the hydrogen and methane analysis, and, on a separate portion, helium carrier gas and a silica gel column heated to 100° were used for the ethane determinations. Polymer was that material which remained after all of the volatile materials had been removed at room temperature by vacuum techniques. In several instances the polymer was analyzed in a high temperature chromatograph. A silicone column and a helium sweep were used. Although we did not quantitatively assay the residue we were able to obtain information about the approximate amount of low molecular weight material in the polymer.

Baker's Reagent Grade iodine was sublimed once before using; its concentration was determined spectrophotometrically (extinction coefficient 0.922 at 515 $m\mu$). Hydrogen iodide, produced by irradiation of an iodine octamethyl tetramer solution, also was determined by means of the spectrophotometer. Hydrogen iodide and iodine were removed from the irradiated solutions by extracting three times with a total of 25 ml. of 0.001 M H_2SO_4 (the acid suppresses hydrolysis of iodine) and iodine was removed from the aqueous phase by extracting three times with a total of 25 ml. of cyclohexane before iodide analysis. The iodide concentration was determined from its absorption at 226 $m\mu$ (ϵ 13,200). This technique does not distinguish between HI and $\equiv Si-I$ but other spectroscopic evidence suggests that the iodide ion probably results from HI.

Results

The yield (G -value) for gas production from a number of irradiated samples was about 3.3 molecules per 100 e.v. Molecular weight distributions were not determined on the residues but the total number of monomer units incorporated into polymer is known. We shall be reporting the G -value for monomer converted to polymer. The polymer yield within a series (10 to 20 samples prepared simultaneously) was reproducible. However, yields varied between series although all samples were prepared utilizing the same degassed

(* Research Division, McDonnell Aircraft Corporation, St. Louis, Missouri. (†) Presently associated with Union Carbide Consumer Products Company, Division of Union Carbide Corporation, Parma 30, Ohio.

(1) W. Barnes, H. W. Dewhurst, R. W. Kilb, and L. E. St. Pierre, *J. Polymer Sci.*, **36**, 535 (1959).

(2) L. E. St. Pierre, H. A. Dewhurst, and A. M. Bueche, *ibid.*, **36**, 105 (1959).

(3) E. L. Warrick, *Ind. Eng. Chem.*, **47**, 2388 (1955).

(4) (a) S. W. Kantor, Abstracts, 130th National Meeting of the American Chemical Society, Atlantic City, N. J., September, 1956, p. 55-O; (b) U. S. Patent 2,766,220.

(5) E. J. Lawton, W. T. Grubb, and J. S. Balwit, *J. Polymer Sci.*, **19**, 455 (1956); W. Burlant and C. Taylor, *ibid.*, **41**, 547 (1959).

(6) A. Charlesby, W. H. T. Davison, and D. G. Lloyd, *J. Phys. Chem.*, **63**, 970 (1959).

(7) A. Charlesby, *Proc. Roy. Soc. (London)*, **A230**, 120 (1955).

(8) E. L. Warrick, J. F. Zack, and G. Knoll, Abstracts, 135th National Meeting of the American Chemical Society, Boston, April, 1959, p. 12-L.

(9) H. A. Dewhurst and L. E. St. Pierre, *J. Phys. Chem.*, **64**, 1063 (1960).

(10) H. A. Dewhurst and L. E. St. Pierre, *ibid.*, **64**, 1060 (1960).

(11) A. A. Miller, *J. Am. Chem. Soc.*, **82**, 3519 (1960).

(12) A. A. Miller, *ibid.*, **83**, 31 (1961).

(13) V. H. Dibeler, F. L. Mohler, and R. M. Reese, *J. Chem. Phys.*, **21**, 180 (1953).

(14) C. J. Hoehandel and J. A. Ghormley, *ibid.*, **21**, 880 (1953).

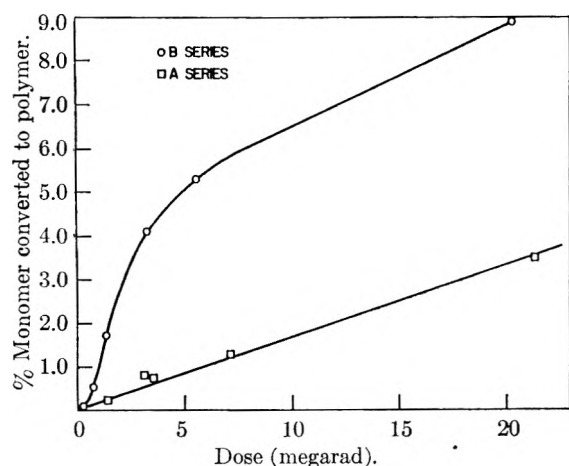


Fig. 1.—Polymer production from octamethylcyclotetra-siloxane as a function of dose.

octamethyl tetramer solutions and essentially similar procedures.

In order to check for air contamination while loading the vessels, an ion gage was connected to the filling system by a stopcock and liquid nitrogen trap. We were unable to observe any non-condensable vapors at pressures greater than 10^{-4} mm. during the filling operation.

For two typical series, the conversion of monomer to polymer as a function of dose is shown in Fig. 1. Chromatographic analysis of the residue from the A series (lower curve) indicated that it was primarily composed of siloxane dimers (cyclic octamethyl tetramer units bonded by a methylene, ethylene, or silicon-silicon bridge). These dimers were produced by a process independent of dose and dose rate (two dose rates were used: 2.05 and 0.095 megarad/hr.). A G -value of 5.5 molecules of monomer converted to dimer per 100 e.v. is calculated from the slope of this line. Chromatographic analysis of the residue from series B (upper curve) indicated that only part of the polymer was siloxane dimer. The majority of the residue was linear polydimethylsiloxanes (identified by infrared analysis). The linear portion of this curve yields a G of 5.9 molecules of monomer converted to polymer per 100 e.v. Radiation delivered at a different intensity alters the shape of the polymer converted *vs.* dose curve. At the lower intensity (0.095 megarad/hr.) the curve has a greater initial slope but reaches the linear region after a slightly smaller dose.

It should be pointed out that the exact difference between the A and B type series is not known. Ten vessels were filled simultaneously with degassed tetramer from a storage reservoir—this constitutes one series; then ten more vessels were filled in an identical manner from the same degassed solution—this constitutes the second series. *A priori* we did not know if a given series would be type A or B. However, if one sample from a given series was type A, the remainder of the samples were of the same type. Similarly, if one sample was of the B type, the remaining nine samples were type B.

The production of hydrogen, methane, and ethane from irradiated octamethyl tetramer is inde-

pendent of dose for doses up to at least 30 megarad. The G -values determined from the slopes of the yield *vs.* dose curve are 0.89, 2.08, and 0.29 molecules per 100 e.v. for hydrogen, methane, and ethane, respectively. The hydrogen, methane, and ethane distribution is given in Table I. Warrick's³ data for an irradiation dose of 52.5 megarads (equivalent to 48.8 megarads) on the octamethyl tetramer is included for comparison.

TABLE I
GAS YIELDS FROM IRRADIATED OCTAMETHYLCYCLOTETRA-SILOXANE

Dose	Warrick 48.8 Mrads % total gas	This work 20.5 Mrads	
		G	% total gas
H ₂	34.05	0.89	27.3
CH ₄	60.4	2.08	63.8
C ₂ H ₆	4.6	0.29	8.9

The gas yields are not dependent on the particular series studied as is the polymer yield. Over the range tested, 2.05 megarads/hr. (1.28×10^{20} e.v./g.-hr.) and 0.095 megarad/hr. (5.9×10^{18} e.v./g.-hr.), gas yields are independent of the radiation intensity for a given dose.

In Fig. 2, the polymer yields (molecules of monomer converted to polymer per 100 e.v.) as a function of the temperature of irradiation are shown for two series. All samples received an irradiation dose of 2.8 megarads at a dose rate of 1.3 megarads/hr. When these octamethyl tetramer samples were irradiated below their melting point (*i.e.*, as solids), the yields were essentially the same for both series. However, when liquid samples were irradiated, the yield of the polymer resulting from siloxane rearrangement increased ~ 8 -fold as the temperature was raised from 17 to 80°; the apparent activation energy for this polymerization is 7 ± 1 kcal./mole. The standard deviation is calculated from three individual series. Over the same temperature range, there was no increase in the yield of dimer. As shown in the plot, at the melting point there was an increase in the yield of both types of polymer; however, in the series producing siloxane rearrangement the effect is much more pronounced.

The gas yields as a function of temperature are the same for both polymerization processes. The hydrogen, methane, and ethane yields as a function of temperature are shown in Fig. 3. All samples received a total dose of 2.8 megarads at a dose rate of 1.3 megarads/hr. The hydrogen yield from solid phase irradiations decreases from a value of 0.71 at -196° to 0.56 at $+15^\circ$, while the methane yield rises from 0.98 to 1.39 and the ethane yield rises from ~ 0 to 0.22 in the same temperature interval. The yields of hydrogen and ethane are independent of temperature when the tetramer is irradiated in the liquid phase, while the rate of methane production increases with an apparent temperature coefficient of about 1 kcal.

High-temperature chromatographic analysis of the residue from polymerizations in which dimers were produced revealed two distinct components. Their approximate boiling points were 257 and 267° and they were present in a ratio of 1:2. These components were probably heptamethylcyclo-

tetrasiloxane groups fused through either a silicon-silicon bond, a methylene bridge, or an ethylene bridge. Since their boiling points do not uniquely identify them, we cannot be certain which two of the three possible dimers were found. Kantor,⁴ who also studied the polymer from the irradiated octamethyl tetramer, believes that the methylene and silicon-silicon bonded dimers are the only ones produced. Although Kantor did not report the formation of any other polymer, our experiments with the "dimer" parallel has. He found a ratio of 2:1 for the amount of higher to lower boiling compound and a yield of about six which did not vary with temperature.

In an attempt to obtain reproducible results, irradiation vessels were carefully treated. They were washed with distilled water, dried at 110° for 24 hr., degassed several hours in a high vacuum system, and then flamed with a hand torch. This procedure did not eliminate the occurrence of the two different types of polymerization.

Attempts were made to determine the effects of trace impurities on the polymer yields. When a trace of water was known to be present during the irradiation, the polymer yields were low in about 60% of the experiments. The remaining 40% of the time, the yields were high. In the presence of oxygen at a pressure of several centimeters of mercury the polymer yields were always low. However, in a series of samples containing traces of oxygen (deliberately added) the radiation still induced siloxane rearrangement. Table II shows this series in which oxygen in concentrations up to $16 \times 10^{-7} M$ has a negligible effect on the polymer and gas yields. The oxygen concentration was calculated from its solubility (measured chromatographically to be 0.324–0.324 ml. of oxygen per ml. of tetramer) and the measured volume of the sample and the void space in the irradiation vessel.

TABLE II
EFFECT OF OXYGEN ON THE GAS AND POLYMER YIELDS FROM IRRADIATED OCTAMETHYL TETRAMER^a

Oxygen concn., mole/l.	$G(\text{H}_2)$	$G(\text{CH}_4)$	$G(\text{C}_2\text{H}_6)$	$G(\text{-monomer})$
0	0.94	2.04	0.32	30
0.3×10^{-7}	0.97	2.04	.34	30
1.7	1.02	2.07	..	28
2.7	1.01	2.05	.31	29
7.2	1.01	2.06	.30	30
8	0.98	2.09	.31	26
15	1.03	2.10	.31	26
16	0.96	2.13	.32	24

^a All samples received an irradiation dose of 3 megarads at a dose rate of 1.2 megarads/hr.

At much higher oxygen concentration (when the oxygen pressure above the solution was in the atmosphere range), Miller¹² found that the yield of cross-linking in irradiated polydimethylsiloxanes decreased.

Irradiation cells were fabricated from nine different types of glass and used to determine whether the chemical composition or active sites of the irradiation vessel walls would have an effect on the siloxane rearrangement reaction. Apparently, these factors are not important since the average

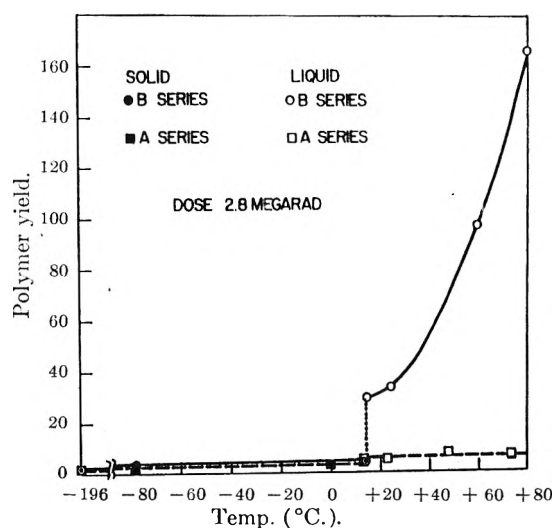


Fig. 2.—Polymer yield from irradiated octamethyl tetramer as a function of irradiation temperature.

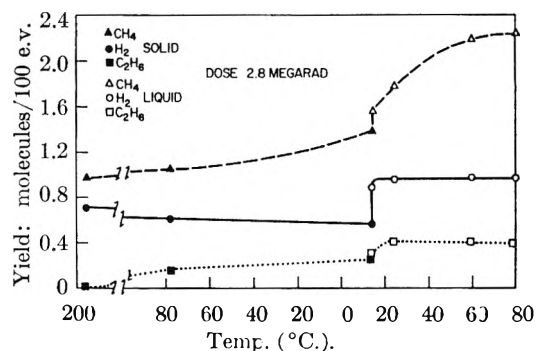


Fig. 3.—Gas yields from irradiated octamethyl tetramer as a function of temperature.

values (Table III) for $G(-M)$ and $G(+ \text{ gas})$ are 20 and 3.36, respectively.

TABLE III
EFFECT OF THE CONSTRUCTION MATERIAL OF THE IRRADIATION VESSEL ON THE POLYMER AND GAS YIELDS FROM IRRADIATED OCTAMETHYLCYCLOTETRASILOXANE^a

Sample	Vessel	$G(-M)$	$G(+ \text{ gas})$
SA-1	Nonex	21	3.35
SA-2	Pyrex	22	3.32
SA-3	No. 7052 glass ^b	19	3.35
SA-4	No. 7991 glass ^b	26	3.35
SA-5	Uranium glass	20	3.32
SA-6	Quartz	16	3.46
SA-7	Cobalt glass	21	3.31
SA-8	No. 7070 glass ^b	18	3.46
SA-9	Vycor	17	..

^a All samples received an irradiation dose of 2.9 megarads at a dose rate of 1.45 megarads/hr. ^b Standard Corning numbers.

The siloxane rearrangement phenomenon is not a post-irradiation effect. The polymerization of the octamethyl tetramer occurs while the solution is being irradiated only; there is no additional polymerization after the sample has been removed from the radiation field. A series of samples was exposed to a dose of 3 megarads at a dose rate of 1.5 megarads/hr., removed from the irradiation field, and then aged for various periods at room temperature. The data are shown in Table IV;

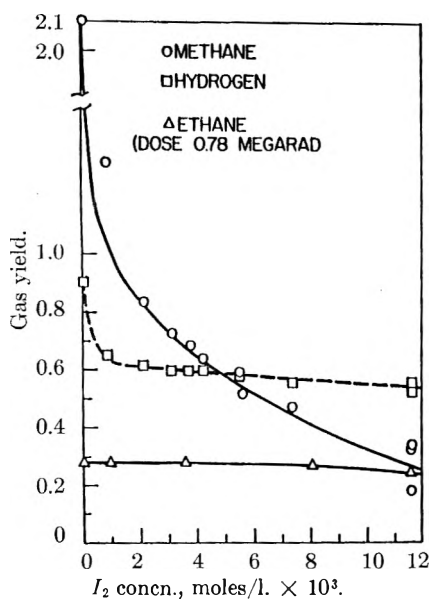


Fig. 4.—Hydrogen, methane, and ethane yields from irradiated iodine octamethyl tetramer solutions as a function of the initial iodine concentration, 28°.

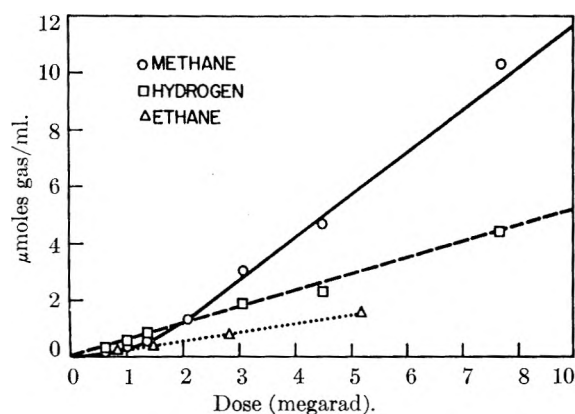


Fig. 5.—Hydrogen, methane, and ethane produced by irradiation of an iodine octamethyl tetramer solution ($11.6 \times 10^{-3} M$) as a function of irradiation dose, at 28°.

the polymer yields are roughly the same (average 25) regardless of the aging period.

TABLE IV

EFFECT OF AGING ON THE POLYMER YIELD FROM IRRADIATED OCTAMETHYLCYCLOTETRASILOXANE (DOSE 3 MEGARADS)

Sample	"Aging" period, hr.	$G(-M)$
P-3	0.5	24
P-5	6.67	20
P-4	19.6	23
P-1	90.5	31
P-2	191.5	27
P-6	595.5	24

In order to obtain information about the radiation induced free radical reactions, a free radical scavenger, iodine, was added to samples of octamethyl tetramer. Figure 4 shows the hydrogen, methane, and ethane yields as a function of initial iodine concentration for a dose of 0.78 megarad (intensity, 1.3 megarads/hr.). The hydrogen yield, $G(H_2)_{I_2} = 0.6$, is essentially independent of the initial iodine concentration for concentrations

greater than $1 \times 10^{-3} M$. This value indicates that about two-thirds of the hydrogen is produced by some process which is not affected by iodine, since the $G(H_2) = 0.9$ in the absence of iodine. The methane yield decreases markedly as the initial iodine concentration increases, dropping from 0.8 to 0.3 as the iodine concentration increases from 2 to $11 \times 10^{-3} M$. The ethane yield, however, is unaffected by the presence of iodine.

For a given initial iodine concentration, the effect of varied dose on the hydrogen, methane, and ethane yields also was studied. This is shown in Fig. 5. The amount of hydrogen produced increases linearly with the dose. The slope of this line gives a hydrogen yield of 0.57. After an induction period of about 1.5 megarads, methane is produced linearly with dose and the slope of the linear portion of the curve gives a methane yield of 1.45. Ethane is produced as a linear function of dose and it is produced at the same rate as in pure tetramer, *i.e.*, 0.29 molecule per 100 e.v. This indicates that ethane is not produced by the combination of two free methyl radicals. The initial iodine concentration of this solution was $11.6 \times 10^{-3} M$ and a dose of 7.5 megarads was sufficient to convert all the iodine to hydrogen iodide and methyl iodide. The production of hydrogen iodide as a function of dose is given in Table V.

TABLE V

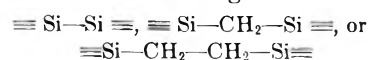
PRODUCTION OF HYDROGEN IODIDE FROM A SOLUTION OF IODIDE ($6 \times 10^{-3} M$) IN OCTAMETHYLCYCLOTETRASILOXANE AS A FUNCTION OF DOSE

Total dose, megarad	Hydrogen iodide concn., μmoles HI/ml.
0	0
0.30	0.9
0.71	1.8
0.83	1.7
1.07	1.9
1.45	2.5
1.96	2.6
2.73	2.7
3.26	2.9
4.00	2.4
4.95	2.4

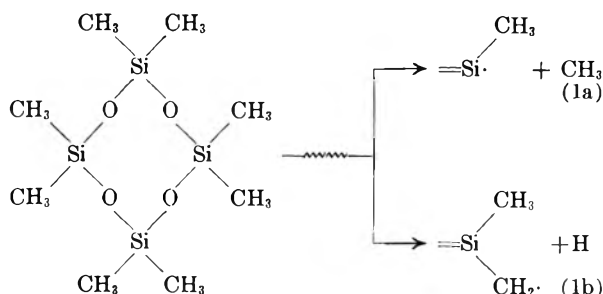
The hydrogen iodide concentration reaches a plateau value of approximately $2.5 \times 10^{-3} M$ after an irradiation dose of about 1.5 megarads. The decrease in the iodine concentration with dose is not shown here but will be discussed in a later publication.

Discussion

The production of hydrogen, methane, and ethane is accompanied by the production of dimeric polydimethylsiloxane structures which could be connected in the following manner

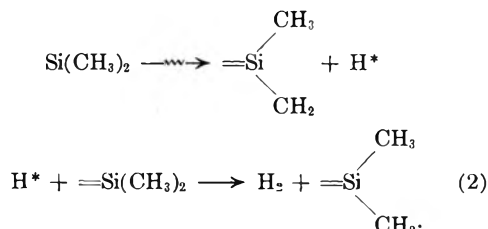


Such linkages could result from the combination of free radicals produced in the radiolysis in which the gaseous products would be, respectively, ethane, methane, or hydrogen



We found that the total gas yield is approximately equal to the dimer yield, which follows since two atoms are required to produce one gas molecule and, of course, two silicon radicals to make a dimer.

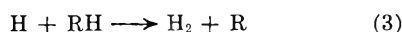
Production of Hydrogen.—Charlesby⁶ has suggested, from a kinetic analysis involving intensity studies of polydimethylsiloxane solutions containing anthracene, that at least part of the hydrogen atoms produced by reaction 1b are "hot-radicals" and can immediately abstract another hydrogen from a neighboring monomer



These two radicals should have a high probability for reaction since they are produced so close together. This would lead to the dimer $\equiv\text{Si}\cdot\text{CH}_2\cdot\text{CH}_2\cdot\text{Si}\equiv$, two heptamethylcyclotetrasiloxyl units connected by an ethylene bridge. However, Kantor⁴ was unable to find this compound in irradiated octamethyl tetramer solutions.

Miller,¹¹ who studied the cross-linking in irradiated polydimethylsiloxane solutions, found cross-links of the types $\equiv\text{Si}-\text{Si}\equiv$, $\equiv\text{SiCH}_2\text{Si}\equiv$, and $\equiv\text{Si}-\text{CH}_2\text{CH}_2\text{Si}\equiv$. Dewhurs⁷ and St. Pierre⁹ also found compounds with all three cross-links in their studies on the radiolysis of hexamethyldisiloxane.

Since the hydrogen yield from irradiations in the solid state (below 17°) and in the presence of iodine is about two-thirds of the maximum hydrogen yield, we believe that as much as two-thirds of the hydrogen is produced by a molecular process. Some of the molecular hydrogen is produced by radical combination with the spur—here the radicals are unaffected by phase and scavengers. However, a large fraction of the molecular hydrogen is formed by a process similar to reaction 2. The remaining one-third of the hydrogen probably is produced by the abstraction reaction of a thermal hydrogen atom with a monomer molecule



Usually abstraction reactions of the type depicted by eq. 3 require activation energies of the order of several kcal./mole. However, if the thermal hydrogen atoms can react in this manner, and in only this manner, the over-all rate of hydrogen production will appear as a temperature independ-

ent process. At the intensities used in this work, the probability of two hydrogen atoms meeting is small except in the solid phase at very low temperatures (−196°) where combination is the most probable reaction producing molecular hydrogen. Thus, we feel that one-third of the hydrogen is produced *via* a thermal abstraction reaction, a process in which the hydrogen atoms are accessible to scavenging by iodine.

Production of Methane.—In the liquid phase methane is produced by a process which has a temperature coefficient of approximately 1 kcal./mole. The temperature dependence suggests that an abstraction reaction may be important; *i.e.*

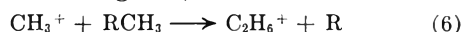


This reaction would be completely inhibited by iodine. In an iodine-tetramer solution during the initial period of radiolysis, little methane is produced. As the radiolysis continues, HI is produced and it reacts with the methyl radicals to produce methane.

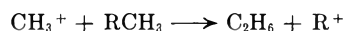


The role of iodine and hydrogen iodide will be discussed fully in a subsequent paper; however, some of the results are given here. The hydrogen iodide concentration rises rapidly with dose and reaches a plateau (see Table V). After the plateau is reached methane is produced at a linear rate. Thus, a steady state is reached in which HI is consumed as quickly as it is produced by the radiolysis. In this same region, the rate of iodine loss is markedly reduced. This arises from regeneration of iodine atoms by reaction 5. After all the molecular iodine is consumed, most of the iodine is in the form of iodide.

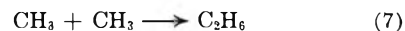
Production of Ethane.—Ethane is produced by some process which is essentially temperature independent (at least in the temperature range 14 to +80°) and is not affected by the presence of iodine. A reaction involving ions, such as



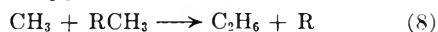
or



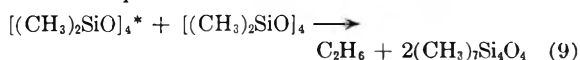
would most likely be influenced by a good electron acceptor such as iodine. Direct thermal radical combination



would be influenced by iodine. An abstraction reaction of the type



has been shown by Rice and Teller¹⁵ to be improbable on theoretical grounds, as this process would require an activation energy of about 2 e.v. If the methyl radical in reaction 8 had excess energy of the order of 2 e.v.; *i.e.*, a "hot radical," it is possible that reaction 8 may be important. It is also possible that a direct molecular reaction



(where $[(\text{CH}_3)_2\text{SiO}]_4$ represents a highly excited octamethyl tetramer molecule and $(\text{CH}_3)_7\text{Si}_4\text{O}_4$ is a

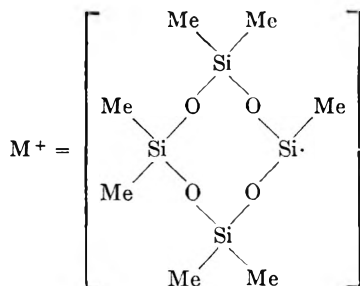
heptamethyl tetramer radical) also may be important. If ethane is produced by reactions similar to those shown in eq. 8 and 9, one might expect that the ethane yield would be temperature independent.

Production of Dimeric Siloxanes.—Warrick,⁸ using electron spin resonance techniques, found evidence for $\equiv\text{Si}\cdot$ and $\equiv\text{SiCH}_2\cdot$ radicals produced in the radiolysis of polydimethylsiloxanes. An extension to the cyclic radicals depicted in eq. 1a and 1b can easily be made.

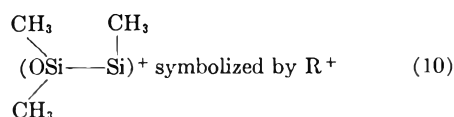
If the silicone radicals, $\equiv\text{Si}\cdot$ and $\equiv\text{SiCH}_2\cdot$, combine at random, three different types of dimer molecules would be formed. In the radiolysis of the octamethyl tetramer, only two dimers have been found by us and by Kantor.⁴ However, Miller¹¹ found all three—the silicon-silicon, the methylene bridged, and the ethylene bridged—cross-links upon radiolysis of polydimethylsiloxane. In the radiolysis of hexamethyldisiloxane Dewhurst and St. Pierre found three dimers with structures containing $\equiv\text{Si}-\text{Si}\equiv$, $\equiv\text{Si}-\text{CH}_2-\text{Si}\equiv$, and $\equiv\text{Si}(\text{CH}_2)_2-\text{Si}\equiv$ bonds. If we consider the dimers proposed by Kantor, $\equiv\text{SiCH}_2\text{Si}\equiv$ and $\equiv\text{Si}-\text{Si}\equiv$, it is very difficult to account for hydrogen production unless it arises entirely from a thermal free radical. If this is the case, and if radical combination can occur, why is not the $\equiv\text{Si}-\text{CH}_2\text{CH}_2-\text{Si}\equiv$ dimer formed? We believe it is formed but have been unable to prove its existence. Furthermore, reaction 2 leads to the formation of $\equiv\text{Si}-\text{CH}_2\text{CH}_2\text{Si}\equiv$, and this reaction can account for the hydrogen yields in iodine solution. This ethylene bridged dimer also would be predicted from Charlesby's⁶ work on linear polydimethylsiloxanes.

Dewhurst, *et al.*,² determined the cross-linking yield in polydimethylsiloxane fluids. They found $G(\text{cross-linking}) = 2.5 \pm 0.3$. Miller¹¹ found a value of 3.0. These values are in agreement with our gas and dimer yields of approximately three. One would expect the cross-linking of cyclic silicones to be similar to that found in linear polydimethylsiloxanes.

Siloxane Rearrangement.—The mechanism which produces siloxane rearrangement is considerably different from that which produces the dimers. In the former, the siloxane ring must open and then open additional rings to produce a linear polymer. The conventional siloxane rearrangement catalysts are ionic in nature. Therefore, we believe that ions produced by the irradiation are responsible for the large yields. For example, the positive ion (which we shall call M^+)



may be the initial ion which opens to form a radical ion



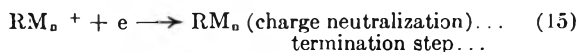
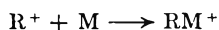
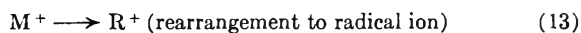
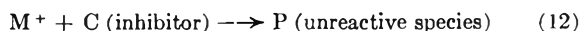
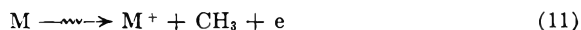
In a gas phase mass spectrometric study of hexamethyldisiloxane $[(\text{CH}_3)_3\text{SiOSi}(\text{CH}_3)_3]$ and octamethyltrisiloxane $[(\text{CH}_3)_3\text{SiOSi}(\text{CH}_3)_2\text{OSi}(\text{CH}_3)_3]$, Dibeler, Mohler, and Reese¹³ found that



was the most probable ionization process.

The difference between the behavior of the A series (low yield) and B series (high yield) can be explained by the presence of a trace quantity of inhibitor in the A series which is consumed by irradiation. In both series as irradiation continues a new inhibitor is formed. Within a given series the concentration of initial inhibitor would be constant but it could vary from one series to another. Thus, in samples where the initial inhibitor concentration was exceedingly small (B series), the rate of polymer production in the early stages of irradiation is high; however, as the irradiation proceeds a new inhibitor which also eliminates siloxane rearrangement is formed.

The radiation-produced inhibitor could be one of the dimer molecules or another product which is produced in small quantities. Such a product could be a silicone hydride such as heptamethylcyclotetrasiloxane, which is known to be produced in small amounts.⁴ The temperature coefficient for the siloxane rearrangement, 7 kcal., indicates that radicals may be involved in the polymerization reaction. We can, therefore, write a qualitative scheme for the production of linear polydimethylsiloxanes



Possibly the inhibitor present during the early stages of radiolysis is oxygen, but only additional work can confirm this.

It also is possible that a negative ion formed by electron attachment is responsible for the siloxane rearrangement. The present work cannot rule out such a possibility.

Acknowledgment.—We are deeply indebted to Dr. J. A. Ghormley for his helpful suggestions and comments given so freely during the course of this work.

HYDRAZINIUM BROMIDE AS A SOLVENT

BY RALPH P. SEWARD

*Department of Chemistry, The Pennsylvania State University, University Park, Pennsylvania^{1a,b}**Received December 22, 1961*

From the lowering of the freezing point of hydrazinium bromide by hydrazinium nitrate, hydrazinium iodide, and ammonium bromide a cryoscopic constant of 8.20 ± 0.1 degree per mole solute per kg. solvent was established. The molal lowerings for the solutes ammonium nitrate and lead iodide were, respectively, twice and three times 8.20. A molal lowering of half of 8.20 for the solute hydrazinium chloride is attributed to solid solution formation. Silver, lead, and mercury(II) bromides cause abnormally large freezing point depressions. Mercury(I) bromide disproportionates. The heat of fusion of hydrazinium bromide calculated from the cryoscopic constant is $3540 \text{ cal. mole}^{-1}$, while a calorimetric measurement gave $3800 \text{ cal. mole}^{-1}$. Hydrazinium bromide is a poor solvent for non-ionic solutes. Water, however, gives the normal freezing point lowering. Hydrazinium bromide and tetrabutylammonium bromide form a system of two liquid layers at temperatures above the melting point of the latter salt.

Observation of solubilities in and the cryoscopic behavior of solutions in the solvent hydrazinium bromide have been made with two objectives. One of these was a comparison of the lowering of the freezing point of this fused salt solvent on addition of a non-ionic solute with the lowerings produced by typical salts. Observations of this type are precluded for simple binary salts by their high melting points. As only for the ammonium nitrate-water² and potassium thiocyanate-water³ systems are data available of adequate precision for such a comparison, further observations seemed desirable. Chretien and Nessius⁴ made cryoscopic measurements with hydrazinium chloride as solvent but their only non-ionic solute was urea, for which the measurements are somewhat uncertain since the freezing points varied with time. Hydrazinium bromide has the conveniently low melting point of 86.5° , but the disadvantage that most organic compounds are not soluble in it. Urea and acetamide were found to be soluble but the solutions appeared unstable, confirming the observations of Chretien and Nessius⁴ in hydrazinium chloride, and the only satisfactory non-ionic solute found has been water.

A second objective of the investigations was that of finding more about the mutual solubilities of fused salts, in particular, whether two salts with a common ion could differ sufficiently that two liquid phases would result. The considerable difference in the nature of the hydrazinium ion and quaternary substituted ammonium ions suggested that hydrazinium bromide and tetrabutylammonium bromide might be immiscible in the liquid state and this proved to be the case. The bromide rather than the chloride system was chosen because of the relative ease of preparing the quaternary ammonium bromide compared to the chloride.

In order to establish the normal cryoscopic behavior of hydrazinium bromide with ionic solutes, measurements were made with $\text{N}_2\text{H}_5\text{NO}_3$, $\text{N}_2\text{H}_5\text{Cl}$, $\text{N}_2\text{H}_5\text{I}$, NH_4Br , NH_4NO_3 , and PbI_2 , and, in order to check certain observations of Chretien and

Nessius,⁴ with AgBr , PbBr_2 , HgBr_2 , and Hg_2Br_2 as solutes.

Finally, as a check on the cryoscopic value, the heat of fusion of hydrazinium bromide was measured calorimetrically.

Experimental

Materials—Hydrazinium bromide was prepared by adding aqueous hydrobromic acid to aqueous hydrazine until the methyl orange end-point was reached. After removing most of the water by heating until the temperature reached about 100° , the salt was recrystallized twice from methanol. Final drying was accomplished by bubbling dry nitrogen through the molten material or more quickly by melting under a vacuum. Hydrazinium bromide is deliquescent only in a quite humid atmosphere. Its melting point was found to be 86.5° . Gilbert and Cobb⁵ reported the m.p. as 84° . The other hydrazine salts were prepared in a similar fashion and had melting points in agreement with previously reported values. Tetrabutylammonium bromide was made from tetrabutylammonium hydroxide and hydrobromic acid. The ammonium salts were commercial "Reagent" chemicals while silver bromide and the lead and mercury salts were prepared by precipitation from aqueous solution.

Freezing Point Measurements.—These were made by the Beckmann technique, in part with a Beckmann thermometer and manual stirring, and in part with a thermistor and d.c. bridge for temperatures and mechanical stirring. The reproducibility was of the order of $\pm 0.01^\circ$ in the most dilute solutions, up to $\pm 0.03^\circ$ at higher concentrations, with both methods but the latter method was more convenient. Supercooling was kept at a fairly constant value of about 0.5° by addition of solvent crystals. As was found by Chretien and Nessius with $\text{N}_2\text{H}_5\text{Cl}$, contact with the atmosphere resulted in a progressive decrease in freezing point. Hence a stream of dry nitrogen was passed over the solutions during measurements. When the solute was water, the solution was covered by a layer of paraffin oil to prevent loss by vaporization.

With water as solute the concentrations of solute were extended to higher values and since the Beckmann technique becomes less reliable as the freezing points depart further from that of pure solvent, solutions over 5 molal in water were stirred with solid solvent in a large constant temperature bath and filtered samples of liquid taken. The composition of these samples was determined gravimetrically by precipitating silver bromide.

Calorimetric Measurements.—These measurements, of only moderate precision, were made by heating samples of hydrazinium bromide, sealed in thin walled glass tubes, to various temperatures in the constant temperature bath and dropping them into the calorimeter. The calorimeter consisted of a 500-ml. dewar jar containing 400 ml. of water and equipped with a mechanical stirrer. Temperatures were read with the aid of a thermistor which was sensitive to better than 0.001° . To reduce heat loss in transfer of the sample to the calorimeter the sample was removed from the bath in a glass sleeve which surrounded it until it was dropped into the calorimeter. The heat capacity of the calorimeter was determined by similar operations with a piece of

(1) (a) Done in part at Bristol, England. The author is indebted to Professor D. H. Everett for making the facilities of the University chemical laboratories available to him; (b) supported in part by the U. S. Atomic Energy Commission under Contract AT(30-1)-1881.

(2) A. G. Keenan, *J. Phys. Chem.*, **60**, 1356 (1956); **61**, 781 (1957).

(3) F. C. Kracek, *J. Wash. Acad. Soc.*, **26**, 307 (1936).

(4) A. Chretien and A. Nessius, *Bull. soc. chim. France*, **7**, 258 (1940).

(5) E. C. Gilbert and A. W. Cobb, *J. Am. Chem. Soc.*, **57**, 39 (1935).

aluminum metal. From several observations with two different samples of the salt the mean heat capacity from room temperature up to the melting point was found to be 25.2 cal. mole⁻¹ deg.⁻¹ and the heat of fusion to be 3800 cal. mole⁻¹. Individual values differed by no more than 2% from these figures.

Results and Discussion

The Cryoscopic Heat of Fusion.—When the freezing point lowerings produced by the solutes N₂H₅Cl, N₂H₅NO₃, N₂H₅I, NH₄Br, NH₄NO₃, and PbI₂ at various molal concentrations were plotted against solute molality, the points for N₂H₅NO₃, N₂H₅I, and NH₄Br all lay close to a straight line which had a slope of 8.20 deg. (moles solute)⁻¹ (kg. solvent)⁻¹. There was no systematic curvature and individual deviations from the line were of magnitudes comparable to the uncertainties in individual determinations. The freezing point lowerings due to NH₄NO₃ and PbI₂ were observed to lie close to straight lines drawn to have, respectively, slopes of twice and three times 8.20. It may be concluded that solutions in the solvent N₂H₅Br behave in the normal manner for molten salts. This behavior is illustrated by the experiments of Van Artsdalen⁶ with NaNO₃ as solvent in which the introduction of solutes having two and three ions foreign to the solvent produced twice and three times the lowering in freezing point produced by equal molalities of solutes having only one ion foreign to the solvent.

A line drawn through the points for the solute N₂H₅Cl would have a slope of about 4. To confirm the suspicion that this difference from the other solutes is due to the formation of solid solutions, freezing points were observed over the complete composition range in the N₂H₅Br–N₂H₅Cl system. With the bromide freezing at 86° and the chloride at 92° a minimum freezing point of 72° was observed. If the system behaved ideally with no solid solution formation, a eutectic point should exist at about 46°. Furthermore, no sign of a eutectic halt could be found in cooling any of the mixtures.

A molal cryoscopic constant of 8.20 for a solvent freezing at 359.7°K., and having a formula weight of 113, leads to a heat of fusion of 3540 cal. mole⁻¹. Although there is a 7% discrepancy between the cryoscopic 3540 and the calorimetric 3800 heat of fusion, the agreement is good enough to indicate that 8.20, rather than some multiple, is the normal cryoscopic constant.

Silver, Lead, and Mercury Bromides in Hydrazinium Bromide.—These bromides as solutes give more than the normal freezing point lowerings, increasingly so with rising concentration in the case of lead and silver as shown in Table I. With these solutes the freezing points were less reproducible and the numerical values of $\Delta T/m$ more uncertain. They are sufficiently consistent to show that the deviations from normal behavior are in the direction which would be expected if the formation of complex ions has decreased the amount of solvent present. There is no sign that at lower concentrations $\Delta T/m$ approaches double its normal value as was reported by Chretien and Nessius⁴ for PbCl₂ and HgCl₂ in their solvent,

TABLE I

LOWERING OF THE FREEZING POINT OF N₂H₅Br BY SILVER, LEAD, AND MERCURY BROMIDES AT VARIOUS MOLAL CONCENTRATIONS

AgBr	<i>m</i>	0.081	0.169	0.275	0.377
	$\Delta T/m$	8.40	8.92	8.95	9.17
PbBr ₂	<i>m</i>	0.080	0.172	0.267	0.377
	$\Delta T/m$	8.45	8.80	9.41	9.52
HgBr ₂	<i>m</i>	0.021	0.121	0.221	0.347
	$\Delta T/m$	9.3	10.5	10.7	10.2
Hg ₂ Br ₂	<i>m</i>	0.047	0.128	0.214	0.301
	$\Delta T/m$	10.1	9.6	10.0	10.7

N₂H₅Cl. The observations with mercury(I) bromide were made to see if the Hg₂⁺⁺ ion could exist in the salt melt. Immediately on addition the mercury(I) bromide turned black and, after stirring, a drop of liquid mercury formed in the tube. From a melt to which 0.00663 formula weight of Hg₂Br₂ had been added there was recovered a drop of mercury amounting to 0.00630 g.-atom. It is apparent that the freezing point lowerings recorded for the Hg₂Br₂ are actually those for the HgBr₂ formed by disproportionation. This behavior agrees with that of Hg₂Cl₂ in N₂H₅Cl as reported by Chretien and Nessius.⁴ The equilibrium Hg₂⁺⁺ + Hg could well be essentially complete to the right owing to the formation of more stable Hg(II) halide complexes.

Water in Hydrazinium Bromide.—Up to a water mole fraction of 0.50, values of minus log of N₂H₅Br mole fraction plotted against the reciprocal of absolute temperature give points lying on a straight line. The straight line corresponds to the equation

$$-\log N_{\text{N}_2\text{H}_5\text{Br}} = \frac{3540}{2.3R} \left(\frac{1}{T} - \frac{1}{359.6} \right)$$

Since the slope of the line depends on the heat of fusion calculated from the freezing point lowerings produced by typical salts, it is seen that solutions with water as solute do not differ significantly from those with salts as solutes. It appears that a small amount of water does not alter the heat of fusion of the solvent salt and that the water is randomly dispersed among the ions. If this is so, water molecules would have the same effect in dilute solution as the addition of an equal number of ions which are foreign to the solvent salt. As this may not be obvious, consider a mixture of *n* moles of H₂O in *n*₀ moles N₂H₅Br. If the salt is completely dissociated, the mole fraction of each ion is *n*₀/(*n* + 2*n*₀). Taking the activity of each ion as the ratio of this mole fraction to the ion mole fraction in the standard state of pure liquid N₂H₅Br where it is *n*₀/2*n*₀, each ion activity becomes 2*n*₀/(*n* + 2*n*₀). The solvent activity, taken as the product of the ion activities, is 1/(1 + *n*/2*n*₀)² and $-\log(\text{solvent activity}) = \log [1 + n/n_0 + 1/4(n/n_0)^2]$ which differs from $-\log(\text{solvent mole fraction}) = -\log [n_0/(n_0 + n)]$ by only 2.4% for a 0.10 solute mole fraction. It is perhaps surprising that the linear relation is followed so well in solutions having a high water concentration. Above 0.50 mole fraction of the water the measured solubilities become slightly smaller than those predicted by the straight

(6) E. R. Van Artsdalen, *J. Phys. Chem.*, **60**, 172 (1956).

line. Even at the lowest temperature, 16° , although this is 70° below the melting point and the salt mole fraction is only 0.285, the solubility predicted by the straight line differs by only 3% from the measured value.

The only salts for which comparable measurements have been made are potassium thiocyanate and ammonium nitrate. For potassium thiocyanate Plester, Rogers, and Ubbelohde⁷ found the heat of fusion to be 3390 cal. per mole by calorimetric measurements. From cryoscopic observations Dingmans⁸ found heats of fusion of 3130 cal. with KCl as solute and 3185 with KBr as solute, while Kordes, Bergmann, and Vogel⁹ report freezing point lowerings by KBr corresponding to a heat of fusion of 2250 cal. Kracek³ found the solubility of KSCN in water near the melting point of the salt to vary with temperature in accordance with a heat of fusion of 2960 cal. In view of the disagreement in the cryoscopic measurements it is not clear whether solutions of water in KSCN behave differently from solutions of salts in KSCN. In ammonium nitrate as solvent, Keenan² found no significant difference between the freezing point lowerings produced by water and those produced by salts.

The Hydrazinium Bromide-Tetrabutylammonium Bromide System.—When tetrabutylammonium bromide was added to hydrazinium bromide no decrease in freezing point could be detected. The solubility of tetrabutylammonium bromide thus must be less than 0.003 molal at a temperature only about 30° below its melting point. At temperatures above the melting point of tetrabutylammonium bromide, two liquid layers were found. Although a number of instances of two liquid layer salt systems have been reported, these involve systems without a common ion. The currently

accepted model of a molten salt is that in which the nearest neighbors of cations are anions and the nearest neighbors of anions are cations, without the long range order existing in the crystalline state and with lower average ion coordination numbers than in the solid form. This picture of the state of the liquid suggests that only the considerable difference in cation size causes liquid-liquid immiscibility in the above system.

The Displacement of Iodide from Solution in Hydrazinium Bromide by Bromide.—On addition of 5.97 mmoles of N_2H_5I , the freezing point of 19.54 g. of N_2H_5Br was lowered by 2.41° . When 2.01 mmoles of $(C_4H_9)_4N \cdot Br$ was added the freezing point of the solution was higher. Eight successive observations of the freezing point showed increasing temperatures, an apparently limiting value 1.60° below the initial freezing point of the solvent being reached. This can be accounted for by the removal of 2.01 mmoles of iodide ion from the solution and its replacement by 2.01 mmoles of bromide ion from the tetrabutylammonium bromide. The slowness of the exchange can be attributed to the fact that two phases were involved. This experiment was done to find further evidence on the effect of ion size on solubility. Coulomb's law predicts a lower energy for a system where the larger cation is associated with the larger anion and the smaller cation with the smaller anion compared to that of the reciprocal salt system. In the system described above the favored pairing would be $N_2H_5 \cdot Br$ and $(C_4H_9)_4N \cdot I$. A qualitative observation with hydrazinium picrate added to the two phase $N_2H_5Br-(C_4H_9)_4N \cdot Br$ system was found to be consistent with the observations on the system containing iodide. In this case the $(C_4H_9)_4Br$ phase acquired a deeper yellow color than did the N_2H_5Br phase which, however, must have retained some of the picrate. As the solubility of hydrazinium picrate in hydrazinium bromide is quite small, freezing point lowering experiments were not attempted.

(7) D. W. Plester, S. E. Rogers, and A. R. Ubbelohde, *J. Sci. Instr.*, **33**, 211 (1956).

(8) P. Dingmans, *Rec. trav. chim.*, **58**, 559 (1939).

(9) E. Kordes, W. Bergmann, and U. W. Vogel, *Z. Elektrochem.*, **55**, 600 (1951).

THE SIGNIFICANT STRUCTURE THEORY OF LIQUID HYDROGEN IN ITS VARIOUS ORTHO-PARA AND ISOTOPIC FORMS¹

BY DOUGLAS HENDERSON,² HENRY EYRING, AND DALE FELIX

Departments of Physics and Chemistry, University of Utah, Salt Lake City, Utah

Received December 26, 1961

The significant structure theory of liquids is extended to include liquid hydrogen in its various ortho-para and isotopic forms. It is assumed that liquid hydrogen has a quasi-lattice structure in which the "lattice sites" are occupied either by hydrogen molecules or holes of molecular size. Such a hole will confer gas-like properties on a molecule which jumps into it and also will give rise to a degeneracy in the solid-like structure. On this basis a partition function can be written down for liquid hydrogen. The thermodynamic properties of para-hydrogen, normal hydrogen, hydrogen deuteride, ortho-deuterium, and normal deuterium are calculated for temperatures ranging from the triple point to temperatures considerably above the boiling point. Critical constants also are calculated. The results are in good agreement with experimental data. In addition, the surface tensions of normal hydrogen, hydrogen deuteride, and normal deuterium are calculated with good results.

Introduction

X-Ray studies of liquids³ indicate considerable short range order with little change in nearest neighbor distance from that of the solid state. For liquids one can, therefore, speak of a quasi-lattice structure with the expansion of the liquid due to the introduction of vacancies or holes into the structure.

To remove a molecule from a lattice and leave a hole behind involves breaking all the bonds binding the molecule to its neighbors. To evaporate molecules requires only half this energy since again all bonds to neighbors are broken but each bond joins two molecules and therefore only half of the energy of a bond should be charged against each neighbor. Thus, the energy of vaporization of a molecule is just half the sum of the bond energies joining it to its neighbors. Clearly, the energy of vaporization could be regained by letting the hole disappear by migrating to the liquid surface or by returning the molecule to the surface. Therefore, it follows that the introduction of a molecular sized hole requires an energy equal to the heat of vaporization. Thus, approximately, a molecular sized hole in the liquid contributes the same enthalpy and entropy as does a molecule in the vapor and therefore it is to be expected that there should be as many molecular sized holes per unit volume of liquid as there are molecules per unit volume of vapor so that the sum of the densities of liquid and vapor should be constant except for a drift toward lower mean densities of the vapor with rising temperature because of the presence of fractional sized molecules in the liquid. This qualitative explanation of the experimental law of rectilinear diameters was first pointed out by Eyring.⁴

The Model

The above considerations can be quantitatively formulated in the following manner. Neglecting the effect of holes other than those of molecular size, then the number of holes present in a liquid is

(1) This is an essential portion of a thesis submitted by D. Henderson to the Physics Department, University of Utah, in partial fulfillment of the requirements for a Doctor of Philosophy Degree. This paper was presented at the National Meeting of the American Chemical Society in Chicago on September 5, 1961.

(2) Corning Glass Foundation Fellow, 1959-1961. Department of Physical Sciences, University of Idaho, Moscow, Idaho.

(3) A. Eisenstein and N. S. Gingrich, *Phys. Rev.*, **62**, 261 (1942).

(4) H. Eyring, *J. Chem. Phys.*, **4**, 283 (1936).

$N(V - V_s)/V_s$ where V_s and V are, respectively, the molar volumes of the solid and liquid phases. Such a molecular sized hole will confer gas-like properties on a neighboring molecule which jumps into it. Assuming a random distribution of holes and molecules, then $N(V - V_s)/V$ of the molecules will possess gas-like properties and NV_s/V of the molecules will have solid-like properties. If the above argument is valid then the specific heat at constant volume of classical liquid would be

$$C_v = 6 \frac{V_s}{V} + 3 \frac{V - V_s}{V} \quad (1)$$

It has been pointed out by Walter and Eyring⁵ that eq. 1 provides a good representation of the specific heat of liquid argon.

The presence of holes in the liquid will not only confer gas-like properties on some of the molecules but also will provide for a solid-like molecule a positional degeneracy equal to the number of neighboring holes multiplied by the probability of the molecule and a hole exchanging positions. On this basis the partition function for a liquid would be

$$Z = \{Z_s(1 + n_h e^{-\epsilon/RT})^N\}^{V_s/V} \{Z_g\}^{(V - V_s)/V} \quad (2)$$

where Z_s and Z_g are, respectively, the partition functions for the solid and gas phases of the substance and ϵ is the energy for a hole-molecule pair to exchange positions. Assuming a random distribution of holes and molecules

$$n_h = z \frac{V - V_s}{V} \quad (3)$$

where $z = 12$ is the coordination number of the lattice. At high temperatures a large entropy in addition to a small energy is required to minimize the Gibbs free energy and therefore the molecules will tend to surround themselves with their full complement of holes. For this situation

$$n_h = n \frac{V - V_s}{V_s} \quad (4)$$

which is the expression used in previous investigations⁶ based on the significant structure theory of liquids. The energy ϵ is assumed to be proportional

(5) J. Walter and H. Eyring, *ibid.*, **9**, 393 (1941).

(6) H. Eyring, T. Ree, and N. Hirai, *Proc. Natl. Acad. Sci. U. S.*, **44**, 683 (1958); E. J. Fuller, T. Ree, and H. Eyring, *ibid.*, **45**, 1593 (1959); C. M. Carlson, H. Eyring, and T. Ree, *ibid.*, **46**, 333 (1960); T. R. Thomson, H. Eyring, and T. Ree, *ibid.*, **46**, 336 (1960); C. M. Carlson, H. Eyring, and T. Ree, *ibid.*, **46**, 649 (1960); H. Eyring and T. Ree, *ibid.*, **47**, 526 (1961).

to the potential energy of the lattice and inversely proportional to n_h .

It is to be emphasized that the significant structure theory of liquids does not imply that a liquid is a mixture of solid and gas. A molecule has solid-like properties for the time it vibrates about an equilibrium position, then it may instantaneously transform into gas-like behavior in one or more of its translational degrees of freedom as it jumps into a neighboring hole.

Application to Liquid Hydrogen

In applying the above theory to liquid hydrogen a Debye partition function was used for the solid-like molecules. At the temperatures of interest, the gas-like molecules are slightly degenerate and therefore a Bose-Einstein partition function was used for the hydrogen and deuterium molecules and a Fermi-Dirac partition function was used for the hydrogen deuteride molecules. The resulting partition function for liquid hydrogen is then

$$\ln Z = N \frac{V_s}{V} \left\{ \frac{E_p}{RT} - \frac{9}{8} \left(\frac{\theta_D}{T} \right) - 9 \left(\frac{T}{\theta_D} \right)^3 \times \int_0^{\theta_D/T} u^2 \ln(1 - e^{-u}) du + \ln \left(1 + z \frac{V - V_s}{V} e^{-\alpha} \right) \right\} + N \frac{V - V_s}{V} \left\{ 1 - \ln y = \frac{y}{2^{3/2}} \right\} + \ln Z_r \quad (5)$$

where the top sign applies to the Bose-Einstein case and the bottom sign applies to the Fermi-Dirac case

$$\alpha = \frac{aE_p}{RT} \frac{V}{V - V_s}$$

E_p is the potential energy of the lattice, a is a proportionality factor.

$$y = \frac{N}{V} \left(\frac{h^2}{2\pi mkT} \right)^{3/2}$$

θ_D is the Debye temperature of the lattice, and Z_r is the rotational partition function for the molecules. If $\theta_r = h^2/8\pi^2Ik$ then the rotational partition functions for ortho-hydrogen (o-H₂) and parahydrogen (p-H₂), respectively, are given by the expressions

$$Z_r^o = 3 \sum_{n=1,3}^{\infty} (2n+1)e^{-n(n+1)\frac{\theta_r}{T}}$$

$$Z_r^p = \sum_{n=0,2}^{\infty} (2n+1)e^{-n(n+1)\frac{\theta_r}{T}} \quad (6)$$

For ortho-deuterium (o-D₂) and para-deuterium (p-D₂) the corresponding expressions are

$$Z_r^o = 6 \sum_{n=0,2}^{\infty} (2n+1)e^{-n(n+1)\frac{\theta_r}{T}}$$

$$Z_r^p = 3 \sum_{n=1,3}^{\infty} (2n+1)e^{-n(n+1)\frac{\theta_r}{T}} \quad (7)$$

For mixtures of ortho and para molecules the rotational partition function is given by the usual expression

$$\ln Z_r = \eta \ln Z_r^o + (1 - \eta) \ln Z_r^p \quad (8)$$

where η is the fraction of the molecules that are in the ortho state. For normal hydrogen $\eta = 3/4$, while for normal deuterium $\eta = 2/3$. Finally for hydrogen deuteride (H-D) the rotational partition function is

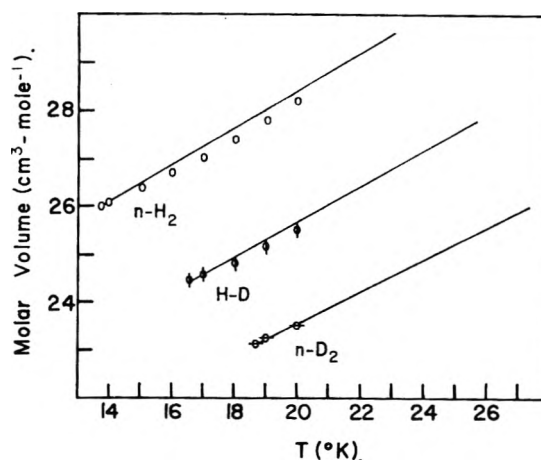


Fig. 1.—Molar volumes of liquid n-H₂, H-D, and n-D₂. The curve consists of the calculated values and the experimental points O, φ, and ⊖ are taken from ref. 9, 5, and 10, respectively.

$$Z_r = 6 \sum_{n=1,2}^{\infty} (2n+1)e^{-n(n+1)\frac{\theta_r}{T}} \quad (9)$$

All the quantities except a and E_p in eq. 5 are known. Values for a and E_p can be obtained by requiring the Gibbs free energy to be a minimum at the observed triple point. The values of the parameters in this investigation are given in Table I. The molar volume of solid o-D₂ and the Debye temperature of H-D are given in parentheses, since experimental data is unavailable and the values given are estimates.

TABLE I

	p-H ₂	n-H ₂	H-D	o-D ₂	n-D ₂
V_s (cm ³ -mole ⁻¹)	23.34 ⁷	23.25 ⁷	21.84 ⁷	(20.58)	20.48 ⁷
θ_D (°K.)	91 ⁸	91 ⁸	(90)	89 ⁹	89 ⁹
E_p (cal.-mole ⁻¹)	384.9	386.3	435.7	475.2	476.8
I (g.-cm. × 10 ⁴¹)	4.67 ¹⁰	4.67 ¹⁰	6.21 ¹⁰	9.31 ¹⁰	9.31 ¹⁰
θ_r (°K.)	85.4	85.4	64.2	42.8	42.8
$a \times 10^2$	0.547	0.554	0.565	0.640	0.647

The Thermodynamic Properties of Liquid Hydrogen

Volume and Pressure.—The Helmholtz free energy is given by

$$A = -kT \ln Z \quad (10)$$

If A is plotted as a function of V for constant T and the points of common tangency found, the calculated vapor pressure will equal the slope of the common tangent and the abscissa of the two points of common tangency will be the volumes of the liquid and vapor. The results of these calculations are plotted in Fig. 1 and 2. In Fig. 1 the calculated molar volumes of n-H₂, H-D, and n-D₂ are compared with the experimental results of Scott and Brickwedde,¹¹ Wooley, *et al.*,⁷ and Clusius and

(7) H. W. Wooley, R. B. Scott, and F. G. Brickwedde, *J. Res. Natl. Bur. Standards*, **41**, 379 (1948).

(8) H. L. Johns on, J. T. Clarke, E. B. Rifkin, and E. C. Kerr, *J. Am. Chem. Soc.*, **72**, 3933 (1950).

(9) E. C. Kerr, E. B. Rifkin, H. L. Johnston, and J. T. Clarke, *ibid.*, **73**, 282 (1951).

(10) A. Farkas, "Orthohydrogen, Parahydrogen, and Heavy Hydrogen," Cambridge University Press, London, 1935, p. 162.

(11) R. B. Scott and F. G. Brickwedde, *J. Res. Natl. Bur. Standards*, **19**, 237 (1937).

TABLE II

	CALCULATED AND OBSERVED BOILING POINT PROPERTIES				
	p-H ₂	n-H ₂	H-D	o-D ₂	n-D ₂
T_b (°K.)	20.58	20.70	22.29	23.65	23.75 calcd.
	20.261 ⁸	20.365 ¹⁴	22.14 ¹³	23.59 ⁹	23.67 ¹⁵ obsd.
	+1.58%	+1.64%	+0.68%	+0.25%	+0.34% Δ
V_b (cm. ³ -mole ⁻¹)	28.829	28.692	26.525	24.955	24.830 calcd.
	28.482 ¹¹	28.393 ¹¹ obsd.
	+1.22%	+1.05% Δ

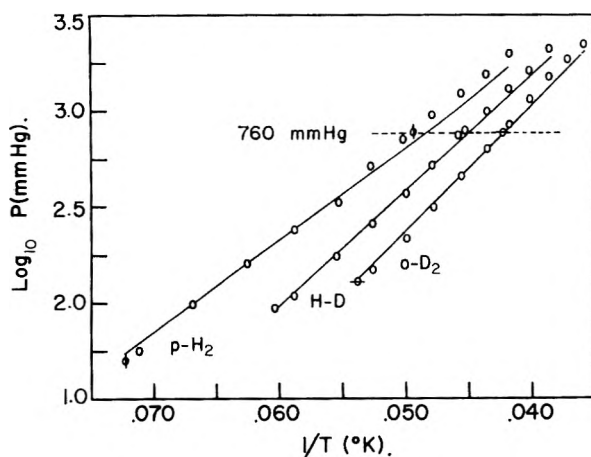


Fig. 2.—Vapor pressures of liquid p-H₂, H-D, and o-D₂. The curve consists of the calculated values and the experiments points O, φ, and ⊕ are taken from ref. 11, 6, and 7, respectively.

Bartholome,¹² respectively. In Fig. 2 the calculated vapor pressures of p-H₂, H-D, and o-D₂ are compared with the experimental results of Hoge and Arnold,¹³ Johnston, *et al.*,⁸ and Kerr, *et al.*⁹ These calculations were not performed right to the critical point since at these higher temperatures and lower densities a random distribution of molecules and holes will no longer be valid and therefore eq. 3 will not be applicable. The calculated and experimental values of the temperatures and volumes at the boiling points of p-H₂, n-H₂, H-D, o-D₂, and n-D₂ are compared in Table II.

Pressures at volumes other than at saturated vapor pressures may be calculated by means of the relation

$$P = - \left(\frac{\partial A}{\partial V} \right)_T \quad (11)$$

Isotherms for normal hydrogen have been calculated at 16.43 and 22.96°K. and for normal deuterium at 19.70 and 27.21°K. and are compared with the data of Bartholome,¹⁶ Johnston, *et al.*,¹⁷ and Friedman, *et al.*,¹⁸ in Fig. 3 and 4. In applying eq. 11 the pressure variation of V_s must be taken

(12) K. Clusius and E. Bartholome, *Z. physik. Chem.*, **B30**, 237 (1935).

(13) H. J. Hoge and R. A. Arnold, *J. Res. Natl. Bur. Standards*, **47**, 63 (1951).

(14) G. W. Moessen, J. G. Aston, and R. G. Aschah, *J. Chem. Phys.*, **22**, 2096 (1954).

(15) E. R. Grilley, *J. Am. Chem. Soc.*, **73**, 843 (1951).

(16) E. Bartholome, *Z. physik. Chem.*, **B33**, 387 (1936).

(17) H. L. Johnston, W. E. Keller, and A. S. Friedman, *J. Am. Chem. Soc.*, **76**, 1482 (1954).

(18) A. S. Friedman, M. Trzeciak, and H. L. Johnston *ibid.*, **76**, 1552 (1954).

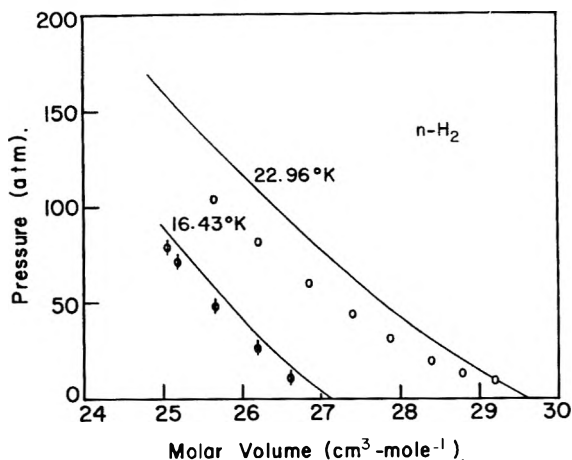


Fig. 3.—Isotherms of liquid n-H₂. The curve consists of the calculated values and the experimental points φ and O are taken from ref. 14 and 15, respectively.

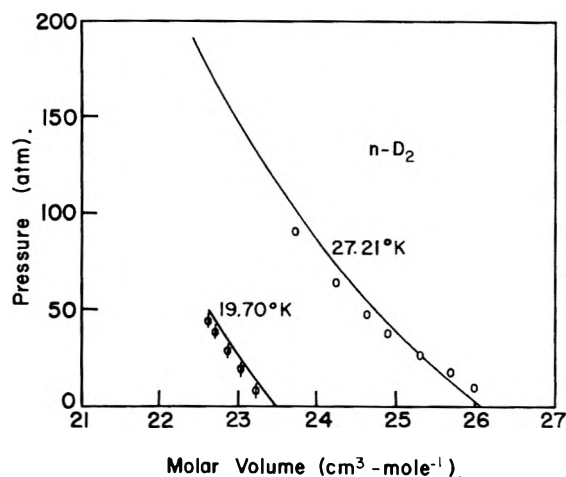


Fig. 4.—Isotherms of liquid n-D₂. The curve consists of the calculated values and the experimental points φ and O are taken from ref. 14 and 16, respectively.

into account. In doing this the compressibility data tabulated by Wooley, *et al.*,⁷ was used.

Specific Heat.—The specific heat at constant volume may be calculated from eq. 5 by the relation

$$C_v = \left(\frac{\partial}{\partial T} kT^2 \frac{\partial \ln Z}{\partial T} \right)_v \quad (12)$$

The most recent and probably the most accurate data is for the more easily measured specific heat at saturated vapor pressures, C_s , which is related to C_v by the expression

$$C_s = C_v + T \left(\frac{\partial S}{\partial V} \right)_T \left(\frac{dV}{dT} \right)_{sat} \quad (13)$$

The calculated values of C_s for p-H₂, H-D, and o-D₂ are compared with the measurements of

TABLE III
CALCULATED AND OBSERVED CRITICAL CONSTANTS

	p-H ₂	n-H ₂	H-D	o-D ₂	n-D ₂	
T _c (°K.)	35.9	36.12	37.6	39.4	39.7	calcd.
	32.934 ²⁰	33.24 ²¹	35.908 ²⁰	38.262 ²⁰	38.24 ²²	obsd.
	+8.81%	+8.90%	+4.71%	+2.97%	+3.82%	Δ
P _c (atm.)	13.6	13.8	15.5	17.1	17.3	calcd.
	12.770 ²⁰	12.797 ²¹	14.645 ²⁰	16.282 ²⁰	16.421 ²²	obsd.
	+6.50%	+7.84%	+5.84%	+5.02%	+5.35%	Δ
V _c (cm ³ -mole ⁻¹)	77.7	77.3	71.5	68.3	68.0	calcd.
	65.5 ²⁰	..	62.8 ²⁰	60.3 ²⁰	..	obsd.
	+18.6%	..	+13.8%	+13.3%	..	Δ

Johnston, *et al.*,⁸ Smith, *et al.*,¹⁹ and Kerr, *et al.*⁹ in Fig. 5.

Critical Constants.—At the comparatively high temperatures and low densities of the critical points of the various forms of liquid hydrogen eq. 4 was assumed valid, *i.e.*, $n = z(V_s/V)$ is a constant. In the calculation of critical constants it was assumed that $^{2/3}z$ was a sufficiently good value for n . Since n appears logarithmically its exact value does not greatly affect the value of the critical constants. The critical constants were calculated in the usual way.

$$P = - \left(\frac{\partial A}{\partial V} \right)_T, \left(\frac{\partial P}{\partial V} \right)_T = 0, \left(\frac{\partial^2 P}{\partial V^2} \right)_T = 0 \quad (14)$$

The calculated and observed critical constants are compared in Table III.

Surface Tension.—Since the partition function which has been used reduces to the gas partition function for $V \gg V_s$, it is to be expected that the partition function will be applicable to the surface layer as well as the bulk liquid. The principal change required arises from the differences in the forces acting on a surface molecule and bulk molecule. This difference is reflected in the value of E_{pi} . If only nearest neighbor interactions are considered, then assuming close-packing

$$E_{pi} = E_p \left(\frac{6}{12} \frac{\rho_i}{\rho} + \frac{3}{12} \frac{\rho_{i-1}}{\rho} + \frac{3}{12} \frac{\rho_{i+1}}{\rho} \right) \quad (15)$$

where E_{pi} is the corrected value for the potential energy of the i -th layer below the surface and ρ_i , ρ_{i+1} , ρ_{i-1} are the densities of the i -th layer and the layers immediately below and above. When $i = 0$ then one can write for the zeroth or first gas layer

$$E_{p0} = E_p \left(\frac{1}{4} \frac{\rho_0}{\rho} \right) \quad (16)$$

since a molecule in the first gas layer has three neighbors in the first liquid layer and none in the first gas layer or in any gas layer above.

The procedure is to assume values for the ρ_i and then by use of (15) and (16) plot the Helmholtz free energy as a function of V . In this manner new values for the ρ_i are obtained and the process is repeated until self consistency is achieved. The Gibbs free energy then is calculated for each layer

(19) A. L. Smith, N. C. Hallett, and H. L. Johnston, *J. Am. Chem. Soc.*, **76**, 1486 (1954).

(20) H. J. Hoge and J. W. Lassiter, *J. Res. Natl. Bur. Standards*, **47**, 75 (1951).

(21) D. White, A. S. Friedman, and H. L. Johnston, *J. Am. Chem. Soc.*, **72**, 3565 (1950).

(22) A. S. Friedman, D. White, and F. L. Johnston, *ibid.*, **73**, 1310 (1951).

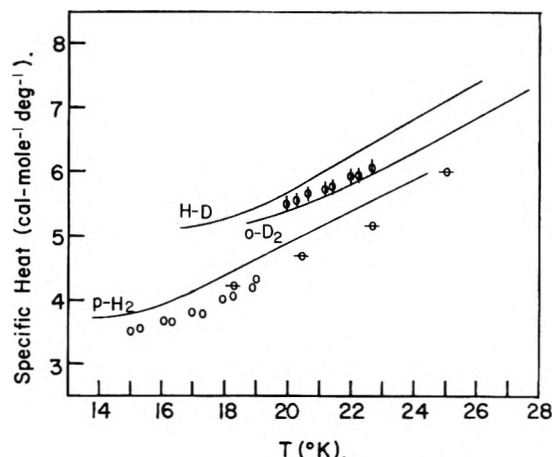


Fig. 5.—Specific heat at saturated vapor pressures of liquid p-H₂, H-D, and o-D₂. The curve consists of the calculated values and the experimental points O, φ, and ⊕ are taken from ref. 6, 17, and 7, respectively.

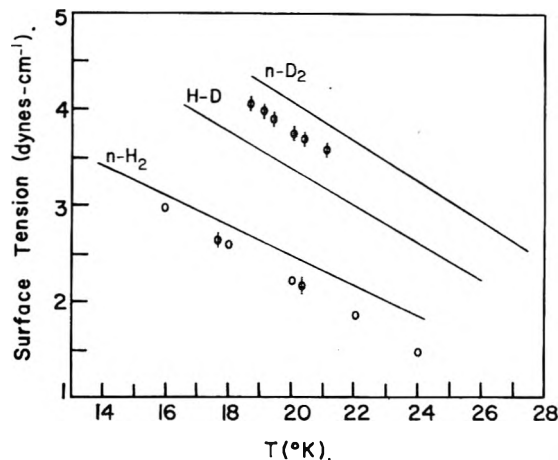


Fig. 6.—Surface tension of liquid n-H₂, H-D, and n-D₂. The curve consists of the calculated values and the experimental points O and φ are taken from ref. 21 and 22, respectively.

and surface tension, γ , is then calculated from the expression

$$\gamma = \sum_i \Delta G_i \frac{0.9165}{V_i} \left(\frac{V_s}{N} \right)^{1/3} \quad (17)$$

where $0.9165 (V_s/N)^{1/3}$ is the thickness of layers of close packing and ΔG_i is the excess Gibbs free energy of the i -th layer over that of the bulk liquid. The calculated values of the surface tension are

compared with the experimental values of Shelton and Man²³ and van Itterbeck.²⁴

It is interesting to note that the values of the critical temperatures obtained by extrapolating the surface tension curves to zero are 36.0, 37.7, and 39.9°K. for n-H₂, H-D, and n-D₂, respectively. These values compare very well with the values calculated above.

Discussion

The agreement between the calculated and experimental values of the thermodynamic properties of liquid hydrogen is, with the exception of vapor pressures at high temperatures, good. However, to obtain satisfactory values for the critical constants of hydrogen it was necessary to use (4) instead of (3). Unfortunately an expression for positional de-

(23) D. B. Shelton and D. B. Man, Report UCRL-3421, Univ. of Calif. Radiation Lab, May 15, 1956, p. 12.

(24) A. van Itterbeck. *Physica*, **7**, 325 (1940).

generacy which is applicable at all temperatures has not yet been obtained. Should such an expression be obtained it would not only provide a more satisfactory basis for the theory but would, in all probability, improve the agreement between the calculated and observed vapor pressures. Equation 5 was based on a random distribution of holes and molecules (Bragg-Williams approximation) and it therefore seems possible that a more satisfactory partition function could be obtained by the use of a better approximation, such as the quasi chemical approximation. This is presently being investigated.

Acknowledgments.—The authors wish to thank the staff of the University of Utah Computing Center for their assistance in programming this research for a Burrough's 205 Datatron computer, and Mrs. Barbara Staker, who assisted in the preparation of the figures.

CHEMISTRY OF COÖRDINATION COMPOUNDS. IV. ENOL STABILITY OF β -DIKETONES AND THE RATE OF FORMATION OF MONOENOLATOCOPPER(II) IONS

BY ALFRED V. CELIANO,

Department of Chemistry, Seton Hall University, South Orange, N. J.

MICHAEL CEFOLA, AND PHILIP S. GENTILE

Department of Chemistry, Fordham University, Bronx 57, N. Y.

Received December 26, 1961

The kinetics of reactions between copper(II) ion and a series of β -diketones in methanol was investigated conductometrically in the temperature range -27 to 0° . The reactions followed second-order kinetics, first order with respect to copper(II) ion and first order with respect to the enol form of the β -diketone. The rate of first complex formation decreases with increasing stability of the enol tautomer. Such behavior is attributed to the electron withdrawing capacity of the various groups substituted at the α - and γ -carbon atoms.

Introduction

In a previous communication¹ the kinetics of formation of monoacetylacetonatocopper(II) ion (first complex) was reported. It was concluded that the reaction involves a direct reaction of Cu(II) ion with the enol form of acetylacetone with no prior ionization of the β -diketone. The present study was undertaken to determine the effect of variation of structural and electronic factors in β -diketones on the rate of first complex formation with the same metal ion. The ligands chosen were benzoylacetone, *p*-chlorobenzoylacetone, *p*-nitrobenzoylacetone, *p*-methoxybenzoylacetone, and dibenzoylmethane. The structural changes, from ligand to ligand, consist of modifications of acetylacetone in positions not directly involved in bonding to the metal ion. It therefore seems reasonable to assume that the rate law applicable to the rate of formation of monoacetylacetonatocopper(II) ion is likewise applicable to the rate of formation of first complexes of copper(II) ion with the remaining β -diketones. This assumption is verified by the fact that the same integrated rate

equation (second order) may be employed successfully, within experimental error, to describe the rate of first complex formation for all the ligands.

Experimental

Experimental details were reported in a previous communication.¹ Eastman Kodak White Label benzoylacetone and dibenzoylmethane were recrystallized twice from methanol. The *p*-chloro-, *p*-nitro-, and *p*-methoxybenzoylacetones were synthesized by the method of Hauser, *et al.*²⁻⁴ The *p*-nitro- and *p*-chlorobenzoylacetones were recrystallized twice from cyclohexane and twice from methanol. *p*-Methoxybenzoylacetone was recrystallized three times from cyclohexane. The solid diketones were all dried, *in vacuo*, over phosphorus pentoxide at temperatures slightly below their melting points. The purity of the ligands was determined by titration following the method of Fritz⁵ and was found to be: dibenzoylmethane, 99.6%; benzoylacetone, 99.0%; *p*-chlorobenzoylacetone, 99.7%; *p*-methoxybenzoylacetone, 99.6%; *p*-nitrobenzoylacetone, 99.5%. The enol content of the ligands in solutions was determined by a modified Kurt Meyer bromine titration method.⁶ The

(2) C. Hauser and J. Adams, *J. Am. Chem. Soc.*, **66**, 345 (1944).

(3) C. Hauser, F. W. Swamer, and E. Ringler, *ibid.*, **70**, 4023 (1948).

(4) C. Hauser and H. Walker, *ibid.*, **68**, 2742 (1946).

(5) J. S. Fritz, *Anal. Chem.*, **24**, 674 (1955).

(6) S. R. Cooper and R. P. Barnes, *Ind. Eng. Chem., Anal. Ed.*, **10**, 379 (1939).

(1) A. V. Celiano, M. Cefola, and P. S. Gentile, *J. Phys. Chem.*, **65**, 2194 (1961).

TABLE I
ENOL CONTENT OF β -DIKETONES IN METHANOL
 $\mu = 0.1$, $[\text{H}_2\text{O}] = 5.56 \times 10^{-1} M$

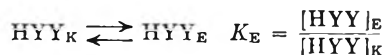
Ligand	0°		-17.08°		-27.42°	
	% Enol	K_E	% Enol	K_E	% Enol	K_E
HAA	77.8 \pm 0.2	3.51	74.9 \pm 0.1	2.98	73.4 \pm 0.1	2.76
HBA	92.5 \pm .2	12.33	91.9 \pm .2	10.99	90.5 \pm .3	9.53
HDBM	97.3 \pm .1	36.04	96.1 \pm .1	24.64	96.4 \pm .1	26.77
HMeOBA	92.6 \pm .2	12.68	90.0 \pm .1	9.42	89.4 \pm .1	8.43
HCIBA	93.1 \pm .1	13.49	95.2 \pm .5	19.83	93.1 \pm .1	10.36
HNO ₂ BA	94.7 \pm .2	17.86

ionic strength of all solutions was set at 0.1 by the addition of NaClO₄. The rates of reaction were followed conductometrically in methanol solutions exactly as reported in a previous communication.¹

Kinetics of First Complex Formation

The following notations shall be used in the ensuing discussions

- [] = concentration
 [HYY]_K = β -diketone in the keto form
 [HYY]_E = β -diketone in the enol form
 [YY⁻] = enolate ion
 [CuYY⁺] = mono-enolato-copper(II) ion
 K_E = concn. quotient for the process



- k_1 = specific rate constant for first complex formation

- HAA = acetylacetone
 HBA = benzoylacetone
 HDBM = dibenzoylmethane
 HMeOBA = *p*-methoxybenzoylacetone
 HCIBA = *p*-chlorobenzoylacetone
 HNO₂BA = *p*-nitrobenzoylacetone

Enol Content of Ligands.—Since it has been shown¹ that the ligand species reacting in the rapid formation of monoacetylacetonato-copper(II) ion is the enol tautomer of the β -diketone, the enol content of all ligands was determined in solutions whose characteristics were similar to those employed in the kinetic determinations. In the latter determinations a period of 2 to 4 hr. elapsed from making up the reactant solutions to the time they were mixed. It has been determined that 2 hr. suffice for the establishment of tautomeric equilibrium. Table I lists the percentage enol and concentration quotient for enolization at the temperatures used in the kinetic determinations.

Kinetics of First Complex Formation.—For the reaction



The specific rate constants for first complex formation were determined graphically from the second-order rate equation for a non-reversible process

$$\frac{2.303}{(a-b)} \log \frac{b(a-x)}{a(b-x)} = k_1 t \quad (2)$$

where a = initial concentration of Cu²⁺, b = initial concentration of enol tautomer, and x = concentration of first complex at time t . The justification for the applicability of eq. 1, at least up to 60% completion of reaction, already has been considered¹ in the case of acetylacetone. That the same approach is valid for the other ligands presently under consideration is not only confirmed by the fact that

linear relationships are obtained well past 60% completion, but also by the fact that of all the complexes concerned, CuAA⁺ is the least stable.⁷ As the position of equilibrium proceeds to the right, the effect of the reverse reaction becomes more negligible, thus allowing eq. 1 to be used to an even higher per cent completion of the reaction. Table II lists the specific rate constants for first complex formation determined graphically. The values are the average of three determinations and the deviation noted is the average deviation of the calculated values from data covering only 60% completion of the reaction.

The temperature coefficients of the specific rate constants (which follow the Arrhenius equation, $k = Ae^{-E_a/RT}$, with good precision) were determined by the method of least squares and the entropies of activation were calculated from the relationship

$$k = (kT/h)e^{-E_a/RT} e^{\Delta S^*R} \quad (3)$$

The precision associated with the values of activation energies and entropies of activation were evaluated from the slope and intercept of the plot of $\log k_1$ vs. $1/T$. Table III lists the values of E_a and ΔS^* for the various ligands.

Effect of Enol Stability on Rate of Complex Formation.—A comparison of the data presented in Tables I and II indicates that in all cases the rate of first complex formation decreases with increasing stability of the enol tautomer of the various ligands. Figure 1, in which $\log K_E$ is plotted vs. $\log k_1$ for the various ligands at 0°, shows the relationship to be linear and therefore to be in the form of a Hammett linear free energy relationship. However, the simple Hammett equation⁸

$$\log(k/k_0) = \sigma \rho \quad (4)$$

utilizing σ values compiled by Jaffe,⁹ does not apply to the specific rate constants of *p*-phenyl substituted benzoylacetones. This may be due to the effect of resonance of the functional groups with the reaction center,¹⁰ but sufficient data for the reaction under study has not been amassed to make this statement more than conjectural.

Table IV lists the slopes of the line obtained from a plot of $\log K_E$ vs. $\log k_1$ as well as the correlation coefficient, r . A value of unity for r in-

(7) A. E. Martell and M. Calvin, "Chemistry of the Metal Chelate Compounds," Prentice-Hall, Inc., New York, N. Y., 1953, pp. 550-551.

(8) L. P. Hammett, "Physical Organic Chemistry," McGraw-Hill Book Co., New York, N. Y., 1940, p. 184.

(9) H. H. Jaffe, *Chem. Rev.*, **53**, 191 (1953).

(10) R. J. Taft in "Steric Effects in Organic Chemistry," M. S. Newman, Editor, John Wiley and Sons, Inc., New York, N. Y., 1956, p. 676.

TABLE II

SPECIFIC RATE CONSTANTS OF FORMATION OF MONOENOLATOCOPPER(II) ION IN METHANOL
 $\mu = 0.1$, $[H_2O] = 5.56 \times 10^{-1} M$, $[Cu^{2+}]_{initial} = 2.46 \times 10^{-3} - 4.93 \times 10^{-3}$; $[HYY]_E_{initial} = 1.7 \times 10^{-3} - 7.60 \times 10^{-3}$

Ligand	k_1 (l. mole ⁻¹ sec. ⁻¹)		
	0.00°	-17.08°	-27.42°
HAA	$1.00 \times 10^4 \pm 0.04$	$2.72 \times 10^3 \pm 0.1$	$1.09 \times 10^3 \pm 0.06$
HBA	$9.3 \times 10^2 \pm .5$	$2.03 \times 10^2 \pm .08$	$6.5 \times 10^1 \pm .3$
HDBM	$1.07 \times 10^2 \pm .5$	$1.50 \times 10^1 \pm .06$	$5.23 \pm .2$
HCIBA	$6.2 \times 10^2 \pm .3$	$1.45 \times 10^2 \pm .06$	$4.7 \times 10^1 \pm .2$
HMeOBA	$8.9 \times 10^2 \pm .5$	$2.09 \times 10^2 \pm .09$	$6.45 \times 10^1 \pm .15$
HNO ₂ BA	$4.50 \times 10^2 \pm .15$

TABLE III

ENERGY AND ENTROPY OF ACTIVATION

Ligand	E_a , kcal. mole ⁻¹	ΔS^* (e.u.) 273°K.
HAA	10.8 ± 0.1	-2.6 ± 0.3
HBA	$12.9 \pm .1$	$+0.4 \pm .4$
HDBM	$14.9 \pm .3$	$+3.2 \pm .6$
HCIBA	$12.5 \pm .2$	$-1.7 \pm .6$
HMeOBA	$12.7 \pm .2$	$-0.2 \pm .4$

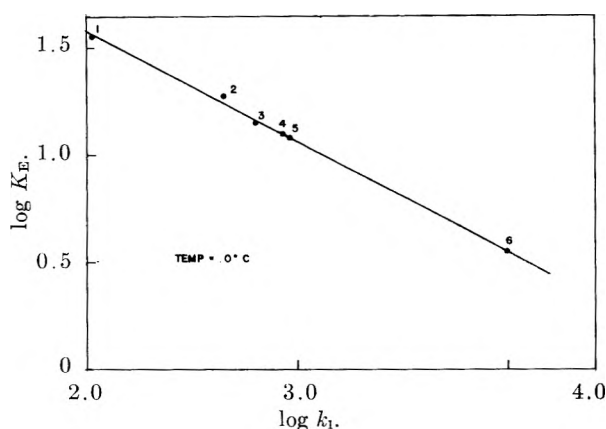


Fig. 1.—Log plot of K_E vs. k_1 for ligands at 0°: 1, HDBM; 2, HNO₂BA; 3, HCIBA; 4, HMeOBA; 5, HBA; 6, HAA.

indicates perfect linear correlation of the form $y = mx + b$. These relationships indicate that the activated complex in the formation of mono-enolato-Cu(II) ion not only involves attraction between the ligand and the metal ion but also a perturbation of the enol chelate ring, a perturbation which becomes more difficult with increasing stability of the enol tautomer.

TABLE IV

t , °C.	$d \log K_E / d \log k_1$	r
0.00	-0.503 ± 0.003	0.92
-17.04	$-.41 \pm .02$.78
-27.42	$-.43 \pm .02$.83

The exact manner in which the thermodynamic parameters E_a and ΔS^* should vary from reaction to reaction so as to indicate that a single mechanism is operative has been the subject of much investigation. Weinstein and Fainberg¹¹ have pointed out that a discussion of these parameters without consistent choice of standard state is not unambiguous. Leffler¹² has shown, however, that a linear relationship between these quantities is

(11) S. Weinstein and A. H. Fainberg, *J. Am. Chem. Soc.*, **81**, 46 (1959).

(12) J. Leffler, *J. Org. Chem.*, **20**, 1306 (1955).

“evidence favoring a constant mechanism for a related series of reactions.” It might be thought that the factors increasing enol stability should affect the rate of complex formation in similar fashion for all ligands. Examination of Fig. 2, in which the activation energy is plotted vs. the entropy of activation, indicates that such is not the case.

As first one methyl group and then the second in acetylacetone is replaced with phenyl groups, enol stability increases while the rate of complex formation decreases, because the energy and entropy of activation both increase. However, as benzoylacetone is substituted in the *para* position with electron withdrawing groups, enol stability increases while the rate of complex formation decreases, but now because the energy and entropy of activation both decrease, the decrease in entropy of activation being the preponderant factor.

The enolic content of any carbonyl compound is greatly modified by two factors, solvent and structure. Some investigators¹³ claim that the enolizing tendency of non-cyclic diketones is more affected by electronic and polar factors than by steric effects. On the other hand, there are investigators who claim that steric factors predominate. Hammond claims¹⁴ that substitution of methyl groups in acetylacetone with bulky substituents favors the *cis* keto form which, from electrostatic consideration, is unfavorable and hence eliminated by enol formation. Zuffanti,¹⁵ on the other hand, attributes the high enol content of dibenzoylmethane to the electron sink capacity of the phenyl groups. Although not underestimating steric factors, the latter explanation seems to have merit when we consider that *p*-nitro- and *p*-chlorobenzoylacetone are more enolic than benzoylacetone. These substituents would tend to increase the electron sink capacity of the phenyl group and therefore increase enol content. If such be the case, the direction in which the energy and entropy of activation change from ligand to ligand may be explained as follows. In the series, acetylacetone, benzoylacetone, dibenzoylmethane, increasing enol stability, attributed to the electron sink capacity of the phenyl groups, is associated with increasing entropy and energy of activation because of the increasing freedom of the electronic system of the phenyl groups to respond to the de-

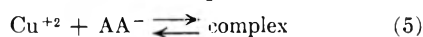
(13) F. Arndt, L. Loewe, and R. Ginkole, *Rev. fac. sci. univ. Istanbul.*, **A11**, No. 4, 147 (1946).

(14) G. Hammond in “Steric Effects in Organic Chemistry,” M. Neuman, Editor, John Wiley and Sons, Inc., New York, N. Y., 1956, p. 442 ff.

(15) S. Zuffanti, *J. Chem. Educ.*, **22**, 230 (1945).

mands of Cu(II) ion and the correspondingly greater difficulty of incipient ionization of the enolic hydrogen in the transition state. On the other hand, comparing *p*-chlorobenzoylacetone to benzoylacetone, increased enol stability of the *p*-chloro derivative, due to the intensification of the electron sink capacity of the phenyl group, is associated with decreasing entropy and energy of activation because of the diminished freedom of the electronic system of the phenyl group to respond to the demands of the Cu(II) ion and an increase in the ease with which the enolic hydrogen may be removed. Although data for *p*-methoxybenzoylacetone have been included in this paper, no attempt has been made to use these data in the discussion because all values for this system fall within the experimental error of the benzoylacetone system. The apparent anomaly in the behavior of this normally electron releasing group can only be explained when more data on the effect of such groups are available for the reaction under study.

Taft and Cook¹⁶ have estimated the minimum value of the specific rate constant for first complex formation between thenoyltrifluoroacetone and Cu²⁺ in water at 25° to be $>3 \times 10^6$ l. mole⁻¹ min.⁻¹. The enol content of this ligand was determined to be 1.8%. Using this value, the specific rate constant for the reaction between Cu²⁺ and the un-ionized enol tautomer of 2-thenoyltrifluoroacetone was estimated to be 10⁸ at 0° in methanol from Fig. 1. Fully recognizing the differences in temperature, solvent, and ionic strength, it still seems rather curious that both rate constants fall within two orders of magnitude of one another and that the rate of complex formation from enolate is slower than from the enol form. One would expect the rate of complex formation with the enolate ion to be much more rapid than complex formation with the enol form, an expectation borne out by the fact that the reaction was too rapid to be measured



with our apparatus. It may be that the limiting value obtained by Taft is in reality the k_1 of formation from the enol form. If one supposes that establishment of equilibrium between the enolate and the enol is rapid (Pearson and Dillon¹⁷ estimate k ion recombination for acetylacetone to be 6×10^8 l. mole⁻¹ sec.⁻¹ at 25°) the enol and enolate mech-

(16) R. J. Taft and H. Cook, *J. Am. Chem. Soc.*, **81**, 46 (1959).

(17) R. Pearson and R. Dillon, *ibid.*, **75**, 2439 (1953).

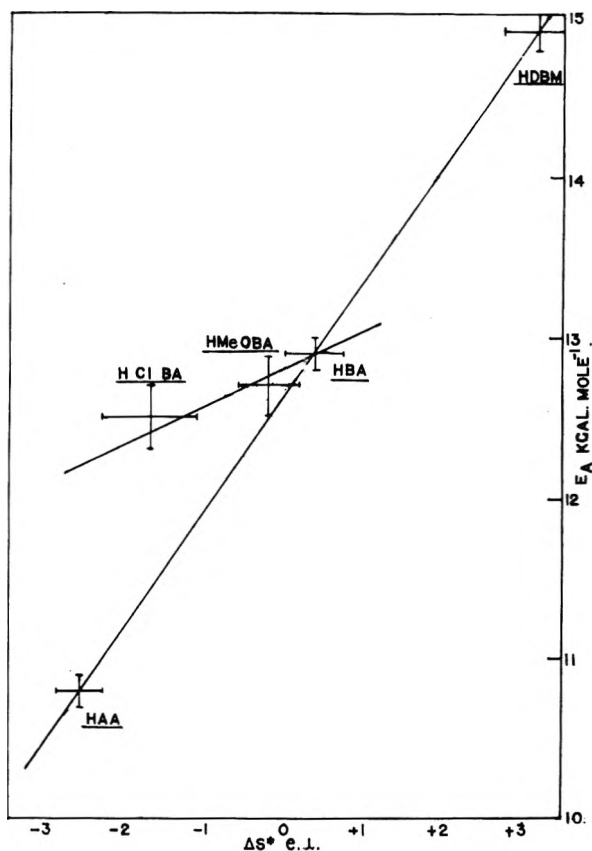
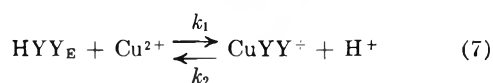
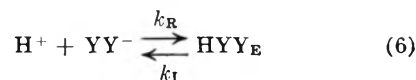


Figure 2.

anisms may be expressed by the same differential rate equation when the hydrogen ion concentration remains constant within a given experiment.



$$\frac{dx}{dt} = k_1[\text{HYY}]_E[\text{Cu}^{2+}] - k_2[\text{CuYY}^+][\text{H}^+] \quad (8)$$

$$= k_1 \frac{k_R}{k_1} [\text{H}^+][\text{YY}^-][\text{Cu}^{2+}] - k_2[\text{H}^+][\text{CuYY}^+] \quad (9)$$

Acknowledgment.—We are grateful to the AEC for support of this work *via* the contract AT-(30-1)-906.

ADSORPTION AND BOUNDARY FRICTION ON POLYMER SURFACES

BY TOMLINSON FORT, JR.

*Fiber Surface Research Section, Textile Fibers Department, E. I. du Pont de Nemours and Company, Inc.
Kinston, North Carolina*

Received January 2, 1962

A study was made of the boundary friction and lubrication of nylon, polyethylene terephthalate, polyacrylonitrile, cellulose acetate, and polytetrafluoroethylene surfaces. Sliding conditions were fixed so that reduction in friction effected by a given lubricant was a function of its adsorption on the polymer. Objects of the work were to (1) determine the frictional behavior of the various polymers and (2) show how different polymeric substrates affect the film forming tendencies and adsorbed film properties of the lubricants. The characteristic friction of clean and lubricated polymers increased with decreasing load and passed through a maximum as speed was raised. Friction decreased linearly with increasing lubricant chain length for homologous series of liquid acids, alcohols, and alkanes. Solid lubricants all reduced friction to a low level. Easy sliding was achieved by slip agents whose molecular skeleton consisted of long, unbranched hydrocarbon chains, and these were most effective when applied from a solvent with this same optimum structure. Elevated temperatures increased friction of both clean and lubricated polymers. Optical and electron micrographs correlated friction level with polymer surface damage. Monomolecular films gave low friction and were quite resistant to abrasive wear. Results are interpreted in terms of the adhesion theory of friction modified to take account of the soft, thermoplastic nature of polymeric solids, and weak adsorption of the lubricant molecules to the relatively inert rubbing surfaces.

Introduction

When one body slides over another, friction always resists the motion. If conditions are such that the rubbing surfaces actually touch (boundary friction), the magnitude of this resisting force is determined by a large number of factors which include the hardness and shear characteristics of the solids and the extent to which their surfaces are covered by an adsorbed lubricant film.¹ Thus, friction measurements provide a useful means of studying both the bulk and surface properties of solids. This paper describes a systematic investigation of the boundary friction and lubrication of polymers.

A number of studies of polymer friction have been reported²⁻⁵ as well as a few on polymer boundary lubrication.⁶⁻⁸ Much of this work has originated from interest in the friction and lubrication of textile fibers. Results (through 1959) are summarized in the recent text by Howell, Mieszkis, and Tabor.¹⁰ Impetus for other work has come from the increasing use of plastics (nylon, "Teflon,"¹¹ etc.) in gears and bearings.¹² Many of the reported studies have emphasized the engineering applications of the results. More work of a fundamental nature, especially in the area of polymer boundary lubrication, is badly needed.

In this investigation, friction coefficients were measured for samples of five different plastics sliding under a variety of conditions of load, speed, and temperature, both in the presence and absence

of boundary lubricants. Results are explained in terms of the adhesion theory of friction, making allowances for the soft, thermoplastic nature of the rubbing solids. The lubricants studied were all classical adsorbing compounds whose properties as monolayers on high energy surfaces are well known. Comparison of these results with those of similar studies on other surfaces showed how the low energy polymer substrates affected the film forming tendencies and adsorbed film properties of the lubricants.

Experimental

A. Apparatus.—The apparatus used is shown schematically in Fig. 1. The basic parts are a rotating, variable speed turntable against which the test film is pressed and a counterbalanced, pivot-mounted lever arm to one end of which is attached a hemispherical polymer slider. As the table rotates, friction between film and slider induces a torque in the arm which is measured by a strain gage and recording system.

The lever arm was mounted on sets of ring and thrust bearings which permit free movement in the vertical plane and rotation in the horizontal plane. On one end of the arm is a chuck which holds the slider and has a flat top on which weights can be placed. At the other end are coarse and fine counterbalancing weights.

The turntable is a Boston Gear Reducer, Model VLW 13, 900:1 gear ratio (Boston Gear Works, Quincy 71, Mass.), with a 5-in. diameter stainless steel plate mounted on the slow speed shaft. A circular slot was cut in the underside of this plate, just large enough to contain a 400-watt "Chromalox" type A ring heating element (Edwin L. Wiegand Co. Pittsburgh, Pa.). Turntable temperature is regulated by an "Amplitrol" heater control unit (Thermo Electric Manufacturing Co., Dubuque, Iowa). The test film is held to the upper side of the plate by a "Teflon" ring gasket and a steel clamp. The drive unit is a 1/2-horsepower "Craftsman" capacitor motor (Sears, Roebuck and Co., Greensboro, N.C.), coupled to a Revco Model 142X "Zero Max" Variable Speed Unit (Revco Inc., Minneapolis, Minn.). The turntable was purposely overpowered to ensure that its speed would not be slowed by high frictional forces.

In order to reduce vibrations to a minimum, the motor and variable speed unit were screwed to one base plate, the rest of the apparatus to another. These plates then were mounted on separate 1-in. thick sheets of foam rubber. The only connection between them is a wide belt cut from a length of soft, thin-walled rubber tubing which effectively insulates the motor from the friction unit.

B. Polymer Films and Sliders.—Friction tests were made on plasticizer-free samples of five different polymers: polyhexamethylene adipamide (nylon), polyethylene terephthalate (P.E.T.), polyacrylonitrile (A.N.P.), cellulose acetate (C.A.), and polytetrafluoroethylene (P.T.F.E.). The films were: nylon, 10-mil Polypence 101 nylon from

(1) F. P. Bowden and D. Tabor, "The Friction and Lubrication of Solids" Oxford at the Clarendon Press, 1950.

(2) K. V. Shooter and R. H. Thomas, *Research* (London), **2**, 533 (1949).

(3) K. V. Shooter and D. Tabor, *Proc. Phys. Soc.*, **B65**, 661 (1952).

(4) R. C. Bowers, W. C. Clinton, and W. A. Zisman, *Mod. Plastics*, **31**, 131 (1954).

(5) M. W. Pascoe and D. Tabor, *Proc. Roy. Soc. (London)*, **A235**, 210 (1956).

(6) R. C. Bowers, W. C. Clinton, and W. A. Zisman, *Ind. Eng. Chem.*, **46**, 2416 (1954).

(7) M. W. Pascoe, Ph.D. Dissertation, Cambridge University, 1954, reported by D. Tabor, in *Wear*, **1**, 5 (1957-1958).

(8) J. A. Greenwood and D. Tabor, *Proc. Phys. Soc. (London)*, **71**, 989 (1958).

(9) T. Fort, Jr., and J. S. Olsen, *Textile Res. J.*, **31**, 1007 (1961).

(10) H. G. Howell, K. W. Mieszkis, and D. Tabor, "Friction in Textiles," Interscience Publishers, Inc., New York, N. Y., 1959.

(11) Registered trademark for Du Pont's TFE-fluorocarbon resin.

(12) A. J. G. Allen, *Lubrication Eng.*, **14**, 211 (1958).

Polymer Corp. of Pennsylvania, Reading, Pa.; P.E.T., 7.5-mil Type D "Mylar"¹³ from E. I. du Pont de Nemours and Co., Wilmington, Del.; P.T.F.E., 2-mil "Teflon" from United States Gasket Co., Camden, N. J.; C.A. and A.N.P., laboratory prepared samples with thicknesses of 1.5 and 1.0 mils, respectively. A new piece of film was used for each experiment.

Sliders were made from bulk samples of these same polymers. They were first machined to 1/4-in. diameter cylinders; then the ends were carefully rounded and polished to a hemispherical shape. The sliders were periodically re-polished between experiments.

Before each measurement, both film and slider were extracted with carbon tetrachloride in a Soxhlet apparatus for a minimum of 45 min. to remove any adsorbed organic contaminants.

C. Lubricants.—The lubricants used were always the best commercially available. Liquids were further purified either by distillation or percolation through silica gel and alumina adsorption columns, and solids by repeated recrystallization from an appropriate solvent, until their physical constants agreed with the accepted literature values.

D. Conditions.—Experiments with liquid lubricants were performed under a pool of the liquid. Solids were applied to the polymer surfaces from hexane solution. After the solvent had evaporated, excess lubricant was removed by wiping the film with successive pieces of clean, dry filter paper. This procedure was not critical, and the friction values listed are the easily reproducible low coefficients observed for each sliding system.

All friction coefficients were measured in a room maintained at 22° and 65% relative humidity. Friction determinations were run at least in duplicate, and values were reproducible to ± 0.02 unit. Unless stated otherwise, all measurements were made at 1000 grams load, room temperature, and 10^{-3} cm./sec. sliding speed. Stick-slip sliding was generally observed with A.N.P., not with the other polymers. Recorded frictions for A.N.P. are static coefficients, obtained from the peak in the stick-slip curves, when average sliding speed was 10^{-3} cm./sec. Data for the other polymers are kinetic coefficients at this same speed and load.

Results and Discussion

A. Nature of Polymer Friction.—According to the adhesion theory of friction as originally worked out for sliding metals,¹ the magnitude of the boundary frictional force may be arrived at as follows. When two solid bodies are pressed together, intimate molecular contact is made, and true cold weld junctions are formed between asperities in their surfaces. The asperities then crush down until the junction area (A) is sufficient to support the applied load (W). If the surfaces then are slid over one another, the frictional force $F = AS$ where S is the shear strength of the junctions. Since metals deform plastically, A is proportional to W or $A = W/P$, where P is a characteristic constant of the metal, called the yield pressure. The friction coefficient $f = F/W = S/P$ is determined by the hardness and shear properties of the metals and is independent of the contact geometry and pressure between them.

Friction coefficients observed at 1000 g. load for the unlubricated polymers tested here were: C.A., 0.59; A.N.P., 0.49; nylon, 0.45; P.E.T., 0.29; P.T.F.E., 0.07. No other data are available for C.A., A.N.P., or P.E.T. However, the nylon coefficient of 0.45 may be compared with the static coefficient of 0.46 and kinetic coefficient of 0.37 observed for this same polymer by Bowers, Clinton, and Zisman,⁴ a value of ca. 0.35 found by Tabor,¹⁴

(13) Registered trademark for Du Pont's polyester film.

(14) D. Tabor, *Wear*, **1**, 5 (1957-1958).

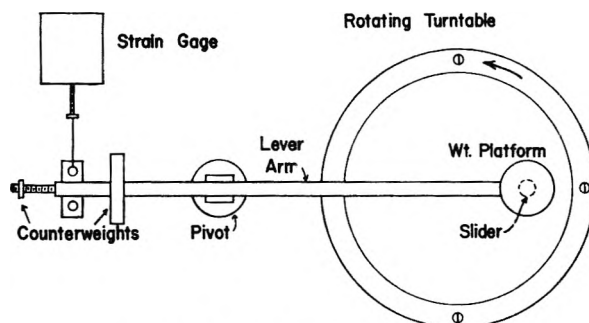


Fig. 1.—Friction apparatus for films.

and the S/P ratio of 0.6 found by Zisman, *et al.*,⁴ from measurements on the bulk polymer.¹⁵

The reasonable agreement (within a factor of two) of the friction coefficients with the S/P ratio for nylon, and similar checks found for other polymers,¹⁰ support the adhesion mechanism. However, P.T.F.E. is exceptional. Measurements by Bowers, Clinton, and Zisman⁴ resulted in an S/P ratio of 0.42 for this plastic; yet the observed friction coefficient was only 0.07. Easy sliding also was found for P.T.F.E. by King and Tabor,¹⁶ Flom and Porile,¹⁷ Allan,¹⁸ and others. The explanation is believed to be this polymer's very low surface energy which, combined with its relatively high yield pressure, leads to weak adhesion over a small contact area so that slip resistance is always low.¹⁰

B. Boundary Friction and Abrasive Wear.—Boundary sliding of metals is associated with much abrasive wear to the rubbing surfaces, the result of breaking the weld junctions formed when they were pressed together. To gain a better understanding of polymer friction, a study was made of the wear scars (scratches, surface damage) produced in the various films by one traverse of an unlubricated polymer slider. This investigation showed the following: 1. There were larger differences in the roughness of the unabraded films, but there was no obvious relationship between film appearance and friction level. 2. There was considerable permanent "grooving" of all the films by the polymer sliders. 3. Some of the film surfaces showed clear evidence of torn adhesive junctions after the slider had passed over them. 4. There was no evidence of increase in polymer surface damage with distance of sliding.

Some representative electron micrographs are shown in Fig. 2.¹⁹

Direction in which the slider moved is the same in each plate. The deep grooves seen in the unabraded nylon and P.T.F.E. surfaces are extrusion marks formed when these films were made. These

(15) To make certain that the metal turntable was not influencing the friction coefficients measured here, experiments were performed on several thicknesses of the various films. No dependence of friction on film thickness was found. If the turntable were a factor, friction of the thin films would have been less than that of the thick ones.⁴

(16) R. F. King and D. Tabor, *Proc. Phys. Soc. (London)*, **B66**, 728 (1953).

(17) D. G. Flom and N. T. Porile, *J. Appl. Phys.*, **26**, 1088 (1955).

(18) A. J. G. Allan, *J. Polymer Sci.*, **44**, 461 (1957).

(19) The electron micrographs shown in Fig. 2, 8, and 9 were made from metal replicas of the film surfaces. Shadowing angle was 30° from the plane of the surface and normal to the direction of abrasion.

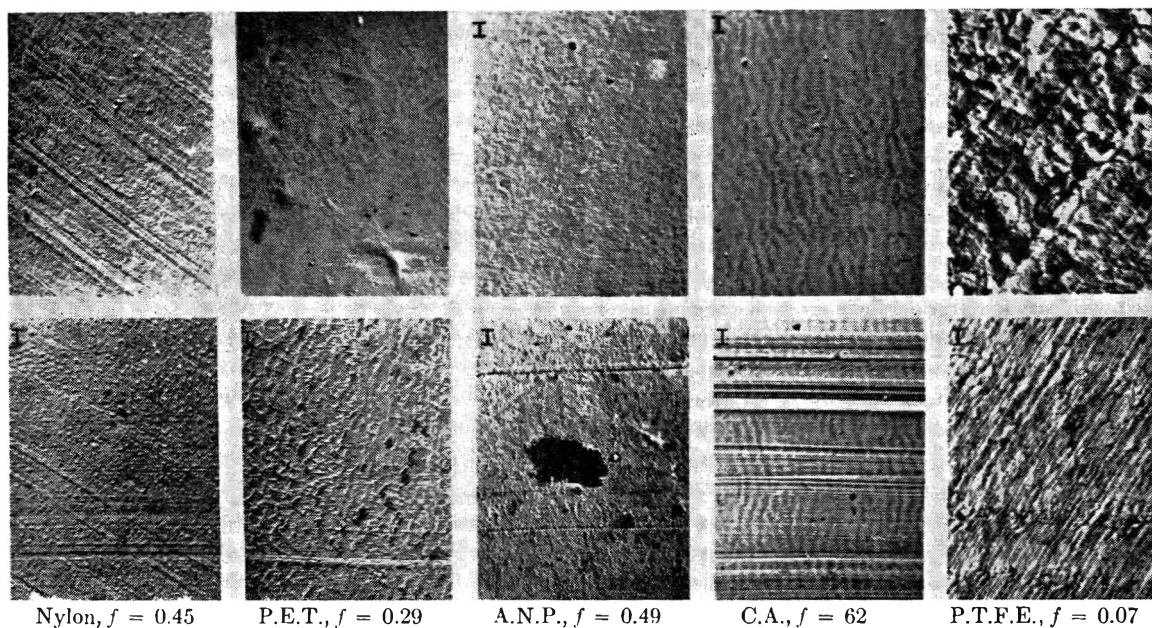


Fig. 2.—Frictional surface damage to polymer films. Electron micrographs made before (upper row of plates) and after (lower row of plates) one traverse of an unlubricated polymer slider. A 1- μ scale is shown in the upper left corner of each plate.

marks are not found on P.E.T., nor on the two solvent-cast films (C.A. and A.N.P.).

The observed tearing of the various film surfaces confirms the adhesion mechanism of polymer friction. Another factor which must contribute to slip resistance is the grooving or ploughing of the films by the sliders. This effect is particularly evident on P.T.F.E., whose surface was actually smoother after abrasion than before.

Inspection of wear tracks on P.E.T. film after *ca.* $1/15$ and $3/4$ in. of sliding (comparison not illustrated) showed no increase in either track width or surface damage as sliding progressed which, contrary to the behavior reported for metals,²⁰ argues against junction growth in polymer friction.

C. Mechanism of Boundary Lubrication.—According to the adhesion theory, when two lubricated surfaces are pressed together, some of the lubricant is trapped between them as they deform. If the surfaces then are slid past one another under high load-low speed conditions, most of the slip agent is pushed aside and has no influence on friction. However, if part of the lubricant is adsorbed, it remains in place and reduces the area of the junctions formed between unlubricated surfaces.¹ Part of the load is supported by junctions of lower shear strength, and the equation for frictional force may be rewritten: $F = A[\alpha S_c + (1 - \alpha)S_L]$, where A is the total area which supports the load, α is the fraction of A not covered by slip agent, S_c is the shear strength of junctions formed between clean surfaces, and S_L is the shear strength of junctions formed between lubricated surfaces. A good boundary lubricant adsorbs strongly to make α small and forms a film whose shear strength (S_L) has a minimum value.

To test this mechanism, a comparison was made of the friction coefficients and wear scars produced on P.E.T. when different boundary lubricants were

applied to this polymer's surface. The lubricants did lower friction and, as predicted, damage to the polymer surface was inversely proportional to ease of sliding. Some comparative pictures for clean and stearic acid lubricated films are shown as part of the high temperature study detailed in Fig. 8 and 9.

D. Friction and Load.—The friction coefficients of sliding metals are independent of the normal load because of the plastic deformation characteristics of these materials which lead to a linear relationship between junction area (A) and load (W). Polymers, which are softer solids that undergo significant elastic deformation ($A \sim W^{2/3}$) before plastic flow begins, exhibit friction coefficients which generally increase as load decreases. Data for the unlubricated plastics studied here are shown graphically in Fig. 3.

It is seen that graphs of friction *vs.* load, plotted on double logarithmic coordinates, yield a series of straight lines. Behavior of each polymer then is represented by the equation $f = F/W = bW^{(c-1)}$, where b and c are constants related to the strength and deformation characteristics of the junctions sheared in sliding. In every case, the value of c lies between $2/3$ and 1 , indicating the partly elastic-partly plastic deformation characteristics of the polymers. The data for nylon, C.A., and P.T.F.E. may be compared with that of Howell and Mazur²¹ and that collected by Allan,¹² who found c values of 0.9 , 0.96 , and *ca.* 0.92 for the three polymers, respectively.

Though most friction coefficients reported here were obtained at 1000 g. load, all polymer-lubricant systems were studied at both 100 and 1000 g. In addition, selected sliding systems were tested at other (intermediate) load levels. All the polymers behaved similarly, and some typical results are shown in Fig. 4. It is seen that: 1. The friction

(20) F. P. Bowden, *Endeavour*, **16**, 5 (1957).

(21) H. G. Howell and J. Mazur, *J. Text. Inst.*, **44**, T59 (1953).

coefficient of both clean and lubricated P.E.T. increased with decreasing load. 2. The lubricants tested did not change the load dependence of P.E.T. friction.

Both these facts are significant; the first because it implies that the minimum friction obtainable with lubricated polymers sliding at light loads may be considerably higher than the value of ~ 0.1 commonly found for metals covered with an adsorbed film; the second because it shows that (a) the action of the slip agents was limited to the surfaces of the polymers; *i.e.*, they did not act as plasticizers, and (b) the sliding conditions effected true boundary friction, even in the presence of hydrodynamic lubricants like hexadecane and oleic acid.

E. Friction and Sliding Speed.—Most experiments were performed at *ca.* 10^{-3} cm./sec. The friction of clean and lubricated P.E.T. was studied over a wide speed range. Results graphed in Fig. 5 show a marked dependence on speed over the entire range tested, with all sliding systems exhibiting a friction maximum at 10^{-2} – 10^{-3} cm./sec.

These results are reminiscent of the work reported by Burwell and Rabinowicz,²² who studied the friction of metals from 10^{-8} to 10^{-2} cm./sec. and noted a similar decrease below 10^{-5} cm./sec. They attributed their results to metallic "creep," or bulk flow of the test material, and hypothesized that all friction should approach zero at zero sliding speed. This same hypothesis may be offered to explain the results for P.E.T. "Creep" occurred at much higher speeds than Burwell and Rabinowicz observed it, but this is not surprising when one considers the differences between polymeric and metallic solids.

The transition from boundary to hydrodynamic sliding is marked by a large decrease in friction¹ and is certainly responsible for the behavior observed above 10^{-2} cm./sec. for liquid lubricated P.E.T. True boundary friction persisted to higher speeds with the mineral oil than with oleic acid, which was expected since the greater viscosity of the acid ($\eta = 30$ cp.) made it better able to support hydrodynamic sliding than the oil ($\eta = 8$ cp.). The relatively soft, easily deformable nature of the polymer also contributed to formation of the hydrodynamic film.

F. Effect of Temperature.—All the experiments described so far were performed at room temperature. It was of interest to study the effects of temperature on polymer friction. Data for the unlubricated plastics is collected in Fig. 6, which shows that elevated temperatures raised the friction of P.E.T., nylon, C.A., A.N.P., and P.T.F.E. and that nylon and A.N.P. exhibited a friction maximum within the temperature range studied (25–150°).²³

As discussed above, the magnitude of the boundary frictional force (F) is determined by two factors, the area of contact between the sliding surfaces (A) and the bulk shear strength of the test material: $F = AS$. The polymers studied here are thermo-

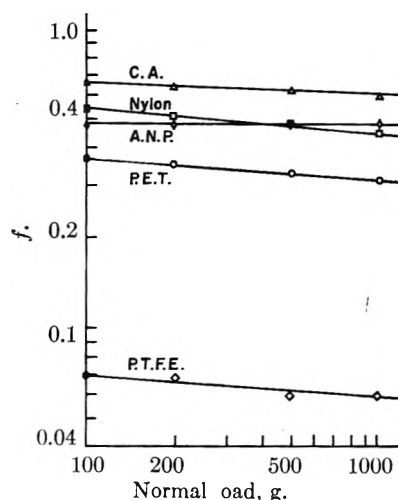


Fig. 3.—Effect of load on the boundary friction of polymers.

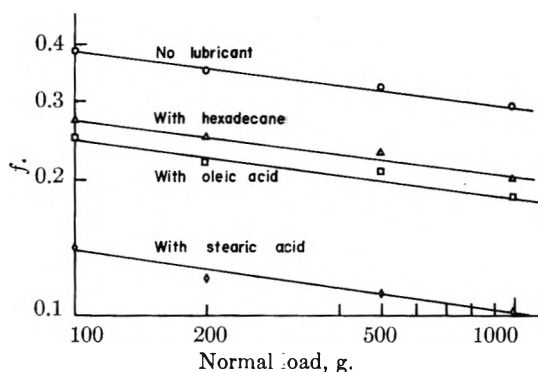


Fig. 4.—Effect of load on the boundary friction of polyethylene terephthalate.

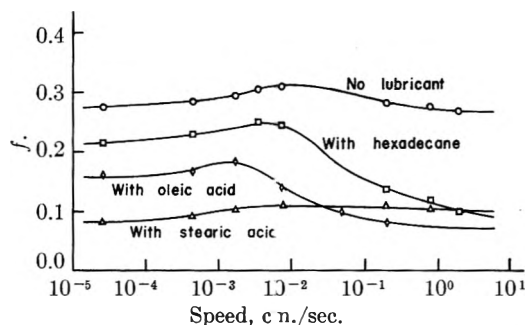


Fig. 5.—Effect of speed on the boundary friction of polyethylene terephthalate.

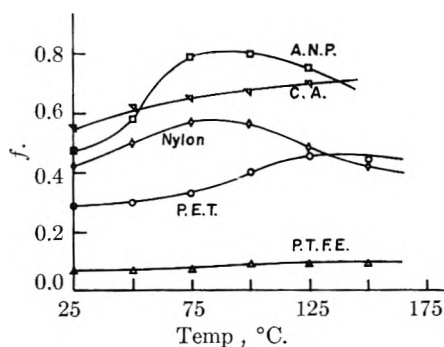


Fig. 6.—Effect of temperature on the boundary friction of polymers.

(22) J. T. Burwell and E. Rabinowicz, *J. Appl. Phys.*, **24**, 136 (1953).

(23) Recorded temperatures are those of the upper surface of the film whose lower surface pressed against an electrically heated plate. Some thermal gradient must have existed in the film.

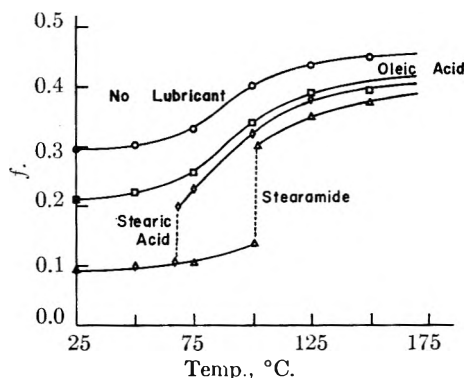


Fig. 7.— Effect of temperature on the boundary lubrication of polyethylene terephthalate.

plastic and softened as the temperature was raised. Softening increased A while decreasing S . When friction increased with temperature, the area factor predominated; when friction decreased, the reduced polymer shear strength was more important.

The effect of temperature on polymer friction and wear was studied in detail on P.E.T. The experiments showed that: 1. Friction of both clean and lubricated P.E.T. increased with temperature. 2. The increase in friction was associated with an increase in wear scar width and in severity of polymer surface damage. 3. All lubricants tested reduced friction over the entire temperature range studied. 4. At a given temperature, the presence of a slip agent did not affect the width of the wear scar but did reduce the severity of surface damage relative to that observed on the unlubricated polymer. 5. Solid lubricants produced lower friction surfaces than did liquids. When the film surface temperature was raised through the melting point of a solid, a large increase in friction was observed. This increased friction was associated with a large increase in abrasive wear.

Friction data and pictures which illustrate these points are shown in Fig. 7, 8, and 9.

Figure 8 confirms the explanation given above for the effect of temperature on polymer friction. At elevated temperatures, the softened P.E.T. allowed increased contact between the sliding surfaces, indicated by increased track (wear scar) width as the film got hotter. This increase outweighed the reduced shear strength of the softened polymer.

Comparison of Fig. 8 with Fig. 9 shows the reduction in surface damage effected by the boundary lubricant. As expected, wear, like friction, was reduced most at the lowest temperature. Comparison of the wear scars produced on stearic acid lubricated P.E.T. at 67 and 69° (just below and above the melting point of the acid) clearly shows the large increase in surface damage associated with the abrupt rise in friction when the lubricant melted.

Track widths listed in Fig. 8 and 9 are nearly the same at any given temperature, which confirms that the effects of the stearic acid were limited to the P.E.T. surface.

G. Lubrication by Homologous Series of Fatty Acids, Alcohols, and Alkanes.—A systematic investigation was made of the lubrication of P.E.T.

by homologous series of fatty acids, alcohols, and alkanes. Results, given in Fig. 10, show that: 1. All the solids tested reduced friction to the same low level and were much more effective than liquid lubricants. 2. At any given hydrocarbon chain length, liquid acids were more effective than liquid alcohols, which were better than liquid alkanes. 3. For each homologous series, friction decreased linearly with increasing liquid lubricant chain length.

This study was similar to those carried out on metals years ago by Hardy²⁴ and later by Bowden and Tabor.¹ The results are similar to those found by Hardy, and Bowden and Tabor, except for the large solid-liquid lubricant difference which was not observed on metals. They are consistent with work reported by Zisman, *et al.*,⁶ who found the friction of nylon was lowered more by polar lubricants like fatty acids than by non-polar materials like alkanes, and by Fort and Olsen,⁵ who observed large differences in the abilities of solid and liquid slip agents to reduce the boundary friction of textile yarns.

Long-chain compounds are classical materials so far as adsorption is concerned. Many studies^{25,26} have confirmed that such materials form oriented arrays at the surfaces on which they adsorb, with the terminal polar groups attached to the substrate and the long hydrocarbon chains extending out from the surface. In this configuration, the adsorbed films present a surface of minimum energy, the terminal methyl groups. The "strength" of such adsorbed films is a function of two factors, the adhesion of the terminal polar groups to the substrate and the cohesion between the adsorbed molecules in the film. The first of these is determined by the dipole moment of the terminal group, the energy of the substrate surface, and any specific interaction such as chemical or hydrogen bonding between substrate and adsorbed molecules. Cohesion between adjacent polar groups is due principally to hydrogen bonding, while interchain cohesion is caused by van der Waal's forces acting between methylene groups on adjacent molecules.

Assuming this model for the adsorbed film structure is correct on polymers, the order of affinities for the P.E.T. surface indicated by Fig. 10 is as expected, because it parallels both the order of dipole moment strengths and hydrogen bonding tendencies²⁷ of the terminal polar groups. Strength of adsorption increases with lubricant chain length as a result of intermolecular cohesion, each methylene group increasing the adsorption tendency by an equal amount because of adlineation of the hydrocarbon chains. Adsorption of liquid slip agents is

(24) Sir W. B. Hardy, "Collected Works," Cambridge University Press, 1936.

(25) N. K. Adam, "The Physics and Chemistry of Surfaces," Oxford University Press, 1941.

(26) E. G. Shafrin and W. A. Zisman, *J. Colloid Sci.*, **1**, 166 (1952).

(27) Steric hindrance prevents intermolecular hydrogen bonding in monolayers of the long-chain alcohols though bonding to the substrate is permitted. Both types of bonding are possible with the acids, neither with the alkanes.²⁸

(28) A. E. Alexander in "Surface Phenomena in Chemistry and Biology," J. F. Danielli, K. G. A. Pankhurst, and A. C. Riddiford, ed., Pergamon Press, New York, N. Y., 1958.

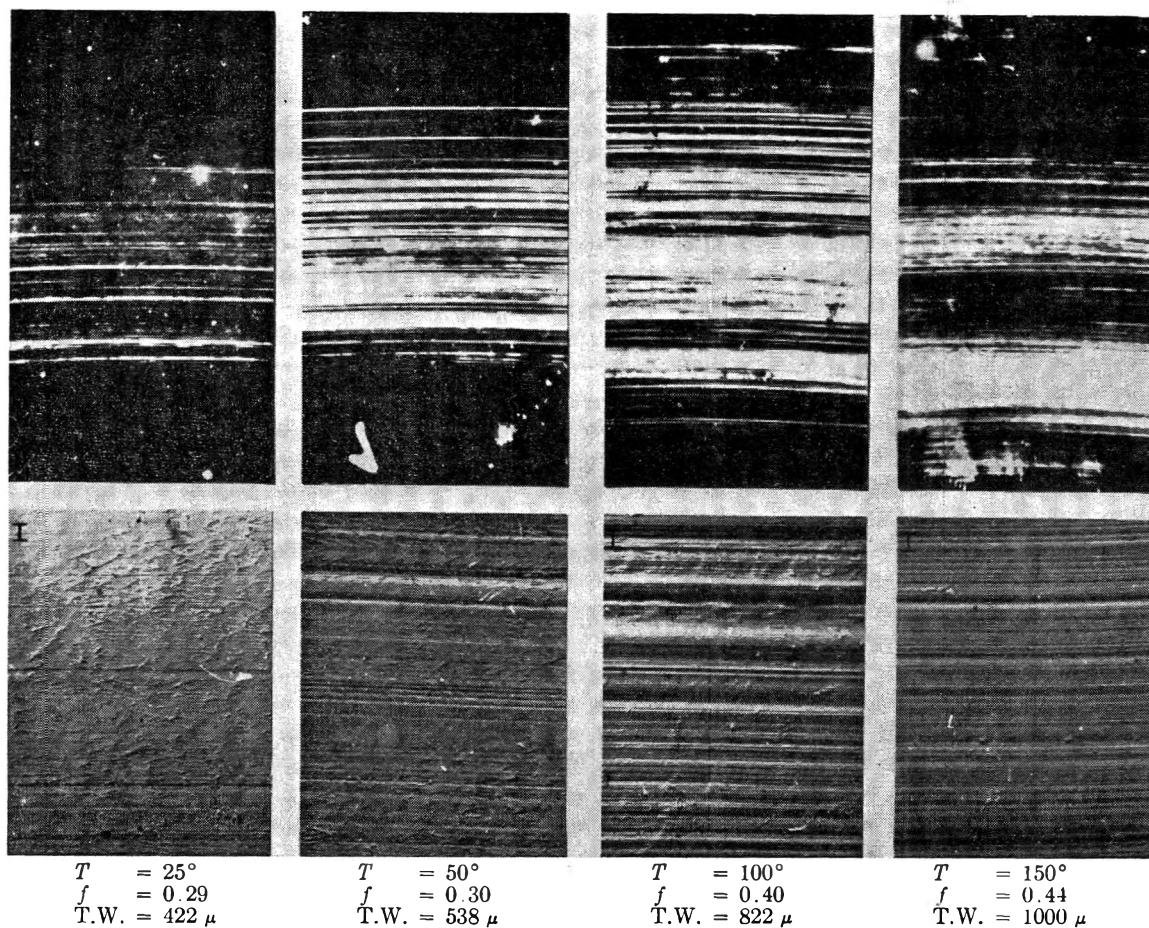


Fig. 8.—Friction and wear on unlubricated P.E.T. film. Optical reflection micrographs (upper row of plates) of the entire width of the wear track and electron micrographs (lower row of plates) of a portion of the wear track after one traverse of an unlubricated P.E.T. slider. Temperature, friction, and track width (T.W.) were as indicated. A 1- μ scale is shown in the plates taken from electron micrographs.

never very high, and friction is consequently never very low, because attraction between polar groups and substrate is always weak. When intermolecular cohesion is strong enough that the lubricants are solids, essentially complete coverage of the surface is effected without the necessity of strong adhesive forces. Friction is reduced to the same low level (*ca.* 0.1) irrespective of the adsorbate's chemical type, which must mean that the shear strength of all these solids is about the same.

H. Durability of the Lubricant Films.—Zisman and co-workers²⁹ found the mechanical durability of lubricant films cast on glass and stainless steel plates was a sensitive measure of the strength of adsorption of the lubricant to the substrate. They found that the number of repeat traverses of the slider which a given film could withstand was directly related to the strength of adhesion of adsorbate to substrate, and to the lubricant's chain length. It was of interest to test the durability of some of the solid fatty acid derivatives on polymers.

Octadecane and octadecyl alcohol were applied to P.E.T. and subjected to 100 repeat traverses of the slider at 0.01 cm./sec. and 1000 g. load. In no case was there evidence of breakdown of the film. (Friction did not increase.) This durability was far

greater than that found for similar materials on metals. Since the affinity of the slip agents for the polymer was small, the explanation must be the small yield pressure of the polymer, which kept the shearing force per unit of contact area (abrasive action) low, compared to metals. An alternate explanation, that of surface migration of the lubricant molecules to repair the film between traverses of the slider, is considered much less likely.

I. Lubrication by Monolayers.—Solid lubricants usually were applied to the polymers from a volatile solvent or sometimes simply rubbed in with a piece of filter paper. Both techniques resulted in an excess of slip agent on the test surface. Other workers have repeatedly shown³⁰⁻³² that a monomolecular lubricant film effects minimum friction of glass and metal surfaces. It was of interest to see whether this also was so for polymers.

A monolayer³³ of octadecyl alcohol was deposited on a sheet of P.E.T. film, by raising the horizontally oriented film through a monomolecular layer of the alcohol spread on water (using oleic acid as piston

(30) J. J. Bikerman, *Proc. Roy. Soc. (London)*, **A170**, 130 (1939).

(31) J. N. Gregory, C.S.I.R.O. (Australia) Tribophysics Division Report A74 (1943).

(32) O. Levine and W. A. Zisman, *J. Phys. Chem.*, **61**, 1068 (1957).

(33) K. B. Blodgett, *J. Am. Chem. Soc.*, **57**, 1007 (1935).

(29) R. C. Cottingham, E. G. Shafrin, and W. A. Zisman, *J. Phys. Chem.*, **62**, 513 (1958).

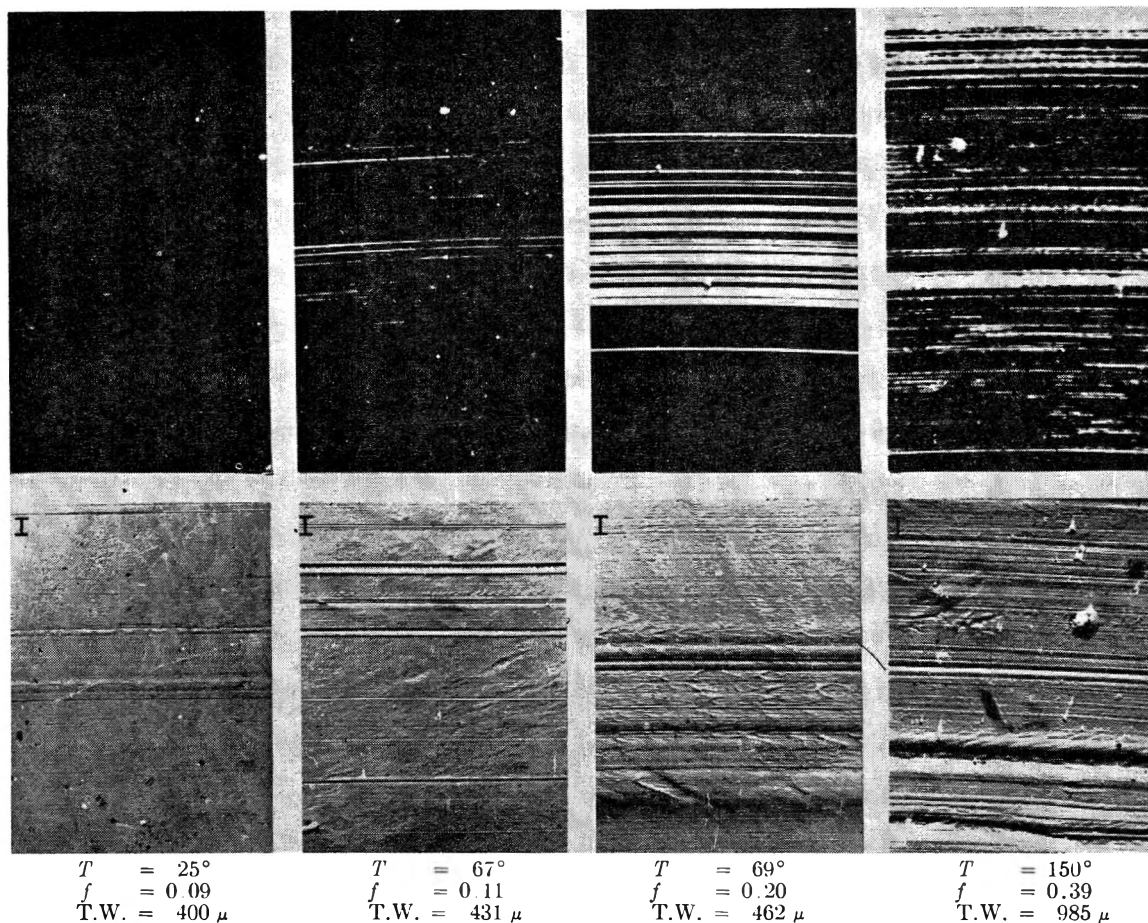


Fig. 9.—Friction and wear on stearic acid lubricated P.E.T. film. Optical reflection micrographs (upper row of plates) of the entire width of the wear track and electron micrographs (lower row of plates) of a portion of the wear track after one traverse of a stearic acid lubricated P.E.T. slider. Temperature, friction, and track width (T.W.) were as indicated. A 1- μ scale is shown in the plates taken from electron micrographs.

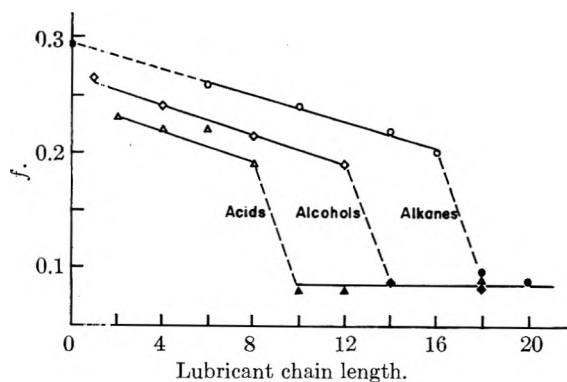


Fig. 10.—Lubrication of polyethylene terephthalate by homologous series of fatty acids, alcohols, and alkanes.

oil). Experiments showed the monolayer reduced friction to the same level as did an excess of the lubricant, and repeat traverse experiments made as described above again failed to break down the adsorbed film. Excessive amounts of slip agents are not, therefore, necessary for low polymer boundary friction.

J. Adsorption from Solution.—Two factors were investigated in studying the reduction in polymer boundary friction effected by solutions of long-chain molecules: (1) the relative abilities of different adsorbates in a given solvent to lower fric-

tion and (2) the relation of solvent type to lubricant efficiency. Saturated solutions of solid fatty acid derivatives in a given solvent showed the same order of efficiencies as did their pure liquid lower homologs. Their effectiveness was strongly dependent on the solvent in which they were dissolved, the best solvents being those which could form "mixed" films. Some results for P.E.T. are collected in Table I.

TABLE I
SOLUTION LUBRICATION OF POLYETHYLENE TEREPHTHALATE

Lubricant ^a	<i>f</i>
None	0.29
Ethyl stearate in hexadecane	.22
Octadecanol in hexadecane	.20
Octadecylamine in hexadecane	.09
Stearic acid in hexadecane	.11
Stearic acid in decane	.17
Stearic acid in hexane	.24
Stearic acid in cyclohexane	.24

^a All solutions were nearly saturated.

The observed order of efficiencies in hexadecane was as expected. Less predictable was the solvent effect which made the friction of P.E.T. lubricated with stearic acid in hexane double that found for the same polymer covered with the same acid in hexadecane. A part of the difference may be ascribed to the solvent alone, for Fig. 10 shows a decrease in

friction with increasing chain length of pure hydrocarbons. However, stearic acid in hexane reduced the friction coefficient of P.E.T. only 0.03 unit more than did the hexane alone, while the corresponding difference for the acid in hexadecane is 0.09, a threefold increase. Decane, of intermediate chain length, showed intermediate behavior. Long-chain solvents thus increase the reduction in friction effected by dissolved lubricants and tend to magnify the differences in lubricating abilities of materials applied from solution to polymer surfaces.

These results may be explained by recalling that the surface of P.E.T. is heterogeneous. Most adsorption of polar molecules, like stearic acid, probably occurs on the relatively active ester links, leaving the remainder of the surface (benzene rings and methylene groups) bare. Interchain cohesion is largely lacking in the resulting film, so individual molecules have a short lifetime on the surface. These effects tend to make friction high.

If the acid is applied from hexadecane solution, solvent molecules adsorb to the adsorbed acid forming a "mixed" film of solvent and solute. If shear occurs at the terminal methyl groups of the mixed film molecules, a low coefficient of friction would be expected.

Mixed films have been postulated before to explain friction results on metals³⁴ and the behavior of stearic acid monolayers on water.³⁵ It is clear that mixed films cannot be formed by cyclic or branched chain molecules. With straight chain molecules, the tendency to adsorb should increase with chain length, as observed.

K. Effect of Polymer Surface Chemistry.—Nine different lubricants were applied to each polymer surface. The slip agents were of widely different chemical type and included solids, liquids, and solutions of solids in liquids. Results of the friction tests are collected in Table II, which shows that: 1. Easiest slip was effected by the solid fatty acid and amine. 2. The least effective lubricant was always hexadecane followed, usually, by butyl stearate. 3. Relative efficacy of fatty acid derivatives in hexadecane solution depended somewhat on the polymer, but generally increased with the polarity of the lubricant. 4. The liquid slip agents did not, in general, reduce friction to the low levels characteristic of adsorbed monolayers on metals ($f \sim 0.10$). 5. No lubricant composition affected the low friction of P.T.F.E.

These results show that the adsorption picture built up for P.E.T. applies equally to all the polymers studied except P.T.F.E., for whose inert surface adsorbate affinity was exceedingly small. No large polymer to polymer differences are apparent,

(34) O. Levine and W. A. Zisman, *J. Phys. Chem.*, **61**, 1188 (1957).

(35) H. D. Cook and H. E. Ries, Jr., *ibid.*, **63**, 226 (1959).

TABLE II

COMPARISON OF LUBRICANTS ON THE DIFFERENT POLYMERS

Lubricant	P.E.T.	Nylon ^a	C.A.	A.N.P.
None	0.29	0.45	0.59	0.49
Hexadecane	.20	.29	.51	.40
Butyl stearate	.18	.22	.42	.39
Oleic acid	.16	.19	.36	.33
Ethyl stearate ^b	.22	.22	.45	.35
Octadecyl alcohol ^b	.20	.20	.43	.38
Stearic acid ^b	.1	.17	.25	.20
Octadecylamine ^b	.09	.13	.30	.17
Solid stearic acid	.10	.13	.10	.06
Solid octadecylamine	.08	.09	.10	.07

^a The friction coefficient of P.T.F.E. was 0.07 and this low value was unaffected by lubricants. ^b Nearly saturated solution in hexadecane.

though their ease of lubrication seems to increase in the order: P.T.F.E., P.E.T., C.A., A.N.P., nylon.

It was of interest to modify one of the polymers to increase the number (and energy) of adsorption sites on its surface, and study the effect on friction. Accordingly, several P.E.T. films were dipped into a concentrated aqueous solution of caustic, neutralized with dilute acid, then washed with distilled water. It was felt that this treatment, known³⁶ to produce carboxyl groups in the P.E.T. surface, might lead to a specific interaction between the acidic surface and a basic adsorbing molecule like octadecylamine. Data (Table III) for different lubricants applied to etched and control surfaces show such an interaction. Octadecylamine, even in hexane solution, was so strongly adsorbed that friction was reduced to a low level. Adsorption of stearic acid from hexane was increased slightly, while friction reduction by hydrocarbons and solids was unaffected by the caustic treatment.

TABLE III

EFFECT OF SURFACE ETCHING ON LUBRICATION OF POLYETHYLENE TEREPHTHALATE

Lubricant	Control surface	Etched surface
None	0.29	0.29
Hexane	.25	.25
Octadecylamine ^a	.18	.10
Stearic acid ^a	.24	.21
Solid octadecylamine	.09	.08
Solid stearic acid	.10	.09

^a Nearly saturated solution in hexane.

Acknowledgments.—The author would like to thank Drs. J. S. Olsen, W. A. Zisman, and H. R. Billica for helpful discussions of this work, and Mr. Grover Morris for the electron and optical micrographs shown in Fig. 2, 8, and 9.

(36) R. C. Golike and S. W. Lasoski, Jr., *ibid.*, **64**, 895 (1960).

THE MECHANISMS OF PHOTOREACTIONS IN SOLUTION. IX. ENERGY TRANSFER FROM THE TRIPLET STATES OF ALDEHYDES AND KETONES TO UNSATURATED COMPOUNDS¹

BY GEORGE S. HAMMOND, NICHOLAS J. TURRO, AND PETER A. LEERMAKERS

Contribution No. 2783 from Gates and Crellin Laboratories, California Institute of Technology, Pasadena, California

Received January 2, 1962

cis ⇌ *trans* isomerization of the piperlyenes, the 1,2-dichloroethylenes, and the 2-pentenenes can be effected by irradiation in the presence of photosensitizers. Various carbonyl compounds have been used as sensitizers and the results form a coherent pattern if it is assumed that the key step in the photochemical reactions is transfer of triplet excitation. Presently available results indicate that transfer of energy probably occurs on every collision between a triplet and a second molecule if the transfer is exothermic. Endothermic transfers may occur but with reduced efficiency.

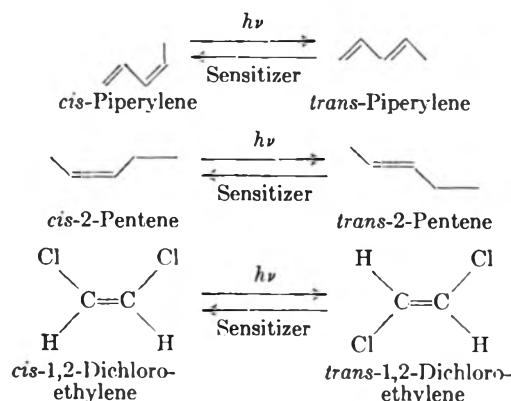
Recent work indicates that irradiation of several aromatic ketones and aldehydes in solution at ordinary temperatures produces triplet states of the carbonyl compounds in high quantum yield.¹⁻³ Among the interesting consequences of this fact is the possibility of making triplet states of other molecules by direct transfer of energy from carbonyl triplets to some second molecule.³⁻⁷ Such an indirect path for the production of triplet states may be uniquely useful for two reasons. First, the quantum yield of triplets produced by direct irradiation may be low, or even vanishingly small, simply because the excited singlet states of many molecules decay directly to the ground singlet states without passing through triplet states. Such a case was observed in the study of the photolysis of ethyl pyruvate.⁵ The quantum yield for decomposition sensitized by benzophenone was twice as large as the quantum yield in direct photolysis. The second advantage of the use of sensitizers in the production of triplets derives from the fact that the separation in energy between singlet and triplet states may vary widely from one system to another. Figure 1 illustrates the point using the comparison of benzophenone and a linear diene as an example. The $S_0 \rightarrow S_1$ transition of benzophenone has a maximum close to 3450 Å. and the phosphorescence spectrum has a maximum at 4100 Å.⁸; there is only a small separation between S_1 and T_1 . On the other hand, the $S_0 \rightarrow S_1$ transition of conjugated, open-chain dienes has a maximum in the vicinity of 2300 Å. and T_1 lies in the vicinity of 4800 Å. The latter conclusion was reached by Evans⁹ by study of the $S_0 \rightarrow T_1$ absorption of butadiene and isoprene in the presence of a high pressure of oxygen. The same conclusion

concerning the location of the triplet states of dienes can be adduced from the studies reported in this paper and communicated earlier in brief form.⁶

A consequence of the situation described in Fig. 1 is the possibility that the triplet state of a diene can be produced by irradiation with long wave length light which is not absorbed by the diene. As will be shown in this and subsequent papers, study of such phenomena can shed light on a variety of significant phenomena. *e.g.*, estimation of the energy levels of the triplet states of both donors and acceptors, clarification of the mechanisms of photochemical reactions, and increasing our understanding of the process of excitation-transfer. There will obviously be many cases in which photoreactions which would be difficult or impossible to carry out by direct irradiation can be run conveniently using light of relatively long wave lengths.

Results and Discussion

We have chosen *cis-trans* interconversion of the piperlyenes (1,3-pentadienes), 2-pentenenes, and 1,2-dichloroethylenes as convenient chemical processes for detection of energy transfer from triplet states of various sensitizers to unsaturated molecules. The most extensive work has been done with the piperlyenes.



(1) (a) Presented at the International Symposium on Reversible Photochemical Processes, Durham, North Carolina, April, 1962; (b) Part VIII of the series is K. R. Kopecky, G. S. Hammond, and P. A. Leermakers, *J. Am. Chem. Soc.*, **84**, 1015 (1962).

(2) G. S. Hammond and W. M. Moore, *ibid.*, **81**, 6334 (1959); G. S. Hammond, W. M. Moore, and R. P. Foss, *ibid.*, **83**, 2789 (1961).

(3) H. L. J. Bäckstrom and K. Sandros, *Acta Chem. Scand.*, **14**, 48 (1960).

(4) G. O. Schenck and R. Steinmetz, *Tetrahedron Letters*, No. **21**, 1 (1960).

(5) G. S. Hammond, P. A. Leermakers, and N. J. Turro, *J. Am. Chem. Soc.*, **83**, 2395 (1961).

(6) G. S. Hammond, P. A. Leermakers, and N. J. Turro, *ibid.*, **83**, 2396 (1961).

(7) K. R. Kopecky, G. S. Hammond, and P. A. Leermakers, *ibid.*, **83**, 2398 (1961).

(8) G. N. Lewis and M. Kasha, *ibid.*, **66**, 2100 (1944).

(9) D. F. Evans, *J. Chem. Soc.*, 1735 (1960).

Benzene solutions containing *cis*-piperlyene and various aldehydes and ketones were irradiated using a medium-pressure mercury arc. Vapor chromatography was used to follow the production of *trans*-piperlyene. In most instances the system reached a photostationary state after a few hours of irradiation. In one experiment pure

trans-piperylene was used with benzophenone as a sensitizer. Conversion to the *cis* isomer was observed and at the termination of the experiment the *trans/cis* ratio was slightly higher than that observed in the experiments in which the *cis*-diene was used as a starting material. The result implies that the photostationary condition may not have been completely achieved in all experiments; however, the data reported in Table I all are derived from experiments in which conversions had become very slow; therefore, the tabulated values are at least close to those for the true photostationary states.

Two striking results emerge. First dibenzalacetone and 9-anthraldehyde, which have very low-lying triplet states, are completely inert as sensitizers; second, *different sensitizers give different photostationary mixtures*. Many hypotheses can be developed to account for these results and it seems inappropriate at this time to discuss all of the possibilities which come to mind. However, the trend suggests that a major controlling variable is the energy level of the lowest triplet state of the sensitizer. We have inferred from data reported elsewhere¹⁰ that excitation transfer from benzophenone triplets to *cis*-piperylene is a diffusion-controlled process. It is reasonable to assume that the same is true of the transfer from benzophenone triplets to *trans*-piperylene. This implies that transfer is essentially a Franck-Condon process; *i.e.*, there is essentially no change in the nuclear position during the actual transfer. The planar triplet states of the dienes produced in this manner would, therefore, be formed in excited vibrational states and would decay by vibrational cascade to one or more unknown twisted forms.¹¹ Ultimately the triplets will return to their ground singlet states by thermal degradation. The latter process will produce the *cis* and *trans* isomers of piperylene in some ratio which cannot be predicted on any *a priori* basis. The data in Table I show that those compounds which have triplets lying 70 kcal. or more above their ground states produce photostationary mixtures in which the *trans/cis* ratio is about 1.25. The postulate which most easily accommodates this fact is the view that all of these sensitizers transfer energy to piperylene in diffusion-controlled reactions and that the factor 1.25 represents the natural¹³ decay ratio. Presumptive evidence that the decay process is not influenced by the sensitizer was obtained in the case of benzophenone. Solutions containing 0.2 *M* piperylene and 0.05, 0.01,

(10) G. S. Hammond and P. A. Leerrakers, *J. Phys. Chem.*, **66**, 1148 (1962).

(11) The stable configuration of the lowest triplet state of linear dienes is unknown. However, the great stabilization (~ 20 kcal.) of the perpendicular form of ethylene¹² suggests that diene triplets probably will suffer distortion from planarity. Because twisting will sacrifice resonance energy, the actual configuration probably will be some compromise between planar and perpendicular configurations.

(12) R. S. Mulliken and C. C. J. Foorthaar, *Chem. Rev.*, **41**, 219 (1947).

(13) The term "natural" is used to indicate the *trans/cis* ratio produced by decay of piperylene triplets undisturbed by external influences. Even if our belief that the decay ratio is not influenced by the sensitizer is completely correct, the results still may not show the "natural" ratio. It is entirely possible that solvent effects on the decay process will be significant. Study of this problem is in progress.

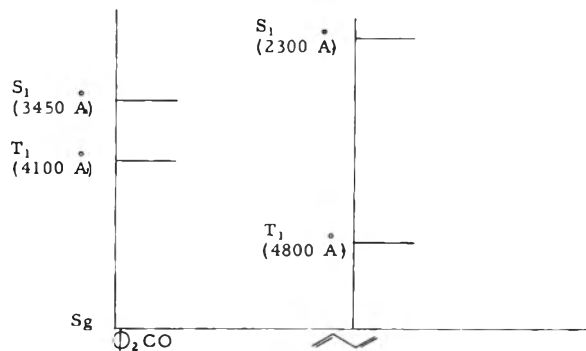


Fig. 1.—Correlation of the excited states of benzophenone and linear, conjugated dienes.

and 0.001 *M* benzophenone were irradiated for long periods of time. Although the rate of isomerization decreased as the concentration of sensitizer was decreased, the same photostationary state was ultimately reached in each of the experiments. This result implies that the fate of the piperylene triplets is not influenced by formation of complexes with the sensitizer.¹⁴

The failure of dibenzalacetone and 9-anthraldehyde to function as sensitizers almost certainly indicates that the triplets derived from them have insufficient energy to promote either of the isomeric piperylenes to triplet states. This clearly marks the $S_0 \rightarrow T_1$ transition of the piperylenes as requiring more than 53 kcal.; *i.e.*, the transition lies at wave lengths shorter than 5400 Å. This conclusion is in good agreement with the observations of Evans,⁹ who assigned the $O \rightarrow O$ band of the $S_g \rightarrow T_1$ transition of butadiene at 4800 Å.

What, then, is responsible for the interesting variations in the photostationary states established in the presence of sensitizers which have triplets lying between 53 and 70 kcal. above their ground states? Scrutiny of the data reveals that there is a monotonic relationship between decreasing energy of the triplets and increasing *trans/cis* ratio at the steady state. A simple hypothesis can be advanced to account for this relationship. *If the excess energy of the ground vibrational T_1 state of the sensitizer is less than the energy of the $O \rightarrow O$ component of the $S_0 \rightarrow T_1$ transition of the receiver, excitation-transfer will be an endothermic process and will, presumably, begin to become measurably inefficient.* There is no reason to expect the efficiencies of the transfer processes involving the *cis*- and *trans*-dienes to decrease at the same rates. The data indicate that transfer to the *trans* isomer becomes inefficient more rapidly than does transfer to the *cis* isomer. *If the energetics of the transfer process were the only controlling factor, we would conclude that the $S_0 \rightarrow T_1$ transition of *trans*-piperylene lies at slightly shorter wave length than the same transition of the *cis* isomer; furthermore, the singlet-triplet transitions of both isomers lie between 4600 and 5400 Å.*

If the inferences are correct, the method provides

(14) The extreme opposite point cannot be rigorously excluded; *i.e.*, if complexes of *very great* stability were formed between the carbonyl compound and piperylene triplets, all of the triplets might be complexed even though the concentration of the former is very low. Semi-intuitive reasoning makes such a condition seem unlikely, especially so since a large number of sensitizers give *trans/cis* ratios close to 1.25.

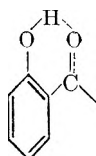
an easy means for estimation of energy levels of the triplet states of compounds for which phosphorescence data are unavailable. Cases in point are acetone, phenanthrenequinone, and fluorenone. The data in Table I indicate tentative assignment of the energies of the triplet states of these compounds as >70, ~65, and ~62 kcal., respectively.

TABLE I
ISOMERIZATION OF *cis*-PIPERYLENE^a

Sensitizer	<i>E_T</i> of sensitizer, kcal. ^b	<i>trans/cis</i> ratio at stationary state
Acetophenone	74	1.23
Benzaldehyde	72	1.23
Acetone	?	1.23
Butanone	?	1.23
3-Pentanone	?	1.23
Cyclohexanone	?	1.23
Cyclopentanone	?	1.23
Benzophenone	70	1.30
Anthraquinone	?	1.30
Ethyl pyruvate	~68	1.35
Phenanthrenequinone ^c	?	1.65
Fluorenone	?	1.95
Benzil ^d	62	2.15
2-Acetonaphthone	59	2.55
2,3-Pentanedione	53	3.10
Biacetyl	56	10-13
1-Naphthaldehyde	57	10-13
Dibenzalacetone ^d	53	No reaction
9-Anthraldehyde	~40	No reaction
Salicylaldehyde	~70	No reaction
<i>p</i> -Hydroxybenzaldehyde	?	1.2
<i>o</i> -Methoxybenzaldehyde ^d	?	1.2
2,4-Dihydroxybenzophenone	?	No reaction
2-Hydroxybenzophenone-4-methoxy	?	No reaction

^a Benzene solutions, 0.1 *M* in sensitizer and olefin.
^b Ref. 8 except that those marked ~ are estimated by us.
^c Ratio of peak heights in chromatograms of incompletely separated mixtures. ^d Olefin slowly consumed during reaction.

The last five entries in Table I show the results of a preliminary study of compounds containing *o*-hydroxybenzoyl groups. Such compounds, notably *o*-hydroxybenzophenone and its derivatives, are widely used as photostabilizers; *i.e.*, when incorporated in materials such as films and fibers they often afford prolonged protection against photochemical degradation. Three compounds: salicylaldehyde, 2-hydroxybenzophenone, and 2,4-dihydroxybenzophenone containing the characteristic structure were studied and found to be completely inactive as sensitizers for the isomerization of the piperyles. In contrast, both *p*-hydroxybenzaldehyde and *o*-methoxybenzaldehyde were very effective sensitizers. From these facts we infer that the excited states of compounds containing the *o*-hydroxybenzoyl group either (1) are not degraded by way of triplet states, or (2) give triplet states incapable of transferring energy to the dienes.



The phenomenon seems to be associated with the presence of internal hydrogen bonds.

The presence of such a structure may favor the $S_1 \rightarrow S_0$ degradation relative to intersystem crossing ($S_1 \rightarrow T_1$). The effect might be due to disturbance of usual relationships between $\pi \rightarrow \pi^*$ and $n \rightarrow \pi^*$ excited states or it might be due to the existence of special, chemical implementation of the $S_1 \rightarrow S_0$ process.¹⁵

Alternatively, the triplet states of the hydrogen bonded molecules might be very short lived or might have very low energies.¹⁷

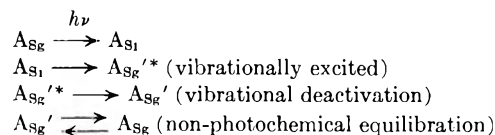
Endothermic Transfer Reactions.—Evans⁹ located the O-O band of the $S_0 \rightarrow T_1$ absorption spectrum of ethylene at 3480 Å. (80 kcal. mole⁻¹). Consequently we anticipated that transfer of excitation from the triplet states of most carbonyl compounds to unconjugated alkenes would be rather inefficient. Such has proven to be the case. Irradiation of benzene solutions containing *cis*- or *trans*-2-pentene and sensitizers such as acetone, benzophenone, or acetophenone effects very slow isomerization. Prolonged irradiation produces in each case mixtures which appear to be fairly close to photostationary states since similar compositions are obtained starting with either isomer. Benzil and fluorenone cause very slow isomerization of *cis*-pentene. 2-Acetonaphthone

TABLE II
PHOTOSENSITIZED ISOMERIZATION OF 2-PENTENES

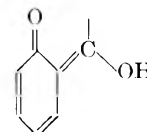
Sensitizer	Starting material	<i>trans/cis</i> Ratio after various times of irradiation ^a		
		2 days	5 days	8 days
Acetone ^b	<i>cis</i> -2-Pentene	0.8	~1.9	1.7
Acetone ^b	<i>trans</i> -2-Pentene	2.2	1.91	1.9
Benzophenone	<i>cis</i> -2-Pentene	3.6	6.1	..
Benzophenone	<i>trans</i> -2-Pentene	7.8	7.7	6.6
Acetophenone	<i>cis</i> -2-Pentene	..	3.2	3.6
Acetophenone	<i>trans</i> -2-Pentene	7.1	5.2	4.6 (10 days—3.9)
Benzil	<i>cis</i> -2-Pentene	0.16	0.3	0.8
Fluorenone	<i>cis</i> -2-Pentene	..	0.15	0.18

^a Reaction run in parallel to effect approximate equivalence of illumination. ^b Reaction run in neat acetone.

(15) For example, tautomers of the parent structure may be produced. Conversion of an excited singlet of a molecule, A, to a vibrationally excited, ground singlet of an isomer, A', may provide a fast route for non-irradiative decay of excited states.



In order for such a mechanism to have any significance in the case at hand, it would be necessary to assume that the tautomer, A', is the non-hydrogen bonded, *trans*-enol.¹⁶



(16) See N. C. Yang, *J. Am. Chem. Soc.*, **83**, 2213 (1961), for evidence that a formally similar reaction occurs with *o*-methylacetophenone.

(17) The compounds in question have relatively low lying $\pi-\pi^*$ singlet states since the compounds have intense maxima ($E \sim 20,000$) near 3500 Å. Consequently the lowest triplets of these molecules may have the $\pi-\pi^*$ configuration and lie at low energy levels. See reference 18 for a discussion of a similar problem.

(18) G. S. Hammond and P. A. Leermakers, *J. Am. Chem. Soc.*, **84**, 207 (1962).

is no sensitizer. The data are summarized in Table II.

Somewhat similar results were obtained with the isomeric 1,2-dichloroethylenes. A number of the higher energy sensitizers produced mixtures which apparently were photostationary. The results are given in Table III. There are, however, interesting contrasts between the experiments obtained with the pentenes on the one hand and with the dichloroethylenes on the other. Experiments run in parallel in which the two compounds were irradiated in acetone solution indicated that the rate of sensitized isomerization of *cis*-2-pentene was somewhat, but not a great deal, more rapid than the rate of isomerization of *trans*-1,2-dichloroethylene. In contrast the dichloroethylenes isomerized much more rapidly than the pentenes in the presence of low energy sensitizers such as fluorenone and benzil. These results show that factors other than energy balance must be important in determining the efficiencies of some of the energy transfers. Further study of the problem is in progress.

TABLE III

PHOTOSENSITIZED ISOMERIZATION OF *trans*-1,2-DICHLOROETHYLENE

Sensitizer ^a	<i>cis/trans</i> in photostationary mixtures
CH ₃ COCH ₃	~2.1
CH ₃ COC ₆ H ₅	3.1
C ₆ H ₅ COC ₆ H ₅	4.5
C ₆ H ₅ COCOC ₆ H ₅	4.0-4.1
β-C ₁₀ H ₇ COCH ₃	No reaction
Fluorenone	2.5 ^b

^a Benzene solutions, except for acetone which was used without solvent. ^b Reaction ceased because of build up of quenchers in the solution.

Lewis and Kasha⁸ reported that *trans*-1,2-dichloroethylene phosphoresces with a O-O band at 3970 Å. (72 kcal.). This position seems anomalously low and conceivably could be due to the presence of impurities; the suspicion is increased by the report that the corresponding dibromo- and diiodoethylenes have almost the same phosphorescence as the dichloro compound. If the assignment is correct, transfer of energy from the triplets of acetone and acetophenone to dichloroethylene would be exothermic and might be expected to be diffusion-controlled. The fact that isomerizations sensitized by the two ketones arrive at

different photostationary states is inconsistent with this view. The rates of isomerization of dichloroethylenes are clearly less than the rates of isomerization of piperylenes under similar conditions. This result, in itself, does not compel the conclusion that energy transfer is inefficient since the latter conclusion may be adduced from the recent report of Cundall and Milne,¹⁹ who observed that dichloroethylenes induce isomerization of the 2-butenes in the vapor phase with concomitant quenching of the isomerization of the former. It is very likely that there is a significant barrier to rotation in the triplets of the dichloroethylenes. This is consistent with the view that the lowest triplet of dichloroethylene has considerable $n \rightarrow \pi$ character; *i.e.*, $\begin{array}{c} \downarrow \\ \text{:}\ddot{\text{C}}\text{I}-\text{CH}=\text{CH}\ddot{\text{C}}\text{I:} \\ \downarrow \end{array}$. Such a configuration should stabilize the planar configuration relative to the perpendicular form.

Experimental

Materials.—Benzene, Mallinckrodt White Label, was used as received. *cis*-2-Pentene, Phillips 95 mole %, was distilled; b.p. 39° at 760 mm. *trans*-2-Pentene, Phillips Technical Grade, was distilled; b.p. 36–38° at 760 mm. Mixed piperylenes, from Matheson Coleman & Bell, were distilled; b.p. 42° at 760 mm. Pure *cis*-piperylene was prepared by the method of Craig.²⁰ *trans*-1,2-Dichloroethylene, Matheson Coleman & Bell reagent grade, was distilled; b.p. 47° at 760 mm.

Analysis.—All mixtures were analyzed by vapor chromatography. In every case it was possible to prepare a column which would separate the pairs of *cis-trans* isomers. Columns used to accomplish such separations were: piperylene, 12 ft. of dimethylsulfalane (20%) (separation not complete); 2-pentenenes, 12 ft. silver nitrate in ethylene glycol or 12 ft. β,β'-oxydipropionitrile (25%); 1,2-dichloroethylenes, 12 ft. Apiezon J or 12 ft. β,β'-oxydipropionitrile (25%).

All experiments reported in this paper were carried out using a Hanovia quartz immersion reactor. In the experiments with piperylene a filter having a cutoff at 2800 Å. was used. Other experiments were carried out with unfiltered light. In experiments designed to establish photostationary states solutions were placed in quartz or Pyrex cells designed for use in the Beckman DU spectrophotometer. The cells were strapped to the inner jacket of the reactor. This technique allows several experiments involving prolonged irradiation to be carried out simultaneously; however, the procedure also makes comparison of rate data inaccurate because the conditions of illumination are not exactly reproducible.

All reactions were run in benzene solution unless otherwise indicated. The concentration of both sensitizer and olefin was approximately 0.1 M in most experiments.

(19) R. B. Cundall and D. G. Milne, *J. Am. Chem. Soc.*, **83**, 3902 (1961).

(20) D. Craig, *ibid.*, **65**, 1006 (1943).

MECHANISMS OF PHOTOREACTIONS IN SOLUTION. X. RELATIVE EFFICIENCIES OF VARIOUS QUENCHERS IN THE PHOTOREDUCTION OF BENZOPHENONE

BY GEORGE S. HAMMOND AND PETER A. LEERMAKERS¹

Contribution No. 2797 from the Gates and Crellin Laboratories of Chemistry, California Institute of Technology, Pasadena, California

Received January 2, 1962

A number of organic compounds quench the photoreduction of benzophenone by benzhydrol. Quantitative study of the effect shows the efficiencies of many active quenchers are very similar. From this fact we infer that transfer of energy from benzophenone triplets to quenchers probably occurs at every collision if transfer of triplet excitation is exothermic.

In the accompanying paper² it was shown that energy transfer from the triplet state of a ketone or aldehyde to an acceptor molecule with concomitant production of the triplet state of the latter can indeed be an efficient process. Such an energy transfer process was employed to promote chemical reaction of the acceptor molecule. The present paper reports the results of an investigation to determine quantitatively the relative rates of energy transfer (or quenching) from benzophenone triplets to other organic molecules with relatively low-lying triplet states. Bäckstrom and Sandros³ previously have observed, using the flash photolytic technique, that certain polynuclear hydrocarbons quench biacetyl phosphorescence with rate constants of the order of 10^9 l. mole⁻¹ sec.⁻¹. Presumably the mechanism of quenching is triplet excitation transfer to the quencher.

It previously has been shown that the chemically active excited state of benzophenone in photoreduction reactions is a triplet.⁴ If triplet-triplet energy transfer is an efficient process in solution, then suitable acceptor molecules ought to compete with a hydrogen donor for benzophenone triplets and thus reduce the quantum yield for photoreduction of the ketone. In the present investigation, the quantum yields for photoreduction of benzophenone by benzhydrol in the presence of various quenchers have been measured. The data have been analyzed to yield quantitative information concerning the relative rates of quenching by the various quencher (acceptor) molecules. Similar observations have been reported by Moore and Ketchum, who used naphthalene as a quencher.⁵

Experimental

Chemicals. 1-Naphthaldehyde (Eastman Kodak White Label) was vacuum distilled and the fraction boiling in the range 110–112° at 3 mm. was collected for use. 2-Acetonaphthone (Eastman Kodak White Label) was recrystallized from petroleum ether, m.p. 55–56°. Benzhydrol (Matheson Coleman & Bell, Reagent Grade) was twice recrystallized from petroleum ether. Benzophenone (m.p. 47–48°), biacetyl, benzil (m.p. 94–95°), naphthalene (m.p. 80–81°), and maleic anhydride (m.p. 53–55°), all Reagent Grade, were used as furnished by Matheson Coleman &

Bell. Azulene (Aldrich Chemical Corp., m.p. 101–102°) and benzene (Mallinckrodt Analytical Reagent Grade) were used as furnished. *cis*-Piperylene was obtained from mixed piperylene furnished by K and K Laboratories. The mixture was heated under reflux with maleic anhydride to remove the *trans*-isomer. The *cis*-isomer then was distilled and a fraction boiling at 43–44° at atmospheric pressure was collected for use. Purified cyclohexene was obtained from Dr. Karl Kopecky. 9-Anthraldehyde (Aldrich Chemical Corp.) was recrystallized from acetic acid, m.p. 104°. Cyclooctatetraene (Aldrich Chemical Corp.) was used as furnished. The preparation of tributylstannane has been described in a previous paper.⁶

Apparatus.—The light source, optical system, reaction cells, etc., for the quantum yield determinations have been described previously.⁴ The filter system, consisting of Corning glass filters 7–60 and 0–52 in series, isolated the 3660 Å. line from the mercury arc.

Actinometry.—A benzophenone–benzhydrol actinometer was employed. Solutions 0.05 *M* in benzophenone and 0.10 *M* in benzhydrol were degassed and irradiated for measured periods of time. The residual benzophenone then was determined spectrophotometrically. A quantum yield of 0.74 for the process is assumed.⁷ The results obtained by this method were consistent with one determination using the uranyl oxalate actinometer. A solution 0.10 *M* in oxalic acid and 0.03 *M* in uranium acetate was irradiated. After 11,160 sec. the residual oxalic acid was titrated with 0.100 *N* permanganate. A quantum yield of 0.49 is assumed for the uranyl oxalate system.⁸

Photoreduction of Benzophenone.—Benzene solutions usually containing 0.05 *M* benzophenone, 0.10 *M* benzhydrol, and a quencher in low concentration ($2\text{--}10 \times 10^{-4}$ *M*) were placed in quartz cells, degassed, and irradiated. After a measured length of time the reaction was stopped and the residual benzophenone was determined spectrophotometrically after appropriate dilution.

Photoreduction of 9-Anthraldehyde.—Benzene solutions containing 1.0×10^{-3} *M* 9-anthraldehyde and 0.148 *M* butylstannane were degassed and irradiated. The cells then were opened and residual anthraldehyde was determined by 25-fold dilution and measurement of its absorbance at 4000–4400 Å. In one experiment azulene (5.0×10^{-3} *M*) was included. In an experiment to identify products a solution containing 7.5 mmoles of tributylstannane in 130 ml. of benzene was irradiated for 8 hr. The solvent then was stripped off and petroleum ether was added. A white solid (0.4 g., 27%) separated, m.p. 220–230°. Chromatography of the entire reaction mixture on alumina yielded this material pure, m.p. 228–232°. The product was shown to be the pinacol, 1,2-(9-anthryl)-glycol by cleavage to 9-anthraldehyde with lead tetraacetate. Treatment of 18 mg. of the compound with lead tetraacetate in acetic acid for 3 hr., followed by the addition of 2,4-dinitrophenylhydrazine reagent, yielded a brick-red solid (not weighed) which was recrystallized from ethanol–ethyl acetate, m.p.

(1) National Science Foundation Predoctoral Fellow, 1958–1961.

(2) G. S. Hammond, N. J. Turro, and P. A. Leermakers, *J. Phys. Chem.*, **66**, 1144 (1962).

(3) H. L. J. Bäckstrom and K. Sandros, *Acta Chem. Scand.*, **12**, 822 (1958).

(4) W. M. Moore, G. S. Hammond, and R. P. Foss, *J. Am. Chem. Soc.*, **83**, 2789 (1961).

(5) W. M. Moore and M. Ketchum, *ibid.*, **84**, 1368 (1962).

(6) G. S. Hammond and P. A. Leermakers, *ibid.*, **84**, 207 (1962).

(7) This assumption is based on the extensive investigation of the system by W. M. Moore, Ph.D. thesis, Iowa State College, 1959, and ref. 4; and on the slight revision of the data by Mr. R. P. Foss of these Laboratories.

(8) C. R. Masson, V. Boekelheide, and W. A. Noyes, Jr., "Technique of Organic Chemistry," ed., A. Weissberger, Vol. II, 2nd Ed., Interscience Publishers, New York, N. Y., 1956.

271–275°. Authentic 9-anthraldehyde-2,4-dinitrophenylhydrazone was prepared, m.p. 277–282°; mixed m.p. 272–280°.

Results and Discussion

From previous work in these Laboratories⁴ it is known that the photoreduction of benzophenone by benzhydrol in the presence of a quencher follows the rate law

$$\frac{1}{\Phi} = \frac{1}{\Phi'} + \frac{k_d}{\Phi'k_r[\text{DH}]} + \frac{k_q[\text{Q}]}{\Phi'k_r[\text{DH}]}$$

where k_d , k_r , and k_q are, respectively, the rate constants for thermal deactivation, hydrogen abstraction, and quenching of the triplet state; [DH] is hydrogen donor concentration; [Q] is quencher concentration; and Φ' is the quantum yield of triplets (unity for the case of benzophenone). Measurement of the quantum yield, Φ , for the photoreduction as a function of quencher concentration at fixed benzhydrol concentration yielded values of k_q/k_r , the ratio of the rates of quenching to hydrogen abstraction. The data are given in Table I.

From recent observations in these Laboratories^{2,9,10} it is clear that the quenching mechanism

TABLE I^a

PHOTOREDUCTION OF BENZOPHENONE BY BENZHYDROL IN THE PRESENCE OF QUENCHERS

Quencher	[Quencher]	[Benzhydrol]	Φ	k_q/k_r	E_T^b	Ref.
2-Acetonaphthone	5×10^{-4}	0.20	0.30	790	59	9
2-Acetonaphthone	5×10^{-4}	.10	.20	730		
Naphthalene	5×10^{-4}	.10	.20	750	61	9
Naphthalene	2×10^{-4}	.10	.34			
cis-Piperylene	5×10^{-4}	.10	.21	750	55–60	c
cis-Piperylene	1.0×10^{-1}	.10	.104			
Benzil	4.4×10^{-4}	.10	.31	436	62	9
Cyclohexene	5×10^{-4}	.10	.67	30	?	
Azulene	5×10^{-4}	.10	.15			
Azulene	2×10^{-4}	.10	.25	1100	?	
Azulene	3×10^{-4}	.10	.20			
1-Naphthaldehyde	5×10^{-4}	.10	.17	880	57	9
1-Naphthaldehyde	2×10^{-4}	.10	.34			
Cyclooctatetraene	5×10^{-4}	.10	.20	630	?	
Cyclooctatetraene	1.0×10^{-3}	.10	.13			
Biacetyl	5×10^{-4}	.10	.41	d	56	9
Maleic anhydride	5×10^{-4}	.10	.58	d	?	
None10	.74	

^a Concentration of benzophenone = 0.05 M. ^b Energy of lowest triplet state (kcal.). ^c Quencher consumed in the reaction. ^d Quencher consumed, probably by the Schenck reaction.¹¹ ^e Reference 12.

must involve energy transfer from the benzophenone triplet to the acceptor (quencher) with production of the triplet state of the latter. Transfer from benzophenone triplets to naphthalene at low temperature has been observed directly by Terenin and Ermolaev¹³ and by Farmer, Gardner, and McDowell.¹⁴ Porter and Wilkinson¹⁵ also have

shown that benzophenone triplets transfer excitation to naphthalene, with production of the triplet state of the latter, in a diffusion controlled process in solution. In every case in which the energy of the lowest triplet state of the acceptor is known, the transfer would be exothermic, since the lowest triplet of benzophenone lies 70 kcal. above the ground state.¹⁶ No information is available concerning the triplet states of azulene, cyclooctatetraene, cyclohexene, and maleic anhydride. However, since the first singlet-singlet transition of azulene is found at 7000 Å. (42 kcal.) the compound must have one, and probably more,¹⁷ triplet states lying below the lowest triplet of benzophenone. It also is highly reasonable that cyclooctatetraene has at least one triplet state lower in energy than that of benzophenone. If the molecule is considered to be two independent butadiene systems, the T_1-S_0 transition energy would be around 60 kcal.¹⁸ The assumption of any conjugation between the butadiene systems would presumably further lower the transition energy. However, it seems very probable that energy transfer from benzophenone to cyclohexene would be endothermic. Evans¹⁷ observed the S_2-T_1 transition of ethylene at 29,000 cm^{-1} (83 kcal.). Incorporation of the ethylenic function in a cyclic system might lower the energy of the triplet state somewhat, but it seems very doubtful that it could be as low as 70 kcal. We believe that the relatively inefficient quenching by cyclohexene is probably characteristic of an energy transfer which is endothermic by a few kcal. If the argument is turned around, we can infer that the S_2-T_1 transition of maleic anhydride, a reasonably efficient quencher, must require 70 kcal. or less.

The quenching efficiencies of most of the compounds tested are grouped remarkably close together. Naphthalene, 1-naphthaldehyde, 2-acetonaphthone, piperylene, and cyclooctatetraene all have values of k_q/k_r around 800; the most efficient quencher of all tested was azulene, in which k_q/k_r was 1100.

The remarkable similarity in the rates of quenching by compounds as different as piperylene (1,3-pentadiene), acetonaphthone, and azulene (rates well within a factor of two of each other) is compelling evidence for the existence of one common, rate-limiting factor. A diffusion controlled process is implied. Bäckstrom and Sandros^{3,19} previously have assumed that energy transfers of this sort are diffusion controlled. The rate constants which they obtained for quenching of the phosphorescence of biacetyl by certain polynuclear aromatic hydrocarbons ($k_q \sim 10^9$ l. mole⁻¹ sec.⁻¹) are of the same order of magnitude as the rate constants of diffusion controlled reactions. Since this process must involve triplet-triplet transfer, it probably is safe to assume that quenching of benzophenone triplets by energy transfer will be at least close to

(9) G. S. Hammond, P. A. Leermakers, and N. J. Turro, *J. Am. Chem. Soc.*, **83**, 2395, 2396 (1961).

(10) K. R. Kopecky, G. S. Hammond, and P. A. Leermakers, *ibid.*, **83**, 2397 (1961).

(11) G. O. Schenck and R. Steinmetz, *Tetrahedron Letters*, **21**, 1 (1960).

(12) G. S. Hammond, P. A. Leermakers, and N. J. Turro, *J. Am. Chem. Soc.*, **83**, 2396 (1961).

(13) A. Terenin and V. Ermolaev, *Doklady Akad. Nauk S.S.S.R.*, **85**, 547 (1952); *Trans. Faraday Soc.*, **52**, 1042 (1956).

(14) J. B. Farmer, C. L. Gardner, and C. A. McDowell, *J. Chem. Phys.*, **34**, 1058 (1961).

(15) G. Porter and F. Wilkinson, *Proc. Roy. Soc. (London)*, **A264**, 1 (1961).

(16) G. N. Lewis and M. Kasha, *J. Am. Chem. Soc.*, **66**, 2100 (1944).

(17) R. Pariser, *J. Chem. Phys.*, **25**, 1112 (1956).

(18) D. F. Evans, *J. Chem. Soc.*, 1735 (1960).

(19) H. L. J. Bäckstrom and K. Sandros, *Acta Chem. Scand.*, **14**, 48 (1960).

diffusion controlled if the process is not significantly endothermic.

As mentioned previously, azulene was observed to be the best of the tested quenchers. Calculations based on three measurements yielded a value of $k_q/k_r = 1100$. Azulene presumably has more than one triplet lower in energy than the lowest triplet of benzophenone. The lowest azulene triplet probably lies in the infrared, a few thousand wave numbers below the lowest excited singlet state which is responsible for absorption at 15,000 cm^{-1} (6000–7000 Å).¹⁶ Two higher triplets, corresponding to the singlets obtained by the transitions at 3500 and 2800 Å,¹⁶ should lie below or near to the benzophenone triplet. It is presumed that benzophenone is quenched by excitation of azulene to an upper triplet, since this process best conserves electronic energy.

It was of interest to determine experimentally if azulene also could quench by energy transfer to its lowest triplet. 9-Anthraldehyde was selected as the donor, since the energy of its lowest triplet must be at least as low as that of anthracene (14,700 cm^{-1} or 42 kcal.¹³) and probably slightly lower. This value would be well below the expected energy

of an upper triplet of azulene, hence energy transfer to an upper triplet would not be anticipated. With no azulene present, 9-anthraldehyde was photoreduced by 0.15 *M* tributylstannane with a quantum yield of 0.045 to give the corresponding glycol, 1,2-di-(9-anthryl)-ethan-1,2-diol. Under similar conditions, in the presence of 5×10^{-4} *M* azulene, the quantum yield was reduced to 0.025 (Table II). Thus, quenching again was found to be significant, with k_q/k_r calculated to be 5300. Since the systems are different, this number cannot be compared directly with the data from the benzophenone-benzhydrol system. The conclusion to be drawn is that quenching by energy transfer to the lowest triplet of azulene does occur.

TABLE II
PHOTOREDUCTION OF 9-ANTHRALDEHYDE BY TRIBUTYLSTANNANE IN THE PRESENCE OF AZULENE

Anthraldehyde	Stannane	Azulene	Φ	k_q/k_r
1.0×10^{-3}	0.148	0.045	..
1.0×10^{-3}	0.148	5×10^{-4}	0.025	5300

Acknowledgment.—We are indebted to Mr. Harold Thomas, who carried out the experiments with cyclooctatetraene.

PROTON MAGNETIC RESONANCE AND INFRARED SPECTRA OF SOME ION-EXCHANGE RESIN-SOLVENT SYSTEMS

BY JOHN E. GORDON

Mellon Institute, Pittsburgh, Pennsylvania

Received January 4, 1962

The proton magnetic resonance spectra of a variety of ion-exchange resins immersed in several liquids and liquid mixtures have been recorded, and these are found to be remarkably well defined. Due to the close similarity of the diamagnetic susceptibilities of water and the resins, rather narrow lines are observed in these systems; due to the fact of slow exchange between water within and without the resin beads, separate lines appear for water in the two environments. These circumstances allow a number of phenomena of importance in the physical chemistry of the exchangers to be observed directly; among these are the exchange of proton-containing counterions, the change of counterion molality with cross-linking, the distribution of mixed solvents between the phases, and the loss of rotational freedom of counterions in the resin phase as a function of the swelling. In addition the spectra provide a powerful tool for the investigation of resin heterogeneity; several interesting cases of the existence of two discrete, though closely similar, fractions in commercial resins are described. Infrared spectra and swelling measurements indicate that hydrogen resinates in anhydrous acetonitrile exists predominantly as the undissociated sulfonic acid, in equilibrium with a small amount of lyonium sulfonate ion pairs, while in dioxane the converse is true.

Introduction

The description of chemical structure within a particle of ion-exchange resin in contact with solvent is a problem of considerable interest and importance. For example, the nature of ion association in water-swollen exchangers, heterogeneity of exchange sites within and between individual resin particles, interaction between counterions and between fixed exchange sites, and the state of the sorbed liquid are incompletely understood topics which have been approached primarily by interpretation of thermodynamic, diffusion, and conductance data.¹ On going to mixed and non-aqueous solvents, these problems are compounded, and new ones emerge, *e.g.*, the degree of solvolysis of $-\text{SO}_3\text{H}$ groups. One might expect spectroscopic methods to contribute rather more

directly to the elucidation of some of these questions; however, only a single report on the infrared spectra of ion exchangers² appears to have been made. The present work consists of attempts to (i) discover what phenomena may be observed in the proton magnetic resonance (p.m.r.) spectra of resin-solvent systems, and (ii) to employ the infrared spectra as a criterion of the chemical state of the resin exchange functions in non-aqueous media. The p.m.r. section contains descriptions of the spectra along with attempts to identify the molecular origins of the effects observed and generally to understand the spectra in terms of known principles of single-phase systems, followed by a discussion of what contribution the spectra can make to understanding the physical chemistry of the exchangers.

(1) See J. A. Kitchener in J. O'M. Bockris, "Modern Aspects of Electrochemistry," Academic Press, New York, N. Y., 1959, p. 87.

(2) A. Strasheim and K. Buijs, *Spectrochim. Acta*, **17**, 388 (1961).

Experimental

Materials.—Resins were principally purified grades of Dowex 50W and Dowex 1 obtained from Bio-Rad Laboratories, Richmond, California as AG 50W and AG 1. They were converted to the desired ionic states by standard column procedures, and when anhydrous materials were desired, were first air dried to 10–20% water, then dried to constant weight at 75–80° and a final pressure of about 10^{-4} mm. (6–8 hr.). Direct potentiometric Karl Fischer titration under methanol showed that the materials so prepared contained no more than 0.04 mmole of water per meq. of resin. Acetonitrile and dioxane were reagent materials distilled from phosphorus pentoxide and sodium, respectively, through a 61-cm. glass helices-packed column; constant-boiling center cuts possessing properties agreeing with published values were used. Water was deionized with a mixed-bed ion-exchange column.

Spectroscopic Measurements.—Infrared spectra were determined on a Beckman IR-4 spectrophotometer equipped with a rocksalt prism. Air-dried resin samples were repeatedly ground in a stainless steel ball mill on a Wig-L-Bug amalgamator, then dried to constant weight as above, and sealed *in vacuo*; opening, mixing with Nujol or the appropriate solvent, and pressing between rocksalt plates was done in a drybox. P.m.r. spectra were recorded on a Varian A-60 spectrometer whose probe temperature was $32 \pm 2^\circ$. Suspensions of resin beads in the appropriate solvent (prepared in the drybox where necessary) were observed in Wilmad Glass Co. semi-precision, 5 mm. \times 15 cm. cells.

Swelling Measurements.—Selected 50–100 mesh beads were dried as above, and the diameters were measured, before and after addition of solvent, with a microscope equipped with an eyepiece micrometer which allowed estimation to about 0.004 mm., the beads being protected from the atmosphere by enclosure between two greased cavity slides.

Results and Discussion

Proton Magnetic Resonance Spectra.—Most of the observations were made on the Bio-Rad Dowex resins and these are summarized in Table I; results with some other materials are described in a later section. Some examples of these spectra, which are seen to be remarkably well defined, are given in Fig. 1 and 2. Several features are common to most of the spectra: (1) Separate signals arising from liquid within and without the resin particles are observed³; the sign and magnitude of the shift of interior relative to exterior liquid depends both on the nature of the proton under observation and the nature of the resin salt. (2) Suspension of the resin in the liquid broadens the exterior liquid resonance and shifts it by *ca.* 2–10 c.p.s. (3) Lines due to interior liquid and to proton-containing counterions are broadened to an extent dependent on structure.

Lines Due to Exterior Liquid.—The shift produced in the position of the exterior liquid line by the presence of the solid can be accounted for to a good approximation as the result of the change in bulk diamagnetic susceptibility of the sample. This is best shown using spheres of pure cross-linked polystyrene, for which the volume suscepti-

(3) Identification of interior and exterior liquid resonances is accomplished by manipulation of the sample cell to place a more dense or less dense suspension of the solid within the probe; the intensities of the two signals then are observed to vary in a continuous, complimentary fashion. Further evidence that production of two lines is not an artifact of the heterogeneous nature of the sample is obtained: (1) using spheres of pure crosslinked polystyrene which are not penetrated by water—in which case water suspensions display only the exterior water line, while suspensions in toluene, which is distributed into the polymer, again give two lines for both methyl and aromatic protons; (2) by observing continuous intensity changes, with changing solvent composition, of the four expected lines in resin-binary liquid systems; and (3) by observing changes with time in the number and positions of lines in mixtures of two different resin salts and water (see below).

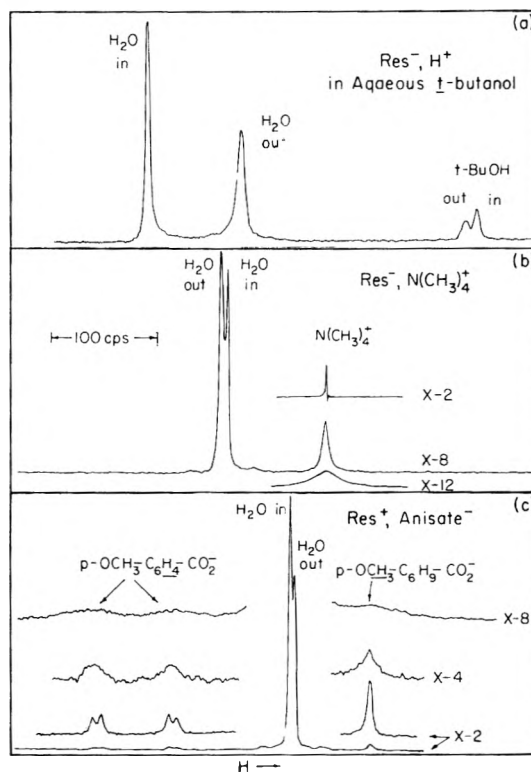


Fig. 1.—Proton magnetic resonance spectra of ion-exchange resin-liquid systems. The scale is the same for a, b, and c. Resins are Bio-Rad AG 1 and AG 50W.

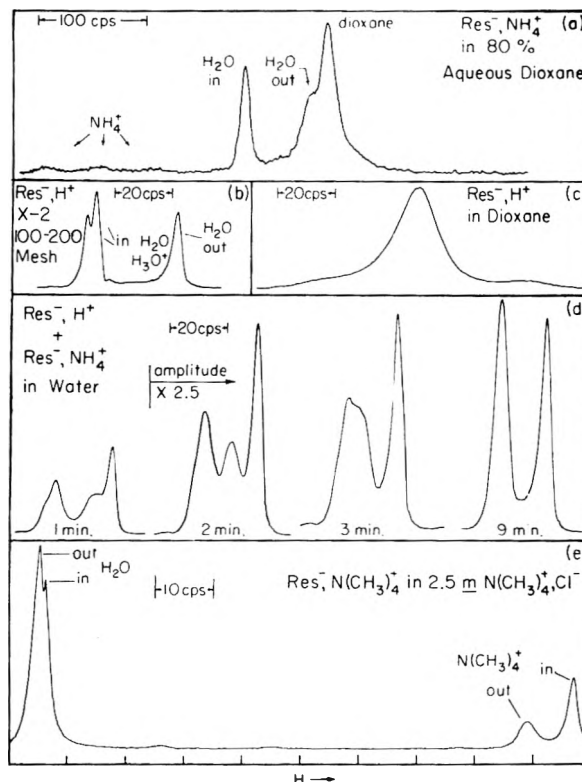


Fig. 2.—Proton magnetic resonance spectra of ion-exchange resin-liquid systems. Resins are Bio-Rad AG 1 and AG 50W.

bility is easier to estimate. Table II shows how the observed shifts for four liquids do indeed fall in the order of their susceptibilities; using these

TABLE I
 DATA FROM 60 MC. P.M.R. SPECTRA OF SOME ION-EXCHANGE RESIN SUSPENSIONS

Resin			Liquid	Shift of interior liquid relative to exterior (c.p.s.)	Width of ^a interior liquid resonance (c.p.s.) H ₂ O	Width of ^a exterior liquid resonance (c.p.s.)	Width of ^a counter-ion resonance (c.p.s.)	Width ^a of interior liquid resonance (c.p.s.)		Width of ^a exterior liquid resonance (c.p.s.)
Counter-ion	% DVB	Particle size ^b						liq. relative to exterior (c.p.s.)	liq. resonance (c.p.s.)	
A. Water and 5% aqueous <i>t</i> -butyl alcohol										
Na ⁺	8	C	H ₂ O	17	4.5	12				
Na ⁺	8	C	H ₂ O- <i>t</i> -BuOH	17	4.5	11		16	<i>c</i>	11
NMe ₄ ⁺	2	B	H ₂ O	~2	<i>d</i>	<i>d</i>	2			
NMe ₄ ⁺	8	C	H ₂ O	6	3	6	7			
NMe ₄ ⁺	12	C	H ₂ O	9	4	6	29			
NMe ₄ ⁺	8	C	H ₂ O- <i>t</i> -BuOH	8	4	6	8	19	<i>c</i>	6.5
H ⁺	2	B	H ₂ O	-24	4.5 ^e	4	4.5 ^e			
				-27						
H ⁺	4	C	H ₂ O	-43	4 ^e	8	4 ^e			
				-47						
H ⁺	8	C	H ₂ O	-79	4 ^e	8	4 ^e			
H ⁺	12	C	H ₂ O	-102	4 ^e	10	4 ^e			
H ⁺	8	A	H ₂ O	-86	3 ^e	7	3 ^e			
H ⁺	8	C	H ₂ O	-79	4 ^e	8	4 ^e			
H ⁺	8	D	H ₂ O	-73	6.5 ^e	16	6.5 ^e			
H ⁺	8	C	H ₂ O- <i>t</i> -BuOH	-89	5 ^e	8	5 ^e	11	5	7
NH ₄ ⁺ (H ⁺) ^f	8	C	H ₂ O	<5	<i>d</i>	<i>d</i>	8 ^g			
NH ₄ ⁺ (NH ₃) ^h	8	C	H ₂ O	-14	4 ^e	7	4 ^e			
NH ₄ ⁺ (NH ₃) ^h	8	C	H ₂ O- <i>t</i> -BuOH	-15	4 ^e	8	4 ^e	18	<i>c</i>	9
Cl ⁻	4	C	H ₂ O- <i>t</i> -BuOH	~4	<i>d</i>	<i>d</i>		~4	<i>d</i>	<i>d</i>
HCO ₂ ⁻	4	C	H ₂ O	-4	4	4	2			
HCO ₂ ⁻	4	C	H ₂ O- <i>t</i> -BuOH	-5	5	4		3	3	4
OH ⁻	2	B	H ₂ O	-9	2.5 ^e	4	2.5 ^e			
OH ⁻	4	C	H ₂ O	-18	5 ^e	4	5 ^e			
Anisate ⁻	2	B	H ₂ O	-3	<i>d</i>	<i>d</i>	13(Ar) ⁱ			
							5(OCH ₃)			
Anisate ⁻	4	C	H ₂ O	-9	4	7	19(Ar) ⁱ			
							15(OCH ₃)			
Anisate ⁻	8	C	H ₂ O	-14	6	7	~50(Ar) ⁱ			
							~50(OCH ₃)			
Anisate ⁻	4	C	H ₂ O- <i>t</i> -BuOH	-8	4	6	21(Ar) ⁱ	9	4	7
							18(OCH ₃)			
<i>p</i> -Nitrobenzoate	4	C	H ₂ O	-8	4	4	27			
<i>p</i> -Nitrobenzoate	4	C	H ₂ O- <i>t</i> -BuOH	-7	4	4.5		15	4	4.5
Polystyrene ^j			H ₂ O- <i>t</i> -BuOH	No interior line		2.5		No interior line ^k		2.5
Polystyrene ^j			Toluene	-6.5(CH ₃)						
				-5.5(Ar)	~6(CH ₃)	~11(CH ₃)				
B. 80% Aqueous dioxane										
					H ₂ O			Dioxane		
H ⁺	8	C		-185	7.5	<i>d</i>	7.5 ^e	<i>l</i>	<i>l</i>	~12
NH ₄ ⁺ (H ⁺) ^f	8	C		-60	9	<i>d</i>	20-25	<i>l</i>	<i>l</i>	~20
NMe ₄ ⁺	8	C		-35	10	~22	19	<i>l</i>	<i>l</i>	~14
Anisate ⁻	4	C		-57	9	<i>d</i>	21 Ar ⁱ	<i>l</i>	<i>l</i>	<i>d</i>
							16 OCH ₃			

^a Width at half-height. Under the conditions used, line widths in homogeneous aqueous solution were (c.p.s.): water, *t*-butyl alcohol, and tetramethylammonium and formate ions, 2; dioxane and ammonium ion, 3; anisate ion, 2 (methoxyl) and 11 (aromatic); *p*-nitrobenzoate ion, 8. ^b Dry mesh range before introduction of electrolyte functions: A, 50-100 mesh; B, 100-200 mesh; C, 200-400 mesh; D, minus 400 mesh. ^c Too weak to measure. ^d Insufficiently resolved. ^e Interior liquid and counterion undergoing rapid chemical exchange. ^f A few per cent. of hydrogen resinates added to repress dissociation and chemical exchange of NH₄⁺. ^g Each component of triplet. ^h A trace of ammonium hydroxide was added to ensure rapid chemical exchange between NH₄⁺ and H₂O. ⁱ Each component of doublet. ^j Spheres, 200-400 mesh, 8% DVB, kindly furnished by Dow Chemical Co. ^k Relative to external water by substitution, since the exterior water line in the suspension was unresolved; this has the effect of increasing the observed shift of the interior water line by about 5 c.p.s. ^l Interior dioxane resonance is buried under exterior dioxane as shown by separating the phases and observing the spectrum of the solid phase alone.

susceptibilities, the value -0.690×10^{-6} for the volume susceptibility of the polystyrene, and the volume fraction of liquid in each of the suspensions obtained by integration of the p.m.r. signal in the

absence and in the presence of the solid, the expected shifts in the liquid line position may be computed, and these are given in Table II. This value for the susceptibility of the polystyrene-

DVB copolymer may be compared with that (-0.736×10^{-6}) estimated from the Pascal constants and the measured density, 1.052 g./cc. Results with the ion exchangers themselves paralleled these results, although with considerable variation from resin to resin due to the fact that the susceptibility of the solid changes with the chemical identity of the electrolyte functions and the degree of swelling. The average shifts for exterior liquid due to the presence of the solid were: water, -2 c.p.s.; 80% dioxane, -6 c.p.s.; dioxane, -7 c.p.s.; acetonitrile, -12 c.p.s.

TABLE II

SHIFTS IN P.M.R. LINE POSITIONS OF LIQUIDS PRODUCED BY ADDITION OF POLYSTYRENE-DIVINYLBENZENE SPHERES^a

Liquid	$\Delta\nu$, c.p.s.		$-\chi^b \times 10^6$	Vol. fr. liquid
	Obsd.	Calcd.		
Water	+ 2.5	+ 2.5	0.721	0.350
Toluene	- 5	- 2.6	.631	.643
Dioxane	- 5	- 6.4	.589	.502
Acetonitrile	-12	-2.4	.483	.525

^a See Table I, footnote j. ^b From ref. 4 except for acetonitrile which was estimated from the Pascal constants (ref. 4, p. 19).

A qualitative account of the broadening of the exterior liquid lines can be given in terms of local field inhomogeneities in the vicinity of particles of diamagnetic susceptibility different from that of the surrounding liquid; the order of observed line widths for the various liquids, acetonitrile > dioxane > aqueous dioxane > water, is indeed the order of solid-liquid susceptibility differences as inferred above, and the exterior liquid line width increases with decreasing particle diameter (decreasing mean distance of liquid molecules from the solid) as expected. The sharpness of the spectra in water is thus a result of fortunate near identity of the liquid and solid susceptibilities.

A quantitative estimate of the line broadening from this source can be made for the simplified model obtained by replacing the real sample by a non-interacting collection of individual, spherical solid particles each surrounded by a spherical shell of liquid, the diameters being chosen to maintain the observed volume fraction of liquid in the sample. This was done by computing the component, in the direction of the applied field, of the field due to the magnetized sphere at radial intervals across the liquid region by numerical integration over the solid sphere of

$$H = H_0 \Delta\chi \int_V (1 - 3 \cos^2 \alpha) r^{-3} dV$$

both in the direction of the applied field and perpendicular to it. Here H_0 is the applied field, $\Delta\chi$ the difference in susceptibility of liquid and solid, α the angle between the induced dipole in the volume element dV of the solid sphere and the line connecting the dipole with the point in the liquid region at which the field is to be calculated, and r is the distance of this point from the dipole. From these results the field at intermediate angular orientations can be obtained and the entire

(4) J. A. Pople, W. G. Schneider, and H. J. Bernstein, "High-Resolution Nuclear Magnetic Resonance," McGraw-Hill Book Co., New York, N. Y., 1959, p. 488.

liquid region thus mapped. The results of this procedure for a liquid fraction of about 0.4, the measured value for several of the resins in water, gave a distribution of local field strengths corresponding to a line width at half-height, $\Delta H = 7.2\Delta\chi H_0$; for the susceptibilities employed above, this is about 17 and 86 c.p.s. at 60 Mc. for water and acetonitrile, respectively (observed: ca. 6 and 40 c.p.s.).⁵ Reverting from this simplified case to the actual sample where each sphere is in contact with several neighbor spheres, the line is expected to be narrower than the above prediction for two reasons: First, the mean distance of the proton from the sphere will increase; and second, the presence of neighboring spheres will decrease the inhomogeneity of the field (*e.g.*, at the center of a void in close-packed uniform magnetized spheres the field due to the spheres is zero). The observed broadening thus can be said to be of the correct order of magnitude for the effect suggested.

The Line Positions of Interior Liquid and Counterion Resonances.—Since, to a good approximation, the resin particles are perfect spheres, there will be no contribution to the observed shifts of interior from exterior liquid resonances due to the difference in diamagnetic susceptibility of liquid and solid.⁶ Two factors which are important are shifts produced by solvation of fixed- and counterions, and anomalous diamagnetic shielding effects produced by the aromatic nuclei⁷ of the resin matrix.

As a first approximation, the first of these factors might be neglected for carbon-bound protons, and we can hope to account for the shifts of the methyl resonance of *t*-butyl alcohol on the basis of the second factor alone. From Table I the observed shifts for *t*-butyl alcohol on entering the resin phase are indeed always positive, *i.e.*, to higher applied fields, as required by the effect under consideration. From the magnitude of the high-field shift observed by Bothner-By and Glick for aliphatic solutes dissolved in aromatic liquids, the densities of the resins,^{8,9} swelling measurements, and the capacity of the resins, one can estimate the following values for the expected shifts due to the diamagnetic anisotropy of the polystyrene matrix: for cation exchangers, $+14$ – 18 c.p.s.; for anion exchangers, $+9$ c.p.s.; for anion exchangers charged with aromatic counterions, $+23$ c.p.s. These estimates are for the case of random orientation of the molecule with respect to the aromatic ring. The observed shifts for *t*-butyl alcohol in the cation exchangers (average = $+16$ c.p.s.) agree well with the prediction, while those for the anion exchangers (4 and 12 c.p.s., without and with an aromatic counterion) are in the correct direction but have about half the

(5) The range of a/a_0 (a = distance of liquid molecule from the center of the solid sphere of radius a_0) included was 1.0185 to 1.2035; neglect of the innermost region affects the intensity of the line at its far extremities but has little influence on the width at half height.

(6) Reference 4, p. 81.

(7) A. A. Bothner-By and R. E. Glick, *J. Chem. Phys.*, **26**, 1651 (1957).

(8) H. P. Gregor, J. Belle, and R. A. Marcus, *J. Am. Chem. Soc.*, **76**, 1984 (1954).

(9) H. P. Gregor, F. Gutoff, and J. I. Bregman, *J. Colloid Sci.*, **6**, 245 (1951).

predicted magnitude. Some analogous information for homogeneous solution in 5% butanol is obtainable from Table III; here also the effect of the aromatic nucleus is smaller for the aromatic cation than for the aromatic anion, though the average shift is very close to that predicted for the anomalous diamagnetic shielding due to 5 *m* aromatic nuclei (22 c.p.s.). These results probably reflect orientation effects in the ion-solvent interaction; the result for sodium chloride shows further that the effect of inorganic ions on methyl proton line positions can be sizeable. These and other effects (*e.g.*, inter-chain orientation effects, exclusion of liquid from regions of high cross-link density) doubtless contribute something to the resin results, though the anomalous shielding of the aromatic matrix, in random orientation, appears to account for the bulk of the shift.

TABLE III

SOLVENT LINE POSITIONS FOR 5.00 *m* SOLUTIONS OF SOME ELECTROLYTES IN 5% AQUEOUS *t*-BUTYL ALCOHOL REFERRED TO PURE EXTERNAL SOLVENT MIXTURE

Solute	Shift (c.p.s.)	
	H ₂ O	(CH ₃) ₃ COH
NaCl	8.5	-12.2
NMe ₄ Cl	2.3	-2.9
C ₆ H ₅ NMe ₃ Cl	8.3	12.8
HCO ₂ Na	-0.9	-1.2
C ₆ H ₅ CO ₂ Na	7.2	31.2
HNO ₃ or HCl	-83.5 ^a	
NaOH	-26 ^b	

^a Interpolated from reference 10; for pure water and corrected for bulk susceptibility. ^b Interpolated from H. S. Gutowsky and A. Saika, *J. Chem. Phys.*, 21, 1688 (1953).

The shifts of interior from exterior water contrast markedly with those for *t*-butyl alcohol, depending strongly upon the resin structure, as expected for a direct chemical interaction with the electrolyte functions present; the observed effects are in all respects analogous to those produced by electrolytes in homogeneous solution. The order of interior water line positions for the various counterions in the resin spectra ($H^+ < N(CH_3)_4^+ < Na^+$ and $OH^- < HCO_2^- < Cl^-$) is the same as that measured (Table III) in homogeneous solution, though there is probably some aromatic high-field shift superimposed upon this variation. Further, taking phenyltrimethylammonium chloride solution, at the concentration prevailing in the resin, as a homogeneous model for the resinium chloride, the expected water line shift, +3.6 c.p.s., is in good agreement with the observed shift of about +4 c.p.s. Finally, the dependence of the interior water shift, for a given counterion, upon the degree of cross-linking of the resin follows the expected pattern for changes in electrolyte concentration paralleling swelling changes dependent on the cross-linking. This can be quantitatively tested for the hydrogen resins by combining the observed shifts with the relation between chemical shift and molality established¹⁰ for strong acids in homogeneous aqueous solution; the molality of hydrogen counterions obtained in this way is 1.34, 2.50, 4.36, and 5.70 for the 2, 4, 8, and

12% DVB resins, in reasonable agreement with swelling measurements¹¹ on similar materials of 1950-1951 vintage which gave 1.07, 2.45, and 4.80 *m* for the first three cases.

In 80% dioxane, the apparent general increase in the shift to lower field of interior relative to exterior water, as compared with the pure water suspensions, is in large part artificial, as it includes a shift of +55 c.p.s. in the position of the exterior water line on going from pure water to 80% aqueous dioxane, a result of the change in hydrogen bonding equilibria. This semi-quantitatively accounts for all of the observed shifts except that in the hydrogen resinate, where replacement of some of the interior water by dioxane has increased the fraction of H₃O⁺ in the H₃O⁺-H₂O rapid exchange system, leading to an additional shift to lower field.

The only case for which the position of the counterion resonance has been measured is the 2% DVB tetramethylammonium resinate (Fig. 2e). Since salt effects on the tetramethylammonium ion resonance in homogeneous solution are small, the line position varying no more than ±2 c.p.s. with concentration over the range 0.5-3 *m*, the shift of the interior line from that displayed by a surrounding tetramethylammonium chloride solution of approximately the same concentration may be expected to result primarily from the anomalous shielding of the resin matrix. The expected shift from this source, estimated from the observed⁹ resin volumes as before (assuming the deswelling due to exterior tetramethylammonium chloride to be the same as that observed⁹ for an equal concentration of ammonium chloride), is +9 c.p.s., in good agreement with the observed +8 c.p.s. shift.

Line Widths of Interior Liquid and Counterion Resonances.—In contrast to the situation for exterior liquid molecules near resin beads considered as magnetized spheres, molecules within the spheres should experience a uniform field¹² and their resonance lines should remain unbroadened, except that in a dense suspension of spheres broadening due to neighboring spheres may become important. The systems at hand indeed show some broadening (about 4 c.p.s. *vs.* 2 c.p.s. for the homogeneous liquid) of the interior water line and this is less than that for exterior water, as expected. Since the interior water line width is nearly independent of the nature of the electrolyte functions present and of the cross-linking, but depends more markedly on the particle size, approaching the line width of pure water at large diameters, it is reasonable to attribute all of the detected broadening (except in the case of chemically heterogeneous resins treated below) to the field inhomogeneity arising from the particulate nature of the sample.

Except for formate, the broadening of the organic counterion lines is generally greater than that of interior water in the same resin, and it increases very rapidly with increased cross-linking (Table

(11) G. E. Boyd and B. A. Soldano, *J. Am. Chem. Soc.*, 75, 6092 (1953).

(12) L. Page and N. I. Adams, Jr., "Principles of Electricity," D. Van Nostrand Co., Princeton, N. J., 3rd Ed., 1958, p. 123.

(10) G. C. Hood, O. Redlich, and C. A. Reilly, *J. Chem. Phys.*, 22, 2067 (1954).

I; Fig. 1). This is presumably the result of increasing viscosity of the gel as the volume fraction of the hydrocarbon network increases accompanying increased cross-linking and concurrent decreased swelling, leading to loss of rotational freedom in the ion and enhanced dipolar broadening¹³ of its resonance. These effects correspond directly to the behavior of self-diffusion coefficients¹⁴ of resin components, where diffusion of counterions is found to be more drastically reduced, relative to homogeneous solution, and more dependent upon the cross-linking, than is diffusion of water. The depression of the equivalent conductance of counterions, which also increases with decreasing swelling of the resin, is attributed to the same source.¹⁵

Figure 3 shows how the counterion line widths extrapolate smoothly to the line widths observed in homogeneous aqueous solution at zero cross-linking, both for the tetramethylammonium ion and for the anisate ion. This is of interest because, though the tetramethylammonium resin appears to be unassociated in water,^{8,9,16} exchange thermodynamics¹⁷ and swelling measurements⁸ have been interpreted as indicating extensive ion association in anion exchangers charged with large organic ions. The absence of a discontinuity, in the width of the anisate ion line, between the resins of low cross-linking and homogeneous aqueous solution indicates that (since the ion association itself does not go to zero at low cross-linking¹⁷) formation of ion pairs between counterions and the charged resin matrix produces no further dipolar broadening of the counterion resonance. It appears that both of the deficiencies which might be anticipated in the investigation of counterion line broadening as an index of ion association in these systems are operative—that is, bound ions retain enough motion to give rather sharp lines while at the same time free and associated ions suffer broadening induced by the physical nature of the medium.

Anhydrous Dioxane and Acetonitrile.—Spectra in these liquids were measured for hydrogen, ammonium and tetramethylammonium resins, and for resinium formate and anisate; all of the spectra are very similar and have the following characteristics: (a) The exterior liquid line is greatly broadened, as previously discussed, the average widths at half height being *ca.* 25 and 40 c.p.s., respectively. (b) No lines due to protons in counterions were detected. (c) No lines plausibly attributable to interior liquid were observed. Shoulders on the high-field side of the exterior liquid line were present in some cases, though it was difficult to separate these completely from the spinning side bands which are virtually impossible to eliminate from these spectra. It seems probable

(13) Reference 4, p. 29.

(14) (a) G. E. Boyd and B. A. Soldano, *J. Am. Chem. Soc.*, **75**, 6091, 6099, 6105, 6107 (1953); (b) M. Tetenbaum and H. P. Gregor, *J. Phys. Chem.*, **58**, 1165 (1954).

(15) A. Despic and G. J. Hills, *Trans. Faraday Soc.*, **51**, 1260 (1955).

(16) H. P. Gregor, D. Nobel, and M. H. Gottlieb, *J. Phys. Chem.*, **59**, 10 (1955).

(17) H. P. Gregor, J. Belle, and R. A. Marcus, *J. Am. Chem. Soc.*, **77**, 2713 (1955).

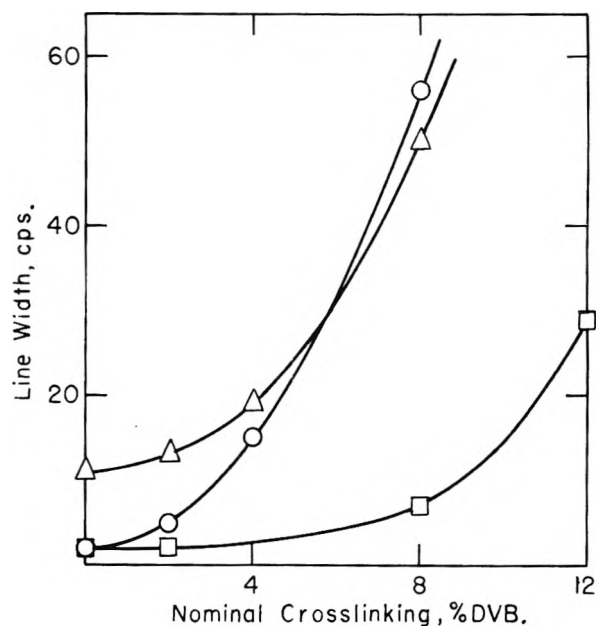


Fig. 3.—Nuclear magnetic resonance line widths for counterions in ion-exchange resin-water suspensions vs. the degree of cross-linking of the resin: □, tetramethylammonium ion; ○, anisate ion (methyl); △, anisate ion (aromatic).

that interior liquid lines, where present at all,¹⁸ are buried under the exterior line; this was shown to be the case for dioxane in 80% aqueous dioxane by direct examination of the solid phase. The absence of counterion resonances doubtless reflects the very low fluidity of the resins in contact with these liquids which would be expected from the swelling measurements.

Resin Homogeneity.—In all of the resins so far described, the interior water line in the spectra of the water suspensions is only slightly broadened compared to the pure liquid, and this broadening is reasonably attributed to the particulate nature of the sample. The presence of a single, narrow line for interior water implies a high degree of homogeneity, both intra- and inter-particulate, in these materials. In the first sense this is an independent confirmation of the internal structure of the swollen resin¹⁸ as a homogeneous phase of considerable fluidity in which the sorbed liquid molecules all have the same time-average environment.¹⁹ This does not mean that cross-linking or other gradients do not exist within a single particle, but only that there is rapid exchange between water molecules in the various physicochemical situations present. On the other hand, since there is no rapid exchange *between* particles, and since there is a strong dependence of the interior water line position upon the counterion molality, especially in the case of the hydrogen resins and resinium hydroxides, the existence of a single, sharp interior water line places narrow limits on the inter-particle heterogeneity of the sample

(18) Reference 1, p. 93.

(19) It is impossible to rule out the presence of a fraction of interior water molecules so tightly bound to the polymer network or so ice-like that its resonance line is dipole-broadened to the point of disappearance; a sizable fraction of this type could not be undergoing rapid exchange with the visible interior liquid, however.

TABLE IV
 P.M.R. DATA FOR VARIOUS ION EXCHANGERS IN WATER

Resin	Particle size	Cross-linking % DVB	Counter ion	Shift of interior from exterior water, c.p.s.	Width of interior water line, c.p.s.	Width of exterior water line, c.p.s.
Bio-Rad AG 50	100-200 ^a	2	H ⁺	-27.5 -31	~4.5	4
Bio-Rad AG 50	100-200 ^a	2	Na ⁺	+7	2.5	5
Bio-Rad AG 50	200-400 ^a	4	H ⁺	-43 -47	4	8
Rexyn AG 50 ^b	16-50 ^c	Medium porosity	H ⁺	-88 -100(sh)	6 >6	6
Rexyn RG 50 ^b	16-50 ^c	Medium porosity	H ⁺	-88 -100(sh)	8 ?	6
Dowex 50 W ^d	50-100 ^a	2	H ⁺	-27 -30	~6	3
Amberlite IR 120 ^e			H ⁺	-84	15	6
Amberlite IR 120 ^e after cycling			H ⁺	-84	9	6
Dowex 50 ^f	100-200	2	H ⁺	-28	15	3
Dowex 50 ^f after cycling	100-200	2	H ⁺	-28	3	3
Dowex 50 ^f	200-400	4	H ⁺	-44	28	6
Amberlite IR 120 CP ^g	20-50 ^c	High porosity	Na ⁺	+ 2	~3	~3
Amberlite IR 120 CP ^g	20-50 ^c	High porosity	H ⁺	-11	2.5	2
Amberlite CG-120 ^h	100-200 ^a		Na ⁺	+16	11	11
Amberlite CG-120 ^h	100-200 ^a		H ⁺	-87	9	8
Permutit Q ⁱ	16-50 ^c		H ⁺	-87	8	6
Rexyn RG 1 ^b	16-50 ^c	Medium porosity	OH ⁻	-15	3	6
Amberlite IR 45			Free base	<i>j</i>	<i>j</i>	10
Amberlite IR C 50			Free acid	<i>j</i>	<i>j</i>	19

^a Dry mesh range prior to sulfonation, etc. ^b Fisher Scientific Co. ^c Actual wet mesh range. ^d J. T. Baker Chemical Co. Cat. No. 1920. ^e Old stock. ^f Purchased in 1956. ^g Mallinckrodt Chemical 3347. ^h Mallinckrodt Chemical 3337. ⁱ Matheson Coleman & Bell 9055. ^j No interior line.

with respect to cross-linking, degrees of sulfonation, etc. With the hydrogen resins for example, the presence of an appreciable fraction differing by 0.1 in counterion molality (0.2-0.4 of a nominal %DVB unit in cross-linking) should be detectable.

Using the present data, this criterion can be applied to a number of different resins. Most of these are the purified Dowex resins supplied by Bio-Rad Laboratories; with two exceptions discussed below these give evidence of a high order of homogeneity when examined directly as supplied; the narrow interior water lines observed also rule out the presence of paramagnetic counterions. Table IV summarizes the information on heterogeneity and on the resins from other sources. The table is divided into four parts; the first lists those resin samples which give evidence of containing two or more distinct fractions. The second part includes resins which displayed an unusually broad interior water line when observed directly as received; in the two cases where it was tried, cycling the resin with sodium hydroxide-hydrochloric acid sharpened the line, suggesting that the broadening was due to the presence of paramagnetic counterions. The third part of Table IV contains materials from other sources whose behavior was normal, and the fourth part consists of resins which show no interior water line.

The type of heterogeneity shown by the materials in the first section of Table IV is unexpected; the resolution of the interior water resonance for

the Bio-Rad AG 50W X2, 100-200 mesh hydrogen resinate into two rather sharp lines is shown in Fig. 2b. There is, however, some previous evidence for the same sort of behavior. Högfeldt²⁰ found that the selectivity coefficients for silver-hydrogen exchange measured by tracer techniques on individual resin beads not only varied from bead to bead, but, with one resin sample, tended to cluster around two distinct values of the selectivity coefficient, probably reflecting clustering about two cross-linkings.

The heterogeneous X2 100-200 mesh resinate was further examined. On cycling, the splitting of the interior water line disappeared in the sodium state as expected (the separation would be less than 1 c.p.s.) but reappeared unchanged in the hydrogen state, ruling out any explanation based on foreign counterions. Table V shows the correlation found between the particle size and the p.m.r. data obtained on fractionation of the sample on standard sieves; this demonstrates the inter-particulate nature of the heterogeneity and shows that the low-field fraction is concentrated among the largest particles. The most likely structural differences involved in producing the different line positions are in the degrees of cross-linking and sulfonation. It is difficult to conceive a chemical process capable of producing, in a single preparation, such a discrete binary mixture of beads with respect to either of these variables.

(20) E. Högfeldt, *Arkiv Kemi*, **13**, 491 (1959).

A more likely source would seem to be combination, during or after polymerization, of similar but distinct lots of nominally identical material.

TABLE V

P.M.R. SPECTRA OF A HETEROGENEOUS RESIN AS A FUNCTION OF PARTICLE SIZE

Wet screen analysis		Interior water line, c.p.s. from exterior water line	Relative intensity
Retained by	%		
45 mesh	Trace	..	
50	15	-27.5	1
		-31	2.5
60	16	-27.5	1.2
		-31	1
70	22	-27.5	2.3
		-31	1
80	29	-27.5	
100	15	-27.5	
120	3	~27 (broad)	
140	Trace	..	

Kinetic Processes.—Observation of separate lines for interior and exterior water sets a lower limit for the mean lifetime of water molecules in either phase; this ranges from 0.004–0.1 sec. for the resins in Table I. Exchange of interior water with exterior deuterium oxide proved too rapid to measure under the present conditions; the half-time for this reaction in a shallow-bed flow system was of the order of 1 sec. in the measurements of Tetenbaum and Gregor.^{14b} Neither has it been possible to observe exchange of ions between the resin and an electrolyte solution. The exchange occurring between resin particles charged with different counterions immersed in deionized water is observable, however, and provides a good illustration of the correctness of our analysis of the line identities in the simple spectra (Fig. 2d).

Other Applications.—Several further uses of spectra of this sort suggest themselves. Figure 1a implies that it should be possible to measure distribution coefficients between solution and resin phases for binary liquid mixtures. The possibility of measuring selectivity coefficients for proton-containing counterions is suggested by Fig. 2e. The molality of proton-containing counterions can be obtained by integration of the counterion and interior liquid lines. Determination of counterion molality for hydrogen resins from the position of the interior water line already has been illustrated.

Infrared Spectra.—Observed infrared bands for various ionic states of the cross-linked polystyrenesulfonic acid exchanger are given in Table VI. It is clear that the sodium, ammonium, and hydrated hydrogen resins have closely similar spectra which are readily distinguished from that of the anhydrous hydrogen resin. These differences agree well with the results of Detoni and Hadži²¹, who find for simple arylsulfonic acids, characteristic bands for the anhydrous acids (ArSO_2OH) near 895,²² 1092, 1165, 1342, 2350, and 2900 cm^{-1} ,

(21) S. Detoni and D. Hadži, *Spectrochim. Acta*, **11**, 601 (1957).

(22) The frequencies quoted here are for *p*-toluenesulfonic acid; a band near 650 cm^{-1} also is apparent in the reproduced spectrum.

while their salts and the hydrated acids (ArSO_3^-) show, instead, absorption near 1130²³ and 1200 cm^{-1} , together with changes in bands near 1050 cm^{-1} .

TABLE VI

INFRARED BANDS OF THE SULFONIC ACID TYPE CATION EXCHANGER AG 50W-X8 IN VARIOUS IONIC STATES^a

H (dry)	H (hydrated) ^b	Na (dry)	NH_4 (dry)
<660's			
	680s	680s	680s
775w	776w	776w	777w
835m	836m	834m	835m
900s			
1012sh	1009s	1009s	1010s
1040sh	1037s	1042s	1038s
1096m			
	1130s	1131s	1129s
1160-	1160-	1170-	1165-
1180s	1170s	1190s	1175s
1195sh	1215sh	1220sh	1215sh
1320m			
1350m	1350w	1350w	1350w
1420w	1419w	1417w	1420sh
1454w	1445w	1448w	1445w
1492w	1494w	1493w	1496w
1596m	1600w	1598w	1600w
1685w	^d	1670w	•
2415m			
/	2930s	/	/
/	3390s	/	/

^a Frequencies in cm^{-1} ; s = strong, m = medium, w = weak, sh = shoulder. ^b Contains ca. 20% water. ^c A strong band whose maximum was slightly beyond the range of the spectrometer was present, doubtless corresponding to the band shown near 650 cm^{-1} in the spectrum of *p*-toluenesulfonic acid. ^d Water absorption 1600–1800 cm^{-1} . ^e Ammonium ion adsorbs. ^f Halocarbon oil mulls were unsatisfactory in this region with the anhydrous resins which had to be ground dry.

In addition to demonstrating that the hydrogen resin dried to constant weight *in vacuo* is indeed the anhydrous sulfonic acid,²⁴ the infrared spectra offer a means of distinguishing the state of ionization of the sulfonic acid residues when the resin is in contact with solvents other than water. The bands at 900, 1096, and 1130 cm^{-1} proved most useful for this purpose when resin samples soaked in acetonitrile and dioxane were examined. With acetonitrile, the 900 and 1096 cm^{-1} absorptions persisted with roughly undiminished intensity, while the band at 1130 cm^{-1} , though weak, was discernible; thus only a small fraction of the sulfonic acid residues appear to have transferred protons to solvent. In dioxane there is greater interference from solvent bands; however, the 900 cm^{-1} band is very weak, if indeed present, and the appearance of the 660–680, 1010, and 1130 cm^{-1} regions confirms this indication of a high degree of solvolysis of $-\text{SO}_3\text{H}$ groups in this solvent.

Swelling Measurements.—The extent of swelling of dry resin upon immersion in a solvent has been

(23) A corresponding line appears at 1125 cm^{-1} in the Raman spectrum of the *p*-ethylbenzenesulfonate ion and the polystyrenesulfonate ion [S. Lapanje and S. A. Rice, *J. Am. Chem. Soc.*, **83**, 496 (1961)].

(24) The only previously described spectrum of a sulfonic acid ion exchange resin (also Dowex 50) is clearly that of the ionized hydronium sulfonate, though the functional groups are labeled $-\text{SO}_3\text{H}$.

considered a measure of the concentration of free or osmotically active counterions, and the deswelling, relative to water, observed on proceeding to less polar solvents has been identified with the onset of ion association in the resin phase.^{8,16} The hydrogen resinate employed in the present work (Bio-Rad AG 50W-X8) displayed swellings of 122, 45, and 56% in water, acetonitrile, and dioxane.²⁵ The swelling in dioxane is quite appreciable in comparison with the near-zero swelling reported¹⁶ for ammonium and substituted ammonium ions in

(25) G. S. Panson and R. Ellsworth (*J. Org. Chem.*, **25**, 1466 (1960)) find 115 and 75% for water and dioxane with Dowex 50-X8. The present result for dioxane (56 ± 3%) obtained on direct swelling of the dry resin agreed with that obtained on deswelling the water soaked resin by exhaustive washing with dioxane (49 ± 4%).

dioxane. It is unlikely, in view of the ammonium resinate results, that this swelling of the hydrogen resinate is connected with any extensive dissociation to free ions in the lyonium resinate; more likely, it is the natural accompaniment of the solvolysis of -SO₃H groups to lyonium sulfonate ion pairs; this would indicate one limitation on the use of swelling measurements as an index of dissociation to free ions. The best representation of the hydrogen resinate in acetonitrile and dioxane appears to be $\text{ArSO}_3\text{H} \cdot \cdot \cdot s \rightleftharpoons \text{ArSO}_3^- \cdot \cdot \cdot \text{Hs}^+$ ($s = \text{solvent}$) with the equilibrium predominantly to the right in dioxane, to the left in acetonitrile.

Acknowledgment.—The writer thanks Dr. A. A. Bothner-By for numerous helpful discussions.

RADIATION-POLYMERIZATION OF ETHYLENE: EVIDENCE FOR ION-MOLECULE CONDENSATION

By C. D. WAGNER

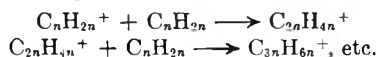
Shell Development Company, Emeryville, California

Received January 8, 1962

Ionizing radiation polymerizes ethylene at -196° to low molecular weight, monoolefinic, mainly branched polymers. Polymerization of a mixture of C₂D₄ and C₂H₄ gives polymer molecules containing deuterium in multiples of four, demonstrating that the initiating species contains four hydrogen atoms. Structure of the C₄, C₆, and C₈ products showed that (1) propagation can occur from either of at least two carbons in the propagating species, (2) no skeletal isomerization occurs, and (3) hydrogen atom migration is limited. This novel type of polymerization is believed to be initiated by the molecule ion, C₂H₄⁺, with propagation by ion-molecule condensation, and termination by electron recombination. However, a mechanism involving excited molecule condensation is not excluded.

Introduction

Ionizing radiation causes α-olefins in the condensed phase to form low molecular weight polymers. Evidence has been obtained that dimeric products are formed in part by condensation of a molecule ion with an uncharged molecule.^{1,2} It was postulated¹ that the trimers, tetramers, pentamers, etc., are formed by the same mechanism, in which charge neutralization is delayed long enough to permit several propagation steps



Collinson, Dainton, and Walker³ in a recent study with 1-hexadecene obtained evidence that the polymers as well as dimer are formed by some type of ionic mechanism.

It has now been found that ethylene also yields low molecular weight polymers when irradiated in solid phase at -196°. These polymers are >90% monoolefins of substantially branched structure.

The same technique used previously with propylene² has now been applied to ethylene. With ethylene it is now possible to test the proposed mechanism to see whether C_nH_{2n}⁺ is the initiating species in the formation of trimer, tetramer, etc., as well as the dimer. A mixture of ethylene and ethylene-d₄ was irradiated at -196°, and the ole-

finic products were examined mass spectrometrically for isotopic species distribution. The results obtained led to further studies on product structures to elucidate the propagation mechanism.

Experimental

Feed Materials.—Ethylene was Phillips Research Grade, analyzed by gas liquid chromatography (GLC) to contain <0.005% of any impurity.

Ethylene-d₄ was obtained from Merck and Co., Ltd. It contained 0.02% of material with the same retention time in a GLC column as butadiene and analysis of radiolysis products provided further evidence that it was, in fact, butadiene-d₆. Another impurity of about 0.03% was present with a retention time similar to a C₆ hydrocarbon. Analysis by mass spectrometry indicated it to be vinyl-d₃ bromide. Neither material was eliminated from the feed in the preparation of the sample for irradiation and they both appeared in the products. The isotopic purity of the C₂D₄ was 96.9%, the 3.1% ethylene-d₃ corresponding to a light hydrogen content in the deuterium of 0.83%.

Both ethylenes were degassed and distilled under vacuum from a bulb at -78° before use.

Irradiation Technique.—The feed ethylene (or mixture of ethylenes), 1.2 g., was distilled into a previously flamed and evacuated 10 mm. o.d. Pyrex tube equipped with a break-off seal. The sample in a dewar at -196° was irradiated by bremsstrahlung from the gold target of a 3 Mev. Van de Graaff. At full power (one mamp. beam), the dose rate was about 40 × 10⁶ rads/hr. (2.5 × 10²¹ e.v./g./hr.). The dose rate with the particular geometry of each experiment was checked by ceric dosimetry in an empty dewar. (The bremsstrahlung path length in the liquid nitrogen was negligible.) When an equimolar mixture of isotopic ethylenes was used, the ethylenes were mixed by shaking while cold before freezing for the irradiation.

Analysis.—Material volatile at -196° was first removed by a Toepler pump after the sample was warmed to fusion and then refrozen. The C₂ fraction was removed by distilla-

(1) Priscilla C. Chang, N. C. Yang, and C. D. Wagner, *J. Am. Chem. Soc.*, **81**, 2060 (1959).

(2) C. D. Wagner, *Tetrahedron*, **14**, 164 (1961).

(3) E. Collinson, F. S. Dainton, and D. C. Walker, *Trans. Faraday Soc.*, **57**, 1732 (1961).

tion from the tube at -78° until the vapor pressure was 5 mm. Both fractions were analyzed mass spectrometrically. A weighed sample (ca. 100 mg.) of highly-purified *n*-pentane (>99.99% pure; only impurity—2-methyl-2-butene) was distilled onto the hydrocarbon product. The product with its pentane carrier then was analyzed by gas chromatography. Products separated by gas chromatography were examined in the mass spectrometer (Westinghouse, Type LV, 75-v. ionizing electrons).

In order to obtain information about the carbon skeletons of the products, a portion of the pentane solution was hydrogenated by allowing it to be in contact with 12 mg. of platinum oxide, 5 mg. of acetic acid, and 2 mmoles of hydrogen at 350 mm. pressure and 110° for 40 hr. The solution, distilled from the oxide through "Ascarite" under high vacuum, then was analyzed by gas chromatography and mass spectrometry.

Results

Product Yields.—*G*-values for hydrogen, methane, C_2 products, and heavier hydrocarbon products by carbon number are given in Table I, for an irradiation to 111×10^6 rads at a dose rate of 37×10^6 rads/hr. Data for hydrogen, methane, acetylene, and ethane were derived from mass spectrometric analysis of the fractions volatile at -196 and -78° . Data for fractions C_4 through C_{14} were derived from a "programmed" gas chromatographic analysis using an 8 m. \times 6 mm. o.d. silicone-filled column at temperatures of 100 – 200° . (cf. Fig. 1.) The C_{16} and C_{18} yields were determined with reference to the C_{12} and C_{14} yields on a 1.5 m. \times 6 mm. silicone column at 170° . (Calibration with *n*-pentane and α -olefins disclosed that area per cent. corresponded to weight per cent. within $\pm 10\%$.)

TABLE I

YIELDS OF PRODUCTS

	<i>G</i>		<i>G</i>
Hydrogen	0.6	C_{10}	0.14
CH_4	.01	C_{12}	.13
C_2H_2	.6	C_{14}	.04
C_2H_6	.6	C_{16}	.002
C_4	0.2–0.3 ^a	C_{18}	.002
C_6	.13	$\Sigma(C_2H_4 \rightarrow \text{polymer})$	2.5
C_8	.08		

^a Value only estimated; method of analysis is inaccurate for this fraction.

Polymers heavier than C_{18} were found to be absent when the product was vacuum-distilled and residue weighed. The upper limit for *G* ($C_2H_4 \rightarrow$ heavy polymer) calculated from this procedure was 0.05.

Species Distribution from C_2D_4 – C_2H_4 .—The equimolar mixture of C_2D_4 and C_2H_4 was irradiated at 44×10^6 rads/hr. for 2 hr. at -196° . Separation of the pentane solution of the polymers on a 12 m. \times 6 mm. o.d. "Ucon" GLC column at 40° made it possible to collect a purified fraction of 1-butene. Separation of a second sample on the same column at 120° provided samples of *trans*-2-hexene, mixed octenes, and decenes.

The mass spectra for the samples in the parent ion region were corrected for contribution by C^{13} , for the light hydrogen in the C_2D_4 , and, with 1-butene, for contributions by fragment ions. The resulting distributions of isotopic species are given in Table II.

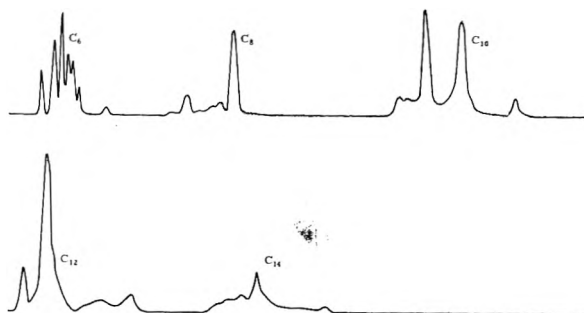


Fig. 1.—Gas chromatogram of C_6 – C_{14} polymers from ethylene (8 m. \times 6 mm. o.d. column, silicone stationary phase, 100 – 200°).

TABLE II

ISOTOPIC SPECIES DISTRIBUTION (Species with deuterium atoms divisible by four are normalized to total one hundred)

	1-Butene	2-Hexene	Octene	Decene
d_0	30	18	10	4
d_1	4	3	1	2
d_2	-2^b	1	1	0
d_3	0	4	1	2
d_4	45	40	30	17
d_5	2	6	4	0
d_6	-4^b	1	1	2
d_7	2	7	4	4
d_8	25	32	36	35
d_9		3	4	0
d_{10}		1	2	2
d_{11}		4	1	4
d_{12}		10	19	30
d_{13}			2	0
d_{14}			1	2
d_{15}			0	2
d_{16}			5	11
d_{17}				0
d_{18}				0
d_{19}				0
d_{20}				2

Probable^a error ± 1 ± 2 ± 2 ± 4

^a Probable error in estimation of ion intensities. ^b Corrections for fragment ion intensities in 1-butene give added error because of unknown isotope effects.

Detailed Structure Analysis.—Information was obtained from non-isotopic experiments on the identity of individual compounds making up the C_4 and C_6 product, and individual carbon skeletons in the C_8 product. Data are assembled in Table III. The C_4 product distribution was determined on a 12 m. \times 6 mm. o.d. column with the Ucon stationary phase at 40° . The C_6 distribution was determined with a 100-m. glass capillary with silicone stationary phase. On this column all C_6 open-chain olefins and paraffins are resolved, either completely or sufficiently to indicate their presence. The two unknown constituents are believed to be cyclic olefins having rings of three or four carbon atoms (see below). The C_8 skeleton distribution was determined on hydrogenated product with a 150-m. nylon capillary column with squalane stationary phase. Absence of other structures is certain; the record with emergence times is shown in Fig. 2. Analysis of the unresolved 3-ethyl-

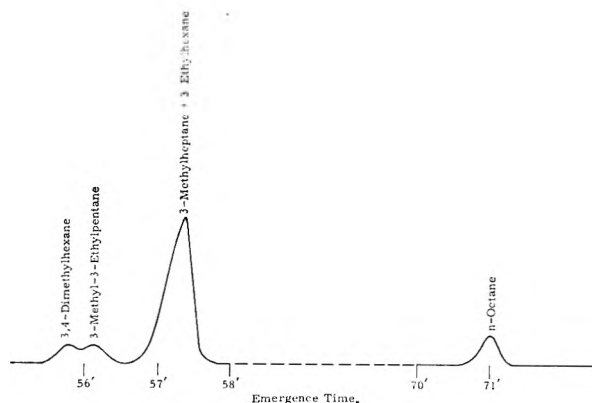


Fig. 2.—Gas chromatogram of hydrogenated C_8 products from ethylene (150 meter nylon capillary with squalane, 25°).

hexane and 3-methylheptane was by mass spectrometry of the trapped fraction.

TABLE III
DETAILED POLYMER ANALYSIS

		% m. in each carbon number
C_4	<i>n</i> -Butane	24
	1-Butene	67
	2-Butene	<1
	Butadiene	9
C_6	3-Methylpentane	14
	<i>n</i> -Hexane	1
	3-Methyl-1-pentene	13
	3-Methyl-2-pentene (low boiling)	5
	3-Methyl-2-pentene (high boiling)	10
	2-Ethyl-1-butene	10
	1-Hexene	11
	<i>trans</i> -2-Hexene	18
	<i>cis</i> -2-Hexene	5
	3-Hexene	1
Unknown no. 1 (cyclic)	5	
Unknown no. 2 (cyclic)	8	
C_8	3,4-Dimethylhexane structure	7
	3-Methyl-3-ethylpentane structure	7
	3-Ethylhexane structure	38
	3-Methylheptane structure	38
	<i>n</i> -Octane structure	11

No attempt was made to resolve components of the C_{10} and C_{12} fractions. Their emergence times made it clear that they were almost all branched compounds; the content of straight-chain product in C_{10} was of the order of 7%.

Further information was obtained on the heavier fractions by direct mass spectrometric examination of the original products. The distribution of ions in the parent ion region provides information on the distribution of hydrogen in the product, shown in Table IV. Open-chain, saturated hydrocarbons and diolefins or cyclic olefins clearly are minor products (note, however, that the parent ion sensitivity of saturates is roughly one-fifth that of olefin, so that they may constitute several per cent. of each product). That cyclic products actually are present was shown by hydrogenation; the C_6 hydrogenated products were 3-methylpentane, *n*-hexane, and small amounts of two hydrocarbons that possessed emergence times correspond-

TABLE IV
MASS SPECTRAL DATA ON THE POLYMERS

	Relative ion intensities			
	C_4	C_6	C_{10}	C_{12}
$C_nH_{2n+2}^+$	3	<10	<1	<5
$C_nH_{2n}^+$	100	100	100	100
$C_nH_{2n-2}^+$	11	<10	9	10

ing neither to open-chain saturates, cyclohexane, nor methylcyclopentane. That they were not olefins was demonstrated by their emergence well ahead of any C_6 olefin from a GLC column containing silver ion in the stationary glycol phase.⁴ Thus they must have a three-membered or four-membered ring, and these must be the hydrogenated products of the unknown constituents in the trimer. It seems likely that cyclic products exist in the other polymer fractions also.

The fragment ion mass spectrum of the C_8 , C_{10} , and C_{12} products clearly showed the prevalence of C_2 branches. Compared to the mass spectrum of 1-decene the C_{10} mass spectrum had C_8 ions 2.5 times normal, C_6 1.5 times normal, and diminished ion intensities at C_6 and C_4 . Compared to the spectrum of 1-dodecene the C_{12} mass spectrum had C_{10} ion intensities three times normal, C_7 ions 1.7 times normal, and C_4 , C_5 , and C_9 intensities diminished.

Effects of Dose and Dose Rate.—Yield by carbon number was determined for two experiments, both carried to 37×10^6 rads, but with irradiations performed at 37×10^6 and 12×10^6 rads/hr. Relative amounts of products by carbon number were identical within experimental error (at this conversion, $\pm 10\%$). The absolute yields were lower in the low dose rate experiment by about 25%.

An experiment was performed to determine whether rate of formation of all products is linear with dose. Two samples of ethylene were irradiated, one to 3.7×10^6 rads at 18.6×10^6 rads/hr., the other to 111.3×10^6 rads at 37×10^6 rads/hr. Yields (*G*-values) of C_8 – C_{12} polymers obtained at low dose were of the order of 40% of those from the high dose, but the distribution was in agreement within 15%, with no trend evident. The reason for the low absolute yield is not known.

Discussion

General Nature of Initiation.—As with 1-hexene,¹ the relative amounts of saturate, mono-olefin, and diolefin in the dimeric product indicate that a mechanism other than free radical recombination must be involved. The experiment with deuterium-labeled ethylene was designed to determine whether the higher polymers really are made up of blocks of C_2H_4 units containing their original hydrogens, as would be required by the postulated ion-molecule mechanism. If this is the case, the species distribution should contain isotopic species with deuterium atoms only in multiples of four. On the other hand, if the mechanism involved, over-all, the union of several C_2H_4 units, a C_2H_3 unit, and an H unit, as would be the case if initiation involves a C_2H_5 ion or radical, the

(4) B. W. Bradford, D. Harvey, and D. E. Chalkley, *J. Inst. Petroleum*, **41**, 80 (1955).

distribution would be less simple. For example, the calculated species distribution for C_8 product from such initiation is given in Table V.

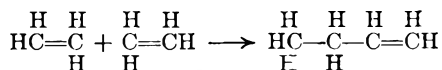
TABLE V

d_0	0.031	d_5	0.094	d_6	0.094	d_{13}	0.031
d_1	.031	d_6	.000	d_{10}	.000	d_{14}	.000
d_2	.000	d_7	.094	d_{11}	.094	d_{15}	.031
d_3	.031	d_8	.188	d_{12}	.125	d_{16}	.031
d_4	.125						

The consequence should be noted that the ratio of the mole fraction of any species with deuterium atoms a multiple of four to the sum of the mole fractions of the two neighboring species should be equal to unity, *e.g.*, $(d_8)/(d_9 + d_7) = (d_4)/(d_3 + d_5) = 1$. This rule is not sensitive to isotope effect. Since these ratios actually are found to be larger by approximately sixfold (from data in Table II), it is concluded that over 70% of the product is initiated by C_2H_4 species.

Since data are at hand, it is of interest to calculate the isotope effect for participation of C_2D_4 compared to C_2H_4 . Calculation from data in Table II from several different product ratios for each product (*e.g.*, d_4/d_0 , d_8/d_4) leads to a value of 0.86 ± 0.08 for the relative probability of reaction of C_2D_4 compared to C_2H_4 . This isotope effect of 14% is rather small, as expected for a reaction in which the rate determining process is not the scission of a carbon-hydrogen bond.

Nature of the Propagation Step.—Information on the nature of the propagation reaction can be obtained from the structure of the products. The only C_4 olefin formed was 1-butene. Some of it may be formed by combination of vinyl and ethyl radicals, but both the isotopic distribution (Table II) and the relative amounts of *n*-butane and butadiene products indicate that the fraction formed by radical combination is small. The direct condensation reaction to form 1-butene must involve over-all the formation of a carbon-carbon bond and at least the 1-3 migration of a hydrogen

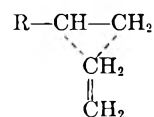


The C_6 products had carbon skeletons divided nearly equally between the straight-chain and 3-methylpentane structures. These would be expected from reaction of ethylene with 1-butene ion under irradiation.¹ Consistency with this picture was further tested in the C_7 products. Molecule ions of the 3-methylpentane-type hexenes should give 3-methylheptane, 3-ethylhexane, 3,4-dimethylhexane, and 3-methyl-3-ethylpentane structures. In complete agreement with this picture, all of these structures were identified, and no others were present.

While the pattern of products fits a single initiation and multiple propagation mechanism, it was necessary to eliminate the possibility that secondary reactions of first-formed products could be responsible. This could happen if olefins other than ethylene were significantly more reactive, perhaps by an energy transfer process. The test was made by irradiating in the usual manner, to 3.3×10^6 rads, a sample of ethylene containing

1% each of 1-pentene and 2-methyl-2-butene. No unusual rate of consumption of the heavier olefins or rate of production of C_7 and C_9 products was noted. It thus is concluded that the polymers arise from single activations of C_2H_4 molecules, with multiple propagation.

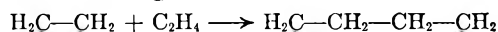
It is, therefore, clear that propagation is not restricted to a single type of carbon atom in the propagating species, and propagation can even result in quaternary structures. Consistency with results from the radiolysis of 1-hexene¹ would require that the propagation involve union of a carbon atom on the double bond of the olefin with either of the two carbon atoms on the electron-deficient double bond of the molecule ion



The result of this mode of propagation is increased branching with degree of polymerization.

The mode of hydrogen atom shift in the propagation is less clear. The isotopic species distribution in Table II requires that the hydrogen atoms originally in the reacting ethylenes be wholly retained in the product. The C_4 products are reasonable in that 1-butene requires a 1,3-shift of a single hydrogen atom, while 2-butene, not found, would require two hydrogen shifts. This principle of least motion quickly fails, however; 3-hexene, which is not formed, should require only a single shift, while 2-hexene, a major product, requires two or more. All of the possible hexenes of the 3-methylpentane structure are formed, including 3-methyl-2-pentene, which should require at least two hydrogen shifts. No explanation for these apparently conflicting observations is at hand.

The Initiating Species.—Several considerations lead to the designation of the molecule ion, $C_2H_4^+$, as the chain initiator rather than some excited state of the molecule. First, there is no precedent for propagation by reaction of an excited molecule with an ethylene. Addition to the lowest triplet state should require activation energy and would seem to lead to separation of unpaired electrons and no branching



On the other hand reaction of the pi electron pair with a positively-charged ion is known to go at a very high reaction rate and to have a negligible temperature coefficient.⁵ Melton and Rudolph⁶ observed ion-molecule condensations of ethylene in the gas phase in the mass spectrometer to give ions as heavy as $C_6H_9^+$ and Field,⁷ in similar studies, observed multiple condensations to give ions as heavy as $C_9H_{11}^+$. Moreover, they found evidence that $C_2H_4^+$ was the initiating ion in the formation of $C_5H_9^+$ as well as others. Thus, polymerization in the gas phase by $C_2H_4^+$ initiation has been observed, and it is confirmed that conventional carbonium ions, *e.g.*, $C_2H_5^+$, are not essential. A significant difference between the

(5) A. G. Evans and M. Polanyi, *J. Chem. Soc.*, 252 (1947).

(6) C. E. Melton and P. S. Rudolph, *J. Chem. Phys.*, **32**, 1128 (1960).

(7) F. H. Field, *J. Am. Chem. Soc.*, **83**, 1523 (1961).

polymers observed in this study in the condensed phase and the ions from those studies in the gas phase is the retention of complete C_2H_4 units in the condensed phase. Apparently the energy dissipation from the ions is fast enough in the condensed phase to avoid loss of hydrogens and splitting of carbon-carbon bonds.

One unexplained problem is the necessity for intramolecular hydrogen migration. In certain instances, two hydrogen migrations must occur in one propagation step to explain the products. Nevertheless, this is a problem that must be explained with any mechanism. At present, it can only be said that the polymerization must be a very fast reaction, rich in energy, and that this must permit at least certain migrations of hydrogens to occur so that olefins are produced at each stage. Observation of small amounts of cyclic materials may well be evidence that occasionally hydrogen migration does not occur and that separation of charge and unpaired electron can be accomplished.

Termination Mechanism.—According to the proposed mechanism, the termination step in the ion-molecule polymerization would be electron recombination. In order that the product distribution be independent of dose rate, it is essential to assume that the recombination rate is not governed by the over-all concentration of positive ions and electrons; this is most easily visualized as a mechanism in which the electrons ejected from a spur return to recombine with the ions in that spur. The degree of polymerization then would depend upon the time between ionization and recombination compared to the time required for propagation.

In applying this idea to this system, it would be necessary to assume that the average energy imparted to the secondary electron drives it away far enough that the propagation proceeds to a pentamer or hexamer, on the average, before recombination. On this basis the scheme shown in Fig. 3 becomes pertinent. It traces the fate of 1000 C_6 positive ions, as determined from Table II. It becomes evident that the probability for recombination rises very strongly at each stage after tetramer, from 44% at pentamer to >80% at heptamer.

It is pertinent to consider the relationship of this mechanism to other recognized radiation-induced ionic polymerizations. One of these, isobutylene, normally is carried to a high degree of polymerization of the order of 12,000, with a G for monomer conversion of 800.⁸ The similarity of the polymer product to that made by chemical initiation makes it likely that *t*-butylcarbonium ion is the initiating species rather than the isobutylene positive ion. If termination occurs by electron recombination in both isobutylene polymerization and ethylene polymerization, it is necessary when comparing

(8) W. H. T. Davison, S. H. Pinner, and R. Worrall, *Chem. Ind.* (London), **38**, 1274 (1957).

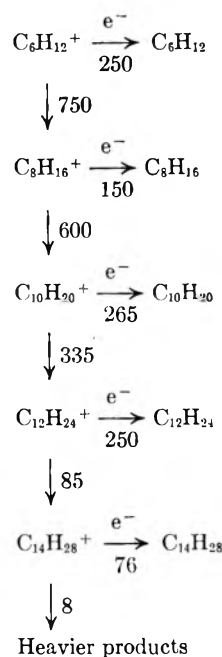


Fig. 3.—Semi-quantitative reaction scheme.

the two polymerizations to assume either that (1) propagation is many times faster with isobutylene, or (2) electron recombination is very much slower. Since ion-molecule condensation should occur with unit collision efficiency, it is difficult to see how (1) can apply unless, as the ethylene polymer increases in size and branching, steric effects markedly reduce reaction rate. As for (2), it is not expected that the ejected electrons would have any greater average energy in isobutylene than those in ethylene; therefore, it would have to be assumed that isobutylene is more efficient in momentarily attaching the electron in its migration to the positive ion. No information is available on this aspect.

Conclusions.—Ethylene in the solid phase at -196° is polymerized by ionizing radiation to low molecular weight olefinic polymers. Initiation is by a C_2H_4 species, thought to be the molecule ion, $C_2H_4^+$. Propagation occurs at either carbon attached to the original double bond, leading to highly-branched polymer structures. Termination is believed to occur on electron recombination. Skeletal rearrangements do not occur in the polymerization. Hydrogen atoms in the products are only those originally in the reacting molecules; however, the required intramolecular migrations of the hydrogen atoms during the polymerization are not yet understood.

Acknowledgment.—The author is grateful to Mr. J. K. MacKenzie for conducting the irradiations, to Mr. V. A. Campanile and Drs. A. G. Polgar and M. A. Muhs for help in the gas chromatographic analyses, and to Drs. J. W. Otvos and P. H. Deming for helpful discussions.

MAGNETIC SUSCEPTIBILITY OF SOME LIQUID METALS, MOLTEN SALTS, AND THEIR SOLUTIONS

BY NORMAN H. NACHTRIEB¹

Institute for the Study of Metals, University of Chicago, Chicago, Ill.

Received January 12, 1962

Measurements are reported for the magnetic susceptibility of the bismuth-bismuth chloride and cadmium-cadmium chloride molten systems for a range of temperatures and compositions and for the sodium-sodium chloride and sodium-sodium bromide systems at a single temperature and composition. Large deviations from additivity relative to the pure components are observed for the bismuth and cadmium solutions, which may be attributed in part to the paramagnetic and diamagnetic contributions of the conduction electrons in the metallic state. The number of free electrons per atom in the liquid metallic state is found to be two for cadmium and three for bismuth. Static susceptibility measurements provide no basis for distinguishing between a solution model in which the metal is in simple physical solution and one in which the formation of cationic species of intermediate valence is assumed to take place. No indication of a paramagnetic contribution to the solution susceptibility is observed in the sodium-sodium bromide system at a metal concentration for which the conduction electrons might be expected to be non-degenerate.

Introduction

When a solution is formed from two or more components the gram susceptibility is ideally a linear combination of the specific susceptibilities of the pure components. This is a statement of Wiedemann's law, which may be written as

$$\chi = \sum_i p_i \chi_i \quad (1)$$

where p_i is the weight fraction of the i th component and χ_i is its gram susceptibility. An empirical law, it has been experimentally verified to within the accuracy of ordinary measurements.² Deviations from it are usually an indication that a chemical reaction has taken place, with a change in the electronic spin state or in the electron density distribution. The original purpose of this study was to measure the magnetic susceptibilities of liquid metals, their molten halide salts, and solutions of the two, and to look for deviations from Wiedemann's law which might shed light upon the state of the "dissolved" metal. As will be shown, large deviations from additivity are observed, but they do not answer this question. Rather, they provide information on the state of the pure liquid metal: in particular, the number of conduction electrons furnished per atom in that state.

Two seemingly quite different kinds of solution appear to form when metals are dissolved in molten halide salts which have a common cation. On the one hand, the alkali, alkaline earth, and rare earth metals dissolve appreciably in their corresponding halides and make a significant electronic contribution to their electrical conductance. The electrons are relatively free, and appear to be bound to comparatively shallow energy traps.^{3,4} Another class of metals, of which bismuth and cadmium are representative, yield purely electrolytic solutions in their respective molten chlorides.^{5,6} Two points of view have been expressed concerning their constitution. Cubicciotti has suggested⁷

that the metal forms a true solution with the salt, in which metal atoms occupy holes in a quasi-crystalline lattice of the halide ions in the melt. The other point of view regards the solutions as mixtures of the salt with a sub-halide, formed by reduction of some of the cations by added metal atoms. Species of intermediate oxidation state such as Bi_x^{+x} or Cd_y^{+2} or complexes of the type $\text{Bi}_x\text{Cl}_y^{-(y-x)}$ and $\text{Cd}_y\text{Cl}_y^{-(y-2)}$ are presumed to exist, in which the metal is univalent. Various lines of evidence provide conflicting clues as to the degree of polymerization, x , for the bismuth system and range from unity to four. Most of this evidence is of thermodynamic character, including measurements of the freezing point depression,⁸ vapor pressure lowering,⁹ and the e.m.f. of concentration cells.¹⁰ An inherent limitation of thermodynamic methods is that they provide no unique answer to the question of molecular constitution, since the colligative properties of solutions are sensitive to intermolecular and interionic forces. Magnetism, by contrast, is a constitutive property which is little affected by such interactions unless they result in extensive polarization or in the redistribution of electron density attending the formation of new molecular species. Paramagnetism arises from the presence of electrons with unpaired spins, and diamagnetism depends classically upon the mean squared radius of the electron orbits, summed over all the electrons in a molecule. Intermolecular potentials are seldom of such a magnitude as to perturb the electron density distribution, although the more sensitive colligative properties may be significantly changed and may lead to activity coefficients markedly different from unity. On the other hand, when a stable molecule is formed by the combination of two or more atoms an appreciable redistribution of electron density may be expected, with a corresponding change in the molecular diamagnetism. In addition, the pairing of electron spins would result in a decrease in paramagnetism, if that process were to occur. Such were the ideas which prompted the study.

Several other investigations of the magnetic

(1) National Science Foundation Senior Postdoctoral Fellow, 1959-1960.

(2) P. W. Selwood, "Magnetochemistry," Interscience Publishers, New York, N. Y., 1943, p. 56.

(3) H. R. Bronstein and M. A. Bredig, *J. Am. Chem. Soc.*, **80**, 2077 (1958).

(4) G. W. Mellors and S. Senderoff, *J. Phys. Chem.*, **64**, 294 (1960).

(5) A. H. W. Aten, *Z. physik. Chem.*, **66**, 641 (1909).

(6) A. H. W. Aten, *ibid.*, **73**, 579 (1910).

(7) D. Cubicciotti, *J. Metals*, **5**, *AIMS Trans.*, **197**, 1106 (1953).

(8) S. W. Mayer, S. J. Yosim, and L. E. Topol, *J. Phys. Chem.*, **64**, 238 (1960).

(9) J. D. Corbett, *ibid.*, **62**, 1149 (1958).

(10) L. E. Topol, S. J. Yosim, and R. A. Osteryoung, *ibid.*, **65**, 1511 (1961).

susceptibility of metal-metal salt systems have been reported. Farquharson and Heymann¹¹ measured the magnetic susceptibility of cadmium in cadmium chloride at 7.6 and 8.7 mole % Cd but made no use of the results beyond noting that the solutions were diamagnetic and concluding therefrom that Cd⁺ ions could not be present. Grjotheim¹² qualitatively confirmed these results, and proposed the presence of either Cd atoms or Cd₂⁺⁺ ions. Corbett, Winbush, and Albers¹³ reported that the solutions of PbI₂, SbCl₃, ZnI₂, and GaBr₂ with their respective metals were all diamagnetic. In the present study the bismuth-bismuth chloride and cadmium-cadmium chloride systems were chosen as typical of those which form purely electrolytic solutions; the sodium-sodium chloride and sodium-sodium bromide systems belong to the class which form solutions that show mixed electronic and electrolytic conductance.

Experimental

The Gouy method was employed, with a Weiss electromagnet capable of yielding inhomogeneous field strengths up to 10,500 oersteds for 20 mm. diameter pole pieces and a gap of 35 mm. The field was calibrated at nine values of the coil current by means of a standard solution of nickel chloride. For the Bi-BiCl₃ measurements the susceptibility tubes were made from Pyrex glass tubing 1.030 cm. i.d. selected for uniformity of bore and wall thickness. Clear quartz tubing about 0.900 cm. i.d. was used for the Cd-CdCl₂ measurements. For the Na-NaCl and Na-NaBr measurements the liquids were contained in a 0.635 cm. i.d. tube of dense alumina of the type used for thermocouple protection sheaths, with a tightly fitting plug of graphite to minimize the escape of the alkali metal vapor; this tube was in turn surrounded by a quartz tube filled with argon to 10 cm. pressure. Corrections were determined for the susceptibility of each type of tube and of the atmosphere displaced by it at each value of the field and temperature. Tests made on various tubes having different end shapes showed that the uncertainties in the blank corrections lay within the weighing error, which was 0.1 mg.

Two furnaces, each designed to fit between the pole pieces, were used. For the Bi-BiCl₃ and Cd-CdCl₂ study a 30 cm. long Alundum tube with an i.d. of 16 mm. was non-inductively wound with No. 22 nichrome wire and jacketed with a 32 mm. o.d. brass tube. A Chromel-Alumel thermocouple was positioned within the furnace just below the magnet axis. To attain the higher temperature needed (~1000°) for the Na-NaBr measurement a furnace with a graphite heating element was constructed. A rod of graphite, 30 cm. long and 20 mm. diameter, was bored to an i.d. of 16 mm. and cut to a 25-turn spiral. This element was held between massive graphite end-pieces and surrounded by a 25 mm. o.d. alundum jacket; asbestos cloth wrapped upon the jacket increased the diameter to 32 mm. and provided thermal insulation and protection for the magnet. Although fragile, this furnace functioned well and reached a temperature of 1055 ± 20°, along the portion occupied by the susceptibility tube for a current of 65 amp.

Bismuth trichloride (anhydrous Analytical Reagent Grade, Carlo Erba Co.) was purified by vacuum distillation and subsequently distilled into the susceptibility tubes on a vacuum line. Refined bismuth metal was weighed into the tubes prior to their attachment to the line. The weight of bismuth chloride was determined by difference from the total weight of the filled tube, the weight of added metal, and the weight of glass recovered at the conclusion of the measurement. A similar procedure was used for the Cd-CdCl₂ experiments, except that purification of the salt (CdCl₂·2.5H₂O) was accomplished by double recrystalliza-

tion followed by conversion to anhydrous CdCl₂ by slow controlled heating to 500° in a current of dry hydrogen chloride. Traces of water remaining after this treatment were removed by fusion in quartz under high vacuum. Both the molten salt and its aqueous solution were completely free of suspended matter. The salt was introduced into the quartz susceptibility tubes by filtration through a capillary under high vacuum.

For the measurements on sodium-sodium chloride and sodium-sodium bromide, the twice recrystallized salts were fused in platinum and cast into 0.635 cm. diameter ingots in a two-part mold of pure graphite for easy introduction into the alundum tubes. Sodium metal was twice-distilled and cast into globules under mineral oil. Degreased in pentane and rapidly weighed, these were added to the susceptibility tube containing the salt for evacuation and seal-off on the vacuum line. Trial experiments indicated that less than 1% of the metal was oxidized during the time of these operations. At the conclusion of the measurements the contents of the alundum tubes were dissolved in water and titrated for alkalinity. The small discrepancy in the weights of sodium originally taken and found was due to the escape of sodium vapor from the alundum tube at the graphite end plug, where it diffused into the surrounding quartz envelope in a narrow band.

All metals and salts were examined spectroscopically for impurities. No ferromagnetic or paramagnetic impurities were detected in the purified bismuth chloride, cadmium chloride, bismuth metal, or cadmium metal; only faint traces of lead were found in the two salts. A trace of potassium was the only impurity detected in the sodium metal and sodium bromide. None of the metals or their salts showed any field-dependence in their magnetic susceptibilities, which might have been expected had there been even small traces of ferromagnetic impurities.

All susceptibility tubes were evacuated to 10⁻⁸ mm. pressure prior to seal-off at constrictions previously provided; as previously noted a pressure of 10 cm. of argon gas was provided for the Na-NaBr and Na-NaCl experiments in an effort to delay the escape of sodium vapor from the molten salt phase. Eyelets of glass or quartz were fashioned at the top of each susceptibility tube to accept a 0.20 mm. diameter platinum suspension wire to the balance hang-down. In each case the volume of metal, salt, or solution was sufficient to fill the tubes to a height of about 10 cm. to ensure that the complete gradient of the inhomogeneous field lay within the specimen length.

The net weight changes of the solutions in the magnetic field ranged from about 3 mg. at 2600 oersteds to about 50 mg. at 10,500 oersteds. Observations were made at nine values of the field strength within this range. Air convection currents within the furnace were the principal source of weighing error, which was generally less than 0.5 mg. Magnetic susceptibilities were evaluated from plots of ΔW vs. H^2 by means of the usual relationship

$$\chi = \frac{2g\Delta W}{\pi r^2 \rho H^2} \quad (2)$$

where ΔW is the weight change (corrected for tube and displaced atmosphere), r is the internal tube radius, ρ is the solution density, and H is the maximum value of the heterogeneous field. Solution densities were calculated from equations of the form $\rho = a + bT$ from the data of Boardman, Dorman, and Heymann¹⁴ for the Cd-CdCl₂ system and of Cubicciotti and Keneshea¹⁵ for the Bi-BiCl₃ system. Densities of the Na-NaCl and Na-NaBr solutions were interpolated from the data of Van Artsdalen and Yaffe.¹⁶ For the pure liquid metals the data available in the Metals Reference Book were used.¹⁷

Results

For the bismuth-bismuth chloride system susceptibility measurements were made at 340 and 407° on pure metal, pure salt, and on solutions

(11) J. Farquharson and E. Heymann, *Trans. Faraday Soc.*, **31**, 1004 (1935).

(12) K. Grjotheim, F. Gronwald, and J. Krogh-Moe, *J. Am. Chem. Soc.*, **77**, 5824 (1955).

(13) J. D. Corbett, S. Winbush, and F. C. Albers, *ibid.*, **79**, 3020 (1957).

(14) N. K. Boardman, F. H. Dorman, and E. Heymann, *J. Phys. Colloid Chem.*, **53**, 375 (1949).

(15) F. J. Keneshea, Jr., and D. Cubicciotti, *ibid.*, **62**, 843 (1958).

(16) E. R. Van Artsdalen and I. S. Yaffe, *ibid.*, **59**, 118 (1955), **60**, 1125 (1956).

(17) C. J. Smithells, "Metals Reference Book," 2nd Ed., Vol. 1, Butterworths Scientific Publications, London, 1955, p. 639.

containing 0.0740, 0.1678, 0.2246, and 0.2849 mole fraction bismuth metal. A separate series of measurements was made on a pure BiCl_3 sample and a solution containing 0.1242 mole fraction bismuth at 280, 330, 380, and 430° to look particularly for a possible temperature dependence in the susceptibility. Table I summarizes the results. Noteworthy is the fact that all the solutions are diamagnetic and not greatly different in value from the susceptibility of the pure liquid salt. There appears to be a small but significant decrease in the diamagnetic susceptibility of the solutions with increasing bismuth content; a linear extrapolation across the immiscibility gap to $X_{\text{Bi}} = 1.00$ gives $\chi = (-0.196 \pm 0.030) \times 10^{-6}$ for the gram susceptibility of "dissolved" bismuth metal. The average value for the gram susceptibility of pure liquid bismuth metal is $(-0.036 \pm 0.001) \times 10^{-6}$, in reasonable agreement with Honda's¹⁸ value $(-0.05 \times 10^{-6}$ from m.p. to 800°), estimated from a graph. No trend in the susceptibility of the 12.42 mole % bismuth solution is apparent between 280 and 430°.

TABLE I

MAGNETIC SUSCEPTIBILITIES OF BISMUTH, BISMUTH CHLORIDE, AND THEIR SOLUTIONS

$t, ^\circ\text{C.}$	Wt. % Bi	X_{Bi}	$\rho, \text{g. cm.}^{-3}$	$-\chi_{\text{obsd.}} \times 10^6$
340	0.00	0.0000	3.669	0.283 ± 0.005
	5.03	.0740	3.324	$.277 \pm .007$
	11.79	.1678	4.358	$.277 \pm .005$
	16.10	.2246	4.208	$.268 \pm .007$
	20.89	.2849	4.391	$.264 \pm .004$
	100.00	1.0000	9.951	$.037 \pm .001$
407	0.00	0.0000	3.522	$.280 \pm .004$
	5.03	.0740	3.383	$.279 \pm .002$
	11.79	.1678	3.320	$.259 \pm .007$
	20.89	.2849	4.248	$.264 \pm .003$
	100.00	1.0000	9.865	$.035 \pm .001$
280	0.00	0.0000	3.801	.279
330	.00	.0000	3.691	.277
380	.00	.0000	3.581	.279
430	.00	.0000	3.471	.284
280	9.39	.1242	4.068	.274
330	9.39	.1242	3.964	.272
380	9.39	.1242	3.860	.273
430	9.39	.1242	3.756	.274

Measurements on the cadmium-cadmium chloride system were made at 550, 600, 650, and 700° for solutions containing 0.0683, 0.0977, and 0.1307 mole fraction cadmium metal. The pure salt was measured at 50° intervals between 600 and 800°, and the pure metal at 100° intervals between 400 and 800°. Table II summarizes the results. To within the precision of measurement there is no temperature dependence of the susceptibility for the pure salt or the solutions. This is not the case for liquid metallic cadmium, however, for which a small monotonic decrease in susceptibility with increasing temperature is observed; the variation is linear neither in T nor $1/T$. The average value of the gram susceptibility of liquid cadmium agrees well with Honda's value¹⁸ $(-0.15 \times 10^{-6}$, m.p. to 800°), however. Like the bis-

muth-bismuth chloride system, the metal, salt, and their liquid solutions are all diamagnetic. The results agree with those of Farquharscn and Heymann¹¹ to within their limits of error.

TABLE II

MAGNETIC SUSCEPTIBILITIES OF CADMIUM, CADMIUM CHLORIDE, AND THEIR SOLUTIONS

X_{Cd}	$t, ^\circ\text{C.}$	$\rho, \text{g. cm.}^{-3}$	$-\chi \times 10^6$
0.00	600	3.366	0.389 ± 0.006
	650	3.324	$.387 \pm .003$
	700	3.282	$.384 \pm .003$
	750	3.240	$.385 \pm .002$
	800	3.198	$.386 \pm .002$
1.00	400	7.93	$.150 \pm .0010$
	500	7.82	$.148 \pm .0006$
	600	7.72	$.145 \pm .0004$
	650	7.66	$.144 \pm .0005$
	700	7.62	$.142 \pm .0007$
	750	7.56	$.140 \pm .0008$
	800	7.50	$.137 \pm .0011$
	0.0683	550	3.468
600		3.426	$.389 \pm .006$
650		3.384	$.385 \pm .006$
.0977	700	3.342	$.390 \pm .006$
	550	3.494	$.393 \pm .004$
	600	3.452	$.392 \pm .003$
.1307	650	3.410	$.395 \pm .005$
	700	3.368	$.399 \pm .003$
	550	3.523	$.374 \pm .004$
.1307	600	3.481	$.394 \pm .006$
	650	3.439	$.388 \pm .004$
	700	3.397	$.385 \pm .003$

For the sodium-sodium chloride and sodium-sodium bromide solutions only two successful experiments were performed, although many were attempted. To within experimental error pure liquid sodium chloride and sodium chloride containing 2.6 atom % sodium metal at 810° have the same susceptibility. Similarly, pure liquid sodium bromide and sodium bromide containing 0.68 atom % sodium metal do not differ by more than the precision of measurement. From 300 to 500° pure liquid sodium has a gram susceptibility of $(0.60 \pm 0.02) \times 10^{-6}$, in fair agreement with the value obtained by Klemm and Hauschulz.¹⁹ Table III summarizes the fragmentary results obtained for these systems.

TABLE III

MAGNETIC SUSCEPTIBILITIES OF SODIUM-SODIUM HALIDES

System	X_{Na}	$T, ^\circ\text{C.}$	$\chi \times 10^{-6}$
Na	1.0000	300	0.597 ± 0.018
	1.0000	400	$.604 \pm .022$
	1.0000	500	$.600 \pm .025$
NaCl	0.0000	810	$-.537 \pm .021$
Na-NaCl	.0259	810	$-.529 \pm .021$
NaBr	.0000	1055	$-.410 \pm .015$
Na-NaBr	.0068	1055	$-.421 \pm .011$

Discussion

Large apparent deviations from Wiedemann's law result for both the bismuth-bismuth chloride and cadmium-cadmium chloride systems when the

(18) K. Honda, "Magnetic Properties of Matter," Syokwabo and Co., Tokyo, 1928, p. 131.

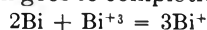
(19) W. Klemm and B. Hauschulz, *Z. Elektrochem.*, **45**, 34f (1939).

experimental gram susceptibilities for the pure components are inserted into eq. 1, together with their weight fractions. The discrepancies are even more obvious if *apparent* gram susceptibilities are calculated for the "dissolved" metal. For bismuth the apparent value is -0.196×10^{-6} , as compared with -0.036×10^{-6} observed for the pure liquid metal. For cadmium the apparent value is -0.447×10^{-6} , as compared with -0.145×10^{-6} observed for pure liquid cadmium at 600° . Although the experimental error is greatly amplified in the calculation of the *apparent* susceptibilities of the dissolved metal in both systems, it is clear that the state of the dissolved metal is not "metallic." Aten's^{6,6} study of the electrical conductance of both systems failed to reveal any indication of free electrons in the solutions, and the magnetic properties are consistent with his conclusions.

Two possibilities may be explored in efforts to account for the deviations from additivity: (a) the formation of cationic species of intermediate valence by chemical reaction of the added metal with cations of the salt, and (b) the formation of a physical solution of metal atoms in the salt phase, taking into account the disappearance of the free electrons of the metallic state by trapping in localized orbitals of the cations. Both procedures are beset with difficulties; in particular, there is no reason to suppose (for the first alternative) that only one species of cation is formed and no experimental susceptibilities exist for such hypothetical species. For the second alternative similar difficulties exist, in that experimental susceptibilities of the neutral atoms or molecules of metal in the free state are unknown. In their absence estimates may be made, based upon the assumed validity of the Wiedemann law together with calculations based upon Slater's method²⁰ for electron density distributions and the Pauli theory of paramagnetism.²¹

Case (A). Cations of Intermediate Valence.—

If the high *apparent* gram susceptibility of dissolved metal arises from its reaction with cations, it is instructive to consider the various species which may be formed. Using the Wiedemann relation, it then is possible to solve for the *apparent* susceptibilities of those species and to compare them with susceptibilities calculated according to some theoretical model. Suppose, for example, that the following reaction goes to completion



Wiedemann's law then takes the form

$$\chi = \chi_{\text{BiCl}_3} \left(p_{\text{BiCl}_3} - \frac{1}{2} \times \frac{\text{BiCl}_3}{\text{Bi}} \times p_{\text{Bi}} \right) + \chi_{\text{BiCl}} \times \frac{3\text{BiCl}}{2\text{Bi}} \times p_{\text{Bi}} \quad (3)$$

The same expression results if a dimer, Bi_2Cl_2 , or any other polymer of BiCl is formed, so that magnetic susceptibility measurements cannot differentiate among them. Alternatively, it might be assumed that BiCl_2 or Bi_2Cl_3 is formed and analogous expressions of Wiedemann's law could be written for them. Such equations are not in-

dependent of eq. 3 or of one another, however, and are related to each other by molecular weight ratios. This being the case, no new information is obtained by calculating *apparent* susceptibilities for BiCl_2 , Bi_2Cl_3 , etc. It will suffice to calculate *apparent* susceptibilities of Bi^{+2} and Cd^{+2} and to compare these with values derived from theory. Average values for the molar susceptibilities of BiCl and Cd_2Cl_2 , calculated from the data of Tables I and II are $(57.2 \pm 4.4) \times 10^{-6}$ and $(121 \pm 7) \times 10^{-6}$, respectively. Subtracting Angus' value of -22.9×10^{-6} for the molar susceptibility of chloride ion²² yields -34.3×10^{-6} and -37.6×10^{-6} for $\chi_{\text{Bi}^{+2}}$ and $1/2\chi_{\text{Cd}^{+2}}$. Molar susceptibilities of Bi^{+3} and Cd^{+2} , calculated in the same way from the data for the pure salts, are -19.6×10^{-6} and -25.2×10^{-6} . Qualitatively, the results are in the correct order: the ions of lower valence have larger diamagnetic susceptibilities.

These values, which have been derived from experiment, may be compared with theoretical estimates of the diamagnetic susceptibilities of Bi^{+2} , Bi^{+3} , Cd^{+2} , and Cd^{+2} . According to the Langevin theory of diamagnetism, the molar susceptibility depends upon the Larmor precession of electrons in closed orbits in the presence of an external field

$$\chi = -\frac{Ne^2}{6mc^2} \sum \bar{r}^2 \quad (4)$$

where the summation extends over all the mean squared radii of the electron orbits. A rough approximation to the mean squared radial distribution is provided by Slater's formula

$$\sum \bar{r}^2 = \frac{(n')^2(n' + 1/2)(n' + 1)}{(Z - s)^2} \quad (5)$$

where n' and s are effective quantum numbers and screening constants, respectively, chosen according to simple rules.²⁰ Such calculations yield $\chi_{\text{Bi}^{+2}} = -60 \times 10^{-6}$, $\chi_{\text{Bi}^{+3}} = -41 \times 10^{-6}$, $1/2 \chi_{\text{Cd}^{+2}} = -46 \times 10^{-6}$, and $\chi_{\text{Cd}^{+2}} = -34 \times 10^{-6}$. The agreement between theory and experiment is poor and is almost certainly attributable to the extreme sensitivity of the Slater calculations to the choice of the screening constant for the electrons of large orbital radius. The calculation serves only to show the relative magnitudes of the susceptibilities of the ions in their two valence states.

Case (B). Physical Solution of Atoms.—Instead of attempting to account for the failure of eq. 1 in terms of new ionic species in the metal-salt solution phase, a different approach may be taken which partially resolves the problem. The observed diamagnetism of liquid metallic bismuth or cadmium is the sum of the magnetic contributions of the ion cores and of the free electrons. The first is a diamagnetic term, and should correspond closely with the susceptibilities found experimentally for Bi^{+3} and Cd^{+2} in their pure salts. The free electrons, to a first approximation, constitute a degenerate gas and only those which lie at the top of the Fermi distribution make a paramagnetic contribution. According to the Pauli theory of paramagnetism²¹ only those electrons whose total energy lies within kT of the Fermi

(20) J. C. Slater, *Phys. Rev.*, **36**, 57 (1930).

(21) W. Pauli, *Z. Physik*, **41**, 81 (1927).

(22) W. R. Angus, *Proc. Roy. Soc. (London)*, **A136**, 569 (1932).

energy are free to align their spins with the impressed magnetic field. In addition, the conduction electrons make a diamagnetic contribution²³ which is equal numerically to one-third of their paramagnetism. The net susceptibility is given by

$$\chi = \frac{NZ\mu_B^2}{kT_F} \quad (6)$$

where μ_B is the magnetic moment of the electron and T_F is the degeneracy temperature. For a free electron gas this is equal to

$$T_F = \frac{\hbar^2}{2mK} \left(\frac{3NZ}{8\pi V} \right)^{2/3} \quad (7)$$

Combining eq. 6 and 7 gives for the molar electron susceptibility

$$\chi = \frac{8m}{\hbar^2} Z^{1/3} N^{1/3} \mu_B^2 \left(\frac{\pi V}{3} \right)^{2/3} \quad (8)$$

Temperature-independent, the susceptibility of the free electrons in one gram-atom of bismuth metal is 13.4×10^{-6} . In terms of the gram susceptibility of bismuth metal this amounts to 0.064×10^{-6} . This value, subtracted from the -0.036×10^{-6} found experimentally for metallic bismuth, yields -0.100×10^{-6} for the gram susceptibility of bismuth atoms stripped of their three valence electrons (*i.e.*, Bi^{+3} ions). The molar value, -20.9×10^{-6} , is in excellent agreement with the value (-19.6×10^{-6}) calculated in (A) from measurements on pure BiCl_3 .

Similar calculations for cadmium metal yield 9.39×10^{-6} for the susceptibility of the free electrons in one gram-atom, or 0.084×10^{-6} per gram of metal. Taking -0.145×10^{-6} as the value for the experimental gram susceptibility of liquid cadmium metal at 600° leads to -0.229×10^{-6} for the gram susceptibility of the metal corrected for the Landau diamagnetism and Pauli paramagnetism of the conduction electrons. In turn, the molar susceptibility is -25.7×10^{-6} , in agreement with -25.2×10^{-6} calculated from measurements on pure liquid cadmium chloride.

For both Cd^{+2} and Bi^{+3} the close agreement in diamagnetic susceptibilities obtained from the liquid metals and the pure salts must be regarded as somewhat fortuitous, in view of the approximate nature of the calculations. Nevertheless, support is provided for the intuitive feeling that the valences of the elements in the metallic state are the same as their familiar chemical values. Moreover, a large fraction of the discrepancy from the additivity law is removed, and nothing anomalous is to be attributed to the metallic state. There remains unexplained some enhanced diamagnetism in both metal-salt solutions, which amounts to -0.096×10^{-6} referred to one gram of bismuth and -0.218×10^{-6} per gram of cadmium. These increments are associated with the transfer of the conducting valence electrons of the metallic state to localized orbitals of ionic or molecular species

in the metal-salt solution. Rough values of the mean orbital radius of these trapped electrons may be estimated by means of the Langevin equation for atomic diamagnetic susceptibility (eq. 4). For bismuth the calculated root mean squared radius is 1.54 \AA , as compared with the accepted value of 1.55 \AA for the metallic radius. For cadmium the agreement is poorer: 2.08 \AA calculated from the excess diamagnetic susceptibility, as compared with the accepted metallic radius of 1.49 \AA . It appears that the magnetic properties of the solutions are reasonably consistent with a model in which neutral atoms or molecules²⁴ are in simple physical solution. The possibility that polymeric ions such as Bi_x^{+x} or Cd_2^{+2} may exist cannot be excluded, however, until means of calculating their electron distribution are devised. The true state of affairs may well be intermediate between the two cases which have been discussed. The fact that both of these systems absorb very strongly in the visible region of the spectrum suggests that this may be so. It is quite possible that this absorption is the long wave length tail of a charge transfer spectrum, such as Davidson²⁵ has observed in aqueous solutions of two cations in different oxidation states. In that event the solute species could be Cd_2^{+2} with an asymmetric charge distribution between the two cores: *i.e.*, resonance hybrids of $\text{Cd} \cdot \text{Cd}^{+2}$, with chloride ions in bridging positions through which charge transfer occurs. It is planned to examine the nuclear magnetic resonance of this system to determine whether there appear to be two different species of cadmium in solution with measurably long lifetimes. Should this prove to be the case, the distinction between a physical solution of metal atoms and the formation of sub-ions would be more conceptual than real.

The sodium-sodium halide solutions are also diamagnetic, and although the experimental errors are quite large there is no indication that the dissolved metal is in a paramagnetic state. Corresponding to 0.68 mole % sodium in sodium bromide is a degeneracy temperature of about 750°K ., and the spin-only paramagnetic susceptibility at 1328°K . should be 275×10^{-6} per gram-atom. The observed gram susceptibility of the solution is $(-0.421 \pm 0.011) \times 10^{-6}$, while the value expected for free spins is -0.387×10^{-6} . The margin for error is large, but the indications are that Na_2 molecules, rather than sodium atoms or Na_2^+ ions, predominate.

Acknowledgment.—The author is greatly indebted to the National Science Foundation for the grant of a Senior Postdoctoral Fellowship. He also wishes to express his appreciation to Professor Roberto Piontelli, Director of the Istituto Di Elettrochimica, Chimica Fisica, e Di Metallurgia Del Politecnico Di Milano, for many kindnesses, and in whose laboratory this study was made.

(24) In the case of bismuth, which has an odd number of electrons, the neutral species cannot be monatomic and the neutral species may be Bi_2 or Bi_4 molecules.

(25) N. Davidson, *J. Am. Chem. Soc.*, **73**, 2361 (1951).

(23) L. Landau, *Z. Physik*, **64**, 629 (1930).

A QUANTITATIVE STUDY OF A ONE-ELECTRON PHOTOÖXIDATION IN A RIGID MEDIUM¹

BY W. C. MEYER² AND A. C. ALBRECHT

Department of Chemistry, Cornell University, Ithaca, N. Y.

Received January 16, 1962

A quantitative study is made of a primary photochemical process—the one-electron photoöxidation of *N,N,N',N'*-tetramethyl-*p*-phenylenediamine (TMPD) dissolved in glassy 3-methylpentane at 77°K. Absolute quantum yields are determined at 5-m μ intervals in the near ultraviolet absorption band. The yield varies from 7×10^{-4} to 6×10^{-3} . The wave length dependence of the quantum yield reveals a structure which is attributed to the specific activity of certain vibrations. Relative quantum yields as a function of exciting wave length have been determined for the fluorescence and phosphorescence of TMPD. The yields are relatively wave length independent. These and other data rule out the role of the triplet state in the one-electron photoöxidation. Instead it is postulated that the electron either tunnels or climbs a barrier separating various excited vibrational levels of the excited singlet state from long lived charge transfer states of a photochemical unit consisting of the solute molecule and an unspecified number of surrounding solvent molecules. Certain quantitative aspects of photochemistry in a rigid system are treated where absorption of photoreactant and photoproduct overlap and their distributions are neither homogeneous nor isotropic.

Introduction

Photochemical studies in condensed phases usually are complicated by the transient nature of the primary photoproducts and the serious intrusion of secondary reactions. When the condensed phase is sufficiently rigid, however, molecular, radical, or ion diffusion is negligible (excluding H and H⁺) and it becomes possible to isolate the primary process and subject it to quantitative study. In fact photochemistry of solute molecules clamped firmly in a rigid, amorphous solvent normally can involve at most some change in a local domain consisting of the solute molecule surrounded by a cluster of solvent molecules. This change may involve photoisomerization, photodissociation (here, the breaking of a molecule into two uncharged fragments) and photoionization (breaking into charged fragments). A very special case of the latter is when one of the charged fragments is an electron—a photoionization which we shall call “photoöxidation” following Lewis and Lipkin.³ The primary photoproducts in each case often can be of rather long life—that is—trapped in the rigid matrix. It is not unreasonable to regard the solute, together with the relevant solvent cluster about it, as a photochemical unit in which light induced transitions are possible leading to metastable states of the unit. The ordinary low energy electronic spectroscopic properties of this unit are normally a super-position of the properties of the solute on the one hand and the solvent cluster on the other (conspicuous charge transfer complexing being of course an exception). Thus photochemical excitation can be carried out through excitation of the solute species, for example; but the steps leading from an excited solute molecule to the primary photoproduct must increasingly involve the solute-solvent system as a unit. By exciting with monochromatic light in a special region where the solute absorbs and monitoring the increase in photoproduct, one can hope to obtain useful quantitative information regarding the primary photochemical

process. For example, one would wish to know whether photochemistry occurs (and with what efficiency) in various excited vibrational levels of the excited electronic state, or whether this state is first thermally equilibrated prior to the chemical change, or possibly internal conversion to the triplet state is prerequisite for the photochemistry. Since with rare exceptions fluorescence and phosphorescence in a rigid glass originate from the thermally equilibrated lowest excited singlet and triplet state, respectively, emission quantum yield studies together with photochemical yields at different wave lengths can provide a means for tracing these paths leading to the primary photoproduct. When, in addition, such data are obtained for a given solute as the solvent is varied and ultimately as temperature is varied, then we hopefully have at hand an initial understanding of the primary process both of electronic (or vibronic) structure of the solute as well as in terms of the solute-solvent system as a unit.

One of the most elementary and basic chemical transformations is the loss of an electron by a molecule, and quantitative investigation of a photooxidation in a rigid medium should be very useful in our understanding of this elementary process. In 1942 Lewis and Lipkin³ reported a number of cases where light of relatively low energies was sufficient to cause electron loss by a solute held in a rigid glass. Among the solutes is *N,N,N',N'*-tetramethyl-*p*-phenylenediamine (TMPD). In an EPA (ether, isopentane, alcohol) glass, 3.5-e.v. photons are sufficient to ionize TMPD to the conjugate free-radical cation, Wurster's Blue (WB). A most surprising aspect of these observations is, of course, how energies far below gaseous ionization potentials succeed in ionizing a molecule when it is contained in a rigid glass, and surely understanding of the one-electron step must succeed, for one, in dealing with this fact. The TMPD-glass system has been studied extensively in our Laboratory from an entirely different point of view. Following the interesting observations of photodichroism in the TMPD-EPA system by Lewis and Bigeleisen,⁴ we have investigated the photodichroism in detail in order to identify electronic⁵ and vibronic⁶ proper-

(1) This investigation was supported (in part) by a PHS research grant A-3415 from the National Institute of Arthritis and Metabolic Diseases.

(2) From the writer's Thesis submitted in partial fulfillment for the Degree of Master of Science, Cornell University, September, 1961.

(3) G. N. Lewis and D. Lipkin, *J. Am. Chem. Soc.*, **64**, 2801 (1942).

(4) G. N. Lewis and J. Bigeleisen, *ibid.*, **65**, 520 (1943).

(5) A. C. Albrecht and W. T. Simpson, *ibid.*, **77**, 4454 (1955).

ties of excited states in TMPD and WB. These studies were not regarded as bearing directly on the mechanism of the photooxidation. However, a quantitative study of the photooxidation along the lines indicated above has now been completed and is the subject of the present report.

In what follows, the wave length dependence of quantum yields of fluorescence, phosphorescence, and photooxidation of TMPD in 3-methylpentane glass at 77°K. is presented. It is seen how the triplet state plays no significant role in the electron ejection; on the other hand quantum yields for the electron ejection rise with increasing photon energy and appear to reveal especially high electron ejection efficiencies for certain vibrational modes. In the Discussion section a model for the primary process is developed to account for our observations. The appendices deal with certain theoretical problems arising in quantitative studies of photochemistry in rigid media where the distributions of reactant and photoproduct are neither homogeneous nor isotropic and where the spectra of both species overlap in the photochemical spectral region.

Experimental

1. **Materials.**—TMPD, obtained as the dihydrochloride salt from Eastman Kodak, was purified by treating the salt with NaOH solution to obtain first the free base, which then was filtered, dried, and sublimed to give colorless, transparent leaflets of TMPD.

3-Methylpentane (Phillips Petroleum, pure grade), used as the solvent in the rigid media, was purified by passing it through a column containing Alcoa Activated Alumina of grade F-1, mesh no. 14. The dimensions of the column were 116 cm. long by 2.5 cm. in diameter. The alumina was reactivated by heating for 8 hr. at 210° while a stream of nitrogen was continuously passed over it. One treatment of the 3-methylpentane rendered it spectroscopically clean down to the far ultraviolet—the transmittancy of a 1-cm. path was better than 90% to 240 μ .

All other reagents were used as received without further purification: esculin from Pfanstiel Chem. Co., KMnO_4 Analytical Reagent from Baker and Adamson, $\text{H}_2\text{C}_2\text{O}_4 \cdot 2\text{H}_2\text{O}$ was Mallinckrodt Analytical Reagent, and $\text{UO}_2(\text{NO}_3)_2 \cdot 6\text{H}_2\text{O}$ was Baker Analyzed Reagent.

2. **Absorption Spectra at Room Temperature.**—All room temperature spectra were taken with the Cary 14 automatic recording spectrophotometer using quartz cells of 1.0-cm. path length. TMPD was studied in isopropyl alcohol and in 3-methylpentane.

3. **Absorption Spectra at 77°K.**—The absorption spectra of TMPD and WB in 3-methylpentane were taken at liquid nitrogen temperatures by molding in the form of a rectangular solid a "dual" rigid glass consisting of the sample and of a blank (solvent only); the glass eliminated the need for a photometer cell and minimized differences in light paths for blank and sample measurements.⁵ Since the presence of moisture in 3-methylpentane results in the formation of ice particles and subsequent opaque glasses, a technique was developed whereby the glasses could be formed in the absence of moisture. The blank and sample were precooled separately in test tubes until highly viscous. The test tubes were flushed out with nitrogen gas after adding the liquids and then stoppered with corks having CaCl_2 drying tubes attached. When a liquid became viscous, it was rapidly poured into a brass mold surrounded by liquid nitrogen. The dimensions of the mold were $1.3 \times 1.3 \times 6.2$ cm. The first phase was solidified in the mold before adding the second one. Clear glasses with sharp boundaries between the phases could thus be made, as evidenced by the sharp dividing line between the blank and sample when viewing sample phosphorescence. Before the second phase was completely solid, a hollow tube with two small holes in the wall near one end was inserted into the upper phase to act as a holder for the cell and also to serve as a liquid nitrogen

feeder to the dewar. The mold containing the rigid glass and holder then was immersed in an oil bath at 130°. This immediately released the rigid glass and holder from the mold; they were quickly immersed in clean liquid nitrogen in a quartz cylindrical dewar, 21 cm. high with an inside diameter of 3.2 cm. The lower portion of the dewar was unsilvered to permit light transmission. The dewar assembly was stoppered with a Pyrex chimney (for effluent gaseous N_2) consisting of a rubber stopper with 3 in. of Pyrex tubing inserted in it. This served well to keep out moisture. A brass platform was fitted in the bottom of the dewar to direct nitrogen bubbles away from the optical path through the system. The liquid nitrogen was added to the assembly from a large dewar by applying nitrogen gas pressure. Thus all contact with water vapor was avoided and the liquid nitrogen remained clear over a period of 8 hr. The holder was centered in the dewar and mounted to a gear assembly which could raise or lower the rigid glass sensitively, leaving the dewar containing the liquid nitrogen stationary during measurements. By thus keeping blank and sample light paths the same, possible errors due to imperfections in the dewar were eliminated. To avoid differences in absorption that might arise between blank and sample because of imperfections in the rigid glass, preliminary measurements were taken at 430 μ , where the sample does not absorb, and positions in the rigid media where transmittancies of blank and sample coincided were marked. In this manner, optical densities could be reproduced to within ± 0.002 density unit.

A Bausch and Lomb 500-mm. focal length grating monochromator with a dispersion of 33 Å. per mm. was used with a General Electric AH-6 mercury lamp to provide monochromatic light for excitation and measuring. The light was focused on the entrance slit of the monochromator using the lens system provided with it. The monochromator was put in the upright position to make the exit slit horizontal. Both the entrance and exit slits were set at 1.0 mm. width to pass a 33 Å. band width. This permitted realistic readings to be taken at 5- μ intervals and at the same time provided sufficient light intensity for photooxidation. After the monochromator exit, two quartz condensing lenses were situated to focus an exit slit image of 0.4 cm. width and 0.75 mm. height on the rigid glass.

In order to avoid possible interference in detection due to emission from TMPD in the blue and near-ultraviolet when measuring ultraviolet spectra, a 1.0-cm. path of an aqueous solution of NiSO_4 (500 g./l.)⁷ and a Corning 9863 filter were inserted between the sample and detector. Light of wave lengths longer than 370 μ is not transmitted.

The detector consisted of the search unit (containing a 1P-21 photomultiplier tube for the visible region and an RCA 7102 tube for the deep-red region) attached to the Photovolt photometer (series 520-M). The search unit was placed such that the diverging light beam from the rigid glass completely covered the entrance of the search unit in order to minimize variations in apparent detector sensitivity from experiment to experiment at a given wave length.

For studies in the 270–360- μ region, a Corning 9863 filter was inserted at the monochromator exit slit to remove possible stray visible light emanating from the interior of the monochromator and originating from the high intensity visible spectrum of the AH-6 lamp. To maintain the identical experimental conditions for the absorption measurements as existed when carrying out the photooxidation, it was necessary to reduce light intensity without changing slit dimensions. This was conveniently accomplished by interposing an integrating screen (which was originally required for determining the wave length dependent light intensities—see below) between the sample and the detector for absorption measurements in the near-ultraviolet. The integrating screen also eliminates the point where the 1P-21 phototube becomes insensitive in the shorter wave length region and thus it was not necessary to change photomultipliers below 300 μ . For the WB spectrum in the 360–480 μ region, it was also necessary to reduce the light intensity striking the photocell. This was done by inserting 5 exposed photographic plates and a blue Corning 5113 filter between the sample and detector, while at the monochromator exit slit, a Corning 7380 filter was used to remove possible ultraviolet stray light. From 480–660 μ , the RCA 7102 phototube was used, and its sensitivity was such that one filtering

(6) A. C. Albrecht, *J. Am. Chem. Soc.*, **82**, 3813 (1960).

(7) M. Kasha, *J. Opt. Soc. Am.*, **38**, 929 (1948).

device was required. A Corning 3385 filter was situated at the monochromator exit to remove stray light and the second-order spectrum of the grating. The results at points of overlap between the various absorption regions utilizing different experimental techniques revealed an accuracy in our technique of about 5%.

Samples of $4.78 \times 10^{-6} M$ solutions of TMPD in 3-methylpentane at room temperature were used for obtaining the spectra. The percentage contraction of the solution upon cooling to 77°K. was found to be 22% in volume, a value also found by Potts⁸ for various glasses. The concentration of TMPD in the rigid medium was thus $6.12 \times 10^{-5} M$. Because of solubility problems Wurster's Blue samples could not be similarly prepared. Instead samples of WB were prepared for spectrophotometry by photooxidizing a broad strip of the above TMPD for 1 hr., being careful to illuminate all sides of the sample and thus to ensure uniform photooxidation and to avoid corrections for anisotropy. Since total conversion of TMPD to WB could not be attained, it was necessary to subtract the contribution of remaining TMPD to the total optical density in the region where both substances absorb, once the concentration of WB was determined. Having a uniform concentration of WB facilitates this correction. The determination of the concentration of WB is now described. While the detailed shape of an absorption curve usually changes on cooling the sample, the integrated intensity for an absorption band should change little because to a first approximation the intensity of a single electronic transition is equal to the square of the pure electronic transition moment, which is temperature independent.⁹ Thus for a given absorption band at two different temperatures, T_1 and T_2

$$\int \epsilon_1 d\nu = \int \epsilon_2 d\nu$$

(ϵ_1 and ϵ_2 are the ν dependent extinction coefficients at T_1 and T_2 , respectively.) After inserting the relations

$$d\nu = \frac{-c}{\lambda} d(\log_e \lambda)$$

and

$$\epsilon = \frac{D}{Cl}$$

where D is optical density, C is concentration, l the path length, and treating $1/\lambda$ as a constant, we obtain

$$\frac{1}{C_1 l_1} \int D_1 d(\log \lambda) = \frac{1}{C_2 l_2} \int D_2 d(\log \lambda)$$

Now $\int D_2 d(\log \lambda)$ can be obtained from the absorption spectrum of Wurster's Blue perchlorate in water at room temperature,⁵ where we know C_2 and l_2 as well. $\int D_1 d(\log \lambda)$ may be obtained from the spectrum in a rigid glass. We know l_1 (thickness of the glass); therefore C_1 is determined. The extinction coefficients at low temperatures thus are determined ($\epsilon = D/Cl$). We do not feel that our implicit assumption of equality of oscillator strengths in two different media is a serious one for the visible band of Wurster's Blue (and one band is sufficient to determine C_1).

4. The Photooxidation.—The same apparatus, technique, and procedure were used for photooxidation as were used in the low temperature spectra determinations, except a rigid glass of sample only was required and the concentration of TMPD in the glass was $6.12 \times 10^{-4} M$. 1.0-mm. monochromator slit widths permitted realistic photooxidation experiments to be done at 5-m μ intervals in the range of interest—295–345 m μ . The production of WB was spectrophotometrically monitored at the 575-m μ peak. The blank readings were taken in an unphotooxidized region of the medium. To monitor it was only necessary to change the wave length dial of the monochromator. The detecting device consisted of the RCA 7102 photomultiplier tube in the Photovolt photometer with a Corning 3385 filter at the monochromator exit.¹⁰ Optical density readings of the

photoproduct were made after time increments of reaction sufficient to produce a change of about 0.03 density unit. Generally, optical density readings were taken at five different times for a given photooxidation experiment (one wave length of excitation at one section of the rigid medium). The rigid glass was large enough and the photooxidized sections small enough to allow 11 separate rate determinations to be taken on one glass. Thus the entire first TMPD absorption band could be covered at 5-m μ intervals on one glass. Instead, however, experiments at one or two wave lengths were repeated on the same glass to test reproducibility. Our estimate of $\pm 5\%$ precision is based on these results and for the repeated wave lengths averaged values are reported.

5. Determination of Lamp Intensity.—The absolute intensity of the AH-6 lamp at 5-m μ intervals from 295–345 m μ for the conditions obtaining during the photooxidation had to be determined before absolute quantum yields of photooxidation could be calculated. The procedure involved obtaining the absolute intensity at one wave length and converting relative intensities of the other wave lengths with respect to this to absolute intensities. Relative intensities were determined using an integrating screen which consisted of an aqueous solution of esculin (1 g./l.)¹¹ in a quartz cell of 1.0-cm. path length. This solution is suitable as an integrating screen in the region 2500–3665 Å., where it absorbs all incident light of these wave lengths and the absorption occurs at the front surface of the solution.

The standard uranyl oxalate actinometer^{12,13} was used to determine the absolute lamp intensity at 315 m μ . It consisted of a 50.0-ml. solution of $1.00 \times 10^{-3} M$ $UO_2(NO_3)_2$ and $5.00 \times 10^{-3} M$ $H_2C_2O_4$ placed in the same dewar used for photooxidation experiments; the solution was continuously stirred during the irradiation. With the monochromator slits set at width of 1.0 mm., the exciting light was not intense enough to cause an observable change in the oxalate concentration after illumination periods of 1 hr. or more. Consequently, the monochromator slits were opened to 1.0 cm. and the actinometer irradiated for 1.00 hr. at 315 m μ . The optical density of the actinometer under the experimental conditions was determined with a water blank. It was found that $96.3 \pm 0.2\%$ was absorbed in all instances.

The volume change in titration of 25.0-ml. aliquots of the actinometer with $KMnO_4$ (following the procedure of Leighton and Forbes¹²) between exposed and unexposed solutions was about 5 ml. The average quantum yield for the actinometer at 315 m μ with monochromator slit widths at 1.0 cm. was taken as 0.56.¹²

To obtain the absolute light intensity with monochromatic slit widths at 1.0 mm. (the settings used for photooxidation), the integrating screen again was used. At 1-cm. slit settings, a band width extending from 282–318 m μ is passed while at 1.0-mm. settings, a band width extending from 312–318 m μ is passed. In either case, all incident light is absorbed by the esculin, and a ratio of readings taken for the two settings gives a direct ratio of the absolute light intensities for the two experimental conditions. The absolute intensities at the other wave lengths then can be calculated from these results, as previously described.

6. Fluorescence and Phosphorescence Intensities.—The relative sum of fluorescence and phosphorescence intensities was first obtained at 5-m μ intervals of excitation in the 325-m μ absorption band of TMPD, and the fluorescence then removed from detection using a suitable filter. The intensities were measured at about a 45° angle from the normal to the sample face. A Corning 3850 filter was used in front of the search unit to eliminate the detection of stray light when the sum of the intensities was being determined; for measurement of the phosphorescence intensities only, a Corning 3387 filter was employed in front of the search unit. In the latter instance complete removal of fluorescence

measurements were taken perpendicular to the sample as oriented for photooxidation, the expression

$$\log(I_0/I) = \epsilon \int C(x) dx$$

would relate to the amount of WB produced in a most awkward and complicated fashion depending on time, distance from the front face, shape of beam, etc.

(11) E. J. Bowen, *Proc. Roy. Soc. (London)*, **A154**, 349 (1936).

(12) W. G. Leighton and G. S. Forbes, *J. Am. Chem. Soc.*, **52**, 3139 (1930).

(13) G. S. Forbes and L. J. Huidt, *ibid.*, **56**, 2363 (1934).

(8) W. Potts, *J. Chem. Phys.*, **21**, 191 (1953).

(9) R. S. Mulliken and C. A. Rieke, *Repts. Progr. in Phys.*, **8**, 231 (1943).

(10) The optical density measurements were taken with the detector aligned behind the sample and coincident with the photooxidizing light beam, to ensure that the Beer-Lambert law is applicable and the total concentration of photoproduct is measured. If, for example, density

(dark blue) was checked visually by alternately observing the phosphorescence through the filter with the exciting light present and absent. No detectable change in the phosphorescence characteristics was noticeable; that is, the filter used in observing the phosphorescence did not cut out any phosphorescence since the intensity and phosphorescence color (pale green) upon cutting off incident light with and without the filter present remained virtually the same. The fluorescence was not visibly discernible through this filter. Thus since the signal for the combined emission was much greater than for the phosphorescence alone, the signal for combined emission was predominantly due to fluorescence. The resolution by difference into fluorescent and phosphorescent components should be accurate in this case. No effort was made to obtain absolute quantum yields for either emission.

Results

The room temperature absorption spectrum of TMPD in 3-methylpentane is given in Fig. 1. There are peaks at 325 and 265 $m\mu$ with molar extinction coefficients 2770 ± 70 and 19200 ± 600 , respectively. This contrasts with TMPD in isopropyl alcohol, which has peaks at 318 and 262 $m\mu$ and extinction coefficients 2152 ± 66 and $16,753 \pm 157$, respectively.^{5,14} The low temperature spectrum of TMPD in 3-methylpentane for the first electronic band is given in Fig. 2. There is no noticeable shift in the peak compared to the room temperature spectrum, although the extinction coefficient at the peak has increased to 3560 ± 90 . In Fig. 3 is given the absorption spectrum of WB in 3-methylpentane at 77°K., which is very similar to that with isopropyl alcohol-isopentane as the rigid solvent.⁵ In 3-methylpentane, WB has peaks at 632, 575, and 325 $m\mu$ with extinction coefficients $19,300 \pm 200$, $16,100 \pm 100$, and $23,400 \pm 800$, respectively.

For calculating quantum yields at several points on the rate curve, *i.e.*, a plot of WB optical density *vs.* time of irradiation, it was convenient to obtain an empirical equation for the rate curve; accordingly, the best equation for each curve was obtained and constants of the equation evaluated. A Burroughs 220 computer was employed for this work. Equations of the form

$$Y = a_0x + a_1x^2 + a_2x^3$$

and

$$Y = bx^c$$

were considered, where the a 's, b , and c are constants. Analysis of the two proposed equations relating optical density of WB to time required to photooxidize to the given density resulted in the selection of

$$D = a_0t + a_1t^2 + a_2t^3 \quad (1)$$

for study because of the larger correlation coefficients obtained for this form. D is the WB density at time t . Our experimental results are presented in Table I by tabulating therein the best fit parameters of eq. 1 together with correlation coefficients for various experiments.

This tabulation represents a concise and useful compilation of our results. It remains to link these analytic expressions for the variation of optical

(14) It has generally been observed that the extinction coefficients are decreased and the absorption peaks shifted to the blue as the solvent for TMPD becomes more acidic in character. The reverse process for TMPD in 3-methylpentane compared with TMPD in isopropyl alcohol thus might be explained if one considers the alcohols more "acidic" than the hydrocarbon solvent.

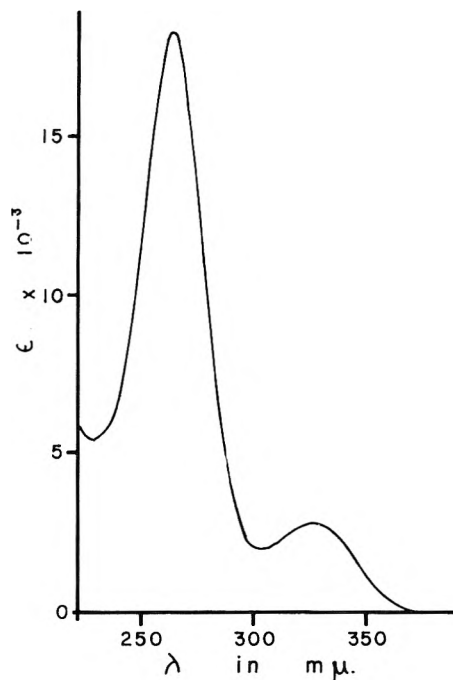


Fig. 1.—The absorption spectrum of TMPD in 3-methylpentane at room temperature.

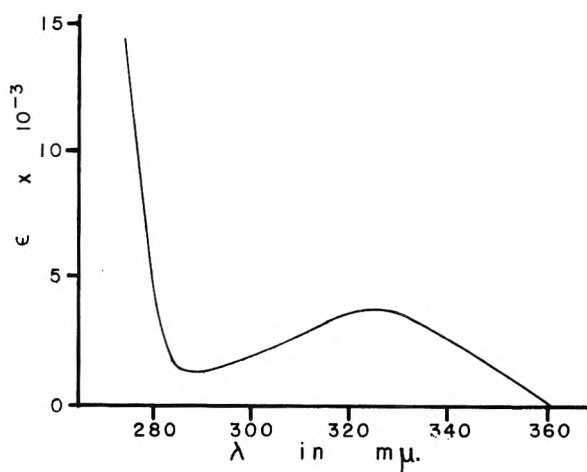


Fig. 2.—The near ultraviolet spectrum of TMPD in 3-methylpentane glass at 77°K.

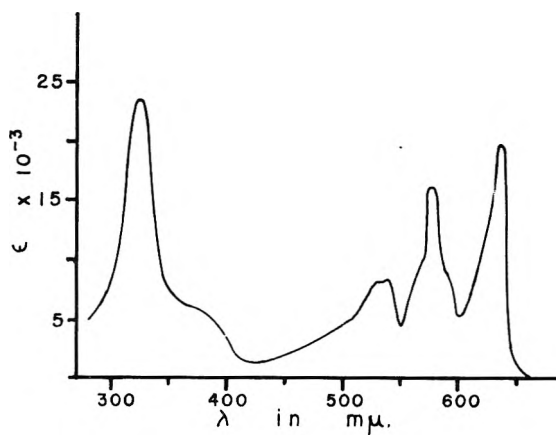


Fig. 3.—The visible and near ultraviolet spectrum of Wurster's Blue in 3-methylpentane glass at 77°K.

TABLE I
EXPERIMENTAL RESULTS

Constants a_0 , a_1 , and a_2 for best fit equation, $D(t) = a_0t + a_1t^2 + a_2t^3$, with the correlation coefficients. $D(t)$ is the optical density of WB at 575 $m\mu$ after t sec. of photooxidation at various ultraviolet wave lengths

Expt.	λ ($m\mu$)	a_0 ($\times 10^4$)	a_1 ($\times 10^7$)	a_2 ($\times 10^{10}$)	Correlation coefficient ^a
1	295	2.70	-1.08	0.347	0.9998
2	300	11.8	-16.8	10.8	.9993
3	305	12.1	-32.9	61.7	.9995
4	310	6.00	-5.42	1.61	.9988
5	315	23.9	-69.5	73.0	.9971
6	320	4.30	-4.25	2.67	.9983
7	325	4.51	-5.52	2.92	.9994
8	330	3.46	-3.56	1.62	.9992
9	335	5.87	-7.97	5.30	.9997
10	340	1.27	-0.172	-0.0507	.9999
11	345	0.983	+0.119	-0.128	.9999
12	300	5.53	+1.16	-13.1	.9979
13	305	6.67	-4.72	2.90	.9998
14	310	3.37	-2.13	1.37	.9999
15	315	18.0	-50.3	61.5	.9999
16	320	3.70	-2.45	0.939	.9996
17	325	3.24	-4.18	2.16	.9926
18	330	1.37	-0.742	0.323	.9997
19	335	2.47	+1.72	-2.97	.9999
20	340	0.929	+0.304	-0.337	.9999

^a The form of the correlation coefficient and the program is described in a report entitled "Multiple Regression and Correlation Analysis for the Burroughs 220 Computer" by E. B. Seidman, Professional Services Department TB 25, Mathematical Report Series, Burroughs Corporation.

density of WB to the total moles of WB produced in time t . This would be a simple matter provided our molecules absorbed isotropically, even though a complicated distribution of WB concentration with depth of sample prevails—especially at large t —because of the rigidity of the medium. Thus we would write

$$D(t) = \epsilon \int_0^l C(x,t) dx \quad (2)$$

where the integral over the complicated function, $C(x, t)$, is just the total moles of WB produced in time t , per unit area of illumination. By dividing the $D(t)$ (Table I) by the extinction coefficient of WB we would have analytical expressions for the time dependence of this integral and computations of quantum yields would simply require division by the total moles of quanta absorbed by TMPD in time t . In fact, however, neither TMPD nor WB absorb isotropically. Fortunately, the anisotropy of absorption as a function of wave length has been determined in the previously mentioned study of the vibronic properties of the first excited state of TMPD.⁶ In Appendix B this problem is discussed in our case and it is shown how the integral we seek is related to $D(t)$ as

$$\int_0^l C(x,t) dx = \frac{10D(t)}{3(3 + \tau_z)\epsilon} \quad (3)$$

where τ_z is related to the probability that TMPD absorbs along its long axis at a given wave length of excitation (and this has been experimentally determined over the near ultraviolet absorption band⁶). The extinction coefficient, ϵ , is the one we

have determined for WB randomly oriented in the rigid glass. Thus, with this correction, our expressions for $D(t)$ do after all provide us with the total moles of WB produced in time t per unit area of illumination. In fact, since τ_z can vary at most from $0 \rightarrow 1$ it is seen that eq. 2 and 3 are not very different. The additional factor in eq. 3 can vary at most from $10/9$ to $10/12$.

Since the quantum yields for the photooxidation show a time dependence, one must distinguish between differential and integral quantum yields. We shall express the differential quantum yield at time t' as

$$\phi(t')_{diff.} = \frac{a \left(\frac{d}{dt} \int_0^l C(x,t) dx \right)_{t'} N^0}{I_A(t')} \quad (4)$$

and the integral quantum yield after time t' has elapsed reads

$$\phi(t')_{int.} = \frac{a \int_0^l C(x,t') dx N^0}{\int_0^{t'} I_A(t) dt} \quad (5)$$

where $I_A(t)$ is the number of photons absorbed per second at time t by the donor species, A, and where the illuminated area, a , is 0.03 cm.^2 in our case and the sample depth is $l \text{ cm.}$ Avogadro's number, N^0 , converts moles of photoproduct to molecules. (If a molar extinction coefficient is used in eq. 3 then a factor of 10^{-3} on the right hand side of eq. 4 and 5 also is required.) The numerators in eq. 4 and 5 are readily determined through eq. 3 and 1 (Table I).

Determination of the light absorbed by the donor molecule at any time, t , is complicated by the fact that there is overlap of a strong band of the photoproduct with the near ultraviolet band of the donor molecule. In addition, the distribution of the photoproduct in sample depth is complicated at large t . These problems are discussed in Appendix A, where the calculation of $I_A(t)$ is outlined. Absolute values for $I_A(0)$ as well as for the incident light intensity, I^0 , at various wave lengths are presented in Table II. The intensities are for the total area of illumination. Table II also contains the raw data concerning fluorescence and phosphorescence intensities as a function of exciting wave lengths. Each emission is on its own relative scale. (We already have indicated that the fluorescence signal was considerably stronger than the phosphorescence signal.)

Table III lists the computed quantum yields (relative) for fluorescence and phosphorescence and the absolute quantum yields for the photooxidation at zero time. Values, uncorrected for anisotropy, are presented for various experiments. Two values are given for most wave lengths. These are computed from data taken from two separate rigid media. With some exceptions there appears to be a tendency for the second member of each pair to be slightly lower than the first and we suspect the presence of determinate errors (rather than changing quantum yields with glass preparation). However this is not certain. For present purposes we have simply averaged the pairs. These averages, corrected for anisotropy, also are presented in Table III. They are plotted in Fig. 4 as the $t = 0$

TABLE II

INCIDENT LIGHT INTENSITY, I_0 , INITIAL LIGHT ABSORBED BY TMPD, I_A , RELATIVE FLUORESCENCE INTENSITY, I_f , AND RELATIVE PHOSPHORESCENCE, I_p , FOR A GIVEN WAVE

λ (m μ)	LENGTH OF EXCITATION			
	I_f (rel.) (arbitrary scale)	I_p (rel.)	I_A ($\times 10^{-14}$) (in photons/sec.)	I_0 ($\times 10^{-14}$)
345	1.38	5.00	1.78	1.83
340	1.46	5.38	1.89	1.91
335	2.47	9.25	3.24	3.25
330	1.67	5.80	2.06	2.06
325	1.81	6.40	2.23	2.23
320	2.21	8.40	2.90	2.90
315	3.47	13.50	4.62	4.64
310	1.51	5.40	1.90	1.91
305	1.82	6.78	2.39	2.43
300	1.60	6.00	2.13	2.22
295	0.80	3.00	1.17	1.28

quantum yields. To illustrate the time dependence of the quantum yields we have arbitrarily chosen to plot in Fig. 4 differential quantum yields at times, depending on wave length, where the optical density of WB is 0.100 (at 575 m μ). Again averages have been taken for the two rigid media. Integral quantum yields also were computed for various times of excitation. In the limit of zero time these agreed with the differential yields at zero time. At other times the integral quantum yields were always higher, when different, than the differential yields, in keeping with the general observation of decrease of yield with time of illumination. Also plotted in Fig. 4 are the relative yields for the two emissions. The contrast between the wave length dependence for the photochemical yields and those for the emission is striking.

TABLE III

RELATIVE FLUORESCENCE AND PHOSPHORESCENCE QUANTUM YIELDS, ϕ_f AND ϕ_p , AND ABSOLUTE PHOTOOXIDATION QUANTUM YIELDS, ϕ_{photo} AND ϕ_{photo}^a (CORRECTED), FOR VARIOUS WAVE LENGTHS OF EXCITATION

Expt.	λ (m μ)	ϕ_f (rel.)	ϕ_p (rel.)	ϕ ($\times 10^3$) photo	ϕ^a ($\times 10^3$) photo
1	295	0.84	0.87	2.5	2.4
2	300	.93	.97	6.2	
12				5.0	5.4
3	305	.95	.98	5.7	
13				4.6	4.9
4	310	.99	.98	3.6	
14				2.8	3.2
5	315	.93	1.00	5.8	
15				6.4	6.1
6	320	.95	0.99	1.7	
16				2.1	1.9
7	325	1.00	.99	2.3	
17				2.2	2.4
8	330	1.00	.97	1.9	
18				1.4	1.8
9	335	0.96	.98	2.0	
19				1.4	1.8
10	340	.96	.98	0.78	
20				0.88	0.89
11	345	.97	.97	0.66	0.71

^a Average yield corrected for anisotropy of photoproduct (see Appendix B).

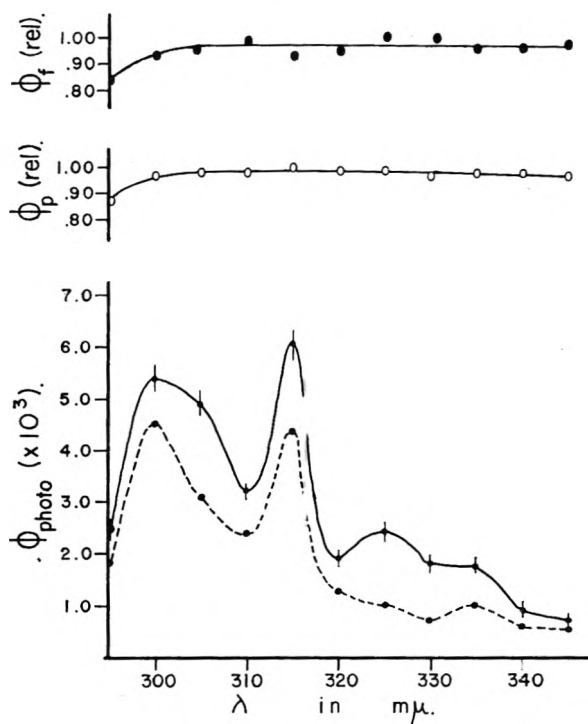


Fig. 4.—●—, the relative yield of fluorescence, ϕ_f ; —○—, the relative yield of phosphorescence, ϕ_p ; —●—, the initial absolute quantum yield of the photochemistry, ϕ_{photo} , with the precision indicated; - -●- -, the differential absolute quantum yield of the photochemistry after about 1% conversion. All measurements made with 3.3 m μ band width (1 mm. slits) of exciting radiation.

Because quantum yields at longer times depend more strongly on the proper correction for absorption of exciting light by the photoproduct (Appendix A), we must be cautious when interpreting this apparent time dependence as reflecting some other intrinsic property of the system. For example, we note that the time dependence is strongest at 325 m μ and this is just where the interference due to WB is at its greatest (see Fig. 2 and 3). On the other hand, the extent of the diminution observed appears to be rather large, even where interference due to WB is much smaller (295 or 345 m μ , for example). We conclude, tentatively, that the decrease with time of ϕ_{photo} reflects partly a genuine tendency (to be discussed below) and partly our inability to correct exactly for the presence of WB.

Finally, the observations of unusual variation with wave length of quantum yields of photooxidation require critical comment. The coincidence of a sharply higher quantum yield at 315 m μ and a strong mercury line in that region is of special concern. Attempts at monochromatic photooxidation with other available sources have not been successful. Instead we have studied photooxidation at 315 m μ using the AH-6 lamp at intensities ranging over an order of magnitude. It was found that the rate of photooxidation is definitely linear with light intensity (as has been assumed). Further, we have independent assurance that no specific determinate errors in our measurement of light absorbed by TMPD appear at high intensities when we note that emission yields (which are based on the same TMPD light absorbed calculations) show a typical

constancy over the entire wave length region. We thus regard the structure in the excitation spectrum for the photochemistry as genuine.

Discussion

The most significant aspects of our results (which are summarized in Fig. 4) would appear to be: the structured excitation spectrum for the photooxidation is very different from that of either fluorescence or phosphorescence; the quantum yields for the photooxidation are low ($\sim 10^{-3}$); these yields are found to diminish with time of photooxidation. These principal observations as well as subsidiary ones shall now be interpreted first in general terms and then through the use of a specific model for our photochemical system.

It generally is regarded that fluorescence and phosphorescence in a system such as ours take place from the thermally equilibrated first excited singlet state and the lowest lying triplet state, respectively. The fact that the excitation spectra for the emission and for the photooxidation are so different indicates that the ejection of the electron waits neither for the thermal equilibration of the excited state nor for the passage into the triplet state.

If we discount (as we shall below) the possible role of weak but direct transitions into new, photochemically active, solute-rigid solvent electronic states, then we are led to say that electron ejection originates from various vibrationally excited levels of the excited singlet state and with especial facility from particular vibrational levels (to account for the structure in the excitation spectrum). This is especially interesting when it is realized that thermal equilibration of vibrationally excited electronic states is orders of magnitude (three, to be conservative) faster than the lifetime of the excited singlet state itself. Thus the intrinsic quantum yield (when the competing processes are taken into account) for the photooxidation climbs very sharply as higher vibrational levels are excited. In the thermally equilibrated excited singlet state (the 340–345 $m\mu$ region) the competing deactivating mechanisms are much slower and yet the quantum yield has dropped to its lowest values. In the simplest terms these results evoke the picture of an energy barrier separating the excited donor species from the ionized donor and the trapped electron. This barrier is either surmounted or penetrated all the more readily the more energetic the donor molecule.

The fact that while the yield does tend to rise with decreasing wave length there nevertheless are points where there is a decline in yield with increasing energies seems to lead to the following interesting conclusions. The nearly wave length independent yields of emission indicate that the absolute yields for emission must be at least an order of magnitude higher than that for the photooxidation. Otherwise the increase of photochemical yields should be reflected by a decrease of emission yields. We conclude that, roughly, for every absorbed photon that brings about electron ejection there are at least ten absorbed photons which ultimately lead to thermally equilibrated electronic states and consequent emission. Now presumably when ex-

iting, say at 310 $m\mu$, the majority of excited molecules are thermally equilibrated and in the process pass through the stage of being at 315 $m\mu$ energy. Then one might ask why is not the excitation spectrum for the photochemistry more an increasing step function with decreasing wave length rather than the observed curve. Thermal cascading always will lead most excited molecules to some lower energy condition having a peak photooxidizing efficiency. The apparent efficiency at higher energies then would be no lower than the highest peak achieved at lower energies. The fact that this is not observed seems to indicate that the 315 "state" achieved through light absorption is not the same as the 315 "state" achieved *via* cascading from higher levels. The vibronic transition probability at 315 $m\mu$ favors certain specific vibronic states which differ from other vibronic states having the same energy but which are reached *via* cascading from higher energies. Thus in the strictest sense of the term our photochemistry can be regarded as vibronic photochemistry.

The decrease with time of the photochemical yields can be explained in at least two ways (apart from the breakdown of our approximations used in Appendix A). First, any photobleaching of WB could bring this about. Light might either cause decompositions of WB or might induce the return of the trapped electron to WB. However, our experience tends to rule out photobleaching because the theoretical limit for the photoconversion of TMPD appears to approach 100%, although the practical limit is less because of the inner filter effect of the photoproduct, WB. For example, in our experiments at a WB optical density of 0.100, where diminution of yield is already noticeable, only 1% of the TMPD has been converted. A second explanation for the time dependence lies in postulating the existence of a variety of TMPD-solvent clusters, some of which are more readily photooxidized than others. The difference among clusters may, for example, be nothing more than the relative proximity of electron traps. A sufficient variation in photooxidizing efficiencies among TMPD solvent clusters, whatever the reasons, is bound to lead to a diminution of yield with time. We suspect that such variation is primarily responsible for the observed time dependence.

It is useful to elaborate in terms of a model. Suppose we speak of TMPD, the donor, surrounded by n solvent molecules, the acceptors, as a photochemical unit DA_n , where we need not specify the magnitude of n . The quartz ultraviolet spectrum of this unit is essentially that of the D molecule (TMPD). This suggests that near ultraviolet excitation of DA_n leads to a condition, D^*A_n , where essentially the donor molecule is vibronically excited. Then, with a certain probability, passage into a charge transfer state, $D^+A_n^-$, may take place. Energetically, $D^+A_n^-$ will lie near or below D^*A_n . If n is fairly large it is likely that there are a number of charge transfer states, some presumably very short lived and others very long lived simply because of the number of A_n^- that are conceivable. Decay from the short lived states (if such have been created) may return the unit to the ground state,

DA_n , or into a longer lived charge transfer state. The photoproduct that we measure must be one of the latter, since we have observed some thermal fading of WB in our system only after a few days. The stability of certain $D^+A_n^-$ relative to conversion to DA_n can be regarded as due to electronic overlap forbiddenness of the coupling between the two states. (The orbital of the transferred electron occupies a different region in space in DA_n than in $D^+A_n^-$; in other words, the electron is distantly removed from the D^+ ion.) Thus, direct optical transitions into the stable low lying $D^+A_n^-$ are not observed. However, what about direct transitions into other low lying $D^+A_n^-$? While in our case such transitions are not spectrally evident in the near-ultraviolet, they may be obscured either by electronic or Franck-Condon weakness. If, though weak, they lead to an intrinsically efficient transfer into the stable $D^+A_n^-$, then perhaps the observed excitation spectrum for the photooxidation has no direct relationship to the first excited state of the donor. We have discarded this possibility first because of the compelling coincidence of the onset of photooxidation with the onset of the conspicuous absorption by the donor in various rigid solvents. Similarly, we find the same coincidence with another donor, *p*-phenylenediamine, in 3-methylpentane glass. Such faithful coincidence would be most remarkable were direct $DA_n \rightarrow D^+A_n^-$ optical transitions dominant in the photochemistry. A second interesting reason for discarding this possibility is now outlined.

Additional evidence that the primary absorption act which leads to the stable $D^+A_n^-$ is $DA_n \rightarrow D^*A_n$ is provided by the polarization of the vibronic transitions which lead to the production of stable $D^+A_n^-$. The mixed polarization that has been found in the near ultraviolet band of TMPD in a rigid glass was in fact detected by observing the orientation of the photoproduct, WB, when polarized exciting light was used.⁶ Strictly speaking, transitions which do not lead to a photoproduct (which lead to emission for example) are not detected by this method. Still our results support theoretical predictions¹⁵ regarding mixed polarization in the near ultraviolet band of (gaseous) TMPD. On these grounds as well, we conclude that absorption first brings about the transition $DA_n \rightarrow D^*A_n$, which then passes by tunnelling or surmounting a barrier into the stable $D^+A_n^-$. A most conclusive proof awaits our study of polarized fluorescence in TMPD excited with polarized light. Here transitions are being studied which ultimately lead to fluorescence (from the thermally equilibrated excited singlet states) and not photochemistry. A mixed polarization found by this technique similar to that found by polarized photochemistry would indicate that the primary absorbing act which leads to photochemistry and which leads to emission is one and the same and in fact involves excitation of the donor species alone.

Possible evidence for the existence of short lived charge transfer states appears to come from our experiments on photoconductivity in TMPD-3-methylpentane glasses first reported in 1959.¹⁶

We have found that the photooxidation of TMPD is accompanied by a current flow which we attribute to electron flow within the glass. On the other hand, the dark conductivity before and after photooxidation is not measurably different. That is, our stable $D^+A_n^-$ does not contribute a charge carrier to our system. But the passage from D^*A_n to $D^+A_n^-$ in a field is accompanied by a current flow—in all likelihood *via* intermediate short lived charge transfer states. Of additional interest is the sharp photocurrent we have just found in the very near ultraviolet (370 m μ) after $D^+A_n^-$ has been formed and not before. We regard this as a transition, $D^+A_n^- \rightarrow D^+A_n^{*-}$ (excitation of the trapped electron) which leads either to another $D^+A_n^-$ or DA_n . Further photoconductivity studies—especially a comparison of the excitation spectrum with that for the photooxidation—should prove especially helpful in clarifying the $D^*A_n \rightarrow D^+A_n^-$ step.

In terms of the DA_n photochemical unit the vibronic structure in the excitation spectrum can be discussed from two points of view. First we note that the equilibrium nuclear configuration of D^+ differs from that of D by a few hundredths of Angstroms of a particular totally symmetric (D_{2h}) ring stretching and compressing mode.¹⁷ It would seem reasonable that excitation of this normal mode in D^* would make electron ejection especially favorable to produce D^+ . If we regard peaks in quantum yield to exist at 335, 325(?), 315, and 300 m μ (Fig. 4) and if we consider the poor resolution of the excitation spectrum, then it is not unreasonable to regard these as representing ring modes somewhere in the 1000 to 2000 cm^{-1} range. It may even be that the ring b_{3g} modes which we know are unusually vibronically active in this transition^{6,15} are accompanied by vibronic activity of that a_g mode which serves as the partner to the b_{3g} mode in D_{6h} symmetry, where both are equally potentially vibronically active e_{2g} species (1596 cm^{-1}). This, in fact, is the particular totally symmetric mode that can carry equilibrium D into the equilibrium D^+ configuration.

A second point of view is to speak in terms of several transient $D^+A_n^-$ states, each being separated by its own barrier from D^*A_n . In these terms, certain vibrational levels of D^* may just be energetically favorable for passage into a particular $D^+A_n^-$ and then on to the stable $D^+A_n^-$. The vibronic structure in the excitation spectrum would, in this case, relate much more to the solvent properties than it would on the basis of the first explanation. We tend to favor the first point of view. We hope that a distinction shall be possible after studies are completed of TMPD in a different glass as well as of another donor in 3-methylpentane. Some evidence already exists to show that the overall quantum yield is strongly dependent on the nature of the rigid environment, A_n . Lewis and Bigeleisen have reported a very rough estimate of an over-all quantum yield for the photooxidation of TMPD in EPA glass.¹⁸ They find an efficiency of

(16) A. C. Albrecht and M. E. Green, *ibid.*, **31**, 261 (1959).

(17) J. D. Turner and A. C. Albrecht, unpublished work on the crystal structure of Wurster's Blue perchlorate.

(18) G. N. Lewis and J. Bigeleisen, *J. Am. Chem. Soc.*, **65**, 2419 (1943).

0.10, a value much larger than ours of, say, 0.003.

Some time ago qualitative studies were carried out to determine whether or not photooxidation in our system occurred from the triplet state of TMPD. It was found that when two identical solutions of TMPD in 3-methylpentane are prepared and one of these is saturated with O₂ under pressure and both are cooled to the glassy state the phosphorescence is nearly completely quenched by the presence of O₂ but the rate of photooxidation appears to be unchanged. The lack of photooxidation from the triplet state has been confirmed by the present work. However, it was conceivable that the low yield electronic photochemistry in the 340–345 mμ region may still be *via* the triplet state and any quenching of this would have been masked by the higher yield vibronic photochemistry at the higher energies. The O₂ experiment was repeated using monochromatic light and making quantitative measurements of the photoproduct. Quenching of the phosphorescence produced no measurable change in yield either at 315 mμ or in the 340–345 mμ region. It may be that the triplet state is simply not sufficiently energetic to permit photooxidation in this medium. The incidental observation that varying oxygen concentration does not alter the efficiency of the photooxidation is of considerable additional interest. Earlier in a search for specific oxygen effects we had prepared oxygen-free glasses and compared rates of photooxidation in these with rates in ordinary glasses. No detectable difference was found.

We hope that further studies along these lines as well as along the lines of the photoconductivity work shall clarify these problems and ultimately provide detailed insight regarding the loss of an electron by a molecule to its environment. In particular we hope that measurements of temperature dependence of quantum yields shall be possible to help distinguish between barrier penetration or tunnelling and barrier crossing in the passage from D^{*}A_n into D⁺A_n⁻. Finally, the nature of A_n⁻ must be elucidated and its role in the energetics of this low energy ionization process must be understood. At present we can say only that a variety of evidence suggests that the electron trap is not some impurity electron accepting chemical species but is rather a property of the glass structure. This would compare with the observations by Linschitz and co-workers^{19,20} of trapped electrons in amine-containing glasses. We shall withhold for the present speculation regarding the origin of relatively deep potential in the glass necessary to account for the low lying D⁺A_n⁻ condition.

Appendix A

Light Absorbed Exclusively by Reactant in a Spectral Region where Reactant and Product Spectra Overlap.—Consider a rigid system consisting of photoreactant, A, and photoproduct, B. Suppose that the spectra of A and B overlap in the photochemical spectral region. In order to compute quantum yields it is of importance to determine the total light absorbed exclusively by species A at any stage in the photochemistry. This problem is complicated by the rigidity of the medium where the distributions of A and B

within the medium become increasingly complex as more and more B is produced. In analytical terms, we seek the integral

$$I_A(t) = \int dI_A(x,t) = \int_0^l I(x,t)\epsilon_A C_A(x,t) dx \quad (\text{A-1})$$

where $dI_A(x,t)$ is the light absorbed by species A at time t in a thickness of sample dx at x . $I(x,t)$ is the total light incident at position x in the sample at time t ; and $C_A(x,t)$ is the concentration of species A at x and time t . Now generalized Beer's law gives

$$I(x,t) = I_0 \exp \left\{ - \left[\int_0^x \epsilon_A C_A(x,t) dx + \int_0^x \epsilon_B C_B(x,t) dx \right] \right\} \quad (\text{A-2})$$

Further, we may write in our case

$$C_A(x,t) + C_B(x,t) = C_0 \quad (\text{A-3})$$

where C_0 is the initial concentration of A.

Thus attempts to integrate eq. A-1 require only some analytic form for $C_A(x,t)$. At this point some form of approximation appears to be necessary.

The rate expression for the production of photoproduct (at time t and at position x in the rigid medium) reads

$$\frac{dC_B(x,t)}{dt} = k_1 C_A(x,t) I(x,t) \quad (\text{A-4})$$

Consider sufficiently low fractional conversion to permit

$$C_A(x,t) \cong C_0 \text{ and } I(x,t) \cong I_0 \exp(-\epsilon_A C_0 x)$$

This gives

$$C_B(x,t) \cong k_1 C_0 I_0 t \exp(-\epsilon_A C_0 x) \quad (\text{A-5})$$

Now consider a wave length where species B alone absorbs with an extinction coefficient ϵ_B' . Beer's law gives

$$\int_0^l C_B(x,t) dx = \frac{D_e}{\epsilon_B'} \quad (\text{A-6})$$

where D_e is $\ln(I_0/I)$ at the wave length under consideration. Integration over x of eq. A-5 gives

$$\int_0^l C_B(x,t) dx \cong \frac{k_1 I_0 t}{\epsilon_A} [1 - \exp(-\epsilon_A C_0 l)] \quad (\text{A-7})$$

or eq. A-6 and A-7 give

$$k_1 I_0 t = \frac{\epsilon_A D_e}{\epsilon_B' [1 - \exp(-\epsilon_A C_0 l)]} \quad (\text{A-8})$$

Thus a measure of D_e and knowledge of ϵ_A , ϵ_B' as well as sample thickness permits a determination of $k_1 I_0 t$ at any time (where our approximations are valid). It is now possible to express $C_A(x,t)$ to a higher order (than $C_A = C_0$) and in terms of the optical density (D_e) of the photoproduct. Thus eq. A-3, A-5 with A-8 give

$$C_A(x,t) \cong C_0 [1 - \alpha \exp(-\epsilon_A C_0 x)] \quad (\text{A-9})$$

where

$$\alpha = D_e \left(\frac{\epsilon_A}{\epsilon_B'} \right) [-\exp(-\epsilon_A C_0 l) + 1]^{-1} \quad (\text{A-10})$$

is readily determined experimentally. Equation A-9 for $C_A(x,t)$ should be adequate for regions of low conversion of A but away from $t = 0$. We apply it to determine $I(x,t)$ (eq. A-2 with eq. A-3) and then in eq. A-1 to determine $I_A(t)$. Thus we find with

$$\beta = \alpha \left(\frac{\epsilon_A - \epsilon_B}{\epsilon_A} \right) \quad (\text{A-11})$$

and

$$\gamma = \epsilon_A C_0$$

that

$$I_A(t) = \gamma I_0 e^{-\beta} \left[\int_0^l e^{-\gamma x} e^{\beta e^{-\gamma x}} dx - \alpha \int_0^l e^{-2\gamma x} e^{\beta e^{-\gamma x}} dx \right] \quad (\text{A-12})$$

With $y = e^{-\gamma x}$ the remaining integrals reduce to ones of a general type, $\int y^n e^{\beta y} dy$, thus

(19) H. Linschitz, M. G. Berry, and D. Schweitzer, *J. Am. Chem. Soc.*, **76**, 5833 (1954).

(20) H. Linschitz, J. Rennert, and T. M. Korn, *ibid.*, **76**, 5839 (1954).

$$I_A(t) = I_0 e^{-\beta} \left\{ \left(\frac{e^\beta - e^{\beta e^{-\gamma t}}}{\beta} \right) + \frac{\alpha}{\beta} (e^{\beta e^{-\gamma t} - \gamma t} - e^\beta) + \frac{\alpha}{\beta^2} (e^\beta - e^{\beta e^{-\gamma t}}) \right\} \quad (\text{A-13})$$

where γt is just the initial ($t = 0$) $\ln I/I$ for the sample at the particular wave length chosen for photochemistry. Through eq. A-11 and A-10, we see how β ultimately relates to the optical density, D_0 , of the photoproduct at any given time. (D_0 is measured in a spectral region where only B absorbs.) Thus the measurement with all other parameters predetermined gives the desired values for light absorbed by species A after t seconds of photooxidation.

While eq. A-13 is valid only at low conversions it is useful for meaningful extrapolations of quantum yields to zero conversion. These extrapolated quantum yields (Fig. 4) are regarded as containing negligible error due to the overlap of photoreactant and photoproduct spectra. Calculated quantum yields at higher conversions are certainly less accurate. It can be seen (Table I) that $D(t)$ at 0.100 is already quite non-linear at some wave lengths (see 325 $m\mu$ at ~ 360 sec., for example). Still the empirical nonlinearity is incorporated into eq. A-13 via β and we feel that error due to overlapping bands may not be too serious and probably accounts for only a small portion of the observed "time dependence" of the quantum yields (Fig. 4). A study of higher order approximations would reveal the magnitude of error. For our primary purpose—the extrapolation to zero time—the present treatment ought to be more than adequate.

Strictly speaking, the present treatment should have considered corrections due to anisotropy of the photoproduct instead of dealing in terms of isotropic extinction coefficients. This correction is discussed in Appendix B where it is small even where it enters most directly into the quantum yield calculations. It would be even smaller in its influence on $I_A(t)$.

In practice molar decadic extinction coefficients are used throughout. For this, eq. A-13 must be altered with the transformations $\beta = 2.303\beta'$, $\alpha = 2.303\alpha'$, and $\gamma = 2.303\gamma'$, where the primed parameters are identical in form to the unprimed (eq. A-10, A-11), except for their exclusive use of molar decadic extinction coefficients.

Appendix B

Correction for Anisotropy of Absorption in the Photoproduct.—In a solution where neither the photoreactant nor the photoproduct are free to rotate and where, as is usually the case, the molecular absorptior is anisotropic, photochemistry (with polarized or unpolarized light) produces an oriented sample. Thus the photoproduct is distributed in a complicated fashion in molecular angle space as well as in depth of sample. An important consequence of this is that one must be careful in defining the molecular extinction coefficient for such a sample. Let us write $\bar{\epsilon}$ for the usual molar decadic extinction coefficient that one would determine for the photoproduct in a fluid solution at a given wave length. Let $C(x,t)$ represent the concentration of photoproduct in a rigid sample as a function of depth and time. The total moles of photoproduct contained (after time t) in a unit area of sample of thickness l is just

$$\int_0^l C(x,t) dx$$

and we seek to determine this integral from optical density measurements, the average extinction coefficient $\bar{\epsilon}$, and our knowledge of the anisotropy of absorption in the photoreactant and photoproduct.

Consider space fixed axes a , b , and c and molecular fixed axes x , y , and z . Suppose that at a given wave length the ratio of apparent extinction coefficients for the three axes of the photoreactant is $r_x:r_y:r_z$ ($r_x + r_y + r_z = 1$). Similarly suppose the ratio of the apparent extinction coefficients (at

the monitoring wave length) of the photoproduct is $q_x:q_y:q_z$ ($q_x + q_y + q_z = 1$). Consider the photochemical light to be incident along the b -axis polarized a fraction p along a and a fraction $1-p$ along c . It can be shown⁶ that optical density measurements of the photoproduct made with light polarized along the a , b , and c axes are proportional to

$$D_a \alpha A = (1-p)B + p[3(r_x q_x + r_y q_y + r_z q_z) + q_x(r_y + r_z) + q_y(r_x + r_z) + q_z(r_x + r_y)]$$

$$D_b \alpha B = r_x q_x + r_y q_y + r_z q_z + 2[q_x(r_y + r_z) + q_y(r_x + r_z) + q_z(r_x + r_y)] \quad (\text{B-1})$$

$$D_c \alpha C = pB + (1-p)[3(r_x q_x + r_y q_y + r_z q_z) + q_x(r_y + r_z) + q_y(r_x + r_z) + q_z(r_x + r_y)]$$

The proportionality constants depend on the nature of the experiment. We note that $A + B + C = 5$.

In the present study the incident light is unpolarized ($p = 1/2$) and the photoproduct absorbs along the z -axis only at the monitoring wave length (575 $m\mu$) ($q_z = 1$, and $q_x = q_y = 0$). Inserting these values into eq. B-1 we find that

$$\begin{aligned} A &= \frac{3 + r_z}{2} \\ B &= 2A - 1 - 2r_z \\ C &= A \end{aligned} \quad (\text{B-2})$$

The proportionality constants linking D_a with A and D_c with C are the same (the ac face is being viewed) so that we see that $D_a = D_c = D$, where D is the optical density observed with unpolarized light incident along b . We may write

$$D = D_a = kA$$

or

$$D = \left(\frac{3 + r_z}{2} \right) k \quad (\text{B-3})$$

where k incorporates in a manner to be determined $\bar{\epsilon}$ and concentration but is not related to any anisotropy.

Consider the hypothetical situation where a given oriented sample is randomized in the molecular angle space (but still with the same $C(x)$). The proportionality constant, k , will not change but the anisotropy parameters A , B , and C will. We shall prime them. For the isotropic situation we have $A' = B' = C'$ and with $A' + B' + C' = 5$ we find that $A' = 5/3$. Thus for the isotropic case we observe that

$$D_a' = D_c' = D' = \bar{\epsilon} \int_0^l C(x,t) dx = kA' = \frac{5}{3} k \quad (\text{B-4})$$

where we may use the "average" extinction coefficient just as we do in fluid solutions. We observe that

$$k = \frac{3}{5} \bar{\epsilon} \int_0^l C(x,t) dx \quad (\text{B-5})$$

and use this in eq. B-3 to find

$$\int_0^l C(x,t) dx = \frac{10}{3\bar{\epsilon}(3 + r_z)} D \quad (\text{B-6})$$

the desired relationship between the integrated concentration, the observed optical density of oriented photoproduct (using unpolarized light), and the "average" extinction coefficient, $\bar{\epsilon}$, corresponding to the one obtained for an isotropic sample. The parameter r_z changes with exciting wave length. This parameter is known for the near ultraviolet band of TMPD in an alcoholic glass (see Table I and eq. 3 of ref. 6). These values are carried over to the hydrocarbon glass after allowing for the shift in the spectrum. In any case the correction turns out not to be serious. The factor $10/[3(3 + r_z)]$, which distinguishes the isotropic case, eq. B-4, from the anisotropic case, eq. B-6, can vary at most from 10/9 to 5/6 as r_z varies from 0 to 1.

SPECTRA OF DILUTE SOLUTIONS OF BISMUTH METAL IN MOLTEN BISMUTH TRIHALIDES. I. EVIDENCE FOR TWO SOLUTE SPECIES IN THE SYSTEM BISMUTH-BISMUTH TRICHLORIDE¹

BY CHARLES R. BOSTON AND G. PEDRO SMITH

Metallurgy Division, Oak Ridge National Laboratory,² Oak Ridge, Tennessee

Received January 18, 1962

Solute bismuth metal in chloride-rich melts of the system Bi-BiCl₃ is found to be partitioned into two chemical species which obey the law of additive absorbances. Absorption spectra from 450 to 750 m μ are reported for molten Bi-BiCl₃ mixtures 0.0027 to 0.7 *M* in solute bismuth metal at path lengths as short as 24 μ and at temperatures of 264, 350, and 433°. The spectrum consists of an intense, broad band with a maximum near 560 m μ . Large apparent deviations from Beer's law are found at all wave lengths. These spectra have the characteristics expected for solutions with two light-absorbing solute species. Phenomenological equations are derived which describe the spectra of solutions consisting of any given number of solute species derived from a common substance.

Introduction

The molecular constitution of the liquid phases of bismuth-bismuth trihalide and related metal-metal salt systems is an unsolved problem which has attracted much recent research and debate. Much of this work is reviewed elsewhere.³⁻⁵ It usually is assumed that bismuth metal dissolves in halide-rich melts to form a single solute species. However, some workers^{4,6} assert that there are two or more solute species which are in equilibrium. No specific solute species has been demonstrated to exist in the halide-rich melts. The species which have been postulated include such diverse entities as bismuth atoms,⁷ polymers of bismuth atoms,⁶ monovalent bismuth ions and their polymers,^{6,8,9} and "ions plus electrons."⁴ The research reported here provides spectrophotometric evidence which clearly favors a two-species model for chloride-rich melts of bismuth in bismuth trichloride.

Experimental

Materials.—Bismuth trichloride was prepared by direct reaction between bismuth metal and chlorine gas. The product was purified by distillation under chlorine followed by purging chlorine from the melt with argon. Analysis of the salt showed 33.68 wt. % Cl as compared with the theoretical value of 33.73%. This material was extremely sensitive to air contamination. Therefore, all handling, including analytical weighing, was performed in a vacuum-type drybox filled with high-purity nitrogen.

Bismuth metal, used as a solute, was deoxidized by bubbling hydrogen through molten, reagent-grade metal held on a sintered glass disk. The oxide-free metal was filtered through the sintered disk into a glass tube, sealed off under vacuum, and later opened in the drybox where the metal ingot was broken up in a mortar and placed in a weighing bottle.

Measurements.—A Cary Model 11MS spectrophotometer

modified for high-temperature work¹⁰ was used to make the spectral measurements. Fused silica cell-insert combinations were used to provide path lengths from 24 to 500 μ . Cells were loaded with weighed amounts (10–12 g.) of Bi-Cl₃ in the drybox and held under a flow of argon during spectral measurements. Melt composition was changed between spectral scans by adding bismuth metal through the top of the cell while keeping a stream of argon passing over the melt.

The possibility that atmospheric contamination significantly influenced the spectra was excluded by the results of measurements on two Bi-BiCl₃ mixtures which were sealed in optical cells under 1/3 atm. of argon. The spectra of these sealed mixtures were quantitatively like the spectra obtained with stoppered cells.

Nomenclature and Units.—All of the melts to be considered lie at the BiCl₃-rich end of the Bi-BiCl₃ binary system. Accordingly, pure BiCl₃ will be referred to as the solvent and the amount of bismuth in excess of that in pure BiCl₃ will be referred to as solute bismuth. The concentration of solute bismuth in moles per liter of melt is calculated from the composition by weight on the basis of the density measurements of Keneshea and Cubicciotti,⁷ and is denoted *M_f*. This is a "formal" measure of solute concentration which may or may not equal the molar concentrations of the atomic, molecular, or ionic species in which the solute bismuth exists in the solution.

The absorbance *A* of a solution is defined in the usual way as log [*I*(solv)/*I*(soln)]. In practice, the absorption of the solvent and the solution were measured separately with an air reference as functions of wave length using the same cell under the same conditions. Then the absorbance of the solution was calculated by subtraction.

The data were recorded as binary numbers punched into paper tape by means of high-precision recording devices. Calculations including the above subtraction were done by a digital computer which read directly the paper-tape output of the spectrophotometer. In the recording operation, absorbance values were sampled at 1-m μ intervals.

The extinction coefficient (molar absorptivity) ϵ of a single solute species is defined in the usual way by the relation $\epsilon = A/bM$ where *A* and *M* are the absorbance and molarity, respectively, ascribed to a specified species and *b* is the path length in cm. The formal extinction coefficient ϵ_f of a solution (which may contain several species) is defined by the relation $\epsilon_f = A/bM_f$, where *A* is the experimentally measured absorbance of the solution.

It may be helpful to know that the composition in mole % of solute bismuth metal is about 8 to 10 times *M_f*. The exact relation depends, of course, on the temperature and the exact *M_f* value.

Results

The bismuth trichloride solvent was essentially transparent at wave lengths between 500 and 750 m μ but a steeply rising absorption edge occurred below 500 m μ which gave a short wave length cutoff. Figure 1 shows the position of this edge at temperatures and path lengths frequently used

(10) C. R. Boston and G. P. Smith, *ibid.*, **62**, 409 (1958).

(1) A preliminary report of this study was presented at the 137th National Meeting of the American Chemical Society, Cleveland, Ohio, April, 1960. A final report was presented at the XVIIIth International Congress of Pure and Applied Chemistry, Montreal, Canada, August, 1961.

(2) Operated for the U. S. Atomic Energy Commission by the Union Carbide Corporation.

(3) D. Cubicciotti, *J. Chem. Educ.*, **37**, 540 (1960).

(4) S. J. Yosim, A. J. Darnell, W. Gehman, and S. W. Mayer, *J. Phys. Chem.*, **63**, 230 (1959).

(5) N. H. Nachtrieb, *ibid.*, **66**, 1163 (1962).

(6) M. A. Bredig, *ibid.*, **63**, 978 (1959).

(7) T. K. Keneshea, Jr., and D. Cubicciotti, *ibid.*, **62**, 843 (1958); **63**, 1112, 1472 (1959).

(8) J. D. Corbett, *ibid.*, **62**, 1149 (1958).

(9) L. E. Topol, S. J. Yosim, and R. A. Osteryoung, *ibid.*, **66**, 1511 (1961).

in this research. From considerations of signal-to-noise ratio, it was concluded that no useful absorbance values could be determined below 400 $m\mu$. The limiting wave length for precise measurement varied between about 420 and 500 $m\mu$ depending on the conditions of measurement. With long path lengths (small M_f) at 433°, the limit for precise measurement was about 500 $m\mu$, while, with short path lengths (large M_f) at 264°, the limit was about 420 $m\mu$.

Typical spectra for different concentrations of bismuth at different temperatures are shown in Fig. 2 in terms of ϵ_f as functions of wave length. The shaded strip at 264° is a region within which lie the spectra for all solutions from 0.0141 M_f down to the lowest concentration measured, 0.0027 M_f . At low concentrations, a strong band is found. The band maximum occurs at a wave length of about 560 $m\mu$ for 264° and at a somewhat longer wave length for higher temperatures. The band is skewed toward longer wave lengths and at 433° has a slight shoulder near 610 $m\mu$ so that it may be a composite of absorptions due to more than one electronic transition. The most striking feature of the spectra is the manner in which the band diminishes with increasing M_f until it is almost indistinguishable against the background of a diffuse absorption edge which rises very slowly with shortening wave length.

Figure 3 shows the manner in which A/b varies with M_f for a wave length near the band maximum for each temperature studied. At quite low concentrations these curves are linear but beyond this brief low-concentration range the departures from linearity are very large. The linear range at 264° is defined by seven spectra with M_f values from 0.00273 through 0.0141 mole/l. of solute bismuth. The slope, which equals ϵ_f over the linear range, has a value of 5820 l./mole-cm. At 350° the linear range, with a slope of 4200, is defined, by six spectra with M_f from 0.00965 through 0.0562 mole/l. At 433° the linear range is not accurately defined.

The shaded strip in Fig. 2 for 264° includes all of those spectra which lie in the linear range of A/b vs. M_f . There is no trend with increasing M_f for the spectra within this strip. Consequently, the strip indicates the precision within which ϵ_f is known for the linear range and, likewise, the precision within which A/b vs. M_f is linear at wave lengths other than that chosen for Fig. 3. A similar shaded strip could be drawn about the lowest-concentration spectrum at the other two temperatures.

Discussion

For solutions with a single solute species, Beer's law usually is obeyed, that is, A/b is proportional to the solute concentration and the molar extinction coefficient ϵ varies with wave length but not concentration. However, for solutions of bismuth metal in fused bismuth trichloride, it is evident from Fig. 2 and 3 that Beer's law is not even approximately obeyed save at the lowest concentrations. We shall show that these very large departures from Beer's law can be accounted for in a quantitative way if one assumes that the

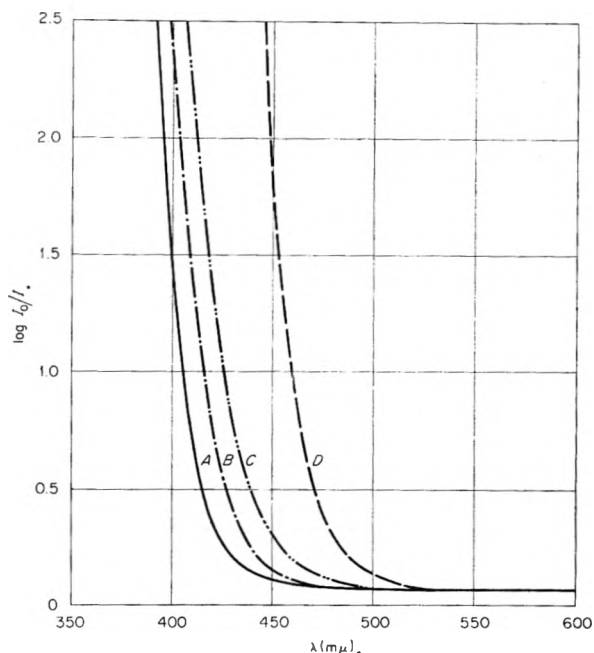


Fig. 1.—Typical absorption spectra of pure molten BiCl_3 plus the silica cell. Spectra A, B, and C are for a path length of 0.00276 cm. and temperatures of 264, 350, and 433°, respectively. Spectrum D is for a path length of 0.0501 cm. and a temperature of 350°.

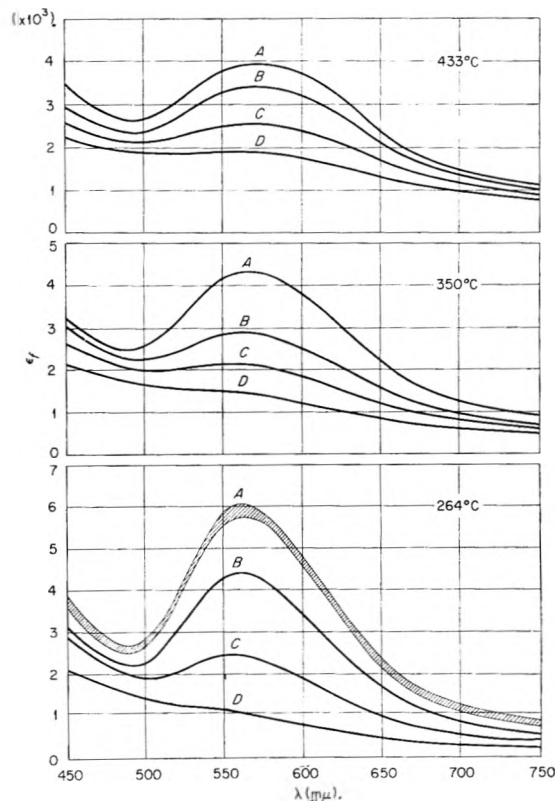


Fig. 2.—Typical spectra of molten Bi-BiCl_3 mixtures in terms of ϵ_f vs. λ with M_f values as follows: at 264°, A = 0.0027 to 0.0141, B = 0.0341, C = 0.113, and D = 0.696; at 350°, A = 0.0485, B = 0.148, C = 0.280, and D = 0.679; and at 433°, A = 0.0099, B = 0.106, C = 0.213, and D = 0.464.

solute bismuth metal is partitioned between two solute species each of which individually obeys

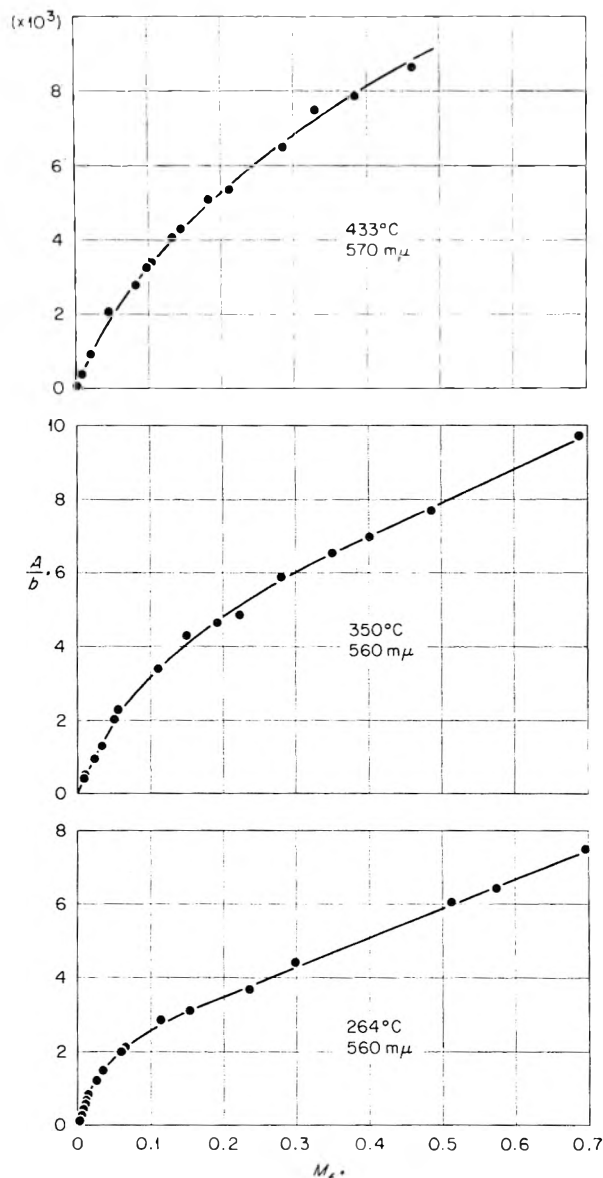


Fig. 3.—Beer's law plots for all values of M_t and for A/b near the band maximum. At 264 and 350°, A/b was determined at 560 $m\mu$ while at 433° A/b was determined at 570 $m\mu$.

Beer's law, that is, a two-species solution with additive absorbances. Since we have no *a priori* way of knowing the molar extinction coefficients of these postulated species, we shall recast the phenomenological law of additive absorbances into a form which does not contain these coefficients.

Let us suppose that the solute bismuth dissolves in or reacts with the fused bismuth trichloride solvent to form two molecular species X_n and X_m . Conservation of mass requires that

$$M_t = D_n M_n + D_m M_m \quad (1)$$

where M_n and M_m are, respectively, the molar concentrations of X_n and X_m , and where D_n and D_m are the numbers of moles of solute bismuth required to form one mole, respectively, of X_n and of X_m . The law of additive absorbances may be written

$$A/b = \epsilon_t M_t = \epsilon_n M_n + \epsilon_m M_m \quad (2)$$

where ϵ_n and ϵ_m are the molar extinction coefficients

of X_n and X_m . At a given temperature, the quantities A and ϵ_t are, of course, functions of wave length and concentration while ϵ_n and ϵ_m are functions of wave length alone. Equations 1 and 2 may be combined to eliminate one concentration variable.

Inasmuch as we have no direct way of measuring separately the two terms on the right-hand side of eq. 2, we shall recast this equation into a form in which ϵ_n and ϵ_m are replaced by the formal extinction coefficients ϵ_f of two solutions which we can measure and which we shall call "reference" solutions. In choosing reference solutions we require only that the algebraic difference between their formal extinction coefficients be significantly larger than experimental errors over most of the wave length range.

Designate quantities pertaining to the two reference solutions by the subscripts 1 and 2 and quantities pertaining to any other solution by the subscript 0. From eq. 2 we have

$$(A/b)_0 = M_{t0}\epsilon_{f0} = M_{n0}\epsilon_{n0} + M_{m0}\epsilon_{m0} \quad (3a)$$

$$(A/b)_1 = M_{t1}\epsilon_{f1} = M_{n1}\epsilon_{n1} + M_{m1}\epsilon_{m1} \quad (3b)$$

$$(A/b)_2 = M_{t2}\epsilon_{f2} = M_{n2}\epsilon_{n2} + M_{m2}\epsilon_{m2} \quad (3c)$$

Define two parameters γ and δ by the equations

$$M_{n0} = \gamma M_{n1} + \delta M_{n2} \quad (4a)$$

$$M_{m0} = \gamma M_{m1} + \delta M_{m2} \quad (4b)$$

Algebraic manipulation of eq. 3 and 4 leads to

$$(A/b)_0 = M_{t0}\epsilon_{f0} = \gamma M_{t1}\epsilon_{f1} + \delta M_{t2}\epsilon_{f2} \quad (5)$$

Using eq. 1 and 4, the parameter δ may be eliminated by the relation

$$\delta = (M_{t0}/M_{t2}) - \gamma(M_{t1}/M_{t2}) \quad (6)$$

The parameter γ may be expressed in terms of concentration variables by solving eq. 4 to give

$$\gamma = (M_{m0}M_{n2} - M_{n0}M_{m2}) / (M_{m1}M_{n2} - M_{n1}M_{m2}) \quad (7)$$

Upon substituting eq. 6 and 7 into eq. 5 and rearranging, we obtain

$$(\epsilon_{f0} - \epsilon_{f2}) = (\epsilon_{f1} - \epsilon_{f2}) \gamma M_{t1}/M_{t0} \quad (8)$$

Equation 8 may be somewhat generalized to give

$$(\epsilon_{f0} - \epsilon_{f1}) = (\epsilon_{f2} - \epsilon_{f3}) \gamma_{021} \gamma_{132} M_{t2} M_{t3} / (M_{t0} M_{t1}) \quad (9)$$

where the subscripts 0, 1, 2, and 3 designate any four solutions, none of which need be regarded as references, and where

$$\gamma_{ijk} = (M_{mi}M_{nk} - M_{ni}M_{mk}) / (M_{mj}M_{nk} - M_{nj}M_{mk}) \quad (10)$$

We shall generally use these equations in the logarithmic forms

$$\log(\epsilon_{f0} - \epsilon_{f2}) = \log(\epsilon_{f1} - \epsilon_{f2}) + \log(\gamma M_{t1}/M_{t0}) \quad (11)$$

$$\log(\epsilon_{f0} - \epsilon_{f1}) = \log(\epsilon_{f2} - \epsilon_{f3}) + \log \zeta \quad (12)$$

where ζ is the collection of concentration terms in eq. 9.

Equations 8, 9, 11, and 12 are alternative descriptions of the behavior of an isothermal family of spectra of solutions of two light-absorbing species in equilibrium which obey the law of additive absorbances. They will be referred to as the two-species model. In principle, ϵ_n/D_n and ϵ_m/D_m constitute the envelopes or extremes of an isothermal family, and all possible spectra of mixtures, that is, all ϵ_t , lie intermediate to these extremes.

There are two simple properties of the two-species model which may be deduced from the

above equations and which serve as tests of the compliance of real solutions. First, if two spectra intersect at any point in the $\epsilon_f - \lambda$ plane, then all spectra intersect at this same point. This is the familiar isosbestic point which has long been used as a test of the two-species model. Unfortunately, the spectral range in our measurements is not wide enough to include an isosbestic point. Second, according to eq. 12 $\log(\epsilon_{fi} - \epsilon_{fj})$ is, to within an additive constant, an invariant function of wave length for every pair of spectra, ϵ_{fi} and ϵ_{fj} . This function is singular at isosbestic points and, hence, is of no practical value for wave length regions where the ϵ_f curves come close together. For this reason, the above two properties are complementary tests of compliance. In the research described here, there are no isosbestic points and, hence, this conventional test is of no aid. For this reason, the second test was developed.

The extent to which the above compliance tests are unique for the two-species model may be ascertained by examining the N -species model. The above procedure for deriving the two-species model is easily generalized for N species in terms of N -reference solutions and gives

$$(A/b)_0 = M_{i0}\epsilon_{i0} = \sum_{j=1}^N \gamma_j M_{ij}\epsilon_{ij} \quad (13)$$

where M_{ij} and ϵ_{ij} are the M_i and ϵ_f of the j -th reference solution and γ_j is one of N parameters which are functions of the concentrations of the N species. Any one and only one γ_j may be eliminated by the relation

$$M_{i0} = \sum_{j=1}^n \gamma_j M_{ij} \quad (14)$$

By substituting the conditions of the compliance tests for the two-species model (for example, $\epsilon_{f1} = \epsilon_{f2} = \dots = \epsilon_{fn}$ at an isosbestic point) into eq. 13 and combining with eq. 14, it may be shown that the multispecies models ($N > 2$) will not, in general, accord with these tests and that an "accidental" accord is possible only for certain unique situations. The situations which give $\log(\epsilon_{fi} - \epsilon_{fj})$ an invariant shape for N greater than two are sufficiently unique so that we regard them as implausible.

It may be worth noting that the equations derived above apply to any solution of two solutes which are in equilibrium or which may be derived in principle from a common substance.

The experimental spectra at each temperature were tested by computing $\log(\epsilon_{fi} - \epsilon_{fj})$ over the full wave length range for many pairs of ϵ_f functions, and then verifying that the shapes of the resultant curves were essentially the same.

Conclusion

The data presented here provide substantial evidence that, in dilute solutions of bismuth metal in fused BiCl_3 , the solute exists as two light-absorbing species.

Acknowledgment.—The authors are indebted to Dr. L. C. Howick, University of Arkansas, who assisted with evaluating the computer results, to Mr. W. M. Ewing who assisted in experimental phases of the research, to Mr. D. E. LaValle who supplied the bismuth trichloride, and to Dr. M. A. Bredig who encouraged this research in many ways.

COMPOUND REPETITION IN OXIDE-OXIDE INTERACTIONS: THE SYSTEM $\text{Li}_2\text{O}-\text{V}_2\text{O}_5$

BY ARNOLD REISMAN AND JOAN MINEO

T. J. Watson Research Center of International Business Machines, Yorktown Heights, N. Y.

Received February 2, 1962

Previous work on compound repetition in oxide-oxide interactions has been extended with studies of the system $\text{Li}_2\text{O}-\text{V}_2\text{O}_5$. It has been found that crystallization from the melt occurs metastably in the high vanadium pentoxide portions of the system with the resultant exclusion of a stable phase, $2\text{Na}_2\text{O}\cdot 17\text{V}_2\text{O}_5$, which melts incongruently at 621° . The phase $2\text{Na}_2\text{O}\cdot 5\text{V}_2\text{O}_5$ has been found to melt congruently at 603° in the metastable equilibria and incongruently at 601° in the stable solid-liquid equilibria. A compound having the composition $\text{Na}_2\text{O}\cdot \text{V}_2\text{O}_5$ melts incongruently at 616° , while another compound having the composition $3\text{Na}_2\text{O}\cdot \text{V}_2\text{O}_5$ melts congruently at 1152° . This phase exhibits three crystallographic inversions, at 724 , 773 , and 1152° . The results of the present work are compared with other reported data on the system $\text{Li}_2\text{O}-\text{V}_2\text{O}_5$ and are used as a basis for prediction of compound repetition in the system $\text{Na}_2\text{O}-\text{V}_2\text{O}_5$.

Introduction

The topic of compound repetition in oxide systems has been the subject of previous reports.¹⁻³ Studies of the system $\text{Li}_2\text{O}-\text{V}_2\text{O}_5$, together with future work on other alkali vanadates, are intended to provide further data on which to evaluate the ideas discussed previously.¹

Based on the results of an incomplete examina-

tion of the solid-liquid equilibria in the system $\text{Li}_2\text{O}-\text{V}_2\text{O}_5$, Canneri⁴ concluded the existence of two lithium vanadates, $\text{Li}_2\text{O}\cdot \text{V}_2\text{O}_5$ and $2\text{Li}_2\text{O}\cdot \text{V}_2\text{O}_5$. More recently, Kohlmuller and Martin,⁵ employing differential thermal, X-ray, and dilatometric techniques, detected three compounds in the system. These were identified as the 1:3, 1:1, and 3:1 salts, the latter exhibiting two phase inversions.

Although the discrepancies evident in the above

(1) A. Reisman, *J. Phys. Chem.*, **66**, 15 (1962).

(2) A. Reisman and J. Mineo, *ibid.*, **65**, 996 (1961).

(3) A. Reisman and F. Holtzberg, *ibid.*, **64**, 748 (1960); *J. Am. Chem. Soc.*, **80**, 6503 (1958).

(4) G. Canneri, *Gazz. chim. ital.*, **58**, 6 (1928).

(5) R. Kohlmuller and J. Martin, *Bull. soc. chim. France*, **4**, 748 (1961).

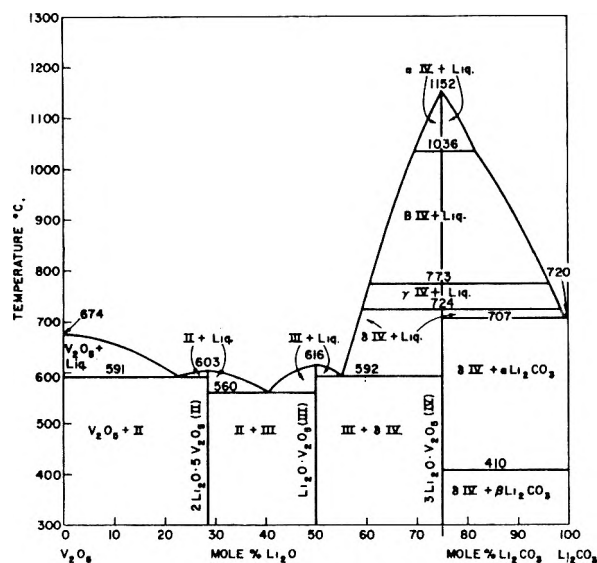


Fig. 1.—The metastable system $\text{Li}_2\text{O}-\text{V}_2\text{O}_5$.

would have, for our purposes, necessitated an independent evaluation, such was actually completed concurrently with publication of the later report. Consequently, both investigations represent essentially concomitant re-appraisals of Canneri's effort. While there are a number of points of agreement among the data obtained in the three investigations, there also exist a number of notable differences.

Experimental Procedure

Differential thermal, powder density, and X-ray analyses were conducted in manners similar to those described in earlier papers.^{3,6-8} Thermal characterizations were effected with heating and cooling analyses. Samples for heating analyses were prepared by first making them molten and then heat treating them at 575° several times. In addition, each cooling curve sample was subjected to a heating study without any further heat equilibration. Heating data derived from each of these kinds of sample were different as will be described below. Cooling studies were conducted on samples reacted and made molten in the DTA apparatus as well as on the solid state heat treated samples after being made molten. Melts were seeded with material obtained from preruns or with heat treated material and were stirred with an oxygen stream.^{6,9}

All experimental samples were examined with X-rays using the Debye Scherrer technique, and density studies were conducted on the heat treated reaction mixtures.

The reagents Li_2CO_3 and V_2O_5 were similar to those described previously.^{6,10}

Experimental Results

A. The System $\text{Li}_2\text{O}-\text{V}_2\text{O}_5$. 1. **DTA Analysis.**—Table I presents data obtained from cooling and heating traces, respectively, on the same samples. Liquidus points were acquired only from cooling curves for obvious reasons, while invariant temperatures were established in both cooling and heating studies. After a complete temperature cycle, the thermocouple and stirring assembly were extracted to just above the melt.

(6) F. Holtzberg, A. Reisman, M. Berry, and M. Berkenblit, *J. Am. Chem. Soc.*, **78**, 1536 (1956).

(7) F. Holtzberg, A. Reisman, M. Berry, and M. Berkenblit, *ibid.*, **79**, 2039 (1957).

(8) A. Reisman, F. Holtzberg, M. Berkenblit, and M. Berry, *ibid.*, **78**, 4514 (1956).

(9) A. Reisman and F. Holtzberg, *ibid.*, **77**, 2112 (1955).

(10) A. Reisman, *ibid.*, **80**, 3558 (1958).

TABLE I

THERMAL AND X-RAY DATA OBTAINED FROM COOLING ANALYSIS SAMPLES IN THE SYSTEM $\text{Li}_2\text{O}-\text{V}_2\text{O}_5$

Mole % V_2O_5	Liquidus	Solidus	Transition	Phase detected with X-rays
100	674	674		V_2O_5
97.5	669	586		$\text{V}_2\text{O}_5 + \text{II}$
95.0	666	586		$\text{V}_2\text{O}_5 + \text{II}$
92.5	657	587		$\text{V}_2\text{O}_5 + \text{II}$
90.0	649	595		$\text{V}_2\text{O}_5 + \text{II}$
87.5	644	592		$\text{V}_2\text{O}_5 + \text{II}$
85.0	635	592		$\text{V}_2\text{O}_5 + \text{II}$
80.0	609	594		$\text{V}_2\text{O}_5 + \text{II}$
77.5	595	595		$\text{V}_2\text{O}_5 + \text{II}$
75.0	597	..		$\text{V}_2\text{O}_5 + \text{II}$
74.0	601	..		$\text{V}_2\text{O}_5 + \text{II}$
73.0	603	..		$\text{V}_2\text{O}_5 + \text{II}$
72.5	603	..		$\text{V}_2\text{O}_5 + \text{II}$
71.43	603	..		II
70.0	600	556		II + III
65.0	589	549		II + III
60.0	567	559	eutectic lies in this interval	II + III
57.5	582	560		II + III
55.0	598	552		II + III
52.5	610	536		II + III
50.0	616	616		III
47.5	610	591		III + δ IV
45.0	596	596		III + δ IV
42.5	652	591		III + δ IV
40.0	735	598	713	III + δ IV
37.5	813	594	716	III + δ IV
35.0	900	588	718 776	III + δ IV
32.5	977	595	714 767	III + δ IV
30.0	1042	591	719 775	III + δ IV
27.5	1091	590	716 774 1032	III + δ IV
26.0		582	719 774 1036	III + δ IV
25.0	1152	1152	728 772 1036	δ IV
24.0		700	728 773 1041	δ IV + β Li_2CO_3
22.5	1132	709	727 776 1036	δ IV + β Li_2CO_3
20.0	1068	707	732 772	407 δ IV + β Li_2CO_3
15.0	988	713	732 774	405 δ IV + β Li_2CO_3
10.0	993	706	774	409 δ IV + β Li_2CO_3
5.0	803	708		410 δ IV + β Li_2CO_3
2.5	749	704	eutectic lies in this interval	410 δ IV + β Li_2CO_3
0	720	720		410 β Li_2CO_3

The sample then was cooled with seeding through the final freezing temperature. X-Ray data obtained from the cooled samples are given in Table I. A few samples were obtained from the crucibles directly after the initial solidification cycle. These gave X-ray data consistent with those shown in Table I. Figure 1 is a graphical interpretation of Table I, and is seen to consist of two separate portions. The region 100–25 mole % V_2O_5 is representative of the system $\text{Li}_2\text{O}-\text{V}_2\text{O}_5$, excepting for the absence of the region $3\text{Li}_2\text{O} \cdot \text{V}_2\text{O}_5-\text{Li}_2\text{O}$. The region from 25–0 mole % V_2O_5 comprises the entire composition interval in which Li_2CO_3 is a pseudo binary component under one atmosphere air pressure. This interval may be depicted as the system $3\text{Li}_2\text{O} \cdot \text{V}_2\text{O}_5-\text{Li}_2\text{CO}_3$ on an appropriate scale.

As seen from Fig. 1, the liquidus for primary crystallization of V_2O_5 is depressed from the latter's melting point till 591°, where it terminates in a eutectic. This composition was established at approximately 77.5 mole % V_2O_5 . A new solubility curve ascends from this point to a maximum at 603°, and approximately 71.5 mole % V_2O_5 . It was difficult to separate the peaks due to liquidus and solidus crystallizations in this region because of the small temperature interval between the two, and the small latent heat associated with the

eutectic melting as the compound location is approached. X-Ray traces revealed the presence of V_2O_5 in the 72.5 mole % sample, no V_2O_5 in the 71.4 mole % sample, and the appearance of a new phase in the 70 mole % sample. Consistent with these data, compound II was assigned the composition $2\text{Li}_2\text{O}\cdot 5\text{V}_2\text{O}_5$ (compound I not seen in Fig. 1 is yet to be discussed). From this congruent melting point, the liquidus is depressed by further addition of Li_2O until another triple point is realized at approximately 59 mole % V_2O_5 and 560° . Ascending from this point the liquidus terminates in a maximum at 50 mole % and 616° . X-Ray analyses revealed the presence of $2\text{Li}_2\text{O}\cdot 5\text{V}_2\text{O}_5$ up to the 47.5 mole % sample and the first appearance of another phase at 52.5 mole %, both in addition to the intense pattern of compound III which was observed pure at 50 mole %. Based on these data, III has the composition $\text{Li}_2\text{O}\cdot \text{V}_2\text{O}_5$. In the region 50–25 mole % V_2O_5 another eutectic intersection develops at approximately 45 mole % and 592° and a final maximum is in evidence at 25 mole % and 1152° . These and the relevant X-ray data indicate that IV is $3\text{Li}_2\text{O}\cdot \text{V}_2\text{O}_5$. Thermal examination of this phase revealed three distinct anomalies, at 724, 773, and 1036° . These effects, detected in the two-phase fields of compound IV, were largest at 25 mole % V_2O_5 and apparently represent crystallographic inversions.

The system $3\text{Li}_2\text{O}\cdot \text{V}_2\text{O}_5-\text{Li}_2\text{CO}_3$ is of the simple eutectic variety with the triple point lying at approximately 1 mole % V_2O_5 and 707° on the scale employed. A thermal anomaly was detected in this system at 410° . This effect was largest in pure Li_2CO_3 and is representative of an inversion in the carbonate.¹⁰

2. Density, X-Ray, and Thermal Analysis of Heat Treated Samples.—In attempting to more precisely define the composition of compound II using powder density techniques,³ samples were prepared as follows: Reaction mixtures were made molten, quenched in liquid nitrogen, and ground. They then were heat treated in air for three 24-hr. intervals at 575° with intermediate air quenching and grinding. X-Ray analysis in the region 100–70 mole % V_2O_5 showed the presence of three solid phases, V_2O_5 , compound II, and an unknown phase. Since these data indicated that equilibrium had not been attained, a second set of samples was prepared in the identical fashion excepting for a final six-day heat treatment at 575° followed by grinding in a drybox. X-Ray analyses then revealed the presence of two two-phase regions in this same composition interval. Table II presents the results of density and X-ray studies on these samples and the former are graphed in Fig. 2. It is seen that in addition to the expected density discontinuity at 71.4 mole % V_2O_5 ($2\text{Li}_2\text{O}\cdot 5\text{V}_2\text{O}_5$), a second discontinuity occurs at 89.5 mole % ($2\text{Li}_2\text{O}\cdot 17\text{V}_2\text{O}_5$). X-Ray examinations of the DTA cooling curve samples subsequent to a heat treatment for one week at 575° gave data in agreement with those of Table II. These observations, indicating that the results depicted in Figure 1 represent a metastable equilibrium in the region from 100–71.4 mole % V_2O_5 , led to attempts at inducing nucleation of the

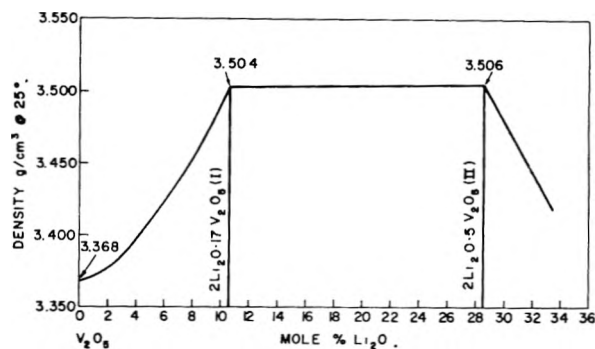


Fig. 2.—Density diagram for the stable system $\text{Li}_2\text{O}-\text{V}_2\text{O}_5$.

stable phases from the melt by seeding with equilibrated material. The data obtained in cooling analysis, however, were identical with those of Table I. Heating analyses then were conducted on the equilibrated samples used for density analyses and these yielded the solidus and/or the peritectic data listed in Table III. After being made molten, these samples again gave cooling and X-ray data in agreement with those of Table I.

TABLE II
DENSITY AND X-RAY DATA FOR THE SYSTEM $\text{Li}_2\text{O}-\text{V}_2\text{O}_5$
FROM SOLID STATE REACTED SAMPLES

Mole % V_2O_5	Density, g./cm. ³ at 25°	Phases detected with X-rays
100	3.368 ± 0.0005 ^a	V_2O_5
97.5	3.380 ± 0.003 ^a	$\text{V}_2\text{O}_5 + \text{I}$
95.0	3.419 ± 0.0025 ^a	$\text{V}_2\text{O}_5 + \text{I}$
92.5	3.445 ± 0.003 ^a	$\text{V}_2\text{O}_5 + \text{I}$
91.0	3.474	$\text{V}_2\text{O}_5 + \text{I}$
90.0	3.491 ± 0.001 ^a	I
89.0	3.503 ± 0.0035 ^a	I
87.5	3.502 ± 0.0005 ^a	I + II
85.0	3.503 ± 0.001 ^a	I + II
82.5	3.499 ± 0.0045 ^a	I + II
80.0	3.505 ± 0.0035 ^b	I + II
77.5	3.504 ± 0.002 ^a	I + II
76.0	3.506 ± 0.002 ^a	I + II
75.0	3.504 ± 0.003 ^a	I + II
74.0	3.505 ± 0.002 ^a	I + II
72.5	3.506 ± 0.002 ^a	I + II
71.0	3.500	II
70.0	3.483	II + III
69.0	3.468	II + III
68.0	3.445	II + III

^a 2 determinations. ^b 3 determinations.

From Table III it is seen that halts were detected at around 621° in the composition interval $\text{V}_2\text{O}_5-2\text{Li}_2\text{O}\cdot 17\text{V}_2\text{O}_5$ and at about 601° in the interval $2\text{Li}_2\text{O}\cdot 17\text{V}_2\text{O}_5-2\text{Li}_2\text{O}\cdot 5\text{V}_2\text{O}_5$. As required thermodynamically, both of these invariant temperatures lie above those for the metastable solubility curve intersection at 591° in the system $\text{V}_2\text{O}_5-2\text{Li}_2\text{O}\cdot 5\text{V}_2\text{O}_5$. Although no liquidus data could be derived from the heating analysis, the congruency or incongruency of melting of the 2:17 and 2:5 phases was deduced from the heating data. The 2:17 ratio, ca. 89.5 mole % V_2O_5 , if congruently melting, should not exhibit either a 621° or 601° thermal anomaly. The data, however, showed the 621° thermal anomaly reaching a maximum at between 90 and 89 mole % V_2O_5 . In addition, both the 621°

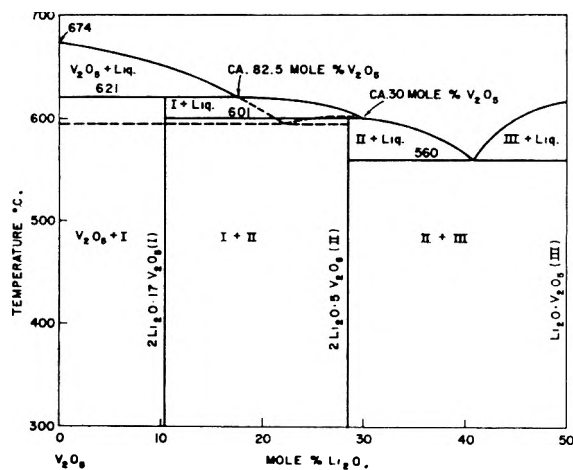


Fig. 3.—The stable system $\text{Li}_2\text{O}-\text{V}_2\text{O}_5$.

and 601° anomalies were in evidence at 89 mole % V_2O_5 , the latter heat effect being much smaller than at higher Li_2O compositions. Consequently, it is evident that the 2:17 phase is incongruently melting. The extent of the incongruity is rather large since the 621° effect is observed to 82.5 mole %. Employing similar reasoning, it is concluded that the 2:5 compound, 71.4 mole %, also melts incongruently, since the 601 and 560° effects were simultaneously present in the heating trace for the 70 mole % sample. The first of these was large and the second small. The extent of incongruity for this compound must be small, since at 69 mole % the 601° effect is no longer in evidence.

TABLE III

HEATING DATA ON SOLID STATE REACTED SAMPLES IN THE SYSTEM $\text{Li}_2\text{O}-\text{V}_2\text{O}_5$

Mole % V_2O_5	Transition	Eutectic
97.5	622	
95.0	617	
92.5	620	
91.0	624	
90.0	618	
89.0	625	
87.5	621 597	
85.0	627 600	
82.5	625 601	
80.0	597	
77.5	604	
76.0	597	
75.0	604	
74.0	605	
72.5	602	
71.4	602	
70.0	600	554
69.0	..	562
68.0	..	567

Based on all of the above, Fig. 3 depicts the proposed equilibrium diagram in the range 100–50 mole % V_2O_5 , Fig. 1 representing the equilibrium fields in the remaining composition interval.

3. "Spitting" in Lithium Vanadate Melts.—Canneri observed that the solidifications of high vanadium pentoxide content samples are attended by eruptive gas evolutions which he termed "spitting." These evolutions were attributed by him to

a reduction of the pentoxide. Because of similar observations, an oxygen stirring stream was utilized during the cooling analyses in the present investigation.⁶ Kohlmuller and Martin also made use of this technique. Since there was some concern that the present conclusions relating to metastability might be attributable to a reduction phenomenon, the following experiments were performed. A sample containing 89.5 mole % V_2O_5 + 10.5 mole % Li_2CO_3 in a platinum crucible was placed in a quartz envelope. The latter was connected to a vacuum pump and the sample reacted and was made molten *in vacuo*. X-Ray analysis of the cooled sample revealed a mixture of V_2O_5 + $2\text{Li}_2\text{O}\cdot 5\text{V}_2\text{O}_5$. The sample was ground, then heat treated *in vacuo* for 48 hr. at 575° . X-Ray analysis then showed a partial conversion to the equilibrium state in that a mixture of V_2O_5 , $2\text{Li}_2\text{O}\cdot 17\text{V}_2\text{O}_5$, and $2\text{Li}_2\text{O}\cdot 5\text{V}_2\text{O}_5$ were simultaneously detected. Further treatment showed increasing conversion. At this point, the sample was made molten *in vacuo* and again analyzed. As initially, only the metastable mixture for this composition was detected. These observations on a sample cycled from metastable toward stable back to metastable states *in vacuo* make it highly improbable that the metastability is related to a reduction phenomenon.

A second sample, having the composition $2\text{Li}_2\text{O}\cdot 17\text{V}_2\text{O}_5$, reacted in the solid state at 575° in air for a sufficient length of time to form the stable phase. It was observed *via* X-ray analyses that even in a solid state reaction process, the metastable state formed first, followed by gradual conversion to the stable state. The equilibrium phase then was examined in air in the simultaneous DTA-TGA apparatus described previously¹¹ at heating and cooling rates of $2^\circ/\text{min}$. Attendant with the melting process, the sample weighing 1.5 g. gained ca. 6 mg. Upon cooling and freezing, 2–3 mg. of this weight was lost and upon remelting, 2–3 mg. was picked up again. Several further repeats showed weight losses of from 1–4 mg. upon freezing and corresponding weight gains upon melting. These data strongly suggest that the phenomenon which Canneri believed to be a manifestation of reduction is really due to expulsion of gases dissolved in the melting process. Since the melts form lava-like crusts upon freezing, it is not unexpected that the weight gain and loss data observed in consecutive recycling show variability, these values depending upon the amount of dissolved gases trapped in the frozen mass. The significant feature of the above, however, is the initial weight gain attendant with the first melting. A more thorough study will be conducted *in vacuo* and a controlled atmosphere DTA-TGA apparatus presently under construction.

B. Discussion of the System $\text{Li}_2\text{O}-\text{V}_2\text{O}_5$.—In the 100–50 mole % V_2O_5 region, there is reasonable agreement between the thermal data obtained by us and Canneri, although the interpretations are different. He found a eutectic at ca. 59 mole % V_2O_5 and 569° which he depicted as the solubility arm intersections of the system $\text{V}_2\text{O}_5-\text{Li}_2\text{O}\cdot\text{V}_2\text{O}_5$. From Fig. 1, it is seen that this triple point, 560°

(11) A. Reisman, *Anal. Chem.*, **32**, 1566 (1960).

and 59 mole % V_2O_5 , occurs in the system $2Li_2O \cdot 5V_2O_5 - V_2O_5 - V_2O_5$. Canneri's reported melting point for the metavanadate, 618° , is in excellent agreement with our value of 616° . Canneri did not, however, detect the 2:17 or 2:5 salts. In the composition interval from 50–25 mole % V_2O_5 , there is again fair agreement of thermal data but little agreement in interpretation. Canneri shows a eutectic at 575° and 35.5 mole % V_2O_5 which is probably the same one we found at 592° and 35 mole %. Extrapolation of his eutectic halt data to zero halt led him to believe that this triple point existed in the system $Li_2O \cdot V_2O_5 - 2Li_2O \cdot V_2O_5$, whereas our data indicate that the system in question is $Li_2O \cdot V_2O_5 - 3Li_2O \cdot V_2O_5$.

There is somewhat better agreement between the present work and that of Kohlmuller and Martin, ignoring the question of metastability for the moment. They find a eutectic at 594° and 79 mole %, in good agreement with our values of 591° and 77.5 mole % V_2O_5 , Fig. 1. Kohlmuller and Martin concluded, however, that this triple point occurs in the system $V_2O_5 - Li_2O \cdot 3V_2O_5$ rather than in the system (metastable) $V_2O_5 - 2Li_2O \cdot 5V_2O_5$. Considering the rather large discrepancy in composition for this phase, its melting point is not in disagreement; 601° reported by the French authors and 603° found here. They also report a eutectic at 67 mole % V_2O_5 and 560° , in good agreement with our values of 69 mole % and 560° . Their reported melting point for the metavanadate, 624° , is not, however, in good agreement with the values given by Canneri and us, since it appears outside the range of expected error, *ca.* $\pm 3^\circ$. One further eutectic is reported by Kohlmuller and Martin, at 46 mole % V_2O_5 and 596° , in good agreement with the presently reported values of 45 mole % and 592° .

They give a melting point for $3Li_2O \cdot V_2O_5$ of 1154° and phase transformations at 662° and 730° . While the melting point determined by us, 1152° , agrees well with their value, the number of and temperatures for the phase inversions do not. We detected an anomaly at 724° which might be correlated with their 730° heat effect, but did not detect one around 662° . Two others were observed, however, at 773° and 1036° . No explanation can be offered for these discrepancies. As for

the failure by previous workers to detect the 2:17 salt, it is to be pointed out that it was not detected by us either in cooling studies, its presence being observed only fortuitously in the process of preparing samples for density analyses.

C. Some Comments on Compound Repetition.—If the working hypothesis on compound repetition in oxide-oxide interactions¹⁻³ has general validity, then the system $Na_2O - V_2O_5$ should definitely contain the compound $2Na_2O \cdot 5V_2O_5$. This phase should melt incongruently and exhibit a greater submergence of its liquidus field than does the corresponding lithium analog. It is not unlikely, based on the slight field submergence evidenced by the lithium salt, that a phase with the same stoichiometry should occur in the system $K_2O - V_2O_5$ with a greatly submerged field. In our previous work on the latter system,⁶ where conventional thermal analysis techniques were employed together with rather cursory X-ray analysis (X-ray studies were conducted only at apparent compound locations), no such phase was detected. This possible omission indicates a re-investigation of the potassium system is warranted, and such is contemplated.

The occurrence of congruently melting 1:1 compounds in both the lithium and potassium systems requires the existence of a congruently melting sodium analog. A similar consideration applies to the occurrence of a congruently melting 3:1 sodium salt. The 2:15 lithium compound presents something of an enigma. While it exhibits a fairly submerged liquidus field, its deduced liquidus curve is not coincident with that for V_2O_5 . This would indicate the possibility of a repetition in the next higher weight system. In the previous work on tantalate systems, however, it has been found that difficulty in generating a stable phase is accompanied by failure of that ratio to repeat in the next higher system. Furthermore, compounds having such high proportions of one component to the other have not been found to repeat to any great extent even when not attended by difficulty in forming them. Based on the above, the occurrence of a 2:15 sodium salt does not appear likely. Certainly no stable potassium analog is to be expected.

NOTES

SURFACE CARBONIUM IONS PRODUCED BY IRRADIATING SILICA GEL

BY HAROLD W. KOHN

Chemistry Division, Oak Ridge National Laboratory, Operated by Union Carbide Corporation for the U. S. Atomic Energy Commission, Oak Ridge, Tenn.

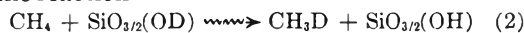
Received December 23, 1961

Recent experiments at this Laboratory have shown that the radiation-induced reactions between hydrogen or methane and well-degassed deuterated

silica gel give relatively large yields of deuterated products. These yields are, depending on pre-treatment of the gel, in the neighborhood of 3 to 5 molecules per 100 e.v. absorbed by the gel for the reaction



and from 0.6 to 1.5 molecules per 100 e.v. absorbed for the reaction¹



(1) H. W. Kohn, *J. Phys. Chem.*, **66**, 1017 (1962).

TABLE I
 COLORS OF ADSORBED COMPOUNDS

Adsorbate	Adsorbed on cracking catalyst	Adsorbed on silica gel and irradiated	Remarks (irradiated samples)
Benzene	Very faint yellow	Not observable	
Phenylmethane	Yellow-pink	Not observable	
Diphenylmethane	Light yellow	Orange and chartreuse	Fades quickly
Triphenylmethane	Bright yellow	Bright yellow	Very stable, 25°
Naphthalene	Pink	Pink	Very stable, 25°
Anthracene	Green	Chartreuse	
Phenanthrene	Blue-gray	Chartreuse	Extensive decomposition
1,1-Diphenylethylene	Chartreuse	Yellow	
Triphenylethylene	Green and brown	Brown and yellow	Extensive decomposition
<i>o</i> -Terphenyl	Turquoise	Turquoise	Fades quickly
<i>m</i> -Terphenyl	Pink	Deep yellow	
<i>p</i> -Terphenyl	Blue-purple	Deep yellow	
<i>p</i> -Quaterphenyl	Buff-orange	Buff-orange	Very stable, 25°
Wurster's blue	Blue	Blue-purple	Very stable, 25°
Biphenyl	Red	Blue-green	Not changed on irradiation
Diphenyl ether	Pink	Pale blue	Fades quickly
Triphenylene	Blue-gray	Blue-gray	

This research demonstrated that these reactions are initiated on the gel surface. Speculation about the mechanism of such reactions led us to the conclusion that the reactive intermediates produced by the radiation probably were ionic in nature. A recent report on the observation of stable surface carbonium ions² prompted us to perform some experiments which indicate that positive ions in the gel formed during the irradiation of silica gel can transfer their charge to adsorbed species, thus leading to stable carbonium ions.

Silica gel and silica-alumina cracking catalysts previously degassed at $520 \pm 10^\circ$ were used as adsorbents. Samples were prepared in pairs using 10 g. of each adsorbent for one member. After the adsorbent had cooled, 100 to 200 mg. of organic adsorbate was distilled from a side-arm onto the adsorbent. In all cases the silica-alumina immediately assumed a definite color, probably characteristic of the carbonium ion formed,³⁻⁵ whereas the silica gel became only a faint off-white.⁶ The silica gel plus organic adsorbate samples then was irradiated for about an hour at -78° in a 600-curie Co⁶⁰ γ source (about 2×10^5 r.). Many irradiated gels plus organic adsorbate samples became the color of their unirradiated silica-alumina counterparts (Table I). On the basis of stability and identical color, several samples (*viz.*, triphenylmethane, naphthalene, *p*-quaterphenyl) when irradiated on silica gel obviously formed the same species as those formed by adsorption on silica-alumina. The similarity in color for others (Wurster's blue, anthracene, triphenylethylene, 1,1-diphenylethylene) was very striking and the small color differences could be due to variations in dispersion, local concentration gradients, or the superimposed slight radiation coloring of the glass and gel.⁷ When diphenyl ether or biphenyl on

silica gel was irradiated, a colored species which differed from that produced by adsorption on silica-alumina was formed. Phenanthrene and triphenylethylene when adsorbed on the cracking catalyst give variable mixtures of dark colors, probably indicative of extensive decomposition. The colors observed are summarized in Table I.

No color was observed upon irradiation if the organic adsorbates were adsorbed on silica gel which was not dehydrated at an elevated temperature. This shows that the color was not due to ions formed by simply irradiating the dispersed organic material. Furthermore, unless the silica gel is dehydrated at an elevated temperature, it initiates little isotopic exchange (reactions 1 and 2). Thus adsorbed water appears to interfere with the charge-transfer process.

If a sample of properly dehydrated silica gel with adsorbed triphenylmethane is exposed to 2537 Å. ultraviolet light, an orange color characteristic of the triphenylmethyl free radical is observed. Since this orange color is noticeably different from the yellow color (characteristic of the triphenylmethylcarbonium ion) observed upon γ -irradiation, one may assume that where the color pairs are similar, the color of irradiated organic compound plus silica gel is not due to the formation of free radicals. In those sample pairs which fail to show similarities, such as diphenyl ether, different modes of carbonium ion formation such as hydride ion abstraction, proton addition, or electron abstraction might account for the color differences, or the color on the irradiated gel in these cases may be due to the presence of free radicals.

Since it is well recognized that silica alumina is a strong acid,⁸ the net effect of irradiating silica may be simply to increase its acidity. The creation of such acid sites may explain the increase of the catalytic activity of the gel upon irradiation.^{9,10}

(2) H. P. Leftin, *J. Phys. Chem.*, **64**, 1714 (1960).

(3) J. K. Fogo, *ibid.*, **65**, 1919 (1961).

(4) J. J. Rooney and R. C. Pink, *Proc. Chem. Soc.*, 70 (1961).

(5) D. M. Brouwer, *Chemistry and Industry* (London), No. 6, 77 (1961).

(6) The adsorption of biphenyl on silica gel gives an immediate red coloration.

(7) H. W. Kohn, *Nature*, **184**, 630 (1959).

(8) H. A. Benesi, *J. Phys. Chem.*, **61**, 970 (1957).

(9) H. Pines and J. Ravoire, *ibid.*, **65**, 1859 (1961).

(10) H. W. Kohn and E. H. Taylor, *ibid.*, **63**, 966 (1959).

A NEW METHOD FOR THE DETERMINATION OF SELF-ASSOCIATION CONSTANTS OF CARBOXYLIC ACIDS IN SOLUTION

BY SHERRIL D. CHRISTIAN¹ AND M. W. C. DHARMAWARDHANA

Department of Chemistry, University of Ceylon, Colombo, Ceylon

Received October 27, 1961

Graddon² has reported recently on the spectra and solubility of a series of complexes between cupric carboxylates and the corresponding carboxylic acids in benzene, chloroform, dioxane, and other organic solvents. Cryoscopic, spectral, and magnetic data^{3,4} suggest that the complexes exist in the form $\text{Cu}_2\text{A}_4(\text{HA})_2$ in non-donor solvents, where A represents the carboxylate radical. We have made use of these complexes in developing a new method for determining self-association constants of carboxylic acids in solution.

If the formation of the cupric carboxylate-carboxylic acid complex is represented by the equation⁵

Cu_2A_4 (solid) + $(\text{HA})_2$ (in soln.) = $\text{Cu}_2\text{A}_4(\text{HA})_2$ (in soln.)
the concentration of acid dimer may be related to that of the dissolved copper through the formation constant

$$K_x = [\text{Cu}]/[(\text{EA})_2]$$

From measurements of the solubility of the complex as a function of total acid concentration, it is possible to infer both K_x and equilibrium constants for association of the acid monomer to form $(\text{HA})_n$. Further, once K_x and the acid association constants are known, the solubility method may be used to study equilibria between dissolved carboxylic acid species and water or other hydrogen-bonding compounds.

We report here the results of a study of the solubility of cupric acetate in chloroform solutions of acetic acid, in the presence of sufficient water to saturate the organic phase. To avoid possible changes in carboxylic acid concentration during equilibration, we determined both the dissolved copper (spectrally, using the absorption maximum at 6800 Å.) and total acid (by titration with NaOH) after equilibrium had been attained. Since titration with strong base results in the precipitation of copper as the hydroxide, the total concentration of titrable acid in the organic phase may be expressed as⁶

$$[\text{A}^T] = [\text{HA}] + 2[(\text{HA})_2] + 6[\text{Cu}_2\text{A}_4(\text{HA})_2]$$

or

$$[\text{A}^T] = \left(\frac{[\text{Cu}]}{K_x}\right)^{1/2} + 2[\text{Cu}]/K_x + 3[\text{Cu}] \quad (1)$$

where K_2 represents the dimerization constant of

(1) Fulbright Grantee on leave of absence from Department of Chemistry, The University of Oklahoma, Norman, Oklahoma.

(2) D. P. Graddon, *J. Inorg. & Nuclear Chem.*, **17**, 222 (1961); **11**, 337 (1959); *Nature*, **186**, 715 (1960).

(3) R. L. Martin and H. Waterman, *J. Chem. Soc.*, 2545 (1957).

(4) R. L. Martin and A. Whitley, *ibid.*, 1394 (1958).

(5) The complex formation reaction is written in terms of $(\text{HA})_2$ rather than HA, since the dimer is frequently the major solute species in solutions of carboxylic acids in organic solvents.

(6) Species of order higher than dimer are neglected.

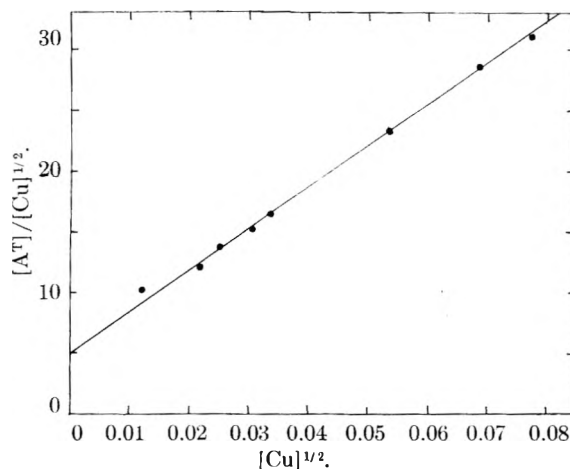


Fig. 1.—Solubility plot for the system acetic acid-chloroform-cupric acetate at 25.4°.

the acid. Actually, since the solution is saturated with water, hydration of the acid monomer and possibly the acid dimer may occur, so that $[\text{HA}]$ and $[(\text{HA})_2]$ represent the total concentrations of monomer and dimer in both the hydrated and unhydrated forms. It should be observed that due to hydration K_2 as it is used here need not be equal to the dimerization constant of the acid in anhydrous solvent.

Equation 1 may be written in the form

$$[\text{A}^T]/[\text{Cu}]^{1/2} = (K_2K_x)^{-1/2} + \left(3 + \frac{2}{K_x}\right) [\text{Cu}]^{1/2}$$

which indicates that a plot of $[\text{A}^T]/[\text{Cu}]^{1/2}$ vs. $[\text{Cu}]^{1/2}$ should be linear, with slope $3 + 2/K_x$ and intercept $(K_2K_x)^{-1/2}$. Equilibrium constants may be calculated from the relations

$$K_x = \frac{2}{\text{Slope} - 3} \text{ and } K_2 = \frac{\text{Slope} - 3}{2(\text{intercept})^2}$$

In Fig. 1, solubility data at 25.4° for the cupric acetate-acetic acid-chloroform system are plotted as indicated above. Values of the constants determined from the straight line are $K_x = 0.0060$ and $K_2 = 6.9$ l./mole. This result for K_2 agrees well with equilibrium constants obtained by Moelwyn-Hughes⁷ and Brown and Mathieson⁸ from partition data for the system water-chloroform-acetic acid. Values of K_2 calculated from their data are 7.0 and 11 l./mole, respectively, at 25°.

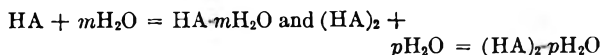
Cupric carboxylate complexes should prove extremely useful as "indicators" for the carboxylic acid dimer. The procedure applied here to the chloroform-acetic acid system leads to results entirely equivalent to those of the partition method. However, the present method may be employed with solvents that are anhydrous or contain arbitrary concentrations of water, whereas with the partition method the organic solvent must be saturated with water.

Preliminary results for the systems acetic acid-chloroform-cupric acetate and propionic acid-benzene-cupric propionate indicate that K_2 is

(7) E. A. Moelwyn-Hughes, *J. Chem. Soc.*, 850 (1940).

(8) C. P. Brown and A. R. Mathieson, *J. Phys. Chem.*, **58**, 1057 (1954).

greater for the anhydrous solvent than for the wet solvent. This implies that dissolved water forms hydrates with one or more of the acid species. A comparison of solubility data for wet and dry solvents should yield values of equilibrium constants for the hydration reactions



in various solvents. We are inclined to believe that hydration of the monomer alone is important in many alkanolic acid-organic solvent systems.

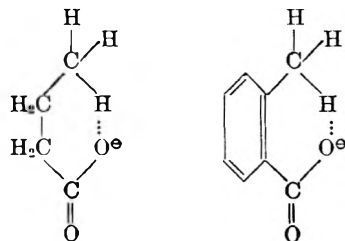
THE STRENGTH OF BUTYRIC AND *o*-TOLUIC ACIDS

By W. J. LE NOBLE, JAMES LUVALLE, AND ASA LEIFER

Department of Chemistry, State University of New York, Long Island Center, and Basic Research Laboratory, Fairchild Camera and Instrument Corporation, Syosset, New York

Received November 18, 1961

The curve of pK_a in water *vs.* chain length of the straight chain aliphatic acids has a significant minimum at butyric acid. Similarly, the acid strength of *o*-toluic acid is known to be much greater than that of the *m*- and *p*-isomers.¹ Two explanations have been advanced to account for these facts. Brown, Taylor, and Sujishi have suggested that the anomalous acid strengths are entropy effects related to a greater steric requirement for the carboxyl group than for the carboxylate²; this may make impossible certain conformations for the undissociated acids that can be accommodated in the anions. Alternatively, weak intramolecular H-bonds have been postulated^{3,4} to account for the facts



In the latter case at least, the usual condition for intramolecular H-bonding (a six-membered, inflexible ring) is satisfied. This interpretation has not become popular, however; the H-bond usually is considered a dipole-dipole interaction and the carbon-hydrogen bonds in a methyl group are not strongly polar.⁵ Since n.m.r. spectroscopy provides an excellent criterion, it was decided to approach the question with this modern tool. Protons engaged in H-bonding appear at rather low applied magnetic fields in the n.m.r. spectrum, presumably because polarization by the base results in a net deshielding. The enol hydrogen of ethyl aceto-

(1) For a recent compilation and discussion of acid strengths, see H. C. Brown, D. M. McDaniel, and O. Hafliger in "Determination of Organic Structures by Physical Methods," by E. A. Braude and F. C. Nachod, Academic Press, Inc., New York, N. Y., 1955, Ch. XIV.

(2) H. C. Brown, M. D. Taylor, and S. Sujishi, *J. Am. Chem. Soc.*, **73**, 2467 (1951).

(3) J. F. J. Dippy, *J. Chem. Soc.*, 1222 (1938).

(4) H. B. Watson, "Modern Theories of Organic Chemistry," 2nd Ed., Oxford University Press, Oxford, 1941.

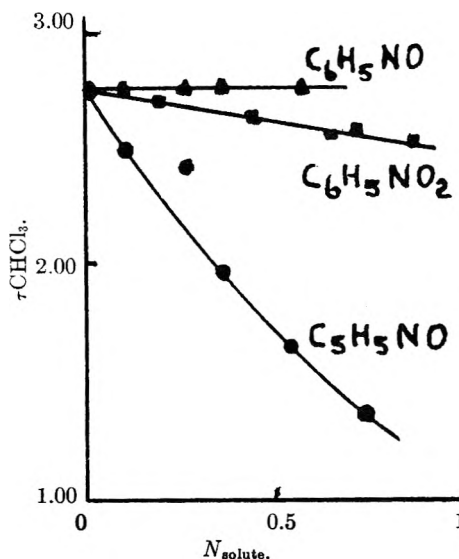


Fig. 1.—Plot of CHCl_3 resonance *vs.* solute mole fraction.

acetate and the acid proton in certain succinate acid anions are examples of this behavior. Nor is it restricted to hydroxylic protons. We found, *e.g.*, that the resonance of the hydrogen atom in chloroform, which is well known for its ability to form weak H-bonds, is shifted to drastically lower fields upon admixture of pyridine-N-oxide, to moderately lower fields by nitrobenzene, and is unaffected by nitrosobenzene (see Fig. 1); the strength of the H-bond is expected to be in this order in view of the decreasing charge on the oxygen atoms. Similar shifts have been observed with a number of aliphatic bases.⁶

The chemical shifts of the methyl hydrogen atoms of the acids and their anions are shown in Table I. Since water was used as solvent for the salts (benzene as external reference) and benzene for the free acids, the differences in δ between the two have only comparative meaning. It is pointed out that in order to ascribe the abnormal acid strength of butyric acid to H-bonding (*i.e.*, a much stronger carbonyl to methyl H-bond in the anion than in the undissociated acid), one should expect a very much greater shift downfield from acid to anion than in propionic acid, the strength of which is not anomalous. A similar remark applies to the toluic acids.

The data do not show the shifts described. The

TABLE I
METHYL RESONANCES

	δCH_3^a (acid)	δCH_3^a (anion)	$\Delta\delta^a$
Propionic acid ^b	6.33	5.45	0.88
Butyric acid ^b	6.46	5.60	0.86
<i>o</i> -Toluic acid	4.63	4.15	0.48
<i>m</i> -Toluic acid	5.18	4.15	1.03
<i>p</i> -Toluic acid	5.24	4.18	1.06

^a In p.p.m. to the benzene signal. ^b Measured to the center of the triplet.

(5) The methyl hydrogen atoms furthermore must compete with water for bonding to the carbonyl group; however, its favorable steric position may interfere with the solvation of this group by water.

(6) G. Korinek and W. G. Schneider, *Can. J. Chem.*, **35**, 1157 (1957).

values of $\Delta\delta$ ($\delta\text{CH}_{3\text{acid}} - \delta\text{CH}_{3\text{anion}}$) are identical for butyric and propionic acid. Similarly, no support is found for the notion of a H-bond in *o*-toluate ion; $\Delta\delta$ is actually *smaller* in that case than for the isomers.

We conclude that these measurements are not consistent with intramolecular H-bonding in butyrate and *o*-toluate anion, and that the strengths of the corresponding acids are best explained as by Brown, *et al.*²

It is interesting to note that the methyl hydrogen resonance of *o*-toluic acid appears at lower field strength than that of its two isomers⁷; a similar difference has been reported for the *cis*- and *trans*-isomers of olefins having methyl and carbonyl groups on the 1- and 2-carbon atoms, respectively.⁸

Experimental

Nitrosobenzene and pyridine-N-oxide⁹ were purified by sublimation; the other chemicals used were commercial materials of satisfactory purity. Nitrosobenzene in chloroform solution was found to obey Beer's law at several wave lengths in the near infrared over nearly the entire concentration range used, so that this material presumably is monomeric under these conditions. The n.m.r. spectra of the chloroform solutions were measured at 20° with tetramethylsilane as internal reference, of the aqueous solutions at 20° with benzene as external reference (one set of tubes being used for all measurements), and of the benzene solutions to the solvent signal. All solutions of the acids and salts were 0.33 *M*. Since only the *differences* in chemical shift were considered of interest in this work, no susceptibility corrections were applied.

(7) As the referee has kindly pointed out, the difference in chemical shift between the methyl protons of the undissociated toluic acids may be the effect of magnetic anisotropy of the carbonyl group.

(8) L. M. Jackman and R. H. Wiley, *Proc. Chem. Soc.*, 196 (1958).

(9) We are indebted to the Reilly Tar and Chemical Corporation for a generous gift of this compound.

SEPARATION FACTORS IN THE NO-NOBr SYSTEM¹

BY ALFRED NARTEN²

Chemistry Department, Columbia University, New York, N. Y.

Received November 15, 1961

The exchange of the nitrogen, oxygen, and chlorine isotopes between the gas and liquid phases of the NO-NOCl system has been studied by Schaeffer and Smith³ and by Yeatts.⁴ The authors point out that a general consideration of the factors affecting suitability of this system for isotope separation suggests that exchange reactions of NOCl might provide an interesting and useful means for the separation of the stable isotopes of nitrogen, oxygen, and chlorine in a simultaneous process.

Whereas the chemistry of nitrosyl chloride is well understood, little is known about nitrosyl bromide. Not even the boiling point of this substance is known with any accuracy.⁵ The thermodynamic properties of gaseous NOBr have been determined from spectroscopic data⁶ and from an

investigation of the reaction $2\text{NO} + \text{Br}_2 = 2\text{NOBr}$.⁷ The data obtained are in good agreement.

At room temperature and atmospheric pressure, gaseous NOBr is 16% dissociated into NO and Br₂. From the analogy with the NO₂-N₂O₄ system it is reasonable to assume that the degree of dissociation in the liquid phase is small as compared with the degree of dissociation in the gas phase at and below room temperature.

The *effective separation factor* is defined as

$$\alpha(X/Y) = \alpha_{\text{eff}} = \frac{[c(X)/c(Y)]_l}{[c(X)/c(Y)]_g} \quad (1)$$

(X = N¹⁵ or O¹⁸, Y = N¹⁴ or O¹⁶, *c* = concn. in moles per liter, *l* = liquid, *g* = gas)

If we restrict the discussion to the exchange of the stable isotopes of nitrogen and oxygen between the two phases of the NO-NOBr system, and if we denote the concentration of the heavy isotope by *c*^{*} and the concentration of the light isotope by *c*, we obtain

$$\alpha_{\text{eff}} = \frac{[c^*(\text{NO}) + c^*(\text{NOBr})]/[c(\text{NO}) + c(\text{NOBr})]_l}{[c^*(\text{NO}) + c^*(\text{NOBr})]/[c(\text{NO}) + c(\text{NOBr})]_g} \quad (1a)$$

Introducing the *individual separation factors*

$$\alpha_1 = \frac{[c^*(\text{NO})/c(\text{NO})]_l}{[c^*(\text{NO})/c(\text{NO})]_g} \quad \alpha_2 = \frac{[c^*(\text{NO})/c(\text{NO})]_l}{[c^*(\text{NOBr})/c(\text{NOBr})]_g} \\ \alpha_3 = \frac{[c^*(\text{NOBr})/c(\text{NOBr})]_l}{[c^*(\text{NOBr})/c(\text{NOBr})]_g} \quad \alpha_4 = \frac{[c^*(\text{NOBr})/c(\text{NOBr})]_l}{[c^*(\text{NO})/c(\text{NO})]_g} \quad (2)$$

and the degree of dissociation $\beta_g(\beta_l)$ of nitrosyl bromide in the gas (liquid) phase according to

$\beta = c(\text{NO})/c^0(\text{NOBr}) = [c^0(\text{NOBr}) - c(\text{NOBr})]/c(\text{NOBr})$ (*c*⁰ being the concentration at $\beta = 0$), using definition (2) and the relation

$$\alpha_1\alpha_3 = \alpha_2\alpha_4$$

we obtain the dependence of the effective separation factor on the individual separation factors and the degree of dissociation in the two phases

$$\alpha_{\text{eff}} = \alpha_3 \frac{1 - \beta_l(1 - \alpha_1/\alpha_4)}{1 - \beta_g(1 - \alpha_3/\alpha_4)} \quad (3)$$

(3) can be further simplified if we make the assumptions

$$\ln \alpha_i \equiv \delta_i \cong (\alpha_i - 1) \ll 1, \beta_l \ll 1$$

The resulting relation is

$$\delta_{\text{eff}} = \delta_4\beta_g + \delta_3(1 - \beta_g) \quad (4)$$

Experimental

Liquid bromine (50 ml.) was equilibrated with nitric oxide in an equilibration vessel, so that the total pressure in the vessel was always atmospheric. After the chemical equilibrium between NO and Br₂ had been established, the mixture was agitated by means of a magnetic stirrer for 1-3 hr. Samples from the gas and liquid phases then were taken. The samples were reacted with mercury to give nitric oxide,⁸ which in turn was reduced to nitrogen in a copper furnace.⁹ Isotopic analysis was carried out in a

(6) W. G. Burns and H. G. Bernstein, *J. Chem. Phys.*, **18**, 1669 (1950).

(7) C. M. Blair, P. D. Brass, and D. M. Yost, *J. Am. Chem. Soc.*, **56**, 1916 (1934).

(8) E. W. R. Steacie and W. McF. Smith, *Can. J. Research*, **16B**, 1 (1938).

(9) T. I. Taylor and W. Spindel, "Proceedings of the Symposium on Isotope Separation," North Holland Publishing Co., Amsterdam, 1957 p. 162.

(1) Supported by a grant from the U. S. Atomic Energy Commission.

(2) Oak Ridge National Laboratory, Oak Ridge, Tennessee.

(3) R. Schaeffer and H. Smith, contract W-7405-eng-82, Ames Laboratory, Ames, Iowa, ISC-887.

(4) L. B. Yeatts, Jr., *J. Chem. Phys.*, **28**, 1255 (1958).

(5) M. Trautz and V. P. Dalal, *Z. inorg. u. allgem. Chem.*, **102**, 149 (1918); **110**, 34 (1920).

CEC 21-210 dual-collector mass spectrometer using the 29/28 ratio. Two sets of equilibrations were carried out at 281 and 253°K. and atmospheric pressure. From five independent equilibrations at each temperature the effective separation factors were evaluated according to (1).

Results

T(°K)	p(mm.)	$\alpha(N^{15}/N^{14})$
281	754	1.0024 ± 0.0008
253	750	1.0046 ± 0.0005

Discussion

The reason for the small values of the effective $\alpha(N^{15}/N^{14})$ is that the degree of dissociation of the gaseous NOBr into NO and Br₂ is comparatively low; the gas phase consists predominantly of NOBr. Since the composition of the gas phase at 253°K. is not known, the approximate determination of the interesting α_4 from the effective $\alpha(N^{15}/N^{14})$ is possible only for 281°K.; according to (4)

$$a_4 = 1.01$$

This result is in good agreement with the spectroscopic data available for the NO-NOBr system.

Although the rate of exchange probably is much faster in the NO-NOBr than in the NO-NOCl system and the liquid NOBr easily could be decomposed by electrolysis or heat (exchange-distillation), the low effective separation factor makes this system unfeasible for the separation of the nitrogen isotopes.

Acknowledgments.—The author is indebted to Prof. T. I. Taylor of Columbia University for his continued interest in this work and for helpful discussions, and to Prof. W. Spindel of Rutgers University for the use of his mass spectrometer.

CATALYTIC HYDROGENOLYSIS OF BENZENE AND TOLUENE

By J. C. ROHRER AND J. H. SINFELT

Esso Research and Engineering Co., Linden, N. J.

Received November 18, 1961

The hydroisomerization of benzene and toluene over a nickel-silica-alumina catalyst has been reported previously by Ciapetta and Hunter.^{1,2} The nickel-silica-alumina catalyst is a typical bifunctional catalyst containing both hydrogenation and acidic components. The products of the hydroisomerization reaction are mixtures of cycloparaffins. At the temperatures investigated by Ciapetta and Hunter, 315 to 427° in the case of benzene and 228 to 372° in the case of toluene, the catalyst was very selective for hydroisomerization. However, the extent of hydroisomerization decreased with increasing temperature, as expected from thermodynamic equilibrium considerations. At still higher temperatures, the equilibrium becomes even less favorable for cycloparaffins, so that only small amounts of cycloparaffins would be expected in the products. As reported in the present study using a platinum on alumina catalyst, the major products are then C₆ and lighter paraffins. The over-all reaction lead-

ing to these products will be termed hydrogenolysis in this paper. In the work reported herein, the hydrogenolysis of benzene and toluene was investigated in a flow reactor as a function of temperature, pressure, and reactant flow rate. The results have given some insight into the kinetics and mechanism of the process.

Experimental

Procedure.—Benzene and toluene were contacted with the catalyst in the presence of hydrogen, using a flow reactor technique described elsewhere.^{3,4} The reaction products were analyzed by a procedure, also described elsewhere,⁴ consisting of a combination of chromatographic columns coupled directly to the reactor outlet.

Materials.—Phillips pure grade benzene and toluene (>99 mole % pure) were used throughout. Both these hydrocarbons and the hydrogen were dried to less than 5 p.p.m. water, using procedures described previously.^{3,4} The platinum-on-alumina catalyst used in the present study contained 0.3 wt. % platinum. The catalyst was prepared by impregnation of alumina with aqueous chloroplatinic acid, followed by calcination in air for 4 hr. at 593°. The surface area of the alumina was 163 m.²/g.

Results

Typical product distribution data for the hydrogenolysis of benzene and toluene are shown in Table I. In the case of benzene, the reaction products are predominantly C₆ and lower carbon number paraffins, while in the case of toluene the products are mainly C₇ and lower carbon number paraffins. Small amounts of cycloparaffins also were observed. In addition, the formation of small quantities of toluene from benzene and of ethylbenzene from toluene indicates that some methylation takes place.

In the case of benzene, the total amounts of cycloparaffins in the reaction products are roughly in accord with equilibrium data.⁵ Furthermore, the average ratio of methylcyclopentane to cyclohexane was found to be 6.2 to 1, which is in rough agreement with equilibrium data⁵ over the temperature range studied. In the case of toluene, only very small quantities of C₇ cycloparaffins were formed for the most part, and the distribution was not well resolved. The distributions of *n*-hexane, 2-methylpentane, and 3-methylpentane in the C₆ paraffin products, and of *n*-heptane, 2-methylhexane, and 3-methylhexane in the C₇ paraffin products were found to be approximately in accord with equilibrium data. However, essentially no dimethylbutanes or dimethylpentanes were observed in the reaction products, which definitely is not in accord with equilibrium data.⁵

Figure 1 shows first-order plots for the hydrogenolysis of benzene and toluene at 499°, 21 atm. total pressure, and 5:1 hydrogen to hydrocarbon ratio. The logarithm of (100 - *x*), where *x* is the % conversion to paraffins, is plotted as a function of a time factor W/F , where *W* is the weight of catalyst in grams and \bar{F} is the feed rate of hydrocarbon reactant in g. moles per hr. The hydrogenolysis reaction appears to follow first-order kinetics reasonably well.

(3) J. H. Sinfelt, H. Hurwitz, and J. C. Rohrer, *J. Phys. Chem.*, **64**, 892 (1960).

(4) J. H. Sinfelt and J. C. Rohrer, *ibid.*, **65**, 978 (1961).

(1) F. G. Ciapetta and J. B. Hunter, U. S. Patent 2,721,226 (1955).
(2) F. G. Ciapetta, R. M. Dobres, and R. W. Baker, "Catalysis," Vol. 6, Reinhold Publ. Corp., New York, N. Y., 1958, p. 586.

(5) "Selected Values of Physical and Thermodynamic Properties of Hydrocarbons and Related Compounds," API Research Project 44, Carnegie Press, Inc., New York, N. Y., 1953.

TABLE I
 TYPICAL PRODUCT DISTRIBUTION DATA^a

Reactant	Benzene					Toluene				
	471	471	499	527	527	471	471	499	527	527
Temp., °C.	471	471	499	527	527	471	471	499	527	527
Pressure, atm.	11	31	21	11	31	11	31	21	11	31
$F/W \times 10^{3b}$	30	30	51	76	76	23	21	48	102	93
Mole % conversion to:										
C ₆ -	2.9	16.2	2.2	1.0	7.6	0.8	11.9	1.8	1.2	3.9
C ₆ paraffins	7.2	18.4	4.3	0.5	6.4		3.9	0.2		0.4
C ₆ cycloparaffins	1.0	2.7	2.4	0.1	2.1		1.1			0.3
C ₇ paraffins						0.3	18.2	1.6		1.2
C ₇ cycloparaffins							4.4			
Benzene						0.7	1.1	1.6	1.0	1.9
Toluene	0.3	0.2	0.4	0.4	0.5					
Ethylbenzene						0.4		0.6		2.1
% Unconverted reactant	88.6	62.5	90.7	98.0	83.4	97.8	59.4	94.2	97.8	90.2

^a H₂:hydrocarbon mole ratio = 5.0. ^b Gram moles hydrocarbon reactant per hr. per g. of catalyst $\times 10^3$.

Figure 2 presents similar first-order plots showing the effects of temperature and pressure. Four curves are shown in all, two for benzene at two different pressures, and two similar curves for toluene. The extent of hydrogenolysis of benzene is somewhat greater than that observed for toluene at a given set of conditions. The data at 527° appear to fall on the same curves as the 471° data or possibly even indicate a lower rate at 527°. At any rate, the effect of temperature on the reaction rate appears quite small. The effect of pressure on the hydrogenolysis is, however, quite strong. Increasing the pressure from 11 to 31 atm. increases the rate of hydrogenolysis by a factor of about 5 to 10.

Discussion

To account for the observed data on the hydrogenolysis of benzene and toluene, the following mechanism is proposed: The benzene or toluene first undergoes a hydrogenation step prior to the splitting of the ring. For example, in the case of benzene the hydrogenation step or steps can lead to the formation of cyclohexadiene, cyclohexene, and cyclohexane. These species conceivably could isomerize to five-membered ring structures such as methylcyclopentadiene, methylcyclopentene, and methylcyclopentane. Any or all of these might be intermediates in the hydrogenolysis. Cyclohexane and methylcyclopentane actually are observed in the reaction products, while the others are not, at least by our analytical methods. The failure to observe these other compounds may be due to a slow rate of desorption from the surface, as suggested by other investigators.⁶

For simplicity in the discussion, assume that the preliminary hydrogenation step leads to a single intermediate I, which then undergoes a ring splitting reaction. In addition, assume that the hydrogenation step is rapid and that an equilibrium is effectively established between the hydrocarbon reactant and the intermediate I. The existence of such an equilibrium is made plausible by the observation that the cycloparaffins formed from benzene are essentially present in equilibrium concentration. The rate-controlling step in the hydro-

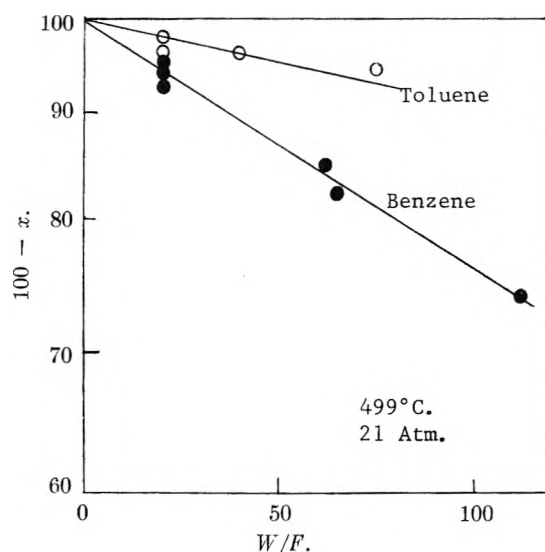


Fig. 1.—Hydrogenolysis of benzene and toluene; x = % conversion to paraffins.

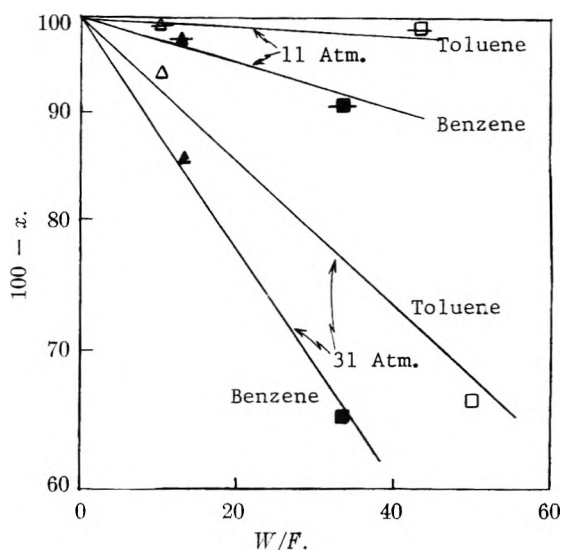
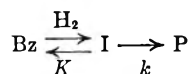


Fig. 2.—Hydrogenolysis of benzene and toluene as a function of temperature and pressure: Δ , \blacktriangle , $-\Delta-$, $-\blacktriangle-$, 527°; \square , \blacksquare , $-\square-$, $-\blacksquare-$, 471°; solid points, benzene; open points, toluene; slashed points, 11 atm.; non-slashed points, 31 atm.

(6) G. A. Mills, H. Heinemann, T. F. Milliken, and A. G. Oblad, *Ind. Eng. Chem.*, **45**, 134 (1953).

genolysis is then the ring splitting of the intermediate I. In the case of benzene, for example, we have



where Bz represents benzene and P represents the primary product of the ring splitting reaction of I. K is an equilibrium constant, and k is a rate constant. The species P conceivably could be a C_6 olefin or diolefin, which undergoes further hydrogenation and hydrocracking reactions to form C_6 and lower carbon number paraffins. A similar scheme could be proposed for toluene. In the preceding discussion it should be appreciated that I really refers to a surface species, which may or may not be detectable in the gas phase.

The simplified kinetic scheme outlined above accounts for the observed effects of temperature and pressure on the hydrogenolysis. According to this scheme, the small or possibly even negative effect of increasing temperature on the rate is due to a decrease in the equilibrium concentration of the intermediate I with increasing temperature; *i.e.*, a hydrogenation step such as that postulated for the formation of the intermediate I would be expected to be exothermic, so that the equilibrium constant K would decrease with increasing temperature. The increase in the specific rate constant k with increasing temperature thus would be opposed by the decrease in the equilibrium concentration of I. If the decrease in the equilibrium constant K with increasing temperature were great enough, the overall rate could even decrease with increasing temperature, which actually might be the case. According to the reaction scheme proposed, the effect of pressure on the rate probably is due in large part to the effect of hydrogen pressure on the equilibrium concentration of I, although the partial pressure of the hydrocarbon reactant also could have some effect.

The observation that the rate of hydrogenolysis of toluene is lower than that of benzene may simply indicate that the equilibrium concentration of the intermediate I is lower in the case of toluene, which is suggested by the fact that the concentration of methylcyclohexane in equilibrium with toluene is less than that of cyclohexane in equilibrium with benzene.⁵

**FLUORINE NUCLEAR MAGNETIC
RESONANCE SPECTROSCOPY. IX.
cis- AND *trans*-2-CHLOROHEPTAFLUORO-
BUTENE-2. THE ASSIGNMENT OF
SHIELDING VALUES AND SPIN-SPIN
COUPLING CONSTANTS IN
FLUOROOLEFIN SPECTRA**

BY GEORGE VAN DYKE TIERS

*Contribution No. 216 from the Central Research Dept. of the Minnesota
Mining and Manufacturing Co., St. Paul 19, Minn.*

Received October 2, 1961

From a preliminary communication¹ of results obtained in the analysis of n.m.r. spin-spin coupling

(1) H. M. McConnell, C. A. Reilly, and A. D. McLean, *J. Chem. Phys.*, **24**, 479 (1956).

constants in fluorinated olefins, values for the *cis* and *trans* F-F coupling constants have been widely quoted.^{2,3} The assignments were based on theoretical calculations, which were not further described, and on shielding values, which were not given in the paper. Confirmatory experimental evidence has not appeared and, in a recent analysis of halopropene spectra,⁴ assignments of *cis* and *trans* structures were made on the basis of the original paper. The suggested assignments remain unconfirmed, at least with reference to *cis* and *trans* structures. Furthermore, no logically unique decision could result solely from the n.m.r. studies; it is necessary to bring into play some absolute method based on, for example, the existence of a center of symmetry, which can be recognized experimentally *via* dipole moment studies or by infrared spectroscopy. Once a structure has been so established, n.m.r. correlations of shielding values and/or coupling constants can be employed (and very powerfully) to extend the assignments to other molecules lacking the elements of symmetry.

Such an original assignment of structure has been made for the *cis* and *trans* isomers of 2,3-dichlorohexafluorobutene-2,⁵ and a carbon-13 satellite study of these isomers has been made⁶ to determine the coupling constants between *cis* and *trans* CF_3 groups. The values obtained, 13.39 ± 0.07 and 1.44 ± 0.02 c./sec., respectively, differ by a power of ten and accordingly may be used as a basis for extending the assignment to related molecules.

In one such case, namely, 2-chloroheptafluorobutene-2, it was found possible to differentiate the *cis* and *trans* couplings between CF_3 and F groups, and thus to establish a link to the self-consistent body of correlations established by Reilly, *et al.*^{1,4} Their unproved assignment now is validated. A similar carbon-13 study of the *cis* and *trans* F-F couplings in the isomers of 1,2-dichloro-1,2-difluoroethylene⁷ also has confirmed their assignment.

Experimental

A sample of 2,2,3-trichloroheptafluorobutane,⁸ obtained from the Hooker Electrochemical Co., was dechlorinated by zinc dust in refluxing *n*-butyl alcohol to give a mixture (*ca.* 50/50) of the *cis* and *trans* isomers of 2-chloroheptafluorobutene-2, b.p. 32° , n_D^{25} 1.2921.⁹ The isomer identified as *cis* by n.m.r. was enriched in the higher-boiling fractions, as had been observed for the *cis* isomer of 2,3-dichlorohexafluorobutene-2.^{6,5} No attempt was made to isolate purified isomers, but separation was achieved by vapor-phase chromatography over "Kel-F" oil KF-3 at 25° , the *trans* isomer being eluted first.

The n.m.r. spectrometer and techniques have been described in previous publications.^{6,10,11} Owing to the wide

(2) J. A. Pople, W. G. Schneider, and H. J. Bernstein, "High-Resolution Nuclear Magnetic Resonance," McGraw-Hill Book Co., New York, N. Y., 1959, p. 335.

(3) L. M. Jackman, "Applications of Nuclear Magnetic Resonance Spectroscopy in Organic Chemistry," Pergamon Press, New York, N. Y., 1959, p. 86.

(4) J. D. Swalen and C. A. Reilly, *J. Chem. Phys.*, **34**, 2122 (1961).

(5) F. Dickinson, R. Hill, and J. Muray, *J. Chem. Soc.*, 1441 (1958).

(6) G. V. D. Tiers, *J. Chem. Phys.*, **35**, 2263 (1961).

(7) G. V. D. Tiers and P. C. Lauterbur, *ibid.*, **36**, 1110 (1962).

(8) R. H. Capps and W. M. Jackson, *J. Phys. Chem.*, **60**, 811 (1956).

(9) A. L. Henne and T. H. Newby, *J. Am. Chem. Soc.*, **70**, 130 (1948).

TABLE I

	1-CF ₃			4-CF ₃			3-F		
	ϕ^{*a}	$J(1,3)^b$	$J(1,4)^b$	ϕ^{*a}	$J(4,1)^b$	$J(4,3)^b$	ϕ^{*a}	$J(3,1)^b$	$J(3,4)^b$
<i>trans</i>	+64.804 ±0.002	24.72 ±0.05	1.27 ±0.02	+68.350 ±0.002	1.33 ±0.01	5.49 ±0.04	+113.369 ±0.005	24.76 ±0.05	5.38 ±0.02
<i>cis</i>	+62.180 ^c ±0.002	8.67 ±0.08	11.32 ±0.07	+66.274 ^c ±0.001	11.43 ±0.08	7.74 ±0.04	+106.761 ±0.008	8.09 ^d ±0.06	8.09 ^d ±0.06

^a Concentration 20% by volume in CCl₃F. ^b The theoretical first order multiplicities were observed in every case. ^c Assigned by analogy to the *trans* case, since the virtual identity of coupling constants for the two CF₃ groups precluded positive identification. ^d The peak is a 7-fold binomial multiplet, resulting from nearly equal coupling to the two CF₃ groups. An explanation for the "J-averaging" phenomenon has been given by J. I. Musher, *J. Chem. Phys.*, **36**, 1086 (1962).

separations of the peaks as compared to the coupling constants, a simple first-order spin-spin analysis was entirely sufficient. Shielding values, ϕ^{*10} and coupling constants for the two isomers are presented in Table I.

The *trans* isomer was identified readily by virtue of the narrow ($J = 1.3$ c./sec.) quadruplet CF₃ peaks.⁶ The large doublet splitting of one of these peaks, $J = 24.74$ c./sec., is not observed for the *cis* isomer and thus must not be $J(3,4)$, since both isomers contain exactly the same structure at these positions and would be expected to show coupling constants of similar magnitude. It therefore must be $J(1,3)$, and thereby identifies the peak due to fluorines at the 1-position. Since this large coupling constant is observed only when fluorine is located *cis* to a CF₃ group, it serves to verify the previously unsupported assignments.^{1,4} The J -values for the *cis* isomer are in satisfactory agreement with the literature values.^{1,4,6} Owing to the accidental near-equivalence of $J(1,3)$ and $J(3,4)$ the assignment of CF₃ peaks must be based on the substantial difference in ϕ^{*} -values between the CF₃ peaks for each isomer. The 3.8 ± 0.3 p.p.m. decrease in shielding, attributed to the presence of Cl rather than F on the olefinic carbon atom bearing the CF₃ group, also is observed in other related compounds.⁶

ADDED IN PROOF.—A recent paper by Andreades¹² also has verified the original assignments.

Acknowledgment.—The author is indebted to R. I. Coon for preparation of the 2-chloroheptafluorobutene-2, to R. B. Calkins for excellent operation of the n.m.r. spectrometer, and to Jane E. H. Tiers for painstaking measurement of the spectra.

(10) G. Filipovich and G. V. D. Tiers, *J. Phys. Chem.*, **63**, 761 (1959).

(11) G. V. D. Tiers, *ibid.*, **62**, 1151 (1958).

(12) S. Andreades, *J. Am. Chem. Soc.*, **84**, 864 (1962).

INTERACTION OF HYDROCARBONS WITH Pt-Al₂O₃ IN THE PRESENCE OF HYDROGEN AND HELIUM

BY J. C. ROHRER AND J. H. SINFELT

Esso Research and Engineering Co., Linden, N. J.

Received November 18, 1961

In studies of the chemisorption of hydrocarbons on various metals, Kemball and co-workers^{1,2} have shown that extensive decomposition takes place, leading to the formation of hydrogen deficient surface residues. The excessive dehydrogenation leading to the formation of such residues also may be accompanied by polymerization reactions. This type of irreversible chemisorption would be expected to limit severely the catalytic activity of the surface for various hydrocarbon reactions. This has been strikingly illustrated in the present work for two different reactions over a platinum on alumina catalyst, the dehydrogenation of

(1) P. G. Wright, P. G. Ashmore and C. Kemball, *Trans. Faraday Soc.*, **54**, 1692 (1958).

methylcyclohexane to toluene and the dehydrocyclization of *n*-heptane to toluene.

Experimental

A micro-reactor technique, similar to that described by other investigators,^{3,4} was used to follow catalytic activity. Small shots of liquid reactant, about 0.05 ml., were injected into either helium or hydrogen in the inlet line leading to the reactor. The pressure was maintained at 1.7 atmospheres. Carrier gas rates of 500 and 1500 cc. (STP) per minute were used for the helium and hydrogen, respectively. A catalyst charge of 1.0 gram was used throughout. The reaction products were analyzed by gas chromatography. Details of the reactor and chromatographic analyses have been presented elsewhere.⁵ The hydrocarbons used were Phillips pure grade (>99 mole % pure) in all cases. Both the hydrocarbons and hydrogen were dried to less than 5 p.p.m. water by procedures described previously.⁵ The catalyst employed in this work contained 0.3 wt. % platinum on alumina, and was prepared by impregnation of alumina with aqueous chloroplatinic acid. The surface area of the alumina was approximately 145 m.²/g.

Results

Successive shots of methylcyclohexane were injected into hydrogen and helium carrier gases, and the activity of the catalyst for dehydrogenation to toluene at 315° was determined.

Shot no.	Carrier gas ^a	Mole % toluene formed
1	H ₂	21
2	H ₂	19
3	H ₂	20
4	He	22
5	He	6.5
6, 7, 8 ^b	He	
9	He	1.7
10 ^c	H ₂	14
11	H ₂	15

^a H₂ rate = 1500 cc. (STP) per min.; He rate = 500 cc. (STP) per min. ^b No product analyses obtained. ^c 48-hour H₂ treatment between periods 9 and 10.

During the period when hydrogen carrier gas was used, the conversion to toluene remained constant at about 20 mole %. Equilibrium conversion at these conditions corresponds to about 85 mole % toluene.⁶ When the carrier gas was switched to helium, the first shot gave about the same conversion as was observed in hydrogen. How-

(2) A. K. Galwey and C. Kenball, *ibid.*, **55**, 1959 (1959).

(3) R. J. Kokes, H. Tobin, Jr., and P. H. Emmett, *J. Am. Chem. Soc.*, **77**, 5860 (1955).

(4) A. I. M. Keulemans and H. H. Voge, *J. Phys. Chem.*, **63**, 476 (1959).

(5) J. H. Sinfelt and J. C. Rohrer, *ibid.*, **65**, 978 (1961).

(6) "Selected Values of Physical and Thermodynamic Properties of Hydrocarbons and Related Compounds," API Research Project 44, Carnegie Press Inc., New York, N. Y., 1953.

ever, since the helium flow rate was threefold lower than that of hydrogen, and the residence time in the case of helium therefore threefold greater, the initial catalytic activity in the presence of helium is substantially lower. Furthermore, the conversion in the presence of helium was found to decline markedly with each successive shot, declining from 22 to 1.7 mole % after six shots. After passing hydrogen over the catalyst for 48 hr., however, about 75% of the catalytic activity was regained, as evidenced by the 15 mole % conversion obtained in the presence of hydrogen.

Some similar data also were obtained with *n*-heptane. In this case, the activity of the catalyst for dehydrocyclization of the *n*-heptane to toluene at 471° was determined for successive shots of *n*-heptane.

Shot no.	Carrier gas ^a	Mole % toluene formed
1	H ₂	15
2	He	11
3	He	0.6
4	He	0.4
5, 6, 7, 8, 9 ^b	He	
10	He	0.1
11	H ₂	6.6

^a H₂ rate = 1500 cc. (STP) per min.; He rate = 500 cc. (STP) per min. ^b No product analyses obtained.

Again, in the presence of helium, the initial catalytic activity was substantially lower than in the presence of hydrogen, and the conversion to toluene declined markedly with successive shots. Also, when the carrier gas was switched back to hydrogen, much of the catalyst activity was regained.

The deactivation observed with successive shots appears quite definitely to be due to the hydrocarbon being passed over the catalyst in the absence of hydrogen, rather than to the presence of helium itself. This is supported by the observation that prolonged treats with pure helium (5 hr.) prior to the first hydrocarbon shot in helium did not affect the initial conversion to toluene.

These studies illustrate in a striking manner the rapid decline in catalytic activity which occurs when a hydrocarbon is contacted with platinum catalyst in the absence of hydrogen. As indicated by the work of Kemball and co-workers,^{1,2} the chemisorption of hydrocarbons on metals is accompanied by extensive decomposition to form hydrogen-deficient surface residues. The role of hydrogen then appears to be one of removal of residues, thus maintaining the surface active for catalytic reactions. Evidence for the removal of surface residues from a platinum catalyst has been obtained by Pitkethly and Goble.⁷ These investigators studied the adsorption of benzene on supported platinum catalysts, and found that the adsorption was almost totally irreversible at temperatures above 200°. However, adsorption sites were recovered by treatment with hydrogen, which removed the adsorbed surface residues by hydrocracking reactions leading to the formation

(7) R. C. Pitkethly and A. G. Goble, Paper No. 91, Section II, Proceedings of the Second International Congress on Catalysis, Paris, France (1960).

of C₁-C₄ hydrocarbons. It was concluded also that hydrogen can maintain a steady-state concentration of hydrocarbon-free platinum sites, which presumably would be active for catalytic reactions.

IONIC ASSOCIATION AND CORRELATION BETWEEN DOUBLE LAYER STRUCTURE AND ELECTRODE KINETICS

BY PAUL DELAHAY AND AKIKO ARAMATA

Coates Chemical Laboratory, Louisiana State University, Baton Rouge 3, Louisiana

Received November 20, 1961

The possibility of ion pair formation *solely in the double layer* region at the electrode in charge transfer reactions was suggested in a previous paper¹ from this Laboratory. It was discussed in some detail by Frumkin^{2,3} to account for certain features of current-potential curves for the reduction of anions. Ion pair formation outside the double layer was not considered. Formation of ion pairs in the bulk of the solution was discussed recently by Joshi and Parsons,⁴ together with other interpretations, to account for the properties of the electrical double layer at the interface between mercury and mixtures of barium chloride and hydrochloric acid. The influence of ion pair formation in the bulk of solution in the correlation between double layer structure and electrode kinetics was also considered *qualitatively* by Gierst⁵ and Parsons⁶ in the interpretation of the minimum which appears in current-potential curves for the reduction of K₂S₂O₈ under certain conditions. A quantitative interpretation of the ion-pair effect is given here for the reduction of iodate on mercury in alkaline solutions of varying composition. This electrode reaction is advantageous because it occurs in a range of potentials in which there is very little specific adsorption of the ions involved. Application is made of the corrected Tafel plot recently mentioned in a previous paper from this Laboratory.⁷

Experimental

Experimental methods were quite conventional and have been reported previously.⁷ Adsorbable impurities (organic) were removed by treatment with activated charcoal as noted before. The solution of KOH was titrated. The K₄Fe(CN)₆ solution was prepared from the dehydrated salt and was titrated for verification.⁸

A five-compartment cell was used with the following electrodes: hydrogen electrode in I; dropping mercury electrode or capillary of Lippmann electrometer and platinum cylinder for differential capacity measurements in III; a high-resistance saturated calomel electrode inserted in IV; and a mercury pool in V. Junctions between compart-

(1) P. Delahay and C. C. Mattax, *J. Am. Chem. Soc.*, **76**, 5314 (1954).

(2) A. N. Frumkin, *Trans. Faraday Soc.*, **55**, 156 (1959).

(3) A. N. Frumkin, "Transactions of the Symposium on Electrode Processes," E. Yeager, ed., John Wiley and Sons, New York, N. Y., 1961, p. 1.

(4) K. M. Joshi and R. Parsons, *Electrochim. Acta*, **4**, 129 (1961).

(5) L. Gierst, ref. 3, pp. 109-144.

(6) R. Parsons, "Advances in Electrochemical Engineering," Vol. 1, P. Delahay, ed., Interscience Division, John Wiley and Sons, New York, N. Y., 1961, pp. 1-64.

(7) K. Asada, P. Delahay, and A. K. Sundaram, *J. Am. Chem. Soc.*, **83**, 3396 (1961).

(8) I. M. Kolthoff and R. Belcher, "Volumetric Analysis," Vol. III, Interscience Publishers, Inc., New York, N. Y., 1957, p. 135.

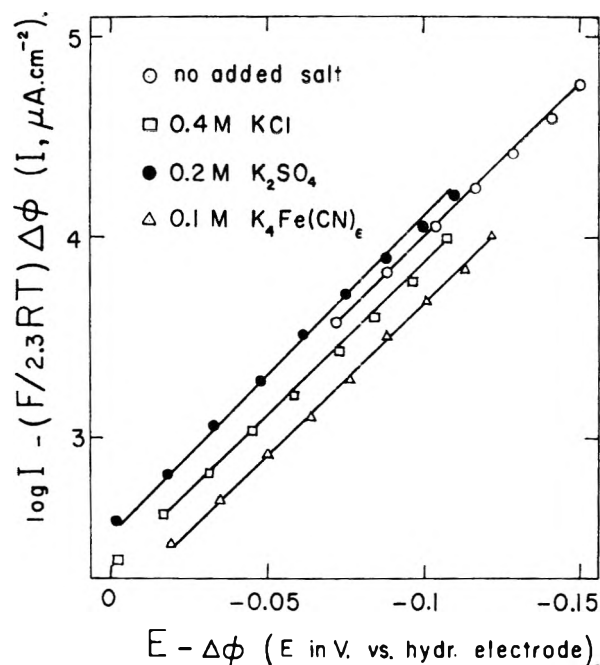


Fig. 1.—Corrected Tafel plots for the solutions of Table I. Correction for ionic association was made for K_2SO_4 and $K_4Fe(CN)_6$.

ments were: a bridge with fritted glass disks for I-II; a 1-mm.-bore capillary for II-III; and fritted glass disks for III-IV and IV-V. Solutions in the compartments were: the solution being studied in II, III, and IV; this solution, but without potassium iodate, in I and the bridge; and KOH in V. All potentials were measured against the hydrogen electrode in I, the electrode in V being the anode of the electrolysis circuit. The potential of the hydrogen electrode was verified against the standard calomel electrode: $E = -0.964$ v. for 5 mM $KIO_3 + 20$ mM KOH; -0.960 v. for the same solution with 0.4 M KCl; -0.963 v. for the solution with 0.2 M K_2SO_4 instead of KCl; and -0.966 v. for the solution with 0.1 M $K_4Fe(CN)_6$ instead of KCl or K_2SO_4 .

Currents did not exceed 10% of the diffusion current and were corrected for mass transfer polarization by use of the factor $[1 - (i/i_d)]$. This correction factor is sufficiently accurate for maximum currents during drop life at the foot of a polarographic wave.⁹

Description and Discussion of Results

Parallel linear Tafel plots were obtained in the current density range, $I = 20$ to $800 \mu A. cm^{-2}$, for the reduction of potassium iodate in the electrolytes of Table I. These plots yielded $\alpha n_a = 0.75$ (α , transfer coefficient; n_a , number of electrons in the activated step), in good agreement with the previously reported¹⁰ value of 0.77. Corrected Tafel plots were prepared according to

$$\ln I + \frac{zF}{RT} \Delta\phi = \ln I^0 + \frac{\alpha n_a F}{RT} E_e - \frac{\alpha n_a F}{RT} (E - \Delta\phi) \quad (1)$$

where I is the current density, I^0 the exchange current density, E the electrode potential, E_e the equilibrium electrode potential, $\Delta\phi$ the difference of potential across the diffuse double layer from the plane of closest approach to solution, z the ionic

valence with sign of the reduced species (iodate), and F , R , and T have their usual significance.¹¹ Values of $\Delta\phi$ were calculated by a previously described method⁷ from the theory of the diffuse double layer, experimental differential capacities,¹² and the point of zero charge. Parallel linear plots were obtained which yielded $\alpha n_a = 0.89$ and the intercepts in Table I. (The difference between $\alpha n_a = 0.77$ for Tafel plots and the corrected value, $\alpha n_a = 0.89$, results from the neglect of the variations of $\Delta\phi$ with E in uncorrected Tafel plots.) The

TABLE I

DATA ON TAFEL PLOTS AND CORRECTED TAFEL PLOTS FOR THE REDUCTION OF 5 mM KIO_3 IN 20 mM KOH ON MERCURY AT 25°

Added salt	$E - \Delta\phi$ for cord. Tafel plot	$E - \Delta\phi$ for cord. Tafel plot with ion-pair corn. ^b
	$\mu A. cm^{-2}$ for Tafel plot v. vs. H.E. ^a	v. vs. H.E.
None	-0.247	-0.036
0.4 M KCl	- .105	- .042
.2 M K_2SO_4	- .121	- .050
.1 M $K_4Fe(CN)_6$	- .132	- .070

^a H.E. = hydrogen electrode in identical solution as for electrolysis but without KIO_3 . ^b For $\log I + (zF/2.3RT) \Delta\phi = 10^3 (I \text{ in } \mu A. cm^{-2})$.

lines without and with 0.4 M KCl are essentially identical within the experimental error of 3–5 mv., but the double layer correction is less satisfactory for 0.2 M K_2SO_4 and, especially, 0.1 M $K_4Fe(CN)_6$. Disagreement for K_2SO_4 was previously noted¹⁰ (without the use of corrected Tafel plots).

Several causes can be invoked for the disagreement between theory and experiment: variation of activity coefficient, ion pair formation in the double layer, influence of ion size, etc. (cf. ref. 4). Further, the calculation of $\Delta\phi$ is based on the Gouy-Chapman theory, *i.e.*, on a very simplified model not unlike that of the Debye-Hückel model for electrolytes. It is surprising, in this respect, that the double layer correction holds so well for concentrations as high as 0.4 M KCl.¹³ Ionic association in the bulk of the solution, which is not negligible for K_2SO_4 and $K_4Fe(CN)_6$, also is to be reckoned with. One has $\log K = 0.96$,^{14a} for formation of $K^+SO_4^-$, and $\log K = 2.3$ ^{14b} for formation of $K^+Fe(CN)_6^{3-}$. Ionic association seems negligible for KOH and KCl.^{14c} The corresponding error in ionic concentrations, if ionic association is not considered, is significant, especially for K^+ ions which are non-specifically adsorbed in the diffuse double layer at the potentials considered here. The corrected Tafel plots of Fig. 1 were obtained after allowance was made for ionic association. The discrepancy for K_2SO_4 noted above disappears and, in fact, there seems to be a

(11) See ref. 5 for a discussion.

(12) Capacities were measured with KIO_3 present as the reaction is so irreversible that the faradaic impedance is very large in comparison with the double layer impedance.

(13) P. Delahay, "Transaction of the Symposium on Electrode Processes," E. Yeager editor, John Wiley and Sons, New York, N. Y., 1961, p. 138.

(14) (a) J. Bjerrum, G. Schwarzenbach, and L. G. Sillén, "Stability Constants, Part II," The Chemical Society, London, 1958, p. 80; (b) *ibid.*, p. 32; (c) *ibid.*, pp. 2 and 93.

(9) J. Koutecky and J. Cizek, *Collection Czechoslov. Chem. Commun.*, **11**, 836 (1956).

(10) M. Breiter, M. Kleinerman, and P. Delahay, *J. Am. Chem. Soc.*, **80**, 5111 (1958).

slight overcorrection. Results for KOH alone, KOH + KCl, and KOH + K_2SO_4 are nearly the same within experimental error. The discrepancy for $K_4Fe(CN)_6$ is decreased but not entirely eliminated. This discrepancy, as given by Fig. 1, is greater than it actually is because formation of the triple ion $(K^+)_2Fe(CN)_6^{2-}$ was not considered. There is evidence for the formation of this ion¹⁵ but no quantitative datum is available. Further, other effects, and particularly the influence of ionic size, could be invoked to explain the remaining small departure from theory. This matter will not be taken up here, though it is being studied at present in this Laboratory.

Ionic association of the reactant, KIO_3 ($K = -0.25$ for formation¹⁶ of $K^+IO_3^-$), also should be considered since the faradaic current is the sum of the currents for the reduction of IO_3^- and $K^+IO_3^-$. These two parallel electrode processes undoubtedly have different exchange densities. Further, the kinetics of dissociation of $K^+IO_3^-$ complicates matters. Double layer corrections for this type of process have been discussed semi-quantitatively,^{10,17} and theoretical analyses have been worked out.^{18,19} This effect is probably minor here because of the weak association between K^+ and IO_3^- .

In conclusion, correction for ionic association of the supporting electrolyte and/or ionic reactants appears to be in order in the correlation between double layer structure and electrode kinetics. However, one would do well to remember the words of caution of Robinson and Stokes²⁰ when using equilibrium constants for ionic association.

Acknowledgment.—This investigation was supported by the Office of Naval Research.

(15) S. R. Cohen, Thesis, Cornell University, Ithaca, N. Y., 1956, p. 34.

(16) Cf. ref. 12, p. 124.

(17) L. Gierst, ref. 11, pp. 109–138.

(18) H. Matsuda, *J. Phys. Chem.*, **64**, 336 (1960).

(19) H. Hurwitz, *Z. Elektrochem.*, **65**, 178 (1961).

(20) R. A. Robinson and R. H. Stokes, "Electrolyte Solutions," 2nd edition, Academic Press, Inc., New York, N. Y., 1959, pp. 421–423.

THE SYSTEM 2,4,6-TRINITROTOLUENE-1,3,5-TRINITROBENZENE

By LOHR A. BURKARDT

Chemistry Division, U. S. Naval Ordnance Test Station, China Lake, California

Received November 21, 1961

The system 2,4,6-trinitrotoluene-1,3,5-trinitrobenzene has been investigated by Efremov¹ and by Shinomiya and Asahina.² Efremov's results are in considerable variance with those reported by Shinomiya and Asahina and those found in the present investigation. Efremov's data indicate a simple system with a eutectic at 56.1% 2,4,6-trinitrotoluene which melts at 48.3°. The lower values reported by Efremov may stem from impure starting components. The 1,3,5-trinitrobenzene had a

(1) N. N. Efremov, *Leningrad. Politekhnikeskii institut imeni M. I. Kalinina*, **28**, 217 (1919).

(2) C. Shinomiya and T. Asahina, *J. Chem. Soc. Japan*, **57**, 732 (1936).

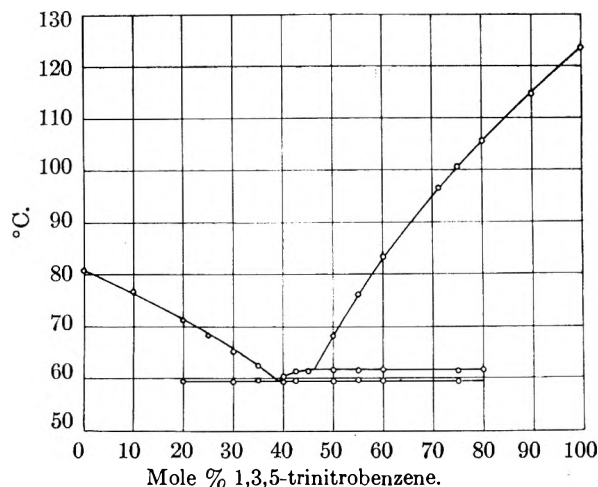


Figure 1.

melting point of 121.4° and the 2,4,6-trinitrotoluene had a melting point of 78.8°. In addition, supercooling difficulties may have occurred. Shinomiya and Asahina obtained their data by the thaw-melt technique. Their results are in fair agreement with those obtained here except in the region of 30–50 mole % 1,3,5-trinitrobenzene. In this region considerable scatter in their data points occurs. These authors make no mention of compound formation. The present study was made with an apparatus³ which permitted a step-wise heating approach to the liquids point. Solid-liquid equilibrium at each thermal step was assured by demonstrating constancy of the light transmission of the sample at each thermal step.

The 2,4,6-trinitrotoluene was recrystallized from benzene and ethyl alcohol. Following recrystallization it was fused and allowed to freeze under a vacuum twice. The melting point was then 80.9°. The 1,3,5-trinitrobenzene was recrystallized from ethyl alcohol, washed with ethyl alcohol, and air-dried. Before use, it was fused and allowed to freeze under a vacuum twice. The melting point was then 123.6°.

Six-gram samples of the required compositions were melted and stirred thoroughly. The temperature of the sample then was allowed to fall until a small amount of solid was formed. The temperature of the sample then was raised stepwise holding the sample at each temperature until the light transmission of the sample became constant. In this manner the temperature was raised to the point at which a few crystals were in equilibrium with the liquid. The temperature then was raised in small increments until these crystals disappeared, the last temperature being taken as the liquidus temperature.

Eutectic melting points were obtained by heating the completely solid sample through the eutectic melting point with a 0.1° temperature gradient between the bath and sample. With a small enough temperature gradient, a flat is obtained at the eutectic melting point.

The system forms a weak equimolar compound with an incongruent melting point of 61.5° at 47 mole % 1,3,5-trinitrobenzene. The eutectic mixture contains 39 mole % 1,3,5-trinitrobenzene and melts at 59.4°. Data for the system are shown graphically in Fig. 1.

(3) L. A. Burkardt, W. S. McEwan, and H. W. Pitman, *Rev. Sci. Instr.*, **27**, 693 (1956).

WATER-RICH EQUILIBRIA IN THE SYSTEM CH₃COONa-CH₃COOH-H₂O¹

BY LEONARD C. LABOWITZ²

Department of Chemistry, New York University, Washington Square
Center, New York 5, N. Y.

Received November 20, 1961

In 1910 it was reported by Balló³ that solid solutions are formed at both the water-rich and acid-rich ends of the phase diagrams in a number of binary mixtures of the type n -RCOOH-H₂O (where n -RCOOH = HCOOH, CH₃COOH, C₇H₅COOH, and n -C₃H₇COOH). The purpose of his work was to support the hypothesis popular at that time⁴ that the deviation of such systems from the simple Raoult-van't Hoff freezing point depression law was due not to molecular association but to solid solution formation. Particular attention was given by Balló to the system acetic acid-water, since it had been the most extensively studied member of the series. In view of the crystallographic differences between acetic acid and ice, it would seem rather improbable that such solid solutions could exist to any appreciable concentrations. Ordinary ice is hexagonal⁵ and acetic acid is orthorhombic.⁶ On the other hand, it is not inconceivable that these differences could be overshadowed by the influence of hydrogen bonding.

Considering the current widespread interest in the existence of solid solutions of ice in which ice is the major component,^{7,8} it is surprising that this early work of Balló evidently has been unnoticed by recent workers. The purpose of the present investigation is to examine the claim made by Balló that solid solutions of ice are formed in the water-rich region of the system acetic acid-water. The original study by Balló was based upon chemical analysis of the phases and use of the tracer method of van Biljert.^{9,10} In the present work, Schreinemakers' method of wet residues^{11,12} is applied to the system sodium acetate-acetic acid-water at -10.2 and -13.9° in order to determine whether the composition of the solid phase in the water-rich region of the system is pure ice or the reported solid solution.

Experimental

Apparatus and Procedure.—The apparatus used for the separation of the liquid phase from the wet residue (Fig. 1) consisted of a long, narrow test-tube fitted with a fritted glass filter stick (F) and a thermocouple well (C). The

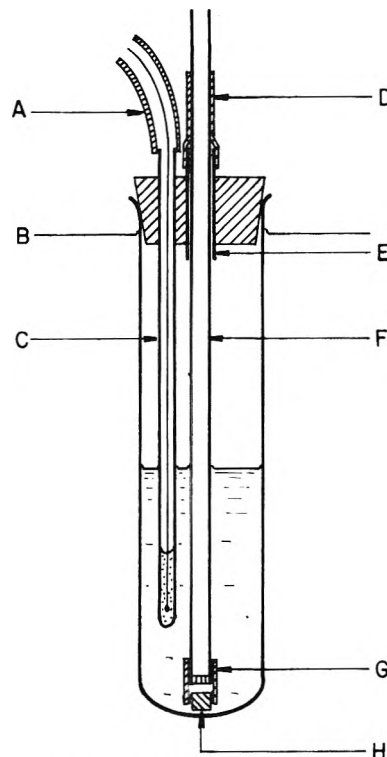


Fig. 1.—Wet residues apparatus.

filter stick was suspended in the test-tube through a short section of glass tubing (E), the point of entry being closed off from the outside atmosphere by means of a short piece of tightly fitting rubber tubing (D). The test-tube was partially filled with sample (about 10 g., completely liquid at room temperature), and the entire assembly shown in the drawing was immersed for periods of 8 to 16 hr. in a low temperature bath to the level indicated by (B). The thermocouple wires were shielded from the bath fluid by plastic tubing (A). In the -10.2° study, the low temperature bath consisted of a well stirred eutectic brine mixture dewar flask. In the -13.9° study, a methanol-containing low temperature bath (Tenney Engineering, Inc., Union, N. J., Model No. 7020) capable of maintaining a given temperature to within $\pm 0.2^\circ$ over the range +70 to -20° was used. During the solidification process, the filter stick was kept in the lowered position as shown. To prevent premature entry of material into the filter stick, the tip was closed by a small glass plug attached with rubber tubing (G). Temperature inside the sample container was monitored with a calibrated single-junction copper-constantan thermocouple and in the bath fluid with a calibrated mercury-in-glass thermometer (in the case of the -10.2° work) and a calibrated pentane-in-glass thermometer (in the case of the -13.9° work). After the attainment of equilibrium, the rubber tubing at (D) was disconnected from the wider tube, and the filter tube was raised until the plug could be disengaged from the tip by the tube (E). The filter stick then was quickly lowered once again to the bottom of the test-tube and as much liquid as possible was withdrawn through the filter stick by suction.

To determine whether equilibrium had been established under the conditions used in these experiments, duplicate samples were subjected to various refrigeration times and starting temperatures (above and below the desired final temperature). The data obtained are self consistent and within the limits of experimental error of the results of other workers on the water solubilities of acetic acid and sodium acetate at -10.2°.

Analysis and Materials.—Acetic acid was determined by titration using a calibrated buret of a weighed sample with standardized 0.1 N NaOH, using phenolphthalein as the indicator. To determine sodium acetate, a separate sample was passed through an ion-exchange resin (Amberlite IR-120, Rohm and Haas Company), thereby converting the

(1) This work was performed at New York University under the auspices of a National Science Foundation Summer Research Program for College Chemistry Teachers.

(2) Department of Chemistry, The City College of New York, New York 31, New York.

(3) R. Balló, *Z. physik. Chem.*, **72**, 439 (1910).

(4) A. Findlay, A. N. Campbell, and N. O. Smith, "The Phase Rule and Its Applications," 9th Ed., Dover Publications, Inc., New York, N. Y., p. 156.

(5) K. Lonsdale, *Proc. Roy. Soc. (London)*, **A246**, 424 (1958).

(6) R. E. Jones and D. H. Templeton, *Acta Cryst.*, **11**, 484 (1958).

(7) L. Pauling, "The Nature of the Chemical Bond," 3rd Ed., Cornell University Press, Ithaca, N. Y., 1960, p. 464.

(8) L. C. Labowitz and E. F. Westrum, Jr., *J. Phys. Chem.*, **65**, 408 (1961).

(9) A. van Biljert, *Z. physik. Chem.*, **8**, 343 (1891).

(10) J. E. Ricci, "The Phase Rule and Heterogeneous Equilibrium," D. Van Nostrand Co., Inc., New York, N. Y., 1951, p. 324.

(11) F. A. H. Schreinemakers, *Z. physik. Chem.*, **11**, 75 (1893).

(12) J. E. Ricci, ref. 10, p. 323.

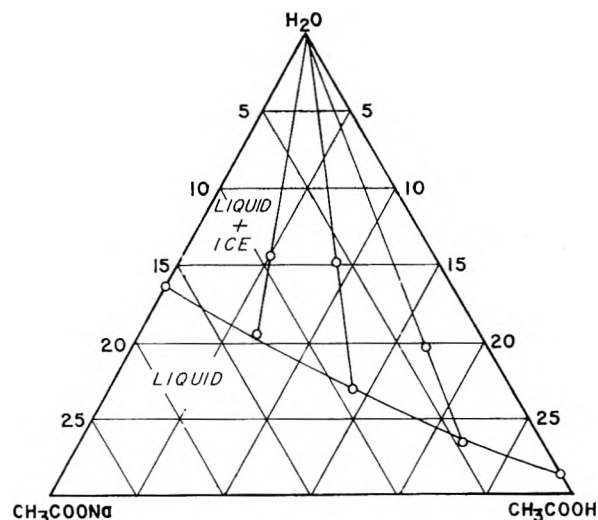


Fig. 2.—Water-rich region of the system $\text{CH}_3\text{COONa}-\text{CH}_3\text{COOH}-\text{H}_2\text{O}$ at -10.2° .

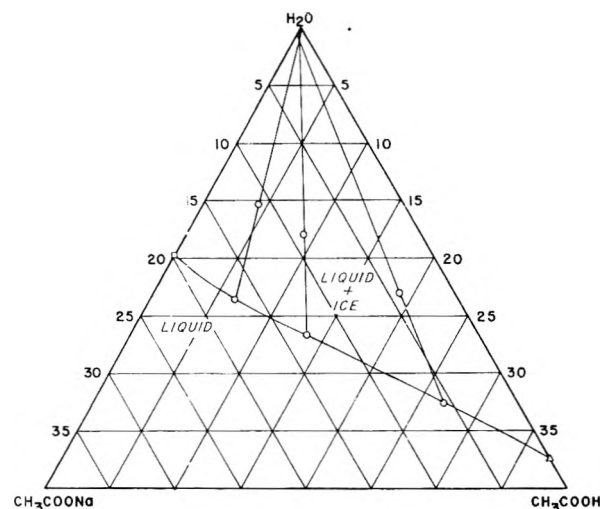


Fig. 3.—Water-rich region of the system $\text{CH}_3\text{COONa}-\text{CH}_3\text{COOH}-\text{H}_2\text{O}$ at -13.9° .

salt to the free acid, and total acetic acid was titrated as described above. The sodium acetate then was estimated by the difference. The method was found to be dependable even in the presence of excess acetic acid. A standard sodium acetate-acetic acid solution was prepared by mixing measured amounts of standardized sodium hydroxide and acetic acid solutions. The results obtained by chemical analysis agreed within 4 parts per thousand of the value predicted on the basis of the concentrations and amounts of the mixed starting materials. In a different experiment, two separate aliquots of a given solution of sodium acetate (excess acetic acid absent, this time) were analyzed by this method and the results agreed within 5 parts per thousand of each other. The relative mean deviation for the sodium acetate determination therefore is estimated to be 2.5 parts per thousand. A calibrated buret was employed for all titrations.

Commercial reagent grade chemicals without further purification were used throughout.

Results and Discussion

According to Balló, the composition of the saturated solid solution at -10.2 and -13.9° would be approximately 14 and 18 weight % CH_3COOH , respectively. The results obtained in the present investigation, given in Table I and Fig. 2 and 3, indicate, however, that the composition of the solid

phase in the water-rich region of the system is, within experimental error, pure ice and not the solid solution claimed by Balló. Aside from some obvious mistakes in the phase diagrams shown by him, it is believed that the results obtained by Balló are incorrect because of misapplication of the method of tracers, misinterpretation of the data, and possible errors made by him in the chemical analysis of the barium acetate tracer.

TABLE I
WET RESIDUES DATA FOR THE SYSTEM $\text{CH}_3\text{COONa}-\text{CH}_3\text{COOH}-\text{H}_2\text{O}$

Tie-line no.		Wt. % CH_3COONa	Wt. % CH_3COOH	Mathematically extrapolated terminus
$-10.2 \pm 0.1^\circ$				
1	Liquid	8.98	13.97	0.57 wt. % CH_3COOH
	Residue	5.73	9.12	
2	Liquid	4.49	21.99	.29 wt. % CH_3COONa
	Residue	3.51	16.90	
3	Liquid	12.61	6.83	.34 wt. % CH_3COOH
	Residue	9.29	5.12	
$-13.9 \pm 0.2^\circ$				
4	Liquid	5.58	27.06	.55 wt. % CH_3COONa
	Residue	4.06	18.90	
5	Liquid	13.10	13.57	.20 wt. % CH_3COONa
	Residue	8.87	9.12	
6	Liquid	17.11	6.57	.17 wt. % CH_3COOH
	Residue	11.04	4.31	

Acknowledgment.—The author wishes to express his sincere appreciation to Profs. John E. Vance and Seymour Z. Lewin of New York University for the generous use of their facilities. The financial support of the National Science Foundation is gratefully acknowledged.

THERMODYNAMIC STUDIES OF THE IODINE COMPLEXES OF *s*-TRITHIANE, THIACYCLOHEXANE, AND THIACYCLOPENTANE IN CARBON TETRACHLORIDE SOLUTION

By J. D. McCULLOUGH AND IRMELA C. ZIMMERMANN

The Department of Chemistry of the University of California at Los Angeles, Los Angeles 24, California

Received December 18, 1961

The present work is an extension of previously reported studies¹⁻³ on systems of the type $\text{D} \cdot \text{I}_2 = \text{D} + \text{I}_2$, where the donor, D, is an organoselenium compound or an organic sulfide.

Experimental

Materials.—Thiacyclopentane and thiacyclohexane were from the same samples used in ref. 1 and were supplied by the American Petroleum Institute Research Project 48A, Bartlesville, Oklahoma.

s-Trithiane was kindly supplied by Professor E. E. Campaigne of Indiana University. The recrystallized solid melted at $220-221^\circ$.

The iodine and carbon tetrachloride and the experimental procedures were those described in ref. 1 and 2.

Method of Calculation.—The method of calculation was

(1) J. D. McCullough and D. Mulvey, *J. Am. Chem. Soc.*, **81**, 1291 (1959).

(2) J. D. McCullough and I. C. Zimmermann, *J. Phys. Chem.*, **64**, 1064 (1960).

(3) J. D. McCullough and I. C. Zimmermann, *ibid.*, **65**, 888 (1961).

TABLE I
ABSORBANCE DATA FOR SOLUTIONS OF DONOR, D, AND I₂ IN CCl₄

(a) D = *s*-Trithiane, C₃H₆S₃

Concn. (moles/l.) × 10 ⁴ at 23.0°		Absorbance per cm. path ^a								
[D]	[I ₂]	15.0°			23.0°			36.6°		
		300 mμ	310 mμ	320 mμ	300 mμ	310 mμ	320 mμ	300 mμ	310 mμ	320 mμ
4.672	29.31	0.978	1.085	0.989	0.720	0.788	0.716	0.548	0.582	0.530
5.860	25.02	0.970	1.092	0.990	0.759	0.833	0.760	0.533	0.598	0.544
6.221	47.94				1.559	1.692	1.526	1.100	1.191	1.088
3.987	38.89	1.090	1.210	1.107	0.840	0.913	0.827	0.633	0.664	0.600
6.867	21.39	1.100	1.237	1.142	0.750	0.832	0.763	0.540	0.588	0.539
6.678	42.13							1.039	1.129	1.034
5.751	60.07				1.728	1.896	1.728	1.284	1.368	1.260
5.056	48.46	1.695	1.882	1.721	1.328	1.405	1.294	0.950	1.022	0.922
3.735	33.20	0.902	1.000	0.914				.510	0.538	.482
4.150	18.39	.540	0.603	.552				.315	.333	.302
3.061	30.41	.688	.755	.687				.409	.422	.378
2.422	16.06	.297	.319	.291				.198	.199	.178
2.099	22.95	.400	.426	.382				.263	.261	.232

(b) D = Thiacyclohexane, C₆H₁₀S

Concn. (moles/l.) × 10 ⁴ at 29.3°		Absorbance per cm. path ^a								
[D]	[I ₂]	13.6°			29.3°			42.7°		
		300 mμ	310 mμ	320 mμ	300 mμ	310 mμ	320 mμ	300 mμ	310 mμ	320 mμ
4.459	1.005	0.302	0.312	0.260	0.159	0.163	0.142	0.0950	0.0970	0.0820
2.783	1.822	.356	.367	.305	.178	.183	.154	.1080	.1095	.0925
7.611	1.164	.580	.597	.495	.295	.305	.257	.1795	.1825	.1550
2.820	1.402	.275	.284	.236	.150	.152	.135	.0895	.0905	.0775
2.047	4.356	.597	.618	.515	.307	.315	.264	.1795	.1810	.1525
3.764	6.524	1.570	1.613	1.339	.812	.840	.702	.479	.490	.415
6.611	1.276	0.540	0.559	0.463	.289	.300	.251	.1700	.1745	.1500
4.565	3.605	1.074	1.123	0.921	.536	.552	.462	.328	.337	.288

(c) D = Thiacyclopentane, C₄H₈S

Concn. (moles/l.) × 10 ⁴ at 30.3°		Absorbance per cm. path ^a								
[D]	[I ₂]	16.0°			30.3°			40.5°		
		310 mμ	320 mμ	330 mμ	310 mμ	320 mμ	330 mμ	310 mμ	320 mμ	330 mμ
9.26	6.491	2.043	1.868	1.400	1.161	1.050	0.797	0.732	0.660	0.498
12.90	3.883	1.656	1.480	1.124	0.899	0.812	.610	.580	.522	.395
23.59	2.736	1.850	1.670	1.258	1.094	.977	.734	.719	.649	.489
12.74	2.627	1.138	1.000	0.757	0.608	.548	.410	.410	.370	.281
15.83	1.846	0.930	0.842	.628	.516	.464	.340	.358	.323	.249
4.80	1.267	0.257	0.232	.178	.135	.122	.093	.090	.081	.061
13.04	3.294	1.398	1.277	.935	.770	.694	.525	.500	.453	.342
15.06	1.210	0.573	0.516	.383	.335	.302	.230	.215	.195	.148
7.26	6.896	1.714	1.539	1.162				.599	.538	.410

^a Absorbance values below ~0.2 were made in 2.000-cm. cells.

that described in ref. 2 and 3 which involves cyclic least-squares treatment of the data by means of a modification of the equation proposed by Scott.⁴

Results and Discussion

Absorbance data for the experimental solutions are given in Table I while the K_c values and derived thermodynamic constants for the dissociation at 25° are given in Tables II and III, respectively. All of the complexes are clearly of the 1:1 type, even when I₂ is present in considerable excess. Data on 1,4-dithiane³ and thiacyclobutane⁵ are included in Table III for comparison purposes.

The increase in the dissociation constants in going from thiacyclohexane to 1,4-dithiane to *s*-trithiane can be explained in terms of the inductive effect. If it is assumed that the availability of electrons on the sulfur atoms is increased by the presence of CH₂ groups in the molecules, it is reasonable to

assume further that the effect will tend to be greater when the ratio of CH₂ groups to S atoms is greater. Thus the availability of electrons at sulfur should fall off in going from thiacyclohexane to 1,4-dithiane to *s*-trithiane. The effect that this has on the dissociation constants is even more pronounced if one makes statistical allowance for the fact that the number of sulfur reaction sites increases from one to two to three in the series. That the ratio of CH₂ groups to S atoms is not the whole story is shown by the fact that the iodine complex of thiacyclopentane is more stable than that of thiacyclohexane. However, the work of Tamres and Searles⁵ has shown that the stabilities of the complexes fall off in going to the four-membered ring, C₃H₆S, and still further in going to the three-membered ring, C₂H₄S.

(4) R. L. Scott, *Rec. trav. chim.*, **75**, 787 (1956).

(5) M. Tamres and S. Searles, *J. Phys. Chem.*, **66**, 1099 (1962).

TABLE II
VALUES OF K_c FOR D-I₂ DISSOCIATION AT VARIOUS
TEMPERATURES AND WAVE LENGTHS

(a) D = s-Trithiane, C ₃ H ₆ S ₃ ($K_c \times 10$)				
λ (m μ)	ϵ	15.0°	23.0°	36.6°
300	61,600	1.011	1.36	1.77
310	70,700	0.990	1.33	1.77
320	65,800	0.982	1.32	1.75
	Av.	0.994	1.34	1.76
(b) D = Thiacyclohexane, C ₆ H ₁₀ S ($K_c \times 10^3$)				
λ (m μ)	ϵ	13.6°	29.3°	42.7°
300	30,900	4.43	8.19	13.7
310	32,200	4.40	8.34	13.8
320	26,900	4.39	7.70	13.4
	Av.	4.41	8.08	13.6
(c) D = Thiacyclopentane, C ₄ H ₈ S ($K_c \times 10^3$)				
λ (m μ)	ϵ	16.0°	30.3°	40.5°
310	13,300	3.28	6.40	11.2
320	15,100	3.34	6.51	11.3
330	13,600	3.35	6.44	11.3
	Av.	3.32	6.45	11.3

TABLE III
THERMODYNAMIC CONSTANTS FOR DISSOCIATION OF D-I₂
COMPLEXES IN CARBON TETRACHLORIDE SOLUTION AT 25°

Donor (D)	K_c , moles/l.	ΔF_c° , kcal./mole	ΔH_c° , kcal./mole	ΔS_c° , cal./deg./ mole
s-Trithiane	1.48×10^{-1}	1.14 ± 0.04	4.6 ± 0.4	11.7 ± 1.4
1,4-Dithi- ane	1.30×10^{-2a}	$2.59 \pm .03$	$6.2 \pm .3$	12.1 ± 1.0
Thiacyclo- hexane	7.40×10^{-3}	$2.92 \pm .03$	$7.1 \pm .3$	14.1 ± 1.0
Thiacyclo- pentane	5.50×10^{-3}	$3.10 \pm .03$	$8.7 \pm .4$	8.7 ± 1.4
Thiacyclo- butane	1.30×10^{-2c}	2.59	$7.03 \pm .17$	14.9 ± 0.6
	1.29×10^{-2d}	2.58	$6.57 \pm .08$	13.4 ± 0.3
	1.15×10^{-2e}	2.66		

^a Ref. 3. ^b Ref. 1, data recalculated by method of present work. ^c Ref. 5, $\lambda = 436$ m μ . ^d Ref. 5, $\lambda = 310$ m μ . ^e Ref. 1.

Acknowledgments.—The authors wish to express their thanks to the National Science Foundation for financial assistance under Research Grant NSF-G12884 and to the Numerical Analysis Research Project of the UCLA Department of Mathematics and the Western Data Processing Center for access to the IBM 7090.

We also wish to thank Professor Tamres of the University of Michigan and Professor Searles of Kansas State University for their cooperation, especially in keeping us informed regarding their own progress and results prior to publication.

THE HEAT OF FORMATION OF DIFLUOROSILYLENE

BY JOHN L. MARGRAVE, ADLI S. KANAAN,
Department of Chemistry, University of Wisconsin,
Madison, Wisconsin

AND DONALD C. PEASE

E. I. du Pont de Nemours and Company, Wilmington, Delaware

Received December 14, 1961

Difluorosilylene (SiF₂) has been prepared in good yield by passing silicon tetrafluoride over silicon, silicon carbide, silicon metal alloy, or binary

silicides of polyvalent metals.¹ SiF₂ radicals are also important species in the decomposition of silicon tetrafluoride, along with SiF and SiF₃, and should be useful in the preparation of new compounds containing silicon and fluorine.

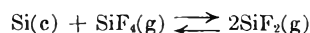
It is essential that SiF₂ be prepared under carefully controlled conditions of temperature, pressure, and quenching. Pease¹ reported a temperature in the range of 1100–1400°, an absolute pressure of not more than about 50 mm., and a quenching of the products to a temperature lower than about 0° within a period of 0.1 to 0.001 sec. as the preferable conditions for a successful reaction. While the product of the SiF₄ + Si (or silicide) reaction is essentially SiF₂ (monomer or polymer), the purity of the difluorosilylene is lowered by the presence of small amounts of silicon monofluoride, SiF, or silicon trifluoride, SiF₃.

The emission spectrum of SiF has been examined by various workers. Johns and Barrow² reported band systems in the Schumann region and in the infrared region as far out as 9000 Å. They estimate the ionization potential for SiF to be 7.3 e.v. and the heat of dissociation, D_{298} , to be about 125 kcal. Other band systems were reported by Johnson and Jenkins³ and some were analyzed by Eyster.⁴

The emission spectrum of SiF₂ in the region 2200–2500 Å. has been observed by Johns, *et al.*⁵ A more recent investigation of the spectrum in the region between 2180 and 5260 Å. has been made by Dasari and Venkateswarlu.⁶ Their analysis of the band system in the region 2755–2179 Å. shows that the SiF₂ molecule is non-linear and the molecular parameters of the lower electronic state are: (1) angle FSiF = $124 \pm 2^\circ$; (2) bond length Si–F = 1.49 ± 0.07 Å.

Compilations of thermodynamic functions for SiF₂ based on estimated molecular parameters are available in the JANAF Thermochemical Tables,⁷ which also report the heat of formation at 298°K. to be -118 ± 10 kcal. mole⁻¹ from bond energy arguments.

The experimental data of Pease¹ may be used to determine a heat of formation based on the reaction



at various pressures and temperatures. Although there is some trend with temperature, as shown in Table I, the heat of formation of SiF₂ must fall in the range -148 ± 4 kcal. mole⁻¹.

From this heat of formation of SiF₂ one computes the average energy of an Si–F bond as 148.5 kcal. This value is in fair agreement with the average bond energy calculated from the new heat of formation of

(1) D. C. Pease, U.S. Patent No. 2,840,588, June 24, 1958.

(2) J. W. C. Johns and R. F. Barrow, *Proc. Phys. Soc. (London)*, **71**, 476 (1958).

(3) R. C. Johnson and H. G. Jenkins, *Proc. Roy. Soc. (London)*, **116**, 327 (1927).

(4) E. H. Eyster, *Phys. Rev.*, **51**, 1078 (1937).

(5) J. W. C. Johns, G. W. Chantry, and R. F. Barrow, *Trans. Faraday Soc.*, **54**, 1589 (1958).

(6) R. R. Dasari and P. Venkateswarlu, *J. Mol. Spectroscopy*, **7**, 287 (1961).

(7) "JANAF Thermochemical Data," Volume 2, December 31, 1960, USAF Contract No. AF 33(616)-6149, Advanced Research Projects Agency, Washington 25, D. C.

TABLE I
 CALCULATED HEAT OF FORMATION OF DIFLUOROSILYLENE

T(°K.)	Equilibrium pressure (mm)			-R ln K	$\Delta \left(\frac{F^0 - H_{298}^0}{T} \right)$ cal. deg. ⁻¹ mole ⁻¹	$\Delta H_{298.16}$ (kcal./mole)	- ΔH_f^0 [SiF ₂ (g)] (kcal./mole)
	System	SiF ₄	SiF ₂ ^a				
1400	50	45	5	14.3	46.96	85.8	150.1
	5	2.5	2.5	11.4	46.96	81.6	152.2
1500	50	45	5	14.3	46.75	91.6	148.2
	5	2.5	2.5	11.4	46.75	87.2	149.5
	3	1.8	1.2	13.6	46.75	90.6	147.8
1600	50	45	5	14.3	46.54	97.4	144.3
	5	2.5	2.5	11.4	46.54	92.6	146.75

^a Estimated from yields of polymerized products.

SiF₄ (-386 kcal. mole⁻¹) as determined by Wise, *et al.*,⁸ using the direct reaction of silicon and fluorine.

(8) S. S. Wise, W. N. Hubbard, and J. L. Margrave, Argonne National Laboratory Report No. 6472, January, 1962.

THE ELECTRICAL CONDUCTIVITY OF SOLUTIONS OF METALS IN THEIR MOLTEN HALIDES. V. PRASEODYMIUM-PRASEODYMIUM TRICHLORIDE¹

BY A. S. DWORKIN, H. R. BRONSTEIN, AND M. A. BREDIG

Chemistry Division, Oak Ridge National Laboratory, Oak Ridge, Tennessee

Received November 24, 1961

The rapid increase in the electrical conductivity with metal concentration in solutions of Ce in CeCl₃² and of La in LaCl₃³ indicates a large proportion of conductance by electrons in the saturated solutions. In solutions of Nd in NdCl₃,³ on the other hand, a very small increase in conductivity indicates very little or no electronic conductance. These results reflect the large, systematic differences in the phase diagrams: no solid phase containing Ce or La in a valence state lower than three was found in the Ce-CeCl₃⁴ or La-LaCl₃⁵ systems, whereas in the Nd-NdCl₃ system an electrically insulating solid, NdCl₂, as well as NdCl_{2.27} and NdCl_{2.37}, exists.⁶ The present report deals with the Pr-PrCl₃ system, which is intermediate in that the phase diagram shows no solid PrCl₂, but only the mixed chloride PrCl_{2.3} stable in the rather small temperature range between 590 and 659°.⁷

Experimental

The reactivity of the solutions with ceramic materials⁸ necessitated the use of a conductivity apparatus in which two rigidly mounted parallel electrodes of molybdenum were im-

mersed in the melt contained in a molybdenum cup. The apparatus, experimental procedure, and determination of the cell constant are described elsewhere.^{2,3} A sapphire capillary cell⁹ was used to confirm the previously established conductivity of Cd-CdCl₂ solutions¹⁰ which served as standards to determine the cell constant of the parallel electrode assembly.^{2,3} Further measurements of the cell constant established its value with a precision of ±1%. The synthetic sapphire cell was used to measure the conductivity of the pure PrCl₃.

The PrCl₃ was prepared from the oxide in the same manner as LaCl₃ and NdCl₃.³

Results and Discussion

The specific conductivity, κ (ohms⁻¹ cm.⁻¹), for PrCl₃ is given by the equation

$$\kappa_{\text{PrCl}_3} = -1.189 + 2.75 \times 10^{-3}t$$

over the temperature range measured, 800-860°. These values and those for LaCl₃,³ CeCl₃,² and NdCl₃³ form a regular series of κ vs. t curves where κ decreases with increasing atomic number or decreasing size of the cation.

Conductivities of LaCl₃, PrCl₃, and NdCl₃ reported by Voight and Biltz¹¹ are considerably lower than ours. In subsequent papers, Biltz, *et al.*,¹² rejected the earlier values as being too low due to polarization. From repeated measurements on LaCl₃, corrections were estimated for the remaining salts. However, their final values, still about 10% lower than ours, were obtained at only one, fairly low frequency, 500 cycles, so that it still is doubtful whether polarization was completely eliminated. This, together with other possible effects such as purity of materials and bubble formation on the electrodes,^{12a} may account for their low results.

Table I lists the specific conductivity of Pr-PrCl₃ solutions at 830° up to a composition near saturation. A short extrapolation of the Pr-PrCl₃ conductivities obtained with the parallel electrode cell to that of pure PrCl₃ yields a specific conductivity in excellent agreement with the value determined by means of the sapphire cell.

The accelerated increase in conductivity with metal concentration in the La and Ce solutions has been attributed^{2,3} to increasing orbital overlap and gradual establishment of a conduction band

(9) H. R. Bronstein and M. A. Bredig, *J. Am. Chem. Soc.*, **80**, 2077 (1958).

(10) (a) A. H. W. Aten, *Z. physik. Chem.*, **73**, 578 (1910); (b) C. A. Angell and J. W. Tomlinson, *Discussions Faraday Soc.*, in press.

(11) A. Voight and W. Biltz, *Z. anorg. u. allgem. Chem.*, **133**, 277 (1924).

(12) (a) W. Biltz and W. Klemm, *Z. physik. Chem.*, **110**, 318 (1924); (b) W. Klemm and W. Biltz, *Z. anorg. u. allgem. Chem.*, **152**, 231 (1926).

(1) Work performed for the U. S. Atomic Energy Commission at the Oak Ridge National Laboratory, operated by the Union Carbide Corporation, Oak Ridge, Tennessee.

(2) H. R. Bronstein, A. S. Dworkin, and M. A. Bredig, *J. Phys. Chem.*, **66**, 44 (1962).

(3) A. S. Dworkin, H. R. Bronstein, and M. A. Bredig, *Discussions Faraday Soc.*, in press.

(4) G. W. Mellors and S. Senderoff, *J. Phys. Chem.*, **63**, 1111 (1959).

(5) F. J. Keneshea and D. Cubicciotti, *J. Chem. Eng. Data*, **6**, 507 (1961).

(6) L. F. Druding and J. D. Corbett, *J. Am. Chem. Soc.*, **83**, 2462 (1961).

(7) L. F. Druding and J. D. Corbett, to be published.

(8) H. R. Bronstein, A. S. Dworkin, and M. A. Bredig, *J. Phys. Chem.*, **64**, 1344 (1960).

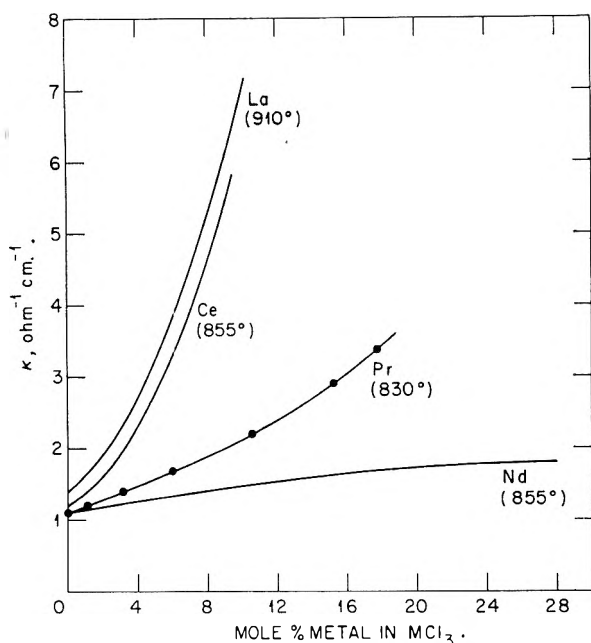


Fig. 1.—Specific conductivity of $M\text{-MCl}_3$ solutions.

TABLE I

SPECIFIC CONDUCTIVITY OF SOLUTIONS OF PRASEODYMIUM IN MOLTEN PRASEODYMIUM TRICHLORIDE AT 830°

Mole % Pr	κ (ohm ⁻¹ cm. ⁻¹)
0	1.09 (sapphire cell value)
0	1.10 (extrapolated, parallel electrode cell)
1.1	1.20
3.2	1.39
6.0	1.68
10.6	2.22
15.3	2.90
17.8	3.37

for electrons from $M \rightarrow M^{3+} + 3e$. These mobile electrons may be in equilibrium ($M^{3+} + e^- = M^{2+}$) with divalent metal ions known to exist in other rare earth systems.^{6,13} Conductivity measurements in the Nd-NdCl₃ system,³ where the stable insulating solid NdCl₂ is known, strongly indicate that the Nd²⁺ is not dissociated into Nd²⁺ + e⁻. Figure 1 shows the electrical behavior of Pr metal dissolved in molten PrCl₃ to be intermediate between La and Ce on the one hand and Nd on the other, but much closer to the latter. This behavior can be explained in terms of a Pr²⁺ ion whose stability in the melt is considerably greater than that of the relatively unstable La²⁺ and Ce²⁺ ions and close to that of stable Nd²⁺ ion. The upward curvature of the specific conductance vs. concentration curve (Fig. 1) for Pr-PrCl₃ can be attributed to the gradual overlap of the orbitals of the conduction electrons as discussed previously.³

(13) J. D. Corbett, L. F. Druding, W. L. Burkhard, and C. B. Lindahl, *Discussions Faraday Soc.*, in press.

INTERMOLECULAR ENERGY TRANSFER IN POLYETHYLENE-POLYBUTADIENE BLENDS DURING γ -IRRADIATION

BY MORTON A. GOLUB

Stanford Research Institute, Menlo Park, California

Received December 16, 1961

Although intramolecular transfer of excitational and/or ionizational energy in high polymers is well known and accounts, for example, for the pronounced radiation resistance of polystyrene compared to polyethylene, few instances of intermolecular energy transfer between different polymer molecules have been reported.

Recently, Dole and Williams^{1,2} found that in the γ -irradiation of a polyethylene-*cis*-polybutadiene blend at 142° the polyethylene was protected to some extent against decay of vinyl groups and evolution of hydrogen while the polybutadiene underwent *cis-trans* isomerization. An even greater protective effect was imparted to polyethylene by *trans*-polybutadiene but no isomerization of this polymer was detected, presumably because the radiostationary equilibrium is far over on the *trans* side³ and what *cis* units would be formed would be difficult to detect by infrared spectroscopy since their absorption coefficient is about one-fourth that of the corresponding *trans* units. Practically no protection or isomerization effects were observed in the room temperature irradiation of polyethylene-polybutadiene blends, apparently because of the non-homogeneous nature of the mixtures, which inhibits energy transfer from crystalline polyethylene to amorphous polybutadiene. These results are analogous to those obtained by Witt⁴ indicating no intermolecular energy transfer from polybutadiene to polystyrene in physical mixtures of these two polymers but considerable intramolecular energy transfer from the butadiene to the styrene segments in corresponding copolymers. Evidently, the physical mixtures of polybutadiene and polystyrene likewise were not sufficiently homogeneous to permit a significant amount of intermolecular energy transfer. Conceivably, a more intimate mixture of these polymers would show such transfer but this has not been achieved.

An estimate by this author³ of the *G*-value for isomerization of 5% *cis*-polybutadiene (CPB) in polyethylene (PE) at 142° gave a yield (based on the energy absorbed directly by CPB) of about four times that in the pure CPB. This result coupled with the observed protection in PE indicated the likely occurrence of intermolecular energy transfer in the PE-CPB blends. In fact, Dole and Williams^{1,2} attributed the reduction in hydrogen evolution to charge transfer, and the reduction in vinyl decay to transfer of excitation energy from the methylene groups in PE to the vinylene units in polybutadiene. The latter groups thus were con-

(1) M. Dole and T. F. Williams, *Discussions Faraday Soc.*, **27**, 74 (1959).

(2) T. F. Williams and M. Dole, *J. Am. Chem. Soc.*, **81**, 2919 (1959).

(3) M. A. Golub, *ibid.*, **82**, 5093 (1960); cf. footnote 5.

(4) E. Witt, *J. Polymer Sci.*, **41**, 507 (1959).

sidered to compete with the saturated paraffinic chains for positive ions and with the vinyl groups for the excitation energy. The purpose of this note is to compare the amount of energy which must have been transferred to CPB to bring about its enhanced isomerization with the amount of energy which had to be removed from PE to produce the observed protection.

Dole and Williams^{1,2} reported that in the 5% CPB-PE blend the increase in *trans*-vinylene content after a dose of 12×10^{20} e.v./g. at 142° was 2.4 times as great as in PE (Marlex 50) alone. The isomerization therefore represented $1.4 \times 3.95 \times 10^{-5}$ mole/g. (the vinylene growth in PE read off from Fig. 2, ref. 2) or $5.53 \times 10^{-5} \times 6.02 \times 10^{23} = 3.33 \times 10^{19}$ *trans* double bonds/g. polymer blend, or 6.66×10^{20} double bonds/g. CPB. For pure CPB γ -irradiated at room temperature to this same dose, 0.94% of the *cis* units are converted to *trans*,⁵ and since 95% of the original unsaturation is of the *cis*-vinylene type, the extent of isomerization is $(0.0094 \times 0.95 \times 6.02 \times 10^{23})/54 = 0.99 \times 10^{20}$ double bonds/g. CPB. It is to be noted that there was no effect of irradiation temperature on the isomerization rate for pure CPB. The isomerization yield in the PE-CPB blend is therefore 6.7 times that in CPB alone. This value is more accurate than the preliminary estimate mentioned above.

Accompanying this enhanced isomerization in CPB, PE was protected^{1,2} to the extent that $G_0(\text{H}_2)$ was reduced from 6.0 to 5.5 and $G_0(-\text{vinyl})$ was reduced from 12.5 to 11.48. The last figure was derived on the basis of the reported reduction in first order constant for vinyl decay from 2.09 to 1.92×10^{-21} g./e.v. Since the yields for the 5% CPB-PE blend apparently were based on the energy absorbed by both polymers, it is necessary for purposes of comparison to consider the effective $G_0(\text{H}_2)$ for PE in the blend as 5.5/0.95 or 5.8, and $G_0(-\text{vinyl})$ as 11.48/0.95 or 12.1.

It should be pointed out here that although the *G*-values for hydrogen evolution and vinyl decay are initial values, the isomerization yield in the polymer blend given above was calculated on the basis of observed integral values for the formation of *trans* units in both the blend and CPB alone. However, the isomerization, which is first order, is not extensive over the particular dose in question, so that the formation of *trans* units is essentially linear with dose. We therefore may consider the initial rate of isomerization in the PE-CPB blend likewise to be 6.7 times that in the pure CPB. Hence, in relating the results for the blend to those for CPB alone, the important quantities all correspond to initial values.

Each molecule of hydrogen evolved represents a consumption² of about 4.2 e.v. so that for each 100 e.v. absorbed in the polymer blend there is $0.95 \times$

4.2 (6.0–5.8) or 0.80 e.v. involved in protection against hydrogen production. Similarly, since the energy involved in activating a vinyl group electronically² is taken to be about 6.5 e.v., the energy removed from PE in protection against vinyl decay is $0.95 \times 6.5(12.5 - 12.1)$ or 2.47 e.v. The combined energy thus diverted from PE is 3.27 e.v./100 e.v. absorbed by the polymer blend. Of this 100 e.v., 5.0 is acquired directly by CPB, of which $0.05 \times 8.0 \times 5/4 \times 3.2$ or 1.6 e.v.⁶ is available for isomerization assuming no energy transfer. If the 3.27 e.v. removed from PE is transferred completely to the vinylene units in CPB the isomerization yield in the blend should be $(3.27 + 1.6/1.6)$ or 3.0 times as great as in the absence of such energy transfer. That this value is not quite half of that (6.7) calculated from the isomerization results indicates that the above estimate for the extent of intermolecular energy transfer in the PE-CPB blend is low by a factor of about 2.8. This discrepancy can be accommodated merely by the transfer of about 6% of the excitational and ionizational energy of PE to CPB over and above that diverted from PE in protection processes, which transfer should be energetically quite easy. The important conclusion to be drawn from this is that about a third of the excess isomerization of CPB in the blend can be accounted for in terms of energy transfer to the vinylene groups from excited vinyl and methylene groups in PE which otherwise would give rise to vinyl decay and hydrogen evolution, respectively. The remaining two-thirds of the energy transfer may be considered to involve other excited or ionized states of methylene groups in PE which, in the absence of CPB, would not normally result in hydrogen production.

The author gratefully acknowledges helpful discussion with Professor Malcolm Dole.

(6) Justification for the 5/4 factor may be seen in ref. 3.

THE RADIATION-INDUCED OXIDATION OF 4-*t*-BUTYLPYROCATECHOL IN AQUEOUS SOLUTIONS¹

BY GEORGE W. BLACK AND BENON H. J. BIELSKI

Department of Chemistry, Brookhaven National Laboratory, Upton, Long Island, New York

Received December 16, 1961

Earlier investigations²⁻⁵ of the effect of ionizing radiations on aqueous solutions of hydroquinones showed that this group of compounds can be used to study the primary decomposition products of water. Since studies of a series of substituted *p*-hydroquinones revealed a selective reactivity toward the free radicals formed during radiolysis of air-saturated 0.8 *N* sulfuric acid, it became the purpose of this study to investigate an *o*-hydroquinone under similar conditions.

(1) Research performed under the auspices of the U. S. Atomic Energy Commission.

(2) N. Waterman and H. Limburg, *Biochem. Z.*, **263**, 400 (1933).

(3) J. Loisleur and R. Latarjet, *Compt. rend. soc. biol.*, **135**, 1534 (1941).

(4) C. Vermeil and L. Salomon, *Compt. rend.*, **249**, 268 (1959).

(5) B. H. J. Przybielski-Bielski and R. R. Becker, *J. Am. Chem. Soc.*, **82**, 2164 (1960).

(5) Based on a revision of data given in ref. 3 involving the use of a new value of 3.65 for the ratio of the *trans* to *cis* absorption coefficients in place of the previous value of 1.89, which necessitated a recalculation of the *cis* contents of all polymer samples examined. As consequences of this revision, an initial *cis* content of 98.9% was reduced, e.g., to 97.9% after a dose of 22.1 Mr., and the $G_0(\text{cis} \rightarrow \text{trans})$ for the solid state isomerization was reduced from the earlier value of 14.6 to 8.0. Also the value of the radiostationary *cis/trans* ratio was changed from 20/80 to 33/67. Further consequences will be discussed in a subsequent publication.

Experimental

Irradiations.—A cylindrical source of Co^{60} γ -rays has been used. The energy absorption in solutions was determined periodically with the Fricke ferrous sulfate dosimeter.⁶ The dose rate for the source was calculated on the basis of $G(\text{Fe}^{+++}) = 15.5$ and was of the order of 2.0×10^{21} e.v./l.-hr. All irradiations were performed in pre-irradiated Pyrex glassware at temperatures between 25 and 30°.

Chemicals.—Triply distilled water and reagent grade chemicals were used throughout. The 4-*t*-butyl-*o*-quinone was prepared by silver oxide oxidation of 4-*t*-butyl-pyrocatechol.⁷ The latter compound was an Eastman Kodak product. Both compounds were purified by sublimation and had these melting points: 4-*t*-butylpyrocatechol 52–56°; 4-*t*-butyl-*o*-quinone 72°.

Analytical.—The radiation-induced disappearance of 4-*t*-butylpyrocatechol and the appearance of the corresponding quinone in 0.8 *N* sulfuric acid solutions were followed spectrophotometrically on a Beckman DU spectrophotometer. All measurements were taken at 25°. The measurements in the ultraviolet region were taken in 1-cm. quartz cuvettes; 10-cm. quartz cells were used in the visible range. The extinction coefficients used in this study are given in Table I.

The hydrogen peroxide formed in this system was determined by the titanium method.⁸ The details of this analytical procedure have been described elsewhere.⁵

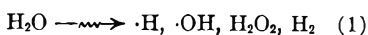
TABLE I
EXTINCTION COEFFICIENTS AT 25° IN 0.8 *N* SULFURIC ACID SOLUTION

Compound	Wave length, Å.	Slit width, mm.	Molar ext. coefficient
4- <i>t</i> -Butylpyrocatechol	2600	0.70	715 ± 10
	2790	.60	2750 ± 20
	4000	.05	5 ± 5
4- <i>t</i> -Butyl- <i>o</i> -quinone	2600	.70	3600 ± 20
	2790	.50	2380 ± 20
	4000	.05	930 ± 25

Results and Discussion

When 4-*t*-butyl-pyrocatechol is irradiated with Co^{60} γ -rays in air-saturated 0.8 *N* sulfuric acid, it is oxidized to the corresponding 4-*t*-butyl-*o*-quinone. Since it had been found experimentally that the ratio $G(4\text{-}t\text{-butylpyrocatechol})/G(4\text{-}t\text{-butyl-}o\text{-quinone}) = 1.02$, only the appearance of the quinone was followed. An investigation for organic products other than 4-*t*-butyl-*o*-quinone gave negative results. It was found that the G -values for the appearance of 4-*t*-butyl-*o*-quinone and hydrogen peroxide were independent of total dose, dose rate, and initial concentration of 4-*t*-butylpyrocatechol above 5.0×10^{-3} mole/l. The G -values for this system reported in Table II were obtained in irradiation experiments in which the exposure time did not exceed 2 min. and the conversion of *o*-hydroquinone to *o*-quinone was less than 1%.

The behavior of an irradiated aqueous system may be described in terms of its decomposition into radical and molecular products. For air saturated 0.8 *N* sulfuric acid irradiated with Co^{60} γ -rays the G -values used were⁵



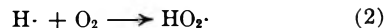
$$G(\text{H}_2\text{O}) = 4.48; G_{\text{H}} = 3.68; G_{\text{OH}} = 2.92; G_{\text{H}_2\text{O}_2} = 0.78; G_{\text{H}_2} = 0.40$$

If it is assumed that the $\text{H}\cdot$ radical formed during radiolysis reacts primarily with molecular oxygen in air-saturated solutions

(6) J. Weiss, *Nucleonics*, **10**, 28 (1952).

(7) R. Willstätter and A. Pfannenstiel, *Ber.*, **37**, 4744 (1904).

(8) G. M. Eisenberg, *Ind. Eng. Chem., Anal. Ed.*, **15**, 327 (1943).



then there are three oxidative species present during irradiation, namely, $\cdot\text{OH}$, $\text{HO}_2\cdot$, and H_2O_2 . From radiation studies of a series of *p*-hydroquinones in 0.8 *N* sulfuric acid, it had been postulated⁵ that hydroquinones can react with the above oxidative species in three distinct ways: A. The hy-

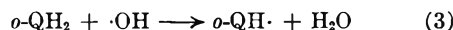
TABLE II

G -VALUES FOR THE IRRADIATION OF 4-*t*-BUTYLPYROCATECHOL IN AIR-SATURATED 0.8 *N* SULFURIC ACID

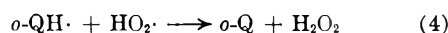
Orig. concn. of <i>o</i> -QH ₂ , mole/l.	$G(\text{Q})$	$G(\text{H}_2\text{O}_2)$
5.0×10^{-4}	2.20 ± 0.07	3.70 ± 0.11
1.0×10^{-3}	$2.52 \pm .06$	$3.86 \pm .16$
2.5×10^{-3}	$2.78 \pm .08$	$3.90 \pm .14$
5.0×10^{-3}	$2.92 \pm .08$	$4.12 \pm .14$
7.5×10^{-3}	$2.91 \pm .06$	$4.22 \pm .10$
1.0×10^{-2}	$2.96 \pm .08$	$4.14 \pm .12$
1.5×10^{-2}	$2.93 \pm .08$	$3.98 \pm .16$

droquinone reacts with $\cdot\text{OH}$ radicals only; B. The hydroquinone reacts with $\cdot\text{OH}$ and $\text{HO}_2\cdot$ radicals; C. The hydroquinone reacts with $\cdot\text{OH}$, $\text{HO}_2\cdot$, and H_2O_2 .

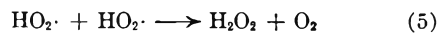
The present investigation indicates that still another possibility exists. 4-*t*-Butylpyrocatechol does not react with hydrogen peroxide in 0.8 *N* sulfuric acid. Experimental results indicate the 4-*t*-butylpyrocatechol (*o*-QH₂) is oxidized only by the $\cdot\text{OH}$ radical to the corresponding semiquinone



Although the $\text{HO}_2\cdot$ radical is not a sufficiently strong oxidizing agent to abstract a hydrogen atom from 4-*t*-butylpyrocatechol, it apparently is able to oxidize the semiquinone formed in reaction 3 to the corresponding *o*-quinone



From the above G -values it is evident that the $\text{H}\cdot$ radical, and hence assuming (2) the $\text{HO}_2\cdot$, is formed in excess over the $\cdot\text{OH}$ radical during radiolysis. The excess of $\text{HO}_2\cdot$ equal to $(G_{\text{H}} - G_{\text{OH}})$ is assumed to disproportionate by the process



The above mechanism predicts these G -values for the formation of 4-*t*-butyl-*o*-quinone and hydrogen peroxide

$$G(4\text{-}t\text{-Butyl-}o\text{-quinone}) = G_{\text{OH}}$$

$$G(\text{Hydrogen Peroxide}) = H_{\text{H}_2\text{O}_2} + \frac{1}{2}G_{\text{OH}} + \frac{1}{2}G_{\text{H}}$$

or

	$G_{\text{calcd.}}$	$G_{\text{obsd.}}$
$G(4\text{-}t\text{-Butyl-}o\text{-quinone})$	2.92	2.93 ± 0.03
$G(\text{Hydrogen Peroxide})$	4.08	4.12 ± 0.03

The close agreement between the calculated and observed values seems to support the suggested mechanism.

Acknowledgments.—We wish to thank Drs. H. A. Schwarz and G. Czapski for stimulating discussions and for reading the manuscript.

THE BISMUTH-SULFUR PHASE DIAGRAM¹

BY DANIEL CUBICCIOTTI

Stanford Research Institute,
Menlo Park, California

Received December 21, 1961

The phase diagram of the Bi-Bi₂S₃ system from pure Bi to mixtures containing as much as 0.55 atom fraction S has been investigated by several workers.²⁻⁴ For mixtures containing more S the pressure became too great for the glass bulbs used by Pélabon and Aten. It is not clear what containers were used by Urazov, *et al.*

We have found that small silica-glass bulbs were strong enough to resist the pressures, so that we could contain even pure sulfur under its own vapor pressure up to the temperatures required for this work. In attempting standard thermal analyses of the mixtures we encountered two problems: (a) the melts showed decided supercooling; and (b) bulbs made with internal thermocouple wells almost invariably broke. Therefore, we decided to determine the liquidus curve by visually observing the point at which the last solid disappeared as the mixture was heated.

Experimental

Weighed amounts of 99.999+ % Bi and S, from American Smelting and Refining Company, were sealed into evacuated silica-glass bulbs. The bulbs were about 7 cm. long and made of 25-mm. o.d., 1-mm. wall tubing for low-S, and of 12-mm. o.d., 2-mm. wall tubing for high-S samples. A Pt-10% Rh thermocouple, calibrated at the Al, Pb, Sn, and Zn points, was tied to the outside. The bulb was heated in a furnace having a 5 mm. longitudinal window-slot with a Vycor tube inside to act as a window. The sample bulb could be manipulated by a handle.

As a sample of Bi and S was heated, the S was observed to melt first, then the Bi. Shortly thereafter a rapid, exothermic reaction occurred between them to form a gray, spongy mass of Bi₂S₃. For all mixtures having less than 0.67 atom fraction S, the sample melted to a silver metallic liquid, from which needles (presumably Bi₂S₃) separated with sufficient cooling. The dissolution of these needles in the metallic liquid was observed as the sample was shaken and heated slowly (2 to 3 degrees per minute near the disappearance temperature). The temperature at which the last solid disappeared was recorded as the liquidus temperature for the mixture. Repeated trials on a sample agreed to better than 3°. Pure Bi was found to liquefy over a short temperature range ending at 271°. Stoichiometric Bi₂S₃ also melted over a short temperature range, as a congruently melting substance, at 775°. These substances would be expected to have sharp melting points. Their melting over a short range of temperature probably was due to temperature gradients in the bulb.

Samples with atom fraction S of 0.15 and 0.40 were cooled after solution temperature determinations and examined under a microscope after being cut and polished. Two phases were observed, a crystalline precipitate and a matrix material. The relative amounts of these two phases agreed with the amounts expected if the precipitate were Bi₂S₃ and the matrix Bi.

X-Ray powder photographs were made of samples that had the composition and (60-hr.) equilibration temperature marked by X's in Fig. 1. All the lines of these samples could be fit to either those of Bi or Bi₂S₃.

These examinations of the cooled samples indicated, therefore, that only two phases were present—Bi and Bi₂S₃. This point may seem belabored; however, it seemed possible that an incongruently-melting compound of stoichiometry

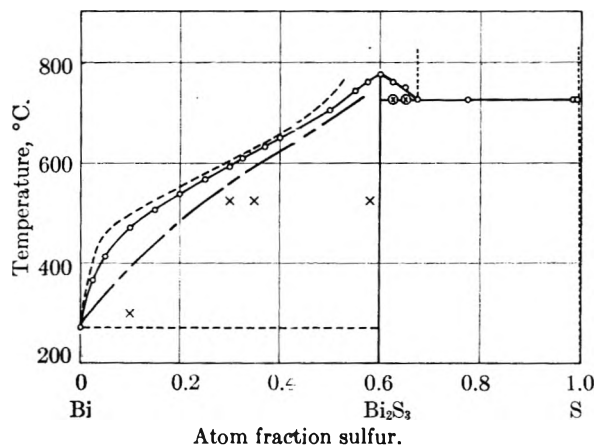


Fig. 1.—The Bi-S phase diagram: full curve, liquidus for the present work; dotted curve indicates region of two immiscible liquids; dashed curve, data of Aten (ref. 2); broken curve, data of Urazov, *et al.* (ref. 4).

Bi₂S might have formed by analogy with BiCl, BiBr, and BiI.⁵ No evidence for such a compound was observed.

Compositions of atom fraction S greater than 0.67 consisted of two liquids above 727°. The denser liquid was silvery (and presumably of composition 0.67 atom fraction S—see Fig. 1). The lighter liquid was dark brown in color and almost pure S. In a sample of 0.992 atom fraction sulfur, the "silver" liquid phase still was observed above 727°, *i.e.*, it had not all dissolved in the S phase. After rapid cooling, the solidified S phase was found to contain small silvery crystals as though some Bi₂S₃ had been in solution in the molten S.

The vapor over the molten samples of atom fraction S about 0.65 and greater was very dark, almost indistinguishable from the liquid S phase. The intensity of the vapor color diminished with reduction of S content below 0.67 such that in the range 0.58 to 0.60 it was difficult to see whether the vapor was colored (because of the background color of the furnace). Below 0.58 the vapor appeared colorless. A rough estimate of the amount of S in the vapor indicated that only a negligible correction was to be applied to the atom fractions of the condensed phases.

Results

The liquidus of the Bi-S phase diagram, under its equilibrium gas pressure, derived from these measurements is given in Fig. 1. The circles represent the temperatures at which the "silver" phase was completely liquefied. The two circles containing crosses represent the temperature at which the "silver" phase appeared completely solidified.

The diagram between Bi and Bi₂S₃ apparently is a eutectic type with the eutectic very close to Bi. Our results are in general agreement with those of other workers. The lack of better agreement may be due to impurities in the materials used by the other workers. Aten reports that his Bi froze at 277°, while recent determinations⁶ of the melting point give 271.0°. Urazov, *et al.*,⁴ report using Bi of 99.8% and "flowers of sulfur." It has been our experience that "flowers of sulfur" when boiled away under nitrogen leaves a substantial amount of charred residue.

The part of the diagram from Bi₂S₃ to S has not been reported before this. The results indicate that Bi₂S₃ is a congruently melting compound. The liquid dissolves S up to an atom fraction of

(1) This work was made possible by the financial support of the Research Division of the United States Atomic Energy Commission.

(2) H. Pélabon, *J. chim. phys.*, **2**, 320 (1904).

(3) A. H. W. Aten, *Z. anorg. Chem.*, **47**, 386 (1905).

(4) G. G. Urazov, K. A. Bol'shakov, P. I. Fedorov, and I. I. Vasilevskaya, *Russ. J. Inorg. Chem.*, **5**, 303 (1960).

(5) (a) S. J. Yosim, A. J. Darnall, W. G. Gehman, and S. W. Mayer, *J. Phys. Chem.*, **63**, 230 (1959); (b) S. J. Yosim, L. D. Ransom, R. A. Sallach, and L. E. Topol, *ibid.*, **66**, 28 (1962).

(6) National Bur. Standards, Circ. 500, 1952.

0.67 and additional S gives rise to a second liquid phase of almost pure S. The limits of miscibility of these two liquids were not investigated and so are represented as dotted lines.

Acknowledgments.—Much of the experimental work was performed by Mr. William E. Robbins. Dr. J. W. Johnson showed us that silica-glass would stand up to these conditions.

THE COLOR OF MERCURIC IODIDE ON ALUMINA

By HARRY GOYA, JOHN L. T. WAUGH, AND HARRY ZEITLIN

*Department of Chemistry, University of Hawaii,
Honolulu, Hawaii*

Received December 22, 1961

The red, tetragonal modification of mercuric iodide undergoes an enantiotropic transformation to a yellow, orthorhombic form when heated above its transition temperature of 127°. When initially precipitated from solution or when formed from the vapor phase, the yellow modification reverts spontaneously to the red, normally stable form. Recently, a red to yellow transition has been observed to take place, apparently similar to the transformation which takes place on heating above the transition temperature, when mercuric iodide is adsorbed on alumina at normal atmospheric temperatures.¹ However, in the adsorbed state under anhydrous conditions, the yellow species remains as such indefinitely. In a preliminary communication, this phenomenon was attributed to a polymorphic conversion, rather than to any change in particle size or to ionization by polarization.^{2,3} It now has been established, by means of X-ray powder, diffraction studies, reflectance analysis, and microscopic examination that the yellow material, which is stable when adsorbed on alumina at atmospheric temperatures, is the same species which results on heating mercuric iodide above 127°.

Experimental

Reagents.—Woelm alumina, grade 1 activity, ground to less than 200 mesh; C.P. grade sodium fluoride, less than 140 mesh; reagent grade mercuric iodide, less than 200 mesh; all mesh sizes refer to U.S. standard screens. The alumina and sodium fluoride were dried for 48 hr. at 115° prior to use and desiccated until required. Samples containing 8% by weight of mercuric iodide adsorbed on alumina were used.

Apparatus and Procedure. The powdered samples were packed into lithium borate glass capillaries of 0.5 mm. diameter and 0.01 mm. wall thickness and mounted in a 114.59 mm. diameter Straumanis-Wilson camera, to record their X-ray powder diffraction patterns, using Cu K α radiation.

The diffuse reflection spectra of the solid mixtures were measured with a Beckman DK-2 automatic recording spectrophotometer, equipped with a reflectance attachment; absorbance as a function of wave length was examined. Concentrations used were 200 mg. of adsorbate mixed with 10 g. of adsorbent. The samples were mixed, mechanically agitated for 6 to 9 min., and poured into 6-ml. cylindrical, quartz cells of 1-cm. light path, which were fitted with ground glass stoppers. The reflection spectra were measured at varying intervals of up to 45 days, after initial mixing.

(1) H. Goya and H. Zeitlin, *Nature*, **18**, 1941 (1959).

(2) E. Weitz and F. Schmidt, *Ber. Deut. Chem. Ges.*, **12**, 2099 (1939).

(3) G. Kortum, J. Vogel, and W. Braun, *Angew. Chem.*, **21**, 651 (1958).

Microscopic examination of the adsorption-desorption phenomena was carried out with a Bausch and Lomb polarizing microscope; photomicrographs (100 \times and 450 \times) of the various samples were taken with an Exa single lens reflex camera with adapter.

Results

Spectral Reflectance.—Mercuric iodide mixed with alumina was found to show a gradual increase in absorbance at 290 m μ , at the same time the absorption peak at 575 m μ decreases steadily and finally becomes unobservable. When adsorbed on sodium fluoride the color of the mercuric iodide remains unchanged, the discrete absorption maxima at 293 and 573 m μ increasing only slightly with time, without any shift in the wave length being detectable. Exposure of the mercuric iodide-alumina mixtures to the moist atmosphere was observed to result in desorption of the iodide. This process also was followed by reflectance measurements and the observed spectra indicated that the changes occurring were essentially the reverse of the adsorption process.

Microscopic Studies.—Red mercuric iodide is soluble in acetone to form a colorless solution. Crystallization from this solution, and the subsequent transformation of the red to the yellow modifications on heating and the reverse conversion from the yellow to the red forms on cooling were carefully observed at various magnifications. Similar observations were made of the yellow material on desorption from alumina and its subsequent reversion to the red variety. This latter effect could be accomplished either mechanically, by suitable prodding with a needle, or by moistening the yellow material adsorbed on alumina; in either case, the yellow material is initially detached from the alumina as yellow crystals, which then transform to the red variety, in a manner very similar to the initial precipitation of mercuric iodide from solution as the yellow form. The homogeneous nature and the stability of the yellow iodide when adsorbed on alumina is quite remarkable.

X-Ray Diffraction Data.—Powder photographs of the red, tetragonal mercuric iodide showed narrow, well-defined diffraction maxima, while those of alumina and of mercuric iodide adsorbed on alumina displayed broader, more diffuse maxima. The relative intensities and the observed interplanar spacing values as obtained from the powder photographs are shown in Table I. The spacings for the mercuric iodide-alumina mixture are those observed after subtracting the spacings which correspond to those due to alumina. The interplanar spacings corresponding to the strongest arcs on the red mercuric iodide photographs are not observed for the yellow mixture and those corresponding to the medium and weak arcs are dissimilar. It was not possible to obtain a powder photograph of the pure, yellow form of mercuric iodide. However, from the unit cell dimensions of the yellow form reported in the literature,^{4,5} interplanar spacings were calculated for a small field of indices hkl with the results shown in the last column of the table.

(4) W. S. Gorsky, *Physik Z. Sowjetunion*, **5**, 367 (1934).

(5) H. J. Verweel and J. M. Bijvoet, *Z. Krist.*, **77**, 122 (1931).

TABLE I
 "d VALUES" FOR MERCURIC IODIDE (RED), ALUMINA, AND
 YELLOW MERCURIC IODIDE ADSORBED ON ALUMINA

Red mercuric iodide		Alumina		Yellow mercuric iodide on alumina		
d_{obsd} (Å.)	Relative intensity ^a	d_{obsd} (Å.)	Relative intensity	d_{obsd} (Å.)	Relative intensity	d_{calc} (Å.)
13.93	w	4.79	md	7.14	s	7.31
9.92		4.38		6.63		6.46
8.25	w	3.12	vwd	4.45	w	4.43
7.05		2.88	md	3.82		3.87
6.02	w	2.69		3.74	m	3.66
4.09	m	2.47	s	3.51	s	3.54
3.53	m	2.33	d	3.41		3.44
2.96	m	2.27	md	2.85	m	2.86
2.73	m	2.15	md	1.96	w	
2.50	w	2.08	d	1.71	vw	
2.17	s	2.01	vsd	1.61	vvw	
2.09	w	1.93	d	1.44	vvw	
2.03	m	1.87	vwd	0.998	vw	
1.92	w	1.56	md	0.811	vw	
1.85	m	1.48	wd	0.796		
1.75	w	1.41	vsd	0.772	w	
1.64	w	1.37	d			
1.54	w	1.14	wd			
1.53	w	1.01	wd			
1.49	m	0.997	d			
1.46	w	0.890	vwd			
1.43	vw	0.871	d			
1.40	m	0.865	vw			
1.36	w	0.812	md			
1.34	w	0.798	d			
1.31	m	0.771	w			
1.26	s					
1.25						
1.23	w					
1.21	vw					
1.19	w					
1.15	w					
1.09	w					
1.08	w					
1.04	vw					
1.03	vvw					
0.977	w					
0.963	w					
0.942	w					
0.922	w					
0.891	w					

^a v, very; s, strong; m, medium; w, weak; d, diffuse.
^b Orthorhombic unit cell with $a_0 = 4.674$ Å.; $b_0 = 13.76$ Å.; $c_0 = 7.32$ Å.

Discussion

On the basis of the evidence reported above, the very marked color transformation from red to yellow, when mercuric iodide is adsorbed on the active adsorbent alumina but not on sodium fluoride, obviously is not due simply to a change in particle size. Two distinct and stable phases are involved before and after adsorption. The stability of the yellow form on alumina is quite remarkable; no trace of decomposition could be observed on heating to 130° in a vacuum oven for several hours, whereas the yellow modification of mercuric iodide itself decomposes substantially under these circumstances. The spectral reflectance measurements as well as the optical and X-ray diffraction data all point to a polymorphic

conversion and to the exclusion of any ionization of the type referred to by Weitz and Schmidt.² It is believed that the energy released on adsorption of mercuric iodide on alumina transforms the red, stable modification to the yellow form, which continues to exist as such in the adsorbed state, as long as moisture is excluded, under the influence of the polarizing action of the crystal field of the alumina.

The work described was supported in part by grants from the Petroleum Research Fund and the Research Corporation of New York (to H.Z.).

WETTING PROPERTIES OF ACRYLIC AND METHACRYLIC POLYMERS CONTAINING FLUORINATED SIDE CHAINS

BY MARIANNE K. BERNETT AND W. A. ZISMAN

U. S. Naval Research Laboratory, Washington, D. C.

Received January 6, 1962

Recent studies^{1,2} have shown that several new types of solid polymers have lower surface energies than polytetrafluoroethylene. These materials are copolymers of tetrafluoroethylene and hexafluoropropylene (HFP) in various molar proportions and a HFP homopolymer. Depending upon the molar proportions of the polymer constituents, the critical surface tension of wetting (γ_c) of the respective copolymer decreases as perfluoromethyl groups in each surface replace perfluoromethylene groups and reaches its lowest value of 16.2 dynes/cm. for poly-HFP, which in this series presents the highest proportion of perfluoromethyl groups in the surface.

The present investigation reports on the wettability of two partially fluorinated polymers. In each polymer the molecular portion determining the surface energy is a linear seven or eight carbon perfluoro chain linked to the polymer backbone by a different group. If such perfluoro chains could orient vertically in close packing at the surface, they should present the lowest surface energy as yet reported for a bulk solid, comparable to the surface energy of monolayers of perfluoroalkanoic acids³ and 17-perfluoroalkylheptadecanoic acids.⁴

Experimental

The two polymers studied were pure experimental compounds generously donated for this investigation by the Commercial Chemicals Department of the Minnesota Mining and Manufacturing Company. Each was in the form of a 20% solution in xylene hexafluoride. The formulas of the respective homopolymers are $C_7F_{15}CH_2OOC-C(CH_3)=CH_2$ (polymer A) and $C_8F_{17}SO_2N(C_3H_7)-CH_2CH_2OOC-CH=CH_2$ (polymer S). The films were cast by pouring measured quantities on smooth Pyrex and stainless steel surfaces, with later slow and controlled evaporating of the solvent at room temperature in a dust-free environment and a final exposure for 24 hr. in a vacuum oven at 50°. The resulting smooth and specular films, which were from 6 to 9 mils thick, adhered well to the underlying surface. They were firm and transparent and could be removed in small fragments only by chipping from the substrate. Liquids for the wetting studies and the procedure for their purification have

(1) M. K. Bennett and W. A. Zisman, *J. Phys. Chem.*, **64**, 1292 (1960).

(2) M. K. Bennett and W. A. Zisman, *ibid.*, **65**, 2266 (1961).

(3) E. F. Hare, E. G. Shafrin, and W. A. Zisman, *ibid.*, **58**, 236 (1954).

(4) E. G. Shafrin and W. A. Zisman, *ibid.*, **66**, 740 (1962).

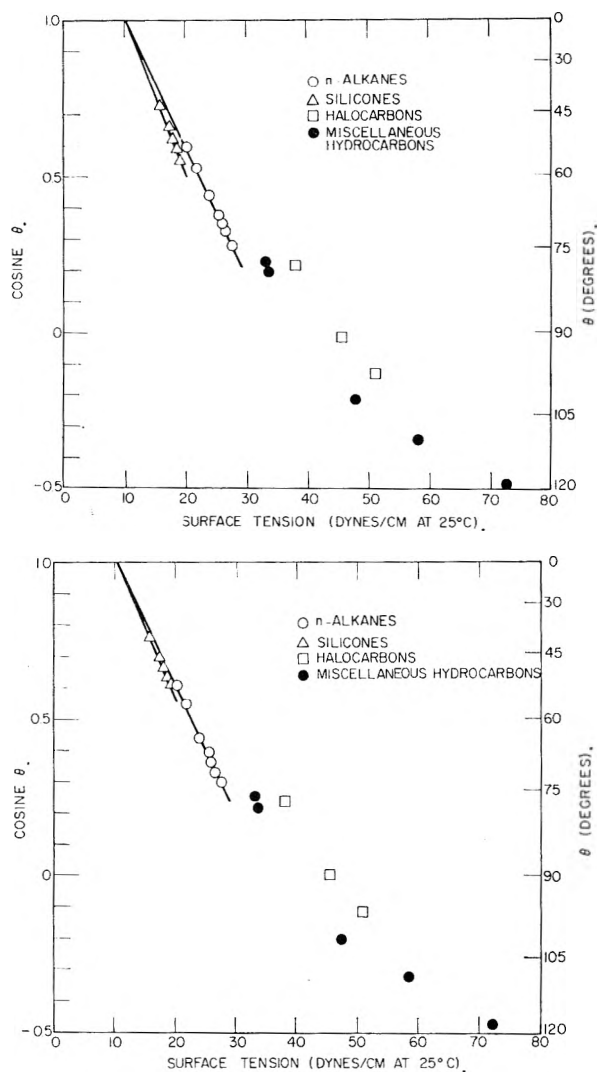


Fig. 1.—Wettability by various liquids of cast films: upper (a) of polymer A; lower (b) of polymer S.

been described previously,^{5,6} as has the method of measuring contact angles.⁷ A series of Dow Corning silicone fluids, DC 200,⁸ of various viscosities and surface tensions ranging from 15.9 to 19.2 dynes/cm. at 25° also were included in this study in order to observe the wetting behavior with liquids having surface tensions below 20 dynes/cm. All measurements were made at 25 ± 1° and 50 ± 2% relative humidity.

Experimental Results and Discussion

The wettability curves for the polymer films are independent of the substrates. These curves are shown in Fig. 1a and 1b for polymer A and polymer S, respectively. Values of γ_c obtained by the homologous series of *n*-alkanes are 10.6 dynes/cm. for polymer A and 11.1 dynes/cm. for polymer S. The DC 200 liquids produced the same value of γ_c as the *n*-alkanes for polymer A and varied only 0.1 dyne/cm. for polymer S. Graphical points for the other families of liquids used each fitted linear curves, but their extrapolated intercepts do not coincide with the value defined by the *n*-alkanes. Similar effects had been observed and discussed in

previous investigations.^{5-7,9} It also can be seen that deviations from a straight line resulted with the hydrogen-bonding liquids, such as formamide and ethylene glycol. Such deviations for liquids having a surface tension above 45 dynes/cm. are in agreement with the results of Ellison and Zisman on halogenated organic solid surfaces.⁹

The critical surface tensions of 10.6 and 11.1 dynes/cm. of these two polymers are by far the lowest ever reported on any bulk solid organic surface. They compare with the γ_c values of 8.6 and 7.9 dynes/cm. characteristic for monolayers of perfluorohexanoic acid and perfluorooctanoic acid,³ and the γ_c values of 8.0 and 11.4 dynes/cm. determined for perfluoroheptyl- and perfluoropentyl-heptadecanoic acids, respectively.⁴ Since the γ_c values of the free surface of these polymeric coatings approach those of the vertically oriented and closely packed monolayers, one must conclude that the orientation and packing of the perfluoro side chains also closely approach those of the acid monolayers. The high contact angles of the cast polymer films thus are due to the adlineation of the long fluorinated side chains. The resulting surface is characterized by a closer packing of the terminal $-\text{CF}_3$ groups than is possible in a linear polymer such as poly-HFP, whose side chains consist of $-\text{CF}_3$ groups only, and whose surface is theoretically constituted of alternating $-\text{CF}_2-$ and $-\text{CF}_3$ groups.

It can be seen in Fig. 1 that the polymer with the $-\text{C}_8\text{F}_{17}$ side chain has a slightly higher γ_c value than the polymer having a $-\text{C}_7\text{F}_{15}$ side chain. From previous studies one would expect the compound with the longer perfluoro chain to exhibit a lower γ_c value than that with the shorter chain. This seeming irregularity can be explained on inspection of Stuart-Briegleb molecular ball models. The $-\text{C}_8\text{F}_{17}$ chains of the polymers pack less closely than the $-\text{C}_7\text{F}_{15}$ chains of polymer A because they are connected to the polymer backbone by much longer and bulkier groups which occupy larger spaces. Thus, the fluorinated chains do not necessarily adlineate since they are allowed a certain amount of freedom in spatial arrangement. On the other hand, the shorter and more compact side chains of polymer A force their perfluoro groups to orient vertically in the closest packing possible. Spatially, then, it is not the length of the perfluoro chain, but the total molecular side group that is determinant in the orientation and packing, and since closer packing can be achieved by the polymer A perfluoro chains it is this polymer that exhibits the lower γ_c value.

(9) A. H. Ellison and W. A. Zisman, *J. Phys. Chem.*, **57**, 622 (1953).

DETERMINATION OF THE STABILITY CONSTANTS OF COMPLEXES BY GAS CHROMATOGRAPHY

By E. GIL-AV AND J. HERLING

Daniel Steff Research Institute, Weizmann Institute of Science, Rehovoth, Israel

Received January 8, 1962

As gas chromatography permits convenient measurement of the partition coefficient between a gas and a liquid phase, it seemed likely that the

(5) H. W. Fox and W. A. Zisman, *J. Colloid Sci.*, **5**, 514 (1950).

(6) H. W. Fox and W. A. Zisman, *ibid.*, **7**, 428 (1952).

(7) E. G. Shafrin and W. A. Zisman, *ibid.*, **7**, 166 (1952).

(8) Dow Corning, Silicone Notes 3-106 b (1960).

method also could be used for the determination of stability constants.¹⁻³ The feasibility of this approach has been demonstrated in an investigation of olefin-silver ion complexes in ethylene glycol solutions.

Making the plausible assumption that the ratio of olefin (B) to silver ion is 1:1,⁴ the relationship between the stability constant $K = [\text{BAg}^+]/[\text{B}][\text{Ag}^+]$ and the partition coefficient (amount of solute per unit volume of stationary phase/amount of solute per unit volume of gas phase) is expressed by

$$K = (k - k_0)/k_0[\text{Ag}^+]$$

where k is the partition coefficient of the olefin between the silver nitrate-glycol and the gas phase, k_0 is the partition coefficient of the olefin between ethylene glycol containing sodium nitrate and the gas phase, and $[\text{Ag}^+]$ is the silver ion concentration (mole/l.).

k and k_0 were calculated from the specific retention volume V_g^s of the olefin on ethylene glycol containing 1.77 mole/l. of AgNO_3 and NaNO_3 , respectively. The stationary phase was coated in the ratio 1:3 on acid treated firebrick of 50-80 mesh, packed into glass tubes of 1 m. length and 4.2 mm. diameter. The temperature was 30° and the flow of helium 80-100 ml./min.

Since the activity coefficient (γ) of a solute can be determined easily by gas chromatography,⁶ it is further possible to calculate from the experimental data the value of $K'_0 = K/\gamma_B$, which is proportional to the thermodynamic equilibrium constant $K_0 = K\gamma_{\text{BAg}^+}/\gamma_{\text{Ag}^+}\gamma_B$. At first approximation the ratio $\gamma_{\text{BAg}^+}/\gamma_{\text{Ag}^+}$ can be considered to be constant for a given ionic strength, and to change relatively little with the nature of the olefin in the series studied.⁷

Olefins coordinate practically instantaneously with silver ion,⁴ and therefore equilibrium conditions were expected to prevail at every point of the column. In order to test this assumption, the stability constants (K) for cyclohexene and octene-1 also were determined in the conventional way^{4,8} by distribution between two liquids (ethylene glycol, containing 1.77 mole/l. silver nitrate, and cyclohexane). The two methods were in good agreement (octene 3.2 and cyclohexene 7.2, as compared with 3.3 and 7.7, respectively, by gas-liquid phase chromatography). In both procedures the largest error is due to the relatively small solubility (corresponding to a small V_g) of the olefins in the solvent containing NaNO_3 . In the experimental conditions, the measurement of K is estimated to be accurate within $\pm 5\%$ and compares favorably with the conventional method.^{4,8}

Except for the obvious interest of readily permitting measurements of complex-stability in organic solvents, the procedure further has the advantage of requiring only a few mg. of substance, which need not be purified previously.

Results are given in Table I. Comparing the data for the 1-alkyl cycloolefins (I and VIII) with the corresponding 3- and 4-alkyl isomers (II, III, IX, and X), it is seen that a methyl substituent at the double bond markedly reduces the stability of the complex, and the same effect is evident from the lower constant of VI as compared with IV. The observed influence of the methyl group is in accord with reported data for metal-olefin complexes, and has been ascribed essentially to steric effects in the case of silver coordination compounds.⁹ As the bulk of the substituent is increased, the stability is further decreased (compare I, V, and VII).

TABLE I
STABILITY CONSTANTS OF OLEFIN-SILVER ION COMPLEXES
AT 30° IN ETHYLENE GLYCOL SOLUTION
(1.77 N AgNO_3)

	Compound	k_0	k	K	γ_B	$K'_0 \times 10^4$
I	1-Methylcyclohexene	27.9	90	1.25	290	43
II	3-Methylcyclohexene	23.0	250	5.5	265	210
III	4-Methylcyclohexene	23.0	230	5.1	265	190
IV	Methylenecyclohexane	24.3	440	9.6	270	350
V	1-Ethylcyclohexene	55.8	185	1.3	405	32
VI	Ethylidenecyclohexane	55.8	355	3.0	450	67
VII	1-Isopropylcyclohexene	69.5	200	1.05	845	12.5
VIII	1-Methylcyclopentene	13.0	80	2.9	165	175
IX	3-Methylcyclopentene	10.0	225	12.0	145	810
X	4-Methylcyclopentene	10.6	115	5.5	140	400
XI	Methylenecyclopentane	13.4	155	6.0	160	370
XII	1-Ethylcyclopentene	24.3	180	3.6	285	125
XIII	3-Ethylcyclopentene	19.2	420	11.8	285	415
XIV	4-Ethylcyclopentene	19.2	260	7.1	285	290
XV	1-Methylcyclobutene	6.3	12.3	0.54	140	38
XVI	Methylenecyclobutane	7.2	110	8.1	140	585

On the other hand, electronic factors would appear to be responsible for the higher tendency for complex formation of the 3-alkylcyclopentenes (IX and XIII), as compared with the 4-alkyl isomers (X and XIV). The same trend is observed in the cyclohexene series.

In parallel with data found in aqueous solutions,⁸ cyclopentenes show a higher affinity for silver ion than corresponding cyclohexenes, and, similarly, the stability of complexes in the methylenecyclohexane series increases in the order cyclohexane \leq cyclopentane < cyclobutane.

1-Methylcyclobutene (XV), for which no data are available in the literature so far, has, however, a lower stability constant than 1-methylcyclopentene, contrary to what could have been expected from its higher ring strain.

(9) J. Chatt, in "Cationic Polymerisation and Related Complexes," P. H. Plesch, ed., W. Heffer & Sons Ltd., Cambridge, England, 1953, p. 46.

THE HEAT OF FORMATION OF $\text{BF}_2(\text{g})$

By JOHN L. MARGRAVE

Department of Chemistry, University of Wisconsin, Madison, Wisconsin
Received January 17, 1962

Appearance potential studies on BF_3 ^{1,2} and on various organo-boron difluorides, including CH_3 -

(1) E. Gil-Av, J. Herling, and J. Shabtai, *J. Chromatog.*, **1**, 508 (1958); **2**, 406 (1959).

(2) R. O. C. Norman, *Proc. Chem. Soc.*, 151 (1958).

(3) G. P. Cartoni, R. S. Lowrie, C. S. G. Phillips, and L. M. Venanzi in "Gas Chromatography, 1960," R. P. W. Scott, ed., Butterworths, London, England, 1960, p. 273.

(4) S. Winstein and H. J. Lucas, *J. Am. Chem. Soc.*, **60**, 836 (1938).

(5) A. B. Littlewood, C. S. G. Phillips, and D. T. Price, *J. Chem. Soc.*, 1480 (1955).

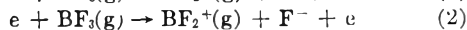
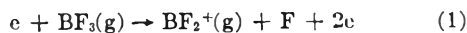
(6) A. I. M. Keulemans, "Gas Chromatography," 2nd ed., Reinhold Publ. Corp., New York, N. Y., 1959, p. 182.

(7) F. R. Hepner, K. N. Trueblood, and H. J. Lucas, *J. Am. Chem. Soc.*, **74**, 1333 (1952).

(8) J. G. Traynham and J. K. Olechowsky, *ibid.*, **81**, 571 (1959).

BF₂ and similar derivatives,³ now allow an experimental evaluation of the heat of formation of the BF₂ radical.

Consider the following reactions which might occur in the ionization chamber of a mass spectrograph to produce BF₂⁺



If reaction 1 holds

$$\text{App. pot. of BF}_2^+ \geq \Delta H_f^0(\text{BF}_2) + I(\text{BF}_2) + \Delta H_f^0(\text{F}) - \Delta H_f^0(\text{BF}_3)$$

With the appearance potential of BF₂⁺ selected as 16.5 ± 0.3 e.v.,^{1,2} the ionization potential of BF₂ given as 9.4 ± 0.1 e.v.,³ ΔH_f⁰(F) = 0.8 e.v.,⁴ and ΔH_f⁰(BF₃) = -11.7 e.v.,⁵ one computes ΔH_f⁰(BF₂) ≤ -5.4 ± 0.4 e.v. ≤ -124 ± 9 kcal./mole.

If reaction 2 holds

$$\text{A.p.}(\text{BF}_2^+) \geq \Delta H_f^0(\text{BF}_2) + I(\text{BF}_2) + \Delta H_f^0(\text{F}^-) - \Delta H_f^0(\text{BF}_3)$$

With ΔH_f⁰(F⁻) = -2.8 e.v.,⁶ one computes

$$\Delta H_f^0(\text{BF}_2) \leq -1.8 \pm 0.4 \text{ e.v.} \leq -42 \pm 9 \text{ kcal./mole}$$

To help choose between the values one can compare the experimentally determined thermochemical properties of CF₂, NF₂, and SiF₂ with those derived from average bond energy calculations. By this latter technique one estimates ΔH_f⁰(BF₂) = -135 kcal./mole; ΔH_f⁰(CF₂) = -23 kcal./mole; and ΔH_f⁰(SiF₂) = -137 kcal./mole, while the heats of formation of CF₂ and SiF₂ are known to be -45 ± 10 kcal./mole⁴ and -148 ± 4 kcal./mole,⁷ respectively. Thus, the average bond energy approach yields too endothermic a heat by 22 kcal./mole for CF₂ and 11 kcal./mole for SiF₂. The heat of formation of NF₃ has been reported as -29 ± 2 kcal./mole,⁸ which yields an average bond energy heat of formation for NF₂ of +18 kcal./mole. The experimentally determined heat of formation of NF₂ is +9 kcal./mole.⁹ It appears that AF₂ molecules are at least as stable as predicted on the basis of average bond energy calculations from AF₃ and AF₄ properties, and there is evidence for π-bonding in CF₂, NF₂, and SiF₂ which should not be so extensive in BF₂.

Thus, the appearance potential study establishes ΔH_f ≤ -124 ± 9 kcal./mole while the average bond energy calculation tends to suggest a slightly more negative heat. As a "best" value, it appears -130 ± 6 kcal./mole is consistent with all available data.

(1) O. Osberghaus, *Z. Physik*, **128**, 366 (1950).

(2) R. Law and J. Margrave, *J. Chem. Phys.*, **25**, 1086 (1956).

(3) W. C. Steele, L. D. Nichols, and F. G. A. Stone, *J. Am. Chem. Soc.*, **84**, 1154 (1962).

(4) JANAF Thermochemical Tables, USAF Control No. AF 33-(616)-6149, Advanced Research Projects Agency, Washington 25, D.C.

(5) S. Wise, W. N. Hubbard, H. Feder, and J. L. Margrave, *J. Phys. Chem.*, **65**, 2157 (1961).

(6) H. O. Pritchard, *Chem. Rev.*, **52**, 529 (1953).

(7) J. L. Margrave, A. Kanaan, and D. Pease, *J. Phys. Chem.*, **66**, 1200 (1962).

(8) G. T. Armstrong, S. Marantz, and C. F. Coyle, *J. Am. Chem. Soc.*, **81**, 3798 (1959).

(9) F. A. Johnson and C. G. Colburn, *J. Chem. Phys.*, **33**, 1869 (1960); *J. Am. Chem. Soc.*, **83**, 7043 (1961).

PRESSURE DEPENDENCE OF ELECTROLYTIC CONDUCTANCE IN TOLUENE

BY CHARLES M. APT, FREDERICK F. MARGOSIAN, IVAN SIMON, JAY H. VREELAND,

Arthur D. Little, Inc., Cambridge 40, Massachusetts

AND RAYMOND M. FUOSS

Department of Chemistry, Yale University, New Haven, Connecticut

Received January 20, 1962

The effect of pressure on the conductance of aqueous solutions was the subject of a number of classical researches by Tamman and others¹; water is, however, an exceptional liquid in most of its properties. Schmidt² measured the conductance of tetramethylammonium iodide in a series of organic solvents and found a rather close parallel between the pressure coefficients of fluidity ϕ and conductance σ for aprotic solvents; for hydrogen-bonding solvents, the values of $(\partial\phi/\partial p)_T$ and $(\partial\sigma/\partial p)_T$ were, as might be expected, considerably different. For the case of dilute solutions of electrolytes in aprotic solvents of high dielectric constant (e.g., acetonitrile, nitrobenzene), one would expect approximate equality of the two coefficients, because conductance is proportional to ionic mobility and the latter increases with increasing fluidity.³ In solvents of low dielectric constant, however, not all of the electrolytic solute contributes to conductance, due to ionic association. The latter is controlled by electrostatic forces which depend inversely on the dielectric constant, and the dielectric constant in turn depends on the pressure. Consequently, we would expect two effects of pressure on electrolytic conductance in solvents of low dielectric constant, one hydrodynamic and one electrostatic. It is the purpose of this note to present some preliminary measurements on the system tetrabutylammonium picrate-toluene at (approx.) 12, 25, and 75° over the pressure range up to 6000 kg./cm.², which will show that both effects are indeed present.

Experimental

The apparatus consisted of a cylindrical pressure bomb (25 mm. i.d., 100 mm. o.d., 250 mm. long), a two-stage pressure generator and a manganin resistance pressure gage. A coaxial, cylindrical conductance cell (57 mm. long, outer electrode 14.3 mm. i.d., inner electrode 12.7 mm. o.d., 0.00327 cm.⁻¹ cell constant) was inserted in the pressure bomb and immersed in the hydraulic fluid (kerosene). The gold-plated electrodes were insulated from each other by sapphire spacers and the lead from the inner electrode was brought out through the high-pressure plug by an optically polished sapphire insulator. The electrolyte in the conductance cell was separated from the hydraulic fluid by a thin-walled Teflon cup fitted over the end of the outer electrode. Sliding of the cup allowed transmission of the pressure without contamination of the electrolyte by the fluid and without appreciable pressure differential. The manganin gage was calibrated previously against an accurate dead-weight gage of the Michels' type. The leakage current of the empty cell was of the order of 10⁻¹² amp. Solutions of tetrabutylammonium picrate (m.p. 89.5°) were made with purified toluene

(1) C. A. Kraus, "Properties of Electrically Conducting Systems. Chemical Catalog Co., New York, N. Y., 1922, pp. 126-143.

(2) E. W. Schmidt, *Z. physik. Chem.*, **75**, 305 (1911).

(3) In second approximation, an electrostatic correction must be made to allow for the effects of dipole relaxation on the ionic motion; R. M. Fuoss, *Proc. Natl. Acad. Sci. U. S. A.*, **45**, 807 (1959).

(solvent conductance of the order 10^{-13} to 10^{-14} ohm $^{-1}$ cm. $^{-1}$).

Conductances were determined by measuring d.c. currents at 6.4 volts, using a Keithley Mod-210 chopper microammeter. The normal pressure conductance at room temperature was measured first; then measurements were made at a series of pressures up to about 7000 kg./cm. 2 gage, first at room temperatures and then at several other temperatures. At the end of a run, the normal pressure-room temperature resistance again was measured; it usually checked the initial value within a few per cent. (if not, the data were discarded).

In Fig. 1 is shown the conductance of tetrabutylammonium picrate in toluene at 28° (solid circles); for comparison, the conductance of tetraisoamylammonium picrate in benzene 4 at 25° (open circles) also is shown. By compensation of two opposite effects (higher viscosity of toluene, smaller size of the $(C_4H_9)_4N^+$ ion), the two curves practically coincide. The 28° conductances (at normal pressure) are as follows: $c = 5.80 \times 10^{-3}$ mole l. $^{-1}$, $\Lambda = 30.0 \times 10^{-4}$; 3.26×10^{-3} , 14.9×10^{-4} ; 7.65×10^{-4} , 3.01×10^{-4} ; 7.65×10^{-5} , 1.57×10^{-4} . The point at the lowest concentration is obviously a little high, but the pressure data for this solution will not be rejected, because our primary interest is in the ratio of the specific conductance σ at pressure p to the conductance σ_0 at normal pressure. The significant result of the experiments is summarized in Fig. 1: the lower curve (half-black points) is the conductance curve for tetrabutylammonium picrate in toluene at 24° and 6000 kg./cm. 2 . Although the viscosity 5 has increased approximately 20-fold, the conductance is decreased to about one quarter instead of to one twentieth (*i.e.*, the curve is displaced downward by about 0.6 log unit instead of by 1.3), as it would be if only hydrodynamic effects were involved.

The explanation of the apparent discrepancy is suggested by the simultaneous shift of the whole conductance curve to the right, *i.e.*, in the direction corresponding to curves for solvents of higher dielectric constant, which decreases ion association both to pairs and triples (which are the main species present in the vicinity of the conductance minimum 6). In this range of concentration, the conductance function is 7

$$\Lambda c^{1/2} = \Lambda_0 K_A^{-1/2} + (\lambda_0/K_A k_3) c \quad (1)$$

where Λ_0 and λ_0 are the limiting conductances for the solute species $(A^+ \cdot B^-)$ and the triple ions $(A_2B^+ \cdot AB_3^-)$, respectively, K_A is the pair association constant, and k_3 is the triple ion dissociation constant. The constant K_A varies as e^b where $b = e^2/aDkT$ (e = charge, a = center-to-center contact distance, D = dielectric constant, k = Boltzmann constant, and T = temperature) while k_3 varies as $e^{-b/2}$. Therefore, at two different pressures, where the dielectric constant has values D and D' and the viscosity values η and η' , the corresponding conductance ratio becomes

$$\Lambda'/\Lambda = \eta(\alpha e^{-b'/2} + \beta)/\eta'(\alpha e^{-b/2} + \beta) \quad (2)$$

where α and β are independent of pressure. At the minimum in conductance, where the two terms on the right side of (1) are equal, the conductance is

$$\Lambda c^{1/2} = 2\alpha e^{-b/2}/\eta \quad (3)$$

Explicitly, K_A is given by 8

$$K_A = (4\pi N a^3/3000) e^b \quad (4)$$

For $a = 6 \times 10^{-8}$ cm., for example, this becomes $K_A = 0.315 \exp(93/D)$ and therefore is extremely sensitive to the dielectric constant. The dielectric constant of toluene increases 9 from 2.375 at 30° and normal pressure to 2.775 at 6000 kg./cm. 2 . This change of only 17% in D changes $e^{b/2}$ by a factor several hundred in order of magnitude. Hence on raising the pressure to 6000 kg./cm. 2 , we may neglect β compared to $\alpha e^{-b'/2}$ in Λ' , giving for the conductance ratio

$$\Lambda'/\Lambda = (\eta/2\eta') \exp[(b - b')/2] \quad (5)$$

The experimental values are $\Lambda'/\Lambda = 1/4$ and $\eta/\eta' = 1/20$;

(4) R. M. Fuoss and C. A. Kraus, *J. Am. Chem. Soc.*, **55**, 3614 (1933).

(5) P. W. Bridgman, *Proc. Am. Acad. Arts Sci.*, **61**, 57 (1926).

(6) R. M. Fuoss and F. Accascina, "Electrolytic Conductance," Interscience Publishers, Inc., New York, N. Y., 1959, Chapter 17.

(7) R. M. Fuoss and C. A. Kraus, *J. Am. Chem. Soc.*, **55**, 2387 (1933).

(8) R. M. Fuoss, *ibid.*, **80**, 5059 (1953).

(9) Z. T. Chang, *Chinese J. Phys.*, **1**, No. 2, 1 (1934).

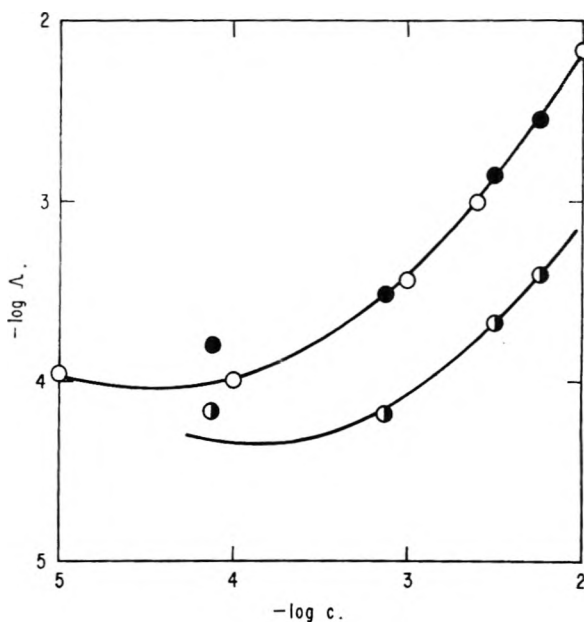


Fig. 1.—Conductance curves: tetraisoamylammonium picrate in benzene at 25° (open circles); tetrabutylammonium picrate in toluene at 28° and normal pressure (solid circles); tetrabutylammonium picrate in toluene at 24° and 6000 kg./cm. 2 (half-black circles).

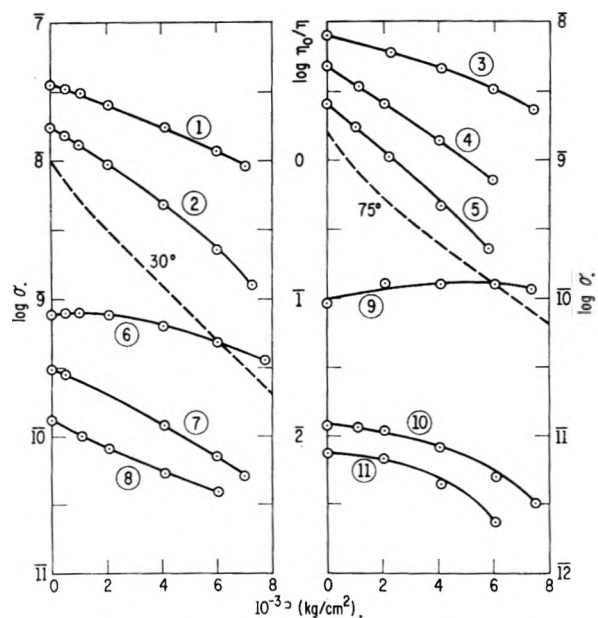


Fig. 2.—Specific conductance of tetrabutylammonium picrate in toluene as a function of concentration, pressure, and temperature: curves 1, 2 for 5.80×10^{-3} N at 77 and 28°; curves 3, 4, 5 for 3.26×10^{-3} N at 75, 28, 13°; curves 6, 7, 8 for 7.65×10^{-4} N at 77, 22, 13°; curves 9, 10, 11 for 7.65×10^{-5} N at 77, 24, 13°.

using $b = 560/aD$ and solving for \bar{a} , the ion pair contact distance, we find 7.4. This value for tetrabutylammonium picrate agrees reasonably well with values obtained from conductance in solvents of higher dielectric constant (for example, $\bar{a} = 5.83$ in ethylene chloride, 10 $\bar{a} = 5.80$ in trisecyl phosphate, 11 and $\bar{a} = 5.60$ in anisole. 12 The agree-

(10) D. J. Mead, R. M. Fuoss, and C. A. Kraus, *Trans. Faraday Soc.*, **52**, 594 (1936).

(11) M. A. Elliott and R. M. Fuoss, *J. Am. Chem. Soc.*, **61**, 294 (1939).

(12) G. S. Bien, C. A. Kraus, and R. M. Fuoss, *ibid.*, **56**, 1860 (1934).

ment shows that the expected electrostatic effect of pressure on conductance *via* the change in dielectric constant is the explanation of the observed discrepancy between $(\partial\phi/\partial p)_T$ and $(\partial\sigma/\partial p)_T$.

We conclude with a brief presentation of the experimental data by means of Fig. 2, where logarithm of specific conductance (mho cm.^{-1}) is plotted against pressure for the four systems studied. For comparison, Bridgman's viscosity data at 30 and 75° are shown as the dashed lines drawn to the same logarithmic scale (numerical scale values in center). If hydrodynamic effects alone were in control, all of the conductance curves would of course be parallel to the viscosity curves at the same temperature. At the higher concentrations and lower temperatures, there is a rough parallel because positive and negative effects of ionic associations tend to cancel, but at the lower concentrations and higher temperatures, the electrostatic effects described above nullify to a considerable extent the effect of increased viscosity due to increased pressure. Incidentally, the complexity of the σ - p - T relationships shown in Fig. 2 demonstrate quite convincingly that changes in the electrical resistance of a lubricated system may not be used as a measure of the viscosity changes in the lubricant. These exploratory measurements do serve, however, to show that the pressure dependence of conductance in non-aqueous systems offers an intriguing field for further experimental and theoretical work.

KINETIC DEUTERIUM ISOTOPE EFFECT IN THE NITROSATION OF ANILINE. THE DEUTERIUM ISOTOPE EFFECT ON THREE EQUILIBRIUM CONSTANTS

BY JOHN O. EDWARDS, KHAIRAT M. IBNE-RASA, ETSUYO ITOKAWA CHOI, AND COLIN L. RICE

*Metcalf Chemical Laboratories of Brown University,
Providence, Rhode Island*

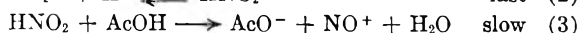
Received February 14, 1962

Part I

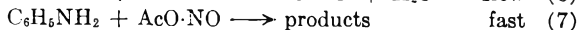
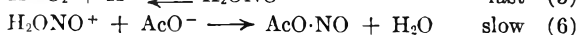
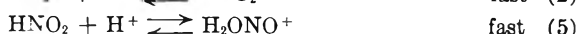
It has been found^{1,2} that the leading term in the rate equation for the nitrosation of aniline in acetate buffers is

$$\text{Rate} = k_{\text{AcO}^-}[\text{AcO}^-][\text{NO}_2^-][\text{H}^+]^2 \quad (1)$$

This rate equation, which is dominant when $[\text{AcO}^-] \gg [\text{NO}_2^-]$, has been interpreted¹ as representing the mechanism



Bunton and Masui³ have suggested an alternative mechanism for the buffer-catalyzed nitrosation



The former mechanism involves an O-H bond breaking in the rate step (eq. 3), while no O-H bond is broken in the slow step (eq. 6) of the latter mechanism. It was hoped that discrimination between these two mechanisms might be possible from the magnitude of the solvent deuterium isotope effect. The deuterium isotope effect on the ionization constant of nitrous acid was measured in connection with this kinetic study.

(1) J. O. Edwards, J. R. Abbott, H. R. Ellison, and J. Nyberg, *J. Phys. Chem.*, **63**, 359 (1959).

(2) F. Seel and W. Hufnagel, *Z. physik Chem.*, **26**, 270 (1960).

(3) C. A. Bunton and M. Masui, *J. Chem. Soc.*, 304 (1960).

Results.—The nitrosation technique described earlier¹ was used. Conditions were chosen to make the buffer-catalyzed path the predominant one; $[\text{C}_6\text{H}_5\text{NH}_3^+] = 5 \times 10^{-4} M$, $[\text{NO}_2^-] = 1 \times 10^{-2} M$, $[\text{AcO}^-] = 2 \times 10^{-1} M$, and $[\text{AcOH}] = 6.4 \times 10^{-2} M$ (from acetic anhydride). The rate of disappearance of aniline at 0° was found to be $2.26 \pm 0.03\%$ min.^{-1} in water, while that in D_2O was found to be $1.49 \pm 0.02\%$ min.^{-1} ; four kinetics runs were made in each solvent. The apparent $k_{\text{H}_2\text{O}}/k_{\text{D}_2\text{O}}$ thus was equal to 1.52 ± 0.04 .

In order to distinguish between the above two mechanisms, a knowledge of the relative acidities ($K_{\text{H}}/K_{\text{D}}$) of the acids HNO_2 , H_2NO_2^+ , and $\text{CH}_3\text{-COOH}$ in the solvents H_2O and D_2O is necessary. The value of the ratio $K_{\text{H}}/K_{\text{D}}$ for nitrous acid was determined by the method of Glasoe and Long.⁴ The $\text{p}K_{\text{H}}$ (where K is the concentration ionization constant) for nitrous acid in water at $\mu = 0.11$ and 25° was found to be 2.99 and $\text{p}K_{\text{D}}$ was found to be 3.53 under identical conditions. Thus $\text{p}K_{\text{D}} - \text{p}K_{\text{H}}$ for nitrous acid is 0.54 and the ratio $K_{\text{H}}/K_{\text{D}} = 3.5$.

The value $K_{\text{H}}/K_{\text{D}}$ for acetic acid, which is known to be 3.3,^{4,5} also was found to be 3.3 at 25°, thus verifying our technique.

Discussion.—Contrary to our hopes, the value of $K_{\text{H}}/K_{\text{D}}$ for aniline nitrosation turned out to be inconclusive as to the mechanism. Taking out the known influence of nitrous acid ionization and acetic acid ionization (twice) in H_2O and D_2O , the mechanism of Bunton and Masui³ ascribes the remaining isotope effect of 2.1 to the ratio of ionization constants of H_2NO_2^+ and D_2NO_2^+ (assuming negligible secondary solvation effects). In view of the fact that the ratio $K_{\text{H}}/K_{\text{D}}$ for ionization constants decreases as the value of $\text{p}K_{\text{H}}$ decreases,⁶ this value of 2.1 is quite reasonable for the ionization of as strong an acid as H_2NO_2^+ .

In the mechanism involving rate determining proton transfer, the ionization constants for nitrous acid and acetic acid ionizations again are applied to the observed rates. The ratio $k_{\text{H}}/k_{\text{D}}$ for the rate step (eq. 3) thus is calculated to be 1.6. This value is close to those reported by Jencks and Carriolo⁷ for the general base-catalyzed hydrolysis of acyl activated esters ($k_{\text{H}_2\text{O}}/k_{\text{D}_2\text{O}} = 2$ to 3), where O-H bond stretching presumably is involved in the transition state. It also is close to the value of the deuterium isotope effect ($k_{\text{H}}/k_{\text{D}} = 1.7$) reported by Butler and Gold⁸ for the acetate-catalyzed hydrolysis of acetic anhydride, where a rate-controlling proton transfer is suggested to be involved.

It is apparent therefore that the solvent deuterium isotope effect cannot be employed to sort out the correct mechanism for aniline nitrosation at the present time.

Part II

Equilibrium constants of two reactions, involving

(4) P. K. Glasoe and F. A. Long, *J. Phys. Chem.*, **64**, 188 (1960).

(5) S. Korman and V. K. LaMer, *J. Am. Chem. Soc.*, **58**, 1346 (1936).

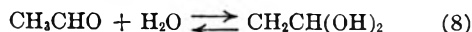
(6) N. C. Li, P. Tang, and R. Mathur, *J. Phys. Chem.*, **65**, 1074 (1961).

(7) W. P. Jencks and J. Carriolo, *J. Am. Chem. Soc.*, **83**, 1743 (1961).

(8) A. R. Butler and V. Gold, *J. Chem. Soc.*, 2305 (1961).

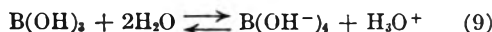
hydration steps, were measured in the solvents H₂O and D₂O.

Results.—An uncomplicated hydration reaction studied was that of acetaldehyde in aqueous solution



using ultraviolet absorption to measure the amount of free carbonyl formed, according to the method of Bell and Clunie.⁹ It was found that $K_{\text{H}} = 1.40$ and $K_{\text{D}} = 1.54$. Thus $K_{\text{H}}/K_{\text{D}}$ is equal to 0.91 (at 20°, no added electrolyte). Using the value of the hydration equilibrium constant in H₂O at 0°⁹ and the data on the relative rates of formation and decomposition of acetaldehyde hydrate in water and deuterium oxide,¹⁰ a value of 0.92 was calculated for this ratio. This agrees well with our directly measured value of 0.91.

The second hydration reaction, the ionization of boric acid, is known to involve a change in coordination number from three to four as in the equation

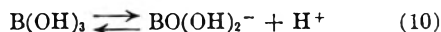


For this reaction the value of 9.27 found here for $\text{p}K_{\text{a}(\text{H})}$ is in good agreement with literature values. The value of 9.79 for $\text{p}K_{\text{a}(\text{D})}$ was observed. Thus $K_{\text{H}}/K_{\text{D}}$ for the boric acid ionization is 3.3.

Discussion.—Hydration of acetaldehyde goes to a larger extent in D₂O than in H₂O. It is not obvious why D₂O should bind more strongly than H₂O, but the fact that the value of $K_{\text{H}}/K_{\text{D}}$ is close to unity seems reasonable.

The observed value of $K_{\text{H}}/K_{\text{D}}$ for boric acid ionization is 3.3, which is less than the value of 4.0 that is interpolated from the data given by Bell¹¹ when the observed $\text{p}K_{\text{a}}$ is used.

In fact, it is necessary to consider separately the isotope effects on two aspects of the boric acid ionizations. These are



From Branch and Calvin¹² we have an estimate for the $\text{p}K_{\text{a}}$ of boric acid as a Brønsted acid: this value of 12.6 can be used to evaluate $K_{\text{H}}/K_{\text{D}}$ for eq. 10, which turns out to be 4.7. Since

$$(K_{\text{H}}/K_{\text{D}})_9 = (K_{\text{H}}/K_{\text{D}})_{10} \times (K_{\text{H}}/K_{\text{D}})_{11}$$

where subscripts denote equation numbers, it can be shown that the estimated value for $K_{\text{H}}/K_{\text{D}}$ for eq. 11 is 0.70. Thus hydration of the borate ion is more favored in D₂O than in H₂O. This is the same direction as found in the acetaldehyde hydration; however, the magnitude is certainly larger.

The data given indicate that a hydration reaction has a different equilibrium constant in D₂O than in H₂O. For this reason, caution must be observed in interpretation of deuterium isotope effects where hydration may be involved.

Experimental

The rates of nitrosation of aniline in D₂O and H₂O, at 0°, were measured according to the method described earlier,¹ except that quantities and aliquots were reduced in size to economize in the use of D₂O. Acetic anhydride was used as a source of acetic acid and the concentrations of all the reactants and the buffering agents, which have been given in the section entitled "Results," were identical in both the solvents within experimental error, and were chosen to make the buffered catalyzed reaction the predominant one.

Measurements of pH and pD were made with a Beckman Model GS pH meter at 25°. Conventional buffer mixtures were used as standards. Reagent grade chemicals were used. The D₂O was 99.5 atom % deuterium. Solutions of roughly 0.05 M HCl in H₂O and DCl in D₂O were prepared and standardized by titration with standard sodium hydroxide. In a typical experiment for the determination of the ionization constant of nitrous acid, a solution containing 0.10 M NaNO₂ and 0.01 M DCl in D₂O was prepared at 25° and the pH measured. pD then was taken as the pH meter reading +0.40.⁴ The electrodes were dried in a mercury bath before immersion in the D₂O solutions. The ionization constants of boric acid were studied similarly except that purified samples of Kernite (Na₂B₄O₇·4H₂O) were employed to give the proper buffer ratio directly.

In aqueous systems pH is defined as $-\log C_{\text{H}^+} - \log f_{\pm}$, where f_{\pm} is the activity coefficient. At a total ionic strength of 0.11, which was maintained during the measurements, $-\log f_{\pm}$ was taken as 0.10.⁶

A Beckman DK-1 spectrophotometer was used to obtain the spectra of acetaldehyde solutions, which were allowed to equilibrate at 20°. The concentration range studied was 0.02–0.12 M. In order to obtain ϵ_0 , the extinction coefficient of the pure, unhydrated acetaldehyde in H₂O, the data of Bell and Clunie⁹ were used to determine the fraction hydrated at 20°. The interpolated value is 0.583, and this was assumed to be correct and was used for the calculation of ϵ_0 . The extinction coefficient obtained for the solution (which was due to the unhydrated fraction of acetaldehyde) in H₂O was 7.47 at the absorption maximum (λ_{max} 276 m μ). Therefore ϵ_0 turns out to be 17.9. By using the experimentally obtained extinction coefficient of the D₂O solutions and ϵ_0 , the fraction of acetaldehyde hydrated in D₂O was found to be 0.606. Thus K_{H} , the hydration equilibrium constant in H₂O, is 1.40 and K_{D} , the hydration equilibrium constant in D₂O, is 1.54. The ratio of the two constants, $K_{\text{H}}/K_{\text{D}}$, is 0.91. The extinction coefficient of acetaldehyde in spectral grade cyclohexane was found to be 17.0, in agreement with the ϵ_0 determined above.

Acknowledgment.—We are pleased to acknowledge the continued support of the U. S. Atomic Energy Commission. K. M. I. is thankful to Forman Christian College (Lahore, Pakistan) and its principal, Rev. R. M. Ewing, for a grant of leave.

(9) R. P. Bell and J. C. Clunie, *Trans. Faraday Soc.*, **48**, 439 (1952).

(10) Y. Pocker, *Proc. Chem. Soc.*, 17 (1960).

(11) R. P. Bell, "The Proton in Chemistry," Cornell Univ. Press, Ithaca, N. Y., 1959, p. 188.

(12) G. E. K. Branch and M. Calvin, "The Theory of Organic Chemistry," Prentice-Hall, Inc., New York, N. Y., 1941, p. 211.

COMMUNICATIONS TO THE EDITOR

THE IONIZATION POTENTIAL OF HYDROGEN DISULFIDE (H_2S_2)¹

Sir:

Hydrogen disulfide was discovered by Scheele in 1777,² and a number of subsequent investigators³ have determined various physical properties of H_2S_2 . In the course of a detailed study of the mass spectrum and the appearance potentials of different ions from 3,4-dithiahexane, we have found that the $m/e = 66$ ion is quite intense. The abundances of $m/e = 68$ and $m/e = 70$, due to the natural abundance of S^{34} , indicate that $m/e = 66$ contains two sulfur atoms, and is nearly entirely due to H_2S_2^+ at 70 e.v.

The appearance potential of the H_2S_2^+ ion was found to be 12.2 ± 0.2 e.v. from measurements on both the $m/e = 66$ and the $m/e = 68$ ions. Our measurements were made using a time-of-flight mass spectrometer⁴ and the appearance potentials were determined by the extrapolated voltages difference method⁵ and the energy compensation technique.⁶

From the rather low appearance potential, the ionization and dissociation process leading to H_2S_2^+ from 3,4-dithiahexane is expected to be relatively simple. Such a process is: $\text{C}_2\text{H}_6\text{SSC}_2\text{H}_5 \rightarrow \text{H}_2\text{S}_2^+ + 2\text{C}_2\text{H}_4$. From our determined appearance potential and from $\Delta H_f(\text{C}_2\text{H}_6\text{SSC}_2\text{H}_5) = -17.42$ kcal./mole⁷ and $\Delta H_f(\text{C}_2\text{H}_4) = 12.496$ kcal./mole,⁸ we calculate $\Delta H_f^+(\text{H}_2\text{S}_2) = 239$ kcal./mole. We compare this value to the value of $\Delta H_f^+(\text{H}_2\text{S}) = 236$ kcal./mole.⁹

Feher and Winkhaus¹⁰ determined $\Delta H_f(\text{H}_2\text{S}_2(l)) = -4.21$ kcal./mole, in fair agreement with a calculated value of -5.5 kcal./mole,⁸ and $\Delta H_f(\text{H}_2\text{S}_2(g)) = 3.83$ kcal./mole. Also, Feher and Hitzemann^{3c} report $\Delta H_{\text{vap}}(\text{H}_2\text{S}_2) = 8.074$ kcal./mole. $\Delta H_f(\text{H}_2\text{S}_2)$ together with $\Delta H_f^+(\text{H}_2\text{S}_2)$ leads to the calculation of $I(\text{H}_2\text{S}_2) = 10.2$ e.v. This

(1) This study was supported in part by the U. S. Atomic Energy Commission, under Contract No. AT(11-1)-751 with Kansas State University.

(2) C. L. Berthollet, *Ann. chim. phys.*, (1) **25**, 248 (1798); "Chemische Abhandlung von der Luft und dem Feuer," Berlin, 1793, p. 162.

(3) See, for example, (a) J. H. Walton and L. B. Parsons, *J. Am. Chem. Soc.*, **43**, 2539 (1921); (b) K. H. Butler and O. Maass, *ibid.*, **52**, 2184 (1930); (c) F. Feher and G. Hitzemann, *Z. anorg. allgem. Chem.*, **294**, 50 (1958).

(4) E. J. Gallegos and R. W. Kiser, *J. Am. Chem. Soc.*, **83**, 773 (1961).

(5) J. W. Warren, *Nature*, **165**, 811 (1950).

(6) R. W. Kiser and E. J. Gallegos, *J. Phys. Chem.*, **66**, 947 (1962).

(7) W. N. Hubbard, D. R. Douslin, J. P. McCullough, D. W. Scott, S. S. Todd, J. F. Messerly, I. A. Hossenlopp, A. George, and G. Waddington, *J. Am. Chem. Soc.*, **80**, 3547 (1958).

(8) F. D. Rossini, D. D. Wagman, W. H. Evans, S. Levine, and I. Jaffe, "Selected Values of Chemical Thermodynamic Properties," National Bureau of Standards Circular 500, U. S. Government Printing Office, Washington, D. C., 1952.

(9) F. H. Field and J. L. Franklin, "Electron Impact Phenomena and the Properties of Gaseous Ions," Academic Press, Inc., New York, N. Y., 1957, p. 300.

(10) F. Feher and G. Winkhaus, *Z. anorg. allgem. Chem.*, **292**, 210 (1957).

result may be compared with the ionization potentials of 10.47 e.v. for H_2S ,^{11,12} 12.60 e.v. for water,¹³ and 11.26 e.v.¹⁴ and 12.1 e.v.¹⁵ for hydrogen peroxide.

It is possible to calculate a value of $I(\text{H}_2\text{S}_2)$ based on Franklin's group orbital method.¹⁶ Taking $I(\text{CH}_3\text{SSCH}_3) = 8.46$ e.v.,¹⁷ the C-S interaction parameter = 1.99,¹⁸ and $I(\text{CH}_4) = 13.31$,^{16,18} we calculate $I(\text{H}_2\text{S}_2) = 10.09$ e.v. If this same calculation is performed with $I(\text{C}_2\text{H}_5\text{SSC}_2\text{H}_5) = 8.27$ e.v.,¹⁷ we calculate $I(\text{H}_2\text{S}_2) = 9.90$ e.v. Both of these calculations agree with our experimental results.

Combining $\Delta H_f(\text{H}_2\text{S}_2) = 3.83$ kcal./mole with $\Delta H_f(\text{SH}) = 33$ kcal./mole,¹⁸ we calculate $D(\text{HS-SH}) = 62$ kcal./mole. The results of Franklin and Lumpkin¹⁹ agree when using the lower limit of their value of $\Delta H_f(\text{SH}) = 38 \pm 5$ as $\Delta H_f(\text{SH}) = 33$ kcal./mole. Our value of $D(\text{HS-SH}) = 62$ kcal./mole is also in agreement with $E(\text{S-S}) = 63.2$ kcal./mole reported by Feher and Winkhaus.¹⁰ If $\Delta H_f(\text{SH})$ should be closer to 30 kcal./mole,²⁰ $D(\text{HS-SH})$ would be more nearly 56 kcal./mole. We conclude then that $D(\text{HS-SH}) = 59 \pm 3$ kcal./mole, a value not too different from $D(\text{HO-OH})$.²⁰

(11) P. G. Wilkinson, *J. Mol. Spectry.*, **6**, 1 (1961).

(12) J. D. Morrison, *J. Chem. Phys.*, **19**, 1305 (1951).

(13) D. C. Frost and C. A. McDowell, *Can. J. Chem.*, **36**, 39 (1958).

(14) L. P. Lindeman and J. G. Guffy, *J. Chem. Phys.*, **29**, 247 (1958).

(15) A. J. B. Robertson, *Trans. Faraday Soc.*, **48**, 229 (1952).

(16) J. L. Franklin, *J. Chem. Phys.*, **22**, 1304 (1954).

(17) K. Watanabe, T. Nakayama, and J. Mottl, "Final Report on Ionization Potential of Molecules by a Photoionization Method," December, 1959; Dept. Army #5B99-01-004 ORD-#TB2-0001-OOR-#1624, Contract No. DA-04-200-ORD 480 and 737.

(18) E. Gallegos and R. W. Kiser, *J. Phys. Chem.*, **65**, 1177 (1961).

(19) J. L. Franklin and H. E. Lumpkin, *J. Am. Chem. Soc.*, **74**, 1023 (1952).

(20) T. L. Cottrell, "The Strengths of Chemical Bonds," Sec. Ed., Butterworths Scientific Publications, London, 1958, pp. 212, 224, and 255.

DEPARTMENT OF CHEMISTRY
KANSAS STATE UNIVERSITY
MANHATTAN, KANSAS

ROBERT W. KISER
BRICE G. HOBROCK

RECEIVED APRIL 23, 1962

THE EFFECT OF GASES ON THE ELECTRON SPIN RESONANCE SPECTRUM OF CHEMISORBED DIPHENYLETHYLENE

Sir:

Radical cation formation in the chemisorption of polynuclear aromatic hydrocarbons on silica-alumina catalysts has been demonstrated by electron spin resonance measurements.¹ A similar species had been suggested earlier² to account for the long wave length (600 m μ) absorption band observed^{2,3}

(1) J. J. Rooney and R. C. Pink, *Proc. Chem. Soc.*, **70**, 142 (1961).

(2) H. P. Leftin and W. K. Hall, *J. Phys. Chem.*, **64**, 382, 1714 (1960).

(3) A. Webb, "Proc. Int. Catalysis Cong. II," Editions Technip, Paris, 1960, Vol. I, p. 1289.

from chemisorbed 1,1-diphenylethylene. In this case an e.s.r. signal was not observed and since the only alternate assignment,³ namely, that of an olefin π -complex⁴ with surface protons, has been discredited^{2,5} the nature of this chemisorbed species remains unsettled.

Recent experiments in this Laboratory have shown that the chemisorbed 1,1-diphenylethylene species is indeed paramagnetic and that the resonance signal is strongly influenced by surface conditions. The effect of oxygen on the e.s.r. from chemisorbed perylene and anthracene has raised serious doubts concerning the ability of silica-alumina to produce radical ions by direct reaction with hydrocarbons.⁶ The present communication reports data which show that although oxygen has a profound and reversible effect on the e.s.r. signal associated with chemisorbed 1,1-diphenylethylene, in this case at least, the effect is in a contradictory sense to that observed by Fogo⁶ and tends to support the hypothesis that radical cations also can be formed by interactions involving only the hydrocarbon and the acid site on the surface of the catalyst.

E.s.r. Spectra of Chemisorbed Diphenylethylene.

—The e.s.r. spectrum of 1,1-diphenylethylene chemisorbed on a (25% alumina, 75% silica) cracking catalyst (Varian V-4500 spectrometer operating with 100 kc. field modulation) consists of a single broad resonance line having a half-width of about 12 gauss and centered at $g = 2.00$ and is similar to the e.s.r. spectrum for the blue compound formed by reduction of diphenylethylene with potassium metal in tetrahydrofuran solution.² This similarity in the e.s.r. and in the optical spectra² of cation and anion radicals is as predicted from the simple MO theory for radical ions.⁷ Failure to detect hyperfine splitting of the resonance line suggests exchange involving the radical ion and excess neutral olefin that is present in a physically adsorbed layer; alternatively it may be due in part to anisotropy of the resonance.

The Effect of Oxygen.—Samples were calcined in oxygen and evacuated for 24 hr. at 500°. A was sealed under vacuum while B was sealed with 5 mm. of oxygen pressure. Samples C and D were further treated in an atmosphere of hydrogen for 24 hr. at 500° prior to final evacuation. C was sealed under vacuum while 8 mm. of hydrogen was added to D prior to sealing. In each case the adsorbate was evacuated separately in a compartment joined to the sample tube through a breakoff seal. Chemisorption was controlled such that each sample ultimately attained the same degree of surface coverage. E.s.r. due to either the quartz sample tube or to the clean catalyst was not detected even when oxygen was present on the catalyst surface. Both absorption intensity and the line widths were dependent on surface environment. Line widths were somewhat greater for those samples having an oxygen history and the

intensities generally were lower. Addition of oxygen to a sample having either an oxygen or a hydrogen history led to a significant decrease in intensity. This effect could be reversed at room temperature either by pumping out the gas or by introducing an oxygen-free gas to the system. These observations are quite the reverse of those reported by Fogo,⁶ who found that exposure of adsorbed anthracene to the air caused an appreciable enhancement in the e.s.r. signal. They are, however, similar to the reversible oxygen effect observed with carbon blacks,⁸ which has been ascribed to broadening due to the interaction of the surface radicals with the unpaired electrons of the oxygen molecules.

We have observed another, hitherto unreported, effect of surface environment on the e.s.r. spectra of adsorbed radicals. While the enhancement of the signal observed when hydrogen (A-4) or argon (B-4) was added to the samples having an oxygen history might be explained on the basis of a dilution of adsorbed oxygen by the adsorption of the other gas, no such explanation can be given for the results obtained with samples C and D. These samples which had a hydrogen history (did not contain adsorbed oxygen) also showed an enhancement of signal intensity upon the addition of gaseous hydrogen or water vapor. This effect was reversible. One possible explanation is that the unpaired electrons of the adsorbed radicals are perturbed by interaction with active sites or with

TABLE I

	Sample and conditions	Intensity (arbitrary units)	Width ^a (gauss)
A	1 Vacuum (O ₂ history)	0	...
	2 1,1-Diphenylethylene chemisorbed	90	11
	3 O ₂ added (10 mm.)	77	12
	4 O ₂ pumped out and H ₂ added (10 mm.)	89	12
B	1 5 mm. O ₂	0	...
	2 1,1-Diphenylethylene chemisorbed	45	12
	3 O ₂ pumped out	65	12
	4 Argon added (10 mm.)	150	11.3
C	1 Vacuum (H ₂ history)	0	...
	2 1,1-Diphenylethylene chemisorbed	65	10
	3 H ₂ added (8 mm.)	109	9.0
	4 H ₂ pumped out and O ₂ added (10 mm.)	83	12
D	1 8 mm. H ₂	0	...
	2 1,1-Diphenylethylene chemisorbed	143	8.6
	3 H ₂ pumped out	85	10.5
	4 H ₂ O added (10 mm.)	188	8.9

^a Peak width at half peak height.

other adsorbed species such as, *e.g.*, the methyl-diphenylcarbonium ions which also^{2,3} are present on the surface. The added gases can shield these surface groups and therefore diminish their effect on the adsorbed radicals. In the case of water vapor the carbonium ions are preferentially desorbed (bleaching of the spectrum at 423 m μ)

(4) A. G. Evans, P. M. S. Jones, and J. H. Thomas, *J. Chem. Soc.*, 104 (1957).

(5) J. A. Grace and M. C. R. Symons, *ibid.*, 958 (1959).

(6) J. K. Fogo, *J. Phys. Chem.*, **65**, 1919 (1961).

(7) S. I. Weissman, E. DeBoer, and J. J. Conradi, *J. Chem. Phys.*, **26**, 963 (1958).

(8) (a) D. E. G. Austin and D. J. E. Ingram, *Chem. Ind. (London)*, 981, (1956); (b) L. H. Piette "NMR and EPR Spectroscopy," Pergamon Press, New York, N. Y., 1960, pp. 212-214; (c) H. Harker, C. Jackson, and W. F. K. Wynne-Jones, *Proc. Roy. Soc. (London)*, **A262**, 328 (1961), and references therein.

whereas the radical ions are substantially unaltered.^{2,3} It has been suggested³ that in this desorption process the carbonium ions are converted to the long wave length species (radical cation). This would be consistent with the increased number of spins observed when argon (B-4), hydrogen (C-3), and water (D-4) were added to our systems.

Table I summarizes some of the relevant data.

The pronounced effect of water vapor on the intensity of the c.s.r. signal (D-4) suggests that a

similar effect (due to atmospheric moisture) may have influenced the earlier⁶ work.

M. W. KELLOGG RESEARCH LABORATORIES H. P. LEFTIN
JERSEY CITY, N. J.
CHEMISTRY DEPARTMENT M. C. HOBSON
UNIVERSITY OF PENNSYLVANIA
PHILADELPHIA, PENNSYLVANIA
E. R. JOHNSON FOUNDATION J. S. LEIGH
UNIVERSITY OF PENNSYLVANIA
PHILADELPHIA, PENNSYLVANIA

RECEIVED MARCH 1, 1962

1961 DIRECTORY OF GRADUATE RESEARCH

The newest edition of this unique directory is the fifth to be prepared by the ACS Committee on Professional Training. It covers the 1959-60 and 1960-61 academic years and provides a useful reference to:

- degrees available
- fields of interest and publications
of 3702 faculty members

in 273 departments or divisions of chemistry, biochemistry, and chemical engineering in United States universities offering the Ph.D. degree.

Under each department heading, degrees offered and fields of specialization appear first. Then faculty members are listed alphabetically with an up-to-date record on their education...general fields of major research interest...subjects of current research...publications during the past two years. You can clearly determine where your own field of interest is most actively represented.

The table of contents lists universities under the three main groups. There is another index by faculty names. A summary table also shows for each graduate department of chemistry the number on the faculty, number of Ph.D.'s in each department, graduate enrollment, and Ph.D. degrees granted in 1959-60 and 1960-61. It offers as a starting point a quick comparison by size.

If you counsel students or seek an advanced degree yourself, or if you are interested in knowing the kind of research done in certain academic centers, for whatever purpose, then this book will answer your questions and save you time.

529 pages.

Paper bound.

Price: \$4.00

Order from:

**Special Issues Sales, American Chemical Society
1155 16th Street, N. W., Washington 6, D. C.**

No. **31** in the
**ADVANCES IN
CHEMISTRY
SERIES**

CRITICAL SOLUTION TEMPERATURES

by **Alfred W. Francis**, consultant to Socony Mobil Oil Co., Inc.

This volume, written by an authority on hydrocarbon chemistry and liquid-liquid phase relations, lists over 6000 critical solution temperatures (the minimum temperature for mixing of two substances in all proportions *as liquids*). Also included are about 800 aniline point observations; methods for determining CST; guides to using CST data and to estimating the CST for untested systems.

Among uses of CST are: screening possible extraction solvents for selectivity; approximating liquid solubility at any temperature below the CST; characterizing hydrocarbons; analysis of mixtures, especially where water is one component, and providing an insight into molecular structure.

CONTENTS

Introduction and six Figures: Critical Solution Temperatures . . .
Aniline and Furfural Points . . . Lower Critical Solution Temperatures . . . Mutual Miscibility of Liquids (tabulations of numerical CST data from charts in five published compilations) . . . Bibliography.

246 pages.

Cloth bound.

Price: \$5.00

Order from: **Special Issues Sales, American Chemical Society**
1155 Sixteenth Street, N.W., Washington 6, D. C.
